

Novel Insights into the Nitrogen Assimilation Pathways in Chickpea (*Cicer arietinum*) Nodules

By

Troy Miller

Bachelor of Science (Honours) (Biotechnology)

Thesis

Submitted to Flinders University

for the degree of

Doctor of Philosophy

College of Science and Engineering

23rd September 2024

Table of Contents

TABLE OF CONTENTS	I
ABSTRACT	VI
DECLARATION	VIII
ACKNOWLEDGEMENTS	IX
ABBREVIATIONS	XI
LIST OF FIGURES	XIII
LIST OF TABLES	XVIII
1 INTRODUCTION	1
1.1 Nitrogen Use and Global Food Security	2
1.1.2 Chickpea agricultural and economic significance	3
1.2 Biological Nitrogen Fixation	5
1.2.1 Nodule organogenesis	7
1.2.3 Determinate and indeterminate type nodules	9
1.2.4 Nitrogenase activity	11
1.2.5 Fixed carbon fuels the bacteroids	12
1.3 Legumes Role in Agricultural Productivity	13
1.4 Pathways of Fixed Nitrogen	15
1.4.1 Ammonium assimilation into amino acids	15
1.4.2 The ureide pathway	18
1.4.3 The amide pathway	21
1.5 The Source-to-Sink Interplay between Carbon and Nitrogen Partitioning	22
1.5.1 What role does nitrogen metabolism, ureides and amides play in chickpea?	23
1.6 Aims	29
2 GENERAL METHODS	30
2.1 General Lab Techniques	31
2.1.1 Reagents	31
2.1.2 Streak & spread plating	31
2.1.3 Bacterial inoculation	31
2.1.4 Glycerol stock preparation	31
2.1.5 TSS buffer preparation	31
2.1.6 Preparation of TSS chemical competent DH5 α E. coli	32
2.1.7 SOC broth preparation	32
2.1.8 Heat shock transformation of chemical competent E. coli	32
2.1.9 Plasmid purification	32
2.1.10 Ammonium acetate precipitation	33
2.1.11 Polymerase chain reaction (PCR)	33
2.1.12 Colony PCR	33

2.1.13 PCR clean-up.....	34
2.1.14 Agarose gel electrophoresis	34
2.1.15 Agarose gel DNA purification	34
2.1.16 Restriction digestion.....	35
2.2 Plant Growth & Harvesting.....	36
2.2.1 Growth conditions.....	36
2.2.2 Tissue harvesting	38
2.2.3 Plant nitrogen growth experimental setup	38
2.3 Gene Expression Analysis	39
2.3.1 Diethyl pyrocarbonate (DEPC) treatment	39
2.3.2 TRIzol RNA extraction	39
2.3.3 ProtoScript cDNA synthesis	40
2.3.4 Quantitative reverse transcriptase PCR (qRT-PCR) primer design	42
2.3.5 qRT-PCR setup & thermocycling.....	43
2.3.6 qRT-PCR standards	43
2.4 Ureide Colorimetric Assay	44
2.4.1 Tissue preparation for ureide quantification	44
2.5 RNA Sequencing	48
2.5.1 RNA sequencing growth conditions and tissue harvesting	48
2.5.2 RNA extraction and sequencing setup	48
2.6 Gateway® Cloning into <i>S. cerevisiae</i>	49
2.6.1 Gateway® vectors	49
2.6.2 Gene amplification for Gateway® cloning.....	49
2.6.3 Overlapping PCR to anneal attB cloning sites to gene products.....	49
2.6.4 Cloning gene products into Gateway® entry plasmids (BP Clonase™).....	50
2.6.5 Cloning gene products into Gateway® destination plasmids (LR Clonase™ II)	51
2.7 <i>S. cerevisiae</i> Expression Experiments	52
2.7.1 <i>S. cerevisiae</i> strains used for characterization experiments	52
2.7.2 <i>S. cerevisiae</i> transformation into mutant and parental strains	52
2.7.3 Preparation of the mutant and parental <i>S. cerevisiae</i> strain	52
2.7.4 Streak plate assay of the amino acid knockout <i>S. cerevisiae</i> strain	53
2.7.5 Spot plate assay of the amino acid knockout <i>S. cerevisiae</i> strain	53
2.7.6 Liquid growth assay of the amino acid knockout <i>S. cerevisiae</i> strain	53
3 NITROGEN METABOLISM, AMIDE AND UREIDE BIOSYNTHESIS IN CHICKPEA	55
Chapter 3: Introduction.....	56
3.1 Legume Classification	56
3.1.1 Distinguishing between ureide and amide producing legumes	56
Chapter 3: Aims	57
Chapter 3: Results.....	58

3.2 Nitrogen Growth Experiments	58
3.2.1 Chickpea nodules exhibit indeterminate type morphology	58
3.2.2 Chickpea nitrogen supplementation time course	59
3.2.3 Chickpea experience rapid nodule senescence after the onset of nitrogen fixation.....	71
3.3 Gene Expression Analysis of Nitrogen Fixation	73
3.3.1 Nitrogen and amide metabolism gene expression in chickpea nodules.....	73
3.3.2 Ureide biosynthesis gene expression in nodules	75
3.3.3 Fixed-N transporter gene expression in chickpea nodules	78
3.4 Ureide Quantification and Transport in N ₂ Fixing Chickpea Nodules.....	81
3.4.1 Comparison of total ureide biosynthesis between chickpea and <i>G. max</i>	81
3.4.2 The effect of nitrogen availability on ureide biosynthesis	84
Chapter 3: Discussion	87
3.5 Limited Evidence for Ureide Biosynthesis in Chickpea Nodule	87
5.6 Experimental Limitations.....	89
Chapter 3: Conclusions.....	89
4 TRANSCRIPTIONAL ANALYSIS OF NITROGEN FIXATION IN CHICKPEA NODULES USING RNA SEQUENCING	91
Chapter 4: Introduction.....	92
4.1 Fixed Nitrogen Transport in Legumes	92
4.1.1 Ureide transport network.....	93
4.1.2 Amino acid and amide synthesis	93
4.1.3 Ureide synthesis	94
4.1.4 Legume transcriptomic databases	94
Chapter 4: Aims	96
4.2 RNA Sequencing Comparisons of Differentially Expressed Genes	97
4.3 Set-Up and Pre-Processing of Chickpea RNA Sequencing Data.....	99
4.4.1 Transcriptional variability and correlation of the total RNAseq dataset.....	101
4.4.2 Statistical significance and transcriptional fold change for RNAseq comparisons.....	103
4.4.3 Analysis of enriched functional gene categories in chickpea during nitrogen fixation.....	110
4.5 RNA Sequencing Reveals an Updated Model of Nitrogen Fixation in Chickpea	114
4.5.1 Imported nodule sucrose supports malate synthesis in the uninfected cell prior to metabolism in the infected cell.....	117
4.5.2 Carbon transport in chickpea	126
4.5.3 Carbon metabolism in chickpea	126
4.5.4 Chickpea nodules exhibit upregulation of the GS/GOGAT cycle and amide synthesis.	128
4.5.5 Upregulation of aminotransferases of the shikimate pathway	129
4.5.6 Non-differential expression of the ureide biosynthesis pathway	134
4.6 Chickpea Predominantly Synthesise Amides from Fixed Nitrogen	137
4.6.1 The synthesis of amino acids and amides in chickpea	137
4.6.2 The synthesis and degradation of ureides in chickpea	140

4.7 Upregulation of Key Amino Acid Transporters from Multiple Gene Families.....	144
4.7.1 Nitrate transporters.....	144
4.7.2 Amino acid permeases	144
4.7.3 Amino acid vacuolar transporters	147
4.7.4 Cationic amino acid transporters	147
4.7.5 Usually multiple acids move in and out transporters.....	147
4.8 Single-cell RNA Sequencing Reveals Possible Localization of Highly Upregulated Transporters	152
4.8.1 Predicted nodule localisation of several chickpea amino acid transporters.....	152
4.9 RNA Sequencing and Single Cell RNA Provides Further Understanding of a Fixed N Transport Network in Chickpea Nodules	157
4.9.1 AAPs, CATs, and AVTs concomitantly coordinate amino acid distribution and export in chickpea nodules.	157
4.9.2 UmamiT/WAT1 transporters in chickpea participate in amino acid transport, nodule development and pathogen defense.....	159
Chapter 4: Conclusions.....	162
5 FUNCTIONAL CHARACTERISATION OF CHICKPEA AMINO ACID TRANSPORTERS IN SACCHAROMYCES CEREVISIAE	163
Chapter 5: Introduction	164
5.1 Amino Acid Transporters are the Key to Improve Nitrogen Fixation	164
5.2 Phylogenetic Analysis of Chickpea Amino Acid Transporters Identified via RNAseq.....	166
5.3 Cloning of Chickpea Amino Acid Transporter Genes and Heterologous Expression in <i>S. cerevisiae</i> ..	176
5.4. <i>S. cerevisiae</i> Streak Plate Assays with Transformants in pYESdest52 Expression Vector	178
5.4.1 Testing different nitrogen supplementation in the pYESdest52 transformants	178
5.4.2 Streak plate amino acid assays of CaAAP6 & CaAVT6C in pYESdest52	181
5.5. Multiple Chickpea Amino Acid Transporters Rescued the Amino Acid Mutant <i>S. cerevisiae</i> Strain in the pDR196 Expression Vector	186
5.5.1 Complementation in pDR196 using spot plate assays	186
5.5.2 Multiple chickpea amino acid transporters rescued the knock-out mutant <i>S. cerevisiae</i> strain in liquid assays.....	191
5.5.3 Liquid assay mutant complementation with Glu, Asp and Ala.....	196
5.5.4 Liquid assay mutant complementation with GABA and Tyr.....	203
5.6. Transport Affinity of Chickpea Amino Acid Transporters at Acid pH	205
5.6.1 Amide complementation under acidic pH conditions.....	205
5.6.2 Glu, Asp, GABA and Ala complementation under acidic pH conditions.....	207
Chapter 5: Discussion	209
5.7 Yeast Complementation Reveals Transport of Amino Acids by Nodule Localised Chickpea Amino Acid Transporters	209
5.7.1 Chickpea nodule transporters exhibit broad transport functionality	209
5.8.1 AAP6	211
5.8.2 AVT.....	211
5.8.3 UmamiT	212

5.9 The Effect of pH and Amino Acid Charge	213
5.10 Limitations of the <i>S. cerevisiae</i> Complementation Results	217
5.10.1 Future directions for amino acid transporter characterization	218
Chapter 5: Conclusions.....	218
6 GENERAL DISCUSSION.....	219
6.1 Thesis in the Broader Context	220
6.2 Chickpea: An Amidic Legume	221
6.2.1 Metabolism of fixed nitrogen.....	221
6.2.2 Transport of amino acids and amides in chickpea	222
6.3 Future Directions	224
6.3.1 Chickpea tissue culture for genetic modification studies	225
6.4 An Updated Model of Nitrogen Fixation in Chickpea.....	227
6.5 Conclusions.....	230
Reference List	231
Appendix 3A.1: Acetylene reduction assay and nodule dry weight.....	264
Appendix 3A.2: GmPur1 expression in leaf and root tissue.....	265
Appendix 3A.3: CaUPS1 & CaPur1 expression in chickpea grown with high and low N supplementation	266
Appendix 3A.4: Total ureide summary data in chickpea leaf, root and nodule tissues.....	268
Appendix 4A.1: Pearson’s correlation analysis.....	269
Appendix 4A.2: Unique and shared differentially expressed gene interactions between comparisons	271
Appendix 4A.3: Gene summary list for each transporter gene family analysed in the RNAseq database	277
Appendix 4a: Single cell mRNA relative expression and cell count data.....	297
Appendix 5a.1: Primers used for yeast cloning pipeline and PCR setup conditions	306
Appendix 5a.2: PCR amplification of amino acid transporters.....	314
Appendix 5a.3: BP Gateway® cloning of chickpea transporters into pDONR	318
Appendix 5a.4: LR gateway ® cloning of chickpea transporters into pDR196.....	326
Appendix 5a.5: Setup of the pYESdest52 expression system.....	331
Appendix 5a.6: Restriction digest validation of pYESdest52 expression clones	336
Appendix 5a.7: Validation of the parental wild type 23344c <i>S. cerevisiae</i> control strains in liquid growth assays.....	339
Appendix 5a.7: Pre-optimized Amide liquid growth assay complementation of the mutant 22Δ10AA yeast strain	347
Appendix 5a.8 Effect of decreasing pH on the mutant 22Δ10AA strain grown with (NH ₄) ₂ SO ₄	351
Appendix 6a.1: Chickpea tissue culture method overview	359
Appendix 6a.2: Multiple chickpea cultivar tissue culture test	364
Appendix 6a.3: Light intensity experiments.....	375

Abstract

Nitrogen is an integral component for effective plant growth, crucial to the synthesis of amino acids, proteins, and chlorophyll, thereby directly influencing crop yield. Modern farming practices rely heavily on synthetic nitrogen fertilisers, which are not only expensive but wasteful due to inefficient nitrogen utilization by plants leading to environmental contamination. Leguminous plants like chickpea (*Cicer arietinum*) possess a symbiotic relationship with soil bacteria, collectively known as rhizobia, with the ability to fix atmospheric nitrogen into a bioavailable form usable by the plant, offering an alternative to fertilisers. This symbiosis takes place in nodules, specialised organs located on roots that house the rhizobia. Within the nodule cells rhizobia differentiate into the symbiotic bacteroids contained in symbiosomes, organelle-like structures surrounded by a plant derived membrane known as the symbiosome membrane. Atmospheric nitrogen is reduced to ammonia in bacteroids and exported through the symbiosome as ammonium, then further metabolised into amides glutamine (Gln) & asparagine (Asn) or ureides allantoin & allantoic acid. These serve as a means to store and remobilise nitrogen to support plant growth. The biosynthesis of amides or ureides differs between legumes and it is unclear in the literature which pathway occurs in chickpea. Previous studies have shown that improving the export of amides or ureides from the nodules of other legumes can significantly improve the rate of nitrogen fixation. However, before this can be accomplished in chickpea, the pathway of nitrogen fixation and transporters responsible in amide or ureide export from the nodules must be known.

A colorimetric assay was employed to quantify total ureides in leaf, root, and nodule tissue under low N conditions (0.5 mM KNO₃). Chickpea exhibited significantly reduced levels of ureides across all tissues compared to soybean, a typical ureide producing legume. Moreover, qRT-PCR showed an apparent upregulation of amide biosynthesis and negligible expression of the ureide biosynthesis pathway in nodules, particularly the enzyme Pur1, a rate limiting step of this pathway.

To back up these observations a model of nitrogen fixation in chickpea was developed via RNA sequencing comparing gene expression from nodule tissue preceding and during nitrogen fixation. A significant upregulation of the entire amide biosynthesis pathway was observed, in contrast to non-differential expression of the ureide pathway. Further analysis identified several (7) promising amide transporters exhibiting significant upregulation during nitrogen fixation. Based on single cell RNA (scRNA) performed in *Medicago truncatula* nodules, these transporters were predictively localised within nodule compartments such as the parenchyma and were likely involved in fixed nitrogen export. *Saccharomyces cerevisiae* complementation assays employing a mutant strain deficient in amino acid transport showed broad amino acid transport properties by the proteins encoded by these genes, particularly the amides, Gln and Asn.

Data suggests that chickpea predominantly synthesise amides over ureides for nitrogen export from the nodules. This export is likely facilitated by the transporters *CaAAP6*, *CaAVT6A*, *CaUmamiT9*, *CaUmamiT18*, *CaUmamiT20*, predictively localised to the nodule parenchyma and shown to transport a broad range of amino acids including the amides Asn and Gln. These transporters present promising targets for future genetic manipulation experiments to improve nitrogen fixation in chickpea.

Declaration

I certify that this thesis:

1. does not incorporate without acknowledgment any material previously submitted for a degree or diploma in any university
2. and the research within will not be submitted for any other future degree or diploma without the permission of Flinders University; and
3. to the best of my knowledge and belief, does not contain any material previously published or written by another person except where due reference is made in the text.

Signed

Date 23rd September 2024

Acknowledgements

To begin with, I would like to thank my supervisors Dr Sunita Ramesh and Prof. David Day for allowing me to learn and develop my research skills under their guidance. They were both always open to chat when needed and I could not have made it to this point without them.

I would also like to express my gratitude to Prof. Peter Anderson for initially giving me the opportunity to work with CRISPR during my honour's degree, which even though we could not achieve the desired outcomes still led me to the point where I am now.

Importantly, to the whole Flinders Plant Molecular Physiology group, I would have not enjoyed my time at Flinders anywhere near as much if it was not for all your support and I will definitely miss you all. This includes Dr Nick Booth, Lauren Philip-Dutton, Barry Rainbird, Shayne Faulkner, Kathryn Schleyer, Alexandra Cunningham and Carly Schramm for all the help and Tavern drink sessions we all shared. As well as always open to chatting in the office when I obviously needed something to do other than looking at my thesis. Which included a lot of moral support from Barry, mostly because he was unlucky enough to sit behind me in our office during the toughest period of my lab work and thesis writing. Also, I would like to extend my thanks to the lab heads who were not directly involved in my project by provided much needed assistance along the way, particularly, Dr Crystal Sweetman, Prof. Peter Anderson, Prof. Kathleen Soole, Assoc. Prof. Colin Jenkins, Dr Yuri Shavrukov. I would also like to acknowledge and thank Ella Brear and Evgenia Ovchinnikova for kindly making some of their past data available to me and allowing me to include this data within my thesis.

It is also worth noting the much-needed lifesaver Adriana Gaeguta-Bierbaum was, along with Carly Schramm and Dr James Herbert for allowing me to use several microplate readers simultaneously in the Biology Discover Centre for an extended period of time. Without their help I would not have been able to collect the final set of data required to finalise my thesis on time.

Lastly, my family and friends have been instrumental in providing me support through an extremely stressful period my of life and I cannot thank them all enough. Most importantly I want to thank my parents for all the support they have given in allowing me to pursue my love for science over the years to get me to this point.

I will miss seeing everyone everyday who supported me throughout my PhD now that I am off onto the next chapter of my life in Perth. I will always endeavour to make it back to the Flinders Tavern for a drink whenever I am back in Adelaide.

I also acknowledge the financial support I received through the Australian Government Research Training Program Scholarship.

Abbreviations

μ l – micro litre	LB – Lysogeny broth
μ M – micro molar	LiAc – Lithium acetate
μ m – microgram	Lj – Lotus japonicus
AA – Amino acids	M – Molar
AAH – Allantoate amidohydrolase	MDH – Malate dehydrogenase
AAP – Amino acid permease	mg – milligram
AGRF – Australian genome research facility	ml – millilitre
Ala – Alanine	mM – milli molar
Ala-AT – Alanine aminotransferase	mRNA – Messenger ribonucleic acid
ALN – Allantoinase	Mt – Medicago truncatula
ANOVA – Analysis of variance	N – Nitrogen
ANU – Australian national university	NA – Nodule apex
AS – Asparagine synthase	NCBI – National centre for biotechnology information
Asn – Asparagine	NEB – New England biolabs
Asp – Aspartate	NF – Nitrogen fixation
Asp-AT – Aspartate aminotransferase	NH ₃ – Ammonia
At – Arabidopsis thaliana	NH ₄ ⁺ – Ammonium
ATP – Adenosine triphosphate	Non-DE – Non-differential expression
AVT – Amino acid vacuolar transporter	NP – Nodule parenchyma
BLAST – Basic local alignment search tool	NRT – Nitrate transporter
C – Carbon	OAA – Oxaloacetate
Ca – Cicer arietinum	OD – Optical density
CAT – Cationic amino acid permease	PAR – Photosynthetic active radiation
cDNA – Complementary DNA	PC – Pearson's correlation
Ct – Threshold cycle	PCA – Principle component analysis
DAI – Days After Inoculation	PCR – Polymerase chain reaction
DE – Differential expression	PE – Paired ends
DEGs – Differentially expressed genes	PEP – Phosphoenolpyruvate
DEPC – Diethyl pyrocarbonate	PEPC - Phosphoenolpyruvate carboxylase
DH5 α – Douglas Hanahan 5 alpha cells	PI – Pre-infected cell
dNTP – Deoxynucleotide triphosphate	Ps – Phaseolus vulgaris
ER – Endoplasmic reticulum	Pur1 - Amidophosphoribosyltransferase 1
FC – Fold change	qRT-PCR – Quantitative real time polymerase chain reaction
FDR – False discovery rate	Rev – Reverse
FPKM – Fragments per kilobase of transcript per million mapped reads	RNA – Ribonucleic acid
Fru – Fructose	RNAseq – Ribonucleic acid sequencing
Fwd – Forward	RPM – Revolutions per minute
g – gram	SARDI – South Australian research and development institute
GABA – Gamma-Aminobutyric Acid	scRNA – Single cell ribonucleic acid
GAP1 – General amino acid permease 1	SOC – Super optimal broth with catabolite repression
Glc – Glucose	Sqrt – Square root
Gln – Glutamine	SuSy – Sucrose synthase
Glu – Glutamate	SUT/SUC- Sucrose transporter
Gm – Glycine max	SWEET – Sugars will eventually be exported transporter
GOGAT – Glutamate oxoglutarate aminotransferase	TCAC – Tricarboxylic acid cycle
GS – Glutamine synthase	Tm – Melting temperature
HIU - Hydroxyisourate hydrolase	
IF – Infected cell	
KNO ₃ – Potassium nitrate	

TSS – Transformation and storage solution
Tyr – Tyrosine
Tyr-AT – Tyrosine aminotransferase
UiC – Uninfected cell
UmamiT – Usually multiple acids move in and out
transporter
UOX – Urate oxidase
UPS – Ureide permease

VA – Vasculature tissue
W/V – Weight/Volume
WAT – Walls are thin
XDH – Xanthine dehydrogenase
YMB – Yeast mannitol broth
YNB – Yeast nitrogen base
YPD – Yeast extract peptone dextrose

List of Figures

Figure 1.1: Chickpea (<i>Cicer arietinum</i>) nodule formation induced by rhizobia infection.	6
Figure 1.2: Soybean nodule electron micrograph showing infected cells housing an abundant population of symbiosomes.	8
Figure 1.3: Organogenesis of determinate and indeterminate nodules.	10
Figure 1.4: Ammonium assimilation into amino acids in the nodule infected cell.	17
Figure 1.5: Ureide biosynthesis beginning with glutamine produced from the GS/GOGAT cycle.	20
Figure 3.1: Chickpea nodules display nodule meristem elongation, indicative of indeterminate nodule morphology.	59
Figure 3.2: Chickpea harvest time course panel grown in sand with low N availability (0.5 mM KNO ₃) and inoculated with rhizobia. Chickpea grown in washed quarry sand and inoculated with rhizobia at sowing. Grown with low nitrogen (0.5 mM KNO ₃) supplemented with McKnight's nutrient solution. Grown under ambient lighting in greenhouse conditions (~20-25°C during the day). Plants harvested (N = 3) at 5-day intervals (10 DAI - 35 DAI).	61
Figure 3.3: Nodule development profile in chickpea shows a rapid senescence of nodules between 20 and 35 DAI when grown in sand supplemented with low nitrogen availability (0.5 mM KNO ₃).	62
Figure 3.4: Chickpea harvest time course panel grown in sand with high N availability (5 mM KNO ₃) and inoculated with rhizobia.	63
Figure 3.5: Chickpea harvest time course panel grown in sand with low N availability (0.5 mM KNO ₃) without rhizobia inoculation.	65
Figure 3.6: Chickpea harvest time course panel grown in sand with high N availability (5 mM KNO ₃) without rhizobia inoculation.	66
Figure 3.7: Chickpea harvest time course panel grown in BioGrow with rhizobia inoculation at sowing.	67
Figure 3.8: Chickpea harvests show no significant effect of low & high nitrogen availability and nodule development on basic growth metrics.	69
Figure 3.9: Chickpea grown symbiotically in sand exhibited significantly less dry weight at 35 DAI compared to chickpea grown in soil.	70
Figure 3.10: Chickpea invest in nodule development despite significantly reduced leghemoglobin expression and nodule senescence post 20 DAI.	72
Figure 3.11: Genes involved in N ₂ fixation of ammonium to amino acids and the amides Gln & Asn are highly expressed in chickpea nodules.	74
Figure 3.12: Chickpea nodules show mostly negligible expression of genes involved in ureide biosynthesis outside of moderate expression of urate oxidase (UOX) and allantoinase (ALN).	76
Figure 3.13: <i>GmPur1</i> , the first step of the ureide biosynthesis pathway is significantly upregulated in <i>G. max</i> nodules, as opposed to insignificant expression in chickpea nodules.	77
Figure 3.14: Chickpea nodules exhibited significantly elevated expression of amino acid transporters AVT6A & UmamiT20, compared to negligible expression of the ureide transporter UPS1.	79
Figure 3.15: Ureide permease 1 (UPS1), was not significantly upregulated in <i>G. max</i> leaf, root and nodule tissues during N ₂ fixation.	80
Figure 3.16: Ureide levels are significantly elevated in N ₂ fixing nodules of <i>G. max</i> compared to chickpea.	82
Figure 3.17: Ureide levels are significantly elevated in both leaf and root tissue in the ureide producer, <i>G. max</i> compared to the same tissues in chickpea.	83

Figure 3.18: Ureide levels are significantly elevated with high nitrogen (5 mM KNO ₃) availability in chickpea leaf tissue at 25 days after inoculation.	85
Figure 3.19: Root ureide levels are significantly elevated in inoculated chickpea grown with high nitrogen (5 mM KNO ₃) availability.	86
Figure 4.1: RNA sequencing comparison overview of differentially expressed genes.....	98
Figure 4.2: Principal component analysis of RNA sequencing variability.....	102
Figure 4.3: Volcano plot distribution of differentially expressed genes for each comparison.	108
Figure 4.4: Enriched MapMan BIN functional categories of differentially expressed genes.	111
Figure 4.5: Nitrogen fixation model in chickpea nodules depicting the change in gene expression related to carbon, ureide, amide and amino acid metabolism.....	116
Figure 4.6: Dot plot array of theoretical nodule localization of chickpea amino acid transporters.	155
Figure 4.7: Nodule overview of theoretical localization of amino acid transporters.....	156
Figure 5.1: Phylogenetic analysis of amino acid transporters; AAP, AVT, CAT and UmamiT from Chickpea.....	171
Figure 5.2: Phylogenetic analysis of AAP transporters from <i>C. arietinum</i> , <i>G. max</i> , <i>P. sativum</i> and <i>A. thaliana</i>	172
Figure 5.3: Phylogenetic analysis of AVT & CAT transporters from <i>C. arietinum</i> , <i>G. max</i> , <i>P. sativum</i> and <i>A. thaliana</i>	173
Figure 5.4: Phylogenetic analysis of UmamiT transporters from <i>C. arietinum</i> , <i>G. max</i> <i>P. sativum</i> and <i>A. thaliana</i>	175
Figure 5.5: Schematic representation of Gateway® cloning chickpea amino acid transporter genes into the <i>S. cerevisiae</i> expression system.....	177
Figure 5.6: <i>S. cerevisiae</i> 22Δ10AA-pYESdest52 and 22Δ10AA- <i>CaAAP6</i> -pYESdest52 can be grown supplemented with adenine as a sole nitrogen source present in the yeast synthetic amino acid minus uracil drop out medium.....	179
Figure 5.7: <i>S. cerevisiae</i> pYESdest52-22Δ10AA/23344c and <i>CaAAP6</i> -22Δ10AA/23344c growth can be supplemented with as little as 0.5 mM (NH ₄) ₂ SO ₄ as a nitrogen source present in the yeast YNB medium at pH 6.2.	180
Figure 5.8: <i>CaAAP6</i> -pYESdest52 compliments aspartate and glutamate but does not compliment the amides glutamine and asparagine in <i>S. cerevisiae</i> 22Δ10AA mutant.	183
Figure 5.9: <i>CaAVT6C</i> -pYESdest52 does not complement the mutant <i>S. cerevisiae</i> 22Δ10AA strain when supplemented with Asn, Gln, Asp and Glu.	185
Figure 5.10: Spot plate growth assay of <i>S. cerevisiae</i> 22Δ10AA strain shows complementation of <i>CaAAP6</i> , <i>CaAVT6A</i> , <i>CaUmamiT9</i> and <i>CaUmamiT18</i> grown with Asp and Glu.....	188
Figure 5.11: Spot plate growth assay of <i>S. cerevisiae</i> 22Δ10AA strain shows complementation of <i>CaAAP6</i> , <i>CaAVT6A</i> , <i>CaUmamiT9</i> and <i>CaUmamiT18</i> grown with Asn & Gln and <i>CaUmamiT20</i> with Gln.....	189
Figure 5.12: Spot plate growth assay of <i>S. cerevisiae</i> 22Δ10AA strain shows complementation of chickpea amino acid transporters grown with GABA, Tyr and Ala.....	190
Figure 5.13: Glutamine liquid 48h growth assay of the mutant (22Δ10AA) <i>S. cerevisiae</i> strain expressing five chickpea amino acid genes, <i>ScGAP1</i> positive control and empty pDR196 negative control.	193
Figure 5.14: Asparagine liquid 48h growth assay of the mutant (22Δ10AA) <i>S. cerevisiae</i> strain expressing five chickpea amino acid genes, <i>ScGAP1</i> positive control and empty pDR196 negative control.	195
Figure 5.15: Glutamate liquid 48h growth assay of the mutant (22Δ10AA) <i>S. cerevisiae</i> strain expressing five chickpea amino acid genes, <i>ScGAP1</i> positive control and empty pDR196 negative control.	198
Figure 5.16: Aspartate liquid 48h growth assay of the mutant (22Δ10AA) <i>S. cerevisiae</i> strain expressing five chickpea amino acid genes, <i>ScGAP1</i> positive control and empty pDR196 negative control.	200

Figure 5.17: Alanine liquid 48h growth assay of the mutant (22Δ10AA) <i>S. cerevisiae</i> strain expressing five chickpea amino acid genes, <i>ScGAP1</i> positive control and empty pDR196 negative control.	202
Figure 5.18: GABA and Tyrosine liquid 48h growth assay of the mutant (22Δ10AA) <i>S. cerevisiae</i> strain expressing five chickpea amino acid genes, <i>ScGAP1</i> positive control and empty pDR196 negative control.	204
Figure 5.19: PH dependent complementation of the amides glutamine & asparagine in the <i>S. cerevisiae</i> mutant (22Δ10AA) strain expressing five chickpea amino acid genes, <i>ScGAP1</i> positive control and empty pDR196 negative control.	206
Figure 5.20: PH dependent complementation of glutamate, aspartate, GABA and alanine in the <i>S. cerevisiae</i> mutant (22Δ10AA) strain expressing five chickpea amino acid genes, <i>ScGAP1</i> positive control and empty pDR196 negative control.	208
Figure 5.21: Basic model of the nodule path of amino acid distribution and nodule export through the inner and outer parenchyma.	216
Figure 6.1: Nitrogen fixation model in chickpea nodules depicting the path of sucrose to the biosynthesis of amino acids and ureides with respective transporters.	228
Figure 3a.1 Acetylene reduction assay depicts plummeting nitrogen fixation rates post 20 DAI despite increasing nodule dry weight. Evgenia Ovchinnikova & Ella Brear, 2017 (Unpublished Data).	264
Figure 3a.2: <i>GmPur1</i> exhibited insignificant expression in both leaf and root tissues from 10 to 35 DAI, suggesting nodule localised function.	265
Figure 3a.3: <i>CaUPS1</i> exhibited significantly inconsistent expression in root and insignificant expression in leaf tissue.	266
Figure 3a.4: <i>CaPur1</i> exhibited negligible expression in chickpea leaf and root tissue.	267
Figure 4a.1: Interactions between each comparison for upregulated DEGs (>1 Log ₂ Fold change).	272
Figure 4a.2: Interactions between each comparison for downregulated DEGs (<-1 Log ₂ Fold change).	274
Figure 4a.3: UpSet plot of gene interactions between each variable (Up or Downregulated genes) within each comparison.	276
Figure 5a.1: Agarose gel electrophoresis of amino acid transporter gene PCR amplifications.	315
Figure 5a.2: Agarose gel electrophoresis of PCR step, annealing attB cloning sites to amino acid transporter gene sequences.	316
Figure 5a.3: Agarose gel electrophoresis of gel purified attB sites annealed to chickpea amino acid transporter gene sequences.	317
Figure 5a.4: Agarose gel electrophoresis of purified pDONR entry plasmids harbouring chickpea amino acid transporter genes inserted via BP clonase.	320
Figure 5a.5: Sanger sequencing confirmation of BP clonase reaction to yield the <i>CaAVT6A</i> -pDONR plasmid.	321
Figure 5a.6: Sanger sequencing confirmation of BP clonase reaction to yield the <i>CaAVT6C</i> -pDONR plasmid.	322
Figure 5a.7: Sanger sequencing confirmation of BP clonase reaction to yield the <i>CaUmamiT9</i> -pDONR plasmid.	323
Figure 5a.8: Sanger sequencing confirmation of BP clonase reaction to yield the <i>CaUmamiT18</i> -pDONR plasmid.	324
Figure 5a.9: Sanger sequencing confirmation of BP clonase reaction to yield the <i>CaUmamiT20</i> -pDONR plasmid.	325
Figure 5a.10: Agarose gel electrophoresis of purified pDR196 destination expression clones harbouring chickpea amino acid transporter genes inserted via LR II clonase.	328

Figure 5a.11: pDR196 destination yeast expression vector (Besnard et al., 2018).....	329
Figure 5a.12: Transformation of pDR196 expressing chickpea and <i>ScGAP1</i> positive control amino acid transporter genes into <i>S. cerevisiae</i> 22Δ10AA strain.	330
Figure 5a.13: SnapGene® viewer plasmid schematical map of the pYESdest52 yeast expression system...	332
Figure 5a.14: Agarose gel electrophoresis of PCR pipeline for BP/LR setup displaying purified PCR product.	333
Figure 5a.15: Sanger sequencing confirmation of BP clonase reaction to yield the <i>CaAAP6</i> -pDONR plasmid.	334
Figure 5a.16: Sanger sequencing confirmation of BP clonase reaction to yield the <i>CaAVT6C</i> -pDONR plasmid.	335
Figure 5a.17: Agarose gel electrophoresis of purified colonies of pYESdest52 plasmids harbouring chickpea amino acid transporters digested via restriction enzymes.	337
Figure 5a.18: Glutamate Liquid 48h growth assay of the parental (23344c) <i>S. cerevisiae</i> strain harbouring six chickpea amino acid genes, <i>ScGAP1</i> positive control and empty pDR196 negative control.	340
Figure 5a.19: Aspartate Liquid 48h growth assay of the parental (23344c) <i>S. cerevisiae</i> strain harboring six chickpea amino acid genes, <i>ScGAP1</i> positive control and empty pDR196 negative control.	341
Figure 5a.20: Alanine Liquid 48h growth assay of the parental (23344c) <i>S. cerevisiae</i> strain harboring six chickpea amino acid genes, <i>ScGAP1</i> positive control and empty pDR196 negative control.	342
Figure 5a.21: GABA Liquid 48h growth assay of the parental (23344c) <i>S. cerevisiae</i> strain harboring six chickpea amino acid genes, <i>ScGAP1</i> positive control and empty pDR196 negative control.	343
Figure 5a.22: Tyrosine Liquid 48h growth assay of the parental (23344c) <i>S. cerevisiae</i> strain harboring six chickpea amino acid genes, <i>ScGAP1</i> positive control and empty pDR196 negative control.	344
Figure 5a.23: Asparagine Liquid 48h growth assay of the parental (23344c) <i>S. cerevisiae</i> strain expressing six chickpea amino acid genes, <i>ScGAP1</i> positive control and empty pDR196 negative control.	345
Figure 5a.24: Glutamine Liquid 48h growth assay of the parental (23344c) <i>S. cerevisiae</i> strain expressing six chickpea amino acid genes, <i>ScGAP1</i> positive control and empty pDR196 negative control.	346
Figure 5a.25: Glutamine Liquid 48h growth assay of the mutant (22Δ10AA) <i>S. cerevisiae</i> strain expressing five chickpea amino acid genes, <i>ScGAP1</i> positive control and empty pDR196 negative control.	349
Figure 5a.26: Asparagine liquid 48h growth assay of the mutant (22Δ10AA) <i>S. cerevisiae</i> strain expressing five chickpea amino acid genes, <i>ScGAP1</i> positive control and empty pDR196 negative control.	350
Figure 5a.27: PH dependent complementation control (NH ₄) ₂ SO ₄ in the <i>S. cerevisiae</i> mutant (22Δ10AA) strain expressing five chickpea amino acid genes, <i>ScGAP1</i> positive control and empty pDR196 negative control.	352
Figure 5a.28: PH dependent complementation of glutamine in the <i>S. cerevisiae</i> mutant (22Δ10AA) strain expressing five chickpea amino acid genes, <i>ScGAP1</i> positive control and empty pDR196 negative control.	353
Figure 5a.29: PH dependent complementation of asparagine in the <i>S. cerevisiae</i> mutant (22Δ10AA) strain expressing five chickpea amino acid genes, <i>ScGAP1</i> positive control and empty pDR196 negative control.	354
Figure 5a.30: PH dependent complementation of glutamate in the <i>S. cerevisiae</i> mutant (22Δ10AA) strain expressing five chickpea amino acid genes, <i>ScGAP1</i> positive control and empty pDR196 negative control.	355
Figure 5a.31: PH dependent complementation of aspartate in the <i>S. cerevisiae</i> mutant (22Δ10AA) strain expressing five chickpea amino acid genes, <i>ScGAP1</i> positive control and empty pDR196 negative control.	356

Figure 5a.32: PH dependent complementation of GABA in the <i>S. cerevisiae</i> mutant (22Δ10AA) strain expressing five chickpea amino acid genes, <i>ScGAP1</i> positive control and empty pDR196 negative control.	357
Figure 5a.33: PH dependent complementation of alanine in the <i>S. cerevisiae</i> mutant (22Δ10AA) strain expressing five chickpea amino acid genes, <i>ScGAP1</i> positive control and empty pDR196 negative control.	358
Figure 6a.1: Chickpea tissue culture workflow.....	362
Figure 6a.2: Grafting of transgenic explants on newly grown rootstock.	363
Figure 6a.3: Bisections of all 7 cultivars placed on B5 co-cultivation media.....	366
Figure 6a.4: Germination of multiple chickpea cultivars on B5 media.	367
Figure 6a.5: Transition of bisected seeds to regeneration cycle 1 media (RS1).	368
Figure 6a.6: Day 6 progression of explant growth after transition to RS1 media.....	369
Figure 6a.7: Progression of Genesis and Yubileny transferred from (A) B5 media RS1 media after (B) 7 days, (C) 9 days and (D) 13 days.	370
Figure 6a.8: Day 9 growth of cultivars prior to RS2, still on RS1 (A) Rupali, (B) Jimbour, (C) Striker, (D) Slasher, (E) Hatrick.	372
Figure 6a.9: (A) Day 9 transition of cultivars to larger magenta containers in RS1 media (Slasher – Rupali – Striker – Jimbour – Hatrick), (B) day 13 transition to RS2 media.....	373
Figure 6a.10: Spectra wavelength using during light intensity experiments.	375
Figure 6a.11: RS1 transition to RS2.	376
Figure 6a.12: Light experiment showing bisected seeds to RS1 media transition.....	376
Figure 6a.13: Plantlets at the end of RS1 cycle grown with red (PAR-240), low (PAR-70) and high (PAR-300) light conditions.	378
Figure 6a.14: Plantlets transitioned from RS1 to RS2 grown with red (PAR-240), low (PAR-70) and high (PAR-300) light conditions.	379
Figure 6a.15: Tissue quality at the end of RS2 when grown with red (PAR-240), low (PAR-70) and high (PAR-300) light conditions.	380

List of Tables

Table 1.1: Overview of Amino Acid Permease (AAP) transporter modifications in plants	25
Table 1.2: Overview of Ureide Permease (UPS) transporter modifications in plants	27
Table 2.1: Mcknight's nutrient solution 100x concentrate, amount per 0.25 L.....	37
Table 2.2: TRIzol-Like reagent composition for RNA extraction.....	40
Table 2.3: Master-mix 1 for cDNA synthesis.	41
Table 2.4: ProtoScript cDNA synthesis reaction master-mix 2.....	41
Table 2.5: Housekeeping primers used for qRT-PCR normalization in <i>C. arietinum</i> and <i>G. max</i>	42
Table 2.6: Preparation of ureide assay standards.	45
Table 2.7: Sequential workflow of the ureide assay protocol.....	46
Table 2.8: Gateway® vectors used for yeast expression experiments.	49
Table 4.1: Total number of significantly (FDR < 0.01) upregulated (>1 Log ₂ FC) downregulated (<-1 Log ₂ FC), and non-DE (log ₂ FC <1, FDR>0.01) genes between treatments.....	109
Table 4.2: Solute transport and nutrient uptake enriched subcategories in nodules.	113
Table 4.3: Carbon transporter DEGs in chickpea.....	118
Table 4.4: Sucrose metabolism DEGs in chickpea.	121
Table 4.5: Glycolysis expression profile in chickpea.....	122
Table 4.6: DEGs of the Citric Acid Cycle in Chickpea.	124
Table 4.7: DEGs involved in nitrogen and amino acid metabolism in chickpea.....	131
Table 4.8: Aminotransferase DEGs in chickpea involved in amino acid biosynthesis and nitrogen metabolism.....	133
Table 4.9: Purine synthesis and degradation pathway expression profile in chickpea.....	135
Table 4.10: Ureide transporter DEGs in chickpea.	136
Table 4.11: DEGs involved in nitrate transport in chickpea.	145
Table 4.12: Amino acid permease DEGs in chickpea involved in amino acid transport.....	146
Table 4.13: Amino acid vacuolar and cationic amino acid transporter DEGs in chickpea.	149
Table 4.14: UmamiT transporters in chickpea.....	150
Table 4.15: Chickpea amino acid and solute transporters chosen for further localisation analysis with <i>M. truncatula</i> spatial scRNA database.....	154
Table 5.1: Amino acid sequence similarity of identified chickpea amino acid transporters to two model legumes <i>G. max</i> & <i>P. sativum</i> , and <i>A. thaliana</i>	168
Table 5.2: <i>S. cerevisiae</i> liquid growth assay summary of the 22Δ10AA mutant strain expressing chickpea amino acid transporters.	210
Table 3a.1: Mean total ureides (nmols/mg Dry Weight) in leaf, root and nodule tissue over 10 to 35 DAI for chickpea and soybean.	268
Table 3a.2: Mean total ureides (nmols/mg Dry Weight) in leaf, root and nodule tissue from plants inoculated (Green) or uninoculated (Orange), treated with either high N (KNO ₃) or low N (KNO ₃).	268
Table 4a.1: Results of the pearson's correlation analysis displaying most and least correlated (r) groups for all 16 samples.	269
Table 4a.2: Summary amino acid permease transporters DEG in chickpea.	277

Table 4a.3: Summary cationic amino acid transporter DEGs in chickpea.....	278
Table 4a.4: Summary usually multiple amino acids transport in and out transporter DEGs in chickpea.	279
Table 4a.5: Summary amino acid vacuolar transporter DEGs in chickpea.....	282
Table 4a.6: Summary sucrose transporter DEGs in chickpea.....	284
Table 4a.7: Summary nitrate transporter DEGs in chickpea.	286
Table 4a.8: Summary ureide permease DEGs in chickpea.	296
Table 4a.9: ScRNA cell cluster relative gene expression and Log2 relative expression.	297
Table 4a.10: ScRNA cell cluster cell count and square root cell count.	301
Table 5a.1: Primers to amplify chickpea amino acid genes, primer Tm °C, annealing temp °C and product size (bp).	306
Table 5a.2: PCR setup to amplify amino acid transporter gene sequences using Q5 high-fidelity polymerase.	308
Table 5a.3: PCR Primers to anneal attB sites in one overhanging PCR step, using during pDR196 cloning. Red text indicates primer overhang.	309
Table 5a.4: PCR setup to anneal attB cloning sites using Phusion polymerase to previously amplified amino acid transporter gene sequences as template.	311
Table 5a.5: PCR primers for attB site annealing using two PCR steps for cloning into pYESdest52. Red text indicated primer overhang.	312
Table 5a.6: BP recombination reaction setup to clone amino acid genes into the pDONR entry plasmid...	319
Table 5a.7: LR clonase II recombination reaction setup to clone amino acid genes into the pDR196 destination plasmid.	327
Table 5a.8: Predicted restriction digest outcome of pYESdest52 harbouring chickpea amino acid genes. .	338
Table 6a.1: Regeneration media composition for chickpea tissue culture.	360
Table 6a.2: B5 co-cultivation media composition for chickpea tissue culture.....	361
Table 6a.3: Summary of cultivar performance under chickpea tissue culture	374
Table 6a.4: B5 to RS1 transition including seed counts and effect of light conditions on transition efficiency (%).....	377
Table 6a.5: RS1 to RS2 transition including seed counts and effect of light conditions on transition efficiency (%).....	377

1 Introduction

1.1 Nitrogen Use and Global Food Security

In the coming years significant pressure will be placed on agriculture, such as breeders and plant researchers to provide increases in crop yields in response to a growing population and a changing environment through climate change. Currently the world population is nearing 8 billion with this number projected to increase to 9.7 billion by 2050 (Gu et al., 2021). If we are to meet the growing food demand over the next decades, advancements in plant productivity will have to be made. In the past, nitrogen (N) supply was discovered as an integral factor in crop productivity directly responsible for increases in yield with its application more beneficial than any other major essential nutrient (Anas et al., 2020). N is the most essential aspect for plant growth and required for the production of all amino acids, proteins and chlorophyll (Anas et al., 2020). Additionally, N improves CO₂ assimilation, crop quality and improves resistance to environmental stresses (Bondada et al., 1996, Anas et al., 2020).

Previously the Green Revolution of the 20th century saw significant improvements in crop production to prevent a global food crisis (Stein & Klotz, 2016). This was achieved with synthetic nitrogen fertilisers, pesticides, better water use efficiency and selective breeding, which lead to improvements in food supply which could feed approximately 48% of the global population (Stein & Klotz, 2016, Anas et al., 2020). As such to combat the growing demand in crop production, fertilisers containing synthetic N are generally used, which has shown an increase of 11.6 Tg in 1961 to 104 Tg in 2006 in cereal crops alone (Mulvaney et al., 2009). However, soil contamination is a major concern due to plants inability to take up all the N supplied, resulting in upwards of 50% of the N content leaching into soils causing environmental contamination (Gruber & Galloway, 2008). To combat this recent work has focused on the generation of crop plants exhibiting an increased efficiency to utilise available N, or termed nitrogen use efficiency (NUE). This is described by the amount of N a plant can take from a source of N and the subsequent capability to assimilate that N and utilise it within the plant (Moose & Below, 2009, Masclaux-Daubresse et al., 2010). A positive correlation has been discovered between the plant's ability to uptake available N and remobilise N-containing compounds from source to sink tissue, and the resulting yield (Carter & Tegeder, 2016, Garneau et al., 2018, Perchlik & Tegeder, 2017, Santiago & Tegeder, 2016, Zhang et al., 2015). Additionally, previous research has found a possible link between the overaccumulation of N-containing compounds to act as a tolerance mechanism towards abiotic stress (King & Purcell, 2005; Alamillo et al., 2010; Gil-Quintana et al., 2013b; Sulieman & Tran, 2013; Watanabe et al., 2014; Lescano et al., 2016; Irani & Todd, 2018; Quiles et al., 2019).

To meet global food demands in the coming years improvements will need to be made with respect to general crop NUE. Relying solely on past advancements from the Green Revolution will likely not be enough to feed the growing global population. Losses of N can be initially minimised by better agricultural planning of precise fertiliser use for specific crops. Whereas major benefits will rely on molecular approaches to enhance N metabolism pathways to improve a plants ability to effectively utilise N stores (Anas et al., 2020). As such legumes like chickpea (*Cicer arietinum*) may be the key to meet the required improvements in global food production. Legumes as a whole exhibit a unique advantage over other crop species with the ability to perform biological nitrogen fixation which can be coupled with rotational farming practices to improve soil N levels without the need for intensive synthetic N fertilisation.

1.1.2 Chickpea agricultural and economic significance

Chickpea is a self-pollinating diploid plant with a genome size of 738Mbp and a widely cultivated leguminous crop part of the Fabaceae family (Varshney et al., 2013). Legumes are distinguished as plants which grow their edible seed in a pod, such as soybean (*Glycine max*), peas (*Pisum sativum*), lentils (*Lens culinaris*), broad beans (*Vicia faba*), common bean (*Phaseolus vulgaris*), and less commonly known, peanut (*Arachis hypogaea*). When the seed is used as a dry grain for human consumption, the seeds are then termed pulses. Pulses are a rich source of dietary fibre, plant protein, micronutrients and a widely consumed staple food around the world most commonly in Middle Eastern and South Asian countries.

Chickpea cultivars are grouped under two main classifications, desi and kabuli, offering differences in seed shape and colour. Kabuli with a beige coloured large circular seed is typically grown in Mediterranean temperate regions, compared to the smaller angular dark seeds of desi in semiarid climates (Singh et al., 2014). There is also a large disparity in cultivation between the desi and kabuli cultivation at approximately 80% and 20%, respectively, mostly driven by cultural cuisine preferences in Middle Eastern and South Asian countries favouring the desi type (Singh et al., 2014, Kaur & Prasad, 2021). Notably, the kabuli type has a significantly greater abundance of digestible protein over desi cultivars, despite being the less consumed (Sánchez-Vioque et al., 1999).

Chickpea is the most widely consumed pulse in the world with approximately 60% of chickpea grown in India alone, followed closely by Australia (Kaur & Prasad, 2021). Globally chickpea is grown by more than 50 countries over an area of 13 m hectares, yielding over 11 m tons on average annually from 2013 to

2017 (Singh et al., 2014, Merga & Haji, 2019). The Australian agricultural industry has been steadily catching up to India as the largest chickpea producer and as of 2022 to present, Australia held the largest export market share (23%) of chickpea in the world at \$547 million AUD in 2022 (DAFF, 2023). Interestingly, as of the last couple years the largest export destinations of chickpea were to Pakistan (46%) and Bangladesh (33%), historically the largest destination was India (DAFF, 2023). Imposed tariffs in 2022 by India made it economically unviable for Australia to export to India, which led to a significant reduction in chickpea cultivation in Australia in recent years. Despite this chickpea remains the second most economically viable pulse export in Australia with noteworthy global economic significance with a unique part to play in ensuring global food security, along with other legumes.

1.2 Biological Nitrogen Fixation

Legumes unlike other crop species possess the ability to bypass the need for synthetic N fertilisers to acquire N, through a symbiotic partnership with microorganisms. This plant-microbe interaction can be thought of as microbial biofertilizers providing a distinct advantage over traditional fertilisers harbouring unregulated bacterial communities compared to a constant and safe bacterial community (González-Andrés and James 2016). This specialised interaction is known as biological nitrogen fixation, where atmospheric N_2 , inaccessible to most organisms is fixed into a bioavailable form as ammonia (NH_3). Molecular N_2 being a fundamental element for life on Earth is abundantly present, making up 78% of the atmosphere and is essentially a limitless source of N to the limited species with the capability to harness it. Biological nitrogen fixation, therefore, serves as the primary mechanism by which to capture atmospheric N and convert or rather fix N_2 into NH_3 , a biologically useful form.

The ability to perform biological nitrogen fixation is limited to a select group of N_2 fixing prokaryotes known as diazotrophs possessing the nitrogenase enzyme, an enzyme complex which catalyses the conversion of N_2 into NH_3 (Vessey et al., 2005). The association of N_2 fixing bacteria with higher plants is not uncommon through free-living bacteria in the rhizosphere providing useful plant-microbe interactions, albeit a mostly opportunistic rather than mutualistic interaction where the rate of transfer of fixed N to the plant is low (Vessey, 2003). Conversely, the real benefits of these plant-microbe interaction take place in a select few species such as legumes with rhizobial bacteria, actinorhizal plants with Frankia, *Parasponia* with rhizobia and cycads as well as non-legumes such as Azolla and Gunnera plant species with cyanobacteria, where a true mutualistic symbiosis is established (Vessey et al., 2005). This is accomplished when the N_2 fixing bacterium is housed in specialised plant organs, known as nodules, located on root structures (Figure 1.1). The ability for legumes to perform biological nitrogen fixation is of significant agricultural and economical importance.



Figure 1.1: Chickpea (*Cicer arietinum*) nodule formation induced by rhizobium infection.

1.2.1 Nodule organogenesis

The ability of plants to fix N_2 begins with a symbiosis developed between a phylogenetic group, in this case, Fabaceae (Legumes), known as the N_2 fixing clade and a N_2 fixing *Proteobacteria* as well as the β -subclass of β -*Proteobacteria* such as belonging to the *Burkholderia* genus of the Rhizobiaceae family (Moulin et al., 2001, Werner et al., 2014). This symbiosis is important as higher plants such as legumes cannot fix atmospheric N_2 and thus rely on N_2 fixing rhizobia, which induce root nodule organogenesis where fixation takes place. The stimulation of root nodule organogenesis begins with the exuding of phenolic flavonoids by the host plant which functions to attract the bacteria to the roots. This then stimulates the activation of rhizobia (*nod*) nodulation gene expression and induces a Ca^{2+} signalling pathway by the legume after sensing nod factors (NF) as lipo-chito-oligosaccharides which bind to specific plant receptor kinases present on the plasma membrane, further increasing NF production (Udvardi & Poole, 2013).

This is seen as the first host specific recognition step to initiate symbiosis. Specific rhizobia respond to compatible NF from select few legumes with some rhizobia species exhibiting a larger host range (Pueppke & Broughton, 1999). After compatible recognition between rhizobia and respective NF nodule development is triggered, generally via rhizobial infection through the tip of an emerging root hair (Downie, 2010). After a process of root hair retraction or curling and the formation of the infection thread, which starts in a root hair and then traverses the underlying cortex cells towards the nodule primordium, the rhizobium is delivered into the cytoplasm of the dividing cortex cells and endocytosed. (Ferguson et al., 2010). Here the bacteria are surrounded by a membrane synthesised by the host plant known as the peribacteroid membrane, forming the symbiosome membrane (Udvardi & Dau 1997). Infected plant cells are eventually inhabited by thousands of symbiosomes as the rhizobia continues to proliferate (Figure 1.2). The rhizobium which have been encapsulated by the plant derived membrane, eventually differentiates into bacterioids after repeated divisions where N_2 fixation will begin (Ferguson et al., 2010).

Mature nodules which are undergoing N_2 fixation are comprised of infected tissue consisting of infected plant cells and simultaneously surrounded by uninfected cells and tissues, some of which include the phloem and xylem (Ferguson et al., 2010). This ensures the developed nodule housing rhizobial infected tissues, such as the bacteroid can exchange material to and from the host plant, as such establishing a symbiosis of a carbon import from the plant in return for fixed N.

This image has been removed due to copyright restriction. Available online from:
<https://doi.org/10.1146/annurev.arplant.48.1.493> (Figure 1).

Figure 1.2: Soybean nodule electron micrograph showing infected cells housing an abundant population of symbiosomes.

Uninfected cell (UC), Air space (AS), Infected cell (IC). (Udvardi & Day, 1997).

1.2.3 Determinate and indeterminate type nodules

Within legumes different NF signalling gives rise to alternative differentiation of cortical root cells resulting in two distinct nodule shapes, dictated by the host plant (Figure 1.3). Alterations in signalling results in either nodules exhibiting a spherical morphology, known as determinate nodule development, compared to persistent meristematic elongation known as indeterminate nodules (Ferguson et al., 2010, Udvardi & Poole 2013). Indeterminate nodules displaying a persistent meristem give rise to the cylindrical shape, whereby the apical meristem continues to generate new cells subsequently infected with rhizobia (Ferguson et al., 2010). Because of this persistent elongation of the apical meristem, indeterminate nodules exhibit a developmental gradient of cells separated into zones, consisting of a heterogeneous population of N₂ fixing bacteroids (Udvardi & Poole 2013). The newly growing tip is known as the meristematic zone, followed by the invasion zone where the rhizobium is delivered into plant cells, the interzone where rhizobia begin to differentiate into bacteroids, nitrogen fixation zone housing N₂ fixing bacteroids and lastly the senescence zone whereby N₂ fixation has ended and the rhizobia become degraded (Ferguson et al., 2010, Udvardi & Poole 2013). Nodules of this type are seen in temperate legumes species such as *P. sativum*, alfalfa (*Medicago sativa*), clover (*Trifolium repens*) and *Medicago truncatula* (Newcomb, 1976, Newcomb, 1979, Ferguson et al., 2010).

Determinate type nodules, however, do not display notable developmental zones and lack a persistent meristem attributing to a spherical appearance (Calvert et al., 1984, Mathews et al., 1989). In the absence of meristem elongation, determinate type nodules harbour a more apparent homogenous population of N₂ fixing bacteroids, whereby senescence occurs simultaneously in the nodule rather than gradual process in indeterminate nodules. As such these nodules have a turnover rate of a few weeks whereby new nodules are reformed on the newly growing roots (Rolfe & Gresshoff, 1988). Legumes such as *G. max* and *P. vulgaris* grown in tropical and subtropical climates is usually an indication of determinate nodules. In addition to the variation in nodule morphology for different legume species, both types also typically synthesise different end products of N₂ fixation for N remobilisation to the rest of the plant.

This image has been removed due to copyright restriction. Available online from:
<https://doi.org/10.1111/j.1744-7909.2010.00899.x> (Figure 1).

Figure 1.3: Organogenesis of determinate and indeterminate nodules.

Illustration depicts the steps from flavonoid secretion and rhizobium invasion through the infection thread (1-9) to the differentiation of pea (indeterminate) and soybean (determinate) nodule morphology (10) via elongation of the meristematic zone. (Ferguson et al., 2010).

1.2.4 Nitrogenase activity

For N₂ fixation to occur, the bacteroid must maintain a stable low oxygen environment, as the nitrogenase complex is highly liable to oxygen and can be rapidly oxidised (Kuzma et al., 1993). Specialised processes are required in order to prevent nitrogenase oxidative damage, given that rhizobia are obligate aerobes. Luckily, nodules require significant mitochondria respiration rates to fuel N₂ fixation in the bacteroid, so much of the free oxygen which makes it past the nodule outer cell layers which imposes a gaseous diffusion barrier, will be immediately exhausted via mitochondrial respiration. The remaining free oxygen will be consumed by the electron transport chain of the rhizobia. Structural changes in intercellular spaces of the nodules have also been determined as a mechanism to prevent easy diffusion of oxygen into the bacteroids. For example, the occlusion of intercellular spaces in the parenchyma could provide increased resistance to oxygen diffusion into the interior of the nodule protecting oxygen-sensitive damage of nitrogenase (Appleby, 1984, Masepohl et al., 1993, Sujkowska et al., 2011). This occurs during early symbiosis of *P. sativum* nodules where an oxygen barrier is formed from material, probably proteins, accumulating in the air spaces in the outer parenchyma, forcing oxygen to flow through the cell body, thereby restricting oxygen diffusion into the symbiotic zone (Sujkowska et al., 2011), since oxygen diffusion through fluid is 10,000 times slower than through air. *P. sativum* nodule infected cells present a characteristic vacuolar shrinkage as the nodules develop during this period. Changes in water flux as a result cause turgor loss and modifies the structure of the cells via radial wall folding influencing the take up or release of water in the apoplast (Sujkowska et al., 2011). The result of these structural changes causes alterations in the permeability of an oxygen diffusion barrier further protecting the bacteroid from free O₂.

Additionally, the most abundant protein in nodules, leghemoglobin, a legume variant of haemoglobin exhibits a very high affinity to bind with free O₂ and can subsequently deliver O₂ directly to the mitochondria of the bacteroid. Leghaemoglobin is also a characteristic sign of nodule senescence, where leghaemoglobin appears bright pink inside nodules while bound to O₂ and becomes green during senescence.

N₂ fixation begins with the reduction of N₂ into NH₃ (ammonia) by the nitrogenase complex within the bacteroid of the nodule infected cells. The following highly energetic reaction takes place where nitrogen gas is reduced to NH₃ requiring 16 ATP per molecule of N₂: $N_2 + 8H^+ + 8e^- + 16ATP \rightarrow 2NH_3 + H_2 + 16ADP + 16P_i$ (Udvardi & Poole, 2013). Following this NH₃ is protonated into NH₄⁺ (ammonium) after possible diffusion or facilitated by protein channels across the bacteroid symbiosome membrane into

the cytoplasm of the infected cell (Day & Udvardi, 1993, Day et al., 2001, Lodwig & Poole, 2003). At this stage the ammonium in the cytosol can be assimilated via several plant metabolism pathways upregulated during N₂ fixation prior to long distance remobilisation to other plant issues.

1.2.5 Fixed carbon fuels the bacteroids

To fuel the highly energetic reaction to reduce N₂ to ammonia the host plant must provide carbon provisions, as such nodules are strong carbon sinks. Indeed, nodules can make up 25% of the plant photosynthate, despite residing as 5% of the typical weight compared to the rest of the plant (Vance, 2008). The supply of carbon is an integral part in maintaining the symbiosis between the host plant and the rhizobium whereby photosynthates as sucrose is delivered via the phloem. Once sucrose enters the nodules it is primarily hydrolysed by sucrose synthase into hexoses. Further metabolism can occur through glycolysis and the tricarboxylic acid cycle to yield malate, fumarate, succinate and additional dicarboxylic organic acids as a carbon source for nodule bacteroids (Udvardi et al., 1988, Vessey et al., 2005). Most carbon sources however are impermeable to the symbiosome membrane and previous *in vivo* studies have shown that malate, fumarate and succinate were permeable, whereas glutamate, malonate, pyruvate and oxoglutarate were not (Price et al., 1987, Udvardi et al., 1988, Day et al., 1989). Succinate and malate are readily transported by transporters located on the symbiosome (Udvardi & Day, 1997). Dicarboxylate transport across the symbiosome membrane in early reports using a silicon oil centrifugation method with [¹⁴C], established the Km for malate and succinate at 2 and 15 µm, respectively, suggesting high affinity to malate as a carbon fuel source (Udvardi et al., 1988).

Hexoses synthesised from sucrose synthase may also be directed towards starch production, since during non-stressful conditions, the excess nodule carbon supply may be redirected towards starch accumulation (Schulze, 2004, Redondo et al., 2009). Starch stores could then subsequently be broken down into sucrose via sucrose phosphate synthase, found to be upregulated during starch breakdown in *M. truncatula* (Aleman et al., 2010). Interestingly, overexpression of this enzyme in *M. sativa* caused an increased in nodule number and higher production of the amino acids aspartate and glutamine, suggesting that increased carbon supply directed towards starch could be beneficial (Gebrill et al., 2015). However, under typical conditions the cycle of sucrose to starch back to glucose may be counterintuitive during heightened N₂ fixation, unless there indeed exhibits a large surplus of photosynthates.

1.3 Legumes Role in Agricultural Productivity

Biological nitrogen fixation in legumes can provide substantial benefits for sustainability agricultural practices as well as providing direct benefits to consumers. Legumes from the Leguminosae family is the third largest family of flowering plants made up of 800 genera and 20000 species (Lock, 2005). Within legumes species some are considered to be weeds, compared to others as major stable grain crops. Major legumes in agriculture with sizable yield metrics in 2014 included faba bean (1.82 t ha^{-1}), chickpea (0.96 t ha^{-1}), groundnut (1.65 t ha^{-1}), soybean (2.62 t ha^{-1}), lentils (1.08 t ha^{-1}), pea (1.65 t ha^{-1}) and french bean (9.32 t ha^{-1}) (Stagnari et al., 2017). Despite large cultivation of legumes, they are still far exceeded by cereal crops such as rice, wheat and maize. For example, soybean a widely cultivated legume around the world in 2014 exhibited a harvested area of 117.72 million ha compared to wheat at 221.62 million ha (Stagnari et al., 2017). During the same period, chickpea harvested area was 14.8 million ha in 2014 and yielded 0.96 t ha , compared to 2.62 t ha of soybean suggesting chickpea yield metrics are significantly greater considering their respective harvested area (Stagnari et al., 2017). The adoption of legume cultivation around the world varies with regions particularly in Europe seeing a decline in legume cultivation compared to an increase in Australia for example. This is in part due to legume susceptibility to various abiotic and biotic stress generating unstable yields (Graham & Vance, 2003).

Introduction of legumes into rotational cropping systems has significant benefits to improving soil properties by increasing available N, suppressing pests and reducing greenhouse gas emissions from fertiliser production (Cernay et al., 2018, Ditzler et al., 2021, Zhao et al., 2022). In Europe using legumes in rotation cropping reduced CO_2 generated from fertiliser production by 277 kg ha^{-1} per year (Jensen et al., 2012). On a global scale fertiliser production releases 300 Tg of CO_2 into the atmosphere per year (Jensen et al., 2012). It is believed that CO_2 respired from legume roots globally could exceed this level, however this respiration is driven from photosynthetic activity rather than a net contribution of released CO_2 from fertiliser production driven by fossil fuel derived energy (Jensen et al., 2012, Stagnari et al., 2017). As such N derived from nitrogen fixation is a significantly less emissive form of N which would in comparison be applied via synthetic N fertilisers (Schwenke et al., 2015).

The amount of N which can be deposited into the soil after legume rotations can be enhanced by up to 20% consisting of 1.93 g N kg^{-1} soil (Yu et al., 2014). In Australia wheat reported higher yields after legume cropping by 30% on average, whereas improvements around the world can vary depending on climatic factors which affect the dynamics of N in the soil (Angus et al., 2015, Stagnari et al., 2017).

Indeed, biological nitrogen fixation with legumes can produce upwards of 200 million tons of nitrogen per year (Peoples et al., 2009). The amount of fixed N released into the soil can differ considerably depending on the legume, with field pea and faba bean containing around 30-60% of total plant N of 130 and 153 kg N ha⁻¹ in below ground organs (Peoples et al., 2009). In addition, differing soil conditions such as salinity and alkalinity can also affect the N deposited from N₂ fixation which has been observed in both chickpea and common bean (Rao et al., 2002, Faghire et al., 2013). Even within one legume species such as groundnut, the amount of fixed N stored belowground can range from 76 and 188 kg ha⁻¹ outlining variability of rotational cropping depending on current soil conditions (Mokgehle et al., 2014). Rotational cropping or even intercropping by which legumes are grown simultaneously to a cereal in close proximity, can be further improved by identifying the legume which is least impacted by related inhibition of nodulation by increasing soil N levels. This is so that N₂ fixation can continue to deposit N into the soil. As such legumes can typically provide up to 15% of the N to the main crop during intercropping, increasing yields and improving carry over effects to the next cropping window by reducing the amount of N fertiliser required (Li et al., 2009, Pappa et al., 2012).

The direct benefits of legume rotation and intercropping systems is integral to increasing NUE in agriculture which can vary from 30 to 53% in modern farming after application of N (Anas et al., 2020). However systematic changes are required to reduce N losses, which come about through poor application of fertilisers and the amount provided which typically far exceeds the amount that can be effectively utilised by the crop. Nitrogen losses through poor agricultural planning can amount to as much as 70% of the N from applied fertilizers and will need to be minimised via effective legume rotational cropping system (Luo et al., 2018). As such effective legume-based cropping systems have been shown to improve main crop yield by upwards of 20%, whereas these yield improvements declined from increasing N fertiliser rates (Zhao et al., 2022). The decreasing effect of rotational cropping via increasing fertiliser rates is attributed to the inhibition of biological nitrogen fixation, thus limiting the impact the legume rotation crop will have in reinvigorating the N soil level (Zhao et al., 2022).

1.4 Pathways of Fixed Nitrogen

Within tropical legume species such as *G. max* and *P. vulgaris*, exhibiting determinate type nodules, allantoin and allantoic acid, known as ureides are the primary end products of symbiotic N₂ fixation (Atkins & Smith, 2007). These ureides serve as a means to remobilise N to the rest of the plant and can encompass 90% of total N containing compounds transported in the xylem (Layzell et al., 1981, Atkins & Smith, 2007, Baral et al., 2016). Conversely, temperate legumes of indeterminate type nodules prefer the biosynthesis of amides, asparagine (Asn) and glutamine (Gln), as well as other amino acids, functioning as the dominant N transport form (Garneau et al., 2018). Asn in particular is the primary amino acid produced, where NH₄⁺ is most readily reduced to Asn making up around 50% of the total amino acid pool in *P. sativum*, as well as *fava bean* (*Vicia faba*) and *M. sativa* (Atkins & Smith, 2007, Garneau et al., 2018).

1.4.1 Ammonium assimilation into amino acids

Irrespective whether a particular legume directs NH₄⁺ towards the biosynthesis of amides or ureides the initial assimilation pathway is the same, where glutamate (Glu) and Gln are synthesised via glutamine synthetase and glutamate oxoglutarate aminotransferase (GS/GOGAT) pathway (Figure 1.4) (Schwember et al, 2019, Todd et al., 2006, Vance, 2000). GS which can be found in both the infected cell cytosol and plastids, catalyses the ATP-dependent amination of Glu resulting in Gln (Temple et al., 1998). However, the cytosolic version of GS can account for 90% of GS nodule activity of *M. truncatula*, highly upregulated under symbiotic N₂ fixation (Melo et al., 2011, Carvalho et al., 2000). Similarly, *L. japonicus*, GS mutants showed strong inhibition of N₂ fixation rates, measured using an acetylene reduction assay (García-Calderón et al., 2012). GOGAT, also localised in the nodule infected cells is responsible for catalysing the transfer of the amide group from glutamine to α-ketoglutarate yielding glutamate (Temple et al., 1998, Trepp et al., 1999). GOGAT mutants in *M. sativa*, saw a significant reduction in N and carbon metabolism and as such a severe reduction in amino acids and amide levels, suggesting the GOGAT pathway is a critical bottleneck in N₂ assimilation (Cordoba et al., 2003). In addition to the GS/GOGAT pathway, Asn is synthesised by asparagine synthetase (AS) using Gln and oxaloacetate (OAA) derived from the TCA cycle, used as the C-skeleton (Suliman et al., 2010, Berry et al., 2011). Asn is also a particularly efficient form of N transport and storage with a C:N ration of 2:4 (Yang et al., 2011). Interestingly, legumes which synthesise primarily ureides, under stress synthesise

Asn, making up 30% of fixed N content in *G. max* under drought stress (Ramos et al., 2005) and 52% in the xylem sap (Lima & Sodek, 2003).

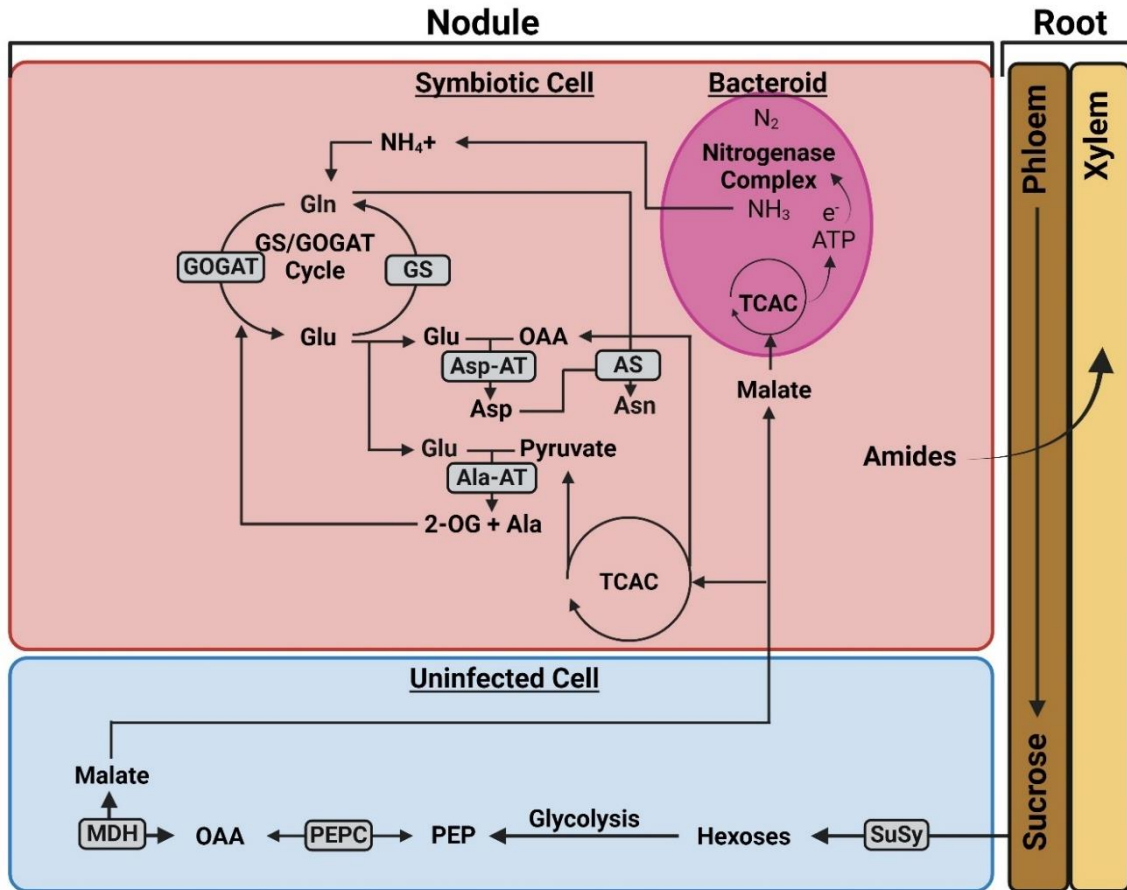


Figure 1.4: Ammonium assimilation into amino acids in the nodule infected cell.

Photosynthates as sucrose is delivered via the phloem, metabolised through glycolysis and the tricarboxylic acid cycle to yield malate and additional dicarboxylic organic acids as a carbon source for nodule bacteriods, fuelling the highly energetic nitrogenase complex. Ammonium (NH_4^+) is assimilated into Gln & Glu driven by the enzymes of the GS/GOGAT cycle, respectively. Additional amino acids, Asp & Ala are synthesized by aminotransferases fueled by Glu, as well as pyruvate and oxaloacetate from the TCAC. Biosynthesis of the primary amide, Asn is then catalyzed by AS from Gln & Asp.

Glutamine (Gln), glutamate (Glu), aspartate (Asp), asparagine (Asn), Alanine (Ala), 2-oxoglutarate (2-OG), glutamate oxoglutarate aminotransferase (GOGAT), glutamine synthetase (GS), asparagine synthase (AS), aspartate aminotransferase (Asp-AT), Sucrose synthase (SuSy), phosphoenolpyruvate carboxylase (PEPC), oxaloacetate (OAA), malate dehydrogenase (MDH), Tricarboxylic Acid Cycle (TCAC). Made with Biorender.com.

1.4.2 The ureide pathway

The biosynthesis of ureides begin with Gln directed towards the plastids of the infected cells for *de novo* purine synthesis, a several enzymatic step pathway yielding xanthine, followed by ureide synthesis (Figure 1.5) (Smith & Atkins 2002). The purine synthesis pathway is an important factor to differentiate the mode of N₂ assimilation in legumes between ureide and amide synthesis, as increased expression of purine synthesis is a notable metabolic feature in ureide-forming legumes (Smith & Atkins, 2002). For example, a significant nodule specific feature of ureide synthesis relates to an upregulation of pur genes encoding important enzymes within the purine synthesis pathway (Smith & Atkins, 2002). Expression of these pur genes have been previously shown to be upregulated during N₂ fixation, such as a 7-fold increase of pur1 (encoding the first enzymatic step of the pathway) expression after a N solute, Gln was added to a culture medium (Schnorr et al., 1996). Similarly, pur5 (encoding AIR synthetase), step five of the pathway was significantly upregulated in cowpea (*Vigna unguiculata*) nodules, whereas other pur genes remained unchanged suggesting the purine pathway may be regulated by transcriptional control of pur5 (Smith & Atkins, 2002).

Ureide synthesis following the purine synthesis pathway begins with the conversion of xanthine into urate via xanthine dehydrogenase (XDH) where it is transported via plasmodesmata into the cytosol of the nodule uninfected cells for the synthesis of allantoin and allantoic acid in peroxisomes (Smith & Atkins, 2002, Baral et al., 2016). Urate is subsequently metabolised in the peroxisome into 5-hydroxyisourate catalysed by urate oxidase (UOX), followed by allantoin synthesis by 5 Hydroxyisourate hydrolase (HIU) (Cheng et al., 2000, Werner et al., 2011). In ureide synthesising legumes such as *G. max* XDH is highly upregulated under N₂ fixation conditions and knockout mutants of both XDH and UOX resulted in a significant deficiency of N₂ fixation and promoted early nodule senescence (Nguyen et al., 2021). Also, when comparing legumes of amide or ureide biosynthesis properties the concentration of the urate oxidase protein in *M. sativa* nodules was also found to be 10% of the concentration in *G. max* nodules (Cheng et al., 2000).

Following the production of allantoin, this can either be exported from the nodules or further catabolised in the uninfected cell endoplasmic reticulum (ER) into the secondary ureide, allantoic acid by allantoinase (ALN) (Werner et al., 2008). A significantly reduced level of ureide production is commonly seen in temperate legumes with indeterminate nodules indicative of amide production, where *M. sativa* and *L. japonicus*, had 0.05 and 0.06 mM of total ureide levels, respectively, compared to 4.82 mM in *G. max* (Cheng et al., 1999, Cheng et al., 2000). Within the ER ureides can be further catabolised through a

relatively complex enzymatic process involved in the N remobilisation of ureides through purine ring catabolism, yielding glyoxylate, ammonium and urea (Voß et al., 2022).

In the absence of catabolism, ureides can then be loaded into the xylem vasculature for transportation to aerial organs and catabolised to yield ammonium during periods of high N demand (Redillas et al., 2019). Ureides are predominantly used as N containing compounds in tropical and sub-tropical legumes such as *G. max*, *P. vulgaris* and *V. unguiculata* due to a 1:1 N:C ratio of allantoin conferring a reduced cost of C to provide N to the plant, which is more efficient over Asn used by temperate legumes (Baral et al. 2016 & Redillas et al., 2019).

Before ureides can be loaded into the xylem for long distance N transport they must be taken up into endodermis cells surrounding the vascular tissue, as their Casparian strip in the cell wall prevents apoplastic transport (Carter & Tegeder, 2016). For this to occur studies have identified membrane-localised ureide permeases (UPS) responsible for ureide transport (Collier & Tegeder 2012, Pelissier et al., 2004). For example, repression of UPS1 in soybean nodules saw an increase of ureide levels by 20-116%, suggesting a key role in ureide export out of the nodules into the xylem (Collier & Tegeder 2012). Likewise, UPS1 overexpression in soybean led to increased nodule N export, metabolism and improved plant biomass (Carter & Tegeder, 2016, Lu et al., 2022). Interestingly *GmUPS1* overexpression appeared to stimulate a whole plant signalling response leading to the upregulation of N₂ fixation to compensate for increased ureide nodule export (Lu et al., 2022).

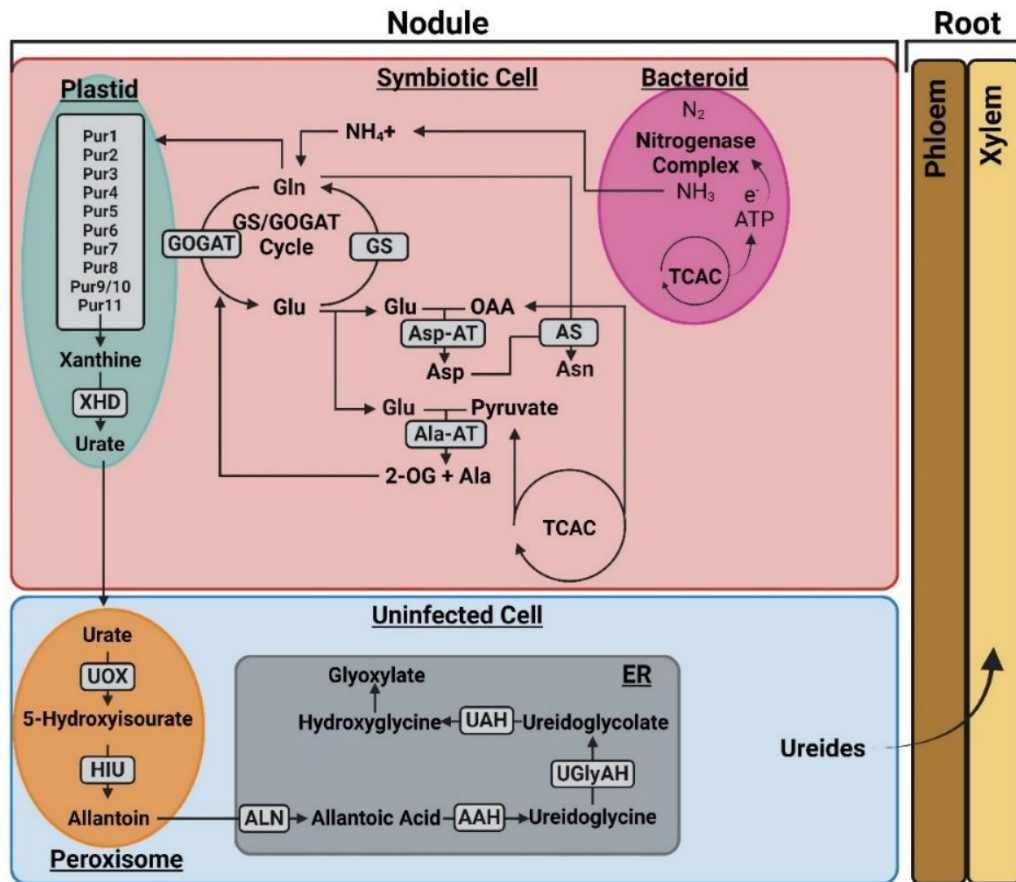


Figure 1.5: Ureide biosynthesis beginning with glutamine produced from the GS/GOGAT cycle.

Gln feeds into the plastid of the symbiotic cells initiating the purine synthesis pathway, yielding urate subsequently transported to the uninfected cell peroxisome. Here the ureide allantoin is synthesized via HIU. Allantoin can be further metabolized into the secondary ureide allantoic acid, catalyzed by ALN.

Glutamine (Gln), glutamate (Glu), aspartate (Asp), asparagine (Asn), Alanine (Ala), 2-oxoglutarate (2-OG), glutamate oxoglutarate aminotransferase (GOGAT), glutamine synthetase (GS), asparagine synthase (AS), aspartate aminotransferase (Asp-AT), Amidophosphoribosyltransferase 1 (Pur1), Phosphoribosylamine glycine ligase (Pur2), Phosphoribosylglycinamide formyltransferase (Pur3), Aminoimidazole RN synthetase (Pur5), Phosphoribosylaminoimidazole carboxylase (Pur6), Succino-aminoimidazole-carboximide RN synthetase (Pur7), Adenylosuccinate lyase (Pur8), Aminoimidazole-carboximide RN transformylase/IMP cyclohydrolase (Pur9/10), Adenylosuccinate synthetase (Pur11), Xanthine dehydrogenase (XDH), Urate oxidase (UOX), 5 Hydroxyisourate hydrolase (HIU), ureide permease (UPS), Allantoate amidohydrolase (AAH), Allantoinase (ALN), Ureidoglycine aminohydrolase (Ugly-AH), Ureidoglycolate amidohydrolase (UAH). Made with Biorender.com.

1.4.3 The amide pathway

Amino acids such as the amides, Gln and Asn function as the dominant form of long distance N transport in temperate legumes species and are integral for the transport of fixed N out of roots to shoots and finally the seeds. Mobilisation of amino acids has also been discovered to function as a feedback regulation mechanism in influencing N uptake, metabolism and allocation to seeds (Santiago & Tegeder, 2016). Within temperate legumes, amides are synthesised in the nodules followed by loading into the xylem for storage in mature source leaves (Perchlik & Tegeder, 2017). Once here the amino-N supply can be used for various metabolic processes throughout different stages in the plant's lifecycle. For example, amino acids are remobilised and loaded into the phloem during the reproductive stage to supply developing sinks, such as flowers, pods and seeds. The mechanism by which amino acids are loaded into the phloem is a crucial bottleneck in the remobilisation of N from source to sink tissue, requiring the use of transport proteins known as Amino Acid Permeases (AAP) (Zhang et al. 2015). Approaches to improve the phloem loading of amino acids by manipulation of AAP genes has been generally successful in improving amino acid partitioning from source to sink tissue with subsequent increases in seed yields. For instance, overexpression of AAP1 in *P. sativum* saw a 39% increase in seed yield, while also significantly more efficient at remobilising N under high N conditions compared to wild-type plants (Perchlik & Tegeder, 2017). The importance of AAPs has also been seen in Arabidopsis through knock-out mutants of *aap8*, whereby a reduction of source to sink N movement was observed through a significant reduction of amino acid phloem loading (Santiago & Tegeder, 2016). Interestingly however, AAP6 in pea appears to function in a similar manner as UPS1, through N retrieval from the apoplasm into the inner cortex cells for nodule xylem export (Garneau et al., 2018). In addition to AAP transporters which are a well characterised broad amino acid transporter (Garneau et al., 2018), other transport families such as amino acid vacuolar transporter (AVT) (Sekito et al., 2014, Tone et al., 2015, Fujiki et al., 2017), usually multiple acids move in and out transporter (UmamiT) (Zhao et al., 2021) and cationic amino acid transporters (CAT) (Rentsch et al., 2007, Yang et al., 2014) are also believed to be involved in amino acid and amide transport.

1.5 The Source-to-Sink Interplay between Carbon and Nitrogen Partitioning

Carbon and Nitrogen partitioning has received attention recently to determine alternative mechanisms for improving plant nitrogen assimilation and enhance source-to-sink transport of amino acids, which involves a complex interplay between C and N status (Lu et al., 2022). Increases in photosynthesis and carbon partitioning have been found to improve N₂ assimilation and additionally the transport of amino acids due to an increased demand within photosynthetically active tissue. For example, overexpression of SUT1 in *P. sativum*, an important sucrose loading gene, saw a combinational increase in photosynthesis rate, leaf nitrogen assimilation and an overall improvement of amino acids levels in plant tissue and seeds from enhanced source-to-sink transport (Lu et al., 2019). Additionally, a knockout of the transporter involved in xylem to phloem transport of amino acids, *aap2*, improved chlorophyll, Rubisco levels, carbon fixation and photosynthetic nitrogen use efficiency (PNUE) in Arabidopsis (Perchlik and Tegeder, 2018). This supports the notion of a coordinated partitioning process between C and N. This partitioning also appears to be interchangeable, where the enhancement of amino acid transport in *P. sativum* saw increases in photosynthesis and C partitioning, in addition to improved seed yield and protein levels (Zhang et al., 2015). The AAP2 knockout in Arabidopsis, however, did not affect seed N levels, but rather improved seed C and oil content, while an improved N allocation to leaves supported the increase in total leaf area and photosynthesis machinery (Perchlik and Tegeder, 2018). This *aap2* knockout approach would be useful in plants primarily used in oil extraction: in the case of legumes which are economically important due to their high protein levels, the unchanged levels of N and seed protein may be counterproductive, however.

For SUT1 overexpression to effectively upregulate N and protein partitioning via increased photosynthesis and C assimilation, a bottleneck may need to be averted if downstream transport cannot accommodate an increase of available C for sinks (Wang et al., 2015; Lu et al., 2020). Indeed, previous research has found that increased sucrose levels can promote an improved delivery of N storage in seeds, however the level of partitioning can likely be improved further through upregulation of N transporters rather than expression of genes involved in N₂ fixation (Weigelt et al., 2008). Lu et al., (2020) found that the overexpression of SUT1 increased protein levels in the seed without any expressional response from N assimilation genes. Thus, supporting the notion that the increase of protein partitioning via increased C sink strength could be improved via a combinational improvement of N transporters for delivery to the seed in tandem to SUT1 overexpression. The increase in sucrose

also appeared to support additional C fixation pathways by providing C for improved amino acid and protein synthesis, thus balancing C flux via the C-N ratio (Lu et al., 2020). This balance is important considering the C donation required for amino acid synthesis, and conversely the amino acid requirement to support the photosynthetic apparatus, highlighting the interconnected partnership between N metabolism and C flux (Ruffel et al., 2008; Figueroa et al., 2016). Interestingly in pea and Arabidopsis, observed increases in amino acids through AAP1 and AAP8 modification respectively, improved photosynthesis only during the reproductive stage, suggesting a combined improvement in C and N partitioning may depend on a large sink requirement such as a developing seed (Zhang et al., 2015; Santiago & Tegeder, 2017). Overall, it may indeed be possible to perform a synergistic upregulation of both SUT and AAP transporters to accommodate potential bottlenecks of amino acid transport to facilitate increased sucrose loading.

1.5.1 What role does nitrogen metabolism, ureides and amides play in chickpea?

Very little is known about the mechanisms of N partitioning in chickpea, with respect to the preference for ureides or amides. That is, the overall importance of UPS1 and AAP transport proteins remain unknown. Depending on the cultivar, chickpea can be classified as a tropical or temperate legume which may exhibit different dominant N forms and the possibility to generate determinate over indeterminate type nodules, however, the latter is unlikely. Considering the importance of this crop within a variety of locations and cultures around the world and significant nutrient content, understanding the role of N from fixation into amides or ureides, loading into the vasculature for root export and transport from source to sink tissue could prove useful. Exploiting this understanding could be used in a variety of ways (1) To improve yields and plant biomass through simultaneous understanding of SUT and AAP's/UPS1 for improved N partitioning and C/N fixation; (2) Production of increased seed protein nutritional content from improvements in N containing compound partitioning from sources to sinks; (3) Reduce costs for farmers and the need for N fertilisers by more efficient N acquisition and partitioning by manipulation of N feedback regulation and transporters; and (4) Reduced environmental impacts of N fertiliser.

To better understand these possible benefits in chickpea, research of amide and ureide transporters in other plants may be of importance, which has been outlined below in Table 1.1. A comprehensive review also describes this table in detail (The et al., 2021). In summary, overexpression studies of AAP1 in pea saw a coordinated improvement in seed yields, biomass, N uptake, phloem and embryo loading of amino acids (Zhang et al., 2015, Perchlik & Tegeder, 2017). Whereas an AAP1 mutant in Arabidopsis

reduced seed N, yield and storage protein, but conversely improved the amino acid composition in the seed coat and endosperm, outlining an importance in import of amino acids into the seed embryo (Sanders et al., 2009). Other instances of knockouts appear to present notable bottlenecks in N partitioning. For example, the knockout of *aap6* in pea saw a reduction in root and shoot N content and presented a notable bottleneck in nodule export through increased amino acid levels (Garneau et al., 2018). Interestingly however, an improvement of nodule metabolism and N₂ fixation also occurred, even under inhibited N export. This indicates that a systemic sink strength signalling mechanism exists under N deficiencies in other tissues resulting in an upregulation of N₂ fixation to compensate. Similarly, knockout of endogenous *OsAAP3* and *OsAAP5* saw improved tillering and grain yield, caused by a rerouting mechanism of amino acids elsewhere such as improving seed yield and stimulated tillering (Lu et al., 2018, Wang et al., 2019).

Studies in *UPS1* have found a multitude of functions for the one transporter, ranging from nodule and root export to phloem source to sink transport of ureides. Repression of this transporter in soybean presented an inhibition of N partitioning to root, shoots and accumulated ureides in the nodules (Collier & Tegeder 2012). Presumably, this accumulation of ureides may have had a possible feedback inhibitory effect on further nodule development and metabolism (Collier & Tegeder 2012). Instances of overexpressing *UPS1* present an impressive potential to improve overall ureide partitioning, with plants exhibiting an increased ability to transport ureides from nodules to shoots and sink tissues (Carter & Tegeder, 2016, Redillas et al., 2019, Thu et al., 2020). The best instance of this was seen by Lu et al (2022), where *GmUPS1* overexpression led to a whole plant rebalancing of the N and C status of the plant, resulting in increased plant biomass, N metabolism and export of fixed N from the nodules. Indeed, this confirms the assumption above regarding signalling mechanism driving up N₂ fixation to compensate for increased sink strength. As such the rate of N₂ fixation does not appear to be a limiting factor in increasing fixed N products, rather a bottleneck resides in the transport of these fixed N products.

Table 1.1: Overview of Amino Acid Permease (AAP) transporter modifications in plants

Transporter	Proposed Function	Modification	Plant	Reference
AAP1	Positive regulator of growth and grain yield	Overexpression: ↑ Grain yield, enhanced tillering Knockout: Opposite phenotype	Rice	Ji et al., 2020
	Amino acid phloem and seed embryo loading	Overexpression: ↑ Shoot & Seed N, biomass, seed yield, N uptake, phloem and embryo loading of AA's	Pea	Zhang et al., 2015 Perchlik & Tegeder, 2017
	Mediates uptake of amino acids by the seed embryo	AAP1 mutant: ↓ Seed N, C, seed weight/number, seed storage protein ↑ Seed coat/endosperm AA's, protein bodies	Arabidopsis	Sanders et al., 2009
AAP2	Xylem to phloem transfer of root amino acids	Knockout: ↑ N remobilisation to leaf tissue	Arabidopsis	Perchlik & Tegeder, 2018
	Xylem to phloem transfer of amino acids and distribution to the embryo	T-DNA insertion: ↓ Seed total N, storage protein ↑ Fatty acids, silique number, seed yield	Arabidopsis	Zhang et al., 2010
AAP3	Regulator of grain yield	Overexpression ↑ AA concentration ↓ inhibited tillering	Rice	Lu et al., 2018

		<p>RNAi:</p> <p>↓Some AAs</p> <p>↑Grain yield</p>		
AAP5	Regulator of grain yield	<p>Overexpression:</p> <p>↑Grain yield</p> <p>RNAi:</p> <p>↑Tiller number and grain yield</p>	Rice	Wang et al., 2019
AAP6	N retrieval from apoplasm into inner cortex cells for nodule export	<p>miRNA:</p> <p>↓ Root, Shoot N</p> <p>↑ Nodule AA's, nodule metabolism and N₂ fixation</p>	Pea	Garneau et al., 2018
	N stress tolerance and N source to sink transport	<p>Overexpression</p> <p>↑ Tolerance to N limitation, source to sink transfer of amino acids under low N, N export from cotyledons and import to sinks at vegetative stage, N import to seed under normal and limited N conditions</p>	Soybean	Liu et al., 2020
AAP8	Source to sink amino acid partitioning for sink development and seed yield	<p>AAP8 mutant:</p> <p>↓ AA's phloem loading to sinks, silique, seed number</p>	Arabidopsis	Santiago, J.P. and Tegeder, M., 2016

Table 1.2: Overview of Ureide Permease (UPS) transporter modifications in plants

Transporter	Proposed Function	Modification	Plant	Reference
UPS1	Transport of ureides out of nodules	<p>Overexpression:</p> <p>↑positively regulated N₂ fixation and C-sink strength of nodules, nodule C supply, N₂ fixation and assimilation and export from nodules</p>	Soybean	Lu et al., 2022
	Transport of ureides out of nodules	<p>RNAi Repression of UPS1-1/2:</p> <p>↑ Ureides in nodules</p> <p>↓ N partitioning to roots and shoots, nodule development, N₂ fixation, nodule metabolism</p>	Soybean	Collier & Tegeder 2012
	Phloem source to sink transport of ureides	<p>Expressed UPS1 in cortex/endodermis cells of nodules:</p> <p>↑ N delivery from nodule to shoot, N₂ fixation per nodule, N assimilation, ureide synthesis and metabolite levels</p>	Soybean	Carter & Tegeder, 2016
		<p>Common bean UPS1 expressed in soybean phloem:</p> <p>↑ Source to sink transport of ureides, ureide synthesis, allantoin/allantoic acid root to sink transport, amino acid assimilation, xylem transport and phloem sink partitioning,</p>	Soybean	Thu et al., 2020

		photosynthesis, sucrose phloem transport		
	Allantoin export out of root cells	<p>Overexpression:</p> <p>↑ Panicle allantoin accumulation, ammonium uptake in roots, increased chlorophyll, tiller number, shoot and root growth under low N</p> <p>Whole-body- overexpression:</p> <p>↑ Allantoin in leaves, stems and roots</p> <p>RNAi:</p> <p>↑ Allantoin in roots</p>	Rice	Redillas et al., 2019
	Source to sink ureide transport	<p>UPS1 mutant:</p> <p>↓ Allantoin in reproductive organs</p> <p>↑ Allantoin synthesis and ureide transport genes in senescing leaves</p>	Arabidopsis	Takagi et al., 2018

1.6 Aims

The overarching aim of this thesis is to determine whether nitrogen fixation in chickpea can be improved and by what means. To determine this, three aims will need to be analysed: (1) Determine if chickpea nodules predominantly synthesise the amides, glutamine and asparagine, or ureides, allantoin and allantoic acid. (2) Identify the key transporters involved in facilitating fixed nitrogen movement out of the nodules and determine localisation of these transporters. (3) Identify the substrates of key transporters, being that of amides or ureides.

To achieve these aims, quantification of ureides (Collier & Tegeder 2012) was measured in leaf, root and nodule tissue of plants grown symbiotically in sand under low nitrogen availability and compared to a typical ureide producing legume, *G. max*. The expression of genes involved in both the amide and ureide biosynthesis pathways were measured using qRT-PCR to determine if expression suggests the path of fixed N metabolism.

RNA sequencing was also performed to obtain a transcriptional model of nitrogen fixation in chickpea nodules and to identify highly upregulated transporters during nitrogen fixation. Identified transporters could be predictively localised using a single cell RNA sequencing database (Ye et al., 2022), which localises gene expression to a particular cellular cluster in nodules. Determining the localisation of highly expressed transporters will help to ascertain function, as such genes facilitating the transport of fixed N out of the nodules would be useful targets for genetic manipulation studies to improve N₂ fixation in chickpea.

Lastly, highly upregulated transporters identified in the RNA sequencing database will be functionally characterised using a mutant yeast strain (Besnard et al., 2016) to determine amino acid transport properties. The combination of each results chapter of this thesis will assist in constructing a nitrogen fixation model in chickpea nodules, determine key transporters of fixed nitrogen and identification of mechanisms to improve nitrogen fixation in chickpea. Overall, this thesis aims to further the current understanding of nitrogen fixation in general, particularly in chickpea, identify key gene families involved in fixed nitrogen transport and to provide applied solutions to increase legume sustainability in modern agricultural systems. There indeed exists the need to improve modern agricultural practices to feed the growing population. Therefore, this critical research provides advancements in biological nitrogen fixation understanding in chickpea and can assist in providing these required improvements, which can also be translated to other legume species.

2 General Methods

2.1 General Lab Techniques

2.1.1 Reagents

Reagents used were supplied from Sigma-Aldrich (USA) unless otherwise stated in the relevant methods.

2.1.2 Streak & spread plating

All *E. coli* plating was conducted under sterile laminar flow conditions using freshly autoclaved LB media (0.1% (w/v) Tryptone, 0.5% (w/v) Yeast Extract, 0.5% (w/v) NaCl, 1.5% (w/v) Agar) using a sterile single use loop or spreader. All bacterial plating was typically accompanied by a control plate with antibiotic selection with autoclaved LB broth (0.1% (w/v) Tryptone, 0.5% (w/v) Yeast Extract, 0.5% (w/v) NaCl), or a plate with no antibiotic selection.

2.1.3 Bacterial inoculation

Bacterial colonies were grown on a streak or spread plate (2.1.2) and a single, well separated colony was used to inoculate into LB liquid broth usually 5-25 ml in 10 ml or 50 ml tubes with appropriate concentrations of antibiotic selection. Cultures were then placed at either 37°C or 30°C for *E. coli* and *S. cerevisiae*, respectively and unless otherwise stated Incubated overnight with high aggregation. Resulting bacterial culture was purified using Wizard® Plus SV Minipreps DNA Purification System (Promega, USA) following the manufactures instruction for extraction of plasmid DNA for downstream applications.

2.1.4 Glycerol stock preparation

Long term storage of bacterial cultures was performed with filter sterilized 50% (w/v) glycerol. Glycerol was added to equal volume of an overnight culture in cryo-storage tubes, mixed several times and snap frozen in liquid nitrogen prior to storage at -80°C.

2.1.5 TSS buffer preparation

TSS buffer was prepared to make chemically competent cells (2.1.6). Prepared 50 ml TSS buffer included, 5 g PEG 3350, 1.5 ml 1M MgCl₂, autoclaved LB broth up to 50 ml and adjusted to pH 6.5. Solution was filter sterilized using a 0.22 µm filter followed by addition of 2.5 ml DMSO. TSS buffer was stored at -20°C and typically remade after multiple freeze thaws or aliquoted prior to freezing.

2.1.6 Preparation of TSS chemical competent DH5α E. coli

DH5α cells inoculated in an overnight culture in autoclaved LB broth (0.1% (w/v) Tryptone, 0.5% (w/v) Yeast Extract, 0.5% (w/v) NaCl) and incubated at 37°C with shaking. Overnight culture then diluted 1:100 into fresh sterile LB broth and grown to an OD₆₀₀ of 0.2 – 0.5. Culture split into two pre-chilled chilled 50 ml falcon tubes and incubated on ice for 10 minutes, followed by centrifugation using a Sigma 3-16PK centrifuge (Sigma-Aldrich, USA) at 1000 g pre-chilled to 4°C. Resulting supernatant was removed and resuspended in pre-chilled TSS buffer (2.1.5) and 50 µl aliquots pipetted into pre-chilled Eppendorf tubes. Eppendorf tubes either used immediately for heat shock transformation (2.1.8) or snap frozen in liquid nitrogen and stored at -80°C.

2.1.7 SOC broth preparation

Super Optimal broth with Catabolite repression (SOC) broth prepared with 1.25 g yeast extract, 5 g tryptone, 1.25 g NaCl, 2.5 ml 250 mM KCl, adjusted to pH 7 and autoclaved. Once cooled, 1.25 ml of 2 M MgCl₂ and 5 ml 1 M glucose was added. SOC broth was stored in aliquots at -20°C.

2.1.8 Heat shock transformation of chemical competent E. coli

Heat shock transformation was performed using pre-prepared competent DH5α cells (2.1.6). Approximately 1-5 µl of template DNA (~100 ng) was added to 25-50 µl thawed DH5α cells in Eppendorf tubes, gently flick mixed and incubated on ice for 30 minutes. Eppendorf tubes placed in a water bath or heat block set at 42°C for 45 seconds and immediately placed back onto ice for 2 minutes. Cells were plated on appropriate antibiotic selection agar plates at 37°C after suspension of DH5α cells in 250 µl LB or SOC broth (2.1.7).

2.1.9 Plasmid purification

Purifications of plasmids were performed by inoculating an overnight LB culture with a single bacterial colony or glycerol stock harboring the desired plasmid. Appropriate antibiotics were added to the overnight culture and incubated at 37°C with shaking. Culture pelleted at max speed using a Sigma 3-16PK centrifuge (Sigma-Aldrich, USA) for 5-10 minutes followed by removal of supernatant. Pellet resuspended in resuspension solution of the Wizard® Plus SV Minipreps DNA Purification System (Promega, USA) and prepped following the manufacturer's instructions. Successful purification and plasmid verification was accomplished by measuring plasmid DNA concentration using a NanoDrop 1000 spectrophotometer (Thermo Fisher Scientific, USA) and visualisation on an agarose gel (2.1.14).

2.1.10 Ammonium acetate precipitation

Ammonium acetate precipitation was used to purify the yeast expression pDR196 plasmid after linearization using restriction enzymes prior to LR Gateway® cloning for improved cloning efficiency. Restriction digest was terminated with 0.5% SDS and 10 µg proteinase K (NEB, USA) and incubated at 50°C for 60 minutes. Linearised plasmid DNA was purified with an equal volume of phenol/chloroform and vortexed briefly, followed by centrifugation for 5 minutes at 16,000 g using an Eppendorf 5425 centrifuge (Eppendorf, USA). The aqueous phase was combined with a 1:10 volume of 5.0 M ammonium acetate and 2 volumes of 100% ethanol, followed by an overnight incubation at -20°C. The linearized plasmid DNA was then pelleted at max speed using an Eppendorf 5425 centrifuge (Eppendorf, USA) at 4°C for 20 minutes, air dried and resuspended in ~20 µl of sterile Milli-Q H₂O. Plasmid DNA concentration and purity was measured using a NanoDrop 1000 spectrophotometer (Thermo Fisher Scientific, USA) and stored at -20°C.

2.1.11 Polymerase chain reaction (PCR)

Polymerase Chain Reaction (PCR) consisted of varying volumes ranging from 15-60 µl depending on the application. A typical PCR using Promega (USA) reagents, unless otherwise stated, consisted of DNA template, 1X GoTaq Flexi Buffer or 5X Green GoTaq® Reaction Buffer, 2 mM MgCl₂, 0.8 mM dNTPs, 2 µM forward and reverse primers, GoTaq polymerase and sterile autoclaved Milli-Q H₂O. Some applications utilised Q5® or Phusion® High-Fidelity DNA Polymerase from New England BioLabs (USA) for reduced chance of PCR base pair mutations for downstream sequencing and cloning. A typical Q5 reaction consisted of DNA template, Q5® Reaction Buffer (NEB #B90275), 10 mM dNTPs, 5 µM forward primer, 5 µM reverse primer, Q5® High-Fidelity DNA Polymerase (NEB #M0491S) and autoclaved Milli-Q H₂O. All PCRs were performed using the MyCycler™ Thermal Cycler (BioRad, USA). Thermocycling conditions generally consisted of; Initial Denaturing at 95°C for 3 mins (98°C – 30 secs for Q5), Denaturing at 95°C for 30 secs (98°C – 10 secs for Q5), Annealing at 35-65°C for 30 secs, Extension at 72°C for 10-60 secs, last 3 steps generally cycled 15-35 times, followed by Final Extension at 72°C for 5 mins (2 mins for Q5). Prior to thermocycling, reactions were setup in a master-mix prepared on ice and pipetted into respective PCR tubes, mixed thoroughly and pulse-spined in a microfuge centrifuge.

2.1.12 Colony PCR

Colony PCR was performed as a rapid means of verifying cloning success from single colonies after heat-shock transformation (2.1.8). Colonies were gently tapped with a sterile pipette tip and swirled in 50 µl

sterile Milli-Q H₂O in a PCR tube to dislodge the bacterial cells in the liquid from the tip. The PCR tube was then incubated at 95°C in a MyCycler™ Thermal Cycler (BioRad, USA) for 5 minutes. A typical PCR reaction (2.1.11) using flanking primers designed to the plasmid and gene insert was performed using the boiled bacterial cells as DNA template and verified via agarose gel electrophoresis (2.1.14).

2.1.13 PCR clean-up

PCR products were purified for sequencing and further PCR/qRT-PCR applications. The Wizard® SV Gel and PCR Clean-Up System (Promega, USA) and manufacturer's instructions were used for PCR purification. Resulting purified product was assessed by either agarose gel electrophoresis (2.1.14) or via a NanoDrop 1000 spectrophotometer (Thermo Fisher Scientific, USA).

2.1.14 Agarose gel electrophoresis

Agarose gel electrophoresis was used to visualise PCR product or DNA/RNA extraction quality. Gels made with 1-1.5% (w/v) agarose (Fisher Biotec, Australia) diluted in 1X TAE buffer, dissolved in a microwave for ~60 seconds and stained with 1 µl GelRed® (Biotium, USA). Agarose solution was left to cool and poured into a gel casting tray left to set for ~30 minutes. Once set, the gel tray was placed into a gel tank apparatus submerged in 1X TAE buffer. Prior to running a gel with extracted RNA, tank apparatus was emptied and soaked in 1% sodium hypochlorite (commercial bleach) and rinsed with sterile Milli-Q H₂O. Gels also containing RNA product were made with 1% (w/v) sodium hypochlorite to prevent contamination and RNA degradation (Aranda et al., 2012). After PCR, 1-5 µl product was usually visualised on gels either supplemented with Blue/Orange 6X loading dye (Promega, USA) or 5X Green GoTaq® Reaction Buffer (Promega, USA). Agarose gel was usually run for 30-70 minutes at 70-120 volts using a PowerPac™ Basic (BioRad, USA) and imaged on a BioRad gel imaging system. Promega 100 bp, 1 kb or lambda DNA ladders (NEB, USA) were used for product size comparison. The 1 kb ladder was used most frequently and made into a stock solution of 20 µl 1 kb ladder, 10 µl Blue/Orange 6X loading dye (Promega, USA) and 60 µl H₂O.

2.1.15 Agarose gel DNA purification

The removal of undesirable secondary products or primer dimer after PCR was accomplished by an agarose gel purification where the desired amplified DNA product was excised from the gel and purified (2.1.13). A typical agarose gel was performed (2.1.14) whereby a smaller volume of the template to be purified was pipetted in the well alongside the remaining product to act as a marker lane. After running the agarose gel, the marker lane was removed from the gel cut out longitudinally and visualized under

UV light to visually observe the DNA band. A small excision was performed where the band was observed, and the gel section re-aligned with the rest of the agarose gel. Using the excised marker as a guide the desired template could be removed from the gel without having to expose the desired DNA template to UV light to prevent DNA mutations. The remainder of the purification was performed following the Wizard® SV Gel and PCR Clean-Up System (Promega, USA) manufacturer's instructions.

2.1.16 Restriction digestion

All restriction enzymes were acquired from NEB (USA) and performed following the manufacturer's instructions. Restriction digests were typically incubated overnight at room temperature and visualized using gel electrophoresis (2.1.14) prior to any downstream applications.

2.2 Plant Growth & Harvesting

2.2.1 Growth conditions

Plants were grown in either BioGrow soil (SARDI, The University of Adelaide, Waite Campus) for seed bulking or control growth experiments, or washed and sterilised quarry sand (SARDI, The University of Adelaide, Waite Campus) for Nitrogen supplemented growth experiments. Chickpea (Cultivar: Slasher) or soybean (Cultivar: Stephens) seeds were germinated in petri dishes on two layers of moist paper towel for 4-5 days prior to sowing and only germinated seeds were subsequently sown. Germinated seeds inoculated with specific plant species rhizobia supplied by Nodulaid® (BASF Crop Solutions Australia) at sowing, by dipping seeds in a rhizobia peat mix slurry unless otherwise stated. Prior to sowing, sand or soil was soaked with McKnight's nutrient (Table 2.1) solution. Chickpea or soybean seeds were placed ~2cm below the surface, with 3 seeds per 18 cm diameter, 4.5 L volume pot. Pots were not watered for at least a week after sowing as to not wash any rhizobia from the germinated seed.

Plants were grown under ambient lighting unless otherwise stated in a controlled temperature greenhouse conditions in ~18-25°C night/day respectively, at Flinders University, South Australia. Plants were only watered with nutrient solution when sand appeared completely dry, typically once or twice a week from ~10-25 Days after inoculation (DAI) then twice-weekly thereon after. Importantly, chickpea grown in sand was very prone to waterlogging during roughly the 1-35 DAI period, then drought stress after this point. Sand was monitored as often as possible to avoid waterlogging and drought issues. Plants grown in BioGrow soil (SARDI, The University of Adelaide, Waite Campus) was watered one or twice a week as the plant developed. For seed bulking or growth experiments where specified, supplemental lighting (~500 PAR, 16/8-hour day/night) was used (Heliospectra AB, Sweden). All other factors were the same as described above, except plants were grown until ready for seed harvesting.

Table 2.1: Mcknight's nutrient solution 100x concentrate, amount per 0.25 L.

Chemical	Amount
CaSO₄·2H₂O	6.75 g
MgSO₄·7H₂O	1 g
KH₂PO₄	4 g
KCL	1.5 g
A-Z Trace Elements	5 ml
D Solution	5 ml
Distilled H₂O	To 250 ml
D Solution (FeCl₂)	10g per L
A-Z Trace Elements Solution (1L)	
H₃BO₃	2.86 g
MnSO₄·7H₂O	2.08 g
ZnSO₄·7H₂O	0.22 g
CuSO₄·5H₂O	0.079 g
NaMoO₄·H₂O	0.079 g

2.2.2 Tissue harvesting

Leaf, root, nodule tissue was typically harvested in triplicates at 5-day intervals (10 DAI-35 DAI) for most growth experiments and snap frozen in liquid nitrogen and stored at -80°C unless otherwise stated for RNA/DNA extraction or ureide quantification. Some leaf, root and nodule tissue were also used for fresh and dry weight measurements, hence, not snap frozen in liquid nitrogen. During harvesting, sand or soil was removed from roots by immersion and/or rinsing in tap water, followed by blotting tissue on paper towel to remove excess water. Typically, after harvesting, root & stem length and nodule & leaf count was recorded alongside photos of the plant and nodules. When dealing with nodules it was important to show an example nodule cut in half to observe either senescing or N₂ fixing nodules via a green or pink interior, respectively.

2.2.3 Plant nitrogen growth experimental setup

For uninoculated growth experiments, seeds were sterilised by first immersing seeds in 70% ethanol (Diluted with sterile H₂O) for 2 minutes while shaking, then a 1% bleach solution (Diluted with sterile H₂O) for 20 minutes with gentle agitation. Bleach washed from seeds with sterile H₂O multiple times, followed by germination on paper towel as described above (2.2.1). Prior to sowing, pots and soil/sand were autoclaved in a kill cycle to remove any present rhizobia. Uninoculated growth experiments were typically separated from inoculated experiments where possible to avoid cross contamination of spores.

Soil growth experiments were grown in BioGrow soil supplied by SARDI, The University of Adelaide, Waite Campus. Seed germination, sowing and growth conditions were conducted as above (2.2.1). However, plants were watered more frequently than plants grown in sand, 2-3 times per week with RO/tap water, depending on plant age.

For nitrogen supplementation growth experiments in sand, plants were grown under either low nitrogen (0.5 mM KNO₃) or high nitrogen (5 mM KNO₃), supplemented with McKnight's nutrient solution (Table 2.1). Low nitrogen was applied to induce efficient symbiotic nitrogen fixation conditions, whereas high nitrogen typically inhibited nodule formation and symbiotic nitrogen fixation.

2.3 Gene Expression Analysis

2.3.1 Diethyl pyrocarbonate (DEPC) treatment

Prior to RNA extraction, cDNA synthesis or the handling of RNA and cDNA, all 1.5 ml microcentrifuge tubes, pipette tips and Milli-Q H₂O were treated with DEPC to remove RNAses to prevent associated degradation. DEPC was handled with appropriate PPE and in a fume hood where possible. DEPC was diluted 1:1000 (1 ml DEPC into 1 L Milli-Q H₂O) prior to use. Microcentrifuge tubes treated by immersing tubes in diluted DEPC making sure solution fills the tubes, in an autoclavable container. Tips treated by filling the underside of pipette tip box after removing the tip tray, so that tips are immersed in DEPC. Tubes, Tips and Milli-Q H₂O was incubated at 37 °C overnight. The following morning the DEPC solution was drained from tips and 1.5 ml tubes and autoclaved to inactive residual DEPC. After this point all treated equipment was only opened in the sterile environment of a laminar flow.

2.3.2 TRIzol RNA extraction

RNA in all cases unless otherwise specified was extracted using the following TRIzol method. All tips, tubes and H₂O were pre-treated with DEPC (2.3.1). Where possible, steps were carried out in a fume hood with appropriate waste containers handy. All steps were also carried out at 4°C or on ice, unless otherwise stated.

Plant tissue following a harvest (2.2.2) and stored at -80°C was first ground to a fine powder in liquid nitrogen in a mortar and pestle or pulverised within a 15 ml falcon tube with 2 Ball-Barings using a vortex. Following this, a maximum of 100 mg of powdered tissue for leaf and nodule, or 130 mg for root was quickly weighed out in a snap frozen RNase free 1.5 ml microcentrifuge tube and placed immediately back into liquid nitrogen. While in a fume hood, 1 ml of TRIzol reagent (Table 2.2) was added to each sample and vigorously shaken on a vortex, then placed on ice. Samples then centrifuged at 12000 g for 5 minutes using an Eppendorf 5425 centrifuge (Eppendorf, USA) at 4°C, and the resulting supernatant was collected into a fresh RNase free tube. If necessary, this step was repeated to remove any unintended pellet transfer. Next 200 µl of chloroform was added to each tube followed by vigorous shaking for 20 seconds, a 3 min ice incubation and centrifugation at 12000 g using an Eppendorf 5425 centrifuge (Eppendorf, USA) for 15 mins at 4°C. After centrifugation, the aqueous phase was collected into a new RNase free tube. This step was typically repeated to reduce any downstream phenol contamination. Following this, 500 µl of 200-proof isopropanol was added and either incubated at room temperature for 10 minutes or overnight at -20°C. Samples were then centrifuged at 12000 g using an

Eppendorf 5425 centrifuge (Eppendorf, USA) for 10 mins at 4°C, with the resulting supernatant discarded. Pellet rinsed with 1 ml 75% ethanol (molecular grade, Sigma, USA) and centrifuged at 12000 g for 5 mins at 4°C, resulting supernatant discarded. This ethanol wash step was also repeated. Washed pellet then air dried in a laminar flow for typically 30 mins or until ethanol had evaporated. Air dried pellet then resuspended in 30 µl DEPC-treated H₂O by pipetting up and down over the pellet until completely resuspended. The quality of the RNA was assessed through a NanoDrop 1000 spectrophotometer (Thermo Fisher Scientific, USA) to determine concentration and purity and run on a 1% bleach agarose gel (2.1.14) at 70 volts for ~1 hour. RNA samples were then continued onto cDNA synthesis (2.3.3) or stored at -80°C.

Table 2.2: TRIzol-Like reagent composition for RNA extraction.

	250 ml	500 ml
Phenol, saturated, pH 4.3	95 ml	190 ml
Guanidine thiocyanate	29.54 g	59.08 g
Ammonium thiocyanate	19.03 g	38.06 g
Sodium acetate, pH 4.5-5.0	8.35 ml of 3 M Stock	16.7 of 3 M Stock
Glycerol	12.5 ml	25 ml
Sterile Milli-Q H₂O	To 250 ml	To 500 ml

2.3.3 ProtoScript cDNA synthesis

CDNA synthesis was conducted on pre-synthesised RNA as describe above (2.3.2). All steps performed in a laminar flow hood and samples kept on ice where possible. All tips, tubes and H₂O were DNase free after treatment with DEPC, described above (2.3.1). Typically filter tips were also used when handling RNA/cDNA from this point. The following master-mix was prepared as per Table 2.3.

Table 2.3: Master-mix 1 for cDNA synthesis.

Component	Volume (μ l)
2 μ g of RNA	X μ l (Max 9 μ l)
50 μ M Oligo d(T) ₂₀ (NEB, USA)	2 μ l
10 mM dNTP (Sigma, USA)	1 μ l
Water	To 12 μ l

Master-mix was prepared for x number of samples and micro-pipetted into PCR tubes containing the required RNA volume (Max 9 μ l) at 2 μ g concentration, followed by the addition of 3 μ l of the master-mix (2 μ l 50 μ M Oligo d(T)₂₀ + 1 μ l 10 mM dNTP) into each tube. Solution was mixed via pipette mixing and incubated at 65°C for 5 mins, then placed on ice for 1 min. Next 1 μ l of DNase 1 (ThermoFisher, USA) was added to each sample, pipette mixed and incubated for 15 mins at room temp. During the 15 min incubation master-mix 2 was prepared as following Table 2.4.

Table 2.4: ProtoScript cDNA synthesis reaction master-mix 2.

	Per Sample	25 Reactions
5 x ProtoScript II Reaction Buffer (NEB, USA)	4 μ l	100 μ l
0.1 M DTT (NEB, USA)	2 μ l	50 μ l
Murine RNaseOut (NEB, USA)	0.5 μ l	12.5 μ l
ProtoScript® II Reverse Transcriptase (NEB, USA)	0.5 μ l	12.5 μ l

After the 15-minute incubation at room temp, 7 μ l of the above master-mix (Table 2.4) was added to each sample for a total reaction volume of 20 μ l and placed in a Thermal Cycler (MyCycler™ BioRad,

USA) under the following conditions: 45 mins @ 42°C for the reverse transcription reaction, then 5 mins at 80°C for enzyme inactivation. Prior to using the synthesized cDNA in qRT-PCR, samples were diluted 1:10 (180 µl DNAase Free H₂O to the 20 µl reaction solution) and separated into 50 µl aliquots for long term storage at -80°C.

2.3.4 Quantitative reverse transcriptase PCR (qRT-PCR) primer design

Primers for use in qRT-PCR were designed using NCBI Primer-Blast (Ye et al., 2012) and synthesized by Sigma-Aldrich (Australia). Primers were designed to bind near the 3' end of the target gene cDNA sequence and spanned exon junctions where possible. For the best efficiency, primers exhibited similar GC content and melting temperatures within 5°C and generated an 80-150 bp product. Housekeeping primers *CaEiF* and *CaHSP90* for *C. arietinum* (Garg et al., 2010) and *GmACT11* and *GmELF1B* for *G. max* (Yin et al., 2015) were used.

Table 2.5: Housekeeping primers used for qRT-PCR normalization in *C. arietinum* and *G. max*.

Gene	Primer (5' to 3')
ELF1B	Fwd-GTTGAAAAGCCAGGGGACA
	Rev-TCTTACCCCTTGAGCGTGG
ACT11	Fwd-ATCTTGACTGAGCGTGGTTATCC
	Rev-AGCTGGTCCTGGCTGTCTCC
HSP90	Fwd-GCAGCATGGCTGGTTACATGT
	Rev-TGATGGGATTCTCAGGGTTGA
EiF	Fwd-TCCACCACTGGTCGTTTTG
	Rev-CTTAATGACACCGACAGCAACAG

2.3.5 qRT-PCR setup & thermocycling

Reactions to measure gene expression were setup in 96 well microplates with 1 μl (2 μM) forward and reverse primer, 5 μl 2 X KAPA SYBR (Fisher Scientific, USA) and 4 μl cDNA. Thermocycling conditions included 95°C for 3 minutes for 1 cycle, 30-40 cycles at 95°C for 5 seconds followed by 60°C for 15 seconds. To assess any unintended amplification a melt curve was also run beginning at 65°C ranging to 95°C in 0.5°C increments every 5 seconds. Data was analysed by calculating relative expression by comparing Ct values to the standard curve (2.3.6) and normalised against the expression of two housekeeping genes (2.3.4), Eif & HSP90 for chickpea and ELF1B & ACT11 for *G. max* (Table 2.5).

2.3.6 qRT-PCR standards

To generate a standard curve to calculate relative expression levels in qRT-PCR, gene products were amplified using PCR, purified (2.1.13) verified on an agarose gel (2.1.14) and concentration measured using a NanoDrop 1000 spectrophotometer (Thermo Fisher Scientific, USA). Promega (USA) BioMath calculator (<http://www.promega.com/a/apps/biomath/?calc=tm>) was then used to determine the concentration of double stranded DNA from $\mu\text{g}/\mu\text{l}$ to $\text{pmol}/\mu\text{l}$ to make 1 $\text{fmol}/\mu\text{l}$ stocks for each gene. A standard curve was then generated by serial diluting 1 $\text{fmol}/\mu\text{l}$ gene stocks from 10^0 to 10^{-8} and performing a qRT-PCR reaction (2.3.5) with the serial dilutions as template.

2.4 Ureide Colorimetric Assay

2.4.1 Tissue preparation for ureide quantification

Harvested plant tissue lyophilization using a Christ Beta 2-8LD+ freeze dryer (John Morris Scientific, Australia) for approximately 48 hours or longer depending on tissue. Tissue was typically kept in 10 ml Eppendorf tubes with the lids removed and one layer of parafilm covering the tube with a small hole puncture to allow equalisation under the vacuum freeze drying chamber. After 48+ hours, lyophilized tissue was then ground up within the 10 ml Eppendorf tube using a thin spatula to crush the tissue into a fine powder. It was important to grind tissue within the Eppendorf tube to ensure the total tissue remains contained, as the lyophilized tissue is exceptionally light and is easily lost.

Freeze dried tissue was weighed into aliquots in 1.5 ml Eppendorf tubes, typically 5-30 mg of tissue. Any tissue weights outside of this range would typically cause considerable data variation. Aliquots were then placed on ice for ~15 minutes prior to processing. Pre-chilled 200 μ l of sterile Milli-Q H₂O was added and while keeping the tubes on ice, tissue was homogenised with a plastic micro-pestle for approximately 20 seconds to disperse the ground powder with the sterile H₂O. Another 800 μ l of sterile H₂O was then pipetted down the micro-pestle shaft into the 1.5 ml Eppendorf tube to rinse off any residual tissue. Tissue + H₂O was pipetted into a new 1.5 ml Eppendorf tube through a single layer of Miracloth (Sigma, USA) to squeeze out remaining liquid separated from solid tissue debris. It was important to clean gloves and the micro-pestle after each sample to prevent cross-contamination. The filtered extract was centrifuged at 20,000 g using an Eppendorf 5425 centrifuge (Eppendorf, USA) for 30 minutes at 4°C to separate the extract from any remaining ground tissue. After centrifugation, the liquid excluding the pellet was transferred into a new 1.5 ml tube and kept on ice. At this stage the extract was either frozen at -80°C, or 100 μ l was transferred into 2 separate tubes, one used for total ureide and the other for allantoic acid determination. Prior to performing the assay, 50 ml of 10 mM allantoic acid stock solutions and the following standards were prepared as per Table 2.6 below. Ureide assay was carried out in steps sequentially outlined as per Table 2.7. This method was adapted from Collier & Tegeder (2012).

Table 2.6: Preparation of ureide assay standards.

Stock	1 mM	300 μM	200 μM	100 μM	50 μM	10 μM	1 μM
Volume of stock solution	5 ml of 10 mM	3 ml of 1 mM	2 ml of 1 mM	1 ml of 1 mM	5 ml of 100 μ M	1 ml of 50 μ M	1 ml of 10 μ M
Volume of H₂O	45 ml	7 ml	8 ml	9 ml	5 ml	4 ml	9 ml

- Green boxes indicate stocks used for standards within assay

Table 2.7: Sequential workflow of the ureide assay protocol.

Standards	Total Ureides	Allantoic Acid
200 µl of standard	100 µl of extracted sample	100 µl of extracted sample
300 µl H ₂ O	400 µl H ₂ O	500 µl H ₂ O
100 µl 0.5 M NaOH	100 µl 0.5 M NaOH	Keep samples on ice while waiting for Total Ureides.
100 °c for 8 mins	100 °c for 8 mins	
Cool on ice (~3 mins)	Cool on ice (~3 mins)	
100 µl 0.65 M HCL	100 µl 0.65 M HCL	100 µl 0.15 M HCL
100 µl 0.33% Phenylhydrazine	100 µl 0.33% Phenylhydrazine	100 µl 0.33% Phenylhydrazine
100°c for 4 mins	100°c for 4 mins	100°c for 4 mins
Cool on ice (~3 mins)	Cool on ice (~3 mins)	Cool on ice (~3 mins)
400 µl Fuming HCL (37%)	400 µl Fuming HCL (37%)	400 µl Fuming HCL (37%)
100 µl 1.67% K-Ferricyanide	100 µl 1.67% K-Ferricyanide	100 µl 1.67% K-Ferricyanide
Leave at room temp for 10 mins	Leave at room temp for 10 mins	Leave at room temp for 10 mins
Read at A ₅₂₀	Read at A ₅₂₀	Read at A ₅₂₀

*Shading indicates shared steps between standards, total ureides and allantoic acid.

Absorbances were read at 520 nm using a SPECTROstar Nano BMG microplate reader (BMG LABTECH, Australia) within 30 minutes of the last step in Table 2.7. Total ureides were calculated using the equation of the line from the standard curve plotted from the six standards (300 µM – 1 µM). Values were converted to nmols/mg of dry weight. OD520 of standards graphed on the y-axis and standard concentration on the x-axis. X amount of tissue was processed in 1 ml of H₂O, only 100 µl was used in the assay, so mg of tissue was converted to 1/10 of the total for conversion. Allantoin was determined

by subtracting allantoinic acid from total ureides. Assay steps were all conducted in a fume hood where possible. Phenylhydrazine 0.33% (w/v) and potassium ferricyanide 1.67% (w/v) were made fresh and used within 3 hours.

2.5 RNA Sequencing

2.5.1 RNA sequencing growth conditions and tissue harvesting

RNA sequencing was performed as mRNA sequencing with 20 million runs per sample with 20x coverage. Included 16 samples (*Cicer. arietinum*, cultivar: Slasher): four reps for root and nodules for two harvest periods (18 DAI & 25 DAI). Chickpea was grown in sterilised washed quarry sand and inoculated with rhizobia (Nodulaid®, BASF Crop Solutions Australia) at sowing after germinating on moist filter paper for four days. Plants grown under low nitrogen 0.5 mM KNO₃ were supplemented with McKnight's nutrient solution (Table 2.1), with ambient lighting in greenhouse conditions (~18-25°C night/day). Sand was only watered with nutrient solution when sand appeared completely dry. During harvesting, nodules were placed into 10 ml microcentrifuges tubes immersed in liquid nitrogen. Root tissue was cut away from the seed, wrapped in aluminium foil and rapidly placed in liquid nitrogen. Tissue ground into a fine powder under liquid nitrogen and was stored at -80°C.

2.5.2 RNA extraction and sequencing setup

RNA was extracted using the Spectrum™ Plant Total RNA Kit (SIGMA, USA), Catalogue number: STRN50 and stored at -80°C. Quality of RNA was assessed through NanoDrop 1000 spectrophotometer (Thermo Fisher Scientific, USA) and agarose gel electrophoresis (2.1.14). RNA sequencing performed by the AGRF at 14 Flemington Road North Melbourne VIC 3051 and performed on the ILLUMINA NOVASEQ 6000. Raw data formatting performed by Darren Wong (ANU) and described in more detail in Chapter: 4.3.

2.6 Gateway® Cloning into *S. cerevisiae*

2.6.1 Gateway® vectors

For *S. cerevisiae* expression experiments, chickpea amino acid transporters were cloned into the pDONR™221 entry vector and either the pYES-DEST52 or pDR196 destination yeast expression vectors. These vectors were maintained in glycerol stocks (2.1.4) and propagated from ccdB Survival™ 2 *E. coli* strain (ThermoFisher, USA) harbouring resistance to the lethal ccdB selection gene located in the vectors in Table 2.8.

Table 2.8: Gateway® vectors used for yeast expression experiments.

Vector	Source	Selection	Cloning Site
pDONR™221	Invitrogen, USA	Kanamycin	attP
pYES-DEST52	Sunita Ramesh, University of Adelaide, Australia	Ampicillin	attR
pDR196-WS	Sunita Ramesh, University of Adelaide, Australia	Ampicillin	attR

2.6.2 Gene amplification for Gateway® cloning

Chickpea amino acid transporters AAP6, AVT6A, AVT6C, CAT1, CAT2, UmamiT9, UmamiT12, UmamiT18, UmamiT20, UmamiT23 and UmamiT41 coding sequences were amplified from nodule cDNA (2.3.3) from chickpea plants grown under low nitrogen 0.5 mM KNO₃ to promote symbiotic conditions. PCR gene amplification was performed using primers and PCR conditions specified in (Appendix 5a.1).

2.6.3 Overlapping PCR to anneal attB cloning sites to gene products

To perform cloning into the Gateway® enabled pDONR221 entry plasmid, previously amplified coding sequences of amino acid genes (2.6.2) were subjected to either one or two rounds of overlapping PCR to anneal attB cloning sites to the 5' and 3' gene sequence. Overlapping PCR involved designed primers

whereby the 5' and 3' end of the forward and reverse primer, respectively contained the attB cloning sites which would be amplified to the respective ends of the gene template through DNA polymerase activity. Primers and PCR conditions used are outlined in the appendix of chapter 5 (Appendix 5a.1). AttB sites are required to enable recombination of gene products into the pDONR221 vector via the enzyme activity of BP clonase™. Forward attB primers were designed to include four guanine (G) residues on the 5' end of the sequence following the attB cloning site. All gene template specific primers were designed using SnapGene Viewer (GSL Biotech LLC, USA) and where possible containing 18-25 bp with a Tm of approximately 60°C, GC content of 50% and GC residues at the 3' end. Following overlapping PCR to anneal attB sites, resulting PCR product was purified via PCR-clean up via Wizard® SV Gel and PCR Clean-Up System (Promega, USA) to remove residual PCR reagents and primer dimer. In some cases, product required a gel purification (2.1.15) to remove and unintended PCR amplification.

2.6.4 Cloning gene products into Gateway® entry plasmids (BP Clonase™)

Cloning of gene sequencing with flanking attB cloning sites performed into attP site containing pDONR221 vector (Appendix: 5a.3) using BP clonase™ following the manufacturer's instructions (Invitrogen Gateway® BP Clonase™ II Enzyme Mix manual) with minor modifications. Gene template amount in the reaction mix was calculated with the size of the gene product plus attB sites (bp) * 0.0165. In addition, 150 ng of pDONR221, 0.5 µl BP clonase and TE buffer or sterile Milli-Q H₂O up to a total volume of 8 µl was added. Reactions were incubated at 25°C overnight or left on the bench overnight at room temperature to perform recombination of the attP to attL sites of the pDONR221 vector. Both incubation options typically generated identical results. The next day, 2 µg proteinase K solution was added to the reaction mix, vortexed briefly and incubated at 37°C for ~10 minutes. The resulting reaction mix was transformed into competent TSS DH5α cells (2.1.6) using a heat-shock protocol (2.1.8) and plated on Kanamycin 50 µg/ml selection media. Resulting colonies were inoculated into LB media (Kanamycin 50 µg/ml) and purified (2.1.9) following sanger sequencing (AGRF, Australia) to confirm successful transformation of gene coding sequences into pDONR221 (Appendix 5a, Figure 5a.5-9).

2.6.5 Cloning gene products into Gateway® destination plasmids (LR Clonase™ II)

Purified pDONR221 plasmids harbouring gene sequences were used as template for cloning into the yeast expression vectors pDR196 and pYES-DEST52 containing attR Gateway® cloning sites and cddB lethal selection gene. Two genes, *CaAAP6* and *CaAVT6C* were cloned into pYES-DEST52 and six genes, *CaAVT6A*, *CaAAP6*, *CaUmamiT9*, *CaUmamiT18*, *CaUmamiT20* and *CaUmamiT41* were cloned into pDR196 using LR Clonase™ II (Invitrogen, USA). The vectors pYES-DEST52 and pDR196 are Gateway® enabled, containing attR cloning sites which transition to attB sites after recombination. LR reactions were performed with a modified protocol with either ½ or ¼ LR reactions (10 µl full reaction), where equal fmol concentrations of entry and destination vectors (150 ng for 10 µL total reaction vol.) were added to enzyme mix containing either 1 or 0.5 µl LR Clonase™ II for ½ or ¼ reaction, respectively. Reaction mix made up to the total volume with TE buffer or sterile Milli-Q H₂O. Prior, the pDR196 vector was first linearised between attR sites with BbvCI (NEB, USA) followed by ammonium acetate precipitation purification (2.1.10), as to improve LR cloning efficiency. The LR reaction was incubated at 25°C overnight and terminated by 1 µg Proteinase K treatment at 37°C for 10 minutes. Heat shock transformation in chemical competent TSS DH5α (2.1.8) was conducted using 2 µl of the LR reaction and plated on Ampicillin 50 µg/ul selection agar media, incubated at 37°C. Resulting single colonies were grown overnight in LB containing Ampicillin 50 µg/ul, purified (2.1.9) and confirmed using a restriction digest (Appendix: 5a.6).

2.7 *S. cerevisiae* Expression Experiments

2.7.1 *S. cerevisiae* strains used for characterization experiments

S. cerevisiae amino acid transporter knockout strain 22Δ10AA (MATα gap1-1 put4-1 uga4-1 can1::HisG lyp1- alp1::HisG hip1::HisG dip5::HisG gnp1Δ agp1Δ ura-) and the parental strain 23344c (MATα ura-), were kindly provided by Guillaume Pilot (Verginia Tech, USA). These strains were stored in Yeast Extract-Peptone-Dextrose (YPD) media containing 2% (w/v) D-glucose, 2% (w/v) peptone and 1% (w/v) yeast extract at -80°C.

2.7.2 *S. cerevisiae* transformation into mutant and parental strains

Transformation into *S. cerevisiae* strains with previously confirmed pDR196 and pYES-DEST52 vectors harboring chickpea amino acid genes (2.6.5) was performed using the lithium acetate (LiAc) method (Gietz & Woods, 2002).

Overnight starter culture of both the 22Δ10AA and 23344c strains in YPD media were grown at 30°C with shaking. The next day 2 ml of the starter culture was again grown in 50 ml of the YPD media until OD₆₀₀ 0.5 - 0.6 and spun down at 3000 g for five minutes using a Sigma 3-16PK centrifuge (Sigma-Aldrich, USA). Supernatant was removed and cells resuspended in 25 ml sterile Milli-Q H₂O and again pelleted at 3000 g for 5 minutes. Supernatant removed and cells resuspended in 1.0 ml 100 mM LiAc and transferred to an Eppendorf tube. Cells pelleted at top speed in an Eppendorf 5425 centrifuge (Eppendorf, Australia) for 15 seconds, followed by resuspension to a final volume of 500 μl with 100 mM LiAc. Suspension vortexed, aliquoted 50 μl into Eppendorf tubes and pelleted, removing LiAc.

Transformation mix prepped by boiling 2 mg/ml salmon sperm DNA and chilling on ice. Transformation mix then setup with 240 μl PEG 3750, 36 μl 1.0 M LiAc, 25 μl salmon sperm DNA (2 mg/ml) and 1 μg plasmid DNA into 50 μl yeast cell aliquots. Transformation mix was vortexed, incubated at 30°C for 30 minutes, heat shocked in a water bath set to 42°C for 25 minutes and pelleted at 8000 rpm for 15 seconds. Cells were then resuspended in 1 ml sterile Milli-Q H₂O and 250 μl grown overnight on 1.7% (w/v) Yeast Nitrogen Base (YNB) without ammonium sulphate, with 2% (w/v) D-glucose and 0.192% (w/v) Yeast Synthetic Drop-out medium minus Uracil at 28°C.

2.7.3 Preparation of the mutant and parental *S. cerevisiae* strain

Single colonies of the *S. cerevisiae* transformants expressing chickpea amino acid transporters were grown on YNB (pH 6.2) with 2% (w/v) D-glucose, 50 mM citric acid, 2% agar and 0.192% (w/v) Yeast

Synthetic Drop-out Medium minus Uracil (Sigma, USA) to bulk up cells for expression assays. Starter cultures were grown overnight in 3 ml liquid YNB as above at pH 6.2 without agar at 30°C with shaking. Cells were then pelleted at 3000 g using a Sigma 3-16PK centrifuge (Sigma-Aldrich, USA), washed twice by resuspending the cell pellet in 5 ml sterile Milli-Q H₂O and diluted to an OD600 of 1 in sterile Milli-Q H₂O. Once at OD600 1, yeast cells expressing chickpea transporters in the mutant and parental strains could be characterised on solid streak plate assays (2.7.4), serial dilution spot assays (2.7.5) or liquid growth assays (2.7.6).

2.7.4 Streak plate assay of the amino acid knockout *S. cerevisiae* strain

Basic *S. cerevisiae* streak plate assays conducted by streaking single colonies of bulked up cells (2.7.3) onto solid YNB media (pH 6.2) with 2% (w/v) D-glucose for pDR196 (or D-galactose for pYES-DEST52), 50 mM citric acid, 2% agar and supplemented with 1, 3 or 6 mM individual amino acids as the sole nitrogen source. Plates incubated at 30°C for ~5-7 days.

2.7.5 Spot plate assay of the amino acid knockout *S. cerevisiae* strain

Overnight cultures grown in liquid YNB (pH 6.2) with 2% (w/v) D-glucose, 50 mM citric acid, and 0.192% (w/v) Yeast Synthetic Drop-out Medium minus Uracil (Sigma, USA) were pelleted at 3000 g and washed twice with sterile Milli-Q H₂O and diluted to OD600 of 1. Cells then plated as 10-fold 5 µl serial dilutions to 10⁻⁴ on solid YNB (pH 6.2) with 2% (w/v) D-glucose, 50 mM citric acid, 2% agar, supplemented with an amino acid at varying concentrations as the sole nitrogen source. Plates incubated at 30°C for 5-7 days.

2.7.6 Liquid growth assay of the amino acid knockout *S. cerevisiae* strain

Cell cultures of the mutant *S. cerevisiae* expressing chickpea transporters prepared as above (2.7.3) to an OD600 of 1. Amino acid stocks of 1, 3 or 6 mM concentration were made in liquid YNB (pH 6.2) media with 2% (w/v) D-glucose, 50 mM citric acid and setup in a 96-well microplate (Costar 96, Sigma, USA) at a 1:10 dilution of YNB + amino acid, and yeast culture, respectively (180 µl : 20 µl). Microplate typically setup with triplicate wells for each mutant strain expressing a chickpea transporter for each amino acid concentration. A positive nitrogen control as (NH₄)₂SO₄, empty vector control and YNB blank in triplicates was also used. Liquid assays conducted using a SPECTROstar Nano BMG microplate reader (BMG LABTECH, Australia) measuring at OD600 with shaking between readings at 30°C, taking data

readings every 15 mins for 48-hours. Relative growth rates were calculated by normalising the linear growth rate against the growth rate of the empty vector expressing 22Δ10AA strain.

3 Nitrogen Metabolism, Amide and Ureide Biosynthesis in Chickpea

Chapter 3: Introduction

3.1 Legume Classification

Legumes are typically classed under two categories, amide or ureide producing, encompassing temperate and subtropical legumes, respectively. Chickpea grown predominately in temperate and semiarid climates may initially show amidic properties (Rachwa-Rosiak et al., 2015). This classification also takes into consideration nodule morphology, whereby determinate nodules of subtropical legumes are indicative of ureide biosynthesis (Pate et al., 1980). Nod factor signalling gives rise to alternative differentiation of cortical root cells, resulting in either spherical nodule morphology as determinate nodule development, compared to persistent meristematic elongation known as indeterminate nodules (Ferguson et al., 2010, Udvardi & Poole 2013). However, there is an exception to the rule of tropical legumes producing determinate nodules: *L. japonicus* is a temperate legume but possesses determinate type nodules (Pacios-Bras et al., 2003). Indeed, the paradigm where all tropical legumes exhibit determinate nodules for ureide biosynthesis, but not all determinate nodules are necessarily from tropical or subtropical legumes, applies here. As such chickpea being a temperate legume is not in itself evidence for both indeterminate nodules and amide biosynthesis and the primary products from N₂ fixation in chickpea is unclear. Consequently, further analysis is needed.

3.1.1 Distinguishing between ureide and amide producing legumes

As discussed previously in the introduction to this thesis, chickpea has received little attention in the literature regarding the fundamental aspects of N₂ fixation, such as basic nodule morphology, whether ammonium is converted predominately into amides or ureides, and the transporters involved in fixed N export out of the nodules. Following symbiotic nitrogen fixation in bacteroids, legumes prioritise either the biosynthesis of the amides glutamine (Gln) & asparagine (Asn) or ureides allantoin & allantoic acid as the predominant form of fixed N to be exported from the nodule. These two distinctions are not always clear, with the two amides having been detected at varying levels within ureidic legumes, particularly Asn in nodule root and leaf tissues (Suliman et al., 2010, Berry et al., 2011). For example, in *G. max* & *L. japonicus* nodules, Asn can make up as much as 32% & 63%, respectively of the total amino acid pool (Harrison et al., 2003, Ramos et al., 2005). The abundance of Gln in ureidic legumes is usually much less significant, presumably because Gln is the precursor to ureide biosynthesis and is sequestered predominately for that purpose.

Because ureidic legumes also synthesise amides, expression of genes involved in the glutamine oxoglutarate aminotransferase (GOGAT) cycle involving ammonium conversion into Gln and/or Glu, as well as asparagine synthase (AS) to yield Asn, is not enough in itself to distinguish between an amidic and ureidic legume. Ureide biosynthesis, however, typically occurs at a significantly reduced rate in amidic legume nodules (Cheng et al., 1999, Cheng et al., 2000). As such, Pur1, the first enzymatic step of the purine synthesis pathway, is a likely regulatory step prior to ureide biosynthesis (Kim et al., 1995, Smith & Atkins 2002). In addition, ureide whole plant transport is believed to be mediated via a single transporter, UPS1, compared to a multitude of likely amino acid transporters (Lescano et al., 2016, Lu et al., 2022). Gene expression of both the enzymatic steps involved in ureide biosynthesis and transport during N₂ fixation may provide additional insight into what N products predominate in chickpea nodules.

Chapter 3: Aims

This section aims to provide evidence to ascertain conclusively whether chickpea should be classified as an amidic or ureidic legume. As such the following questions will be answered. (1) Do chickpea exhibit determinate or indeterminate type nodules. (2) What is the expression profile of genes involved in N₂ fixation, ureide & amide biosynthesis. (3) Is the level of nodule ureides similar or dissimilar to that of *G. max*, a common ureide producing legume. It is hypothesised that chickpea can be classed as an amidic legume possessing indeterminate nodules with insignificant ureide biosynthesis.

These questions were answered by performing chickpea and soybean (*G. max*) growth experiments in sand (General Methods: 2.2) to control the amount of nitrogen availability to promote symbiotic nitrogen fixation. Using this system nodule morphology could be observed, and subsequently the nodules were harvested to both synthesise cDNA for qRT-PCR and perform ureide quantification (General Methods: 2.4) via a colorimetric assay (Collier & Tegeder 2012).

Chapter 3: Results

3.2 Nitrogen Growth Experiments

Chickpea and *G. max* plants were grown in washed quarry sand supplemented with KNO_3 as the sole nitrogen source at a concentration of 0.5 mM to promote symbiotic nitrogen fixation and nodule formation (General Methods: 2.2). Higher nitrogen conditions were applied at a concentration of 5 mM KNO_3 . Sufficient nitrogen availability inhibits the establishment of nodules, since the plant has no need to invest in nodule development. The purpose of providing high nitrogen growing conditions was to determine if there are any growth deficiencies associated with the low nitrogen nodulating plants, or if ureide production occurs in the absence of nodulation under high N availability.

Growth experiments were typically performed up to 35 DAI (Days After Inoculation) and harvested at 5-day intervals to capture nodule development and the establishment of N_2 fixation for ureide quantification and gene expression analysis. *G. max* was grown in conjunction with chickpea as a ureide producer and determinate type nodule control.

3.2.1 Chickpea nodules exhibit indeterminate type morphology

Chickpea plants grown in sand supplemented with low (0.5 mM KNO_3) availability displayed characteristics of indeterminate nodule morphology (Figure 3.1). Symbiotic nitrogen fixation appeared to begin at 15 DAI when nodules were first observed in both chickpea and *G. max* (Figure 3.1). Nodules harvested from 25 DAI began clumping together with the initiation of meristematic elongation (Figure 3.1). At 30 - 35 DAI, harvested chickpea nodules displayed clear indeterminate nodule elongation morphology, whereby nodule appeared to display an expanding cylindrical structure. In comparison, *G. max* nodules maintained a spherical structure, indicative of determinate nodules, at all harvest time points (Figure 3.1).

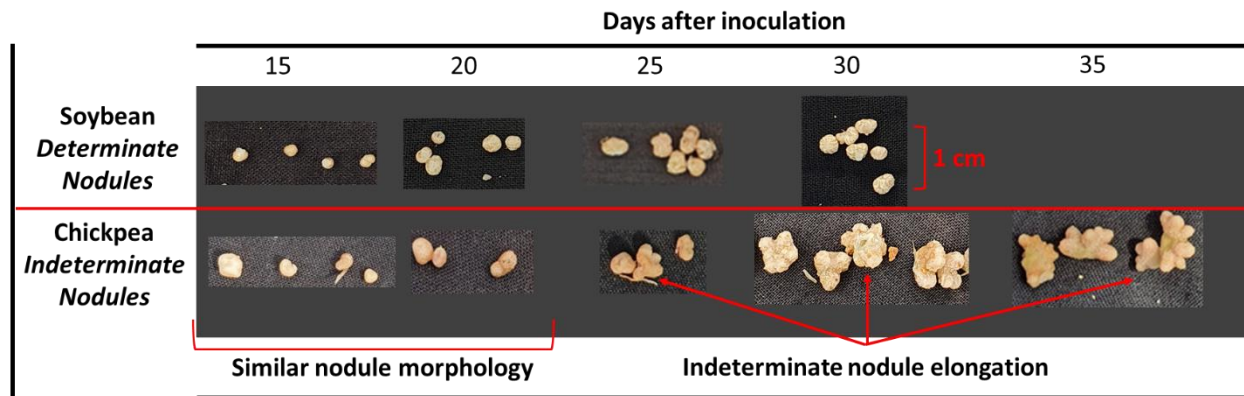


Figure 3.1: Chickpea nodules display nodule meristem elongation, indicative of indeterminate nodule morphology.

Chickpea & soybean grown in washed quarry sand, inoculated with rhizobia at sowing and grown with low nitrogen (0.5 mM KNO₃) supplemented with McKnight's nutrient solution. Nodules harvested at 5-day intervals from 15 to 35 DAI.

3.2.2 Chickpea nitrogen supplementation time course

Chickpea grown in sand supplemented with low N (0.5 mM KNO₃) and watered with McKnight's nutrient solution exhibited no signs of sand growth related stress over a 10 to 35 DAI time course (Figure 3.2). The McKnight's nutrient solution supplemented with 0.5 mM KNO₃ was sufficient to promote normal growth conditions in the absence of soil. Efficient nodulation was also observed with nodules developing at approximately 15-20 DAI and continuing to develop until 35 DAI (Figure 3.3). Nodules appeared to be healthy and fixing nitrogen as indicated by the presence of pink leghemoglobin in bisected nodules (Figure 3.3). The onset of leghemoglobin senescence appeared at approximately 35 DAI visualised by a green pigment forming in nodule bisections. This may indicate a short and rapid period of initial nitrogen fixation in young vegetative stage chickpea plants. Rapid senescence of nodules may also occur because of the indeterminate type morphology, whereby there is a rapid turnover of mature nodules. For example, there appears to be elongation of the meristem as the nodule matures, followed by senescence making way for young nodules. At the 35 DAI time point harvested nodules were observed at varying levels of developmental stages from early development to elongated and senescing (Figure 3.3).

Chickpea grown in sand supplemented with high N availability (5 mM KNO₃) showed no visible signs of stress over 5-day harvest intervals from 10 to 30 DAI (Figure 3.4). When grown in sand with abundant N levels, there were no signs of nodulation present at any harvest, due to high N related nodulation

inhibition. Despite this these plants appeared healthy, similar to that of the low N nodulating plants, indicating no N related stress when nodules are present (Figure 3.2, 3.4).



Figure 3.2: Chickpea harvest time course panel grown in sand with low N availability (0.5 mM KNO₃) and inoculated with rhizobia.

Chickpea grown in washed quarry sand and inoculated with rhizobia at sowing. Grown with low nitrogen (0.5 mM KNO₃) supplemented with McKnight's nutrient solution. Grown under ambient lighting in greenhouse conditions (~20-25°C during the day). Plants harvested (N = 3) at 5-day intervals (10 DAI - 35 DAI).

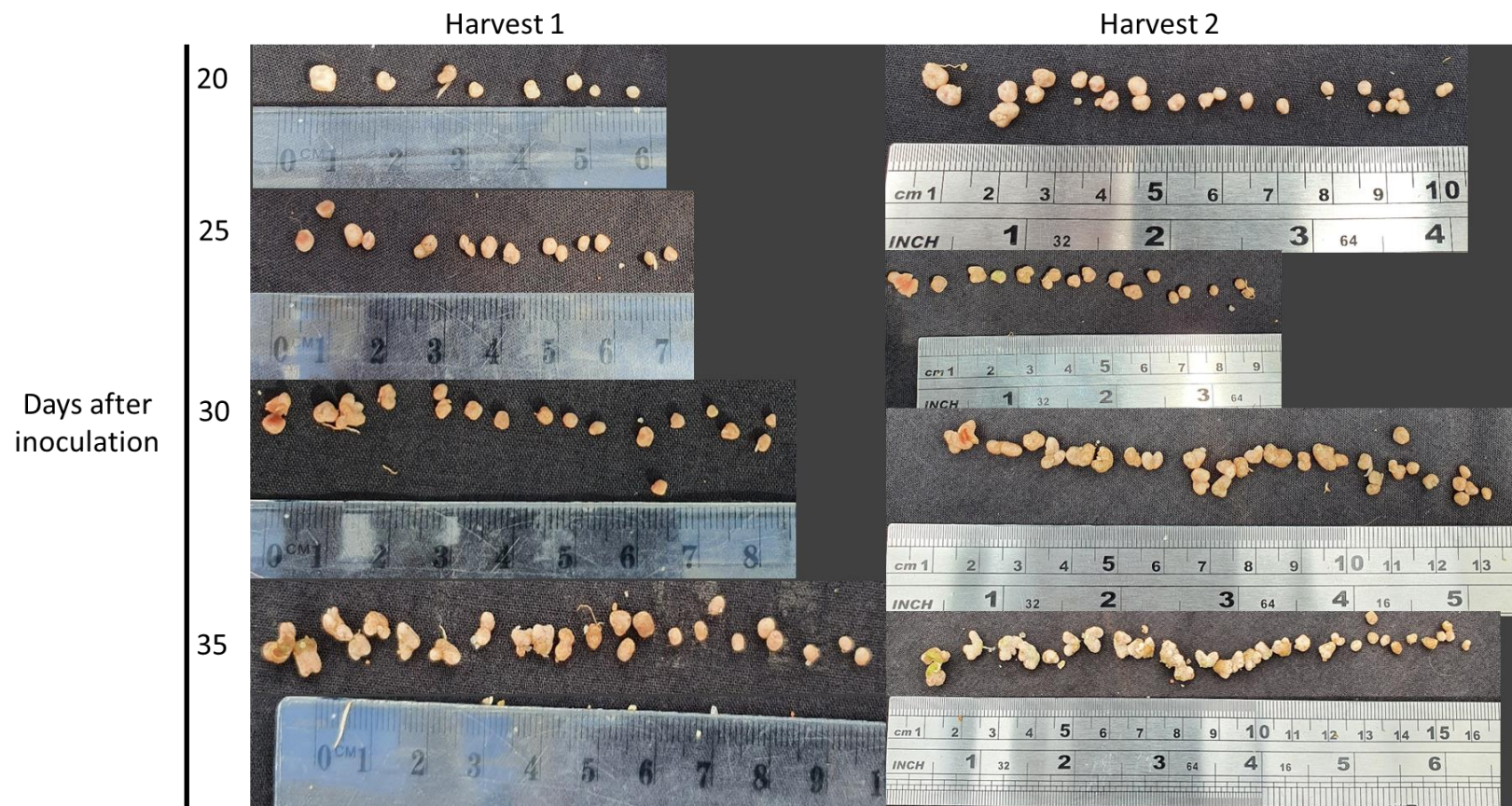


Figure 3.3: Nodule development profile in chickpea shows a rapid senescence of nodules between 20 and 35 DAI when grown in sand supplemented with low nitrogen availability (0.5 mM KNO_3).

Image displays a representative spread of nodule and does not include the total number of nodules from each harvest. N = 3 for both harvests at 5-day intervals from 20 to 35 DAI.

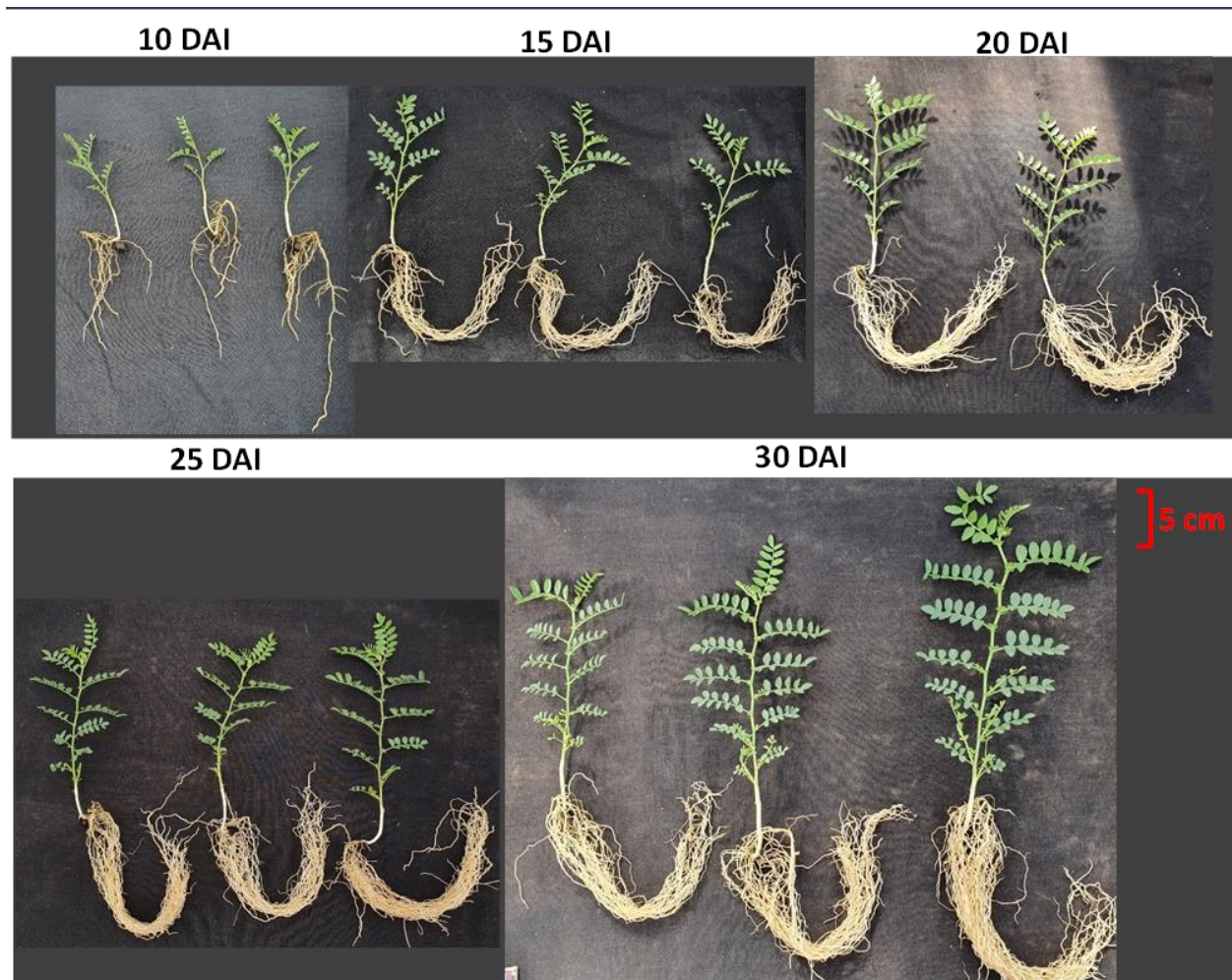


Figure 3.4: Chickpea harvest time course panel grown in sand with high N availability (5 mM KNO₃) and inoculated with rhizobia.

Chickpea grown in washed quarry sand and inoculated with rhizobia at sowing. Grown with high nitrogen (5 mM KNO₃) supplemented with McKnight's nutrient solution. Grown under ambient lighting in greenhouse conditions (~20-25°C during the day). Plants harvested (N = 3) at 5-day intervals (10 DAI - 30 DAI).

Chickpea plants were also supplemented with both high and low N without inoculation with rhizobia (Figure 3.5, 3.6). A combination of low N availability and the absence of nodulation appeared to cause a minor stress phenotype at 25 DAI (Figure 3.5). Stress was observed as reddening of the stem and the outside borders of leaflets, likely anthocyanin pigment accumulation (Figure 3.5). This stress phenotype was likely attributed to low N availability in the absence of nodules to facilitate effective vegetative growth in the already harsh conditions of sand as opposed to soil. This stress was prevented under low N when nodules provided the required N demand of the growing plant (Figure 3.2).

No initiation of a stress response was observed when rhizobia were withheld from plants grown in sand supplemented with high nitrogen availability (Figure 3.6). This outcome, as expected, was the same as the plants mentioned above with rhizobia supplemented with high nitrogen, where nodulation was inhibited (Figure 3.4). Under 5 mM KNO_3 , chickpea could efficiently establish vegetative growth in sand without the need of additional N supplied via N_2 fixation.

In comparison to sand growth, chickpea grown in soil under the same growth conditions did appear to have more expansive and healthy-looking roots (Figure 3.7). Similarly at 25 DAI, soil grown plants appeared to have increased vegetative growth with more leaflets and secondary stem branching (Figure 3.8). Chickpea grown in sand does appear to exhibit minor growth deficiencies even when supplemented with appropriate nutrients via the McKnight's solution and N supplemented as KNO_3 .



Figure 3.5: Chickpea harvest time course panel grown in sand with low N availability (0.5 mM KNO₃) without rhizobia inoculation.

Chickpea grown in washed quarry sand and grown with low nitrogen (0.5 mM KNO₃) supplemented with McKnight's nutrient solution. Grown under ambient lighting in greenhouse conditions (~20-25°C during the day). Plants harvested (N = 3) at 5-day intervals (10 DAI - 25 DAI).



Figure 3.6: Chickpea harvest time course panel grown in sand with high N availability (5 mM KNO₃) without rhizobia inoculation.

Chickpea grown in washed quarry sand and grown with high nitrogen (5 mM KNO₃) supplemented with McKnight's nutrient solution. Grown under ambient lighting in greenhouse conditions (~20-25°C during the day). Plants harvested (N = 3) at 5-day intervals (10 DAI - 25 DAI).

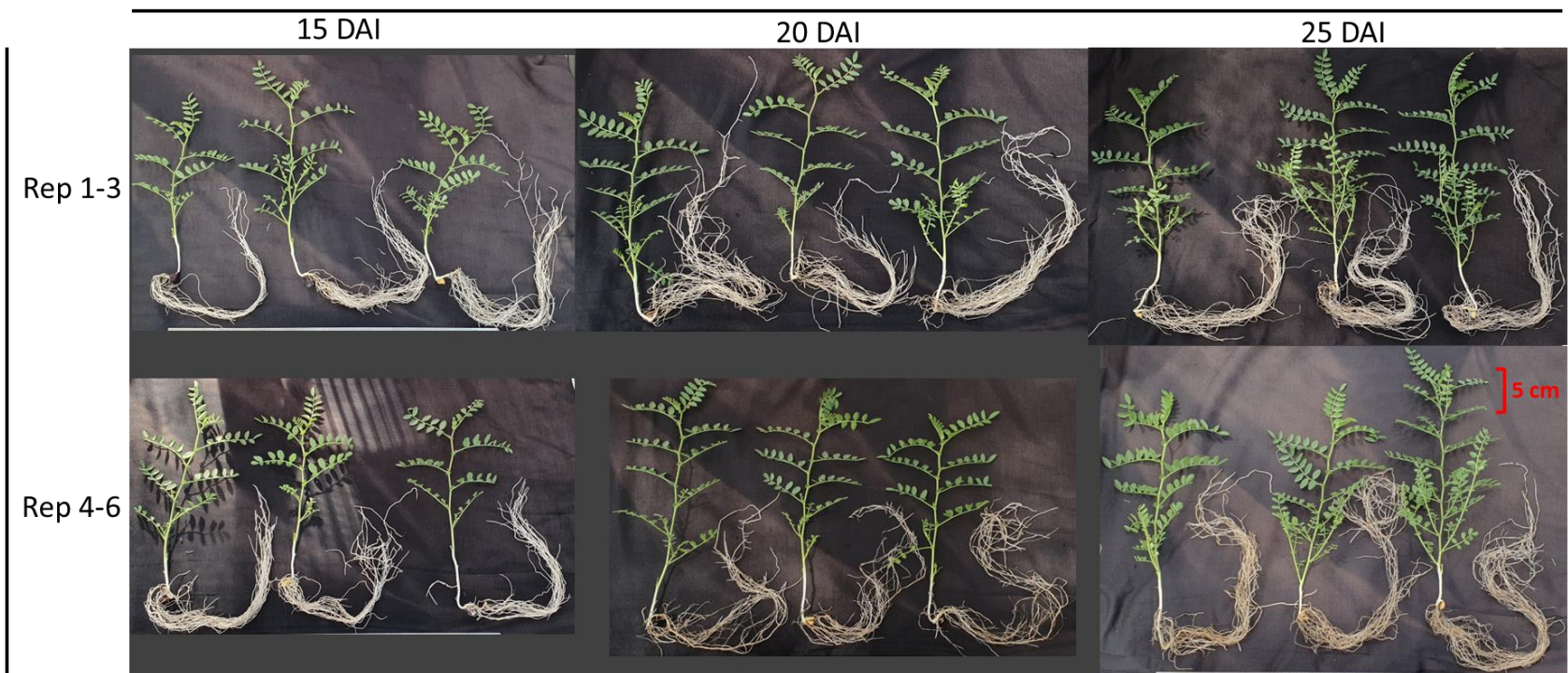


Figure 3.7: Chickpea harvest time course panel grown in BioGrow with rhizobia inoculation at sowing.

Chickpea grown in BioGrow soil supplemented with McKnight's nutrient solution. Grown under ambient lighting in greenhouse conditions (~20-25°C during the day). Plants harvested (N = 6) at 5-day intervals (10 DAI - 25 DAI).

Chickpea grown in sand under high or low N availability and with or without rhizobia saw no significant penalties in basic growth metrics (Figure 3.8). Even though the low N uninoculated plants showed visible stress, this did not cause any significant deviations in plant height, root length or leaf number (Figure 3.8A-C). Notably as would be expected without inoculation and high nitrogen, only the low N inoculated plants developed nodules in sand (Figure 3.8D). The soil grown plants did produce some nodules, however very minor nodulation was observed due to an abundance of N in the BioGrow soil used. In addition, the soil grown plants began to exhibit an increased average root length and leaf number, though not statistically significant (Figure 3.8B, C). This was more apparent in dry weights between the low N inoculated sand plants compared to soil plants, where a significant growth penalty was measured at 35 DAI when grown in sand (Figure 3.9). This difference was attributed to increased root growth and an increase of stem branching in the soil grown plants.

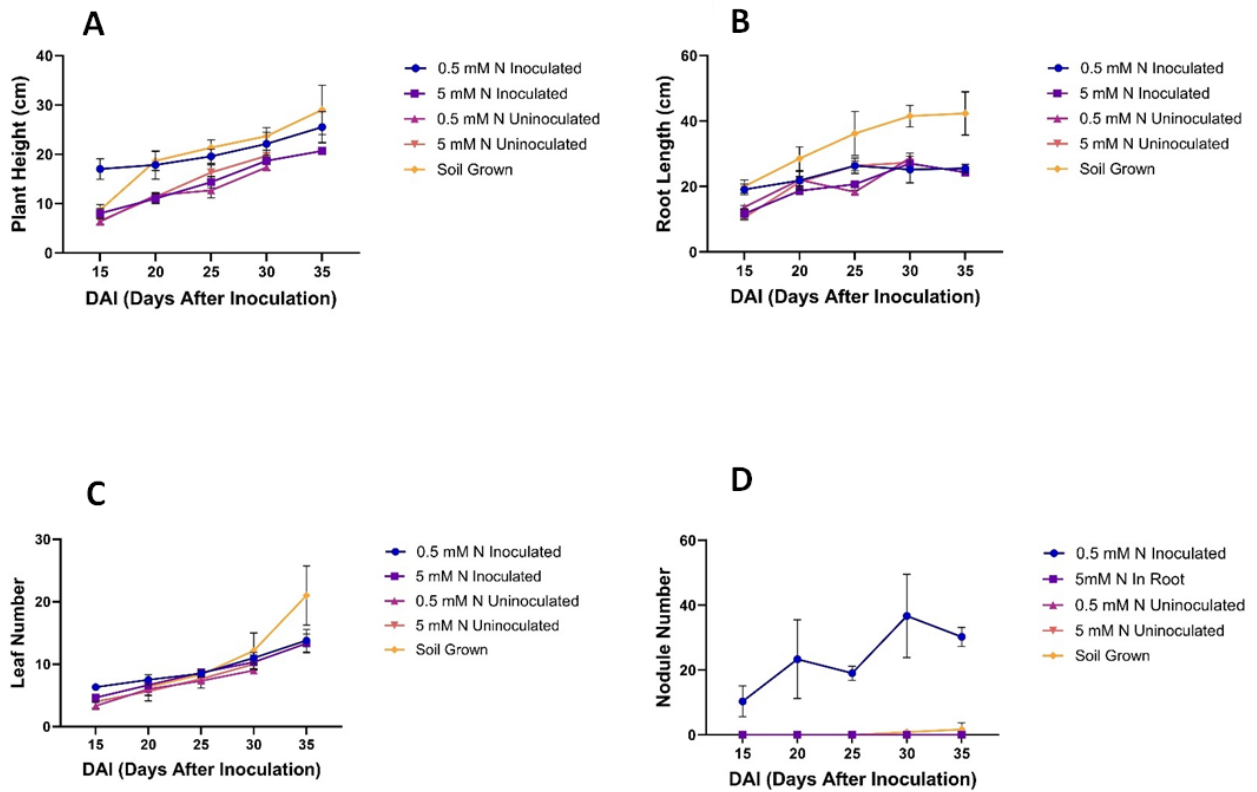


Figure 3.8: Chickpea harvests show no significant effect of low & high nitrogen availability and nodule development on basic growth metrics.

Chickpea harvested at 5-day intervals from 15 to 35 DAI to measure (A) plant height (cm), (B) root length (cm), (C) leaf number and (D) nodule number with respective standard deviation at each harvest point (N = 6). Chickpea grown in sand watered with McKnight's nutrient solution supplemented with low (0.5 mM) and high (5 mM) KNO_3 availability and grown with or without inoculum at sowing.

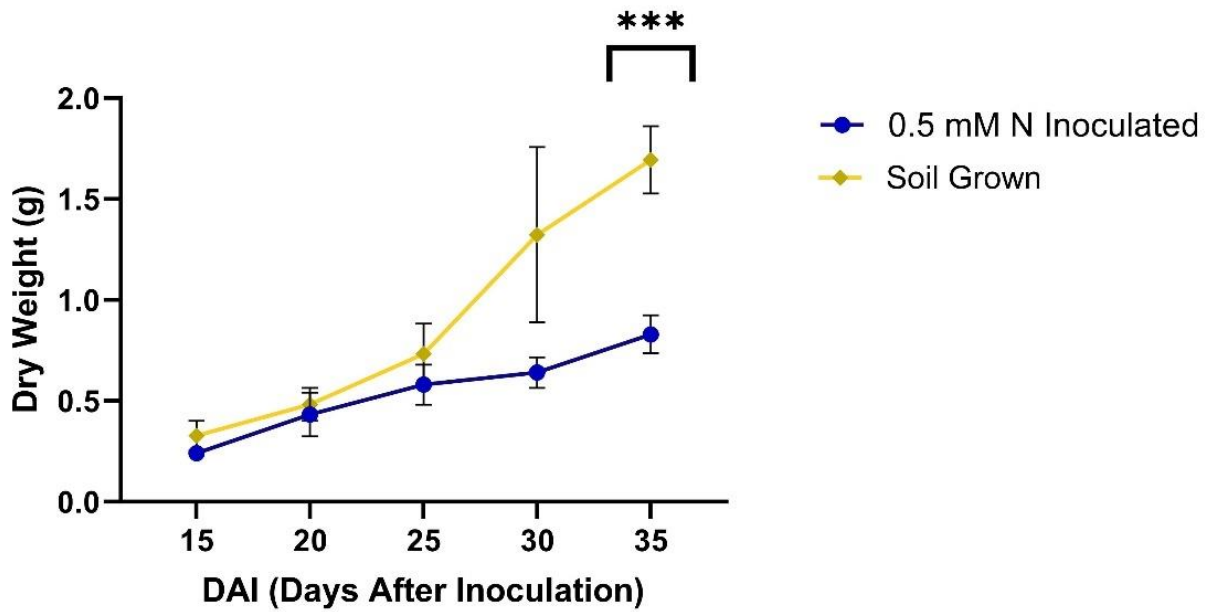


Figure 3.9: Chickpea grown symbiotically in sand exhibited significantly less dry weight at 35 DAI compared to chickpea grown in soil.

Chickpea grown in sand or soil watered with McKnight's nutrient solution supplemented with low (0.5 mM) KNO_3 availability and grown with inoculum at sowing. Tissue harvested at 5-day intervals ($N = 6$) from 15 – 35 DAI and dried in a 50°C oven for several days. Standard deviation depicted at each harvest timepoint and One-Way ANOVA ($* < 0.05$, $** < 0.005$, $*** < 0.0005$) performed to depict significant difference in dry weight between growth medium.

3.2.3 Chickpea experience rapid nodule senescence after the onset of nitrogen fixation

As observed above, chickpea appeared to exhibit rapid nodule senescence at 30-35 DAI (Figure 3.10E). As the plant develops through the vegetative stage, plant and nodule dry weight significantly increases (Figure 3.10A, C). The number of nodules also increases, however the count depicted in figure 10B does not consider nodule clumping where multiple nodules clump into one mass as they elongate. This makes accurate nodule counts ambiguous past 25 DAI but is reflected in the increasing nodule dry weight (Figure 3.10A). Despite the significant carbon sink associated with nodule development, leghemoglobin begins to senesce at 30 DAI by the appearance of an internal pink to green transition (Figure 3.10E). Nodule development is a significant energy and carbon intensive process, and this observation is a seemingly wasteful investment of the plant's resources.

Mean leghemoglobin gene expression from the pool of nodules per plant also reflects this, evidenced by a significant (p -value <0.05) reduction from 20 DAI to 25, 30 and 35 DAI (Figure 3.10D). This significant transcript reduction also coincides with the onset of nodule leghemoglobin senescence (Figure 3.10E). It could be assumed gene transcript is decreasing because the number of nodules is increasing, in turn generating a greater spread in the developmental stages of nodules harvested. However, this would presumably be reflected by a heightened expression level of leghemoglobin production to supplement the newly developing nodules. This result has also been corroborated in similar experiments where N_2 fixation rates significantly decreased at approximately 25 DAI in chickpea nodules using an acetylene reduction assay, which coincided with increasing nodule dry weight (Appendix 3A: Figure 3a.1).

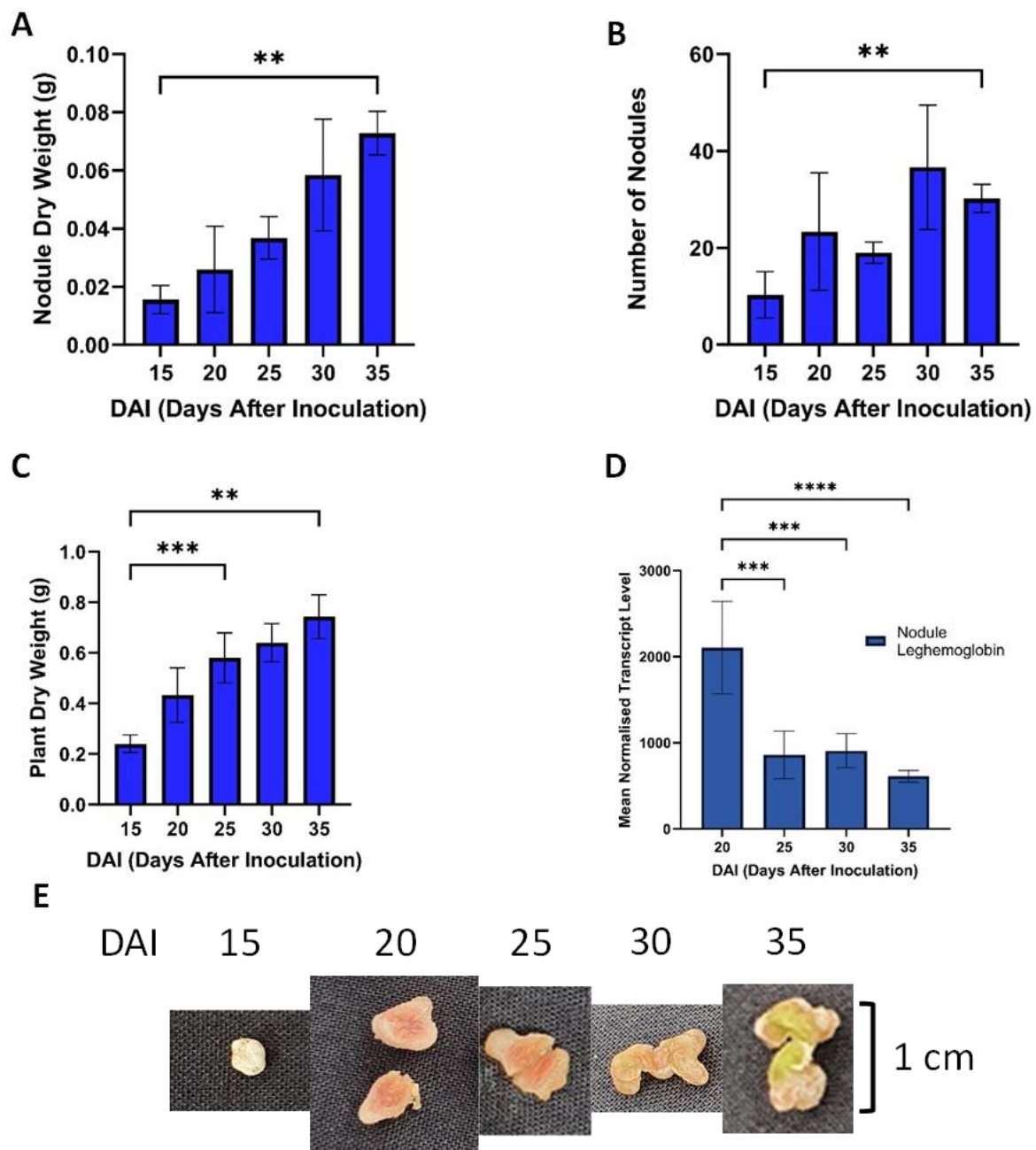


Figure 3.10: Chickpea invest in nodule development despite significantly reduced leghemoglobin expression and nodule senescence post 20 DAI.

Chickpea grown in sand and inoculated with rhizobia at sowing. Grown with low nitrogen (0.5 mM KNO_3) supplemented with McKnight's nutrient solution and provided ambient lighting in greenhouse conditions ($\sim 20\text{-}25^\circ\text{C}$ during the day). Plant tissue harvested (N = 6) at 5-day intervals (15 DAI-35 DAI) for nodule dry weights (A), number of nodules (B) and plant dry weight (C). All nodules from each plant were harvested to measure the reflective leghemoglobin expression at the given harvest window (D) with representative photos to observe leghemoglobin senescence (E). Error bars depicted as the standard deviation at each harvest timepoint. Leghemoglobin transcript data normalised against *CaEiF* and *CaHSP90*. Statistical significance calculated for plant growth metrics overtime and transcript level of leghemoglobin between harvest intervals via One-Way ANOVA with multiple comparisons test (Tukey) ($* < 0.05$, $** < 0.005$, $*** < 0.0005$).

3.3 Gene Expression Analysis of Nitrogen Fixation

To assist in addressing whether chickpea nodules synthesise ureides or amides, gene expression of several enzymes of the N₂ assimilation pathway and ureide biosynthesis was conducted. High transcript levels of genes which encode enzymes of amide biosynthesis does not necessarily indicate the absence of ureide production as described in the introduction above (3.1). However, significant transcript levels will indicate N₂ fixation is occurring, which can be compared to the expression levels of ureide biosynthesis genes during the same period. It is also important to note that nodules harvested for cDNA synthesis for qRT-PCR were a representative spread of the current developmental profile of nodules and not only mature nodules.

3.3.1 Nitrogen and amide metabolism gene expression in chickpea nodules

Mean normalised transcript levels of genes encoding enzymes of amide synthesis were highly expressed in chickpea nodules from 20 to 35 DAI (Figure 3.11A, B). Expression of the GS/GOGAT cycle (Glutamine synthetase/Glutamine oxoglutarate aminotransferase) where ammonium is assimilated into Gln and Glu was highly expressed from 20 to 35 DAI (Figure 3.11A). GOGAT mean normalised transcript level significantly increased from 20 to both 30 and 35 DAI (Figure 3.11A). Notably both enzymes showed the greatest mean transcript level at 30 & 35 DAI, which coincides with increasing nodule senescence in the mature nodules (Figure 3.10E).

The biosynthesis of Asn driven by AS (Asparagine synthase) requires both Gln yielded by the GOGAT cycle, and Asp synthesised via Asp-AT (Aspartate aminotransferase). Both AS & Asp-AT were significantly upregulated from 20 to 30 DAI and in addition Asp-AT expression significantly decreased from 25 to 35 DAI when nodules senescence was observed (Figure 3.11A). High gene expression of ASNase (Asparaginase), Ala-AT (Alanine aminotransferase), and moderate expression of Try-AT (Tyrosine aminotransferase) was not significantly different between time points (Figure 3.11A, B). Moderate expression of NR (Nitrate reductase) also significantly increased from 25 to 30 DAI, as nodule senescence was occurring (Figure 3.11B).

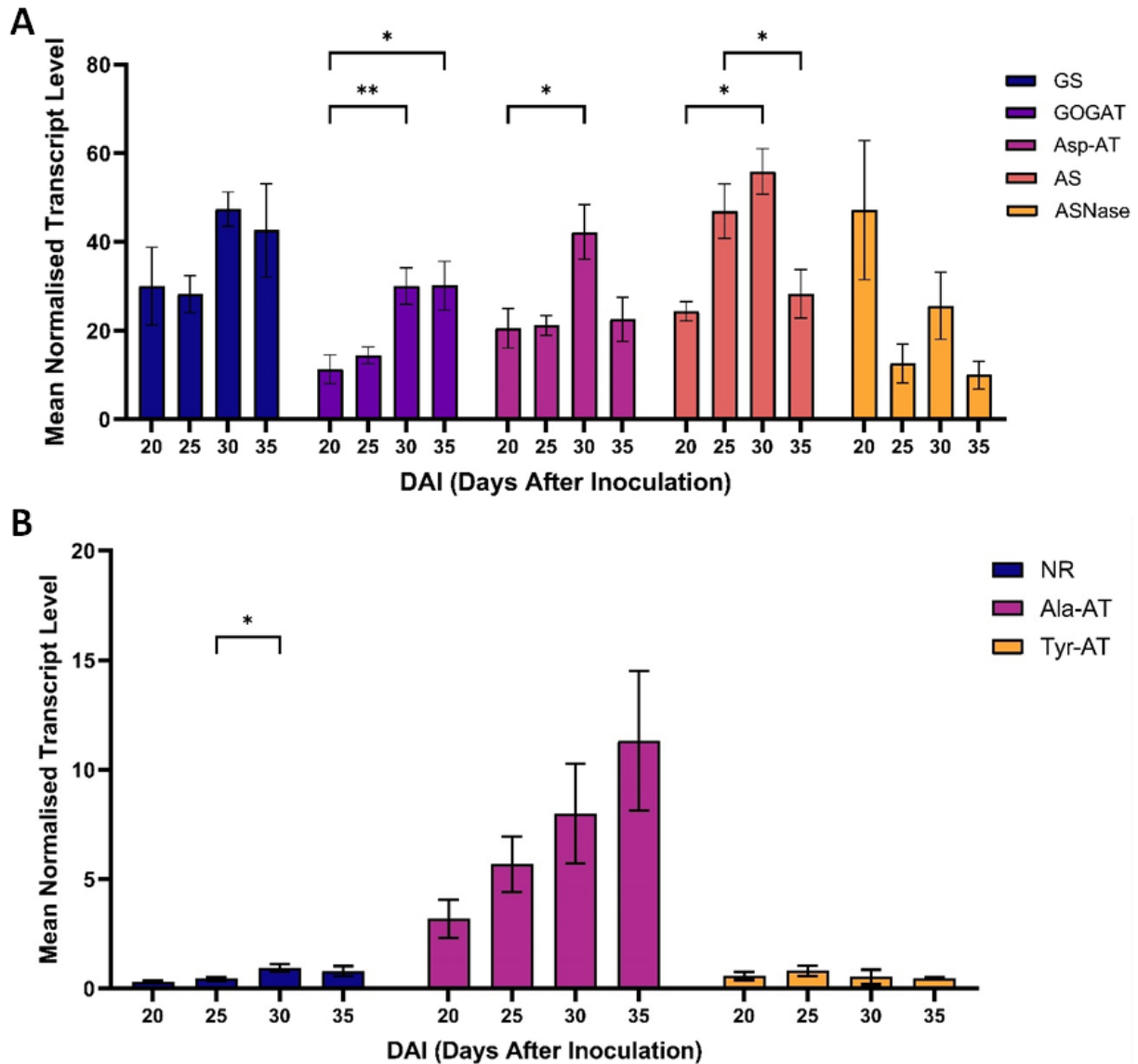


Figure 3.11: Genes involved in assimilation of ammonium to amino acids and synthesis of the amides Gln & Asn are highly expressed.

Transcript levels measured in nodule cDNA from 20 to 35 DAI in 5-day intervals and normalised against *CaEif* & *CaHSP90* (N = 3). Plants grown in sand supplemented with 0.5 mM KNO₃. Error bars depicted as the standard deviation at each harvest timepoint. Statistical significance calculated for transcript level of genes between harvest intervals via One-Way ANOVA with multiple comparisons test (Tukey) (*<0.05, **<0.005, ***<0.0005). GS: glutamine synthetase, GOGAT: glutamine oxoglutarate aminotransferase, Asp-AT: Aspartate aminotransferase, AS: Asparagine Synthase, ASNase: Asparaginase, NR: Nitrate reductase, Ala-AT: Alanine aminotransferase, Tyr-AT: Tyrosine aminotransferase.

3.3.2 Ureide biosynthesis gene expression in nodules

Chickpea nodules exhibited some gene expression of key ureide biosynthesis genes (Figure 3.12). UOX (Urate oxidase) and ALN (Allantoinase) involved in the biosynthesis of allantoin and allantoic acid, respectively were moderately expressed with an increasing mean normalized transcript level from 20 to 35 DAI (Figure 3.12). Mean transcript level of UOX also significantly increased from 20 to 30 DAI (Figure 3.12).

AAH (Allantoate amidohydrolase) which catalyses the catabolism of allantoic acid was only moderately expressed but significantly increased from 25 to 30 DAI (Figure 3.12). Possibly suggesting remobilisation of N during the onset of nodule senescence. HIU (5 Hydroxyisourate hydrolase) responsible for urate biosynthesis and XDH (Xanthine dehydrogenase) catalysing allantoin production were both insignificantly expressed at a negligible transcript level (Figure 3.12). Importantly, Pur1, a rate limiting step in the initiation of the purine synthesis pathway prior to ureide biosynthesis also exhibited insignificant negligible expression at all time points (Figure 3.12). In contrast, in *G. max*, a common ureide producer, *GmPur1* was highly expressed with a significantly elevated normalised transcript at 35 DAI from 20, 25 and 30 DAI (Figure 3.13). During the onset of N₂ fixation in *G. max* the purine synthesis pathway is upregulated over time presumably as the rate of N₂ fixation increases, which did not occur in chickpea nodules. *GmPur1* enzyme activity also appeared to be localised only in the nodules, as leaf and root transcript was insignificantly expressed overtime at a low level (Appendix 3A: Figure 3a.2) Similarly, *CaPur1* exhibited negligible transcript levels in both leaf and root tissue when plants were supplemented with high (5 mM KNO₃) and low (0.5 mM KNO₃) nitrogen growth conditions (Appendix 3A: Figure 3a.4). This may suggest chickpea do not perform purine biosynthesis in any plant tissue.

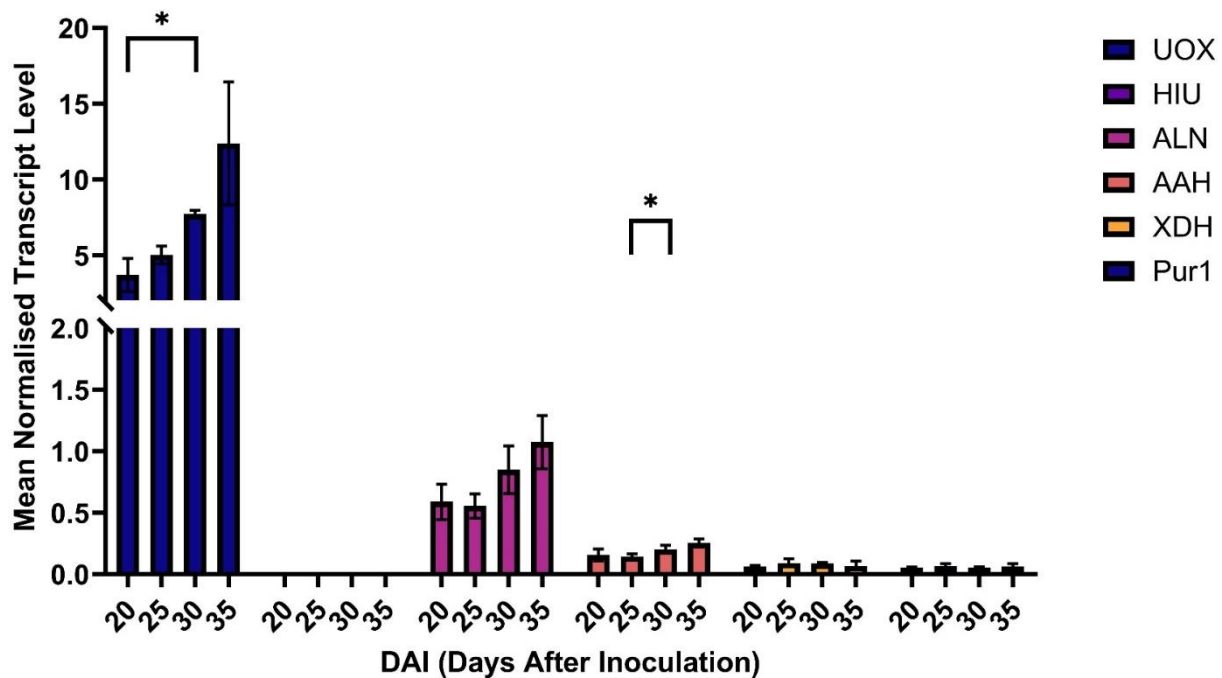


Figure 3.12: Chickpea nodules show mostly negligible expression of genes involved in ureide biosynthesis outside of moderate expression of urate oxidase (UOX) and allantoinase (ALN).

Transcript levels measured in nodule cDNA from 20 to 35 DAI in 5-day intervals and normalised against *CaEiF* & *CaHSP90* (N = 3). Plants grown in sand supplemented with 0.5 mM KNO₃. Error bars depicted as the standard deviation at each harvest timepoint. Statistical significance calculated for transcript level of genes between harvest intervals via One-Way ANOVA with multiple comparisons test (Tukey) (*<0.05, **<0.005, ***<0.0005). UOX: Urate oxidase, HIU: 5 Hydroxyisourate hydrolase, ALN: Allantoinase, AAH: Allantoate amidohydrolase, XDH: Xanthine dehydrogenase, Pur1: Amidophosphoribosyltransferase 1.

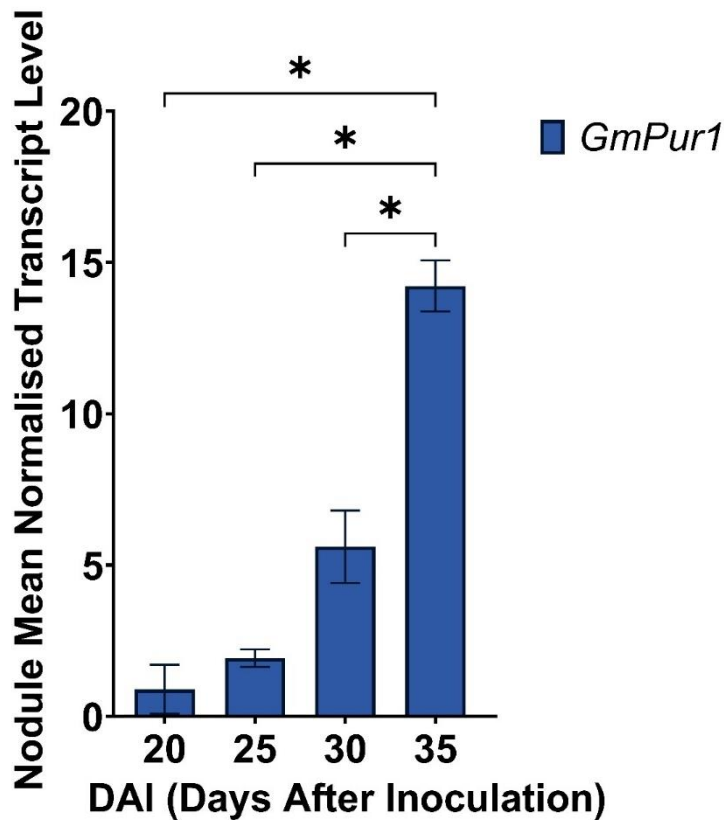


Figure 3.13: *GmPur1*, the first step of the ureide biosynthesis pathway is significantly upregulated in *G. max* nodules, as opposed to insignificant expression in chickpea nodules.

Transcript levels measured in nodule cDNA from 20 to 35 DAI in 5-day intervals and normalised against *GmELF1B* & *GmACT11* (N = 3). Plants grown in sand supplemented with 0.5 mM KNO₃. Error bars depicted as the standard deviation at each harvest timepoint. Statistical significance calculated for transcript level of *GmPur1* between harvest intervals via One-Way ANOVA with multiple comparisons test (Tukey) (*<0.05, **<0.005, ***<0.0005).

3.3.3 Fixed-N transporter gene expression in chickpea nodules

Transcripts of several known amino acid transporters, as well as ureide permease 1 (UPS1), were measured in chickpea nodules over 20 to 35 DAI to observe gene expression during the onset of N₂ fixation (Figure 3.14). Transporters of amino acids displayed moderate to high levels of expression, while the ureide transporter, UPS1, and amino acid permease 6 (AAP6), displayed a minor transcript level and did not significantly increase in expression across harvest time points (Figure 3.14). *GmUPS1* was also expressed at a low level in nodule, root and leaf tissue (Figure 3.15).

The amino acid transporters, amino acid vacuolar transporter 6A (AVT6A) and usually multiple acids move in and out transporter 20 (UmamiT20) both displayed a significant mean normalised transcript level increase from 20 to 30 and 35 DAI, respectively (Figure 3.14). In addition, AVT6A was highly expressed with a mean normalised transcript level above 20 compared to approximately 8 for the cationic amino acid transporter 1 (CAT1) and nitrate transporter 2 (NRT2) at 35 DAI (Figure 3.14).

UPS1 expression was notably absent compared to multiple amino acid transporters during a period of N₂ fixation, possibly indicating a lack of ureides to export from the nodules as evidenced by negligible *CaPur1* expression (Figure 3.14). However, the biosynthesis of allantoin and allantoic acid is probably still occurring, albeit at a low level after significantly increased expression of UOX and AAH (Figure 3.14).

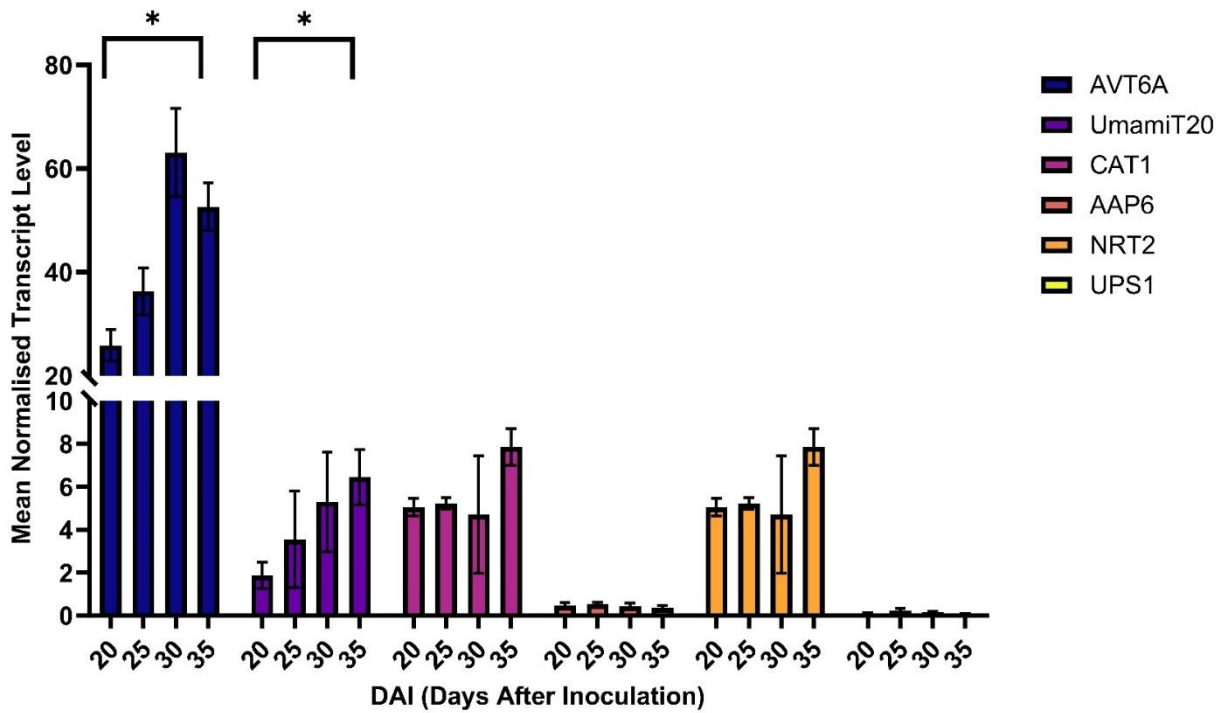


Figure 3.14: Chickpea nodules exhibited significantly elevated expression of amino acid transporters AVT6A & UmamiT20, compared to negligible expression of the ureide transporter UPS1.

Transcript levels measured in nodule cDNA from 20 to 35 DAI in 5-day intervals and normalised against *CaEiF* & *CaHSP90* (N = 3). Error bars depicted as the standard deviation at each harvest timepoint.

Statistical significance calculated for transcript level of genes between harvest intervals via One-Way ANOVA with multiple comparisons test (Tukey) (*<0.05, **<0.005, ***<0.0005). Plants grown in sand supplemented with 0.5 mM KNO₃. AVT6A: Amino acid vacuolar transporter, UmamiT20: Usually multiple acids move in and out transporter, CAT: Cationic amino acid transporter, AAP6: Amino acid permease, NRT2: Nitrate transporter, UPS1: Ureide permease.

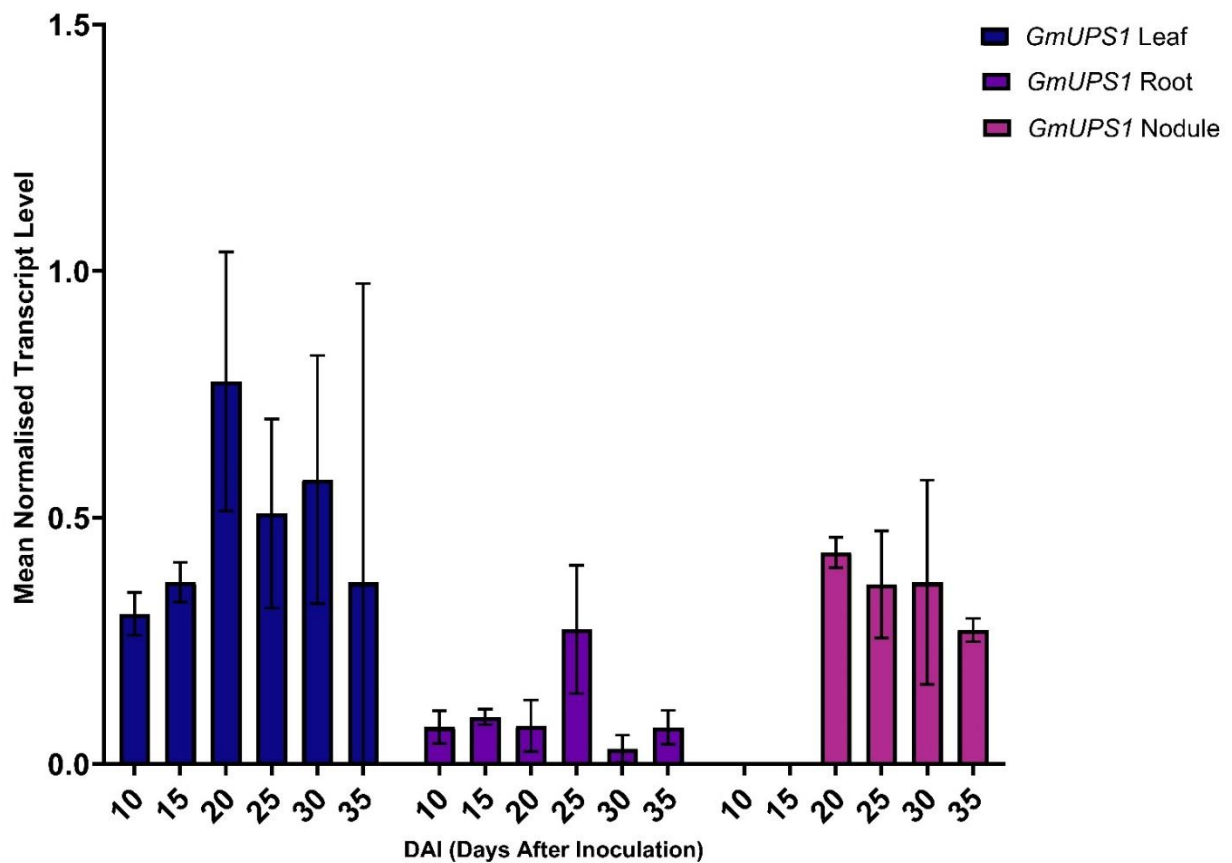


Figure 3.15: Ureide permease 1 (UPS1), was not significantly upregulated in *G. max* leaf, root and nodule tissues during N2 fixation.

Transcript levels measured in nodule cDNA from 20 to 35 DAI in 5-day intervals and normalised against *GmELF1B* & *GmACT11* (N = 3). Plants grown in sand supplemented with 0.5 mM KNO₃. Error bars depicted as the standard deviation at each harvest timepoint. Statistical significance calculated for transcript level of *GmUPS1* between harvest intervals via One-Way ANOVA with multiple comparisons test (Tukey) (*<0.05, **<0.005, ***<0.0005).

3.4 Ureide Quantification and Transport in N₂ Fixing Chickpea Nodules

To determine if ureide biosynthesis is occurring in chickpea, since significant expression of UOX and AAH in nodule tissue was observed, a colorimetric assay (General Methods: 2.4) was performed in nodule, leaf and root tissue to quantify total ureide levels. *G. max* tissue was also harvested to act as a ureide control. Both chickpea and *G. max* were grown under identical growth conditions (General Methods: 2.2) and harvested in 5-day intervals from 10 to 35 DAI.

3.4.1 Comparison of total ureide biosynthesis between chickpea and *G. max*

The mean level of total ureides (nmols/gm dry weight), which includes allantoin and allantoic acid, in *G. max* nodules was elevated compared with chickpea nodules at every time point from 20 to 35 DAI (Figure 3.16A, Appendix 3A: Table 3a.1). *G. max* total ureide levels were significantly elevated (p-value <0.005) at 30 (136.07 & 26.71) & 35 (144.19 & 13.21) DAI (Figure 3.16A, Appendix 3A: Table 3a.1). *G. max* also displayed an increasing level of ureides over time whereas chickpea total ureides increased up to 20 DAI then decreased thereafter (Figure 3.16A). This coincides with nodule senescence observed previously (Figure 3.10E).

Both chickpea and *G. max* nodules continued to develop over the 20 to 30 DAI growth period at a similar rate, with no significant difference in both nodule dry weight or nodule number at any time point (Figure 3.16B, C). This suggests both plants exhibited identical nodule development and presumably similar rates of N₂ fixation, during which the ureidic plant, *G. max* readily synthesized ureides unlike that of chickpea where levels remained low. The low total ureide level does explain the expression of the UOX and AAH enzymes measured in the qRT-PCR experiments, suggesting chickpea does synthesize ureides to some extent (Figure 3.12).

Ureide production in *G. max* appeared to also occur in root and leaf tissue, significantly elevated over that of chickpea at 10 & 15 DAI (Figure 3.17A, B, Table 3a.1). Interestingly, this period preceded nodule development, meaning ureide biosynthesis for N remobilization and storage occurs in other tissues in the absence of nodules in *G. max*, and chickpea to a lesser extent. It also appears that ureides synthesized in the nodules during this period are not exported to the root or leaf tissue, particularly in *G. max* as the total ureide levels in these tissues decreases overtime. Perhaps nodule synthesized ureides are stored in the nodules during this period before remobilizing to other tissues to support increased vegetative growth or seed development. This may also explain why *GmUPS1* exhibited low transcript levels (Figure 3.15).

Alternatively, ureides may be rapidly metabolized to yield N to fuel vegetative growth during this period, seen as a linear increase in plant dry weight overtime (Figure 3.17C).

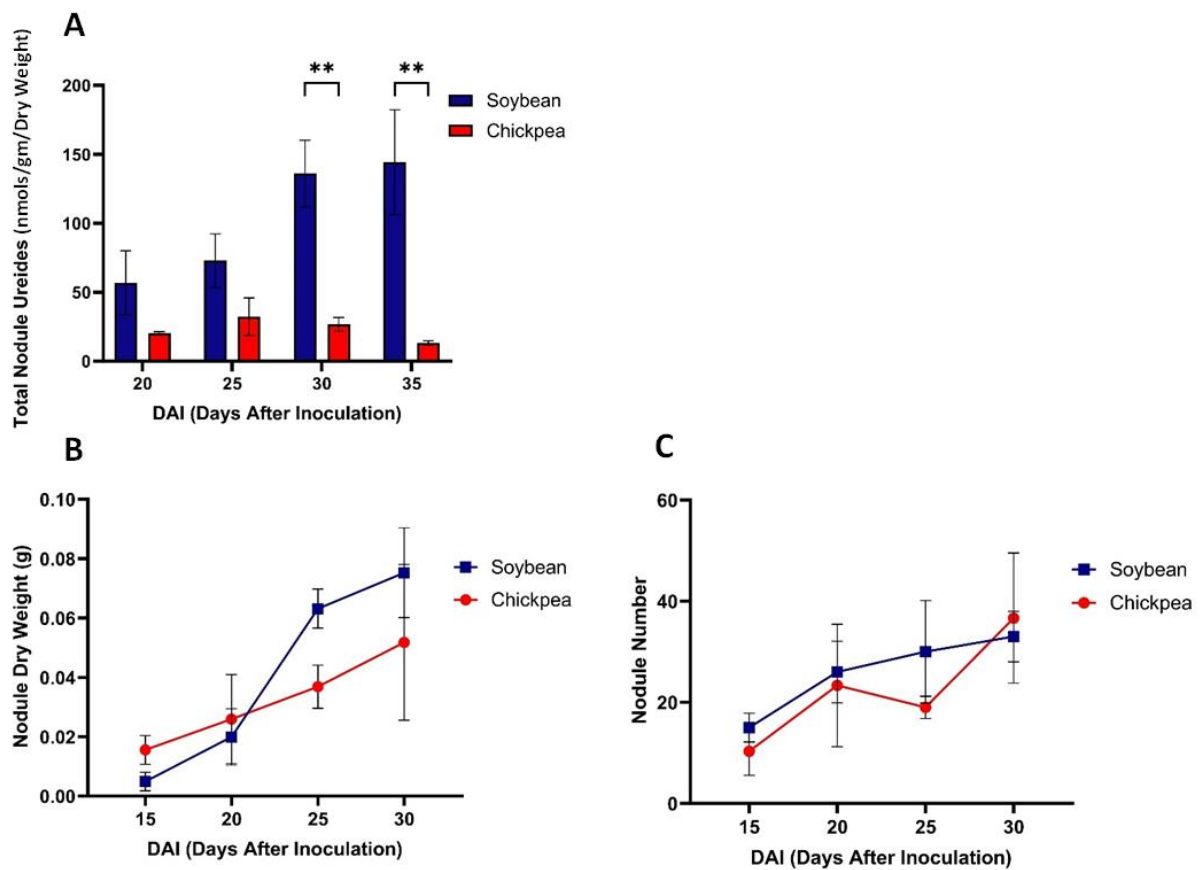


Figure 3.16: Ureide levels are significantly elevated in N_2 fixing nodules of *G. max* compared to chickpea.

(A) Total Ureides includes both Allantoin and Allantoic Acid, N = 6. (B) Mean nodule dry weight and (C) mean nodule number at each harvest period, N = 6. Plants grown in sand and inoculated at sowing, grown with low nitrogen (0.5 mM KNO_3) supplemented with McKnight's nutrient solution. Nodule tissue harvested in 5-day intervals (15 DAI - 35 DAI). Ureide assay adapted from Collier & Tegeder (2012). Statistical significance calculated for the difference in total ureide levels in chickpea and *G. max* nodules between harvest intervals via Two-Way ANOVA with multiple comparisons test (Tukey) (*<0.05, **<0.005, ***<0.0005).

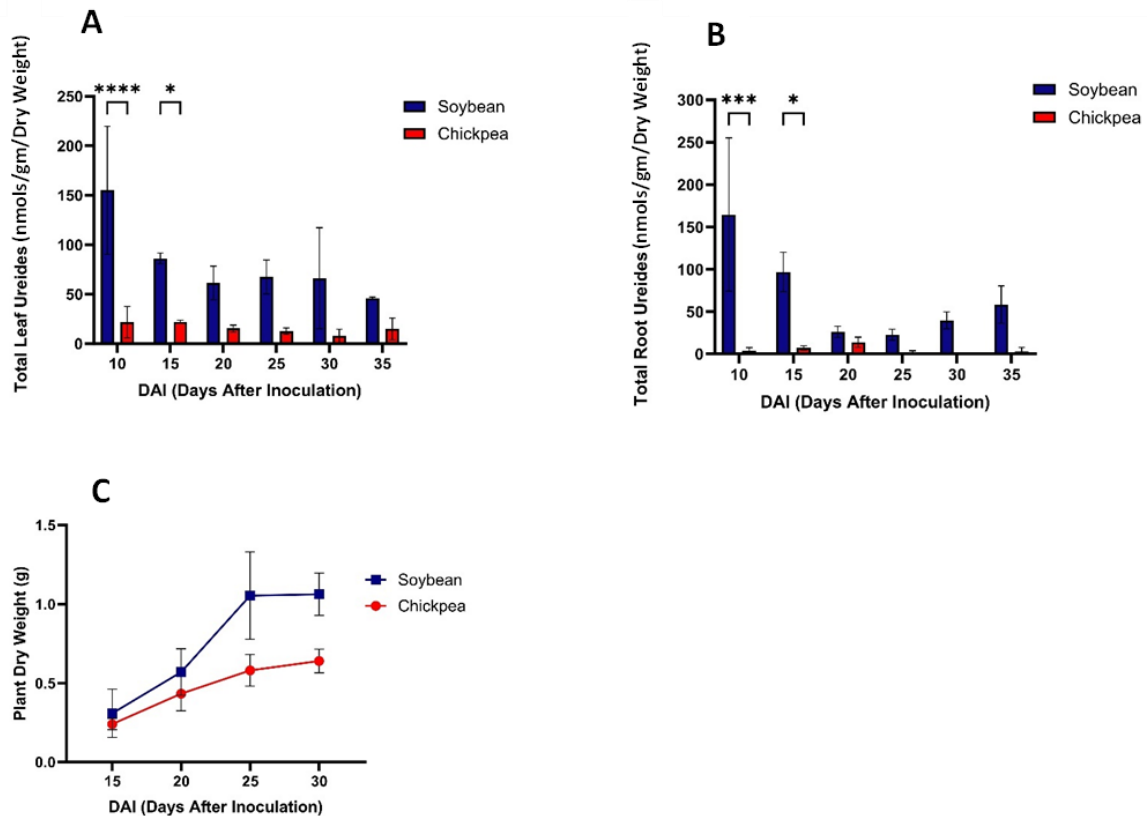


Figure 3.17: Ureide levels are significantly elevated in both leaf and root tissue in the ureide producer, *G. max* compared to the same tissues in chickpea.

Total Ureides includes both Allantoin and Allantoic Acid in (A) leaf and root (B) tissue, and compared against (C) plant dry wight, N = 6. Plants grown in sand and inoculated at sowing, grown with low nitrogen (0.5 mM KNO₃) supplemented with McKnight's nutrient solution. Leaf and root tissue harvested in 5-day intervals (10 DAI - 35 DAI). Ureide assay adapted from Collier & Tegeder (2012). Statistical significance calculated for the difference in total ureide levels in chickpea and *G. max* leaf and root tissue between harvest intervals via Two-Way ANOVA with multiple comparisons test (Tukey) (*<0.05, **<0.005, ***<0.0005).

3.4.2 The effect of nitrogen availability on ureide biosynthesis

Ureide levels were measured in leaf and root tissue after chickpea plants had been supplemented with high (5 mM KNO₃) or low (0.5 KNO₃) N availability. This was performed to determine if the plant switches to preferentially synthesise ureides when external N is abundant. Notably nodule data was not measured in high N plants, as high N levels in the external environment inhibited nodulation. Plants were also inoculated with or without rhizobia at sowing, but as mentioned this had no effect on nodulation in the high N plants. Hence, the only plants which nodulated were plants inoculated and supplemented with low N, identical to the previous experiments.

Plants supplemented with high N, with or without rhizobia had on average a greater abundance of total ureides in leaf and root tissue compared to the low N grown plants (Figure 3.18, 3.19). In leaf tissue of the high N inoculated and uninoculated plants the level of total ureides at 25 DAI (39.28 & 49.76 nmols/mg dw) was significantly greater than that of both low N inoculated or uninoculated plants (12.67 & 7.81 nmols/mg dw) (Figure 3.18, Appendix 3A: Table 3a.2). Similarly, the level of total ureides measured in root tissue of high N & inoculated plants was significantly greater than that of the low N & inoculated plants at 25, 30 and 35 DAI, and 25 DAI of the low N & uninoculated plants (Figure 3.19, Appendix 3A: Table 3a.2).

Transcript levels of UPS1 in these plants showed minor differences as a result of N availability (Appendix 3A: Figure 3a.3A). Leaf UPS1 from low N & inoculated plant tissue was significantly lower at 35 DAI compared to the high N uninoculated plants, however the transcript levels were near housekeeping gene levels (Appendix 3A: Figure 3a.3A). No significant difference was measured in root tissue for UPS1 (Appendix 3A: Figure 3a.3B). Pur1 expression in leaf tissue of low N inoculated plants exhibited a significantly increased expression over all growth treatments at multiple time points, however at very low transcript level (Appendix 3A: Figure 3a.4A). Root expressed Pur1 was also elevated at 15 DAI compared to each growth treatment but at near housekeeping transcript level (Appendix 3A: Figure 3a.4B).

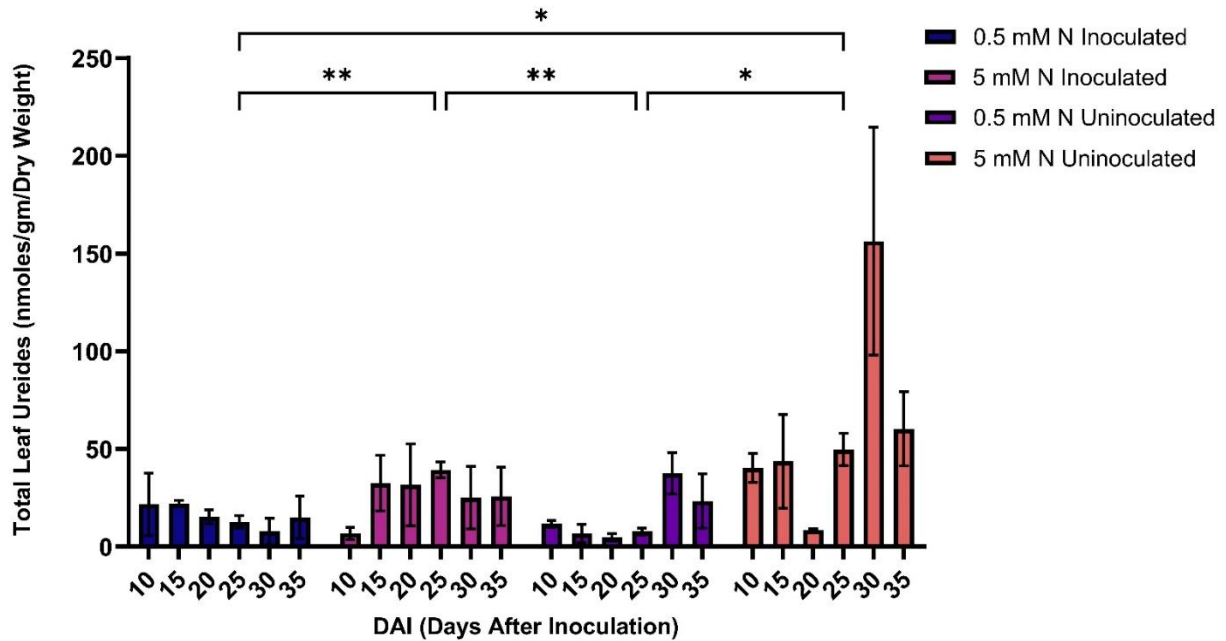


Figure 3.18: Ureide levels are significantly elevated with high nitrogen (5 mM KNO₃) availability in chickpea leaf tissue at 25 days after inoculation.

Total Ureides includes both Allantoin and Allantoic Acid, N = 3. Plants grown in sand and inoculated at sowing, grown with high nitrogen 5 mM KNO₃ supplemented with McKnight's nutrient solution. Leaf tissue harvested in 5-day intervals (10 DAI - 35 DAI). Tissue lyophilised for three days through freeze drying and ground into a fine powder prior to analysis. Ureide assay adapted from Collier & Tegeder (2012). Statistical significance calculated for the difference in total ureide levels in chickpea leaf tissue at individual timepoints between nitrogen growth and inoculation conditions via Two-Way ANOVA with multiple comparisons test (Tukey) (* < 0.05, ** < 0.005, *** < 0.0005).

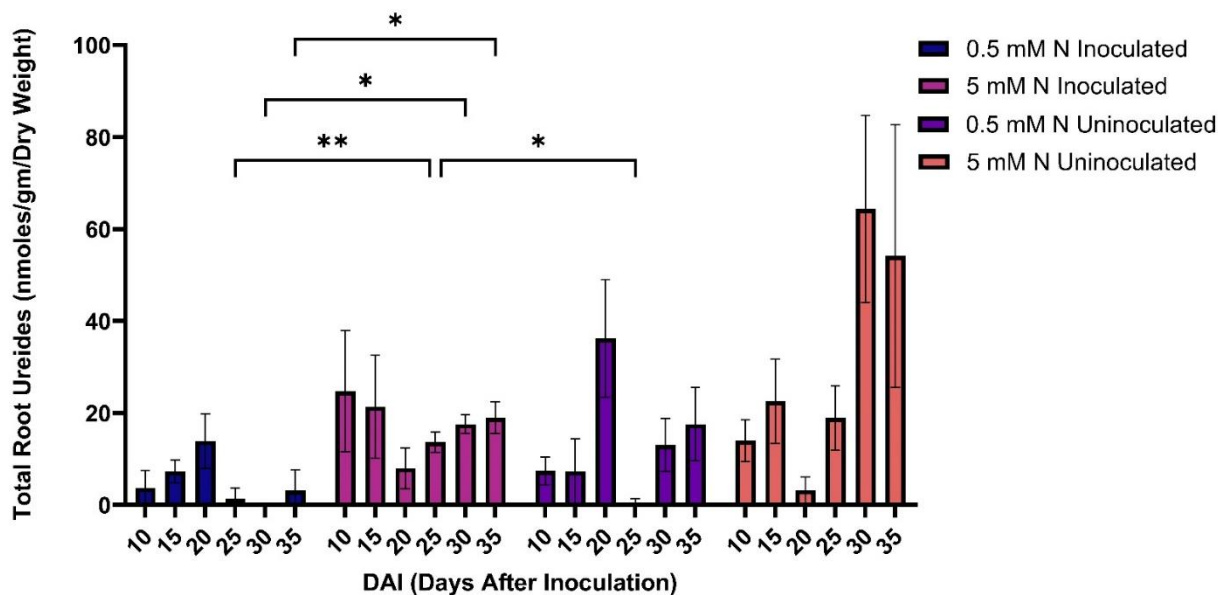


Figure 3.19: Root ureide levels are significantly elevated in inoculated chickpea grown with high nitrogen (5 mM KNO₃) availability.

Total Ureides includes both Allantoin and Allantoic Acid, N = 3. Plants grown in sand and inoculated at sowing, grown with high nitrogen 5 mM KNO₃ supplemented with McKnight's nutrient solution. Root tissue harvested in 5-day intervals (10 DAI - 35 DAI). Tissue lyophilised for three days through freeze drying and ground into a fine powder prior to analysis. Ureide assay adapted from Collier & Tegeder (2012). Statistical significance calculated for the difference in total ureide levels in chickpea root tissue at individual timepoints between nitrogen growth and inoculation conditions via Two-Way ANOVA with multiple comparisons test (Tukey) (*<0.05, **<0.005, ***<0.0005).

Chapter 3: Discussion

3.5 Limited Evidence for Ureide Biosynthesis in Chickpea Nodule

The data presented in this chapter provide convincing evidence that chickpea do not synthesize ureides predominantly in the nodules as a product of N_2 fixation. Gene expression was observed for UOX and ALN and minor expression for AAH, indicating some enzymatic activity of the ureide biosynthesis pathway. UOX is responsible for catalyzing the reaction of urate, the end product of the purine synthesis pathway to 5-hydroxyisourate in the peroxisomes of the uninfected cells and does not have any alternative functions, or any meaningful activity in other plant tissues (Werner et al., 2011). Urate does possibly exhibit a strong scavenging ability of ROS production which would occur from intensive mitochondrial activity in the nodules (Sautin & Johnson, 2008, Voß et al., 2022). The UOX protein has also been measured in the nodules of other amidic species such as *M. sativa*, albeit much lower than that of *G. max* (Cheng et al., 2000). This enzymatic step precedes the production of the ureide allantoin driven by HIU which exhibited virtually housekeeping expression levels in the nodules, whereas expression of ALN responsible for allantoinic acid synthesis may have been responsible for the measured ureides. Perhaps control of HIU expression is a regulatory step in amidic legumes preventing the production of allantoin which in turn limits the biosynthesis of allantoinic acid. The levels of total ureides measured compares to other amidic legumes, such as *M. sativa* and *L. japonicus*, where 0.05 & 0.06 mM, respectively, of total ureides was present in the xylem sap, in comparison to 4.82 mM in *G. max* (Cheng et al., 1999, Cheng et al., 2000).

Ureide biosynthesis in the form of allantoinic acid could be primarily used as another source of N to support nodule development. The catabolism of ureides yields glyoxylate, ammonium and urea via a several step enzymatic pathway (Voß et al., 2022). Beginning with the hydrolyzation of allantoin to S-ureidoglycine via AAH (Serventi et al., 2010), which exhibited minor expression in nodule tissue. It does however seem unusual that allantoinic acid would be synthesized for it to subsequently catabolized immediately after. Expression of the enzymes involved in both ureide biosynthesis and catabolism all increased on average from 20-35 DAI and may also be upregulated as a senescence response to remobilize as much N as possible. In saying this, ureide export from the nodule does not appear to be occurring due to essentially no expression of UPS1, the sole ureide transporter in legumes (Lescano et al., 2016, Lu et al., 2022). Total ureides in root and leaf tissue also did not reflect an increase that would be supplemented from nodule export. Unless exported ureides were immediately metabolized to yield N to support the growing plant. It would have been useful to measure whether allantoin or allantoinic acid was the predominant ureide in the nodules. Unfortunately, it was difficult to find a reliable and affordable source of allantoinic acid to use as a standard, hence the assay can only measure total ureides and cannot discern allantoinic acid from allantoin.

A greater abundance of allantoic acid would have matched the measured expression of the ureide biosynthesis pathway.

Insignificant expression of *Pur1* also implied a lack of ureide biosynthesis, whereby *GmPur1* has been suggested as a regulatory step and significantly upregulated in the presence of Gln (Kin et al., 1995). This was also observed here where *GmPur1* significantly increased overtime in nodule tissue, while *CaPur1* was unchanged, suggesting limited activity of the purine synthesis pathway. Hence it would appear that Gln produced from the GS/GOGAT pathway is used as an amide export product rather than metabolized for ureide biosynthesis. In addition, there was significantly increased expression of AVT6A and UmamiT20 transporters in chickpea nodules, known to be involved in amide transport (Sekito et al., 2014, Tone et al., 2015, Fujiki et al., 2017, Zhao et al., 2021, Garcia et al., 2023).

Conversely, genes involved in the production of amides were highly upregulated. GS, GOGAT and AS are responsible for the production of the amides Gln & Asn and displayed the highest mean normalized transcript level of the genes measured. High expression of these enzymes would not necessarily be indicative of an amidic legume, as Gln is the precursor to the purine synthesis pathway and Asn typically makes up a large portion of the amino acid pool in ureide producing legumes (Harrison et al., 2003, Ramos et al., 2005). A major distinguishing factor between an amidic and ureidic legumes appears to be the absence of ureide biosynthesis for amide species, whereas ureide species appear to synthesize both.

5.6 Experimental Limitations

The data in this chapter provides evidence that chickpea do not synthesise ureides at a notable level. An attempt to measure amide levels in chickpea nodules in collaboration with UWA, was thwarted by equipment failures, preventing the direct comparison of ureide and amide biosynthesis. It would be expected for *G. max* to still exhibit notable levels of Asn in the nodules which has been measured in the literature (Harrison et al., 2003, Ramos et al., 2005). However, a clear indication of high Gln and Asn levels compared to the negligible levels of total ureides would have greatly strengthened the conclusions stated below.

Many of the conclusions made here are based on qRT-PCR data of expression of enzymes involved in the ureide biosynthesis pathway or N metabolism. No protein data was obtained to back up transcript levels due to cost and availability of antibodies for western blot analysis. This would have been particularly useful to validate *CaPur1* and *CaUPS1* expression, as it is generally accepted that gene expression does not necessarily relate to translation of the respective protein. In saying this the lack of expression is in agreement with the total ureide quantification experiments.

Something that also needs to be addressed is the rapid senescence of nodules. It is possible that this is a symptom of growing in sand imposing a moderate stress causing a rapid turnover of nodules. Even though the plants were supplemented with an appropriate nutrient solution there was still a minor growth penalty compared to soil grown plants, particularly at 35 DAI. This unusual nodule senescence profile was also observed in similar growth experiments in sand conducted by Evgenia Ovchinnikova, Ella Brear and Brent Kaiser in 2017 (personal communication, Appendix 3A: Figure 3a.1). This identification of a brief window before senescence allowed critical timing for the RNA sequencing that is described in the following chapter.

Chapter 3: Conclusions

Quantitative RT-PCR of gene expression and ureide assays conducted on chickpea grown in sand supplemented with low nitrogen conditions to stimulate symbiotic nitrogen fixation, supported the hypothesis that chickpea grow indeterminate nodules. Genes encoding the enzymes urate oxidase and allantoinase displayed greater expression than what was expected, indicating minor ureide biosynthesis. Despite this, ureide levels were significantly reduced compared to *G. max*, a common ureide producer. In comparison, the GS/GOGAT cycle and asparagine synthase involved in amide biosynthesis were highly expressed in chickpea nodules over 20-35 DAI. It was also observed that chickpea nodules displayed a rapid onset of senescence from 30 DAI when grown in sand.

In summary, the experiments conducted here provide convincing evidence that chickpea exhibit characteristics of an amidic legume. Additional experiments are required to further confirm the evidence

here. If chickpea do predominantly synthesise amides, identifying key nodule localised transporters would be vitally important to further understand N₂ fixation in chickpea and to provide possible targets for genetic engineering studies.

4 Transcriptional Analysis of Nitrogen Fixation in Chickpea Nodules Using RNA Sequencing

Chapter 4: Introduction

4.1 Fixed Nitrogen Transport in Legumes

The transport of fixed Nitrogen in legumes has been largely examined in traditional legume species such as soybean (*Glycine max*) and pea (*Pisum sativum*) identifying key transporters involved. However, similar research in chickpea is lacking. It is unclear which genes are involved in nodule fixed nitrogen export and whole plant partitioning and whether chickpea follows the typical convention in other legumes where amino acids are predominately transported via amino acid permeases (AAPs) or if amino acid transport is facilitated by other transporter families. For example, studies have identified AAP6 to be a major player in amino acid transport through retrieval of nitrogen from the apoplasm into inner cortex cells for nodule export in pea, and likely function similarly in the phloem and xylem parenchyma cells in roots of soybean (Garneau et al., 2018, Liu et al., 2020). Additionally, AAP1, which functions in amino acid transport in the leaf phloem and cotyledon epidermal cells in pea, doesn't appear to be as important in soybean, further illustrating the importance of research to identify key transporters on a plant-by-plant basis (Lu et al., 2020, Grant et al., 2021).

Outside of the typical AAPs studied in traditional legumes, there are other large gene families involved in amino acid transport in plants, namely the amino acid/auxin permease (AAAP) family, major facilitator superfamily (MFS), ATP-binding cassette (ABC) and amino-polyamine-choline (APC) (Su et al., 2004, Swarup et al., 2004, Sekito et al., 2008). The complex nature of amino acid transport is further accentuated through smaller subfamily of transporters such as vacuolar amino acid transporters (AVTs) and vacuolar basic amino acid transporters (VBAs) from the AAAP and MFS family, respectively (Sekito et al., 2008). Importantly, AAPs fall under the AAAP family alongside the lysine/histidine transporter (LHT), proline transporter (ProT), γ -aminobutyric acid transporter (GAT), aromatic and neutral amino acid transporter (ANT) and auxin resistant (AUX) transporter subfamilies (Rentsch et al., 2007, Lee et al., 2007, Grallath et al., 2005, Meyer et al., 2006). The APC family consists of cationic amino acid transporters (CAT) that have been found to have possible similar amino acid transport properties as AAPs, through sequence similarity and observed function (Garneau et al., 2018). Notably, *PsCAT6* is believed to be involved in phloem loading of amino acids that are not substrates of *PsAAP1* (Zhang et al., 2015, Hammes et al., 2006). In summary, the amino acid transport network in legumes, particularly chickpea, is likely more complex and diversified than just the AAP transporters, outlying the importance of a total transcriptomic analysis approach such as the mRNA sequencing experiment conducted in this chapter.

4.1.1 Ureide transport network

The ureide transporter network in legumes is much simpler with only two known transporters from a single gene family - either UPS1 or UPS2, that are responsible for allantoin and allantoic acid transport in all plant tissues. Arabidopsis is known to have additional UPS transporters such as *AtUPS5*, believed to be of importance in salt stress tolerance, but UPS variants outside of UPS1/2 in legumes are uncommon (Lescano et al., 2016). Studies of UPS1 have found a multitude of functions for the one transporter, ranging from nodule and root export to phloem source to sink transport of ureides (Lu et al., 2022). Repression of this transporter in soybean inhibited N partitioning to root, shoots and led to accumulation of ureides in the nodules (Collier & Tegeder 2012). Compared to amino acid transport, there is convincing evidence to suggest UPS is the only transporter involved in ureide transport in legumes, allowing for a much simpler mechanism for genetic manipulation and subsequent increase in productivity of fixed nitrogen transport in the form of ureides (Pélissier et al., 2004, Collier & Tegeder, 2012, Carter & Tegeder, 2016).

4.1.2 Amino acid and amide synthesis

Irrespective of what form of fixed nitrogen is exported from the nodules, either amides or ureides, the initial metabolism is the same until the amide Gln is either exported or directed to the plastids of the infected cell to drive purine synthesis. Before this point symbiotic nitrogen fixation takes place in the bacteroid, as explained in more detail in chapter 1 (Introduction: 1.2), where NH_4^+ is exported from the symbiosome membrane of the bacteroid into the cytosol of the infected cell. NH_4^+ in higher plants is assimilated into Glu and/or Gln through the combined action of the GS/GOGAT cycle (Temple et al., 1998). Both enzymes of this pathway are independent of each other, whereby GS catalyses the ATP-dependent amination of Glu producing the amide Gln (Trepp et al., 1999). Conversely, GOGAT catalyses the production of Glu from a reductive transfer of the amido group from Gln to 2-oxoglutarate (Lea et al., 1990).

Gln and Glu can be further utilised by various aminotransferases to synthesise amino acids within the nodules. The synthesis of alanine is catalysed by the reversible action of alanine aminotransferase yielding alanine and 2-oxoglutarate from pyruvate and Glu (Rocha et al., 2010). Aspartate, another essential amino acid is also produced from Glu and oxaloacetate derived from the TCA cycle in infected cell mitochondria. This reaction to yield Asp is achieved through aspartate aminotransferase and as mentioned previously, also generates additional 2-oxoglutarate which can then feed back into the GS/GOGAT cycle (Torre et al., 2014). The resulting Asp is also used in the synthesis of another amide, Asn, an important fixed-N product in amide producing legumes. Asp, along with the amide Gln, acts as an amino donor and is converted to Asn via asparagine synthetase (Gaufichon et al., 2010, Duff et al., 2011). In amide producing legumes such as *P. sativum* and *M. truncatula*, Asn and Gln encompass the primary product of N-fixation for the storage and transport of N to the rest of the plant, whereas in legumes such as *G. max*, Gln is further metabolised into ureides.

4.1.3 Ureide synthesis

The ureides allantoin and allantoate (or allantoic acid) are the primary export product of N-fixation of tropical legumes. Despite encompassing a more complicated and involved biosynthesis pathway in comparison to amides, ureides have a higher N:C ratio and are thus a more efficient means of nitrogen transport (Quiles et al., 2019). However, as previously discussed in this thesis the route of fixed-N is species specific, typically related to nodule structure (determinate or indeterminate) and geographical location (tropical or temperate). Even so, all legumes likely have the capacity to synthesise ureides within the nodules, albeit at a reduced rate when comparing amide and ureide species.

The route of fixed-N in the form of Gln is important where the majority of the nodule supply is subsequently imported into the purine pathway for ureide synthesis (Smith & Atkins 2002). This route begins with Gln movement into the plastids of the nodule infected cells to initiate the purine synthesis and degradation pathway. This pathway consists of several enzymatic steps through the activity of Pur genes beginning with phosphoribosylpyrophosphate amidotransferase (PRAT) or otherwise known as Pur1, also believed to be a regulatory step with significant activity increase during nodule development and measured in this thesis (Chapter 3.3.2) (Kim et al., 1995). The result of these enzymatic steps yields xanthine which is further metabolized into urate catalyzed by xanthine dehydrogenase (XDH) located in the infected cell plastids (Todd et al., 2006). XDH has been detected in both infected and uninfected cells, however the following step involving uricase catalyzing an irreversible oxidative transfer of urate to the ureide allantoin has not been found in the infected cells suggesting transport of urate into the uninfected cell peroxisomes or cytosol (Smith & Atkins 2002, Tajima et al., 2004). Allantoin can then be further metabolized via allantoinase to yield an additional ureide species, allantoic acid (Diaz-Leal et al., 2012). Finally, the product of ureide biosynthesis, namely allantoic acid can be degraded either in the nodules or after export to other plant tissues to yield glyoxylate and ammonia through several possible pathways (Diaz-Leal et al., 2012, Todd et al., 2006, Werner & Witte 2011).

4.1.4 Legume transcriptomic databases

Evidence presented earlier in this thesis (Chapter: 3.2.3) suggests that chickpea exhibits an onset of nitrogen fixation at 15-20 DAI and a subsequent rapid senescence of nodules at ~30 DAI. This identifies a critical window in which to assess the underpinnings of nitrogen fixation in chickpea. Understanding nitrogen fixation in chickpea within this period can be used to better identify key genes and metabolic pathways for future research, such as through genetic manipulation. Such instances of genetic manipulation have been studied in other legumes with varying success as described in chapter (Introduction: 1.5, but no such attempts have yet been made in chickpea. Genetic manipulation studies of chickpea have been difficult due to a lack of fundamental understanding of N-fixation and limited transcriptomic data for further research. This contrasts with the comprehensive transcriptomic databases

available for other legumes such as soybean, lotus, pea and Medicago. Chickpea is also notoriously difficult to transform efficiently (Das Bhowmik et al., 2019).

Several transcriptomic databases exist for other legumes such as Soybase (Grant et al., 2010) for soybean, LotusBase (Mun et al., 2016) for lotus and Symbimics (Roux et al., 2014) for Medicago. Geneinvestigator (Hruz et al., 2008), is also an extensive database consisting of tissue or cell type gene expression, and biotic and abiotic stress genetic data, a useful tool for bioinformatic analysis of legumes such as soybean and Medicago. Similarly, databases such ePlant (Waese et al., 2017) and the Expression Atlas (Kapushesky et al., 2010) that provide visual representations of where specific genes are expressed during developmental stages, are also not available for chickpea. There are more genetic databases to assist legume researchers, such as the Legume Information System (Dash et al., 2016) and Legume IP (Dai et al., 2021), both of which contain some chickpea transcriptome data, but with very limited datasets, especially in terms of nodule data. Chickpea has two main transcriptome databases known as the Chickpea Portal (Edwards, 2016) and Chickpea Transcriptome Database (Garg et al., 2011, Agarwal et al., 2012, Jhanwar et al., 2012), both of which present comprehensive genome information for gene annotations, but as mentioned above, limited nodule data, which is critical for nitrogen fixation research. The most comprehensive nodule dataset currently available was published by researchers from ICRISAT in India (Kudapa et al., 2018) comprising all tissues from seeds 24 hours after germination to tissue senescence at 90-100 days after germination. While this dataset is excellent for transcriptome analysis of most tissues, the first nodule harvest point is during the plant reproductive stage at 40-50 days after germination, which our results suggest may be past the period of peak N₂ fixation. There also now exists newly established techniques providing pinpoint single cell accuracy of gene expression within nodules, through spatial transcriptomic techniques (Frank et al., 2022, Liu et al., 2022, Ye et al., 2022). A spatial transcriptomic database in Medicago will be used later in the chapter to pinpoint possible cellular locations of AMINO ACID transporters in nodules (Ye et al., 2022).

Chapter 4: Aims

The aim of this chapter was to perform mRNA sequencing on chickpea (Cultivar: Slasher) nodules grown under low nitrogen (0.5 mM KNO₃) conditions and harvested at 2 timepoints depicting a period preceding or early fixing (18 DAI) and heightened fixing (25 DAI) nodules (General methods: 2.5). This was performed to answer aims two and three of this thesis: Determine if chickpea nodules predominantly synthesize the amides, glutamine and asparagine, or ureides, allantoin and allantoic acid. (2) Identify the key transporters involved in facilitating fixed nitrogen movement out of the nodules and determine localization of these transporters. Root tissue was also analyzed under the same parameters to ascertain whether genes were primarily nodule located.

The mRNA data analyzed here encompasses a small, but important, time window in chickpea nodule development and symbiotic N-fixation. Providing a high-resolution overview of the chickpea transcriptome, allowing for the detection and analysis of both known and novel genes and metabolic pathways. The resulting data were used to accurately quantify the expression levels of important genes to develop a detailed outline of nitrogen fixation in chickpea on a transcriptomic level. It was hypothesized that during a period of peak nitrogen fixation, important metabolic gene pathways, namely nitrogen, amide and ureide metabolism and respective transporters can be identified through transcriptional changes between 25 to 18 days after inoculation (DAI) with rhizobia.

4.2 RNA Sequencing Comparisons of Differentially Expressed Genes

To present an overview of N₂ fixation in chickpea, the resulting mRNA sequencing data was subjected to four comparisons, whereby significant DEGs (Differentially Expressed Genes) could be identified between the two time-points harvest for both nodule and root tissues (Figure 4.1).

Comparisons 1-4 were chosen to identify DEGs expressed in either nodule or roots during a period of increased N₂ fixation or preceding N₂ fixation. Comparison 1 (C1) identifies DEGs up or downregulated from early nodulation to a period of heightened N₂ fixation in nodules, mainly to identify genes involved in ureide and/or amide transport. Comparison 1 was also important to establish a model of N₂ fixation in chickpea involving N, ureide, amino acid, amide and carbon metabolism pathways.

Comparison 2 (C2) was used in a similar manner as comparison 1, primarily to identify root transporters of fixed nitrogen exported from the nodules to the rest of the plant or import of sucrose into the nodules.

Comparisons 3 (C3) and 4 (C4) identified transporters and metabolism genes with root or nodule function preceding or during a period of N₂ fixation, respectively. These comparisons identified many transporters with high expression values, however, were not linked to N₂ fixation due to a fold change between 1 and -1. For example, transporters likely exhibiting constitutive expression, irrespective of N₂ fixation activity.

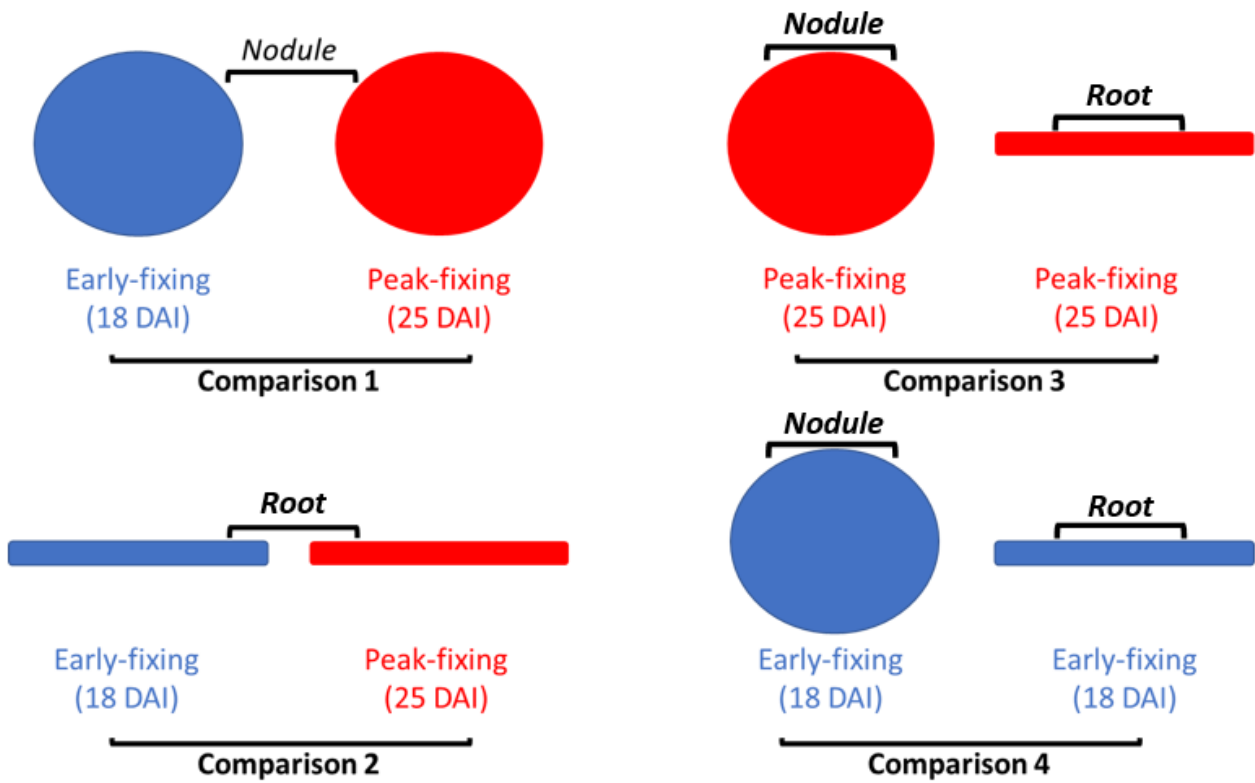


Figure 4.1: RNA sequencing comparison overview of differentially expressed genes.

The following comparisons were tested where early-fixing and peak-fixing refers to root and nodule tissue harvested at 18 and 25 DAI, respectively. Root data are also referred to as early or peak fixing even though roots do not undergo nitrogen fixation, the labeling is merely used to represent the fixation period for consistency. The following comparisons were conducted : (1) Early-fixing nodules compared to peak-fixing nodules; (2) early-fixing roots to peak-fixing roots; (3) peak-fixing nodules to peak-fixing roots; (4) early-fixing nodules to early-fixing roots. From here on, the comparisons will be noted as C1-C4.

4.3 Set-Up and Pre-Processing of Chickpea RNA Sequencing Data

A total of four biological replicates for root and nodule tissues from two harvest periods (early nodulation 18 DAI & N fixing nodules 25 DAI) were selected for transcriptome analysis. Total RNA was extracted from 100 mg snap-frozen root and nodule powder using the SIGMA Spectrum™ Plant Total RNA Kit (Sigma-Aldrich, USA) and stored at -80°C. Preliminary RNA quality were assessed through NanoDrop and agarose gel electrophoresis and final confirmation via an Agilent Bioanalyzer (Agilent, USA) at the Australian Genome Research Facility (AGRF) (Melbourne, Australia). All samples passed a minimum RIN quality of 7 and were used for subsequent Poly(A) mRNA isolation and cDNA library construction according to AGRF's optimized protocol. RNA sequencing was performed by the AGRF on an ILLUMINA NOVASeq 6000 platform to ensure a minimum of 20M 150bp paired-end (PE) reads/sample.

The following RNAseq data formatting was performed by Darren Wong (ANU). Removal of the adaptor sequences, sliding-window trimming, read size and quality filtering of the raw 150bp paired ends (PE) reads in each sample were performed with fastq v0.20.0 (Chen et al., 2018) using default settings. Surviving reads were mapped onto the Desi assembly reference genome (Desi uwa-V3.0 genome) using HISAT2 v2.2.1 (Kim et al., 2015) with default settings and read alignment were pooled across all sequenced libraries and subjected to genome-guided transcriptome assembly was performed using Trinity v2.14.0 with default settings (Grabherr et al., 2011). The identification of accurate gene sets and protein-coding region prediction as well as assembly redundancy removal of contigs were achieved using the EvidentialGene tr2aacds4 pipeline (Gilbert, 2013) using default settings. Read summarization of the final reference transcriptome (hereafter genes) were derived from contigs classified as 'primary' sets by EvidentialGene was performed using FeatureCounts (Liao et al., 2014) with default parameters except for the -B (both ends must be aligned) and -C (exclude chimeric fragments) option enabled for each species. Functional annotation was achieved with MapMan4 functional BIN categories using Mercator4 with default settings (Schwacke et al., 2019). Differential expression (DE) between treatment groups were identified using edgeR (Robinson et al., 2009) with the quasi-likelihood F-test method in R (<http://www.r-project.org>).

A combined false discovery rate (FDR) threshold < 0.01 and a $\log_2FC > 1$ (upregulated) and $\log_2FC < -1$ (downregulated) indicates DE between treatment groups. The Fragments Per Kilobase of transcript per Million mapped reads (FPKM) were chosen as the unit of gene expression throughout this analysis. Enrichment of MapMan4 functional BIN categories in DE genes between treatment groups were based on a hypergeometric distribution adjusted with FDR for multiple hypothesis correction in R as previously described (Wong, 2020). A false discovery rate (FDR) threshold < 0.05 indicates an enriched functional category.

Genes that exhibited an FPKM <10 were generally omitted from tables and figures representing individual genes unless it was deemed important to show a low level of expression for a particular gene of interest. As such, many gene accessions were excluded to avoid redundancy in this chapter, whereas genes of importance that correlated with an increase in N-fixation were prioritized. Additionally, many genes not mentioned here are nonetheless present in chickpea nodules but were deemed of lesser importance. These can be viewed in Appendix 4a.

4.4 Transcriptomic Analysis of Nodule and Root Tissue During Nitrogen Fixation

4.4.1 *Transcriptional variability and correlation of the total RNAseq dataset*

A total of 580M high-quality PE reads (ranging between 27 – 42M PE reads/sample) were successfully obtained from RNA sequencing of two nodules and root harvests (2 harvests x 2 tissues x 4 biological replicates). A very high mapping rate (ca 97.8 – 98.6% of total reads) to the reference Desi assembly reference genome (Desi uwa-V3.0 genome) were observed across individual samples. Due to the poor/uncertain gene annotation quality of the reference, a genome-guided transcriptome assembly approach was undertaken revealing a consolidated transcriptome reference set of 25240 genes amendable for various downstream analysis. To present an overview of N-fixation in chickpea, the resulting mRNA sequencing data was subjected to four comparisons, whereby significant DEGs could be identified between the two time-point harvests for both nodule and root tissues (Figure 4.1).

Principle Component Analysis (PCA) (Figure 4.2A) highlighted that tissue-specificity (Nodule & Root) presented large transcriptomic differences. Nodule transcriptional variance was clearly shown when compared against the root tissue, presenting large separation from each other with PC1 and PC2 explaining 83 and 8% of the total variation, respectively (Figure 4.2A). Following this, nodule tissue also exhibited significant variation between the two harvest timepoints of 18 and 25 DAI. Only minor differences between the two root harvests were evident, indicating minimal transcriptional variability between 25 to 18 DAI in root tissue (Figure 4.2A). Replicates of nodule 25 DAI and both root replicates were all tightly clustered in their respective groups, indicating limited variability within each of the four replicates (Figure 4.2A). Nodules (18 DAI) did present a single replicate slightly placed outside of the group cluster of the other three replicates, indicating some minor transcriptional variability during nodule tissue harvesting (Figure 4.2A). Overall, the experimental design presented the intended outcome in nodule tissue.

Pearson correlation (Figure 4.2B) measured the strength of the linear relationship between all replicates of root and nodules together. Strong linear correlations between all nodule-to-nodule variables and root-to-root variables were evident, with r values close to 1 (Figure 4.2B, Appendix 4A.1 Table 4a.1). Unsurprisingly, the correlation between the time-point harvests for nodule-to-root variables were more weakly correlated, with a Pearson's Correlation bordering on the negative and $r = 0.3$ or lower (Appendix 4A.1 Table 4a.1). A distinct difference in the whole genome transcriptional profile occurs between genes residing in nodule compared to root tissue, indicating unique, tissue-specific biological processes in relation to nitrogen fixation.

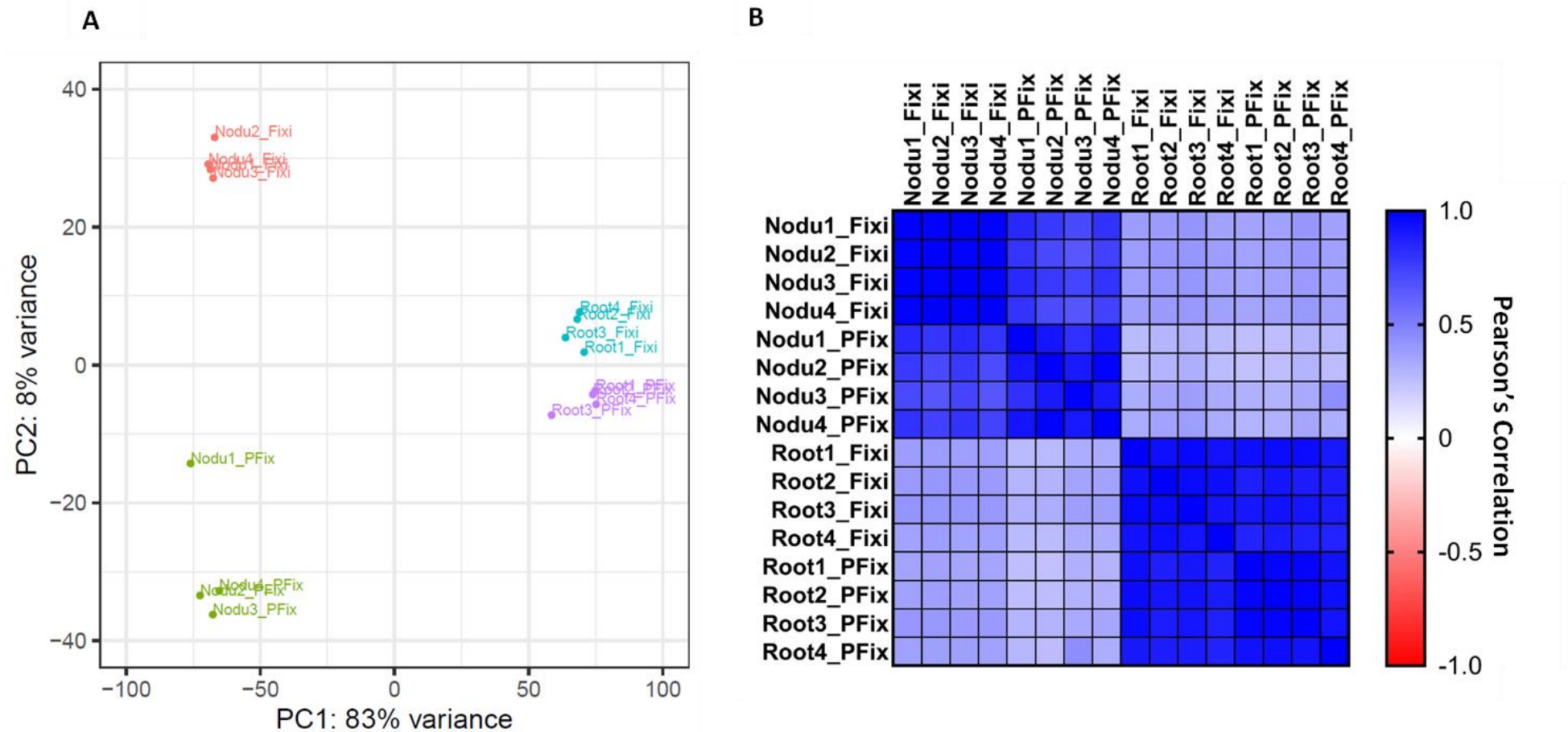


Figure 4.2: Principal component analysis of RNA sequencing variability.

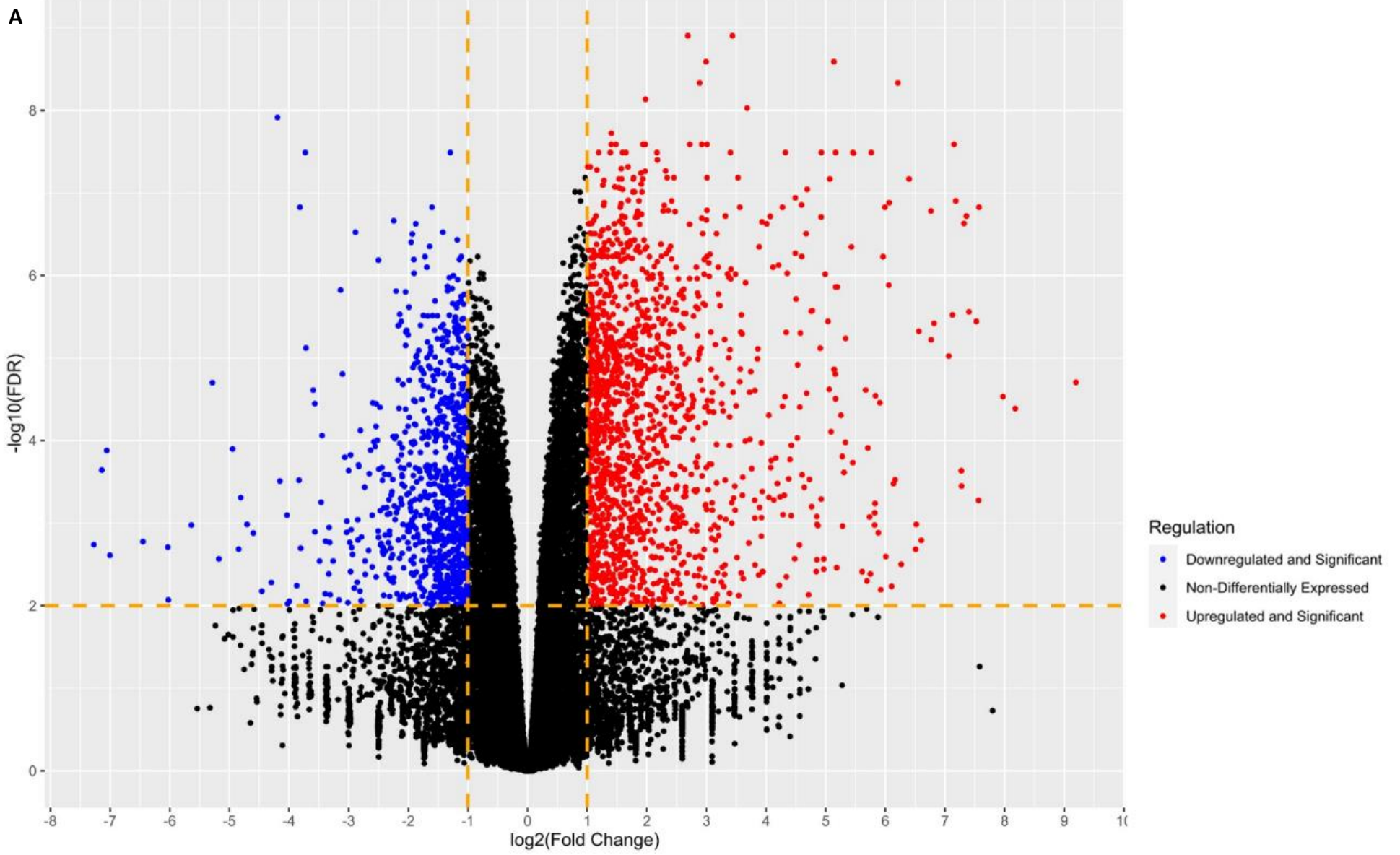
(A) PCA (Principal Component Analysis) plot displaying variability for all 16 samples of nodule and root tissue for both time periods, with portion of variance for PC1 and PC2 at 83% and 8%, respectively, within the RNAseq dataset. PC analysis was calculated on the FPKM (fragments per kilobase of exon per million mapped fragments) using the Log₂ fold change. Each point represents an individual replicate of Nodule 18 DAI (Green), Nodule 25 DAI (Red), Root 18 DAI (Purple) and Root 25 DAI (Blue). (B) Correlation (r) visualised between each sample through a Pearson's Correlation plot.

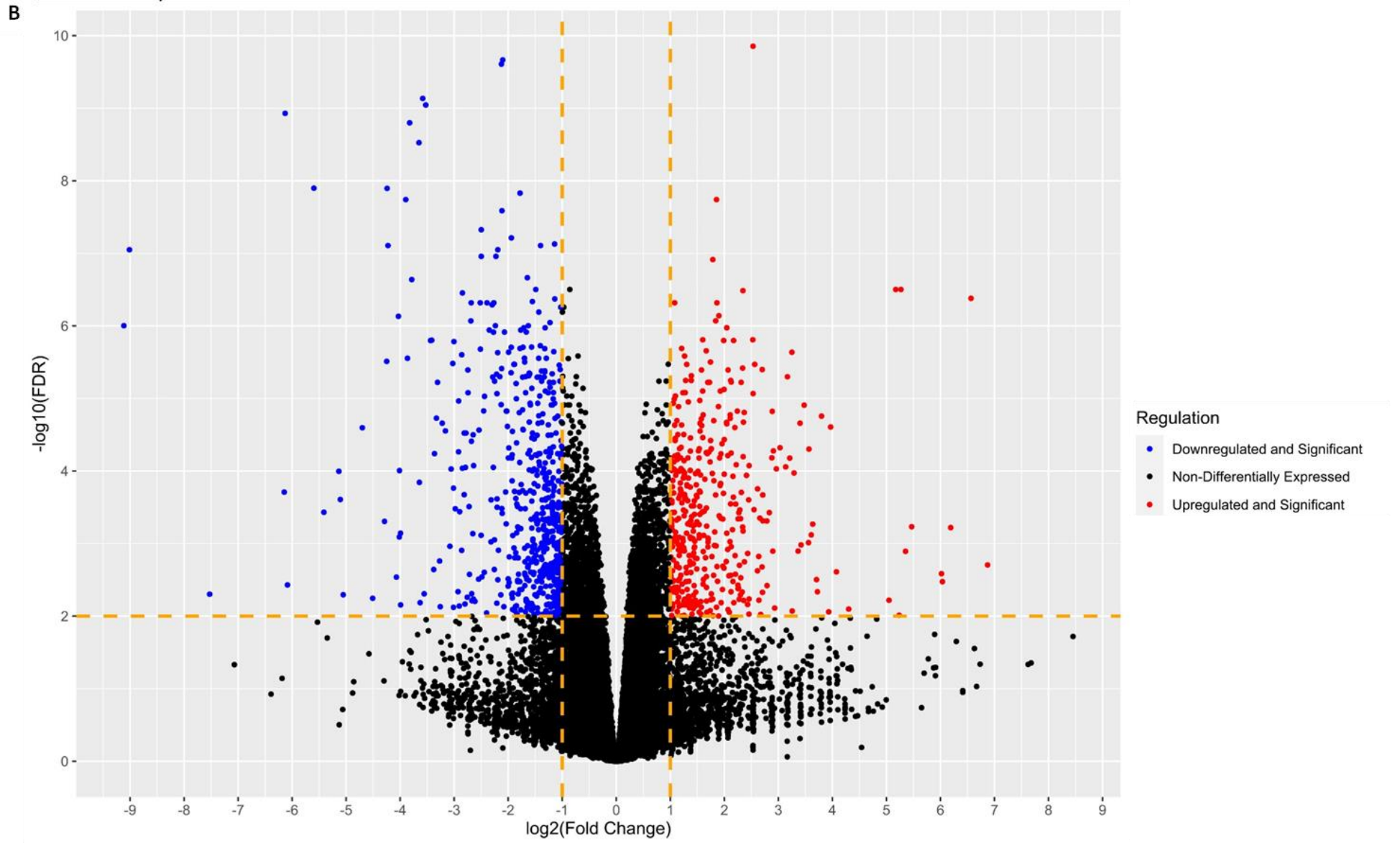
4.4.2 Statistical significance and transcriptional fold change for RNAseq comparisons

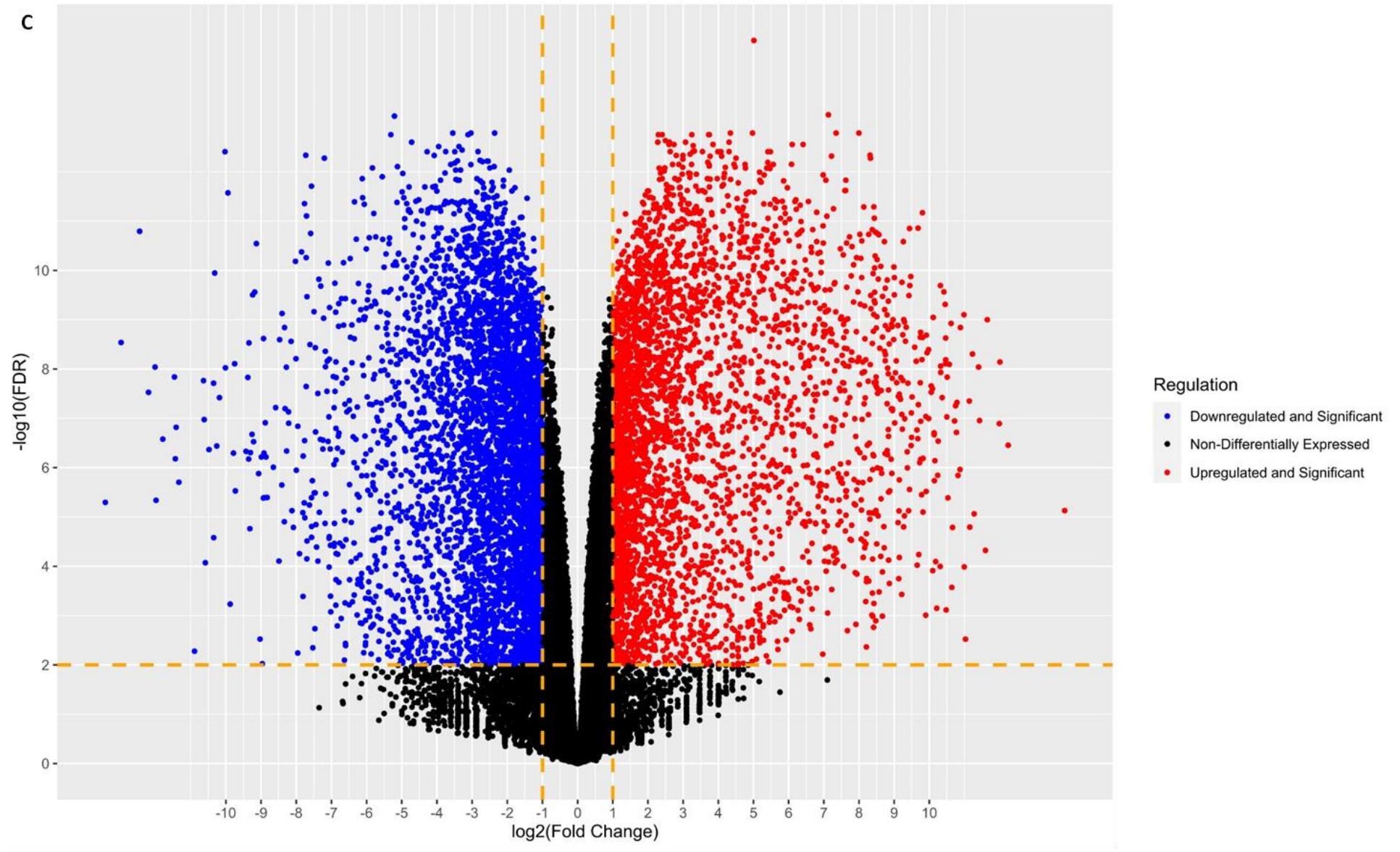
A total of 25240 genes were mapped and annotated to the RNAseq library across all comparisons with overall statistical significance vs magnitude of fold change depicted in Volcano plots (Figure 4.3A-D). Venn diagrams and an UpSet plots depicting the unique and shared differentially expressed gene interactions between each comparison was also analyzed in Appendix 4A.2: Figures 4a.1-3. Comparison 1 (C1) comparing early nodulation to fixing nodules showed 1541 significantly upregulated and 879 downregulated DEGs (Table 4.1) with a $-\log_{10}(\text{FDR})$ greater than 2 and $\log_2\text{FC} >1$ or <-1 , respectively (Figure 4.3A). C1 contained 22782 non-differentially expressed genes with a $\log_2\text{FC}$ between -1 & 1, & $-\log_{10}\text{FDR} <2$ (Table 4.1, Figure 4.3A).

Comparison 2 (C2) volcano plot (Figure 4.3B) depicting 25 to 18 DAI roots showed a smaller DEG group than C1, with marginally more downregulated DEGs at 592 compared to 423 significantly upregulated DEGs. (Table 4.1). Genes with non-differential expression totalled 24187, compared to the 25240 totally mapped genes (Table 4.1). The disparity of upregulation of DEGs in roots is likely attributed to minor physiological changes in root development during this brief period compared to a more prominent developmental change in nodules from 25 to 18 DAI.

Comparison 3 and 4 (C3 & C4) comparing fixing nodules (25 DAI) to 25 DAI roots and early nodulation (18 DAI) to 18 DAI roots, exhibited a considerably larger DEG group than C1 & C2, with 3663 and 3939 significantly upregulated genes, respectively (Figure 4.3C-D, Table 4.1). There were marginally more significantly downregulated genes for C3 & C4 than upregulated genes for C3 & C4 (4664 vs 5231), while the total number of non-differentially expressed genes were 16912 and 16069 (Figure 4.3C-D, Table 4.1). The notable increase in DEGs when comparing C3 & C4 to C1 & C2 is unsurprising when examining two specialised plant tissues with very different biological functions.







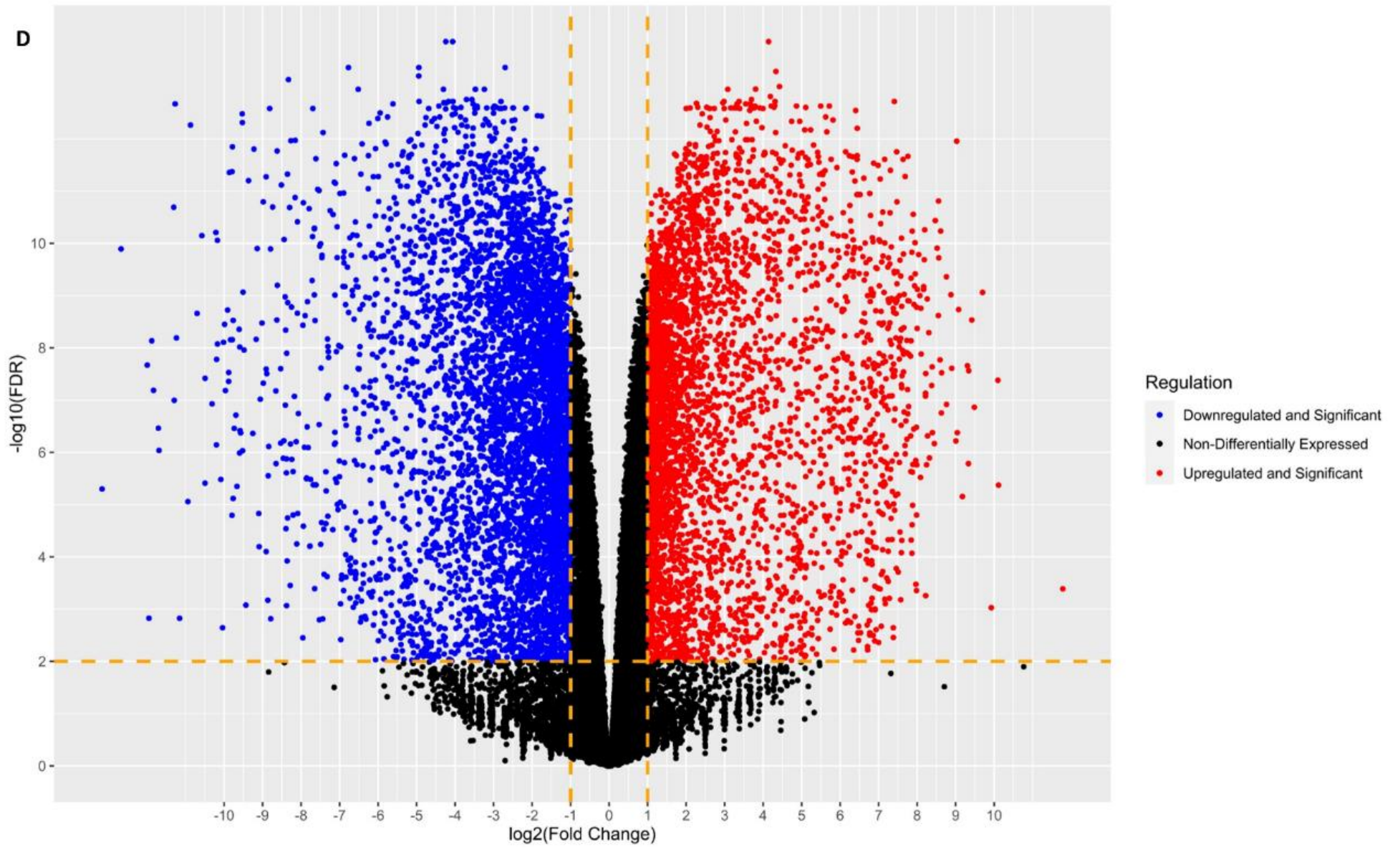


Figure 4.3: Volcano plot distribution of differentially expressed genes for each comparison.

Volcano plot distribution of the total number of genes and differentially expressed genes (DEGs) from chickpea nodule and root comparisons. Red dots: Significant upregulated DEGs (<0.01 $-\log_{10}\text{FDR}$ & >1 Log_2FC), Blue dots: Significant downregulated DEGs (<0.01 $-\log_{10}\text{FDR}$ & <-1 Log_2FC): Black dots: Non-differentially expressed DEGs (>0.01 $-\log_{10}\text{FDR}$) & (<0.01 $-\log_{10}\text{FDR}$ & between 1 & -1 Log_2FC). Orange dotted lines indicate the barriers between a significant $-\log_{10}\text{FDR}$ of 2 (or 0.01 adjusted P-value) and differential expression of >1 & <-1 Log_2FC . (A) Comparison between 25 DAI Nodules and 18 DAI nodules – Comparison 1; (B) 25 DAI Roots and 18 DAI Roots – Comparison 2; (C) 25 DAI Nodules and 25 DAI Roots – Comparison 3; (D) 18 DAI Nodules and 18 DAI Roots – Comparison 4. Dots placed further left or right indicate a larger fold change in expression, higher the dot the more significant the expression.

Table 4.1: Total number of significantly (FDR < 0.01) upregulated (>1 Log₂FC) downregulated (<-1 Log₂FC), and non-DE (log₂FC <1, FDR>0.01) genes between treatments.

False Discovery Rate (FDR) = P-adjusted value <0.01.

	25 vs 18 DAI Nodules (C1)	25 vs 18 DAI Roots (C2)	25 DAI Nodules vs 25 DAI Roots (C3)	18 DAI Nodules vs 18 DAI Roots (C4)
Number of Upregulated DEGS	1541	423	3663	3939
Number of Downregulated DEGs	879	592	4664	5231
Number of Non- Differentially Expressed Genes	22782	24187	16912	16069
Total Number of Genes	25240	25240	25240	25240

4.4.3 Analysis of enriched functional gene categories in chickpea during nitrogen fixation

To gain a fundamental understanding into the biological pathways relevant in the mediation N-fixation in chickpea, enrichment analysis of Mapman BIN categories (FDR < 0.05) were performed on various up and down regulated gene lists. For example, significantly upregulated genes of Nodule 25 vs 18 DAI showcased five enriched categories such as “RNA biosynthesis”, “solute transport”, “nutrient uptake”, “enzyme classification” and “photosynthesis” (Figure 4.4A). This signified a period of increased movement of solutes within the nodules, likely pertaining to amino acids, amides, ureides and carbon. Conversely, during this period, significantly downregulated genes were often enriched in processes involved in “carbohydrate metabolism”, “phytohormone action”, “cell wall organisation” and again “enzyme classification” (Figure 4.4A). The “enzyme classification” enriched category was further broken down into child BIN subcategories, showing significant upregulation of enzymatic genes exhibiting transferase and oxidoreductase activities, indicating heightened activity of aminotransferases and subsequent amino acid biosynthesis from fixed N (Figure 4.4B).

During the same 25 vs 18 DAI period in root tissue there was downregulation of genes enriched in processes of “cell wall organisation”, “solute transport”, “nutrient uptake” and “enzyme classification”, likely a result of a larger portion of the harvested tissue in a more mature growth state in the growing roots (Figure 4.4A). Notably, there was also an upregulation of genes enriched within categories such as “solute transport” and “nutrient uptake” genes, indicating some classes of transporters are modulated during this period, possibly reflecting both transport of fixed N such as amides or ureides out of the nodules to the rest of the plant, and transport of carbon towards the nodules (Figure 4.4A). Of the most prominent categories enriched in nodules identified from 25 vs 18 DAI, “Solute transport” contained 295 and 48 up and downregulated DEGs, respectively (Table 4.2) whereas “Nutrient uptake” exhibited 75 upregulated DEGs only. Many of the DEGs upregulated within these enriched categories are likely key transporters critical in the maintenance of N assimilation. In addition, 16 and 25 of the upregulated DEGs within “solute transport” were annotated as UmamiT and APC gene families, respectively (Table 4.2). In the nodules it was, however, unexpected to observe no enrichment of the “carbohydrate metabolism” category when considering the import and metabolism of photosynthetic carbon as sucrose in nodules to drive the nitrogenase enzyme in the bacteroid. For example, the production of hexoses, such as sucrose are metabolised into malate to fuel the TCA cycle of the bacteroid, whereas oxaloacetate from phosphoenolpyruvate carboxylase (PEPC) and 2-oxygutarate via the TCA cycle are both important for amino acid biosynthesis (Lodwig et al., 2003, Udvardi & Poole, 2013).

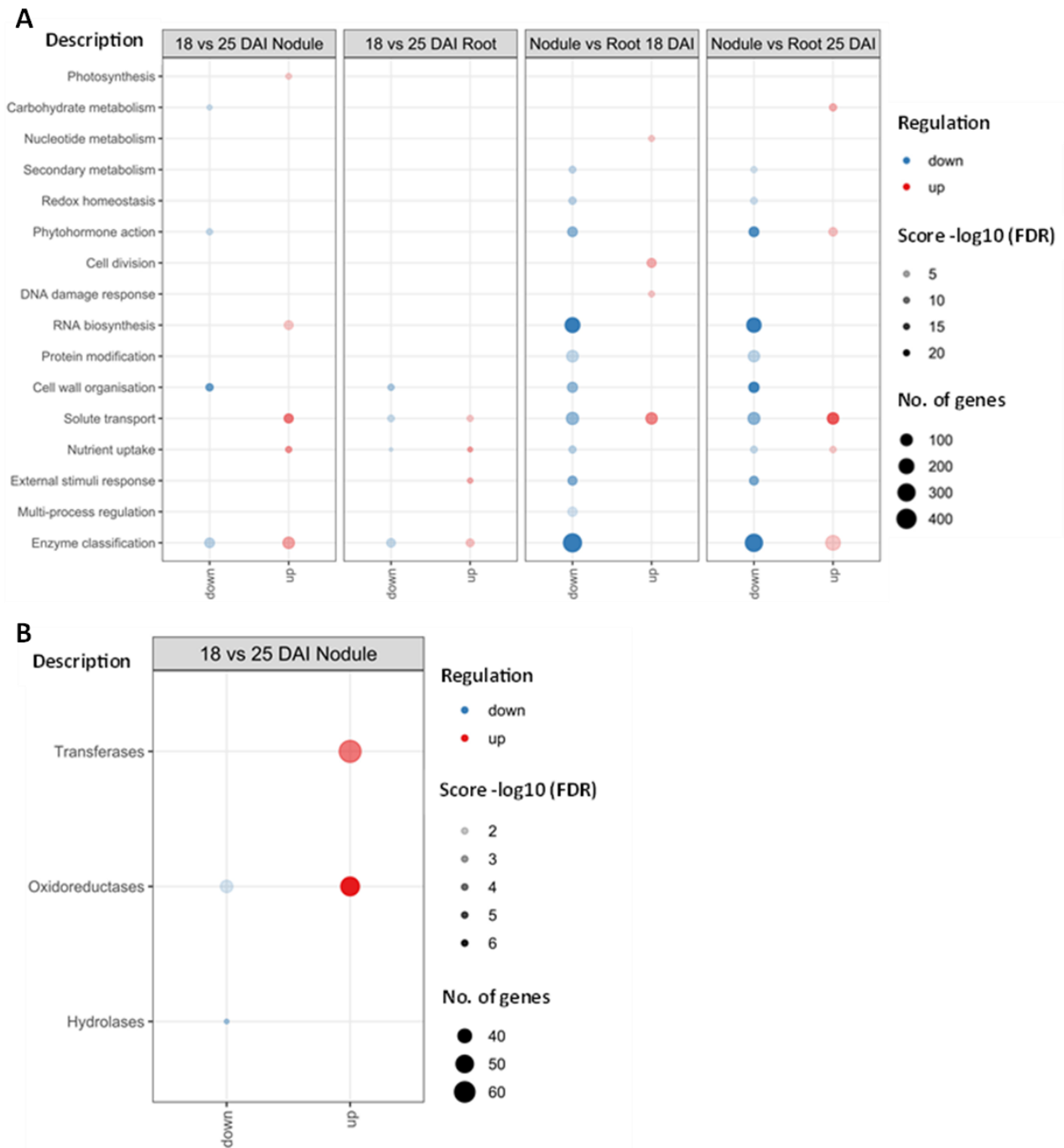


Figure 4.4: Enriched MapMan BIN functional categories of differentially expressed genes.

Functional categories of differentially expressed genes mediating the N_2 fixation process in chickpea. Red points signify upregulated DEGs, whereas blue points represent downregulated DEGs. Larger points indicate more genes in a particular enrichment category, while the intensity of the colour indicates increasing significance ($-\log_{10}FDR$). Enriched (A) Parent and (B) child BIN subcategories within “enzyme classification” for 25 vs 18 DAI nodules are indicated.

Of the 295 total solute transporter genes upregulated in C1, 102 of are classed as carrier mediated transporters in the RNAseq annotation and 136 were classified as broad solute transporters (Table 4.2). Sixteen of the upregulated genes belong to the DMT superfamily, including UmamiTs (Table 4.2). Similarly, the APC superfamily, copper anion channel (COPT) and metal cation transporters of ZIP's had 25, 5 and 11 upregulated genes, respectively (Table 4.2). For nutrient uptake transporters, 34 were classed as transitional metal homeostasis transporters and five as copper transporters (Table 4.2).

Comparisons 3 and 4, which compared nodule to root tissues, identified extensive down regulation of multiple enrichment categories including "RNA biosynthesis", "protein modification", "cell wall organisation", "solute transport", and "nutrient uptake" (Figure 4.4A). Comparisons C3 and C4 identified approximately 200 upregulated and downregulated solute transport genes, suggesting ~200 genes may have specific nodule or root localisation and functions, respectively (Figure 4.4A). C4 in comparison to C3 did not show any upregulation of nutrient uptake genes within the period of early nitrogen fixation (Figure 4.4).

Table 4.2: Solute transport and nutrient uptake enriched subcategories in nodules.

Comparison 1 (Nodule tissue 25 vs 18 DAI) enriched subcategories for solute transport and nutrient uptake and the total number of up or downregulated genes.

Enriched Categories	Number of Genes	
	Solute Transport (Upregulated)	Solute Transport (Downregulated)
Solute Transport		
Solute transport	136	0
Carrier-mediated transport	102	48
DMT superfamily solute transporter (UmamiT)	16	0
APC superfamily	25	0
Copper cation channel (COPT)	5	0
Metal cation transporter (ZIP)	11	0
Nutrient Uptake	Nutrient Uptake (Upregulated)	Nutrient Uptake (Downregulated)
Nutrient uptake	36	0
Transition metal homeostasis transport	34	0
Copper transporter (COPT)	5	0

4.5 RNA Sequencing Reveals an Updated Model of Nitrogen Fixation and Assimilation in Chickpea

By focusing on metabolism genes of sucrose, ureides, amides and amino acids, a model of nitrogen fixation in chickpea nodules was established centred around Figure 4.5 using comparison 1 and 2. Comparison 1 was predominantly used to determine genes important to nodule function whereas C2 was used to identify possible importers of sucrose or other solutes to support N_2 fixation. The established model outlines the path of imported sucrose to the uninfected cell to the synthesis of malate directed to the TCA cycle in the bacteroid of the infected cell. The exported product of N_2 fixation, ammonium, is synthesised into amino acids and amides, that are either exported as a plant N source or the amide Gln is used for the biosynthesis of urate in the purine synthesis pathway. Lastly urate is transported to the peroxisome of the uninfected cell where ureides are synthesised and exported as a plant N source or catabolised in the endoplasmic reticulum.

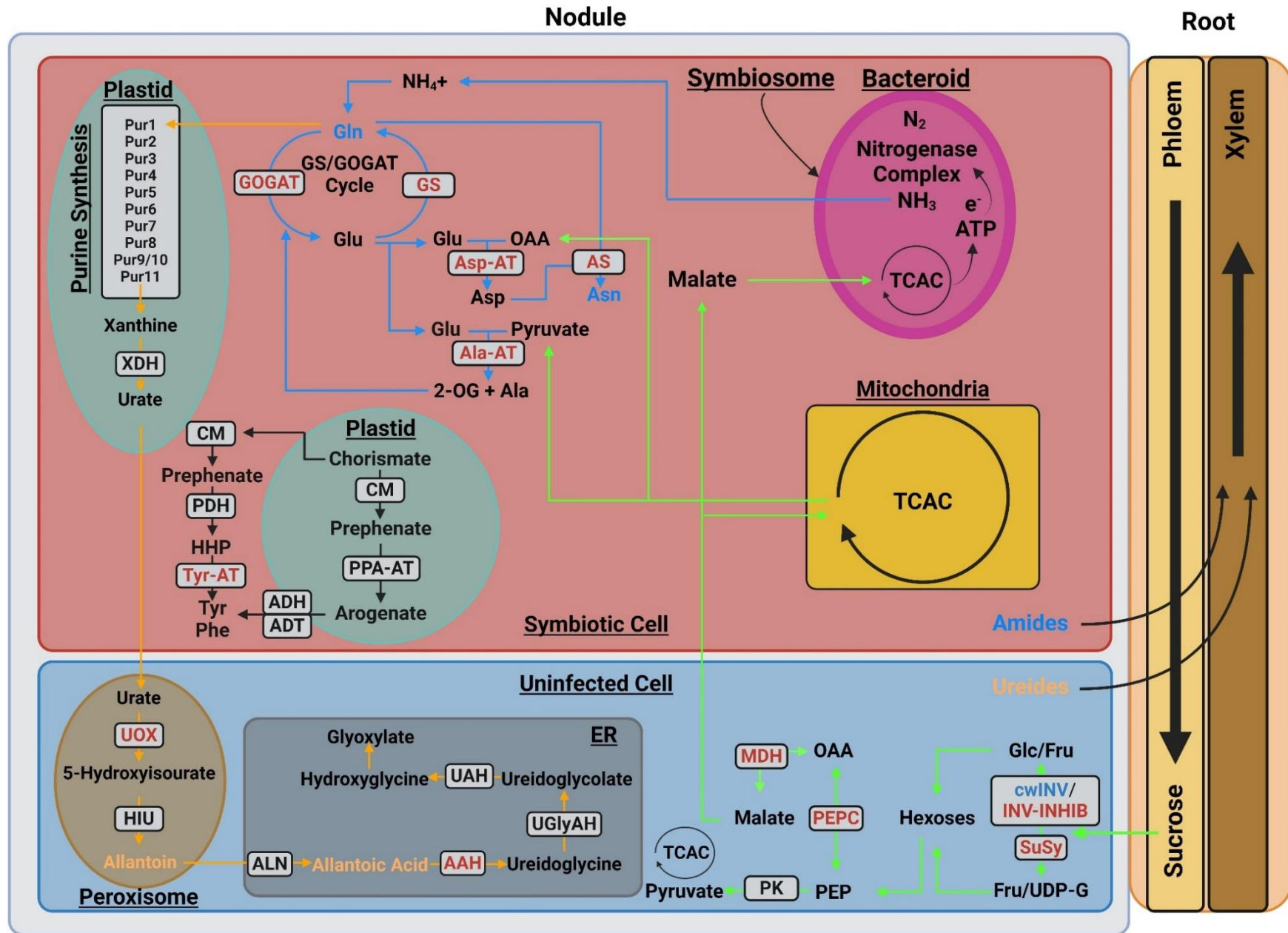


Figure 4.5: Nitrogen fixation model in chickpea nodules depicting the change in gene expression related to carbon, ureide, amide and amino acid metabolism.

Gene expression shown based on the FPKM fold change from 25 vs 18 DAI nodules and are depicted as enzymes (Grey boxes) as either upregulated (Red), downregulated (Blue) and non-differential (Black) expression. Upregulated genes exhibited a $\log_2FC >1$, downregulated <-1 and non-differential expression $>2 -\log_{10}FDR$ (or 0.01 P-value) & $<2 -\log_{10}FDR$ & between 1 & -1 \log_2FC . Carbon metabolism depicted with green arrows, key amino acids and amides in blue and ureide biosynthesis in orange.

Sucrose synthase (SuSy), fructose (Fru), sucrose-specific invertase (cwINV), glucose (Glc), invertase inhibitor (cwINHIB), phosphoenolpyruvate (PEP), oxaloacetate (OAA), malate dehydrogenase (MDH), Tricarboxylic Acid Cycle (TCAC), ammonia (NH_3) atmospheric nitrogen (N_2), ammonium (NH_4^+), asparagine (Asn), glutamine (Gln), glutamine synthetase (GS) glutamate oxoglutarate aminotransferase (GOGAT), Asparagine synthase (AS), glutamate (Glu), aspartate (Asp), aspartate aminotransferase (Asp-AT), alanine (Ala), alanine aminotransferase (Ala-AT), tyrosine (Tyr), phenylalanine (Phe), prephenate dehydrogenase (PDH), chorismate mutase (CM), prephenate amino transferase (PPA-AT), arogenate (AGN), arogenate dehydrogenase (ADH), arogenate dehydratase (ADT), 4-hydroxyphenylpyruvate (HPP), prephenate-specific dehydrogenase (PDH), tyrosine aminotransferase (Tyr-AT), Amidophosphoribosyltransferase 1 (Pur1), Phosphoribosylamine glycine ligase (Pur2), Phosphoribosylglycinamide formyltransferase (Pur3), Aminoimidazole RN synthetase (Pur5), Phosphoribosylaminoimidazole carboxylase (Pur6), Succino-aminoimidazole-carboximide RN synthetase (Pur7), Adenylosuccinate lyase (Pur8), Aminoimidazole-carboximide RN transformylase/IMP cyclohydrolase (Pur9/10), Adenylosuccinate synthetase (Pur11), Xanthine dehydrogenase (XDH), Urate oxidase (UOX), 5 Hydroxyisourate hydrolase (HIU), Allantoate amidohydrolase (AAH), Allantoinase (ALN), Ureidoglycine aminohydrolase (Ugly-AH), Ureidoglycolate amidohydrolase (UAH). Made with Biorender.com

4.5.1 Imported nodule sucrose supports malate synthesis in the uninfected cell prior to metabolism in the infected cell

Initial import of sucrose to support an increase of N₂ fixation may be directed by multiple sucrose transporters but only two genes were correlated to an increase of N₂ fixation at 25 compared to 18 DAI in nodules (Table 4.3). Sugars will eventually be exported transporter 1 (SWEET1) and SWEET2 were significantly upregulated with a Log₂FC increase of 3.4 and 1.0, respectively (Table 4.3). All SWEET genes except SWEET13 depicted were expressed at a higher level in nodules than roots. Similarly, SWEET13 was the only of the SWEET family not found to be located on the plasma membrane via TargetP/WolfPsort analysis (Table 4.3).

The remaining SWEET genes, sucrose transporters (SUC/SUT), monosaccharide transporters and sugar transport protein (STP) family were also likely involved in sucrose transport but were non differentially expressed (between 1 and -1 Log₂FC) at 25 compared to 18 DAI (Table 4.3). Particularly, SWEET2 and SWEET14 were highly expressed at the 25 DAI period, but with a Log₂FC of <1 or 1.0 for SWEET2 (Table 4.3). Conversely, SWEET13, UDP-galactose/UDP-glucose transporter 3, bidirectional sugar transporter 3 (BiSTP3) and sugar transporter ERD6 were significantly downregulated at 25 compared to 18 DAI (Table 4.3). In roots there was no significant upregulation of sucrose or other monosaccharide transporters during the 25 vs 18 DAI timeframe, whereas SWEET13 and SUC/SUT1 were significantly downregulated (Table 4.3).

Table 4.3: Carbon transporter DEGs in chickpea.

Data displayed as Log₂ fold change as a heatmap with corresponding average FPKM for each gene.

mRNA Acc.	Gene Name	AVERAGE FPKM				LOG ₂ FOLD CHANGE		
		25 DAI Nodule	18 DAI Nodule	25 DAI Root	18 DAI Root	Nodule 25 DAI vs 18 DAI	Root 25 DAI vs 18 DAI	Nodule 25 DAI vs Root 25 DAI
XM_004502 518.3	^{Plas} SWEET1	21.1±1.7	2.0±1.3	0±0	0±0	*3.4	1.9	*9.2
XM_027330 330.1	^{Plas} SWEET2	95.7±18.7	49.3±18.6	0.3±0.1	0.6±0.7	*1.0	-0.9	*8.4
XM_004502 010.2	^{Plas} SWEET7	22.2±1.5	12±1.1	1.9±0.2	1.3±0.1	*0.9	*0.5	*3.6
XM_004503 721.1	^{ER} SWEET13	10.3±0.6	44.7±1.5	36.4±1.	112.8±0	*-2.1	*-1.6	*-1.8
XM_004501 759.3	^{Plas} SWEET14	152.5±7.1	214.6±34.	3	0.9±0.2	-0.5	-0.1	*7.4
XM_004492 633.3	^{Plas} UDP-galactose/UDP-glucose transporter 2	26.1±1.3	13.9±1.7	13.5±1.	15.7±1.	*0.9	-0.2	*0.9
XM_004489 957.3	^{Plas} UDP-galactose/UDP-glucose transporter 3	60.7±2.7	145.9±15.	9	11±1.4	*-1.3	-0.3	*2.5
XM_004486 983.3	^{Vacu} UDP-galactose/UDP-glucose transporter 5	26.4±2.4	18.2±0.4	4.5±0.6	5.2±0.2	*0.5	-0.2	*2.5
XM_004502 823.3	^{Vacu} UDP-rhamnose/UDP-galactose transporter 4	23.3±1.4	17±1.9	33.1±2.	24.9±1.	*0.5	*0.4	*-0.5
XM_004496 381.3	^{Plas} UDP-rhamnose/UDP-galactose transporter 6	15.4±1.5	21.7±2.3	11.9±2	15.3±1.	*-0.5	-0.4	0.4
XM_004508 491.3	^{Plas} GDP-fucose transporter 1	44.7±1.1	47.1±2.5	30.3±2	31.1±0.	-0.1	0.0	*0.6
XM_004502 793.3	^{Plas} UDP-xylose transporter 3	27.2±0.7	18.9±1.3	19.2±1	18.2±0.	*0.5	0.1	*0.5
XM_004496 325.3	^{Plas} STP3	44.5±9.6	152.1±13.	5	11.2±4	*-1.8	-0.3	*2.0

XM_004508					16.6±2.			
267.3	^{Plas} Sugar transporter ERD6	12.4±1.9	29.8±2.2	8.7±1.3	6	*-1.3	*-0.9	*0.5
XM_004496				43.5±5.	90.4±5.			
325.3	^{Plas} SUT/SUC	42.8±4.5	56.3±2.7	2	5	*-0.4	*-1.1	0.0

Significant (P-adjusted value <0.01) DEG log₂ fold change displayed with an *. TargetP/WolfPsort peptide localisation analysis, Pero: Peroxisomal, Mito:

Mitochondria, Chlo: Chloroplast, Cyto: Cytoplasmic, Nucl: Nuclear, Vacu: Vacuolar, Extr: Extracellular, Plas: Plasma Membrane, ER: Endoplasmic Reticulum.

Sucrose conversion to hexoses after import into nodule uninfected cells could occur either via sucrose synthase (SuSy), or sucrose-specific invertase (cwINV) (Figure 4.5). SuSy was upregulated whereas cwINV was downregulated with a Log₂FC of 1.2 and -1.3, respectively (Table 4.4). The invertase inhibitor (cwINHIB) of cwINV was upregulated with a Log₂FC of 1.6 (Table 4.4). Importantly, SuSy exhibited a large average FPKM from 25 to 18 DAI at 641.7 to 1509.5, suggesting heightened expression of sucrose metabolism to Fru or UDP-G (Table 4.4). Sucrose biosynthesis directed via sucrose phosphate synthase (SPS) was non-differentially expressed with a Log₂FC of 0.4 (Table 4.4).

Hexoses synthesized from sucrose are metabolized into phosphoenolpyruvate (PEP) and pyruvate during glycolysis. The glycolysis pathway expression was mostly non-differentially expressed but multiple steps consisted of a high average FPKM (Table 4.5). Synthesis of oxaloacetate (OAA) from PEP was upregulated through the reversible action of phosphoenolpyruvate carboxylase (PEPC) Log₂FC expression of 2.3 (Table 4.4). Similarly, the reversible synthesis of malate from oxaloacetate (OAA) via malate dehydrogenase (MDH) was upregulated with a Log₂FC increase of 1.2 (Table 4.4).

Malate export into the infected cell, is either fed into the mitochondria or passes through the symbiosomal membrane to the Tricarboxylic Acid Cycle (TCA) of the bacteroid to support N₂ fixation (Bryce & Day 1990). Indeed, it appeared malate biosynthesis from PEP occurred in the cytosol rather than the mitochondria because the relevant gene contained a TargetP/WolfPsort localisation signal specific for cytosolic localisation (Table 4.4). Genes encoding TCA-related pathway enzymes were generally not DE at 25 compared to 18 DAI, with MDH the only upregulated gene (Table 4.6). However, genes encoding many enzymatic steps had high expression levels, particularly those involved in the pyruvate dehydrogenase complex (PDC), Oxoglutarate dehydrogenase complex (ODC), succinyl-CoA ligase (SCoAL), succinate dehydrogenase (SDH) and succinyl-CoA (SucCoA) (Table 4.6).

Table 4.4: Sucrose metabolism DEGs in chickpea.

Data displayed as Log₂ fold change as a heatmap with corresponding average FPKM for each gene. Data presented for all nodule and root comparisons, 18 DAI (Early-Fixing) and 25 (Peak-Fixing).

mRNA Acc.	GENE NAME	AVERAGE FPKM				LOG ₂ FOLD CHANGE			
		25 DAI Nodule	18 DAI Nodule	25 DAI Root	18 DAI Root	Nodule 25 DAI vs 18 DAI	Root 25 DAI vs 18 DAI	Nodule 25 DAI vs Root 25 DAI	Nodule 18 DAI vs Root 18 DAI
XM_02733 5766.1	^{Cyto} PEP carboxylase (PPC)	207.4±1.7	41.4±26.6	50.1±1.5	88.8±1.5	*2.3	-0.8	*2.0	*-1.1
XM_00449 5513.3	^{Cyto} PPCK PEP carboxylase kinase (PEPCK)	693.5±1.7	233.2±3.4	61.8±1.5	96.6±8.8	*1.6	-0.6	*3.5	*1.3
XM_02733 4755.1	^{Cyto} Alkaline sucrose-specific invertase (cwINV)	1.6±0.6	3.9±0.2	1.3±1.1	1.5±0.3	*-1.3	-0.3	*0.3	*1.3
NM_0013 64991.1	^{Extr} Vacuolar invertase inhibitor (VINV-INHIB)	41.3±3.5	13.9±3.7	15.7±5.1	7.6±0.5	0.7	-0.4	*-4.4	*-5.5
XM_00450 7978.3	^{Chlo/Mito} Sucrose synthase (SuSy)	1509.5±103.6	641.7±25	339.6±43.4	386.1±36.9	*1.6	*1.0	*1.4	*0.9
XM_00450 8392.3	^{Nucl} Sucrose phosphate synthase (SPS)	14.2±0.2	10.5±0.7	15.8±2.6	19.5±0.3	*1.2	-0.2	*2.2	*0.7
XM_00449 5321.3	^{Cyto} Malate dehydrogenase (MDH)	134.1±7.3	58.6±12.1	86.8±1.8	118.1±9.2	*0.4	-0.3	-0.2	*-0.9

Significant (P-adjusted value <0.01) DEG log₂ fold change displayed with an *. TargetP/WolfPsort analysis, Pero: Peroxisomal, Mito: Mitochondria, Chlo:

Chloroplast, Cyto: Cytoplasmic, Nucl: Nuclear, Vacu: Vacuolar, Extr: Extracellular, Plas: Plasma Membrane, ER: Endoplasmic Reticulum.

Table 4.5: Glycolysis expression profile in chickpea.

Data displayed as Log₂ fold change as a heatmap with corresponding average FPKM for each gene. Data presented for all nodule and root comparisons, 18 DAI (Early-Fixing) and 25 (Peak-Fixing).

mRNA Acc.	GENE NAME	AVERAGE FPKM				LOG ₂ FOLD CHANGE			
		25 DAI Nodule	18 DAI Nodule	25 DAI Root	18 DAI Root	Nodule 25 DAI to 18 DAI	Root 25 DAI to 18 DAI	Nodule 25 DAI vs Root 25 DAI	Nodule 18 DAI vs Root 18 DAI
XM_0045 12996.3	CytoHexokinase-1	13.2±0. 8	10.5±0. 8	4.9±0. 2	4.6±0. 2	*0.3	0.1	*1.4	*1.2
XM_0273 31919.1	CytoGlucose-6-phosphate isomerase, cytosolic	30.5±0. 9	24.1±3. 2	33.9±4 .2	33.7±1 .7	0.3	0.0	-0.2	*-0.5
XM_0044 98138.3	Cytocytosolic phosphofructokinase		97.9±7. 85±4.9	41.5±3 .8	48.6±4 .7	-0.2	-0.2	*1.0	*1.0
XM_0045 17220.3	CytoATP-dependent 6- phosphofructokinase 3	178.3±6 .6	107.9±1 5	53.9±1 .2	38±5.5	*0.7	*0.5	*1.7	*1.5
XM_0127 18397.2	CytoATP-dependent 6- phosphofructokinase 5, chloroplatic	34.6±0. 6	22.4±2	29±2.5	27.1±1	*0.6	0.1	*0.3	*-0.3
XM_0127 15948.2	NuclCytosolic fructose- bisphosphate aldolase			17.7±2 .2	17.7±2 .4	*1.4	0.0	-0.1	*-1.5
XM_0044 96959.3	ChloFructose-1,6-bisphosphate aldolase	123.5±4 .7	156.7±4 .6	131.5± 14.7	139.9± 8.6	*-0.3	-0.1	-0.1	0.2
XM_0273 33843.1	ChloFructose-bisphosphate aldolase	677.9±3 4.5	202.7±1 07.3	199.9± 58.3	267.1± 48.4	*1.7	-0.4	*1.8	-0.4
XM_0044 89080.3	Transaldolase	125.9±3 .7	123.5±5 .1	209±7. 5	200±4. 9	0.0	0.1	*-0.7	*-0.7
XM_0044 86950.3	Chlotriose-phosphate isomerase	281.2±6 .5	267.9±1 8.3	204.2± 27	278.1± 21.4	0.1	*-0.4	*0.5	-0.1
NM_0013 65164.1	CytoGlyceraldehyde phosphate dehydrogenase 1 cytosolic	780.3±3 3.4	520.3±5 8.5	380.8± 45.3	411.4± 25.3	*0.6	-0.1	*1.0	0.3
XM_0044 88706.2	ChloPhosphoglycerate kinase 1	58.4±3. 8	43.2±2. 3	29.4±3 .7	29.2±2 .4	*0.4	0.0	*1.0	*0.6

XM_0273 36585.1	Nucl Phosphoglycerate mutase	42.1±1. 7	30.3±4. 9	13.1±1 .5	14.2±1 .9	*0.5	-0.1	*1.7	*1.1
XM_0045 14917.3	Cyto Enolase 2	155.4±2 .3	90±18.2	17.8±0 .5	33.9±3 .5	*0.8	*-0.9	*3.1	*1.4
XM_0044 96443.3	Chlo Plastidial pyruvate kinase 2	45.2±1. 9	43.4±0. 8	24.7±1 .6	24.4±1 .3	0.1	0.0	*0.9	*0.8
XM_0044 91873.3	Cyto Pyruvate kinase 1, cytosolic	70.9±2. 5	44.6±5. 6	22.9±2 .4	21.3±1 .4	*0.7	0.1	*1.6	*1.1

Significant (P-adjusted value <0.01) DEG log₂ fold change displayed with an *. TargetP/WolfPsort analysis, Pero: Peroxisomal, Mito: Mitochondria, Chlo:

Chloroplast, Cyto: Cytoplasmic, Nucl: Nuclear, Vacu: Vacuolar, Extr: Extracellular, Plas: Plasma Membrane, ER: Endoplasmic Reticulum.

Table 4.6: DEGs of the Citric Acid Cycle in Chickpea.

Data displayed as Log₂ fold change as a heatmap with corresponding average FPKM for each gene. Data presented for all nodule and root comparisons, 18 DAI (Early-Fixing) and 25 (Peak-Fixing).

mRNA Acc.	GENE NAME	AVERAGE FPKM				LOG ₂ FOLD CHANGE			
		25 DAI Nodule	18 DAI Nodule	25 DAI Root	18 DAI Root	Nodule 25 DAI to 18 DAI	Root 25 DAI to 18 DAI	Nodule 25 DAI vs Root 25 DAI	Nodule 18 DAI vs Root 18 DAI
XM_0044 97046.3	^{Chlo} Pyruvate dehydrogenase complex (PDC)	58±3.4	84.5±3.6	47.1±3	49.4±4.7	*-0.5	-0.1	*0.3	*0.8
XM_0044 86724.3	^{Chlo} Malic enzyme (ME)	46.8±2	81.8±5.9	3.8±1	4.1±0.8	*0.7	-0.1	*-0.7	*-1.5
XM_0044 99943.3	^{Chlo} Citrate synthase (CYS)	19.1±0.8	27.3±2.7	26.5±2	28.5±2.4	*-0.3	-0.2	*-0.7	*-0.5
XM_0127 18003.2	^{Nucl} Aconitase (ACO)	42.2±1.8	50.4±2.1	55.8±3	59.9±2.7	0.3	0.1	0.1	-0.1
XM_0044 97460.3	^{Mito} Isocitrate dehydrogenase (IDH)	37.8±1.7	46.6±3.2	38.8±2	34.2±2.6	*0.5	0.1	*0.6	0.2
XM_0273 32745.1	^{Mito} Oxoglutarate dehydrogenase complex (ODC)	4±0.1	2.4±0.2	6.4±0.4	7±0.4	0.1	*0.3	*-0.4	-0.2
XM_0044 95017.3	^{Mito} Succinyl-CoA ligase (SCoAL)	6.8±0.5	10.9±1.1	70±6.9	98.4±2.8	-0.1	0.1	*0.3	*0.6
XM_0044 88880.3	^{Mito} Succinate dehydrogenase (SDH)	2.3±0.3	3.7±0.4	22.7±2	29.3±2.6	*0.6	-0.1	0.2	*-0.4
XM_0044 95875.3	^{Mito} Fumarase (FUM)	15.8±0.4	12.8±0.7	13.4±1	13.7±0.4	-0.2	-0.1	0.0	0.1
XM_0044 95321.3	^{Cyto} Malate dehydrogenase (MDH)	36.9±1.5	46.2±1.1	59.3±2	66.6±2.3	*1.2	-0.4	*0.6	*-1.0
XM_0044 93061.3	^{Chlo} Acetyl-CoA (AcCoA)	67.8±4.9	92.1±5	61.9±8	90.7±5.9	*1.3	*0.5	*1.2	*0.4
XM_0045 05118.3	^{Cyto} 2-oxoglutarate-dependent dioxygenase (2OG)	17.6±1.3	14.4±1.4	16.4±0	15.4±0.4	*3.0	0.4	*2.5	-0.1

XM_0044 95017.3	^{Mito} Succinyl-CoA (SucCoA)	22.9±1.1	15.7±2.5	14.6±0.7	13.7±1.1	-0.1	0.1	*0.3	*0.6
XM_0045 14815.2	^{Chlo} Mitochondrial pyruvate carrier (MPC)	100.4±2	91.8±6.2	129.4±4	102.8±3.9	*1.7	0.1	*-1.8	*-3.4

Significant (P-adjusted value <0.01) DEG log₂ fold change displayed with an *. TargetP/WolfPsort analysis, Pero: Peroxisomal, Mito: Mitochondria, Chlo:

Chloroplast, Cyto: Cytoplasmic, Nucl: Nuclear, Vacu: Vacuolar, Extr: Extracellular, Plas: Plasma Membrane, ER: Endoplasmic Reticulum.

4.5.2 Carbon transport in chickpea

Sucrose is the primary import from photosynthetic carbon into sink tissues such as nodules in legumes (Ayre, 2011). In chickpea particularly, the carbon import into nodules and between nodule compartments is poorly understood. SWEET3 is highly expressed in *L. japonicus* during nodule development but was found to be non-differentially expressed in the RNAseq dataset here in both nodules and root tissue (Sugiyama et al., 2017). Similarly, SWEET3 is believed to fall under clade 1 of the 4 SWEET clades established in *Arabidopsis* and appears to be involved in sucrose transport across the plasma membranes, mediating sucrose transport towards nodules (Chen et al., 2010, Sugiyama et al., 2017). This clade is also thought to be made up of both SWEET1 and SWEET2, where SWEET1 here was found to be the only one of three previously reported upregulated sucrose transporters in nodules and upregulated in roots (Doidy et al., 2019). Therefore, it appears that SWEET1 may be important in sucrose import into chickpea nodules during a period of heightened nitrogen fixation.

SWEET13 was upregulated in nodules from 30-day old chickpea under phosphate deficiency (La et al., 2022), indicating a possible stress related function in nodules. It has been suggested that SWEET13 in *M. truncatula* and *P. sativum* may also participate in loading of sucrose from source to sink organs (Doidy et al., 2019). However, SWEET13 in this study was downregulated at 25 compared to 18 DAI in both roots and nodules. It is possible *CaSWEET13* is a stress induced sucrose transporter, as La et al., (2022) also noticed that *CaSWEET13* was highly upregulated in both dehydrated and drought stressed roots. Similarly, *CaSWEET13* may be involved in early carbon import into nodules, as indicated by its high average FPKM in 18 DAI roots.

The overall function of these SWEET genes, particularly SWEET1 may be to import sucrose from the apoplast to either the infected or uninfected cells. The SWEET transporters, SWEET11 and SWEET3 from *M. truncatula* Kryvoruchko et al., (2016) and *L. japonicus* Sugiyama et al., (2017), respectively, were both found to be expressed in the nodule vasculature, meaning they could move sucrose through the apoplast. Ultimately, SWEET1 and other SWEET genes identified here likely behave in this manner, but their specific localisation in chickpea nodules remains unknown.

4.5.3 Carbon metabolism in chickpea

After sucrose import into nodules, it is typically broken down into hexoses via a cytosolic sucrose synthase and invertases (Gordon et al., 1999). SuSy converts sucrose to UDP-G and fructose (Fru), whereas invertases yields glucose (Glu) and fructose (Yarnes & Sengupta-Gopalan, 2009, Stein & Granot, 2019). Importantly, SuSy is typically correlated with the sink strength of the plant and can be a rate limiting step in nodule carbon metabolism (Yarnes & Sengupta-Gopalan). A SuSy mutant in pea with a 90% reduction in gene activity rendered those plants incapable of performing N₂ fixation, although they still produced nodules that appeared normal (Gordon et al., 1999). In chickpea nodules, sucrose is most likely converted

into UPD-G and Fru through the action of SuSy since it was significantly upregulated and exhibited one of the highest levels of expression in nodules at 25 DAI within in the RNAseq database. This is in contrast with the action of invertase in nodule tissue, since a vascular invertase inhibitor was found to be upregulated at 25 DAI compared to 18 DAI. The hexoses synthesised from the highly expressed action of SuSy may also be directed towards starch, since during non-stressful conditions, excess nodule carbon supply is redirected towards starch accumulation (Schulze, 2004, Redondo et al., 2009). It does not appear that sucrose biosynthesis is occurring from starch breakdown since sucrose phosphate synthase (SPS) was non-differentially expressed. This enzyme was found to be upregulated during starch breakdown in *M. truncatula* (Aleman et al., 2010). Interestingly, SPS overexpression in *M. sativa* caused an increased in nodule number and higher production of Asp and Gln, suggesting that increased carbon supply directed towards starch could be beneficial (Gebrill et al., 2015). This cycle of sucrose to starch back to glucose may be counterintuitive during heightened N₂ fixation, since there is evidence that the path of hexoses from upregulated SuSy activity is likely directed ultimately towards the production of malate. For example, PEPC and MDH were both significantly upregulated, whereas SPS was not, in my data set. Also, PEPC and MDH expression has been found to be directly related to N₂ fixation rates, where MDH strongly favors the production of malate from OAA (Vance, 2008). This suggests that chickpea nodules preferentially direct C metabolism to malate production under non-stressed conditions and may have no need of starch accumulation and C recycling, at least during the 18-25 DAI period used here.

The synthesis of malate is integral to nodule function since malate is fed to the infected cell bacteroids as the primary carbon fuel source to support N₂ reduction into ammonia (Udvardi & Poole 2013). Malate import into the bacteroid is believed to be mediated via dicarboxylic transporters (Dct) Udvardi & Poole (2013) particularly in soybean, Udvardi et al., (1988). SuSy as mentioned above was highly upregulated and would produce hexoses that can be converted into OAA by PEPC, then into malate via MDH, which was also highly upregulated. Regarding the model developed above (Figure 4.5), the specific localisation of these integral carbon metabolism enzymes is likely more widespread than depicted. For example, SuSy could be localised in both the infected and uninfected cells, although it was reported localised to a much greater extent in uninfected cortical cells compared to the infected cells (Zammit & Copeland 1993). This suggests that the conversion of sucrose to dicarboxylates such as malate occurs primarily in the uninfected cells. Similarly, immunogold labelling found greater intensity of labelling of SuSy in the cytosol of uninfected cells (Gordon et al., 1992). In *M. truncatula* indeterminate type nodules, SuSy promoter activity was found to be most active in the infected cells but was also observed in the uninfected cell region (Hohnjec et al., 2003).

If SuSy is found to be expressed in both the infected and uninfected cells, it is likely that glycolysis, the production of glucose, and the enzymes PEPC and MDH are also localised to both. Vance (2008) found that nodule enhanced MDH mRNAs were significantly more abundant in infected cells, while the cytosolic isoforms of MDH was found in uninfected cells. Similarly, the cytosolic form of MDH in *Lupinus angustifolius*

nodules showed enhanced activity under phosphorus deficient conditions, likely assisting in the amount of malate to maintain N₂ fixation (Le Roux et al., 2014). It would also be logical to assume that PEPC also exhibits an isoform in both cell types. Through immunogold cytochemistry in *Medicago sativa*, PEPC as expected was localised evenly in both the infected and uninfected cells (Robinson et al., 1996).

In addition to SWEET13 upregulation, there were two Sugar Transport Protein (STP) genes of interest, STP10 and STP13. STPs are a sugar transport family belonging to the Monosaccharide Transporters (MSTs) (Saier et al., 2016). They are believed to function as plasma membrane hexose symporters, facilitating the transport of glucose primarily as well as fructose, galactose, xylose and mannose (Büttner 2010, Schubert et al., 2011). *MtSTP13* has been found highly expressed in both root and nodule tissue in *M. truncatula*, particularly in nodules under photosynthate limiting conditions by Komaitis et al., (2020), and was induced during nodule development (Kryvoruchko et al., 2016). Conversely, STP13 in *P. vulgaris* was correlated with an accumulation of sugars under Fe/Zn stress (Urwat et al., 2021).

STPs are thought to be induced in a coordinated manner with cell wall invertases (cwINVs) involved in sucrose cleavage into hexoses, since both STP and cwINV gene expression increased in a coordinated response (Gupta et al., 2021). However, the function of STP13 in this study is not clear since there was essentially no cwINV activity. It is believed that STPs may be localised in the infected cells of the nodules due to the transporter's low pH optimum, and functions to export Glc to symbiotic bacteria during early N₂ fixation or to salvage monosaccharides lost in cell wall biosynthesis (Schubert et al., 2011, Kryvoruchko et al., 2016). It could therefore be concluded that the STPs identified here may be involved in glucose transport in or out of the infected or uninfected cells.

4.5.4 Chickpea nodules exhibit upregulation of the GS/GOGAT cycle and amide synthesis.

During nitrogen fixation within the bacteroids of the infected nodule cells, ammonia (NH₃) is reduced from atmospheric N₂ through the action of nitrogenase driven by ATP synthesised from the malate fed into the bacteroid TCA Cycle as mentioned previously (Figure 4.5). NH₃ is exported out of the bacteroid and transitioned into ammonium (NH₄⁺) by protonation after moving through the symbiosomal membrane. The resulting NH₄⁺ can then be used to synthesise fixed N as amino acids and amides to support overall nodule function and provide a nitrogen source for the rest of the plant in amidic legumes. Alternatively, products of amino acid synthesis, namely the amide glutamine (Gln) can be driven to the plastids within the infected cells as precursors to purine synthesis and subsequently ureide production. The RNAseq dataset in chickpea nodules showed significant upregulation of amino acid and amide synthesis pathways but non-differential and low expression of both the purine synthesis pathway, ureide synthesis and ureide catabolism (Figure 4.5), suggesting that the path of NH₄⁺ assimilation in chickpea is into amides. In this context, GS/GOGAT expression was highly upregulated in chickpea nodules with a Log₂FC increase of 1.5 and 1.8, respectively

(Table 4.7). Both enzymes also exhibited a high level of expression with an average FPKM of 121.1 to 349.9 and 22.8 to 81.8 from 25 to 18 DAI for GS and GOGAT, respectively (Table 4.7). Gln is either used for purine synthesis, exported from the nodule or used in the synthesis of the primary amide, Asn, via asparagine synthase (AS) (Figure 4.5). Both the root and nodule annotated AS genes were significantly upregulated in the nodule at a Log₂FC increase of 3.4 and 2.8, respectively (Table 4.7). Both genes also displayed a high level of expression with an average FPKM of 145.3 and 269.2 at 25 DAI (Table 4.7). Similarly, NH₄⁺ could be directed to the production of Glu via a Bi-functional glutamate prephenate aminotransferase (GluPAA-AT), which showed a Log₂FC increase of 2.2 (Table 4.8).

Along with GOGAT, several other aminotransferases were also highly upregulated, indicating increased amino acid production in chickpeas nodules at 25 compared to 18 DAI. The probable exported product of the TCA Cycle in the infected cell mitochondria, OAA, can be directed to the synthesis of aspartate (Asp) via aspartate aminotransferase (Asp-AT) (Figure 4.5). Asp-AT was significantly upregulated with a Log₂FC increase of 1.5 and average FPKM of 138.6 at 25 DAI (Table 4.8). The amino acid Glu is also responsible for the synthesis of the neutral amino acid, alanine (Ala). This reaction is catalysed via the reversible action of alanine aminotransferase (Ala-AT), also significantly upregulated with a Log₂FC increase of 3.0 (Table 4.8).

4.5.5 Upregulation of aminotransferases of the shikimate pathway

Other amino acids such as tyrosine (Tyr) and phenylalanine (Phe) are likely to be synthesised in the plastids via the shikimate pathway or through the cytosolic prephenate dehydrogenase (PDH) enzyme (Figure 4.5). The synthesis of prephenate from chorismate via chorismate mutase (CM) was found to be non-differentially expressed in chickpea nodules at 25 compared to 18 DAI (Table 4.7). Importantly, bifunctional glutamate/aspartate-prephenate aminotransferase (BiGluAspPPA-AT), the next step in the shikimate pathway for the transamination of arogenate (AGN) to form prephenate, was significantly upregulated at a Log₂FC increase of 2.2 (Table 4.8). This step could also be catalysed by the upregulated Glutamate/Prephenate aminotransferase (GluPAA-AT) mentioned previously (Table 4.8). The plastidic arogenate dehydrogenase (ADH), for the oxidative decarboxylation of AGN to Tyr, was not found in the RNAseq database but arogenate dehydratase (ADT), which catalyses the conversion to Phe, was found to be non-differentially expressed at a Log₂FC of -0.4 (Table 4.7). Tyrosine can, however, be synthesized by the 4-hydroxyphenylpyruvate (HPP) pathway in the cytosol after chorismate and prephenate cytosol synthesis, via prephenate conversion to HPP by prephenate-specific TyrAp dehydrogenase (PDH), which was also non-differentially expressed at 0.8 Log₂FC (Table 4.7). Following this, HPP can be synthesised to Tyr via transamination, catalysed by tyrosine aminotransferase (Tyr-AT), which was found to be highly upregulated with a Log₂FC increase of 4.6 at 25 DAI compared to 18 DAI (Table 4.8). The shikimate pathway did not appear to be as upregulated as other pathways within the nodules and the only upregulated enzymes were aminotransferases, which likely perform additional functions outside of the pathway. It is also unclear if

these bifunctional aminotransferases were upregulated because of their alternative function rather than Tyr or Phe synthesis.

Table 4.7: DEGs involved in nitrogen and amino acid metabolism in chickpea.

Data displaying DEGs as a Log₂ fold change as a heatmap with corresponding average FPKM for each gene. Data presented for all nodule and root comparisons, 18 DAI (Early-Fixing) and 25 (Peak-Fixing).

mRNA Acc.	GENE NAME	AVERAGE FPKM				LOG ₂ FOLD CHANGE			
		25 DAI Nodule	18 DAI Nodule	25 DAI Root	18 DAI Root	Nodule 25 DAI vs 18 DAI	Root 25 DAI vs 18 DAI	Nodule 25 DAI vs Root 25 DAI	Nodule 18 DAI vs Root 18 DAI
XM_0044 98962.3	CytoL-asparaginase (ASPG)	279.8±3 5.1	731.4±1 16.9	240.0± 47.0	169.3± 32.5	*-1.4	0.5	0.2	*2.1
XM_0044 90556.3	CytoGlutamine-dependent asparagine synthetase (AS) Root	145.3±1 8.0	14.0±7. 7	303.6± 39.2	288.6± 48.3	*3.4	0.1	*-1.1	*-4.4
XM_0045 00222.3	CytoGlutamine-dependent asparagine synthetase (AS) Nodule	269.2±5 4.7	37.5±10 .0	104.8± 24.4	72.7±1 6.2	*2.8	0.5	*1.4	*-1.0
XM_0045 12714.3	CytoGlutamine synthetase nodule isozyme (GS)	349.9±1 7.8	121.1±4 8.9	46.3±4 .0	57.6±1 .1	*1.5	-0.3	*2.9	*1.1
XM_0045 03065.3	CytoGlutamine synthetase nodule isozyme (GS)	264.5±1 1.4	143.9±1 9	239.3± 30.9	233±1 8.2	*0.9	0.0	0.1	*-0.7
XM_0127 15195.2	ChloNADH-dependent glutamate synthase (NADH-GOGAT)	81.8±11 .4	22.8±6. 7	36.0±4 .7	21.7±2 .5	*1.8	0.7	*1.2	0.1
XM_0044 86045.3	ChloPlastidial glutamine synthetase (GLN2)	186.4±1 9.5	221.8±1 7.4	94.0±1 7.4	64.7±9 .6	*-0.3	0.5	*1.0	*1.8
NM_0013 09686.1	ChloThreonine synthase 1, chloroplasmic	65.4±1. 8	19.5±5	34.1±2 .7	23.2±3 .1	*1.7	0.6	*0.9	-0.3
XM_0045 13774.2	PeroNitrate reductase	45.1±6. 4	5.8±1.7	467.3± 81.7	229.8± 62.2	*3.0	*1.0	*-3.4	*-5.3
XM_0044 90073.3	ChloChorismate mutase (CM)	7.6±1	11.1±0. 9	10.4±1 .2	9.7±0. 9	*-0.5	0.1	*-0.4	0.2
XM_0045 06077.3	MitoArogenate dehydratase (ADT)	21.2±1. 8	27.3±2. 3	52.6±4 .4	72.4±3 .9	*-0.4	*-0.5	*-1.3	*-1.4
XM_0127 18045.2	ChloArogenate dehydrogenase (ADH)	45.3±4. 5	26.5±2. 5	0.7±0. 1	0.8±0. 2	*0.8	-0.2	*6.1	*5.1

XM_0044 91260.3	^{Chlo} Hydroxyphenylpyruvate dioxygenase (HPPD)	135.1±9 .9	86.9±18 .1	87.2±7 .3	85.4±6 .9	*0.6	0.0	*0.6	0.0
--------------------	---	---------------	---------------	--------------	--------------	------	-----	------	-----

Significant (P-adjusted value <0.01) DEG log₂ fold change displayed with an *. TargetP/WolfPsort analysis, Pero: Peroxisomal, Mito: Mitochondria, Chlo: Chloroplast, Cyto: Cytoplasmic, Nucl: Nuclear, Vacu: Vacuolar, Extr: Extracellular, Plas: Plasma Membrane, ER: Endoplasmic Reticulum.

Table 4.8: Aminotransferase DEGs in chickpea involved in amino acid biosynthesis and nitrogen metabolism.

Data displayed as Log₂ fold change as a heatmap with corresponding average FPKM for each gene. Data presented for all nodule and root comparisons, 18 DAI (Early-Fixing) and 25 (Peak-Fixing).

mRNA Acc.	GENE NAME	AVERAGE FPKM				LOG ₂ FOLD CHANGE			
		25 DAI Nodule	18 DAI Nodule	25 DAI Root	18 DAI Root	Nodule 25 DAI to 18 DAI	Root 25 DAI to 18 DAI	Nodule 25 DAI vs Root 25 DAI	Nodule 18 DAI vs Root 18 DAI
XM_004492477.3	PeroAlanine/glyoxylate aminotransferase	46.8±7.6	5.8±1.4	52.7±10.3	61.7±6.9	*3.0	-0.2	-0.2	*-3.4
XM_004489730.3	PeroGlutamate/glyoxylate aminotransferase	32.3±2.0	24.9±1.5	32.3±2.6	34.7±1.0	*0.4	-0.1	0.0	*-0.5
XM_004510513.3	MitoAlanine aminotransferase (Ala-AT)	136±4.2	88.4±1.7	73.8±7.5	71.3±7.0	*0.6	0.1	*0.9	0.3
XM_004498719.3	Chlo/MitoAspartate aminotransferase 3 (Asp-AT)	138.6±8	50.0±1.8	12.6±1.9	14.4±0.9	*1.5	-0.2	*3.5	*1.8
XM_004503990.3	Chlo/MitoBifunctional glutamate/aspartate-Prephenate aminotransferase (BiGluAspPPA-AT)	93.4±17.4	20.0±6.4	12.5±1.4	18.0±1.0	*2.2	-0.5	*2.9	0.1
XM_004503990.3	Chlo/MitoGlutamate/Prephenate aminotransferase (GluPAA-AT)	126.2±2.8	28.2±9.2	18.0±2.2	25.4±1.9	*2.2	-0.5	*2.8	0.2
XM_004511195.3	ChloTyrosine aminotransferase (Try-AT)	25.2±4.9	1.1±0.8	3.0±1.1	2.6±1.5	*4.6	0.1	*3.1	*-1.4

Significant (P-adjusted value <0.01) DEG log₂ fold change displayed with an *. TargetP/WolfPsort analysis, Pero: Peroxisomal, Mito: Mitochondria, Chlo:

Chloroplast, Cyto: Cytoplasmic, Nucl: Nuclear, Vacu: Vacuolar, Extr: Extracellular, Plas: Plasma Membrane, ER: Endoplasmic Reticulum.

4.5.6 Non-differential expression of the ureide biosynthesis pathway

The amide Gln is either exported from the nodules as a source of fixed N for the plant or used in the purine synthesis and degradation pathway, prior to ureide synthesis (Figure 4.5). The expression of all enzymatic steps of the multistep purine synthesis pathway in the plastid of the infect cells were non-differentially expressed in the RNAseq database and also exhibited a low level of expression (Figure 4.5). Similarly, many of the enzymes from the purine synthesis pathway were close to downregulated expression, Pur5, Pur6 and Pur8 had a Log₂FC of -0.7, -0.9 and -0.7, respectively, indicating very minor overall conversion of Gln to xanthine (Table 4.9). Conversion of xanthine to urate via Xanthine dehydrogenase (XDH) also showed non-differential gene expression with an FDR >0.01 (Table 4.9).

Ureide synthesis occurs after urate transport into the peroxisome of the uninfected cell via two enzymes, one of which was upregulated (Figure 4.5). Uricase responsible for the synthesis of 5-hydroxyisourate was significantly upregulated with a Log₂FC increase of 1.8 and a high average FPKM of 49.5 to 173.6 at 18 to 25 DAI (Table 4.9). The production of the ureide (S)-Allantoin from 5-Hydroxyisourate via 5 Hydroxyisourate hydrolase (HIU) exhibited a non-differentially expressed Log₂FC with a FDR >0.01 (Table 4.9).

Allantoin from this point would either exported from the nodules to the rest of the plant as a N source or catabolised in the endoplasmic reticulum of the uninfected cells (Figure 4.5). The export of allantoin out of the nodules was likely directed by ureide permease (UPS) 1 or 2, however both found to be non-differentially expressed with a Log₂FC of 0.9 and 0.3 for UPS1.1 and UPS2, respectively (Table 4.10). Both UPS1.1 and UPS2 had a minor level of expression at 25 DAI at 36.9 and 33.1, respectively (Table 4.9). Allantoin catabolism in the endoplasmic reticulum is directed by four enzymatic steps. Step one, three and four directed by Allantoinase (ALN), Ureidoglycine aminohydrolase (Ugly-AH) and Ureidoglycolate amidohydrolase (UAH) were all non-differentially expressed with an FDR >0.01 (Table 4.9). Lastly step two via Allantoate amidohydrolase (AAH), was only marginally significantly upregulated with a Log₂FC of 1.0 and with a low average FPKM (Table 4.9). In summary, the enzymatic steps involved in ureide synthesis and catabolism showed either low expression levels with a Log₂FC <1 or were non-differentially expressed at 25 compared to 18 DAI. This indicated a lack of nodule activity towards the production of ureides as opposed to amino acids and amides discussed above.

Table 4.9: Purine synthesis and degradation pathway expression profile in chickpea.

Data displaying DEGs as Log₂ fold change as a heatmap with corresponding average FPKM for each gene. Data presented for all nodule and root comparisons, 18 DAI (Early-Fixing) and 25 (Peak-Fixing).

mRNA Acc.	GENE NAME	AVERAGE FPKM				LOG ₂ FOLD CHANGE			
		25 DAI Nodule	18 DAI Nodule	25 DAI Root	18 DAI Root	Nodule 25 DAI to 18 DAI	Root 25 DAI to 18 DAI	Nodule 25 DAI vs Root 25 DAI	Nodule 18 DAI vs Root 18 DAI
XM_004 494921.3	^{Chlo/Mito} Amidophosphoribosyltransferase 1 (Pur1)	33.9±2.3	53.3±3.7	37.3±1.8	38.1±3.1	*-0.7	0.0	-0.1	*0.5
XM_004 498225.3	^{Chlo/Mito} Phosphoribosylamine glycine ligase (Pur2)	1.8±0.1	2.5±0.7	1.1±0.3	1.1±0.1	*-0.5	0.0	0.7	*1.2
XM_004 498402.3	^{Chlo} Phosphoribosylglycinamide formyltransferase (Pur3)	12.3±0.5	12.0±1.1	10.7±0.5	9.8±0.6	0.0	0.1	0.2	*0.3
XM_004 509813.3	^{Chlo} Aminoimidazole RN synthetase (Pur5)	16.9±0.6	27.6±2.7	16.5±1.2	17.9±0.8	*-0.7	-0.1	0.0	*0.6
XM_004 495540.3	^{Chlo} Phosphoribosylaminoimidazole carboxylase (Pur6)	10.6±1.5	20.0±1.6	9.9±0.8	8.4±0.5	*-0.9	0.2	0.1	*1.2
XM_004 505667.2	^{Chlo/Mito} Succino-aminoimidazole-carboximide RN synthetase (Pur7)	10.6±0.6	11.7±1.1	9.5±0.8	7.9±0.3	-0.1	0.3	0.1	*0.6
XM_004 490607.3	^{Chlo} Adenylosuccinate lyase (Pur8)	9.2±0.3	15.3±1.1	9.1±0.6	8.0±0.5	*-0.7	0.2	0.0	*0.9
XM_004 516521.3	^{Chlo} Aminoimidazole-carboximide RN transformylase/IMP cyclohydrolase (Pur9/10)	27.6±1.4	28.6±2.2	20.1±2.8	15.5±0.5	-0.1	0.4	*0.5	*0.9
XM_004 493468.3	^{Chlo} Adenylosuccinate synthetase (Pur11)	20.4±0.5	24.6±0.8	14.1±0.3	12.2±0.8	*-0.3	0.2	*0.5	*1.0
XM_004 486904.3	^{Chlo} Xanthine dehydrogenase (XDH)	3.2±0.4	3.0±0.4	7.1±0.4	7.2±0.1	0.1	0.0	*-1.1	*-1.3
NM_001 279099.1	^{Pero} Urate oxidase/uricase (UOX)	173.6±17.3	49.5±7.6	24.2±3.5	31.3±3.9	*1.8	-0.4	*2.8	*0.7
XM_004 510143.3	^{Nucl} 5 Hydroxyisourate hydrolase (HIU)	16.1±1.7	15.1±1.2	12.7±1.9	14.6±0.2	0.1	-0.2	0.3	0.1

XM_004 485692.3	Vacu	Allantoinase (ALN)	17.3±2. 2	14.9±1. 7	12.8± 2.8	17.3± 1.8	0.2	-0.4	0.4	-0.2
XM_004 487850.3	Chlo	Allantoate amidohydrolase (AAH)	1.9±0.3	1.0±0.3	5.8±0. 2	3.6±0. 4	*1.0	0.7	*-1.6	*-1.9
XM_004 508907.3	Chlo	Ureidoglycine aminohydrolase (UGly-AH)	14.7±0. 9	17.5±1. 3	9.7±0. 8	8.0±0. 6	-0.2	0.3	*0.6	*1.1
XM_004 495288.3	Extr	Ureidoglycolate amidohydrolase (UAH)	34.5±1. 8	26.2±0. 7	25.7± 1.8	22.2± 0.7	*0.4	0.2	*0.4	*0.2

Significant (P-adjusted value <0.01) DEG log₂ fold change displayed with an *. TargetP/WolfPsort analysis, Pero: Peroxisomal, Mito: Mitochondria, Chlo:

Chloroplast, Cyto: Cytoplasmic, Nucl: Nuclear, Vacu: Vacuolar, Extr: Extracellular, Plas: Plasma Membrane, ER: Endoplasmic Reticulum.

Table 4.10: Ureide transporter DEGs in chickpea.

Data displayed as a Log₂ fold change heatmap with corresponding average FPKM for each gene. Data presented for all nodule and root comparisons, 18 DAI (Early-Fixing) and 25 (Peak-Fixing).

mRNA Acc.	GENE NAME	AVERAGE FPKM				LOG ₂ FOLD CHANGE			
		25 DAI Nodule	18 DAI Nodule	25 DAI Root	18 DAI Root	Nodule 25 DAI to 18 DAI	Root 25 DAI to 18 DAI	Nodule 25 DAI vs Root 25 DAI	Nodule 18 DAI vs Root 18 DAI
XM_00449 0134.3	PlasUreide Permease 1 (UPS1.1)	36.9±4.7	19.7±9.0	30.8±3. 8	37.9±6. 1	*0.9	-0.3	0.3	*-0.9
XM_00449 0134.3	PlasUreide Permease 1 (UPS1.2)	10.7±2.2	6.3±2.2	8.3±1.2	11.0±1. 7	0.8	-0.4	0.4	*-0.8
XM_02733 2154.1	PlasUreide Permease 2 (UPS2)	33.1±2.3	26.0±2.5	41.2±1. 1	39.1±3. 3	*0.3	0.1	*-0.3	*-0.6

Significant (P-adjusted value <0.01) DEG log₂ fold change displayed with an *. TargetP/WolfPsort analysis, Pero: Peroxisomal, Mito: Mitochondria, Chlo:

Chloroplast, Cyto: Cytoplasmic, Nucl: Nuclear, Vacu: Vacuolar, Extr: Extracellular, Plas: Plasma Membrane, ER: Endoplasmic Reticulum.

4.6 Chickpea Predominantly Synthesise Amides from Fixed Nitrogen

The scheme developed above (Figure 4.5) based on the RNAseq analysis shows evidence to suggest that chickpea can be classified as an amide producer rather than a ureide producer. Chickpeas harbour indeterminate type nodules typical of other amide-producing legumes, as discussed in chapter 1.2.3 and described in the literature (Liu et al., 2018). However, transcript expression profiles of amide, purine and ureide metabolism genes was previously unknown in the early onset on N₂ fixation in chickpea. Understanding the pathway of fixed N in chickpea nodules can open avenues for further research and genetic improvement to improve N₂ fixation.

4.6.1 The synthesis of amino acids and amides in chickpea

While the activity of the nitrogenase enzyme cannot be determined through the RNAseq database here due to the bacterial enzyme origin, other indicators of nodule N₂ fixation were upregulated in the RNAseq database. Irrespective of amide or ureide synthesis, the initial metabolism of NH₄⁺ is the same with the conversion to Glu and Gln via the glutamine synthetase and glutamate synthase (GS-GOGAT) pathway (Schwember et al, 2019, Todd et al., 2006, Vance, 2000).

GS is responsible for catalysing the ATP-dependent amination of Glu yielding Gln (Temple et al., 1998). Immunocytochemical localisation in *M. sativa* by Carvalho et al., (2000), found two isoforms, separated by subcellular location, as cytosolic or plastidic (Melo et al., 2011). In my study, two GS isozymes were found to be significantly upregulated, while expression of a single plastidic version was non-differentially expressed. The cytosolic GS in the central infected cells of *M. truncatula* is highly upregulated during N-fixation and accounts for up to 90% of GS enzymatic activity within the nodules (Melo et al., 2011, Carvalho et al., 2000). It is likely therefore, that the two chickpea nodule isozymes are cytosolic localised, accounting for their significant upregulation. Because GS plays a key role in the subsequent assimilation of essentially all nitrogenous compounds, GS activity can be an indirect indication of the rate of N₂ fixation (Lea et al., 2010, García-Calderón et al., 2012). In *L. japonicus*, GS mutants showed strong inhibition of acetylene reduction, a measure of nitrogenase activity, and the number of nodules, resulting in significant limitations in carbon metabolism and nitrogen fixation (García-Calderón et al., 2012).

GOGAT, the second step of the GS/GOGAT pathway is responsible for catalysing the transfer of the amide group from glutamine to α -ketoglutarate yielding glutamate; immunochemical localisation found it to be located in the infected cells amyloplasts (Temple et al., 1998, Trepp et al., 1999). The GS/GOGAT pathway, along with MDH and PEPC are thought to be critical steps in carbon-nitrogen metabolism in legumes and are all highly induced during nitrogen fixation (Udvardi & Poole, 2013, Vance & Gantt, 1992). In line with this, GOGAT, MDH and PEPC expression was significantly upregulated in a coordinated manner at 25 compared to 18 DAI nodules indicating a period of increased N₂ fixation and ammonium assimilation.

It is important to note that the upregulation of GOGAT is likely related to increased amide production here in chickpea. For example, the GS-GOGAT pathway is involved in the production of the amides Gln and Asn, which are important in indeterminate type nodules of temperate legumes (Schwember et al, 2019). Antisense inhibition of NADH-GOGAT in *M. sativa*, an amide producer, saw a concomitant reduction in N assimilation and carbon metabolism with nodules exhibiting a significant reduction of amino acids and amides (Cordoba et al., 2003). Additionally, the nodules in the study also showed an increase in sucrose accumulation showing a critical bottleneck of N assimilation during impaired GOGAT activity (Cordoba et al., 2003).

Asn which is synthesised by AS using OAA as the C-skeleton and Gln, is the principle amino acid for N export out of the nodules, accounting up to 25% of the total amino acid pool in temperate legume nodules (Suliman et al., 2010, Berry et al., 2011). Asn also contains a high N:C ratio of 4:2 making it a very efficient form of N transport and storage (Yang et al., 2011). AS was found here to be significantly upregulated with upwards of a 3.3-fold increase at 25 compared to 18 DAI nodules. This may suggest heightened amide synthesis and possible export of Asn out of the nodules to serve as the primary source of long distant N supply in chickpea. Interestingly, however, legumes with determinate type nodules, particularly under stress, appear to also utilise Asn for N transport, with upwards of 30% nodule content seen in *G. max*, under drought stress (Ramos et al., 2005) and 18% for N-stress *G. max* nodules and 52% in the xylem sap (Lima & Sodek, 2003).

Various aminotransferases (ATs) were also significantly upregulated in chickpea nodules at 25 compared to 18 DAI. These ATs function to synthesise amides from products of N assimilation such as Glu mentioned above, biosynthesis or catabolism of Asp and synthesis of amino acids from the TCAC products, namely OAA (Bryan, 1980, Ryan & Fottrell, 1974, Farnham et al., 1990, Silvente et al., 2003). ATs are known to play important roles in amide production in indeterminate nodules but are still present in ureide producing legumes such as *G. max* (Gebhardt et al., 1998) and *P. vulgaris* (Silvente et al., 2003). Asp-AT was significantly upregulated in chickpea nodules and catalyses the reversible reaction of 2-oxoglutarate and Asp synthesis by amino group transfer from glutamate to oxalacetate (Givan, 1980). Asp-AT is also primarily localised to the infected cell plastids with a much lower frequency in the uninfected cells (Givan, 1980, Robinson et al., 1994, Yoshioka et al., 1999). Interestingly, in the ureide producer *P. vulgaris*, the nodule enhanced Asp-AT-2 showed increased abundance in nodules where there was an increase in amide production and downregulated in conditions where ureides accumulated (Silvente et al., 2003). These authors also found that the expression of AS involved in the production of the amide Asn was unaffected by feedback mechanisms by either amide or ureide synthesis.

Expression of Ala-AT, which is involved in the reversible reaction of alanine and 2-oxoglutarate from pyruvate and Glu, was non-differentially expressed here (Ricoult et al., 2006). Ala-AT may function to

synthesise alanine for nodule export to the rest of the plant or could be associated with N remobilisation by converting alanine to pyruvate for gluconeogenesis (Sakagishi, 1995). It has been suggested that legumes with both determinate and indeterminate nodules secrete fixed nitrogen as Ala and Asp from the bacteroid as well as ammonia, possibly through Ala production from Ala-AT (Allaway et al., 2000). However, Ala is not considered to be the main form of N secretion after alanine dehydrogenase deletions had no effect on symbiotic performance (Kumar et al., 2005).

Other ATs were also upregulated in chickpea nodules, namely Alanine-glyoxylate aminotransferase, bifunctional glutamate/aspartate-prephenate aminotransferase, glutamate-prephenate aminotransferase and tyrosine aminotransferase. These ATs have lesser-known functions in relation to N₂ fixation, but likely have some association, perhaps in supporting general nodule function due to the significant upregulation at 25 compared to 18 DAI in nodules.

Alanine-glyoxylate aminotransferase has reported functions in the photorespiratory pathway, where it catalyses transamination reactions with L-serine, L-alanine and L-asparagine as an amino acid donor and glyoxylate, pyruvate and hydroxypyruvate as amino acid acceptors (Zhang et al., 2013). This aminotransferase has somewhat overlapping functions with two additional aminotransferases, namely serine-glyoxylate aminotransferase and glutamate-glyoxylate aminotransferase, differing by their donor acceptors as serine and glutamine, respectively (Liepman et al., 2019). Glutamate-glyoxylate and serine-glyoxylate were both non-differentially expressed. These aminotransferases also appear to play important roles in the regulation of amino acid metabolism. The GS/GOGAT pathway was found to be involved in the reassimilation of ammonia released from the conversion of glycine to serine in photorespiration (Igarashi et al., 2003). Serine-glyoxylate aminotransferase has been postulated to function in a similar manner as AS with a high V_{max} with Asn, and Arabidopsis AS mutants grew normally with increased expression of serine-glyoxylate aminotransferase. Perhaps the reason why serine-glyoxylate aminotransferase was non-differentially expressed here was that the nodule isozyme of AS has a much greater affinity to metabolise Asn. It has also been found that alanine-glyoxylate aminotransferase mediates the reverse reaction of alanine aminotransferase in nodules of *L. japonicus* (Takanashi et al., 2012). It is important to note that these enzymes are most abundant in leaf tissue, not nodules.

A bifunctional glutamate/aspartate-prephenate aminotransferase (BiGluAspPPA-AT) was also significantly upregulated in chickpea nodules during the onset of N₂ fixation. *Nicotiana benthamiana* plants in which aspartate-prephenate aminotransferase was silenced, saw a severe reduction in plant growth, significantly reduced levels of Asn and reduced phenylalanine metabolism (Torre et al., 2014). The authors Torre et al., (2014) hypothesised that the bifunctional aminotransferase is involved in both the biosynthesis of Asp and the production of phenylalanine, possibly through the shikimate pathway. Similarly, in Arabidopsis a plastidic glutamate/aspartate-prephenate aminotransferase was found to be directly involved in the

synthesis of phenylalanine and Tyr (Graindorge et al., 2010). The above pathway is typically involved as part of the shikimate pathway known to take place in the plastids beginning with chorismate and production of prephenate via chorismate mutase, followed by the production of aroenate via a prephenate aminotransferase (PPA-AT) (Maeda & Dudareva, 2012). Aroenate can then be synthesised into the aromatic amino acids, Tyr, and phenylalanine, important in the synthesis of proteins (Maeda & Dudareva, 2012). Prephenate dehydratase (PDT) and prephenate dehydrogenase (PHD), which function in the synthesis of phenylalanine and Tyr, respectively, from aroenate, were both significantly non-differentially expressed. A GluPPA-AT was also significantly upregulated here at an almost identical rate as BiGluAspPPA-AT and may share a similar function as part of the shikimate pathway, whereas BiGluAspPPA-AT may have additional functions mentioned above.

In addition to the ATs discussed above, Tyr-AT was also significantly upregulated; it catalyses the reversible transamination of tyrosine from 4-hydroxyphenylpyruvic acid (HPP) (Xu et al., 2020). Try-ATs are diversely distributed in plants, catalysing the removal of the amino group of Tyr (Wang & Maeda, 2018). Unlike the activity of PDH in the shikimate pathway in the plastids, legumes have been found to possess a non-plastidic version of PDH converting PPA into HPP, followed by Tyr-AT transamination of HPP into Tyr (Schenck et al., 2015). PDH was non-differentially expressed here irrespective of its localisation. It is possible that the cytosolic version of PDH is not annotated correctly within the RNAseq reference genome here, or that it is not important in nodulating chickpea. *G. max* and *M. truncatula* have both been found to possess a cytosolic PDH, though, mutants in *M. truncatula* found that PDH had no significant effect on rhizobia symbiosis or N₂ fixation (Schenck et al., 2015, Schenck et al., 2020). The *M. truncatula* variant has also been found upregulated in nodules after nitrate treatment, which is known to stimulate senescence (Schenck et al., 2020). Without evidence of PDH activity in the cytosol, the upregulated Tyr-AT may alternatively be involved in the production of HPP which is a precursor to produce tocopherols and plastoquinone important for antioxidant and electron transport functions (Xu et al., 2020).

4.6.2 The synthesis and degradation of ureides in chickpea

Upregulation of GS/GOGAT, which produces Gln, is not in itself an indicator of an amidic legume, as Gln is also directed to the plastids in the infected cell for *de novo* purine synthesis and subsequent ureide synthesis (Smith & Atkins 2002). In determinate type legumes such as *G. max* and *P. vulgaris*, whose primary N export are the ureides allantoin and allantoic acid, these ureides can account as much as 80% of the nitrogenous compounds that are exported from nodules. (Rainbird et al., 1984, Atkins & Smith 2007, Collier & Tegeder 2012). It is evident in the nodule scheme developed above, however, that enzymes of purine and subsequent ureide synthesis are not expressed at a level that would be expected in determinate nodules. It can also be assumed that Gln synthesis via the significant GS/GOGAT upregulation is not being directed towards the purine synthesis pathway, in line with the data presented in chapter 3 regarding the

lack of ureide levels measured in chickpea nodules (Chapter 3.4.1). The entirety of the *de novo* purine synthesis pathway, which begins in the infected cell plastids and is a crucial step in the production of xanthine (Smith & Atkins, 2002, Collier & Tegeder, 2012), was found to have non-differential gene expression. Pur1, encoding the first step of the purine synthesis pathway, was found in early reports to be upregulated up to 7-fold in the presence of Gln in *G. max*, as opposed to show non-differential expression here (Kin et al., 1995). A recent study by Voß et al., (2022) outlined the importance of Pur1 in common bean nodules, with a very high nodule to root ratio of transcript abundance. However, the RNAseq data here showed no significant fold change comparing root to nodule transcript levels. This was corroborated by the same study where there was no significant transcript difference for Pur1 when comparing nodule and root tissue in *L. japonicus* or *M. truncatula*, both amide legumes (Voß et al., 2022). It was also discussed in chapter 3 that *GmPur1* showed significant upregulation over a time course during the onset of N₂ fixation in *G. max* (Chapter 3.3.2). Similarly, xanthine dehydrogenase (XDH) which synthesises urate in the infected cell plastids was also highly upregulated in *G. max* nodules, and non-differentially expressed here (Nguyen et al., 2021). Knockout mutants of XHD and urate oxidase/uricase (UOX) in *G. max* had a significant deficiency in N₂ fixation and displayed early onset of nodule senescence (Nguyen et al., 2021). This severe phenotype likely contributed to a cascading effect of nodule metabolism and an inability to establish effective N fixing nodules.

Interestingly, UOX, which is responsible for the synthesis of 5-Hydroxyisourate from urate prior to allantoin synthesis via 5 Hydroxyisourate hydrolase (HIU), was significantly upregulated here. In amide legumes *M. sativa* and *L. japonicus*, the levels of combined allantoin and allantoic acid in xylem sap have been measured at 0.05 and 0.06 mM, respectively, albeit much less than levels in *G. max* at 4.82 mM (Cheng et al., 1999, Cheng et al., 2000). The concentration of the uricase protein in *M. sativa* nodules was also found to be 10% of the concentration in *G. max* nodules (Cheng et al., 2000). The UOX gene from the RNAseq database showed 85% sequence similarity to nodulin 35 (Uricase) and uricase-2 in *G. max*. This may suggest that ureide production does occur at some degree in amidic legumes, possibly accounting for the upregulation of UOX. UOX does not appear to have alternative functions other than to produce 5-Hydroxyisourate in the uninfected cell plastids, as well as in other plant tissues (Werner et al., 2011). Urate or uric acid, the substrate of UOX has been noted to be a strong scavenger of reactive oxygen species (ROS) due to particularly large mitochondria intensive function to support N₂ fixation in nodules, generating ROS (Sautin & Johnson, 2008, Voß et al., 2022). Hence, it could be hypothesized that there may be an accumulation of urate for ROS scavenging purposes, indirectly driving up the activity of UOX. This is purely speculation, as the genes responsible for the preceding enzymatic step of XDH was non-differentially expressed. Another hypothesis for the UOX activity could be attributed to possible associations of uric acid toxicity, promoting metabolism of uric acid. Accumulation of uric acid in Arabidopsis has been found to reduce seed germination, cotyledon development and peroxisome maintenance (Hauck et al., 2014). It

could be concluded that the low levels of ureides that can be measured in amidic legumes and seen in chapter 3.4.1 may be attributed to UOX expression even if HIU, the next step involved in allantoin production was non-differentially expressed. Without knowing the concentration of uric acid in chickpea nodules or the relative protein level of UOX, these hypotheses cannot be tested further.

Following the production of allantoin in the plastids of the uninfected cells, allantoin can either be exported from the nodules or transported into the endoplasmic reticulum of the uninfected cells. Here allantoin can be hydrolysed into allantoate, also known as the ureide allantoic acid via allantoinase (ALN), which was non-differentially expressed here in chickpea (Werner et al., 2008). Ureide permeases (UPS) are well characterised to be involved in allantoin and allantoic acid export from the nodules which are located in the endodermis for symplast import into the vasculature tissue (Pélissier, et al., 2004, Collier & Tegeder, 2012, Lu et al., 2022). UPS1 was non-differentially expressed with a moderately low level of expression, possibly accounting for nodule export for the low levels of ureide production discussed above.

Ureide catabolism in the endoplasmic reticulum after allantoin production is a relatively complex enzymatic process involved in the N remobilisation of ureides through purine ring catabolism, yielding glyoxylate, ammonium and urea (Voß et al., 2022). The first step hydrolysing allantoate to S-ureidoglycine via allantoate amidohydrolase (AAH) showed a significant fold change in expression, however exhibited very low expression level (Serventi et al., 2010). Next S-ureidoglycine is cleaved hydrolytically to S-ureidoglycolate also yielding ammonium via Ureidoglycine aminohydrolase (UGlyAH), which was non-differentially expressed (Werner et al., 2010). S-ureidoglycine, however can also decay into glyoxylate, ammonia and urea over time without enzyme assistance (Werner et al., 2013). Lastly glyoxylate and ammonia are again produced via ureidoglycolate amidohydrolase (UAH) with non-differential expression, which hydrolyses S-ureidoglycine (Werner et al., 2010). Overall, at least in chickpea nodules, the purine ring remobilisation pathway of N is likely not occurring at any significant rate. This is not unexpected as most of the purine catabolism occurs in above ground tissue for the remobilisation of N from ureides, particularly in tropical ureidic legumes (Todd et al., 2006).

Although this process has been well studied there is some discussion around the final step involving Ureidoglycolate amidohydrolase (UAH) to hydrolyse S-ureidoglycolate, yielding presumably S-hydroxyglycine which may degrade nonenzymatically to glyoxylate and ammonia (Werner & Witte, 2011, Werner et al., 2013). Interestingly, it was first reported that chickpea possessed an enzyme that bypassed UAH and cleaved S-ureidoglycolate into glyoxylate and urea (Munzo et al., 2001). The activity of this enzyme was showed to exhibit highest activity levels in pods for nitrogen remobilisation. The authors Munzo et al., (2001) hypothesised that amidic legumes such as chickpea have no need for the additional step to yield ammonium because they export amides which can be readily catabolised into ammonium.

This notably provides additional evidence to suggest why the purine and subsequently ureide production in chickpea and amide legumes is not regulated as much as in ureidic legumes.

4.7 Upregulation of Key Amino Acid Transporters from Multiple Gene Families

4.7.1 Nitrate transporters

Several transporter families were identified in the RNAseq database relating to amino acid, nitrate, or diverse solute transport. Several transporters under the nitrate/peptide (NRT/PTR) transporter family were identified upregulated in either the nodules or roots tissues. Four transporters NR1/PTR 2.1, 5.2, 7.2 and 7.3 were significantly upregulated in nodule tissue at 25 compared to 18 DAI with a Log_2FC increase >1 , particularly NRT/PTR 2.1 and 7.3 at a Log_2FC of 5.4 and 4.6, respectively (Table 4.11). NRT2.1 was also significantly upregulated in root tissue (1.4 Log_2FC) and expressed at a high level with an average FPKM of 482.1 at 25 DAI (Table 4.11). Several other transporters were also identified from the NRT/PTR family but had low and/or non-differential expression (Appendix: Table 4a.6). It was, however, evident that nitrate and peptide transport processes were significantly upregulated in the chickpea nodules during a heightened period of N_2 fixation.

4.7.2 Amino acid permeases

Many amino acid permeases (AAPs) were identified, though several exhibited very low expression or were non-differentially expressed (Appendix: Table 4a.2). Surprisingly, there were no standout members of the AAP family that were highly upregulated in response to an increase in N_2 fixation. AAP3 and AAP6.2 were significantly upregulated in the nodules between 25 to 18 DAI, however, with a low level of expression (Table 4.12). Similarly, AAP1 and AAP2 had significantly altered expression between the two timepoints but with a low FPKM and <1 Log_2FC (Table 4.12). Two transporters AAP6.3 and AAP8 were expressed at a moderate level in the nodules irrespective of an increase in N_2 fixation, both with a Log_2FC <1 (Table 4.12). In the roots, only AAP6 and AAP7 were significantly expressed at a moderate to high level with a Log_2FC <1 (Table 4.12). AAP6.1 expression, on the other hand, was non-differentially expressed between 25 to 18 DAI but exhibited a moderate FPKM of 79.2 at 25 DAI. This suggests that the AAP6.1 isoform may be root localised and is downregulated in the nodules (-1.8 Log_2FC) (Table 4.12).

Table 4.11: DEGs involved in nitrate transport in chickpea.

Data displayed as Log₂ fold change as a heatmap with corresponding average FPKM for each gene. Data presented for all nodule and root comparisons, 18 DAI (Early-Fixing) and 25 (Peak-Fixing).

GENE NAME	AVERAGE FPKM				LOG ₂ FOLD CHANGE			
	25 DAI Nodule	18 DAI Nodule	25 DAI Root	18 DAI Root	Nodule 25 DAI to 18 DAI	Root 25 DAI to 18 DAI	Nodule 25 DAI vs Root 25 DAI	Nodule 18 DAI vs Root 18 DAI
Nitrate Transporter (NRT2.1)	111.3	2.6	482.1	187.6	*5.4	1.4	*-2.1	*-6.2
NRT1/PTR FAMILY 2.13	54.0	30.7	16.1	12.1	*0.8	0.4	*1.7	*1.3
NRT1/PTR FAMILY 3.1	102.0	73.3	5.9	5.9	0.5	0.0	*4.1	*3.6
NRT1/PTR FAMILY 4.6	82.9	68.0	11.1	6.3	0.3	*0.8	*2.9	*3.4
NRT1/PTR FAMILY 5.2	154.4	21.3	0.4	0.2	*2.9	1.2	*8.7	*7.0
NRT1/PTR FAMILY 7.1	107.7	54.0	0.2	0.2	*1.0	-0.3	*9.3	*7.9
NRT1/PTR FAMILY 7.3	101.6	4.2	45.0	21.2	*4.6	1.1	*1.2	*-2.3

Data with significant differences (P-adjusted value <0.01) displayed with a * as a log₂ fold change >1 or <-1.

Table 4.12: Amino acid permease DEGs in chickpea involved in amino acid transport.

Data displayed as Log₂ fold change as a heatmap with corresponding average FPKM for each gene. Data presented for all nodule and root comparisons, 18 DAI (Early-Fixing) and 25 (Peak-Fixing).

mRNA Acc.	GENE NAME	AVERAGE FPKM				LOG ₂ FOLD CHANGE			
		25 DAI Nodule	18 DAI Nodule	25 DAI Root	18 DAI Root	Nodule 25 DAI to 18 DAI	Root 25 DAI to 18 DAI	Nodule 25 DAI vs Root 25 DAI	Nodule 18 DAI vs Root 18 DAI
XM_004501077.3	^{Plas} AAP1	38.0±6.9	22.6±6.3	0.5±0.1	0.8±0.2	*0.8	-0.7	*6.4	*4.9
XM_004502924.3	^{Plas} AAP2	14.9±1.5	8.6±0.9	20.9±1.1	19.7±1.6	*0.8	0.1	*-0.5	*-1.2
XM_004498293.3	^{Plas} AAP3	6.9±0.9	1.0±0.2	10.5±1.1	11.1±0.8	*2.7	-0.1	*-0.6	*-3.4
XM_004501019.3	^{Plas} AAP6.1	4.2±1.7	14.1±2.6	79.2±14.6	71.1±6.3	*-1.8	0.2	*-4.2	*-2.3
XM_004496803.3	^{Plas} AAP6.2	21.9±3.1	2.0±2.2	0.1±0.0	0.1±0.0	*3.5	-0.1	*7.7	*4.1
XM_012715204.2	^{Plas} AAP6.3	74.9±8.0	60.6±3.3	78.4±4.7	103.8±2.7	*0.3	*-0.4	-0.1	*-0.8
XM_004491492.3	^{Plas} AAP7	16.7±1.3	19.5±1.4	42.2±7.4	74.5±5.5	-0.2	*-0.8	*-1.3	*-1.9
XM_004501037.3	^{Plas} AAP8	58.8±1.8	70.5±11.3	17.9±2.0	19.1±2.7	-0.3	-0.1	*1.7	*1.9

Significant (P-adjusted value <0.01) DEG log₂ fold change displayed with an *. TargetP/WolfPsort analysis, Pero: Peroxisomal, Mito: Mitochondria, Chlo: Chloroplast, Cyto: Cytoplasmic, Nucl: Nuclear, Vacu: Vacuolar, Extr: Extracellular, Plas: Plasma Membrane, ER: Endoplasmic Reticulum.

4.7.3 Amino acid vacuolar transporters

Several Amino acid vacuolar transporters (AVTs) were identified and exhibited significant upregulation between 25 to 18 DAI. Four were found to be upregulated in the nodules, namely AVT1A, AVT6A, AVT6C.1 and AVT6C.2, however, only AVT6A showed a high level of expression (Table 4.13). AVT6C.1, AVT6C.2 and AVT1A had a Log_2FC increase >1 , but with a low average FPKM, suggesting minor activity in amino acid transport in the nodules despite a fold increase (Table 4.13). AVT6C.1 was also slightly upregulated in the roots but with a much lower Log_2FC of 1.3, compared to a Log_2FC of 4.0 in the nodules (Table 4.13). AVT6A presented possible nodule and root tissue functionality with the highest level of expression in both tissues with an average FPKM of 248.2 and 204.9 at 25 DAI in nodules and roots, respectively (Table 4.13). The other AVTs likely function in both tissues as there was no clear indication of specific localisation expression.

4.7.4 Cationic amino acid transporters

Two notable members of the Cationic amino acid transporter (CAT) family, closely related to AAPs were identified in the RNAseq dataset (Table 4.13). Both CAT1 and CAT2 were significantly upregulated in the nodule tissue at 25 compared to 18 DAI with a Log_2FC increase of 1.6 and 1.5, respectively (Table 4.13). CAT1 displayed a moderate level of expression at 25 DAI and was expressed only in nodule tissue, while CAT2 showed a low level of expression in both nodules and roots but was not significantly upregulated during N_2 fixation in roots (Table 4.13).

4.7.5 Usually multiple acids move in and out transporters

Several other amino acid transporters were identified and jointly annotated as UmamiT (Usually Multiple Acids Move In And Out Transporter) and WAT1 (Walls Are Thin 1). These transporters showed a large range of expression with eight candidates showing localised expression in the nodules, three in the roots and seven with inconclusive localisation or constitutively expressed in both tissues. Additionally, 14 exhibited a significant Log_2FC expression increase in the nodules and only two with a Log_2FC increase and one decrease in the roots (Table 4.14). Several more were identified under this annotation but displayed very low average FPKM expression and were omitted (Appendix: Table 4a.4).

Four of the UmamiT/Wat1 genes were particularly promising: UmamiT9.2, UmamiT20.1, UmamiT18.1 and UmamiT23.2 (Table 4.14). UmamiT9.2 and UmamiT20.1 are likely the most promising transporters since expression was correlated with increased N_2 fixation in nodules, assuming that they in fact do transport amino acids. Both had a significant Log_2FC increase of 3.1 and 4.4 and a high average FPKM of 212.5 and 93.7 at 25 DAI, respectively (Table 4.14). Notably, these genes also displayed similar levels of expression in the roots possibly pertaining to a dual expression profile but did not show a significant Log_2FC at 25 compared to 18 DAI (Table 4.14). UmamiT18.1 and UmamiT23.2 were also highly upregulated with a significant Log_2FC increase of 2.1 and 2.0 with an average FPKM of 90.9 and 104.5 at 25 DAI, respectively

(Table 4.14). UmamiT18.1 also had near identical levels of expression in root tissue at 25 DAI but did not show a significant Log₂FC, whereas UmamiT23.2 had no root expression (Table 4.14).

Several more UmamiT genes from table 4.14 showed a significant Log₂FC increase at 25 from 18 DAI with moderate to low levels of expression. For example, UmamiT41.2 and UmamiT23.1 had moderate expression with an average FPKM of 55.4 and 60.3 for 25 DAI, respectively (Table 4.14). UmamiT41.2 had very similar expression in the roots but was not significantly upregulated (Table 4.14). UmamiT23.3 conversely had a high level of expression but was just short of a significant Log₂FC increase at 0.9; however, it may still be important for amino acid transport (Table 4.14).

One gene, UmamiT9.3, was marginally downregulated in the nodules (Log₂FC -0.80) but is likely still important during early nodule development, with an average FPKM of 92.5 at 18 DAI (Table 4.14). Out of the remaining seven genes from table 4.14, UmamiT9.4, UmamiT34, UmamiT12 and UmamiT24.1 appeared to display high or moderate levels of expression in the nodules over both time points but did not exhibit a significant Log₂FC. UmamiT9.4, UmamiT34 and UmamiT24.1 expression was also only localized to the nodules with no distinguishable expression in roots (Table 4.14). None of the UmamiT/WAT1 genes were significantly upregulated (>1 Log₂FC) in the roots from 25 to 18 DAI, however UmamiT9.2, UmamiT20.1, UmamiT18.1 and UmamiT18.2 were still highly expressed at both time-points with UmamiT18.2 only exhibiting root expression (Table 4.14). Out of all the potential amino acid transporters identified in the RNAseq dataset, the UmamiT genes presented the most promising expression profiles correlated with N₂ fixation. It does, however, remain in question whether this family exhibits any level of redundancy regarding what amino acids are transported by each member, or if each gene transporter has substrate specificity. With so many candidate genes, effective genetic improvement approaches may be problematic until their function and redundancy has been established.

Table 4.13: Amino acid vacuolar and cationic amino acid transporter DEGs in chickpea.

Data displayed as Log₂ fold change as a heatmap with corresponding average FPKM for each gene. Data presented for all nodule and root comparisons, 18 DAI (Early-Fixing) and 25 (Peak-Fixing).

mRNA Acc.	GENE NAME	AVERAGE FPKM				LOG ₂ FOLD CHANGE			
		25 DAI Nodule	18 DAI Nodule	25 DAI Root	18 DAI Root	Nodule 25 DAI to 18 DAI	Root 25 DAI to 18 DAI	Nodule 25 DAI vs Root 25 DAI	Nodule 18 DAI vs Root 18 DAI
XM_004513 689.3	^{Plas} AVT1 A	20.2±0.8	7.3±2.9	0.9±0.4	1.3±0.2	*1.5	-0.5	*4.4	*2.4
XM_004512 221.3	^{Plas} AVT3 C	54.6±3.0	35.2±1.5	106.6±9.	6 69.4±5.0	*0.6	*0.6	*-1.0	*-1.0
XM_004491 908.3	^{Plas} AVT6 A	248.2±22. 4	71.7±10.6	204.9±2 1.9	92.1±5.7	*1.8	*1.2	0.3	-0.4
XM_004507 217.3	^{Plas} AVT6 B	16.8±0.3	13.5±0.9	22.2±2.3	16.3±0.2	*0.3	*0.4	*-0.4	*-0.3
XM_027332 179.1	^{Plas} AVT6 C.1	23.5±5.3	1.5±0.9	13.3±2.1	5.4±0.9	*4.0	*1.3	*0.8	*-1.9
XM_004500 482.3	^{Plas} AVT6 C.2	42.7±3.8	9.1±2.4	27.0±4.7	39.2±3.3	*2.2	-0.5	*0.7	*-2.1
XM_004504 134.3	^{Plas} CAT1	91.0±6.8	29.2±4.8	0.1±0.1	0.1±0.2	*1.6	-0.3	*9.8	*7.9
XM_004493 158.3	^{Plas} CAT2	13.2±1.2	4.7±0.8	29.0±4.5	28.2±6.1	*1.5	0.0	*-1.1	*-2.6

Significant (P-adjusted value <0.01) DEG log₂ fold change displayed with an *. TargetP/WolfPsort analysis, Pero: Peroxisomal, Mito: Mitochondria, Chlo:

Chloroplast, Cyto: Cytoplasmic, Nucl: Nuclear, Vacu: Vacuolar, Extr: Extracellular, Plas: Plasma Membrane, ER: Endoplasmic Reticulum.

Table 4.14: UmamiT transporters in chickpea.

Data displayed as Log₂ fold change as a heatmap with corresponding average FPKM for each gene. Data presented for all nodule and root comparisons, 18 DAI (Early-Fixing) and 25 (Peak-Fixing).

mRNA Acc.	GENE NAME	AVERAGE FPKM				LOG ₂ FOLD CHANGE			
		25 DAI Nodule	18 DAI Nodule	25 DAI Root	18 DAI Root	Nodule 25 DAI vs 18 DAI	Root 25 DAI vs 18 DAI	Nodule 25 DAI vs Root 25 DAI	Nodule 18 DAI vs Root 18 DAI
XM_00449 3270.2	PlasUmamiT9.1 (At5g07050)	10.3±2.1	1.5±0.8	16.3±0.9	23.6±3.2	*2.9	-0.5	-0.7	*-4.1
XM_00451 1031.3	PlasUmamiT9.2 (At5g07050)	212.5±19.9	25.3±14.6	119.2±16.0	95.7±23.7	*3.1	0.3	0.8	*-1.9
XM_01271 4375.2	ERUmamiT9.3 (At5g07050)	53.1±1.4	92.5±10.6	5.5±0.3	4.6±0.5	*-0.8	0.3	*3.3	*4.3
XM_00449 9751.3	VacuUmamiT9.4 (At5g07050)	93.7±5.2	112.2±16.3	0.4±0.1	0.7±1.0	-0.3	-0.5	*7.8	*7.6
XM_01271 4274.2	PlasUmamiT12 (At2g37460)	78.4±2.8	80.1±7.2	36.7±3.1	34.2±4.4	0.0	0.1	*1.1	*1.2
XM_00449 8271.2	PlasUmamiT18.1 (At4g08300)	90.9±11.3	21.9±8.8	94.8±21.4	103.0±29.6	*2.1	-0.1	-0.1	*-2.2
XM_01271 5912	PlasUmamiT18.2 (At4g08300)	8.0±1.1	0.2±0.1	242.3±49.0	134.8±13.5	*5.5	*0.8	-*4.9	*-9.5
XM_02733 3859.1	PlasUmamiT20.1 (At4g08290)	70.8±16.4	3.5±2	70.7±15.4	34.9±7.7	*4.4	1.0	0.0	*-3.3
XM_00448 5472.3	PlasUmamiT23.1 (At1g68170)	60.3±7.5	26.6±6.5	1.3±0.3	1.3±0.6	*1.2	0.1	*5.5	*4.4
XM_02733 6232.1	VacuUmamiT23.2 (At1g68170)	104.5±5.9	26.6±14.3	0.3±0.1	0.5±0.5	*2.0	-0.8	*8.6	*5.9
XM_00448 6185.3	PlasUmamiT23.3 (At1g68170)	88.0±5.1	46.1±11.9	0.3±0.1	0.3±0.2	*0.9	0.0	*8.4	*7.5
XM_01271 6950.2	PlasUmamiT24.1 (At1g25270)	39.2±2.2	57.3±9.5	0.1±0.1	0.3±0.6	-0.5	-1.5	*8.6	*7.6
XM_00448 5472.3	PlasUmamiT24.2 (At1g25270)	23.7±3.0	9.3±3	0.6±0.2	0.6±0.4	*1.4	0.1	*5.3	*4.0

XM_00451 0068.2	Plas UmamiT34 (At4g30420)	136.3±11 .4	85.1±16. 3	0.3±0.2	0.5±0.8	0.7	-0.6	*8.8	*7.5
XM_00450 2530.2	Plas UmamiT36 (At1g70260)	0.9±0.5	0.2±0	21.9±4. 5	6.1±1.3	*2.5	*1.8	*-4.6	*-5.2
XM_00449 8750.3	Vacu UmamiT40 (At5g40240)	5.0±0.9	6.8±0.9	50.8±6. 3	88.8±2. 9	-0.5	*-0.8	*-3.4	*-3.7
XM_00449 1696.3	Plas UmamiT41.1 (At3g28050)	17.9±1.3	5.7±1.1	26.0±2. 3	31.7±1. 8	*1.7	-0.3	*-0.5	*-2.5
XM_00449 1696.3	Plas UmamiT41.2 (At3g28050)	55.4±2.7	16.1±4.3	52.2±4. 7	55.4±2. 3	*1.8	-0.1	0.1	*-1.8
XM_00451 4393.3	Plas UmamiT41.3 (At3g28050)	16.3±0.9	6.1±1.0	13.6±1. 9	12.6±1. 4	*1.4	0.1	0.3	*-1.0

Significant (P-adjusted value <0.01) DEG log₂ fold change displayed with an *. TargetP/WolfPsort analysis, Pero: Peroxisomal, Mito: Mitochondria, Chlo:

Chloroplast, Cyto: Cytoplasmic, Nucl: Nuclear, Vacu: Vacuolar, Extr: Extracellular, Plas: Plasma Membrane, ER: Endoplasmic Reticulum.

4.8 Single-cell RNA Sequencing Reveals Possible Localization of Highly Upregulated Transporters

Several noteworthy transporter genes were identified in chickpea nodules during the onset of N₂ fixation through analysis of the RNAseq database. However, the localisation of these transporters, particularly their distribution between infected and uninfected zones, is unknown with no simple way to overcome this shy of further time-consuming characterisation via methods such as GUS staining. In *M. truncatula* a single-cell RNA sequencing (scRNA) database was recently made available with an extensive dataset of gene expression coupled with single cell localisation within specific nodule cell clusters (Ye et al., 2022). This provided the opportunity to compare upregulated transporters from my RNAseq analysis of chickpea with scRNA in *M. truncatula* nodules.

M. truncatula is an amidic legume with indeterminate nodules, providing a good comparison with chickpea. Noteworthy transporter genes from chickpea were evident (Table 4.15) and orthologs were identified in *M. truncatula* using the NCBI BLAST program to search within the scRNA database. The transporters in Table 4.15 were chosen based on the following reasoning: medium to high significant expression, significant fold change in expression at 25 compared to 18 DAI, and/or genes of important amino acid transporter families such as AAP. It is important to note that there are some limitations to this approach. Even though chickpea and *M. truncatula* nodules are comparable, some gene discrepancies may be present in localisation, expression, and function. The nodules used in the study by Ye et al., (2022) were from 14 DPI (Days post inoculation), and several transporters from the chickpea RNAseq data were not expressed significantly in the scRNA database. All gene orthologs had very high sequence similarity (>80%) to their respective genes in *M. truncatula*, but despite this some orthologs could not be identified in the scRNA database.

The scRNA expression matrix and meta data were imported into RStudio; gene relative expression and cell locations were identified and formatted for further analysis and visualisation using a dotplot matrix (Figure 4.6). To appropriately visualise the data without any large skew in values, relative expression and cell count were normalised using Log₂ and square root conversion, respectively (Figure 4.6).

4.8.1 Predicted nodule localisation of several chickpea amino acid transporters

Nodule parenchyma (NP) exhibited the highest average relative expression among the genes visualised followed by the uninfected cell 2 (Uic2), Infection (IF) and Pre-infection (PI), respectively (Figure 4.6). Presumably the high activity in the NP is related to transport of possibly amino acids towards the vascular tissue for export from the nodule, or distribution to symbiotic or uninfected cells. NP contained the most genes with a log₂ relative expression level >1, at 11 with five uniquely expressed, as all UmamiT transporters (Figure 4.6). Of these, AVT6A was the most widely expressed with a Log₂ relative expression

distributed across four cell clusters, highest in the UiC2 at 3.4 (Appendix: Table 4a.9) but also >1 in NP, uninfected cell 1 (UiC1) and PI (Figure 4.6 & 4.7). Four genes of the UmamiT/WAT1 family UmamiT20.1, UmamiT24.2, UmamiT23.1 and UmamiT23.3 were also uniquely expressed in the NP with Log₂ values >3 for UmamiT20.1 and UmamiT23.3 (Appendix: Table 4a.9).

Uninfected cells which include UiC1 and UiC2 had the second highest average expression but with no unique genes (Figure 4.6). In UiC2, AVT6A showed the highest Log₂ value in that cluster at 3.3 and was also expressed in UiC1 and vascular tissue (VA) at 1.5 & 1.7 (Figure 4.6 & 4.7, Appendix: Table 4a.9). Similarly, AAP2, AAP3, AAP6 and AVT3C were highly expressed in UiC2 with Log₂ values of 1.6, 1.7, 1.1 and 1.2, respectively (Appendix: Table 4a.9).

Symbiotic cells which encompass nitrogen fixation 1 (NF1), nitrogen fixation 2 (NF2), PI and IF clusters contained four uniquely expressed transporters belonging to the AAP, CAT and UmamiT family (Figure 4.7). UmamiT41.2 and UmamiT12 were both expressed in NF1 region with a Log₂ value of 1.0, whereas CAT1 showed a Log₂ value of 1.3 in the NF2 region (Appendix: Table 4a.9). AAP8 was also marginally expressed in the PI cluster at 1.0 relative Log₂ expression (Appendix: Table 4a.9).

Nodule apex 1 & 2 (NA1 & NA2) showed uniquely expressed transporters as AAP7.2 exhibited a Log₂ of 1.0 and AAP2 expressed with a Log₂ value above 1 (Figure 4.6, Appendix: Table 4a.9). Lastly, the VA contained three genes, AVT6A, AAP2 and AAP3 all with Log₂ values above 1, however no unique transporters were identified in this region from the genes tested (Figure 4.6 & 4.7).

Table 4.15: Chickpea amino acid and solute transporters chosen for further localisation analysis with *M. truncatula* spatial scRNA database.

Genes chosen based on fold change at 25 compared to 18 DAI, medium to high FPKM expression level and genes from prominent transporter families.

GENE NAME	AVERAGE FPKM		LOG ₂ FOLD CHANGE
	25 DAI Nodule	18 DAI Nodule	Nodule 18 DAI to 25 DAI
NRT1/ PTR FAMILY 7.3	101.6	4.2	*4.6
NRT2.1	111.3	2.6	*5.4
Amino acid permease (AAP1)	38.0	22.6	*0.8
Amino acid permease (AAP2)	14.9	8.6	*0.8
Amino acid permease (AAP3)	6.9	1.0	*2.8
Amino acid permease (AAP6)	21.9	2.0	*3.5
Amino acid permease (AAP7)	16.7	19.5	-0.2
Amino acid permease (AAP7)	3.6	1.8	*1.0
Amino acid permease (AAP8)	58.8	70.5	-0.3
Amino acid transporter (AVT1A)	20.2	7.3	*1.5
Amino acid transporter (AVT3C)	54.6	35.2	*0.6
Amino acid transporter (AVT6A)	248.2	71.7	*1.8
Amino acid transporter (AVT6C)	23.6	1.5	*4.0
Amino acid transporter (AVT6C)	42.7	9.1	*2.2
Cationic amino acid transporter (CAT1)	91.0	29.2	*1.6
Cationic amino acid transporter (CAT2)	13.2	4.7	*1.5
UmamiT9.2/WAT1 (At5g07050)	212.5	25.3	*3.0
UmamiT20.1/WAT1 (At4g08290)	70.8	3.5	*4.4
UmamiT18.1/WAT1 (At4g08300)	90.9	21.9	*2.1
UmamiT24.2/WAT1 (At1g25270)	23.7	9.3	*1.4
UmamiT41.2/WAT1 (At3g28050)	55.4	16.1	*1.8
UmamiT34/WAT1 (At4g30420)	136.3	85.1	0.7
UmamiT12/WAT1 (At2g37460)	78.4	80.1	0.0
UmamiT23.1/WAT1 (At1g68170)	60.3	26.6	*1.2
UmamiT23.2/WAT1 (At1g68170)	104.5	26.6	*1.9
UmamiT23.3/WAT1 (At1g68170)	88.0	46.1	*0.9
UmamiT/WAT1.1	29.6	8.0	*1.9

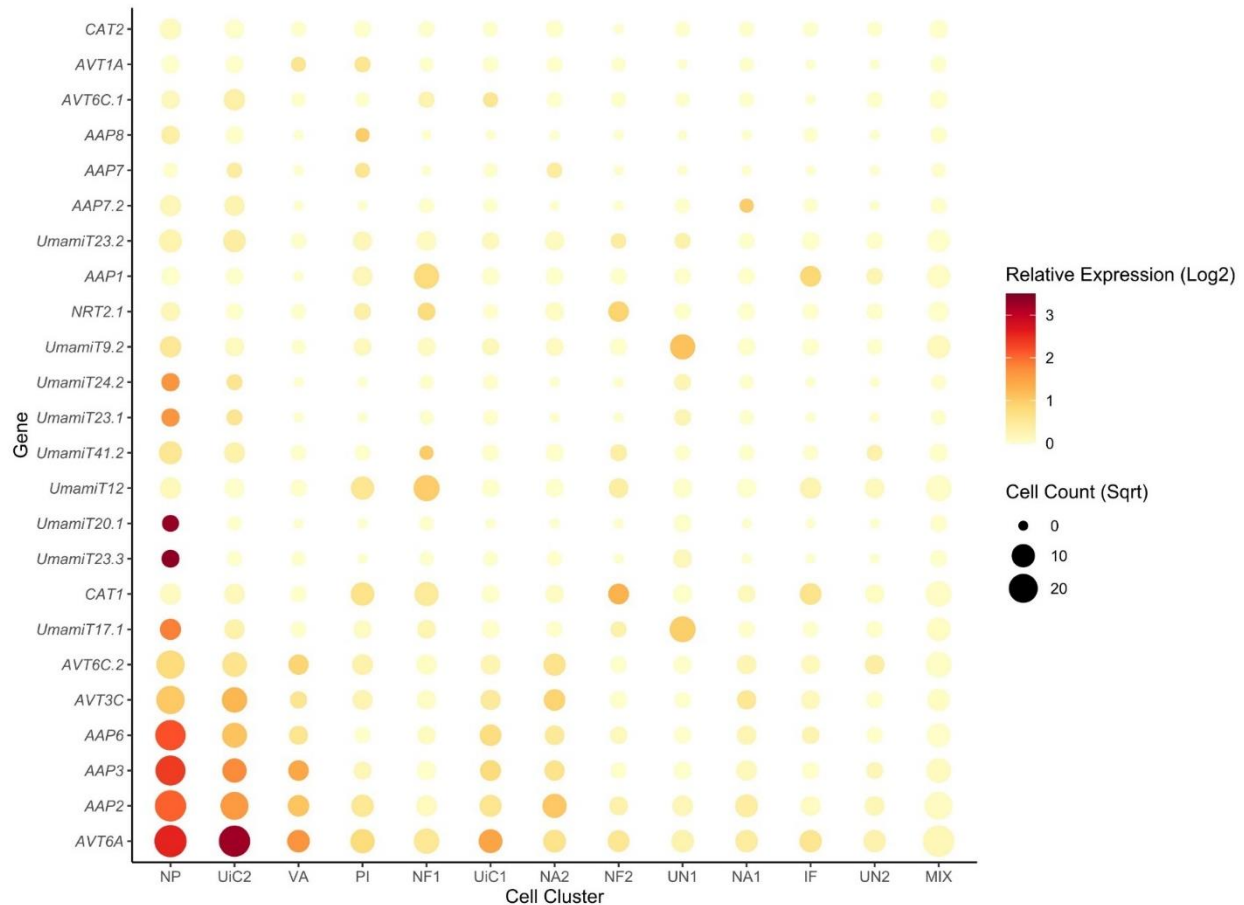


Figure 4.6: Dot plot array of theoretical nodule localization of chickpea amino acid transporters.

Dot plot array depicting relative expression and cell count of *M. truncatula* orthologs from significant highly expressed transporters in chickpea nodules. Chickpea transporter gene orthologs found in *M. truncatula* using NCBI database via BLAST search. Relative expression data and cell count collated from downloaded scRNA expression matrix and meta data (Ye et al., 2022). Gene relative expression data and cell count formatted and analysed using RStudio and dot plot visualised via ggplot2. Gene expression and cell count normalised as Log_2 relative expression and square root, respectively (Appendix 4A: Table 4a.9 & 4a.10). Cell cluster abbreviations, NP: Nodule Parenchayma, UiC1 & 2: Uninfected Cell 1 & 2, PI: Pre-Infection, IF: Infection, NF1 & 2: Nitrogen Fixation 1 & 2, NA1 & 2: Nodule Apex 1 & 2, VA: Vascular Tissue, UN1 & 2: Unknown 1 & 2, MIX: Mix Location. Relative expression values >80 omitted from analysis as outliers. Dot plot arranged with the cell clusters displaying the greatest overall relative expression to the least from left to right.

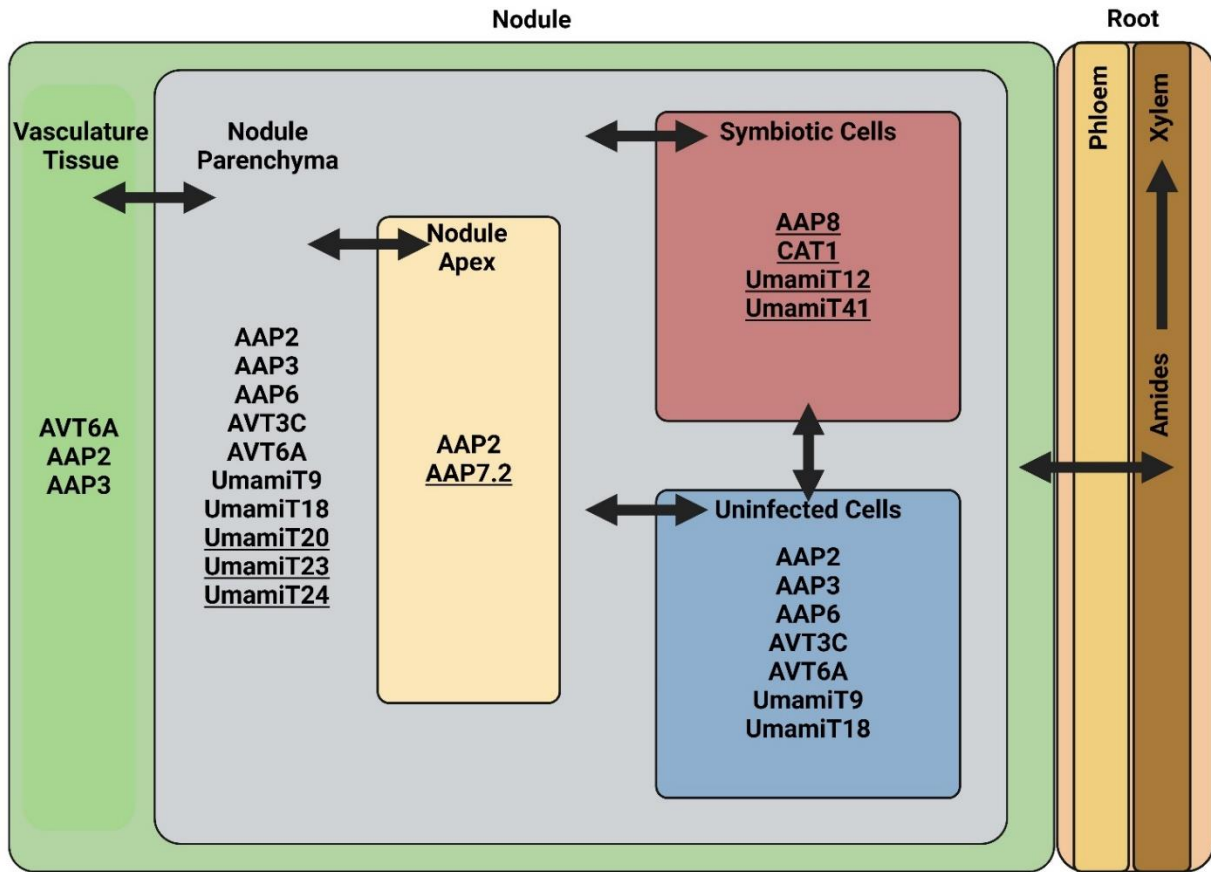


Figure 4.7: Nodule overview of theoretical localization of amino acid transporters.

Theoretical cell cluster localisation of significant highly expressed amino acid transporters in chickpea nodules. Symbiotic cells encompass Nitrogen Fixation 1 & 2, Pre-Infection, and Infection zones. Uninfected cells: Uninfected Cells zone 1 & 2. Nodule apex: Nodule Apex zones 1 & 2. Transporters depicted in shaded boxes in the respective colours of each cell cluster zone. Underlined genes indicate unique expression to a specific cell cluster. Chickpea transporter gene orthologs found in *M. truncatula* using NCBI database via BLAST search. Cell cluster expression data collated from scRNA expression matrix and meta data (Ye et al., 2022). Gene expression data and cell locations formatted using RStudio. Only genes with a Log₂ normalised relative expression level >1 were depicted (Appendix 4A: Table 4a.10). Made with Biorender.com

4.9 RNA Sequencing and Single Cell RNA Provides Further Understanding of a Fixed N Transport Network in Chickpea Nodules

This RNAseq performed on chickpea nodules has assisted in the identification of several key amino acid transporter families, with some promising gene candidates for further study. The transport network for amino acids in chickpea nodules is unknown and sparsely studied. On top of this very little is known about the cellular location of transporters of amino acids in chickpea thus the use of the scRNA database from Ye et al., (2022) has provided some useful clues of various highly expressed transporters in nodules. Even though transporters such as in the AAP family have been reasonably well studied in relation to their link to nitrogen fixation (Zhang et al., 2015, Santiago & Tegeder 2016, Perchlik & Tegeder 2017, Lu et al., 2022) their nodule localisation is mostly unknown. It is important to know the specific role of various transporters for further studies. For example, if the goal is to improve fixed N export from nodules, upregulation of transporters located in the cortex or vasculature may be of most importance.

4.9.1 AAPs, CATs, and AVTs concomitantly coordinate amino acid distribution and export in chickpea nodules.

The RNAseq described here provides some evidence that the extensively studied AAP amino acid transporters may be important also in chickpea nodules. Of the AAPs found, only AAP3 and AAP6 were significantly upregulated but at low levels of expression. AAP8 showed moderate expression but was not upregulated in response to an increase of N₂ fixation. Without knowing how the transcript levels relate to translation of the respective proteins, the importance of the AAPs is purely speculative. However, transporter functions can be extrapolated from their roles in other plants.

AAP1 in Arabidopsis roots imports glutamate and neutral amino acids as N source from the rhizosphere, (Lee et al., 2007, Perchlik et al., 2014) and are expressed in the seed coat and endosperm for amino acid uptake for protein storage and seed yield (Sanders et al., 2009). In rice, AAP1 is highly expressed in buds, leaves and young panicles where it is localised to plasma membranes, transporting neutral and acidic amino acids important for growth, grain yield and seed protein (Ji et al., 2020, Grant et al., 2021). Little is known about AAP2, but it has been shown to be localised to the phloem in Arabidopsis and is important for source to sink allocation of amino acids (Zhang et al., 2010). In Arabidopsis APP3 is localised to the plasma membrane of root phloem and major veins of leaves, but knockout mutants had no altered phenotype, suggesting compensation by other transporters (Okumoto et al., 2004). On the

other hand, overexpression of AAP3 in rice saw elevated total amino acid content (Lu et al., 2018). AAP5 transports basic amino acids and is expressed in the roots (Jämtgård 2010), where mutants in *Arabidopsis* affected the uptake of arginine and lysine (Svennerstam et al., 2011). It is possible that AAP1, 2 and 3 identified in my RNAseq study may coordinate amino acid transport in a similar manner in chickpea nodules, where knocking out one may be compensated by the another. Additionally, AAP2 and AAP3 were expressed together in most cell types in *M. truncatula*, possibly indicating redundancies.

AAP6, which was also found in the database and expressed in uninfected and nodule parenchyma, is a notable amino acid transporter believed to be involved in transport of amino acids out of the infected cells to the vasculature inner cortex for subsequent nodule export in *P. sativum* (Garneau et al., 2018). In non-symbiotic plants such as *Arabidopsis*, AAP6 mutants had a reduction in lysine, phenylalanine, lucine and aspartic acid in phloem (Hunt et al., 2010). In rice (Peng et al., 2014) and wheat (Jin et al., 2018) AAP6 functions as a regulator of grain protein and yield and enhances low N tolerance and seed N status in *G. max* (Liu et al., 2020). AAP6 has also been found to reside in clade 1 of the *Arabidopsis* AAP family, alongside AAP1 and notably AAP8 which was found here to be in the symbiotic cells (Zhou et al., 2020). Similarly, AAP2 and AAP3 are a part of clade 2 (Zhou et al., 2020) perhaps explaining the close relative expression association the two had in the uninfected cells, nodule parenchyma and vascular cells. In *P. sativum* AAP6 is located in the nodule inner cortex and knockout led to a down regulation of AAP2 and AAP3 in nodules, suggesting that those transporters may be involved upstream of AAP6 in phloem or xylem loading (Garneau et al., 2018). Lastly, AAP8, which was not upregulated here but still showed a moderate level of expression, is believed to facilitate phloem loading of amino acids (Santiago & Tegeder 2016), particularly for seed development (Okumoto et al., 2002, Schmidt et al., 2007). Further studies, particularly into AAP2, AAP3 and AAP6 and how they interact together in chickpea would be interesting to elucidate a possible role as key amide export pathway from the nodules. For example, if AAP2 and AAP3 function upstream from AAP6 as seen in *P. sativum*, then they may be good targets for genetic improvement of amino acid distribution and export in chickpea nodules.

Cationic amino acid transporters (CAT), which are highly similar to the AAP family, are from the amino acid polyamine-choline (APC) family and likely play similar roles as the AAPs discussed above (Rentsch et al., 2007). CATs typically transport neutral and some basic amino acids, while AAPs transport neutral amino acids and glutamate of (Rentsch et al., 2007). Two CAT genes, CAT1 & CAT2, were found in the scRNA database but only CAT2 showed a notable expression level in the symbiotic cells. CAT2 has been proposed to function in the regulation of amino acid levels in leaves and is located to the vacuolar

membrane (Yang et al., 2014). However, the scRNA data above indicates that CAT2 may also be found in nodules. CAT6 in contrast has been found in *P. sativum* nodules and may function in a similar manner to AAP2 and AAP3 in chickpea, although the specific localisation of the transporter is still unknown (Garneau et al., 2018). Studies with *Arabidopsis* found evidence for CAT5 as a basic amino acid transporter in plasma membranes, and CAT3, CAT6 and CAT8 as neutral or acidic amino acid transporters (Su et al., 2004, Yang et al., 2010). In tomato, CAT9 has been identified as a tonoplast transporter of the amides Glu and Asp and is induced during fruit development (Snowden et al., 2015). Overexpression of *AtCAT9* saw increased soluble leaf amino acid pools under low nitrogen conditions and it was localised to vesicular membranes (Yang et al., 2015). CAT11 in poplar may also have a role in facilitating Glu loading into the phloem during senescence and is a key transporter in N remobilisation (Couturier et al., 2010). In summary, CAT2 was the only CAT gene identified in the scRNA database and may prove to be a key amide transporter in chickpea nodules, but more work is needed to determine what amino acids are transported by CAT2.

Another family of transporters identified in the RNAseq database were amino acid vacuolar transporter family (AVT). Three members of this family, AVT1A, AVT6A, AVT6C, were found to be significantly upregulated, one AVT3C was non-differentially expressed and another, AVT6A showed high expression at 25 DAI. AVT6A was found to be expressed in the vascular tissue, nodule parenchyma and in the uninfected cells, whereas AVT3C was found in the uninfected and nodule parenchyma cells. The AVT family has been previously characterised in yeast, where AVT1 functions as a vacuolar antiporter of the neutral amino acids Tyr, Gln and Asn (Tone et al., 2015), while AVT3 and AVT4 export both neutral and basic amino acid from the vacuole (Sekito et al., 2014). Notably, AVT6 which displayed high expression here, is involved in Glu and Asp efflux in yeast cells under nitrogen starvation (Rusnak et al., 2001, Chahomchuen et al., 2009). AVT7 which was not identified in the RNAseq database was also found located on the vacuolar membrane of yeast cells involved in the export of Gln (Tone et al., 2015). It would be useful to determine whether AVT1 and AVT3 transport Gln & Asn, and if the highly upregulated AVT6 transports Glu and Asp in chickpea nodules, which could make AVT6 an important amide and amino acid transporter.

4.9.2 Umamit/WAT1 transporters in chickpea participate in amino acid transport, nodule development and pathogen defense.

Another group of transporter genes of particular interest here are classed under two transport families and have received little attention in the literature, until recently. The RNAseq annotation jointly labelled

UmamiT (Usually multiple acids move in and out) and WAT1 (Walls Are Thin) genes together. UmamiT are typically classed as broad specificity bidirectional amino acid transporters while WAT1 are typically vacuolar auxin transporters (Fang et al., 2022). Importantly, the name for this gene family derives from the umami taste associated with the amino acid glutamate, and not related to the taste receptors T1R1/T1R3 in animals (Li et al., 2002). Interestingly, a WAT1 gene was first identified in Arabidopsis as a homolog from *M. truncatula*, NODULIN21, as part of the Drug/Metabolite Transporter superfamily (Ranocha et al., 2010). Presumably some nodulin genes that are involved in legume nodulation are also important in non-leguminous plant development, such as auxin and amino acid transport, giving rise to the WAT1 auxin transporters, adding to the diversity of UmamiT. *M. truncatula* NODULIN21 is the founding member of 44 such proteins in Arabidopsis encompassing both UmamiT and WAT1 transporters (Ladwig et al., 2012). *MtNODULIN21* was originally found to be induced during nodulation, emphasising the potential role of this extensive family in N₂ fixation (Gamas et al., 1996, Denancé et al., 2014).

The UmamiT family are known to have broad functionality in amino acid seed loading (Müller et al., 2015), bidirectional phloem transport (Besnard et al., 2018), vacuolar transport of auxin for WAT1/UmamiTs (Ranocha et al., 2013) and amino acid export in a range of tissues (Besnard et al., 2016, Yao et al., 2020). However, little is known about them outside of Arabidopsis, with no reported characterisation in chickpea. Outside of auxin and amino acid transport, UmamiT transporters have been found to play a part in pathogen infection (Denancé et al., 2013), specifically nematode infestation, by involvement in the activation of the salicylic acid pathway (Pan et al., 2016) and Lignin deposition (Tang et al., 2019). Importantly for the current study, *MtNodulin21*, a homolog of *AtUmamiT9*, was upregulated by the presence of rhizobium, suggesting diverse roles in the roots and during N₂ fixation (Ranocha et al., 2010). These transporters may also play an important role in plant-microbe interactions through amino acid sensing and signalling for nutrient acquisition and pathogen defence (Moormann et al., 2022).

Ten UmamiT genes of interest were identified in the chickpea RNAseq database, while several others did not present any significant expression (Appendix: Table 4a.4). From the notable UmamiTs expressed, UmamiT23 and UmamiT24 are grouped into clade D of the UmamiT phylogeny in Arabidopsis, UmamiT9, UmamiT12, UmamiT18 and UmamiT20 in clade C, UmamiT34 in clade F and UmamiT41 in clade J (Ladwig et al., 2012, Zhao et al., 2021). The UmamiTs from clade C are of particular interest since they showed considerable fold increase in expression during N₂ fixation in my study. Interestingly, the scRNA

in *Medicago* shown above located each UmamiT to the nodule parenchyma, presumably signifying importance in amino acid export from the nodules.

All the UmamiT/WAT1 genes discussed above (Table 4.15, Figure 4.6 & 4.7) are annotated against their respective Arabidopsis related protein, pointing to possible functions. UmamiT9 along with UmamiT20 from clade C are highly enriched in poplar phloem parenchyma cells (Chen et al., 2021), and UmamiT20 in the bundle sheath cells in maize as an amino acid efflux transporter (Bezruczyk et al., 2021).

UmamiT9 has also been found to be upregulated in the roots of pathogen resistant olive cultivars (Ramírez-Tejero et al., 2021), and are induced in rose in response to powdery mildew (Chandran et al., 2021), possibly linked to auxin transport. UmamiT9 is phylogenetically close to *MtUmamiT14* which may participate in nodule formation in *M. truncatula* (Garcia et al., 2023). *MtUmamiT14* is a putative transporter within the MtNodulin21/EamA-like/UmamiT family, with proposed functionality in nodule formation and N₂ fixation located in the infection zone of *M. truncatula* nodules (Garcia et al., 2023). In Arabidopsis, UmamiT14 along with UmamiT11, UmamiT18 and others have been shown to be involved with import/export of amino acids and are expressed in the root pericycle for phloem unloading (Besnard et al., 2016, Besnard 2018, Tegeder & Hammes 2018, Moormann et al., 2022), as well as amino acid export to developing seeds (Müller et al., 2015, Karmann et al., 2018).

A Siliques are Red1 (SIAR1) gene again belonging to the *MtNodulin21* family is a close paralog to UmamiT18 from clade C and was found to translocate amino acids bidirectionally likely located in plasma membranes of vascular tissues (Ladwig et al., 2012). In Arabidopsis, UmamiT18 and UmamiT12 are also from clade C and are enriched in the phloem parenchyma where they secrete amino acids into the apoplasm (Kim et al., 2021). Similarly, UmamiT12 (Kisko et al., 2015) and UmamiT23 (Ibarra-Laclette et al., 2013) are also believed to encode proteins related to *MtNodulin21* and EamA-like transporter family. The EamA-like family may be involved in the transport of solutes, amino acids and plant hormones (Denancé et al., 2014).

Of the Arabidopsis clade D, UmamiT24 and UmamiT25 transfer amino acids to developing seeds, and are located in the seed coat and endosperm, respectively, where mutants saw a reduction in pollen number (Besnard et al., 2018, Tsuchimatsu et al., 2020). Little is known about UmamiT34 and UmamiT41 found in the RNAseq database, outside of possible location in the root cortex in Arabidopsis for UmamiT35 (Zhao et al., 2021), whereas UmamiT41 may exhibit roles in response to auxin for root formation (Carretero-Paulet et al., 2015).

Chapter 4: Conclusions

From the RNAseq analysis conducted here, the following conclusion can be made: **(1)** Chickpea nodules convincingly express metabolism genes related to amide and amino acid biosynthesis with little evidence of glutamine feeding into the purine synthesis pathway for ureide biosynthesis. The purine and ureide biosynthesis pathways exhibited non-differential expression, outside of a couple genes, and with very minor expression. Conversely, aminotransferases and the GS/GOGAT pathways were highly upregulated and are important for synthesis of the amides asparagine and glutamine. **(2)** Transporters whose expression was upregulated in response to increased N₂ fixation are also likely to transport amides and amino acids rather than ureides. Notably ureide transport is mediated by a single transporter family that was non-differentially expressed in response to an increase in N₂ fixation here, in line with the small levels of ureides detected in chapter 3. **(3)** Expression of several key transporters was correlated with an increase in N₂ fixation indicating that they are likely to play important roles in amide and amino acid distribution within nodules as well export from nodules.

5 Functional Characterisation of Chickpea Amino Acid Transporters in *Saccharomyces Cerevisiae*

Chapter 5: Introduction

5.1 Amino Acid Transporters are the Key to Improve Nitrogen Fixation

To facilitate improvements to N₂ fixation in legume crops such as chickpea, the nodule transporters which function in the distribution and export of amino acids, such as the amides Gln and Asn, are of particular interest. Multiple studies have found evidence suggesting that the rate of N₂ fixation is not necessarily a limiting factor, but rather there may be a bottleneck in the rate of fixed nitrogen export (Lu et al., 2022, Garneau et al., 2018). Indeed, there appears to exist systemic signaling mechanisms which can detect a deficiency in shoot N supply leading to significant upregulation in nodule N₂ fixation activity and the production of fixed N (Garneau et al., 2018). This brings into question whether amino acid transporters are the key to enhancing N₂ fixation, rather than metabolic pathways. For example, it could be hypothesized that if amides can be exported from nodules to a greater degree via upregulation of amide transporters, the nodule N₂ fixation rates may subsequently increase to compensate for increased amide flux. A similar rationale was discussed by Tegeder & Masclaux-Daubresse, (2018).

Several candidate genes to achieve this hypothesis were identified in the previous chapter (Chapter 4: Table 4.15), encompassing multiple genes from the UmamiT family (Zhao et al., 2021) and the well-studied AAP6 (Hunt et al., 2010, Garneau et al., 2018, Liu et al., 2020). What remains in question here is do these transporters facilitate the movement of amides and/or a broad range of amino acids? If this is the case, a number of these genes such as *CaAVT6A*, *CaAAP6*, *CaUmamiT18* and *CaUmamiT20* that were theoretically localised to the nodule parenchyma from the scRNA database in *M. truncatula* (Chapter 4: Figure 4.7) (Ye et al., 2022), would be of particular interest. Transporters localised on the parenchyma are likely to be involved in amide flux out of the nodules towards the roots and subsequently shoots, representing promising targets for overexpression studies.

Six highly upregulated genes identified from RNA sequencing (Chapter 4: Table 4.15) that potentially encode transporters of amides and amino acids were characterized through functional complementation in an amino acid transport deficient *S. cerevisiae* strain 22Δ10AA (MAT α gap1-1 put4-1 uga4-1 can1::HisG lyp1- alp1::HisG hip1::HisG dip5::HisG gnp1Δ agp1Δ ura3-118) (Besnard et al., 2016). This strain has 10 amino acid transporters deleted, however, can still be rescued when supplemented with Arg & Orn, and partially rescued with Val, Phe, Trp, Tyr, Asp and Gln at 3 mM (Besnard et al., 2016). Partial rescue by these amino acids can be monitored by performing complementation growth assays in combination with a negative vector control in the mutant strain to assess false positive complementation. The mutant

grows well in medium supplemented with NH_2SO_4 (1.5-3 mM) or medium with the Yeast Synthetic Dropout minus uracil supplement after transformation with a gene of interest. Successful complementation of this mutant strain expressing chickpea amino acid genes would support *S. cerevisiae* growth on solid and liquid media supplemented with individual amino acids, particularly the amides Gln & Asn. Complementation results were compared against the parental *S. cerevisiae* strain (23344c; positive control) expressing chickpea genes and empty vectors pYESdest52 or pDR196 (negative controls) in 22 Δ 10AA & 23344c strains (Appendix 5a.7). Growth assays (48-h) in liquid media were conducted to assess a range of different amino acid concentrations and at different pH to determine transporter characteristics.

5.2 Phylogenetic Analysis of Chickpea Amino Acid Transporters Identified via RNAseq

To determine possible function of the genes of interest identified in the previous chapter (Chapter 4: Table 4.15) amino acid sequence similarity comparisons and a phylogenetic analysis approach were undertaken. If the amino acid sequences showed high similarity and clustered together in phylogenetic clades to previously characterised transporters, then their respective function could be postulated. I also thought it would be useful to compare these chickpea amino acid sequences to homologs from two model legumes that exhibit amide (*P. sativum*) and ureide (*G. max*) biosynthesis and transport properties. I hypothesised that the genes identified here would most likely exhibit higher similarity with those from *P. sativum* rather than *G. max*, given that chickpea appears to be an amidic legume based on results presented in this thesis.

Comparing amino acid sequence similarity of the putative chickpea amino acid transporters, it was observed that the most dissimilar orthologs were from the model plant *A. thaliana*, except *CaUmamiT40* and *CaAAP6.2* with 49% and 66% sequence similarity, respectively (Table 5.1). *G. max* exhibited the greatest sequence similarity with *CaUmamiT9.4* (82), *CaUmamiT18.2* (85), *CaUmamiT23.3* (63) and *CaAAP6.3* (86) (Table 5.1). The most similarity was with *P. sativum*, where *CaAAP6.1* (94), *CaUmamiT18.1* (91) *CaAVT6C.2* (90), *CaAAP3* (89), *CaUmamiT9.1* (88) and *CaAVT6A* (88) exhibited the greatest percentage similarity (Table 5.1). The sequence similarity of 94% between *CaAAP6.1* and *PsAAP6* is particularly notable considering that *PsAAP6* is a well characterised transporter of amino acids, particularly the amide Asn (Tegeder et al., 2018). In general, amino acid sequence similarity was highest for *P. sativum* compared to that of *G. max*. This may indicate greater genotypic associations with other amide transporting legumes over ureide legumes. Phylogenetic analysis of amino acid transporters of the AAP, AVT CAT and UmamiT families further supported this observation where almost all chickpea genes exhibited parallel evolution to *P. sativum* compared to slightly more divergence from *G. max* depicted in a maximum likelihood tree (Figure 5.1-5.4). As observed in table 5.1 both the legumes *G. max* and *P. sativum* presented greater evolutionary similarity to chickpea than the *A. thaliana* counterparts (Figure 5.2, 5.3, 5.4). This observation seems reasonable when considering these transporters were identified from nodule RNA, an organ unique to legumes.

The phylogenetic analysis of all the chickpea transporters from table 5.1 showed that genes pertaining to the UmamiT and CAT families diverged only a little from the AVT and AAP families (Figure 5.1). This may indicate similar transport functions or localisations for these transporters. The AVT and AAP clades were

also highly similar with a bootstrap value of 99 at the branching node between the two clades (Figure 5.1).

Within each clade, the six AVTs were highly similar to each other, only differing with a bootstrap of 80 at the branching node between the AVT1 & AVT6 genes (Figure 5.1). In the AAP family clade, the AAP6 homologs, which typically encompass the greatest attention in the literature, were separated from the other AAP members of the family by a bootstrap of 35, possibly accounting for a unique role of AAP6 (Hunt et al., 2010, Garneau et al., 2018, Liu et al., 2020) (Figure 5.1). In comparison, the UmamiT family exhibited notable variability within members, likely suggesting a range of functions (Figure 5.1).

UmamiT9, UmamiT17 and UmamiT20 split from the other UmamiT genes with a bootstrap value of 25 (Figure 5.1). Two distinct alternative groups encompassing UmamiT23 & UmamiT24 diverged from UmamiT36 UmamiT40 and UmamiT41 (Figure 5.1).

It would be interesting to determine if these transporter families have a diverse range of transport properties or if chickpea has a large redundancy built in. For example, there appear to be several transporters in chickpea from the same family genetically similar to each other with respect to the amino acid gene sequence, all exhibiting high expression. It almost seems wasteful for an organism to invest in so many transporters that may facilitate the same function unless many are purely stress responsive or used for signalling purposes rather than bulk movement of fixed N in the form of amino acids. To help answer this question, several genes from table 5.1 were chosen for functional characterisation using an amino acid knockout *S. cerevisiae* expression system (Besnard et al., 2016).

Table 5.1: Amino acid sequence similarity of identified chickpea amino acid transporters to two model legumes *G. max* & *P. sativum*, and *A. thaliana*.

Arabidopsis (At), Soybean (Gm) and Pea (Ps) protein sequences obtained on NCBI via BLAST® queries compared to the respective chickpea gene identified from the RNAseq database (Chapter 4: Table 4.15). Ortholog similarity percentage determined by percentage identity output from the BLAST® query with greatest protein similarity in red and least in blue. Genes with * were characterised in this chapter.

Gene Name	Chromosome	Exon Count (At/Gm/Ps)	Locus Tag	Protein Accession	Amino Acid Count	At Ortholog (%) Similarity	Gm Ortholog (%) Similarity	Ps Ortholog (%) Similarity
CaUmamiT9.1	Ca3	7 (7/7/12)	LOC101503274	XP_004493327.1	392	AtUmamiT9 (61)	GmUmamiT9 (84)	PsUmamiT9 (88)
CaUmamiT9.2*	Ca7	7 (7/7/12)	LOC101512262	XP_004511088.1	403	AtUmamiT9 (63)	GmUmamiT9 (74)	PsUmamiT9 (83)
CaUmamiT9.3	Ca4	7 (7/7/12)	LOC101515211	XP_012569829.1	355	AtUmamiT9 (41)	GmUmamiT9 (76)	PsUmamiT9 (80)
CaUmamiT9.4	Ca5	7 (7/7/12)	LOC101504704	XP_004499808.1	398	AtUmamiT9 (68)	GmUmamiT9 (82)	PsUmamiT9 (74)
CaUmamiT12*	Ca4	7 (6/7/7)	LOC101496299	XP_012569728.1	351	AtUmamiT12 (65)	GmUmamiT12 (73)	PsUmamiT12 (76)
CaUmamiT18.1*	Ca4	7 (6/7/7)	LOC101510267	XP_004498328.1	383	AtUmamiT18 (66)	GmUmamiT18 (84)	PsUmamiT18 (91)
CaUmamiT18.2	Ca5	8 (6/7/7)	LOC101494594	NP_001296593.1	393	AtUmamiT18 (65)	GmUmamiT18 (85)	PsUmamiT18 (84)
CaUmamiT20*	Ca4	6 (7/7/7)	LOC101512949	XP_027189660.1	392	AtUmamiT20 (44)	GmUmamiT20 (63)	PsUmamiT20 (83)
CaUmamiT23.2	Ca6	6 (7/7/7)	LOC101515033	XP_027192033.1	391	AtUmamiT23 (37)	GmUmamiT23 (57)	PsUmamiT23 (73)
CaUmamiT23.3	Ca1	7 (7/7/7)	LOC101502165	XP_004486242.1	391	AtUmamiT23 (42)	GmUmamiT23 (63)	PsUmamiT23 (63)

CaUmamiT24.1	Ca1	7 (7/7/7)	LOC101499714	XP_004485529.1	413	AtUmamiT24 (47)	GmUmamiT24 (50)	PsUmamiT24 (79)
CaUmamiT24.2	Ca6	7 (7/7/7)	LOC101488446	XP_012572404.1	345	AtUmamiT24 (40)	GmUmamiT24 (49)	PsUmamiT24 (70)
CaUmamiT34	Ca7	15 (7/7/7)	LOC101507140	XP_004510125.2	766	AtUmamiT34 (51)	GmUmamiT34 (66)	PsUmamiT34 (69)
CaUmamiT36	Ca5	7 (7/7/7)	LOC101491579	XP_004502587.1	357	AtUmamiT36 (49)	GmUmamiT36 (76)	PsUmamiT36 (84)
CaUmamiT40	Ca4	7 (7/7/7)	LOC101506522	XP_004498807.1	326	AtUmamiT40 (49)	GmUmamiT40 (42)	PsUmamiT40 (41)
CaUmamiT41.1*	Ca3	7 (7/7/7)	LOC101511733	XP_004491753.2	358	AtUmamiT41 (59)	GmUmamiT41 (79)	PsUmamiT41 (86)
CaUmamiT41.3	Unlocalised	8 (7/7/7)	LOC101506171	XP_004514450.1	369	AtUmamiT41 (45)	GmUmamiT41 (74)	PsUmamiT41 (77)
CaAAP1	Ca5	7 (6/7/6)	LOC101488323	XP_004501134.2	465	AtAAP1 (52)	GmAAP8 (67)	PsAAP1 (80)
CaAAP2	Ca5	8 (7/7/6)	LOC101499396	XP_004502981.1	487	AtAAP2 (65)	GmAAP2 (77)	PsAAP2 (87)
CaAAP3	Ca4	6 (7/6/6)	LOC101489194	XP_004498350.1	487	AtAAP3 (74)	GmAAP3 (79)	PsAAP3 (89)
CaAAP6.1	Ca5	7 (6/7/6)	LOC101495138	XP_004501076.1	481	AtAAP6 (76)	GmAAP6 (90)	PsAAP6 (94)
CaAAP6.2*	Ca4	7 (6/7/6)	LOC101511648	XP_004496860.1	468	AtAAP6 (66)	GmAAP6 (64)	PsAAP6 (63)
CaAAP6.3	Ca4	8 (6/7/6)	LOC101498275	XP_012570658.1	471	AtAAP6 (76)	GmAAP6 (86)	PsAAP6 (85)
CaAAP7	Ca2	7 (7/7/7)	LOC101497359	XP_004491549.1	468	AtAAP7 (62)	GmAAP7 (82)	PsAAP7 (84)
CaAAP8	Ca5	7 (6/7/7)	LOC101500657	XP_004501094.1	472	AtAAP8 (53)	GmAAP8 (77)	PsAAP8 (79)
CaAVT1A	Unlocalised	11 (11/12/12)	LOC101507365	XP_004513746.1	530	AtAVT1A (62)	GmAVT1A (80)	PsAVT1A (82)
CaAVT3C	Ca8	1 (1/2/1)	LOC101501025	XP_004512278.1	425	AtAVT3C (64)	GmAVT3C (78)	PsAVT3C (86)
CaAVT6A*	Ca3	6 (6/6/6)	LOC101508190	XP_004491965.1	465	AtAVT6A (69)	GmAVT6A (88)	PsAVT6A (88)
CaAVT6B	Ca6	6 (5/7/10)	LOC101503435	XP_004507274.1	463	AtAVT6B (67)	GmAVT6B (82)	PsAVT6B (86)
CaAVT6C.1*	Ca2	5 (5/5/5)	LOC101493057	XP_027187980.1	453	AtAVT6C (59)	GmAVT6C (75)	PsAVT6C (83)
CaAVT6C.2	Ca5	5 (5/5/5)	LOC101515343	XP_004500539.1	435	AtAVT6C (59)	GmAVT6C (83)	PsAVT6C (90)

CaCAT1	Ca6	2 (3/3/3)	LOC101491468	XP_004504191.2	586	AtCAT1 (66)	GmCAT1 (77)	PsCAT1 (84)
CaCAT2	Ca3	14 (14/14/14)	LOC101496734	XP_004493215.1	612	AtCAT2 (68)	GmCAT2 (78)	PsCAT2 (85)

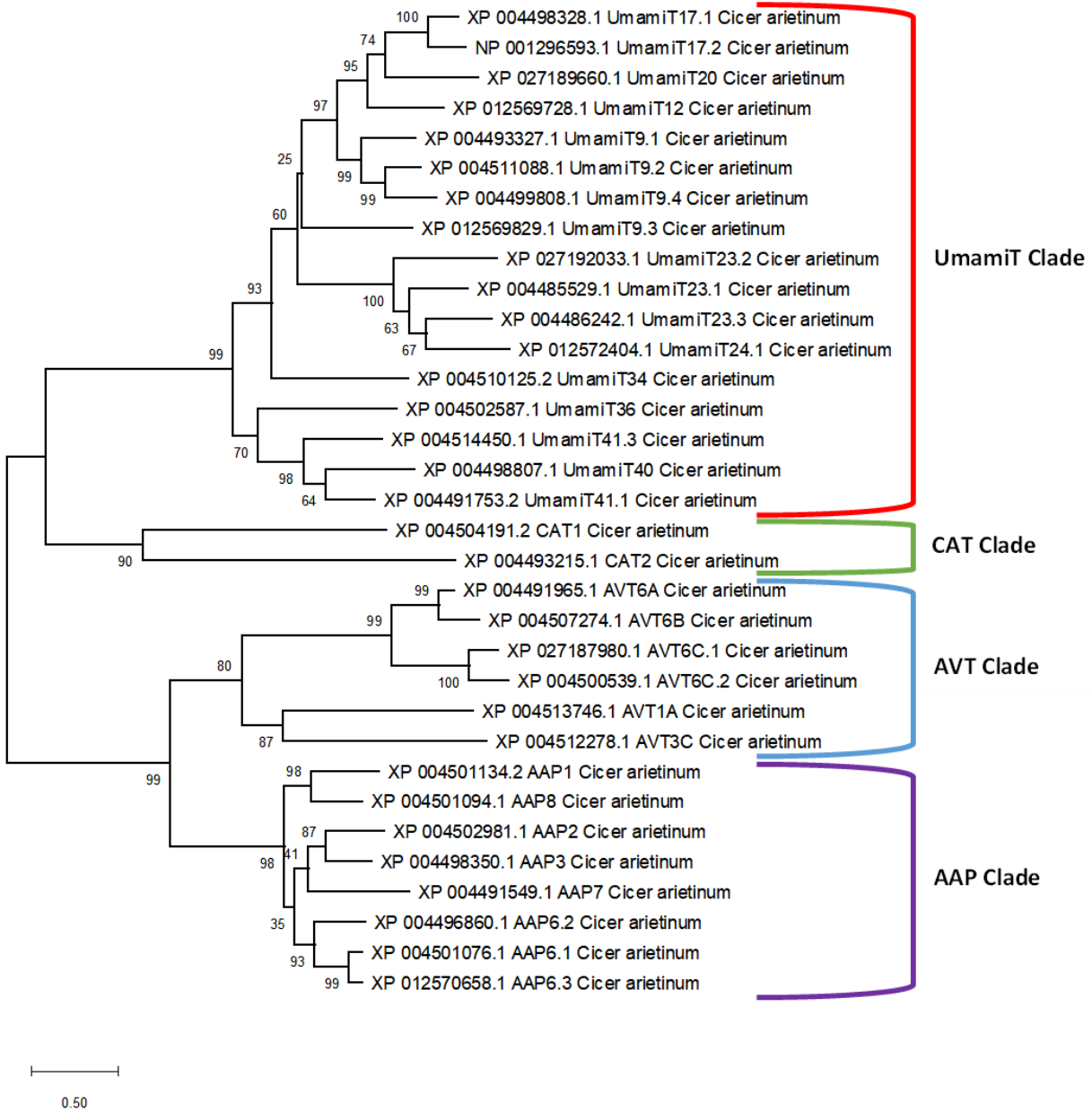


Figure 5.1: Phylogenetic analysis of amino acid transporters; AAP, AVT, CAT and UmamiT from Chickpea.

Maximum likelihood phylogenetic tree constructed on MEGAX 10.0 (Kumar et al., 2018), after amino acid sequences of amino acid genes aligned using MUSCLE. Tree constructed with 1000 bootstrap replications with respective bootstrap values displayed with a maximum of 100 at each node. Publicly available gene amino acid sequences obtained on NCBI. UmamiT clade: Red, CAT clade: Green, AVT clade: Blue and AAP clade: purple.

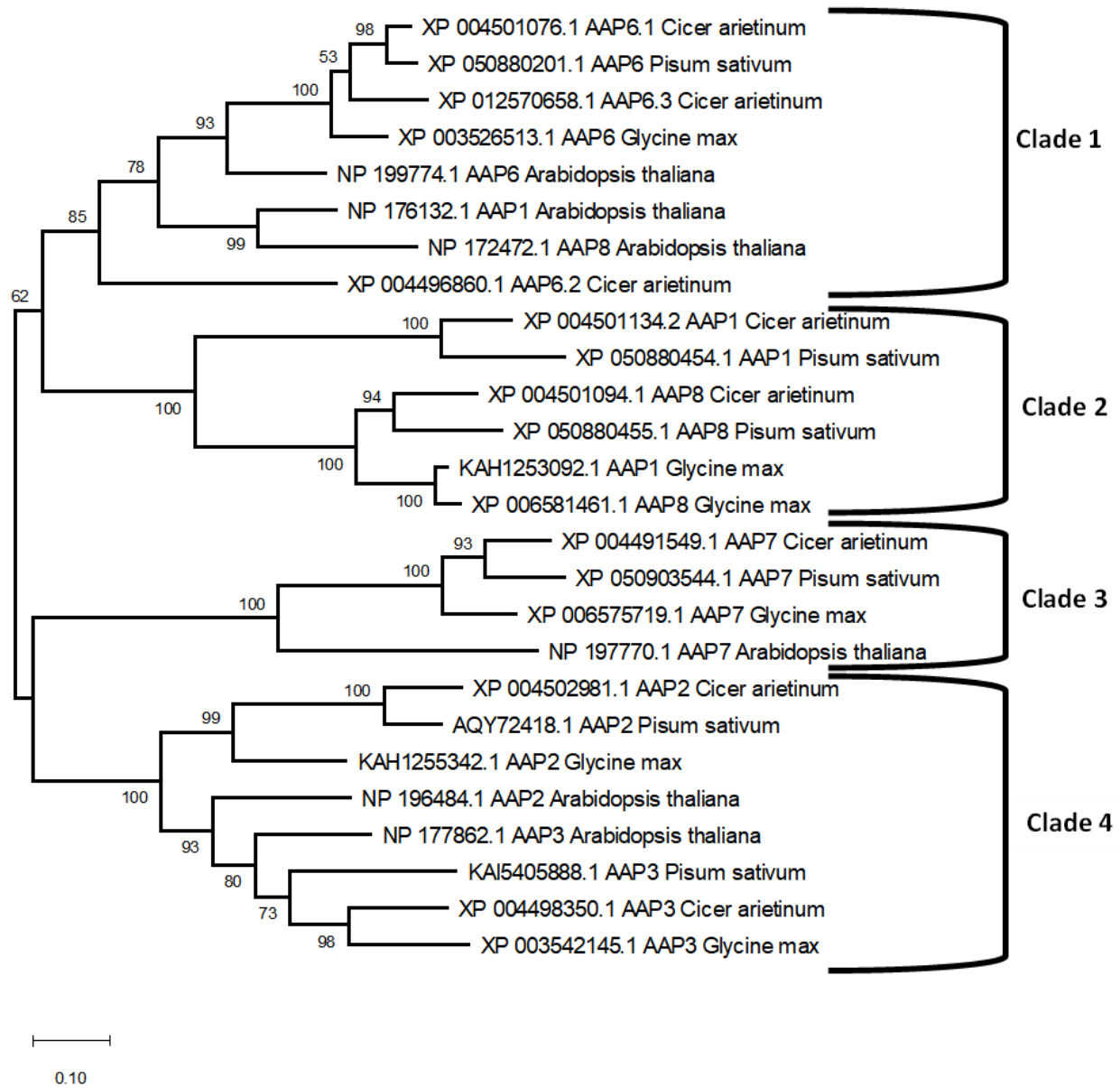


Figure 5.2: Phylogenetic analysis of AAP transporters from *C. arietinum*, *G. max*, *P. sativum* and *A. thaliana*.

Maximum likelihood phylogenetic tree constructed on MEGAX 10.0 (Kumar et al., 2018), after amino acid sequences of AAP genes aligned using MUSCLE. Tree constructed with 1000 bootstrap replications with respective bootstrap values displayed with a maximum of 100 at each node.

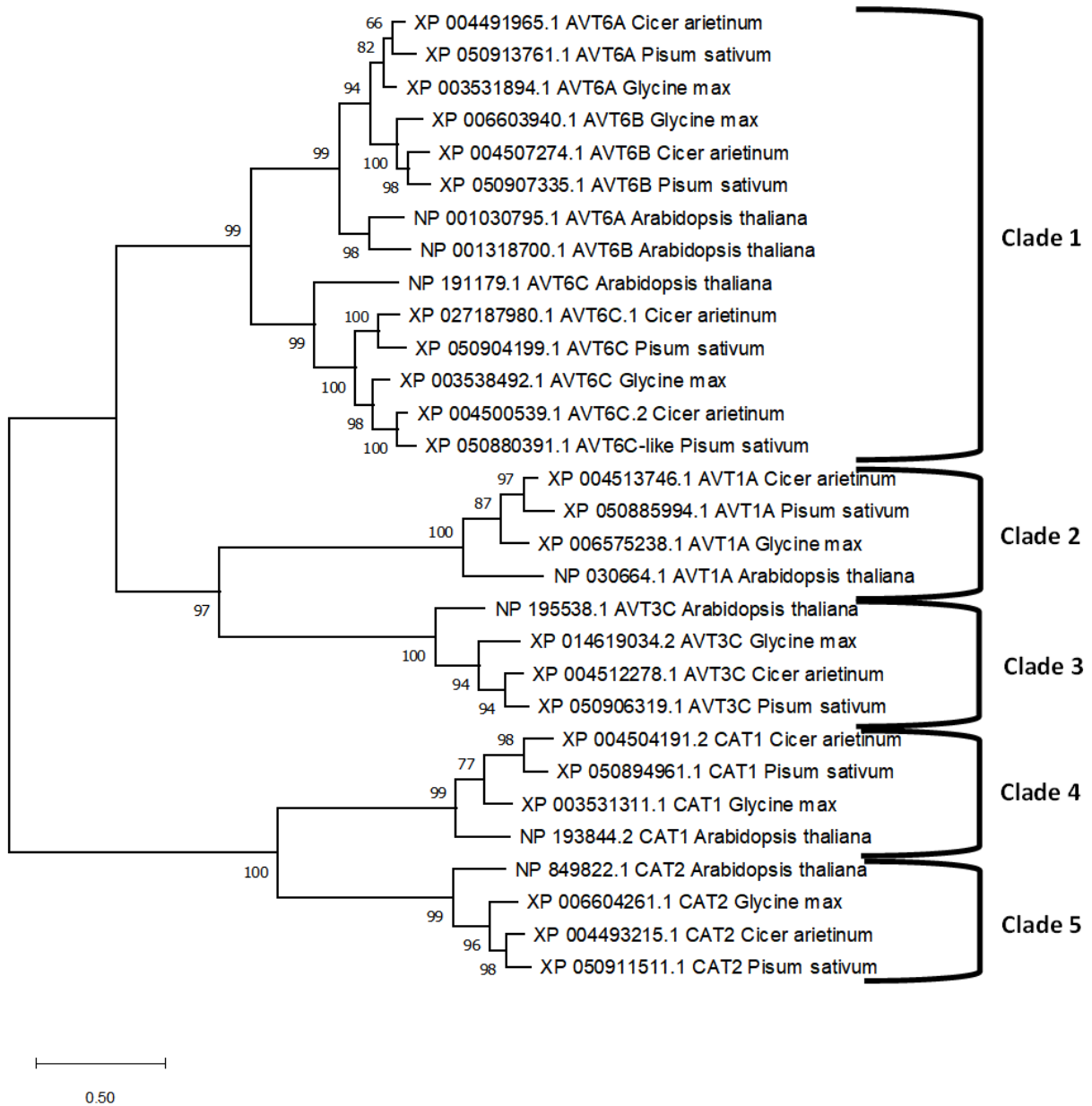
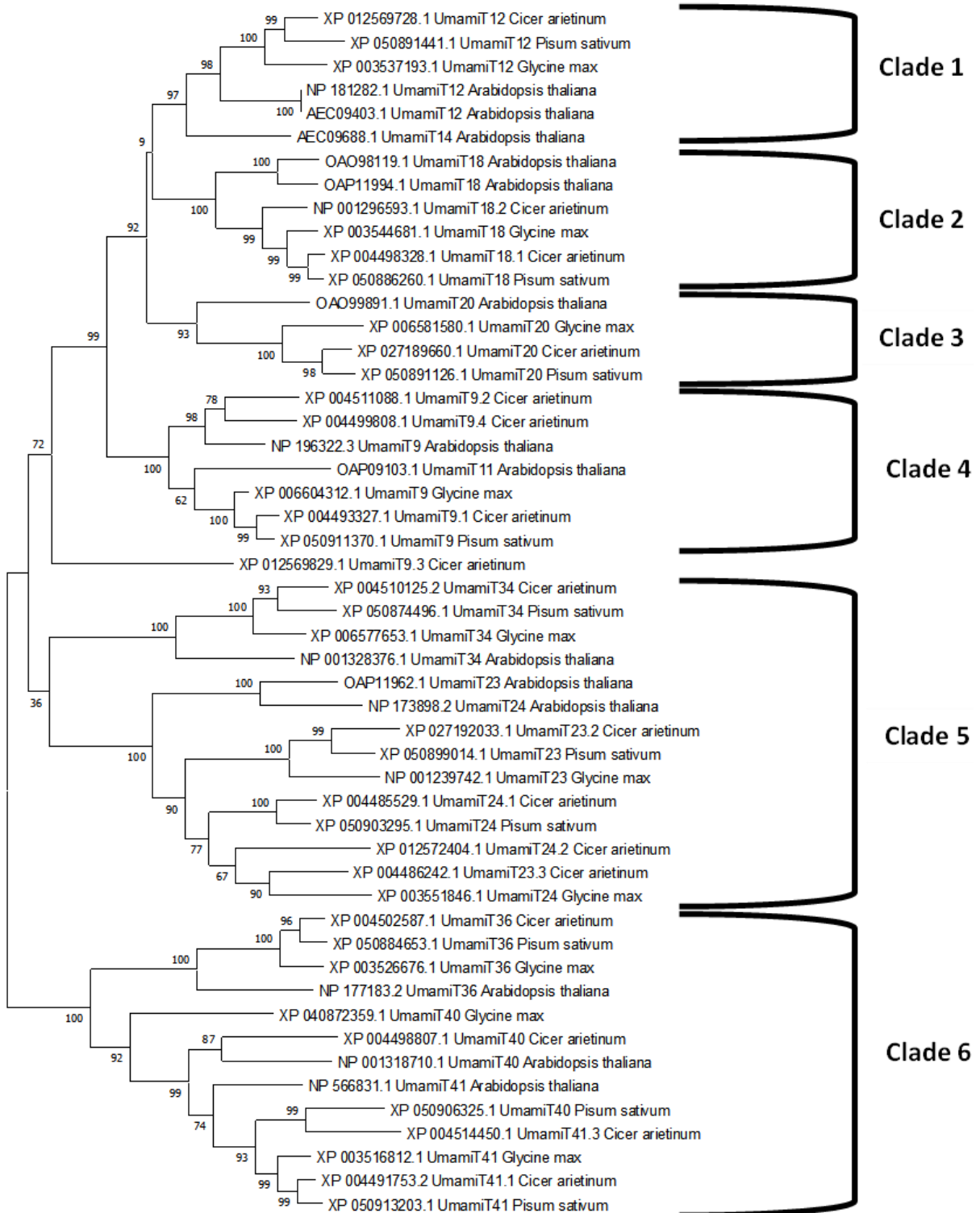


Figure 5.3: Phylogenetic analysis of AVT & CAT transporters from *C. arietinum*, *G. max*, *P. sativum* and *A. thaliana*.

Maximum likelihood phylogenetic tree constructed on MEGAX 10.0 (Kumar et al., 2018), after amino acid sequences of AVT & CAT genes aligned using MUSCLE. Tree constructed with 1000 bootstrap replications with respective bootstrap values displayed with a maximum of 100 at each node.



0.20

Figure 5.4: Phylogenetic analysis of UmamiT transporters from *C. arietinum*, *G. max P. sativum* and *A. thaliana*.

Maximum likelihood phylogenetic tree constructed on MEGAX 10.0 (Kumar et al., 2018), after amino acid sequences of UmamiT genes aligned using MUSCLE. Tree constructed with 1000 bootstrap replications with respective bootstrap values displayed with a maximum of 100 at each node.

5.3 Cloning of Chickpea Amino Acid Transporter Genes and Heterologous Expression in *S. cerevisiae*

To functionally characterise transport, six genes of interest were cloned into a yeast expression system (Besnard et al., 2016) and growth assays were performed by supplementation of various amino acids. The protocol is outlined below (Figure 5.5) and in more detail, General Methods: 2.6 & 2.7. Genes of interest were amplified via PCR from primers designed to bind to the start and stop codon to amplify the amino acid sequence from nodule cDNA. AttB Gateway® adaptor cloning sites were amended using overlapping PCR primers to the 5' and 3' ends of the amplified amino acid sequences for recombination into the entry vector pDONR then the yeast expression vectors pYESdest52 and pDR196 (Figure 5.5). These expression vectors were transformed using a lithium acetate protocol (General Methods: 2.7.2) into two yeast strains (223344c-Parent & 22Δ10AA-Mutant) for functional complementation assays (Figure 5.5). The full procedure is described in the appendix of this chapter (Appendix 5a.1-5a.6).

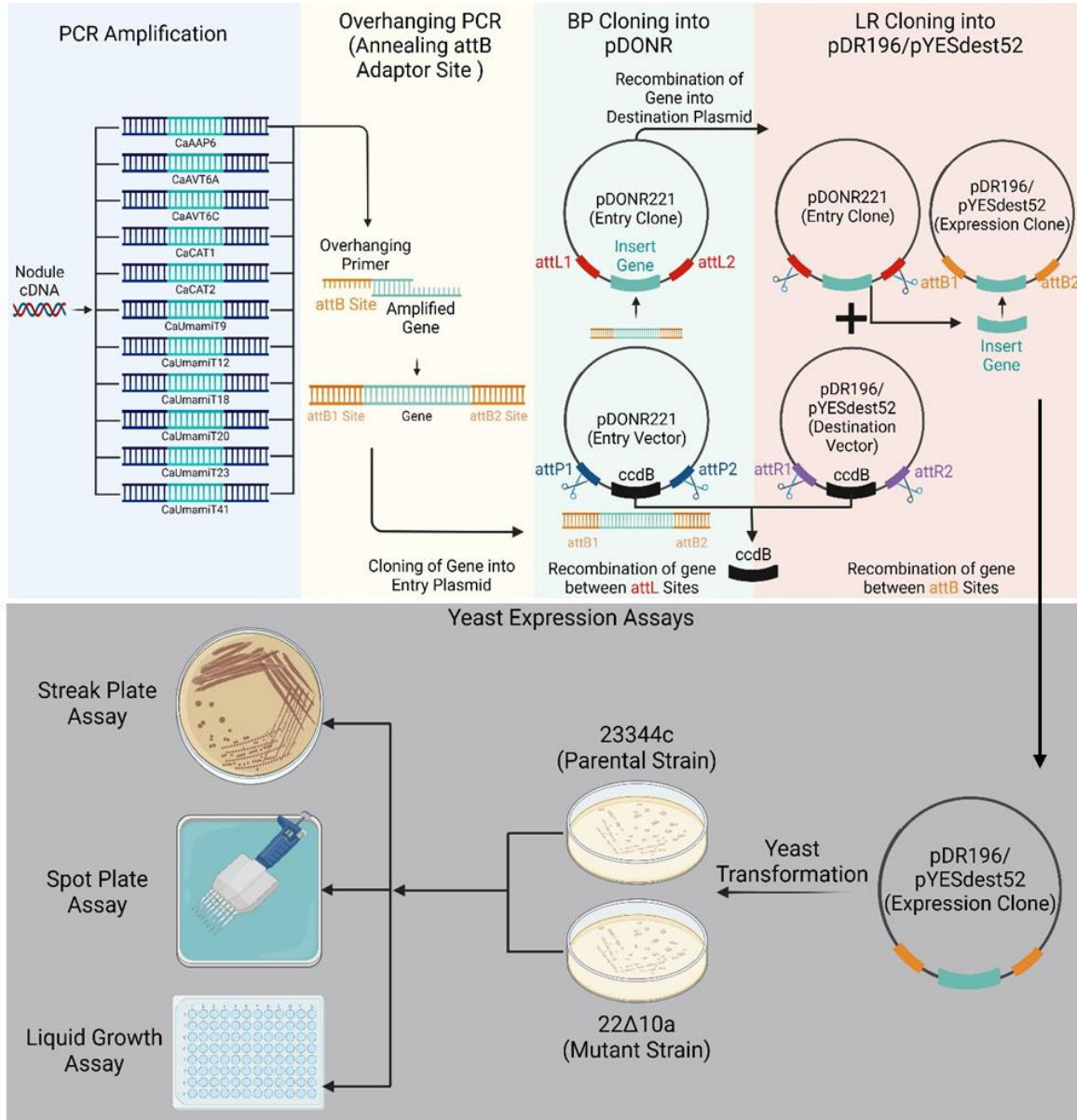


Figure 5.5: Schematic representation of Gateway® cloning chickpea amino acid transporter genes into the *S. cerevisiae* expression system.

Chickpea amino acid transporter genes were amplified from nodule cDNA and attB Gateway® adaptor cloning sites attached via overlapping PCR. Gene sequences cloned into the entry vector, pDONR221 via recombination between the attL sites using BP II clonase. LR II clonase reaction was then performed to allow recombination of the gene of interest between attB sites of the yeast expression destination vectors pDR196 or pYESdest52. Destination vectors were subsequently transformed into both the parental (23344c) and mutant (22Δ10AA) *S. cerevisiae* strains used for complementation experiments involving streak & spot plate assays and more robust liquid growth assays. Created with BioRender.com.

5.4. *S. cerevisiae* Streak Plate Assays with Transformants in pYESdest52 Expression Vector

5.4.1 Testing different nitrogen supplementation in the pYESdest52 transformants

Since low affinity amino acid transporters may struggle to initiate growth of the severe mutant 22Δ10AA strain, even when appropriate amino acids are supplemented, Yeast Synthetic drop-out medium minus uracil was used to provide nitrogen to “jump start” initial growth in the complementation assays.

Adenine, which is not an amino acid but can be used as a nitrogen source, was tested as a supplementation to initiate yeast growth with *CaAAP6*-pYESdest52 (Figure 5.6). 22Δ10AA and 23344c strains harbouring *CaAAP6*-pYESdest and empty pYESdest52 were grown on YNB solid media, 2% galactose at pH 6.2 with adenine supplementation as a sole N source at concentrations of 0.1, 0.5, 1.0 and 3.0 mM (Figure 5.6).

Adenine supplementation showed some growth at a concentration of 0.5 mM for all the transformants except for *CaAAP6*-23344c, whereas transformants on 0.1 mM adenine exhibited negligible growth (Figure 5.6). Both the empty vector parental (23344c) and *CaAAP6* expressing parental (*CaAAP6*-23344c) transformant appeared to have the least amount of growth with adenine supplementation compared to the empty vector mutant (22Δ10AA) and mutant strain expressing *CaAAP6* (*CaAAP6*-22Δ10AA) transformant. It could be possible that in the mutant strain, 22Δ10AA, other transporters that have not been deleted may have upregulated to facilitate greater adenine transport over the parental strain, promoting more growth with adenine supplementation. All transformants used grew at a similar rate when supplemented with a typical nitrogen control (NH₂SO₄) (Figure 5.6). This outcome suggested that using 0.5 mM adenine as a nitrogen source to initiate growth under amino acid assay conditions may help to off-set the severe growth phenotype of the 22Δ10AA strains. However, an additional 0.5 mM adenine control will need to be employed under all assay conditions to identify any false positive complementation.

As an alternative, simply using lower concentrations of NH₂SO₄ was also tested (Figure 5.7). At the lowest concentration tested (0.5 mM), NH₂SO₄ supplementation still exhibited substantial growth in both *CaAAP6* and empty transformants of the 23344c and 22Δ10AA strains (Figure 5.7). Indeed, using NH₂SO₄ in this manner may interfere too much with complementation to establish an initial jump start in growth without overcompensating for the mutant phenotype. Despite the severe growth phenotype of the 22Δ10AA strains, streak assays were conducted initially without using a N source supplementation.

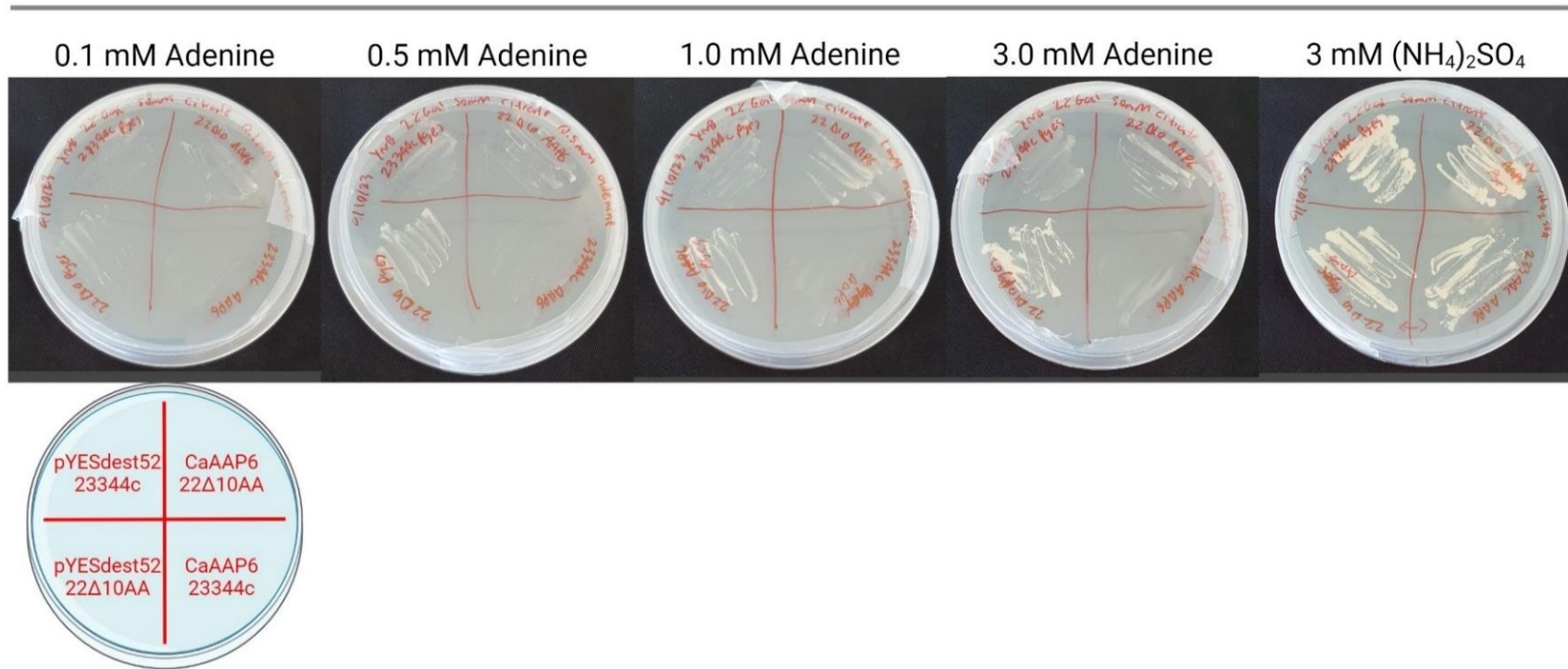


Figure 5.6: *S. cerevisiae* 22Δ10AA-pYESdest52 and 22Δ10AA-CaAAP6-pYESdest52 can be grown supplemented with adenine as a sole nitrogen source present in the yeast synthetic amino acid minus uracil drop out medium.

Streak plate assay of *S. cerevisiae* transformants containing *CaAAP6*-23344c, *CaAAP6*-22Δ10AA and empty 23344c and 22Δ10AA in the pYESdest52 vector. *S. cerevisiae* transformants grown on YNB medium at pH 6.2 supplemented with 2%-Gal, 50 mM citric acid and supplemented with 0.1, 0.5, 1 or 3 mM adenine. Streak plates performed from single colonies of transformants previously grown on YNB medium at pH 6.2 supplemented with 2%-Gal, 50 mM citric acid and yeast synthetic amino acid minus uracil drop out medium. Control YNB medium plates supplemented with 3 mM (NH₄)₂SO₄ as the sole nitrogen source. Top Left: 23344c-pYESdest52; Bottom Left: 22Δ10AA-pYESdest52; Top Right: *CaAAP6*-22Δ10AA-pYESdest52; Bottom Right: *CaAAP6*-23344c-pYESdest52

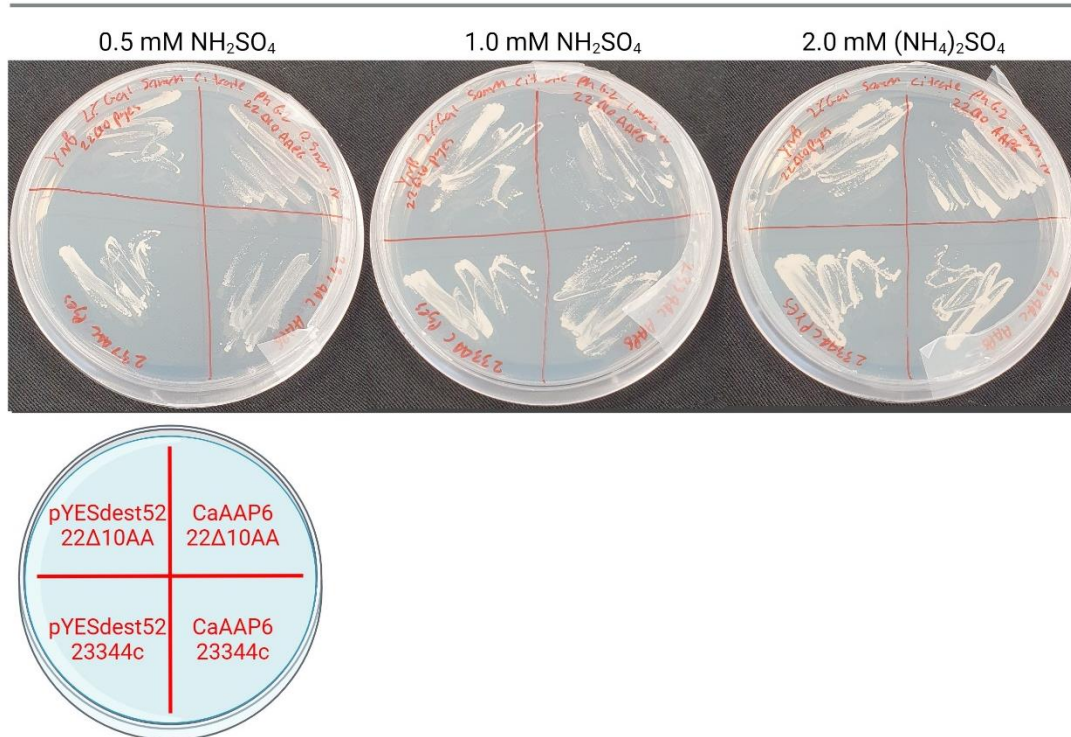


Figure 5.7: *S. cerevisiae* pYESdest52-22Δ10AA/23344c and CaAAP6-22Δ10AA/23344c growth can be supplemented with as little as 0.5 mM (NH₄)₂SO₄ as a nitrogen source present in the yeast YNB medium at pH 6.2.

Streak plate assay of *S. cerevisiae* transformants containing CaAAP6-23344c, CaAAP6-22Δ10AA and empty 23344c and 22Δ10AA in the pYESdest52 vector. *S. cerevisiae* transformants grown on YNB medium at pH 6.2 supplemented with 2%-Gal, 50 mM citric acid and supplemented with 0.5, 1 or 2 mM (NH₄)₂SO₄. Streak plates performed from single colonies of transformants previously grown on YNB medium at pH 6.2 supplemented with 2%-Gal, 50 mM citric acid and yeast synthetic amino acid minus uracil drop out medium. Top Left: pYESdest52-22Δ10AA; Bottom Left: pYESdest52-23344c; Top Right: CaAAP6-pYESdest52-22Δ10AA; Bottom Right: CaAAP6-pYESdest52-23344c.

5.4.2 Streak plate amino acid assays of *CaAAP6* & *CaAVT6C* in *pYESdest52*

Initial streak assays were performed on *pYESdest52* expressing *CaAAP6* & *CaAVT6C* as a rapid means to determine amino acid complementation prior to spot and liquid growth assays. The streak assay was conducted by streaking single colonies of each the *CaAAP6*-*pYESdest52* & *CaAVT6C*-*pYESdest52* of the 23344c & 22 Δ 10AA strains on plates with YNB medium supplemented with yeast synthetic amino acid minus uracil drop out medium to bulk up the single colony (General Methods: 2.7.4). Cells from each plate were then again streaked on YNB medium supplemented with individually, or in combination, the amides Gln & Asn or the amino acids Glu & Asp as the sole N source.

CaAAP6 complemented the amino acid knock-out phenotype of the 22 Δ 10AA strains when grown with Glu and Asp but not the amides Gln & Asp (Figure 5.8). *CaAAP6* complemented the growth phenotype when supplemented with three Asp concentrations of 3, 10 and 20 mM, visualised by the growth of M2 (*CaAAP6*-*pYESdest52*-22 Δ 10AA) (Figure 5.8). In contrast, the yeast mutant strain containing the empty vector, M1 (*pYESdest52*-22 Δ 10AA), did not show any growth. Glu complementation was not as convincing since the positive control in the P2 (*CaAAP6*-*pYESdest52*-23344c) strain showed no growth (Figure 5.8). P1, yeast parental strain containing the empty vector (*pYESdest52*-23344c) on the other hand, grew as expected on all plates (Figure 5.8).

The *pYESdest52*-22 Δ 10AA expressing *CaAAP6* complemented the amino acid deletion of the mutant strain in all tested concentrations using a combination treatment of all four amino acids, likely driven by Asp. However, the empty mutant transformant (M1) also grew here, suggesting that the large N input via combinational supplementation of all four amino acids was enough to rescue the knock-out mutant (Figure 5.8). However, it is possible that P2 and M1 were miss-labelled here explaining the unexpected lack of growth for the P2 control (Figure 5.8).

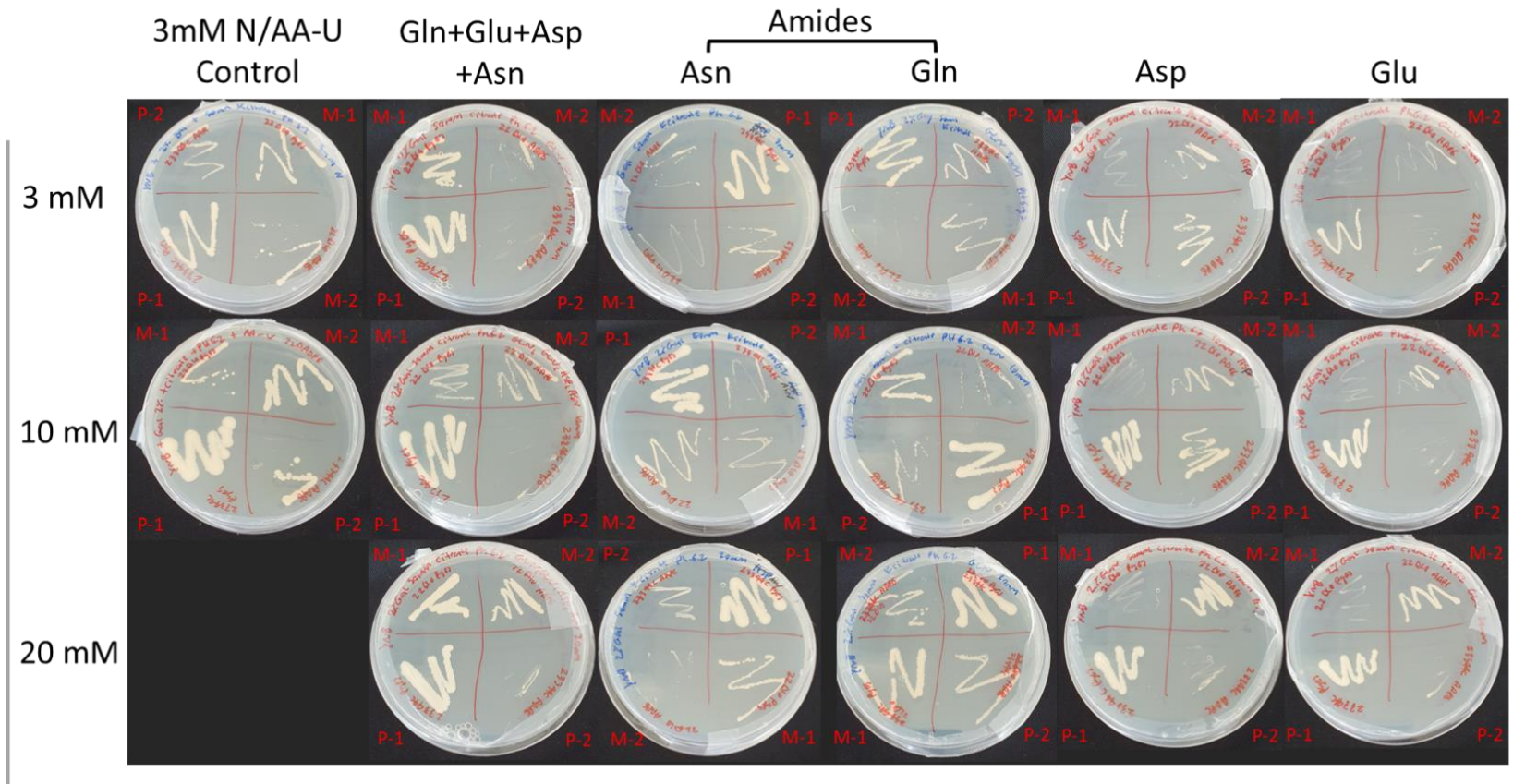


Figure 5.8: *CaAAP6*-pYESdest52 compliments aspartate and glutamate but does not compliment the amides glutamine and asparagine in *S. cerevisiae* 22Δ10AA mutant.

Streak plate assay of *S. cerevisiae* transformants containing *CaAAP6*-23344c, *CaAAP6*-22Δ10AA and empty 23344c and 22Δ10AA in the pYESdest52 vector supplemented with the amides Gln and Asn as well as the amino acids Glu and Asp. *S. cerevisiae* transformants grown on YNB medium at pH 6.2 supplemented with 2% Gal, 50 mM citric acid and various amino acids added together and separately, at 3, 10 and 20 mM concentrations. Streak plates performed from single colonies of transformants previously grown on YNB medium at pH 6.2 supplemented with 2% Gal, 50 mM citric acid and yeast synthetic amino acid minus uracil drop out medium. Control YNB medium plates supplemented with either 3 mM (NH₄)₂SO₄ or yeast synthetic amino acid minus uracil drop out medium as the sole N source. **P1:** 23344c-pYESdest52; **P2:** *CaAAP6*-pYESdest52-23344c; **M1:** 22Δ10AA-pYESdest52; **M2:** *CaAAP6*-pYESdest52-22Δ10AA.

The mutant yeast strain expressing *CaAVT6C* did not grow on media supplemented with any of the four amino acids tested, including the two amides (Figure 5.9). Growth was observed for the two parental control transformants (Figure 5.9). Gln transport appeared to be still somewhat available to the knockout mutant strain in the empty transformant, as minor growth was still observed at 3 mM, with noteworthy growth at 10 and 20 mM (Figure 5.9). Similarly, the Asn plates also rescued the empty and *CaAVT6C-22Δ10AA* mutant phenotype at 20 mM but not 3 and 10 mM (Figure 5.9). The Gln and Asn complementation may also be due to passive diffusion of these neutral amino acids or via Na⁺ carriers and particularly, AVT transporters which have not been removed from the mutant strain (Bianchi et al., 2019).

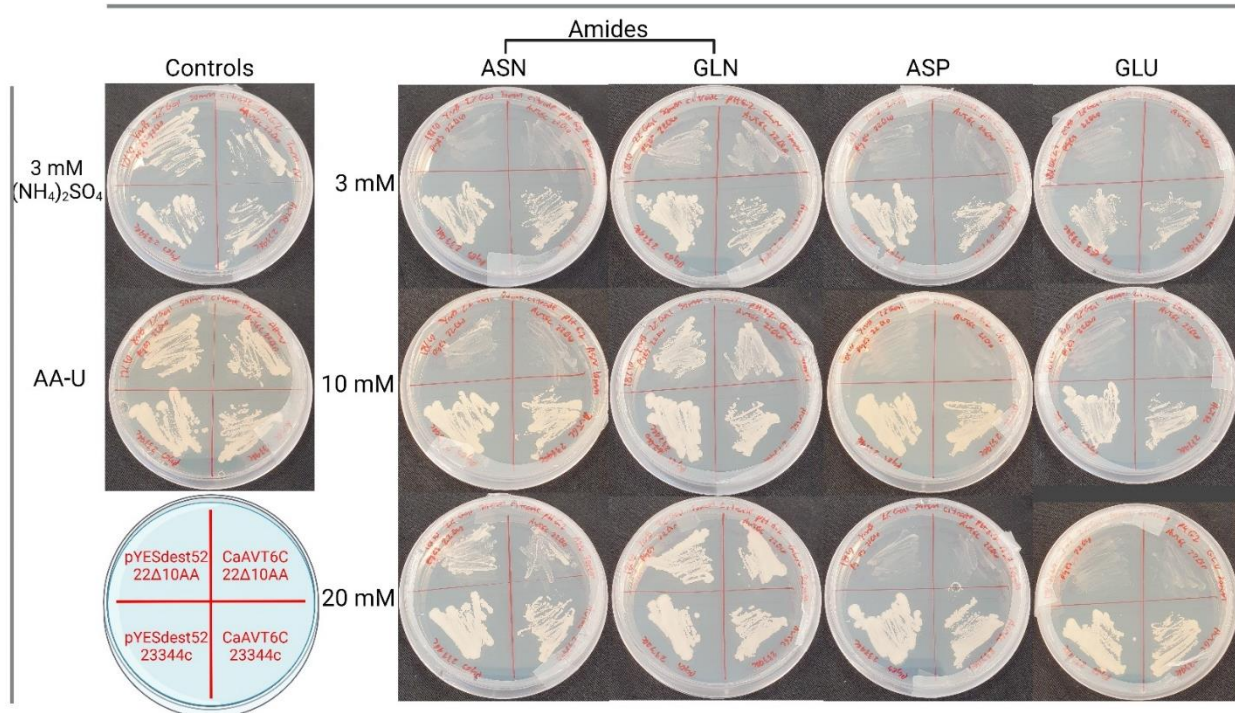


Figure 5.9: *CaAVT6C*-pYESdest52 does not complement the mutant *S. cerevisiae* 22Δ10AA strain when supplemented with Asn, Gln, Asp and Glu.

Streak plate assay of *S. cerevisiae* transformants containing *CaAVT6C*-23344c, *CaAVT6C*-22Δ10AA and empty 23344c and 22Δ10AA in the pYESdest52 vector supplemented with the amides Gln and Asn as well as the amino acids Glu and Asp. *S. cerevisiae* transformants grown on YNB medium at pH 6.2 supplemented with 2% Gal, 50 mM citric acid and various amino acids, at 3, 10 and 20 mM concentrations. Streak plates performed from single colonies of transformants previously grown on YNB medium at pH 6.2 supplemented with 2% Gal, 50 mM citric acid and yeast synthetic amino acid minus uracil drop out medium. Control YNB medium plates supplemented with either 3 mM (NH₄)₂SO₄ or yeast synthetic amino acid minus uracil drop out medium as the sole N source.

5.5. Multiple Chickpea Amino Acid Transporters Rescued the Amino Acid Mutant *S. cerevisiae* Strain in the pDR196 Expression Vector

Further complementation assays were conducted in the pDR196 transformants, due to cloning difficulties in establishing an effective positive control into the pYESdest52 plasmid. Here the *S. cerevisiae* GAP1 gene was used as a positive growth control, as previously used by (Besnard et al., 2016), cloned into pDR196. To help complete the nodule amino acid transport network model, six chickpea amino acid genes AAP6, AVT6A, UmamiT9, UmamiT18, UmamiT20 and UmamiT41 were successfully transformed into the pDR196 expression vector (Appendix 5a.4 Figure 5a.12) for use in both serial diluted spot plates and liquid growth assays (General Methods: 2.7.5, 2.7.6).

5.5.1 Complementation in pDR196 using spot plate assays

Complementation assays of the 22Δ10AA amino acid knockout strain examined on spot plates were performed on solid YNB media (pH 6.2) supplemented with one of seven amino acids: Gln, Glu, Asn, Asp, Ala, GABA or Tyr as the sole nitrogen source. Overnight grown cultures of *S. cerevisiae* 22Δ10AA strain expressing each of the six chickpea transporters, *ScGAP1* and empty pDR196 negative control were pelleted and washed twice then 10-fold serial diluted from OD600 1 to 10⁻³ on each plate.

Supplementation of the seven amino acids resulted in the *ScGAP1* positive control growing efficiently as expected at all concentrations and at the lowest dilution of 10⁻³ at pH 6.2 (Figure 5.10-12). The empty vector pDR196 control exhibited minor growth with 6 mM Glu at a dilution of 10⁻⁰ and moderate growth when supplemented with Gln at 1, 3 and 6 mM at pH 6.2 (Figure 5.10, 5.11). The Gln growth phenotype was also observed in the streak assays using pYESdest52, backing up the assumption that the 22Δ10AA strain was still able to take up Gln, perhaps by passive diffusion (Figure 5.11). Empty vector pDR196 also did not rescue the mutant strain when supplemented with GABA and only exhibited very minor growth with 3 and 6 mM concentrations of Ala (Figure 5.12). An unusual result was observed for Tyr where the empty pDR196 grew effectively under the 1 mM concentration up to the 10⁻³ serial dilution (Figure 5.12). This contradicts the liquid assay results which will be discussed later and was only observed on solid media. On the same plate *CaAAP6*-22Δ10AA showed no growth with supplemented with Tyr at any concentration where it would be expected that if the empty vector complemented the mutant strain so would all other mutants (Figure 5.12). The assays in the panel encompassing GABA, Tyr and Ala were conducted on the same day with the same empty pDR196 culture eliminating any notable variability in

the growth phenotype. Conversely, the N-positive control (3 mM $(\text{NH}_4)_2\text{SO}_4$) rescued the mutant strain as expected in all cases at a near identical rate up to a dilution 10^{-3} (Figure 5.11).

The amino acid knockout of the $22\Delta 10\text{AA}$ *S. cerevisiae* strain was rescued by four chickpea amino acid transporters: AAP6, AVT6A, UmamiT9 and UmamiT18 when grown on media supplemented with the two amides (Gln & Asn) as well as Glu and Asp at a pH of 6.2 (Figure 5.11). Minor complementation was also observed for *CaUmamiT20-22\Delta 10\text{AA}* at 6 mM Glu & Gln with a single colony growing up to the 10^{-1} dilution (Figure 5.10, 5.11). *CaUmamiT41-22\Delta 10\text{AA}* may also have displayed a very minor complementation phenotype for Asp & Glu with colonies at a concentration of 3 mM at dilutions of 10^0 (Figure 5.10, 5.11). *CaUmamiT41-22\Delta 10\text{AA}* complementation when supplemented with Glu & Gln at 6 mM matches the pDR196 empty vector, indicating background transport via the mutant strain and likely not a complementation response (Figure 5.10, 5.11). Irrespectively, possible *CaUmamiT41-22\Delta 10\text{AA}* complementation may indicate very low transport affinity of Asp and Glu.

Complementation was also observed for *CaUmamiT20-22\Delta 10\text{AA}* from 1 mM GABA, Tyr and alongside *CaAAP6-22\Delta 10\text{AA}* for Ala (Figure 5.12). Only a single colony at 1 mM was observed for *CaUmamiT9-22\Delta 10\text{AA}* on the GABA plate (Figure 5.12). Tyr presented notable complementation at all concentrations for all mutants tested except *CaAAP6-22\Delta 10\text{AA}* and very minor yeast growth for *CaUmamiT41-22\Delta 10\text{AA}* at 6 mM Tyr (Figure 5.12). As mentioned above, the empty pDR196 yeast growth was also rescued on the Tyr spot plate, likely indicating a false positive Tyr complementation on the spot plate assay.

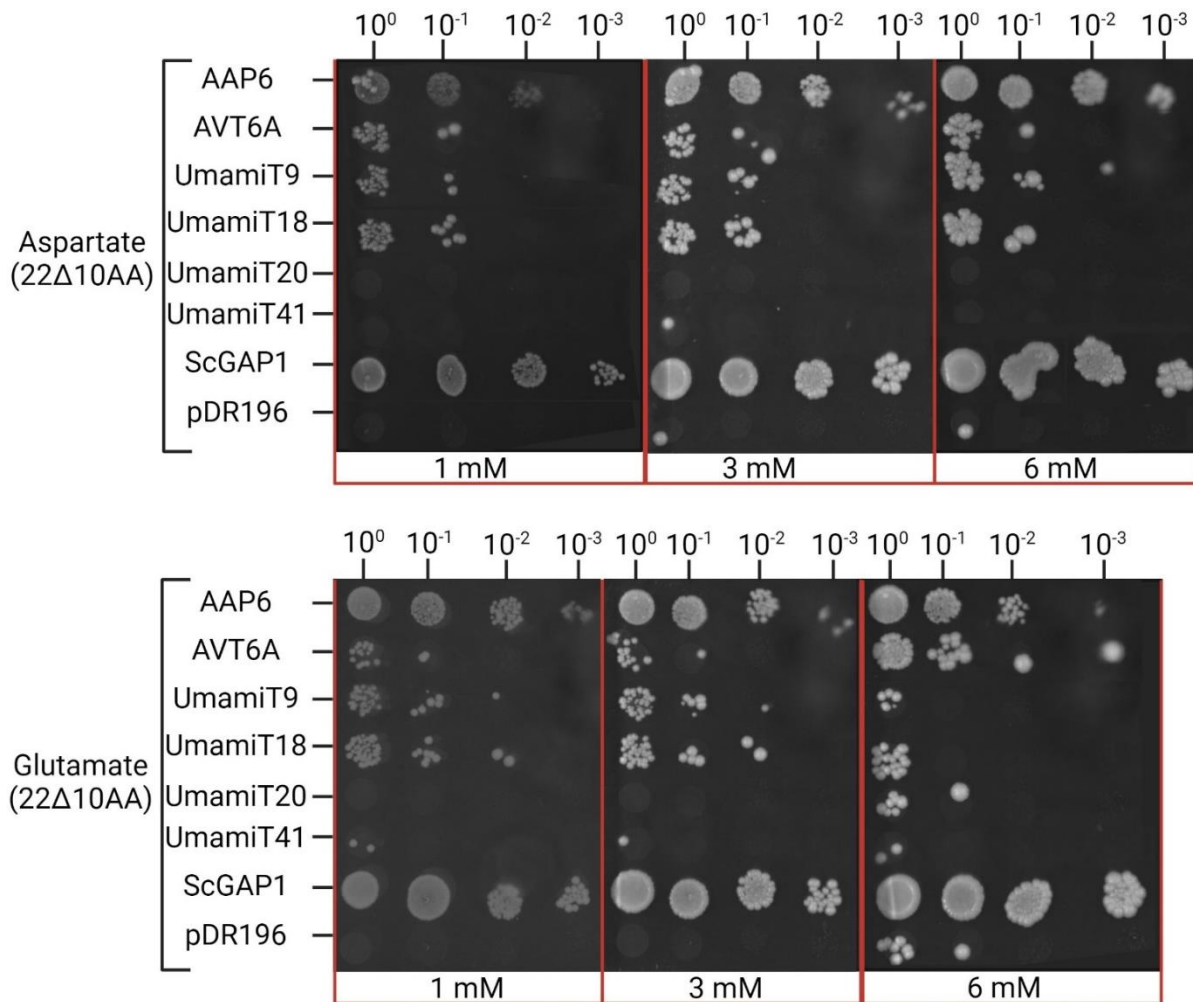


Figure 5.10: Spot plate growth assay of *S. cerevisiae* 22Δ10AA strain shows complementation of *CaAAP6*, *CaAVT6A*, *CaUmamiT9* and *CaUmamiT18* grown with Asp and Glu.

Spot plate assay of *S. cerevisiae* transformants expressing six chickpea amino acid transporters and *ScGAP1* positive control in the pDR196 expression vector transformed into the 22Δ10AA strain. Empty pDR196 in 22Δ10AA was used as a negative empty vector control. *S. cerevisiae* transformants were previously grown overnight in liquid YNB medium at pH 6.2 supplemented with 2% glucose, 50 mM citric acid buffer and yeast synthetic amino acid minus uracil drop out medium as a N source. Culture pellet washed then diluted to an OD600 of 1 and serial diluted up to 10^{-3} for plating on solid YNB medium supplemented with either Asp or Glu at 1, 3 and 6 mM concentrations.

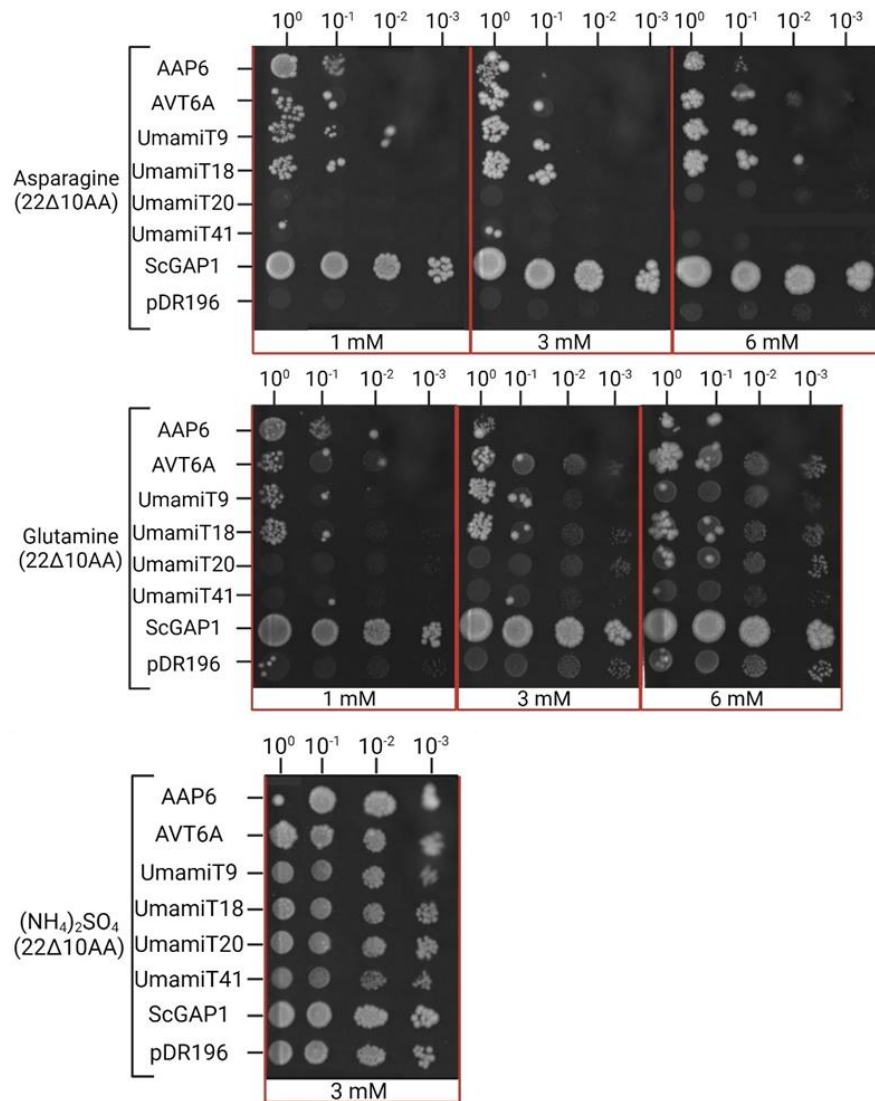


Figure 5.11: Spot plate growth assay of *S. cerevisiae* 22Δ10AA strain shows complementation of *CaAAP6*, *CaAVT6A*, *CaUmamiT9* and *CaUmamiT18* grown with Asn & Gln and *CaUmamiT20* with Gln.

Spot plate assay of *S. cerevisiae* transformants expressing six chickpea amino acid transporters and *ScGAP1* positive control in the pDR196 expression vector transformed into the 22Δ10AA strain. Empty pDR196 in 22Δ10AA was used as a negative empty vector control. *S. cerevisiae* transformants were previously grown overnight in liquid YNB medium at pH 6.2 supplemented with 2% glucose, 50 mM citric acid buffer and yeast synthetic amino acid minus uracil drop out medium as a N source. Culture pellet washed then diluted to an OD₆₀₀ of 1 and serial diluted up to 10⁻³ for plating on solid YNB medium supplemented with either Asn or Gln at 1, 3 and 6 mM concentrations.

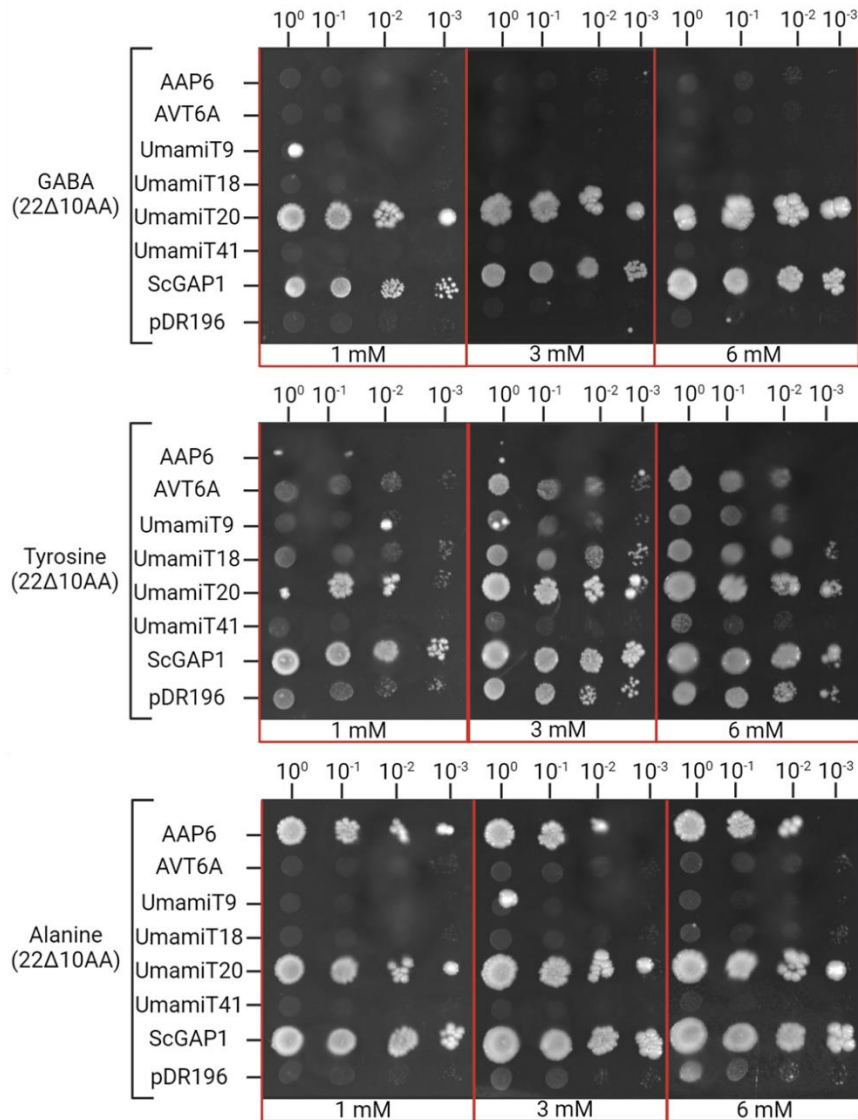


Figure 5.12: Spot plate growth assay of *S. cerevisiae* 22Δ10AA strain shows complementation of chickpea amino acid transporters grown with GABA, Tyr and Ala.

Spot plate assay of *S. cerevisiae* transformants expressing six chickpea amino acid transporters and *ScGAP1* positive control in the pDR196 expression vector transformed into the 22Δ10AA strain. Empty pDR196 in 22Δ10AA was used as a negative empty vector control. *S. cerevisiae* transformants were previously grown overnight in liquid YNB medium at pH 6.2 supplemented with 2% glucose, 50 mM citric acid buffer and yeast synthetic amino acid minus uracil drop out medium as a N source. Culture pellet washed then diluted to an OD600 of 1 and serial diluted up to 10^{-3} for plating on solid YNB medium supplemented with either GABA, Tyr or Ala at 1, 3 and 6 mM concentrations.

5.5.2 Multiple chickpea amino acid transporters rescued the knock-out mutant *S. cerevisiae* strain in liquid assays.

Following optimization of the liquid assay (Appendix: 5a.7), a number of amino acids successfully complemented the amino acid deficient yeast mutant including the two amides Gln and Asn observed previously in pre-optimized conditions (Figure 5a.25-3a.26). *CaAAP6-22Δ10AA*, *CaAVT6A-22Δ10AA*, *CaUmamiT9-22Δ10AA*, *CaUmamiT18-22Δ10AA* and *CaUmamiT20-22Δ10AA* all grew effectively in YNB liquid media (pH 6.2) supplemented with 1, 3 and 6 mM Gln and Asn using the optimized conditions (Figures 3.13, 3.14). These transporters appeared to exhibit a high affinity for both Gln and Asn where a concentration dependent increase of the relative growth rate was statistically significant for *CaAAP6-22Δ10AA*, *CaAVT6A-22Δ10AA*, *CaUmamiT9-22Δ10AA*, *CaUmamiT20-22Δ10AA* and *ScGAP1-22Δ10AA* from 1 to 3 mM & 1 to 6 mM with Asn (Figure 5.14) and for all mutants with Gln (Figure 5.12). That is, both amides effectively rescued the amino acid knockout mutants up to 3 mM concentration with no significant increase from 3 to 6 mM. In both Asn and Gln the *ScGAP1-22Δ10AA* and empty pDR196-22Δ10AA control grew as expected (Figure 5.13, 3,14). There was, however, minor growth recorded for the empty pDR196 control at 3 and 6 mM Gln, but this was observed substantially later compared to the chickpea genes tested (Figure 5.13). *CaUmamiT41-22Δ10AA* was found to not complement the mutant strain with any of the amino acid assayed and was therefore excluded from following analyses. The parental 23344c yeast strain was also validated under liquid growth assay conditions for all the measured amino acids (Appendix: 5a.7).

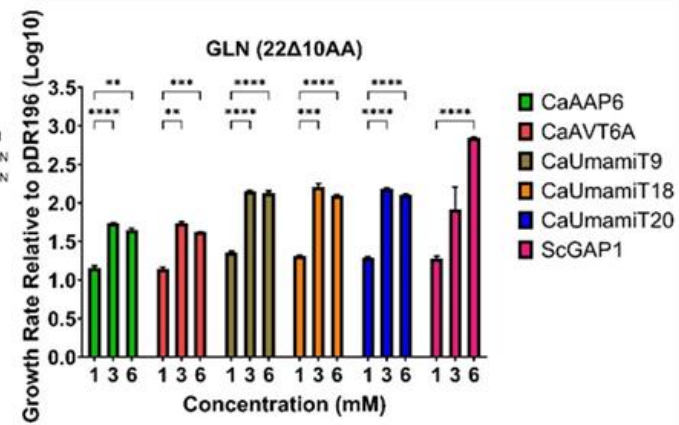
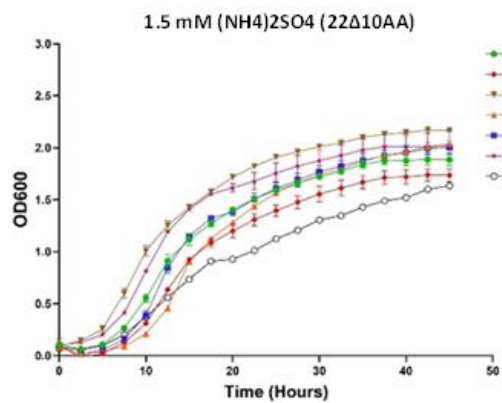
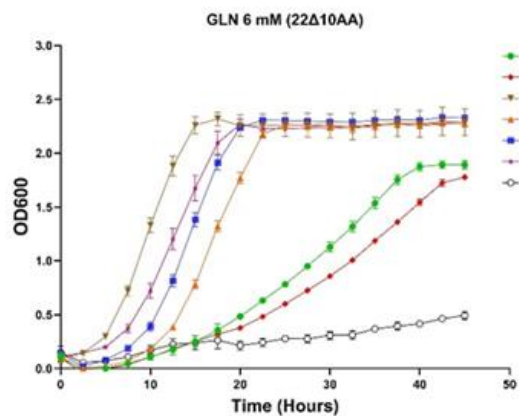
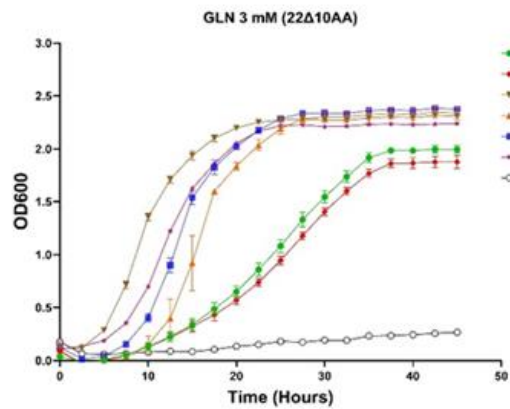
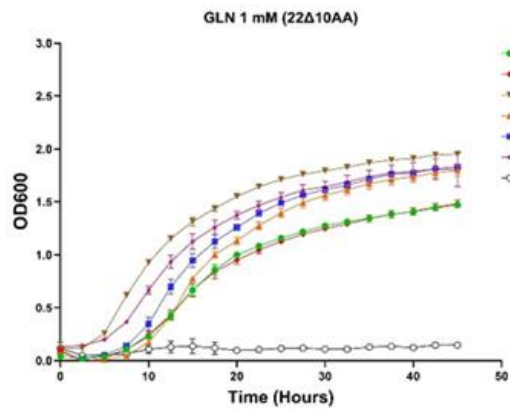


Figure 5.13: Glutamine Liquid 48h growth assay of the mutant (22Δ10AA) *S. cerevisiae* strain expressing five chickpea amino acid genes, *ScGAP1* positive control and empty pDR196 negative control.

Assay measured at OD600 at three separate concentrations of Gln (1, 3 & 6 mM) and 1.5 mM (NH₄)₂SO₄ as a N control. *S. cerevisiae* 22Δ10AA transformants expressing amino acid genes and the empty pDR196 control grown overnight in 2% glucose, 50 mM citric acid buffer and YNB (pH 6.2) supplemented with yeast synthetic amino acid minus uracil drop out medium, washed twice with sterile milli-Q water and diluted to an OD600 of 1. Assay performed with a 1:10 dilution of culture (20 μl) to liquid YNB (180 μl) made as previously, replacing synthetic amino acid medium with Gln, and run at 30°C with shaking. Statistical significance of relative growth rates for genes at differing Gln concentrations was calculated via One-Way ANOVA with multiple comparisons test (Tukey) (*<0.01, **<0.001, ***<0.0001). N = 6.

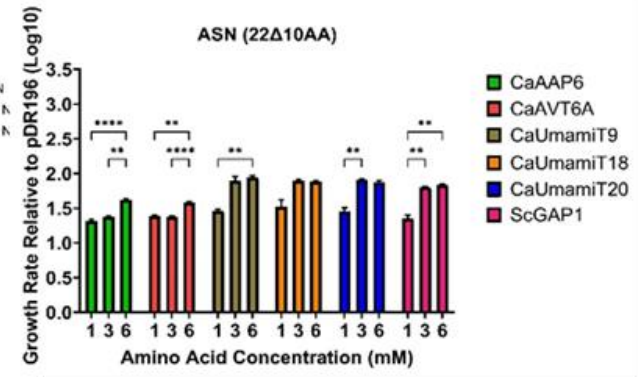
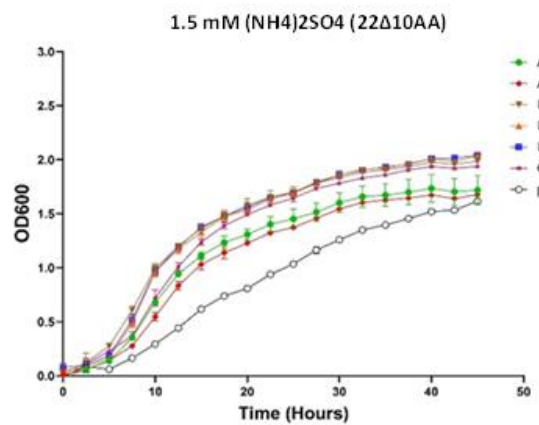
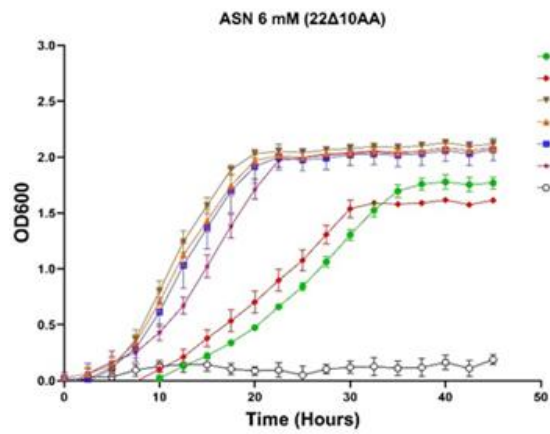
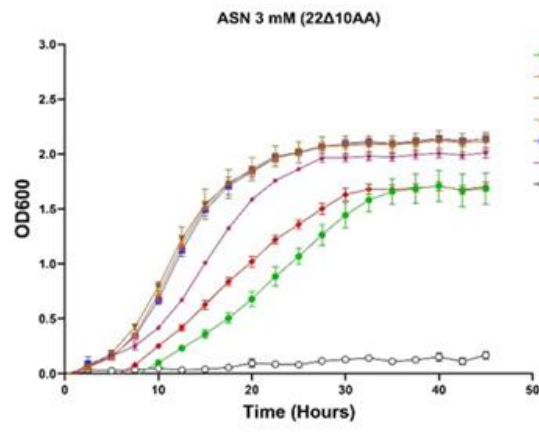
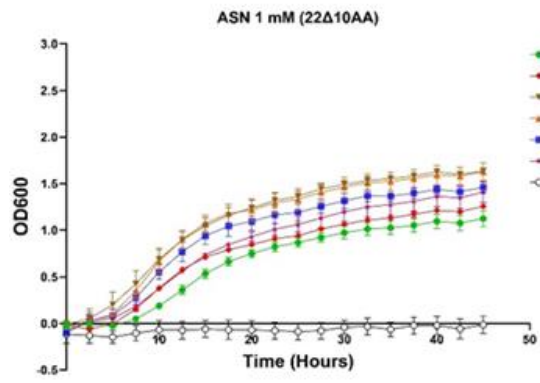


Figure 5.14: Asparagine liquid 48h growth assay of the mutant (22Δ10AA) *S. cerevisiae* strain expressing five chickpea amino acid genes, *ScGAP1* positive control and empty pDR196 negative control.

Assay measured at OD600 at three separate concentrations of Asn (1, 3 & 6 mM) and 1.5 mM (NH₄)₂SO₄ as a N control. *S. cerevisiae* 22Δ10AA transformants expressing amino acid genes and the empty pDR196 control grown overnight in 2% glucose, 50 mM citric acid buffer and YNB (pH 6.2) supplemented with yeast synthetic amino acid minus uracil drop out medium, washed twice with sterile milli-Q water and diluted to an OD600 of 1. Assay performed with a 1:10 dilution of culture (20 μl) to liquid YNB (180 μl) made as previously, replacing synthetic amino acid medium with Asn, and run at 30°C with shaking. Statistical significance of relative growth rates for genes at differing Asn concentrations was calculated via One-Way ANOVA with multiple comparisons test (Tukey) (*<0.01, **<0.001, ***<0.0001). N = 6

5.5.3 Liquid assay mutant complementation with Glu, Asp and Ala

Under pH 6.2 liquid assay conditions *CaAAP6-22Δ10AA*, *CaAVT6A-22Δ10AA*, *CaUmamiT9-22Δ10AA*, *CaUmamiT18-22Δ10AA* and *CaUmamiT20-22Δ10AA* all complemented the amino acid mutant phenotype supplemented with nodule abundant amino acids Glu, Asp and Ala (Figure 5.15, 3.16 & 3.17). These amino acids triggered a significantly increased relative growth rate in a concentration dependent manner from 1 to 6 mM (Figure 5.15, 3.16 & 3.17). Glu and Asp relative growth rates plateaued at approximately a Log_{10} of 2.0 (Figure 5.15 & 3.16), while slightly lower for Ala (Figure 5.17) at approximately 1.5. For Glu the relative growth rate of all genes outside of the empty vector control all significantly increased from 1 to 3 mM similar to the two amides previously observed (Figure 5.15). *CaUmamiT9-22Δ10AA*, *CaUmamiT18-22Δ10AA*, *CaUmamiT20-22Δ10AA* and *ScGAP1-22Δ10AA* also significantly increased from 3 to 6 mM Glu (Figure 5.15). The concentration dependent increase in the relative growth rate was more evenly distributed for Asp, particularly from 3 to 6 mM, with all mutants again showing a significantly increasing relative growth rate (Figure 5.16). However, supplementation of 1 mM Asp, *CaAAP6-22Δ10AA* and *CaAVT6A-22Δ10AA* exhibited very minor growth only just above that of the empty vector control (Figure 5.16). Relative growth of the mutants supplemented with Ala was similar to that of the amides, whereby the rate significantly increased up to 3 mM for all mutants and plateaued thereafter (Figure 5.17). This shows that 3 mM is sufficient to establish a peak growth rate.

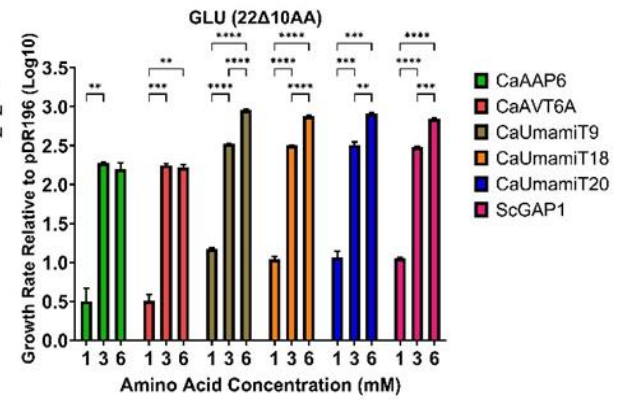
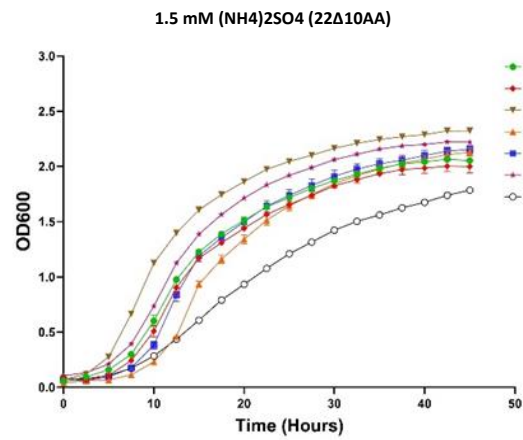
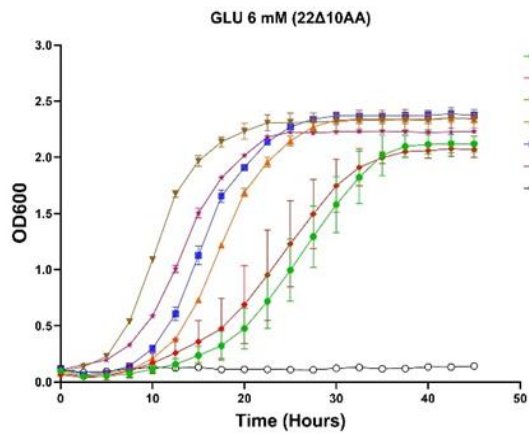
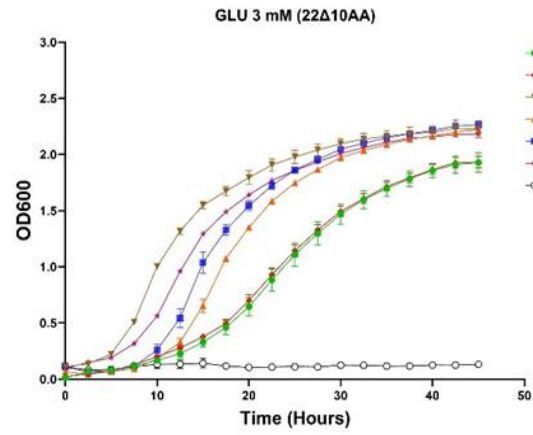
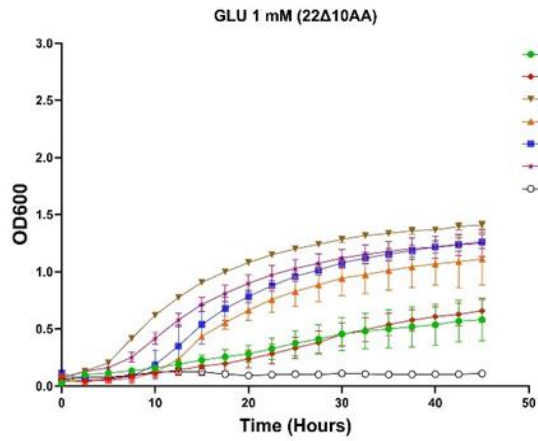


Figure 5.15: Glutamate liquid 48h growth assay of the mutant (22Δ10AA) *S. cerevisiae* strain expressing five chickpea amino acid genes, *ScGAP1* positive control and empty pDR196 negative control.

Assay measured at OD600 at three separate concentrations of Glu (1, 3 & 6 mM) and 1.5 mM (NH₄)₂SO₄ as a N control. *S. cerevisiae* 22Δ10AA transformants expressing amino acid genes and the empty pDR196 control grown overnight in 2% glucose, 50 mM citric acid buffer and YNB (pH 6.2) supplemented with yeast synthetic amino acid minus uracil drop out medium, washed twice with sterile milli-Q water and diluted to an OD600 of 1. Assay performed with a 1:10 dilution of culture (20 μl) to liquid YNB (180 μl) made as previously, replacing synthetic amino acid medium with Glu, and run at 30°C with shaking. Statistical significance of relative growth rates for genes at differing Glu concentrations was calculated via One-Way ANOVA with multiple comparisons test (Tukey) (*<0.01, **<0.001, ***<0.0001). N = 6

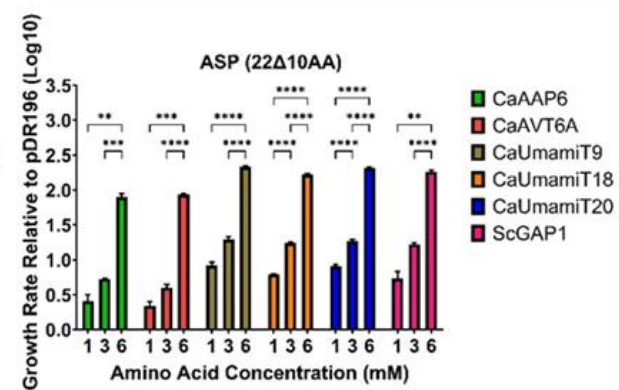
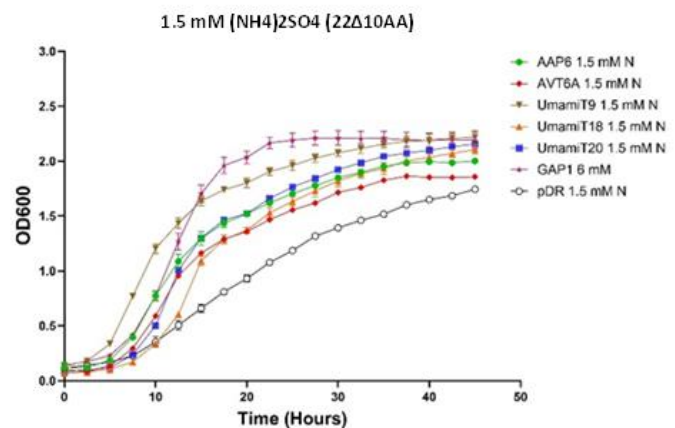
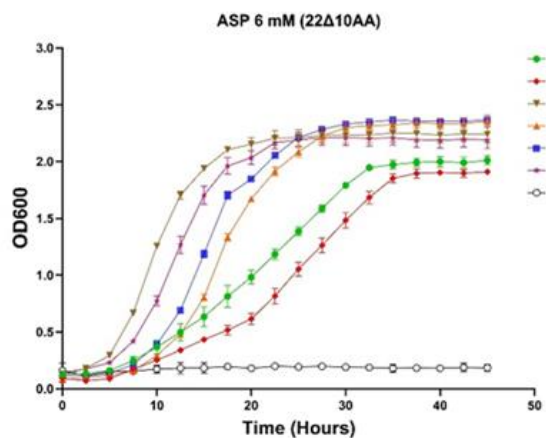
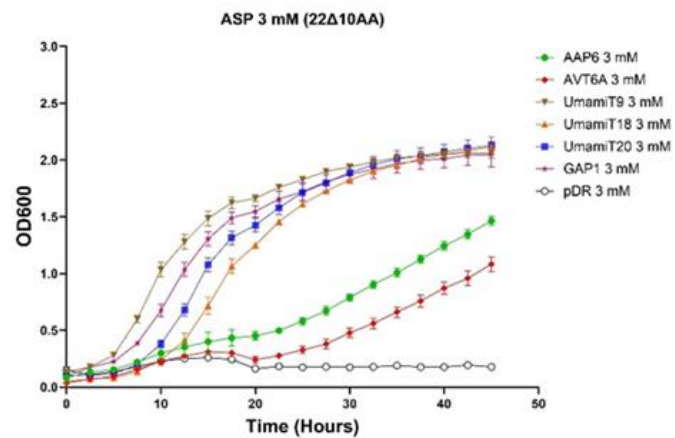
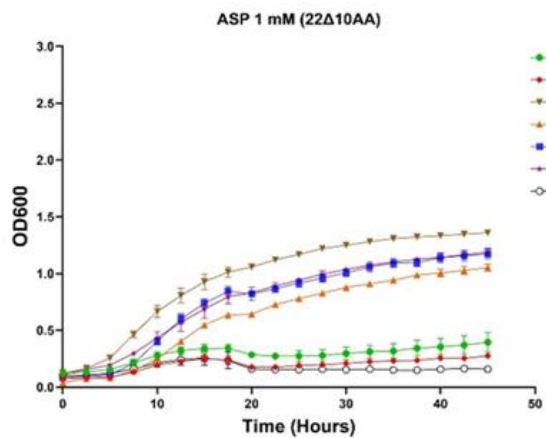


Figure 5.16: Aspartate liquid 48h growth assay of the mutant (22Δ10AA) *S. cerevisiae* strain expressing five chickpea amino acid genes, *ScGAP1* positive control and empty pDR196 negative control.

Assay measured at OD600 at three separate concentrations of Asp (1, 3 & 6 mM) and 1.5 mM (NH₄)₂SO₄ as a N control. *S. cerevisiae* 22Δ10AA transformants expressing amino acid genes and the empty pDR196 control grown overnight in 2% glucose, 50 mM citric acid buffer and YNB (pH 6.2) supplemented with yeast synthetic amino acid minus uracil drop out medium, washed twice with sterile milli-Q water and diluted to an OD600 of 1. Assay performed with a 1:10 dilution of culture (20 μl) to liquid YNB (180 μl) made as previously, replacing synthetic amino acid medium with Asp, and run at 30°C with shaking. Statistical significance of relative growth rates for genes at differing Asp concentrations was calculated via One-Way ANOVA with multiple comparisons test (Tukey) (*<0.01, **<0.001, ***<0.0001). N = 6.

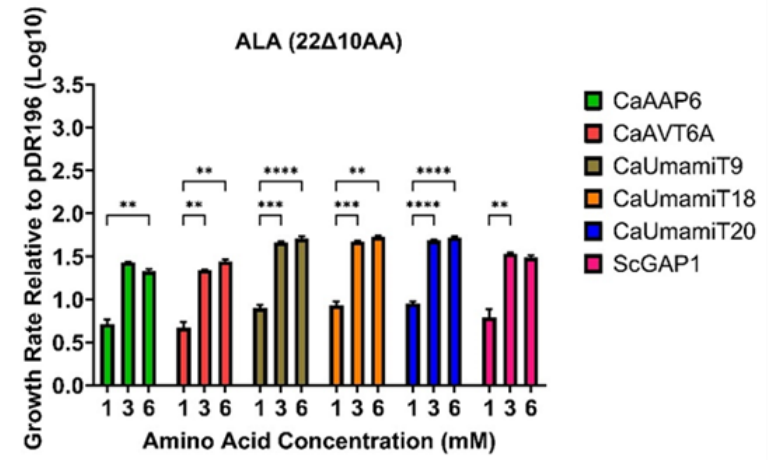
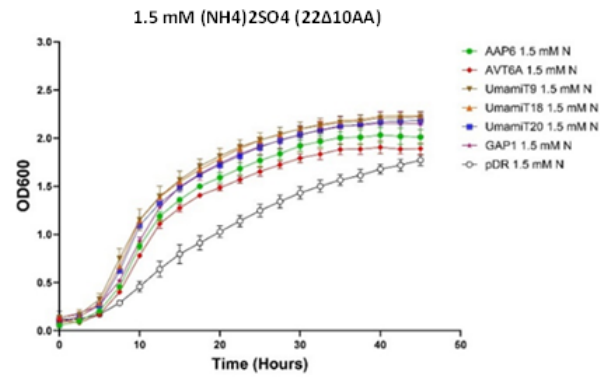
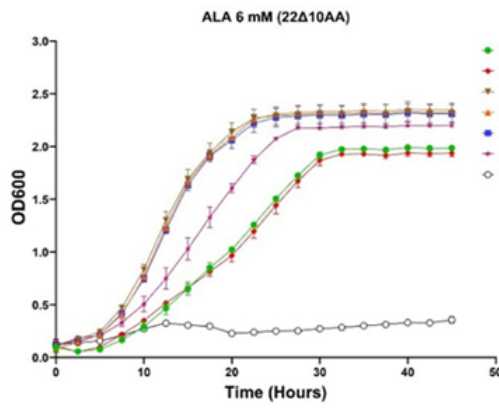
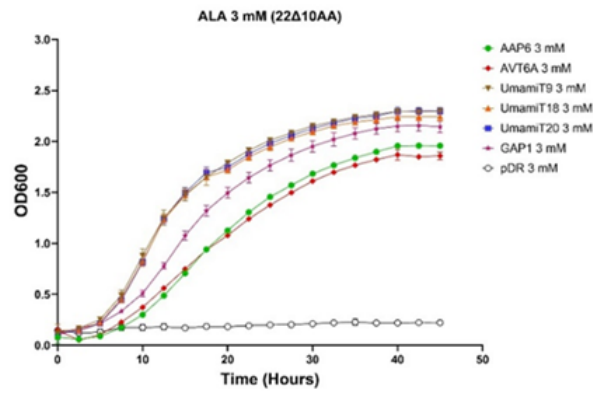
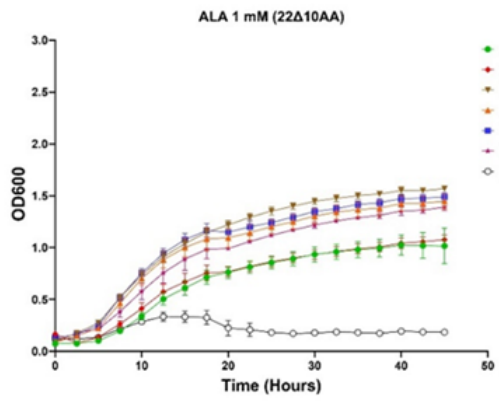


Figure 5.17: Alanine liquid 48h growth assay of the mutant (22Δ10AA) *S. cerevisiae* strain expressing five chickpea amino acid genes, *ScGAP1* positive control and empty pDR196 negative control.

Assay measured at OD600 at three separate concentrations of Ala (1, 3 & 6 mM) and 1.5 mM (NH₄)₂SO₄ as a N control. *S. cerevisiae* 22Δ10AA transformants expressing amino acid genes and the empty pDR196 control grown overnight in 2% glucose, 50 mM citric acid buffer and YNB (pH 6.2) supplemented with yeast synthetic amino acid minus uracil drop out medium, washed twice with sterile milli-Q water and diluted to an OD600 of 1. Assay performed with a 1:10 dilution of culture (20 μl) to liquid YNB (180 μl) made as previously, replacing synthetic amino acid medium with Ala, and run at 30°C with shaking. Statistical significance of relative growth rates for genes at differing Ala concentrations was calculated via One-Way ANOVA with multiple comparisons test (Tukey) (*<0.01, **<0.001, ***<0.0001). N = 6.

3.5.4 Liquid assay mutant complementation with GABA and Tyr

Due to time and equipment restraints, GABA and Tyr complementation for all mutants was examined only at 3 mM (Figure 5.18). *CaAAP6-22Δ10AA* and *CaAVT6A-22Δ10AA* failed to complement the mutant under liquid assay conditions for both GABA and Tyr at 3 mM, with no significant growth over that of the empty vector control (Figure 5.18). Spot plates conducted also generated no complementation evidence for both *CaAAP6-22Δ10AA* and *CaAVT6A-22Δ10AA* when supplemented with GABA (Figure 5.18). Conversely, the spot plates did show complementation when supplemented with Tyr (Figure 5.18) which had not been observed here under liquid conditions (Figure 5.18). *CaAVT6A-22Δ10AA*, did appear to begin growing post 40 hours and therefore may have experienced a slow start to a linear growth phase in liquid as opposed to growth on solid media (Figure 5.18). Whether such a late growth phase is evidence of complementation would need to be verified in alternative systems such as a *Xenopus* oocyte expression system in the future.

CaUmamiT9-22Δ10AA, *CaUmamiT18-22Δ10AA* and *CaUmamiT20-22Δ10AA* rescued the mutant strain supplemented with both GABA and Tyr at a concentration of 3 mM, with a growth rate matching the $(\text{NH}_4)_2\text{SO}_4$ positive growth control (Figure 5.18).

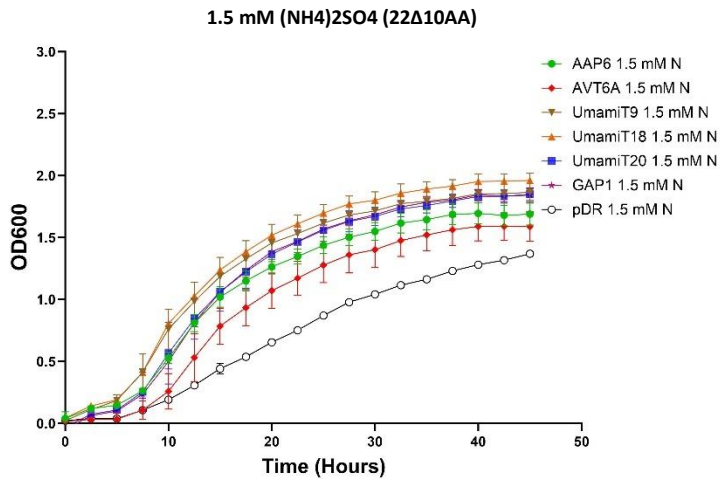
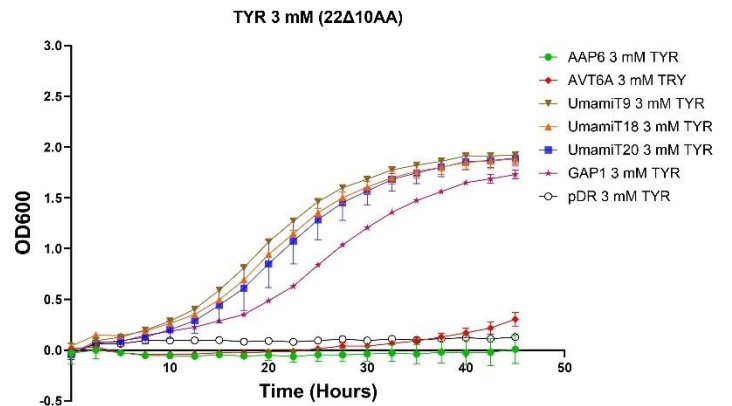
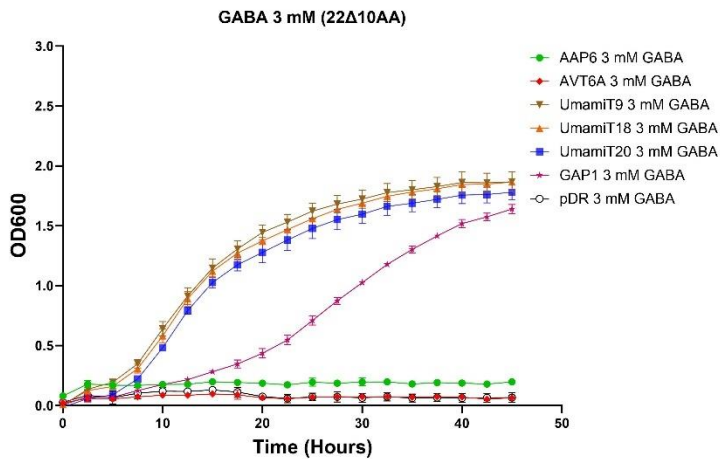


Figure 5.18: GABA and Tyrosine liquid 48h growth assay of the mutant (22Δ10AA) *S. cerevisiae* strain expressing five chickpea amino acid genes, *ScGAP1* positive control and empty pDR196 negative control.

Assay measured at OD600 a single concentration of GABA & Tyr (3 mM) and 1.5 mM (NH₄)₂SO₄ as a N control. *S. cerevisiae* 22Δ10AA transformants expressing amino acid genes and the empty pDR196 control grown overnight in 2% glucose, 50 mM citric acid buffer and YNB (pH 6.2) supplemented with yeast synthetic amino acid minus uracil drop out medium, washed twice with sterile milli-Q water and diluted to an OD600 of 1. Assay performed with a 1:10 dilution of culture (20 μl) to liquid YNB (180 μl) made as previously, replacing synthetic amino acid medium with either GABA or Tyr, and run at 30°C with shaking. N = 3.

5.6. Transport Affinity of Chickpea Amino Acid Transporters at Acid pH

5.6.1 Amide complementation under acidic pH conditions

An increasing acidity of the YNB medium supplemented with the amide Gln, showed a significant relative growth rate increase for *CaAVT6A-22Δ10AA* when grown at pH 4 compared to pH 6 (Figure 5.19A). No growth penalty or increased relative growth rate were observed for the remaining mutants at pH 4, 5 or 6 (Figure 5.19A). Some growth was observed in the empty pDR196 control, explaining why the relative slope values at pH 6 were lower than measured at pH 6.2 previously (Appendix 5a.8: Figure 5a.28 & 5a.29).

The chickpea transporters catalysed uptake of Asn better under a slightly acidic pH as evidenced in the liquid assay (Figure 5.19B). When grown in liquid YNB at pH 6 supplemented with Asn as a sole nitrogen source all mutants maintained a near identical significant increased relative growth rate compared to liquid YNB at pH 4 (Figure 5.19B). In addition, the relative growth rate of *CaUmamiT18-22Δ10AA* and *CaUmamiT20-22Δ10AA* significantly increased in a pH stepwise manner from pH 4 to 6 (Figure 5.19B). In both the Gln and Asn assays, *CaAAP6-22Δ10AA* and *CaAVT6A-22Δ10AA* initiated a linear growth phase several hours later than the rest of the mutants, more apparent with Gln as a N source (Appendix 5a.8: Figure 5a.28, 5a.29). A linear growth phase became less delayed with Asn as the pH became more acidic, hence *CaAAP6-22Δ10AA* and *CaAVT6A-22Δ10AA* may be better suited to more acidic conditions in the case of Asn availability (Appendix 5a.8: Figure 5a.29). It could be assumed that the UmamiT family is better suited to a larger range of pH alterations, whereas the AAP and AVT transport affinity for amino acids is more susceptible to variations in pH. Indeed, under pH 6.2 in the previous amino acid concentration assays, the initiation of a linear growth rate also occurred at approximately 20 hours (Figure 5.13, 5.14).

All amino acids evaluated under increasing acidity showed that the empty vector control consistently displayed increasing growth rate particularly at pH 4 post 20-25 hours into the assay (Appendix 5a.8: Figures 5a.28 – 5a.33). This typically occurred after a linear growth rate had already been established and therefore not influencing the relative growth rate of the mutants. The empty vector control did show some growth with Gln and Asp coinciding with *CaAAP6-22Δ10AA* and *CaAVT6A-22Δ10AA* (Appendix 5a.8: Figure 5a.28, 5a.31).

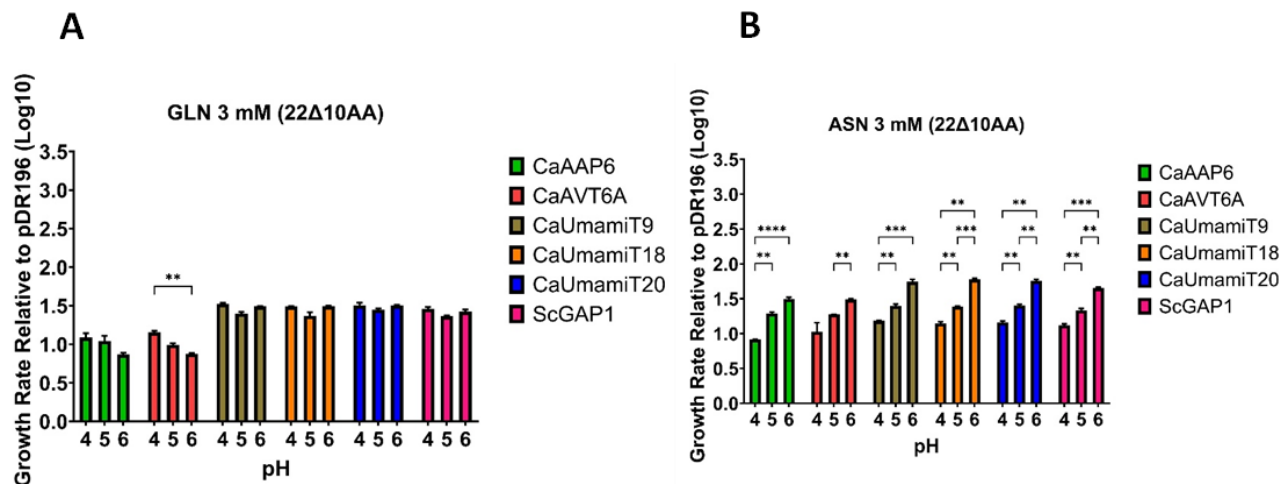


Figure 5.19: PH dependent complementation of the amides glutamine & asparagine in the *S. cerevisiae* mutant (22Δ10AA) strain expressing five chickpea amino acid genes, *ScGAP1* positive control and empty pDR196 negative control.

Linear growth rates were normalized against the empty pDR196 control to calculate relative growth rates. Assay measured at OD600 under increasingly acidic conditions (pH 6, 5 & 4) when supplemented with 3 mM Gln (A) or Asn (B) as the sole nitrogen. *S. cerevisiae* 22Δ10AA transformants expressing amino acid genes and the empty pDR196 control grown overnight in 2% glucose, 50 mM citric acid buffer and YNB (pH 6.2) supplemented with yeast synthetic amino acid minus uracil drop out medium, washed twice with sterile milli-Q water and diluted to an OD600 of 1. Assay performed with a 1:10 dilution of culture (20 μl) to liquid YNB (180 μl) made as previously, replacing synthetic amino acid medium with 3 mM Gln or Asn, and run at 30°C with shaking. Statistical significance calculated for relative growth rates of each gene compared between the three pH levels via One-Way ANOVA with multiple comparisons test (Tukey) (*<0.05, **<0.005, ***<0.0005). N = 3.

5.6.2 Glu, Asp, GABA and Ala complementation under acidic pH conditions

As observed with the two amides, *CaAAP6-22Δ10AA* and *CaAVT6A-22Δ10AA* had a delayed initiation of the linear growth rate as the pH became more acidic when Glu and Asp were substrates (Appendix 5a.8: Figure 5a.30, 5a.31). Empty pDR196 control initiated growth earlier when supplemented with Glu and Asp as the pH became more acidic, in turn influencing the relative growth rate of *CaAAP6-22Δ10AA* and *CaAVT6A-22Δ10AA* (Appendix 5a.8: Figure 5a.30, 5a.31). The remaining mutants linear growth phase preceded any growth of the empty vector control (Appendix 5a.8: Figure 5a.30, 5a.31).

Glu as a nitrogen source under increasing acidity saw less of an impact on relative growth rates in comparison to Asp which saw a significant penalty in the initiation of growth (Figure 5.20A & B). Relative growth was significantly increased from pH 5 to 6 in the case of *CaAAP6-22Δ10AA*, *CaUmamiT20-22Δ10AA* and *ScGAP1-22Δ10AA* and from pH 4 to 5 for *CaAVT6A-22Δ10AA*, when grown supplemented with Glu (Figure 5.20A). With Asp as a nitrogen source all mutants saw significant growth benefits in increasing pH up to 6 (Figure 5.20B).

GABA was unable to rescue the *CaAAP6-22Δ10AA* and *CaAVT6A-22Δ10AA* mutants when pH was decreased to pH 4 in the YNB media (Appendix 5a.8: Figure 5a.32). A stepwise increase in relative growth rates in the remaining mutants was measured indicating an increased dependence on pH facilitated transport of GABA (Figure 5.20C). Minor growth of the empty pDR196 occurred at pH 4 post initiation of a linear growth phase by the transporter mutants, hence not influencing relative growth rates (Appendix 5a.8: Figure 5a.32). The initiation of linear growth rates in the remaining mutants was not affected by changes in pH (Appendix 5a.8: Figure 5a.32).

Ala complementation via the mutants was less dependent on changes in pH, since only *CaAVT6A-22Δ10AA* and *CaUmamiT20-22Δ10AA* were significantly influenced by an increase in pH to pH 6 (Figure 5.20D). All mutants also initiated a linear growth phase within approximately five hours of each other with no pH related alterations and prior to growth observed by the empty vector control (Appendix 5a.8: Figure 5a.33).

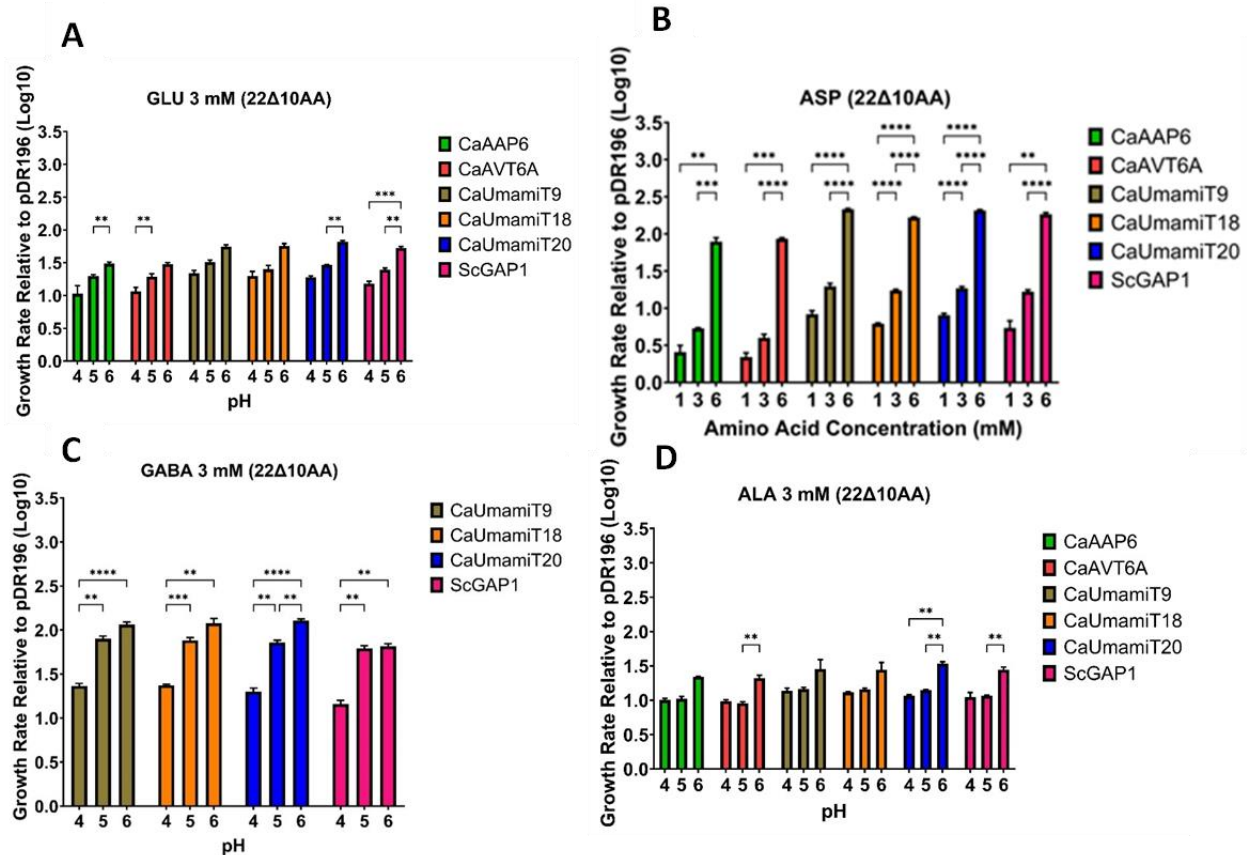


Figure 5.20: PH dependent complementation of glutamate, aspartate, GABA and alanine in the *S. cerevisiae* mutant (22Δ10AA) strain expressing five chickpea amino acid genes, *ScGAP1* positive control and empty pDR196 negative control.

Linear growth rates were normalized against the empty pDR196 control to calculate relative growth rates. Assay measured at OD600 under increasingly acidic conditions (pH 6, 5 & 4) when supplemented with 3 mM Glu (A), Asp (B), GABA (C) or Ala (D) as the sole nitrogen source. *S. cerevisiae* 22Δ10AA transformants expressing amino acid genes and the empty pDR196 control grown overnight in 2% glucose, 50 mM citric acid buffer and YNB (pH 6.2) supplemented with yeast synthetic amino acid minus uracil drop out medium, washed twice with sterile milli-Q water and diluted to an OD600 of 1. Assay performed with a 1:10 dilution of culture (20 μl) to liquid YNB (180 μl) made as previously, replacing synthetic amino acid medium with 3 mM Glu, Asp, GABA or Ala and run at 30°C with shaking. Statistical significance calculated for relative growth rates of each gene compared between the three pH levels via One-Way ANOVA with multiple comparisons test (Tukey) (*<0.05, **<0.005, ***<0.0005). N = 3.

Chapter 5: Discussion

5.7 Yeast Complementation Reveals Transport of Amino Acids by Nodule Localised Chickpea Amino Acid Transporters

Previously it was not known whether chickpea nodules utilized a broad range of amino acid transporters outside the AAPs. Not only this, but there had not been a clear indication that chickpea nodules exported amino acids (amides) over ureides. This was shown to be the case with compelling evidence in Chapters 3 & 4. I subsequently identified a broad range of amino acid transporter families highly expressed under N₂ fixing conditions, using RNAseq. Seven of these genes have now been functionally analyzed (Table 5.2). Importantly, these seven genes encompass three of the most prominent families identified from the RNAseq database. This includes AAP6 (Amino Acid Permease), a well characterized and significant broad amino acid transporter (Garneau et al., 2018). AVT6A & AVT6C (Amino Acid Vacuolar Transporter), a lesser studied family, (Sekito et al., 2014, Tone et al., 2015, Fujiki et al., 2017), and lastly UmamiT9, UmamiT18, UmamiT20 and UmamiT41 from the Usually Multiple Acids Move in and Out Transporter family, from an extensive 40+ member gene family originally characterized from *Arabidopsis* (Zhao et al., 2021). Very few studies have characterized UmamiTs in legumes (Garcia et al., 2023), with no reported characterization in chickpea.

5.7.1 Chickpea nodule transporters exhibit board transport functionality

The data presented here provided evidence that five of the seven genes rescued growth in the yeast mutant strain with amide (Gln & Asn) supplementation (Table 5.2). Gln complementation growth rate was the greatest up to 3 & 6 mM with no growth rate change from pH 4, 5 or 6. Asn complementation for the five genes was not completely abolished at pH 4 but preferentially grew at pH 5 & 6. In other amide producing legumes such as *M. truncatula* and *P. sativum*, Asn has been measured to make up approximately 65% of the total amino acid pool in the nodules, with Gln significantly less at around 5% (Suliman & Schulze, 2010, Garneau et al., 2018). Genes facilitating the transport of Asn are crucial for sustained nodule function and fixed N export out of the nodules.

The examined chickpea transporters also facilitated the transport of Glu, Asp and Ala, all playing critical functions in support of N₂ fixation and biosynthesis of amides (Table 5.2). Interestingly GABA was the only amino acid assessed that could not rescue the mutant strain expressing *CaAAP6* and *CaAVT6A*

when grow in liquid and spot plate growth assays. *CaUmamiT9* & *CaUmamiT18* saw no pH related growth penalties for both Glu, as well as *CaAAP6* for Ala (Table 5.2). *CaAAP6* did however preferentially transport Glu at pH 6, as did *CaUmamiT18* & *CaUmamiT20* with Asp transport (Table 5.2).

Based on the growth assays that were conducted here only limited inference of transporter affinity for a particular amino acid can be determined. The primary conclusions which can be made here is evidence that the examined genes rescued an amino acid deficient yeast strain when supplemented with various amino acids, inferring basic transport properties and concentration preference. For more comprehensive complementation results future work is required, summarized in 5.10.1.

Table 5.1: *S. cerevisiae* liquid growth assay summary of the 22Δ10AA mutant strain expressing chickpea amino acid transporters.

Green indicates complementation with the respective amino acid, red indicates no complementation.

Gene	Gln	Asn	Glu	Asp	Ala	Tyr	GABA
<i>CaAAP6</i>	Green	Green	Green	Green	Green	Green	Red
<i>CaAVT6A</i>	Green	Green	Green	Green	Green	Green	Red
<i>CaAVT6C</i>	Red						
<i>CaUmamiT9</i>	Green						
<i>CaUmamiT18</i>	Green						
<i>CaUmamiT20</i>	Green						
<i>CaUmamiT41</i>	Red						
<i>ScGAP1</i>	Green						

5.8 Complementation of Notable Transporter Families

5.8.1 AAP6

The ability of *CaAAP6* to transport the amino acids Gln, Asn, Glu, Asp and Ala is consistent with previous studies in both amide and ureide producing legumes. *GmAAP6*, *PsAAP6* and *AtAAP6* overexpression and knock-out transgenic lines both saw significant respective increase or decreases in the amino acids Gln, Asn, Glu, Asp and Ala in either nodule or leaf tissues (Hunt et al., 2010, Garneau et al., 2018, Liu et al., 2020). These studies measured Asn in the greatest abundance at approximately 90 nmol/mg in *P. sativum* followed by Glu at 15 nmol/mg, with a similar difference in *G. max* (Garneau et al., 2018, Liu et al., 2020). Interestingly, the *PsAAP6* knockout did not significantly reduce the concentration of Gln in nodule tissue, compared to a significant increase of Gln abundance in *GmAAP6* overexpression, suggesting that *GmAAP6* transport properties may have diverged from *PsAAP6*. This may be the case for *CaAAP6* also. Alternatively, in *P. sativum* other amino acid transporters may have facilitated Gln transport in place of the *PsAAP6* knock-out, indicating levels of redundancy. This seems likely, given that five of the seven chickpea genes tested here rescued the mutant yeast strain when supplemented with Gln as the sole N source.

Phylogenetic relationship and protein sequence of three homologs of *CaAAP6* were highly similar to *PsAAP6* and slightly less so to *GmAAP6*. Hence it is tempting to speculate that *PsAAP6* & *CaAAP6* from amidic legumes have evolved in parallel, where *GmAAP6* has begun to diverge due to different selective pressures associated with being temperate and tropical legumes, respectively. Regardless, it can be hypothesized that the reason Liu et al (2020) saw significantly elevated levels of Gln in *GmAAP6* overexpressing plants was that *GmAAP6* transports Gln into plastids in the nodule symbiotic cells to feed into the purine synthesis pathway driving ureide production. These studies unfortunately did not measure GABA abundance to verify the null complementation observed here.

5.8.2 AVT

CaAVT6A had a similar complementation profile as *CaAAP6*, with similar growth rates and no complementation when supplemented with GABA. AVT3 & AVT4 when expressed in yeast facilitated neutral amino acid export from vacuoles, whereas basic and acidic amino acids were largely not affected (Fujiki et al., 2017). Notably for the current study, *ScAVT6* in yeast functioned as an efflux transporter out of acidic organelles for the acidic amino acids, Glu and Asp, requiring a proton electrochemical gradient

(Rusznak et al., 2001). AVT7 was also found to transport neutral AAs such as Gln (Tone et al., 2015). With regards to *CaAVT6A* examined here, nodule vacuoles vary in pH depending on the maturity of the nodule and whether they are housed in the infected or uninfected cells (Sujkowska et al., 2011, Fedorova, 2023). *CaAVT6A*, from the previous chapter was possibly localised to both the nodule parenchyma and vascular tissue, hence *CaAVT6A* may facilitate the transport of acidic amino acids on the plasma membrane of the vacuoles in these compartments.

5.8.3 *UmamiT*

CaUmamiT41 was the only gene that could not rescue the yeast mutant strain with any amino acid evaluated. Under the same expression system used here, Zhao et al., (2021) also could not rescue the mutant strain expressing *AtUmamiT41* and hypothesized that *UmamiT41* could be considered a housekeeping transporter. On the other hand, the *UmamiT* genes from the *A. thaliana* clade C encompassing *UmamiT9*, *UmamiT18* and *UmamiT20* were found to exhibit the greatest transport activity in the yeast expression system by Zhao et al., (2021), which was also observed here with the respective chickpea orthologs.

These *UmamiT* members may exhibit a more diverse role than AAP6 which is already considered a broad amino acid transporter. *CaUmamiT9*, *CaUmamiT18* and *CaUmamiT20* exhibit high sequence similarity to *P. sativum* and only marginally less similarity with their *G. max* counterparts, possibly indicating a minor divergence from ureide legumes. This divergence may be significant enough to change what amino acids are transported, but perhaps more likely their affinity. *AtUmamiT18* characterized in a *Xenopus* oocyte expression system and the 22Δ10AA (Besnard et al., 2016) and 22D8AA (Ladwig et al., 2012) yeast mutants observed functional complementation with Asp, Asn, Gln and Ala, but not with Glu and GABA as observed here. In addition, *AtUmamiT9* and *AtUmamiT20* did not complement the 22Δ10AA yeast mutant when supplemented with Ala and GABA and *AtUmamiT20* also did not transport Gln (Zhao et al., 2021). This may suggest that legume orthologs, particularly chickpea members of the *UmamiT* family, may have diverged to better suit the physiological demands of nodules. This is not unreasonable considering *A. thaliana* *UmamiT* orthologs were only 60% similar to the *CaUmamiT* amino acid sequences. Glu and Gln are vitally important as part of the GS/GOGAT pathway and Ala biosynthesis which subsequently feeds back into the GS/GOGAT pathway (Schwember et al, 2019). GABA has lesser understood functions but is likely involved in maintaining C/N balance to sustain the significant C cost of N₂ fixation via the GABA shunt pathway (Sulieman & Schulze 2010, Sulieman et al., 2024). Hence, chickpea and other legumes may have evolved transporter redundancy to fulfill N₂ fixation demands.

5.9 The Effect of pH and Amino Acid Charge

Studies of the UmamiT family typically localise these transporters to either the plasma membrane or tonoplast with the ability to export amino acids from the cytosol across a membrane to the apoplast along their electrochemical gradient (Müller et al., 2015, Besnard et al., 2016, Zhao et al., 2021). GFP fusion of all 44 *A. thaliana* UmamiT genes localised 15 to the plasma membrane, 19 to the tonoplast and 31 either ER or Golgi bodies (Zhao et al., 2021). Within the same study, *AtUmamiT9*, *AtUmamiT20* and *AtUmamiT41* analysed here, were localised to both the tonoplast and plasma membranes, whereas *AtUmamiT20* was undetermined (Zhao et al., 2021). UmamiT transporters likely also function as bidirectional transporters moving amino acids in both directions (Müller et al., 2015).

The pH of the symbiosomes that house bacteroids in the nodules, has been found to range from 4.5 to 5.0 in *M. truncatula* indeterminate nodules (Pierre et al., 2013), backed up by previous analysis of symbiosomes isolated from *G. max* (Udvardi & Day 1989). In contrast, the vacuoles of the symbiotic cells sit at a neutral pH, compared to acidic vacuoles of pH 5 - 5.5 within the uninfected cells (Gavrin et al., 2014). As the symbiotic cells establish and progressively mature this pH may begin as more acidic around pH 5 and become neutral once the infected cell matures (Sujkowska et al., 2011, Fedorova, 2023). Uninfected cells and the inner parenchyma cells house acidic vacuoles which neighbour the symbiotic cells, suggesting similar functionality of both the uninfected cells and nodule parenchyma (Sujkowska et al., 2011).

From the complementation data collected here it would seem that the analyzed transporters preferentially transport amino acids at pH 5 or 6, but typically a greater affinity at pH 6. Yeast expressing chickpea amino acid transporters saw significantly increased relative growth rates for amino acids exhibiting a negative charge or the capability to become negatively charged as the pH of the external environment approached neutral. However, these observations are based on initial findings and further work would be required to determine more comprehensive substrate specificity of these transporters.

Both amides were facilitated by *CaAAP6*, *CaAVT6A*, *CaUmamiT9*, *CaUmamiT18* and *CaUmamiT20* with similar relative growth rates. Asn growth rate under these transporters was however significantly gated at a more acidic pH of 5 and 4 possibly due to changes in electrostatic interactions, while Gln remained unchanged and transport affinity was not greatly influenced by the external pH. It is possible that the physiological protein properties of these transporters impede Asn movement as the external pH becomes more acidic, in combination with the charge of Asn which would remain neutrally charged.

All examined transporters saw the greatest affinity for Asp in a negatively charged state at pH 6 and exhibited significant reductions in the relative growth rates of Asp as it became increasingly uncharged at pH 5 & 4, with complementation virtually abolished with yeast expressing *CaAAP6* & *CaAVT6A* at pH 4. *AAP6* has been shown to have a high affinity for neutral and acidic amino acids and also exhibited a high affinity to Asp, seen here (Fischer et al., 2002).

CaAAP6, *CaAVT6A* and *CaUmamiT20* showed a significantly greater affinity to Glu at pH 6, or pH 5 for *CaAVT6A*, indicating a preference for increasing availability of negatively charged Glu. Conversely to this result, Arabidopsis Glu transport by multiple UmamiT transporters showed a pH dependence in acidic conditions whereby uptake was almost abolished at neutral conditions (Müller et al., 2015). Additionally, all the examined chickpea transporters outside of *CaAVT6A* and *CaUmamiT20* at pH 6 saw a low affinity for the neutral amino acid Ala with no pH complementation dependence. This may be as suggested above that these transporters prefer negatively charged amino acids, whereby Ala remains neutral irrespective of the external pH. However, perhaps physiological properties of *CaAVT6A* and *CaUmamiT20* provide more affinity to Ala at an increasingly neutral pH.

CaUmamiT9, *CaUmamiT18* and *CaUmamiT20* all exhibited a high affinity for GABA again at pH 6, while the remaining transporters could not rescue the mutant yeast line. Under these conditions GABA remains predominantly zwitterionic maintaining a neutral charge. The only instance of a UmamiT gene transporting GABA was found at very minor levels in the same yeast mutant expressing Arabidopsis UmamiTs (Zhao et al., 2021). Here it seems nodule localised UmamiT's from chickpea transport GABA more readily than seen in Arabidopsis at increasingly neutral pH levels.

Nodule cellular compartments host a range of pH conditions possibly gating the transport of various amino acids. In addition, the previous chapter, scRNA analysis from *M. truncatula* provided theoretical location of highly expressed transporters in chickpea, which could be further examined here with regards to amino acid complementation. In summary the scRNA localized *CaAVT6A* to the vasculature, parenchyma and uninfected cells, *CaAAP6*; parenchyma and uninfected cells, *CaUmamiT9*; parenchyma, *CaUmamiT18*; parenchyma and uninfected cells, *CaUmamiT20*; parenchyma and *CaUmamiT41*; infected cells. In addition, all the transporters examined here were predictively located to the plasma membrane via TargetP/WolfPsort analysis of the protein sequence (Chapter 4: Table 4.12 – 4.14). Initial assumptions about these transporters suggest they export amino acids out of the nodules via import into the vasculature from the nodule parenchyma or bidirectional transport of amino acids in and out of the

uninfected cells or infected cells, as the nodule parenchyma borders both the uninfected cells and the infected cells (Figure 5.23) (Sujkowska et al., 2011).

Given that these characterized transporters preferentially complemented growth supplemented with amino acids of negative charge at an increasingly neutral pH, this could be explained if located on the plasma membrane of the parenchyma under typical neutral cytosolic pH conditions. Asn is the most abundant amino acid in nodules and was most preferentially complemented at increasingly neutral pH (Suliman & Schulze, 2010, Garneau et al., 2018). If this is the case then it may seem that chickpea do exhibit a significant redundancy of amide transport by multiple transporters.

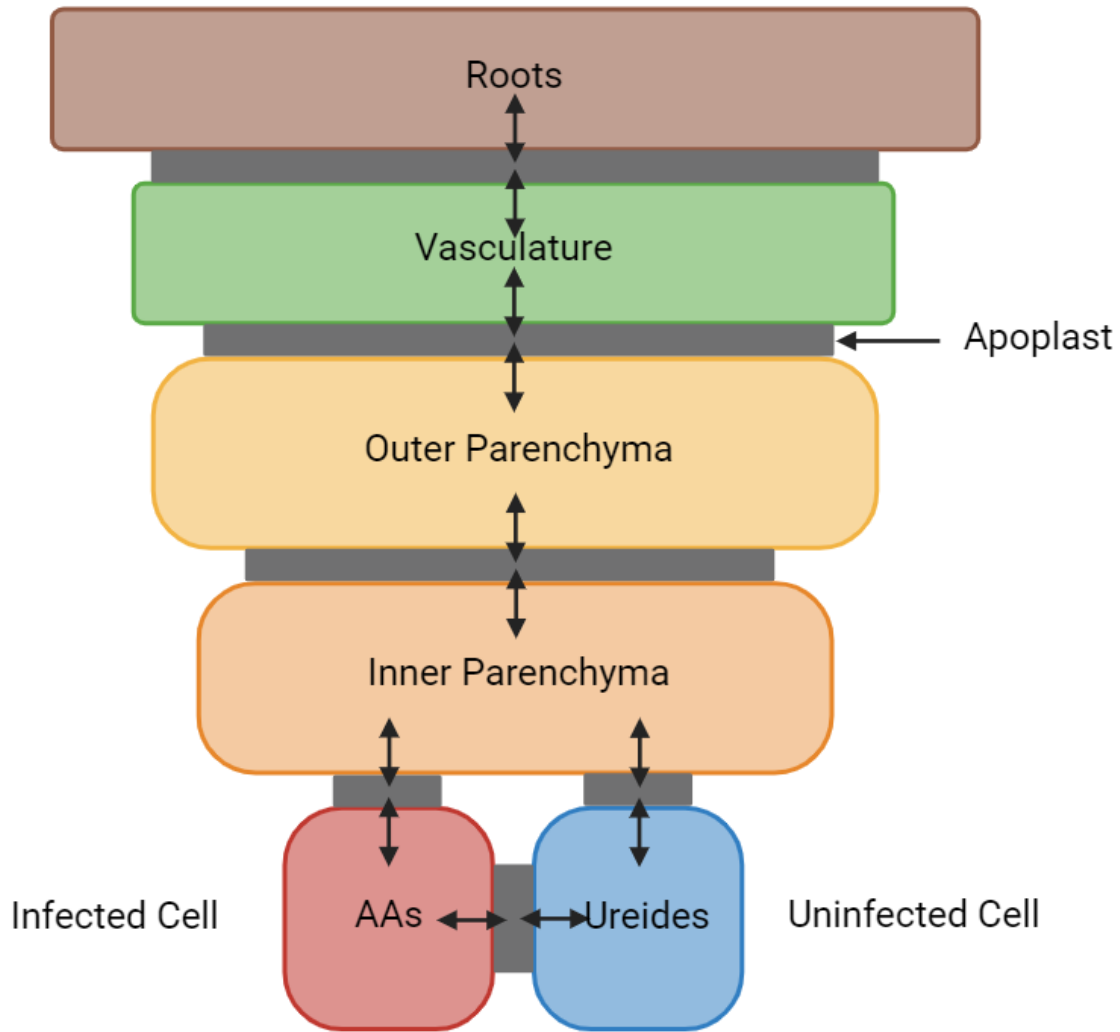


Figure 5.1: Basic model of the nodule path of amino acid distribution and nodule export through the inner and outer parenchyma.

Amino acids including amides are synthesised from the nodule cytoplasmic GS/GOAGT cycle (Schwember et al, 2019), or via plastid localised enzymes of the GS/GOGAT cycle (Trepp et al., 1999). Transporters on the plasma membrane, possibly AAPs, AVTs or UmamiTs are involved in exporting amino acids from the infected cells into the apoplast between the inner parenchyma, followed by plasma membranes transporters importing these amino acids into the inner parenchyma. From here the inner parenchyma borders the infected and uninfected cells and the outer parenchyma to distribute amino acids via plasma membrane bound transporters. Amino acids transported towards the outer parenchyma border the vasculature or nodule cortex where amino acids can be exported from the nodule to the roots via the xylem.

5.10 Limitations of the *S. cerevisiae* Complementation Results

There were some limitations of the yeast complementation performed in this chapter, although a good foundation of chickpea transporter functionality was established. The mutant *S. cerevisiae* strain was particularly difficult to rescue in some instances, evidenced by variability in the liquid and spot plate growth assays. This required the selection of the examined genes as detailed above where the mutant strain was grown on an amino acid spot plate prior to overnight inoculation for liquid growth assay. Performing this step helped to select for the expression of the cloned chickpea transporter, greatly reducing growth variation and improved repeatability. Importantly the empty vector pDR196 control in the mutant strain was prepared in a similar manner to account for the possibility of the mutant reverting back to the parental state.

Unfortunately, due to equipment restraints in performing several 48-h growth assays, a wider range of pH levels could not be conducted which decreased the scope of the obtained data. Increasingly neutral pH levels would have been useful to see if complementation under typical cytosolic conditions was improved. In addition, would complementation be completely abolished under increasingly acidic conditions.

Some variations in results were still present between assay techniques. *CaUmamiT20* could not rescue the mutant when grown on solid YNB media with Asn and Asp supplementation in contrast to its successful complementation in liquid assays, generating complementation uncertainty. *CaUmamiT20* would need to be examined in the future with Asn & Asp as substrates to confirm reproducibility of the assays. Additionally, results obtained with *CaUmamiT18* using GABA as substrate and *CaAVT6A* & *CaUmamiT18* with Ala, were inconsistent between spot plate and liquid growth assays limiting the validity of complementation.

Inconsistencies with the pYESdest52 and pDR196 vectors were apparent since *CaAAP6* in pYESdest52 did not rescue the mutant when grown on streak plates supplemented with amides, compared to successful complementation in pDR169 spot and liquid assays. This inconsistency may be due to the inducible promoters of both vectors, whereby pYESdest52 required galactose compared to glucose of pDR196 to drive gene expression.

Gateway cloning difficulties meant that a number of genes could not be evaluated including *CaAAP3*, *CaUmamiT23*, *CaUmamiT12*, *CaCAT1* and *CaCAT2*, limiting the original scope of the experiments described in this chapter. Complementation of the CAT gene family would have been a useful addition to

this chapter encompassing each of the prominent families identified from the RNAseq dataset. *CaAVT6C* null complementation on streak plates in the pYESdest52 vector supplemented with Asn, Gln, Asp and Glu could also not be verified in pDR196 due to unsuccessful cloning.

5.10.1 Future directions for amino acid transporter characterization

To increase confidence of the generated complementation results a *Xenopus* oocyte expression system could be used in the future as a secondary assay technique. Müller et al., (2015) previously used an oocyte expression system to examine Glu uptake in four *AtUmamiT* transporters. In addition, it would be interesting to determine directionality and affinity of these transporters which could be accomplished via competitive inhibition of transport using radiolabeled [¹⁴C] amino acids, particularly the amides Gln & Asn, in the yeast system. Secretion assays can also be performed via the yeast mutant (Besnard et al., 2016) to infer export.

Chapter 5: Conclusions

Utilization of the amino acid transporter deficient *S. cerevisiae* 22Δ10AA mutant strain identified five chickpea amino acid transporters: *CaAAP6*, *CaAVT6A*, *CaUmamiT9*, *CaUmamiT18* and *CaUmamiT20*, able to rescue growth supplemented with the amides Gln & Asn as the sole nitrogen source. In comparison *CaAVT6C* in pYESdest52 and *CaUmamiT41* in pDR196 were unable to rescue the mutant under any examined amino acid supplementation. The five transporters which rescued the mutant with amides as substrates also rescued growth with Glu, Asp, Ala and Tyr. However, GABA could not complement growth for either *CaAAP6* & *CaAVT6A*. In summary, the results here showcased the broad amino acid transport properties of five highly expressed chickpea nodule localized transporters that potentially play critical roles in sustaining nitrogen fixation.

6 General Discussion

6.1 Thesis in the Broader Context

Legumes possess the remarkable ability to harness atmospheric nitrogen through a symbiosis with Rhizobia bacteria. The capacity to both harness and utilize nitrogen in this manner which is unavailable to non-leguminous plants is of vital importance in modern agriculture. Even though non-leguminous crops cannot fix atmospheric nitrogen, legumes provide a direct benefit to them via rotational cropping systems, whereby legumes can revitalize the soil with nitrogen (Zhao et al., 2022). Rotational cropping systems can improve main crop yield by up to 20%, as well as suppressing pests, diseases, and impose improved soil properties (Cernay et al., 2018, Ditzler et al., 2021, Zhao et al., 2022). Synthetic nitrogen fertilizers are also vastly overused in developed nations causing a whole host of environmental issues from contamination of ground water and water ways to impacting the mounting problem of climate change (Gruber & Galloway, 2008). In addition to this, nitrogen fertilization limits the effect legume rotations can have on farming systems due to nitrogen related repressed nodulation and subsequent N_2 fixation (Zhao et al., 2022). As such a better understanding or improvement of N_2 fixation in popular legumes such as chickpea is critical to provide direct agricultural improvements on a global scale.

In terms of understanding N_2 fixation in chickpea, this project aimed to firstly determine the main products of N_2 fixation, either of the ureides allantoin and allantoic acid or the amides glutamine and asparagine. Knowing which product of N_2 fixation predominates in chickpea nodules can then focus our attention on the transporters responsible in exporting these products out of the nodule towards long distance plant remobilization of nitrogen to support effective plant growth and yield. For example, modification of both *GmUPS1* and *PsAAP6* in other legumes showed that signaling mechanisms exist in legumes where the plant can increase the rate of N_2 fixation to compensate either shoot or nodule nitrogen deficiencies (Carter & Tegeder, 2016, Garneau et al., 2018, Lu et al., 2022). A similar signaling mechanism probably exists in chickpea opening avenues for improvements in not only N_2 fixation and yield but beneficial improvements for rotational cropping systems. Within this project, I have shown convincing evidence that chickpea can be classified as an amidic legume with a developed model of fixed N_2 metabolism and highly expressed amino acid transporters in nodules (Figure 6.1). Several of these amino acid transporters were shown to facilitate amide transport and possible nodule export.

6.2 Chickpea: An Amidic Legume

Legumes can be grouped under two main classifications, amide or ureide producers. Geographical localisation and nodule morphology typically dictates what route fixed N_2 takes. Legumes from tropical and subtropical conditions are generally ureide producers, with determinate type nodules (Pate et al., 1980). In contrast, legumes from temperate and semiarid climates are generally amide producers with indeterminate type nodules (Rachwa-Rosiak et al., 2015). The differences in nodule morphology are dictated by differing nod factor signaling of cortical cell differentiation causing either spherical (determinate) nodules or continued meristematic elongated (indeterminate) nodules (Ferguson et al., 2010, Udvardi & Poole 2013). In this thesis I show that chickpea has indeterminate type nodules predominantly synthesising amides, albeit with minor ureide biosynthesis. This is important not only for understanding the route of fixed N_2 metabolism but also the ability to focus on the transporters at play in nodule amide export. Evidence acquired in this thesis from observing nodule morphology, measuring the expression profile of key enzymes and transporters is critical in grouping chickpea as an amidic legume and opening up future research avenues.

6.2.1 Metabolism of fixed nitrogen

Metabolism of fixed N_2 begins after NH_4^+ is exported from the symbiosome into the infected cell and the initial steps are the same irrespective of amidic or ureidic legume origin. Through the action of glutamine synthetase and glutamine oxoglutarate aminotransferase, commonly known as the GS/GOGAT couple, NH_4^+ is converted to glutamine and glutamate, respectively (Schwember et al, 2019, Todd et al., 2006, Vance, 2000). Asparagine which is typically the principal nitrogen export product can also be synthesized via asparagine synthase from glutamine and oxaloacetate as the C-skeleton (Suliman et al., 2010, Berry et al., 2011). In this thesis, expression of genes involved in these enzymatic steps from both qRT-PCR and RNA sequencing convincingly displayed heightened expression of the biosynthesis of the amides, asparagine and glutamine. As stated previously, glutamine biosynthesises would also be important in ureidic legumes to fuel the purine synthesis pathway and would not be enough of a distinction by itself of an amidic legume without further analysis. Pur1, a regulatory step of this pathway metabolising glutamine (Kin et al., 1995, Smith & Atkins, 2002) was virtually non-expressed in qRT-PCR and RNAseq. Expression of not only Pur1 but the entire purine synthesis pathway in fixing nodules was extremely low. In both chapters 3 and 4 minor expression was observed for urate oxidase and allantoin amidohydrolase, enzymes after the purine synthesis pathway responsible in the biosynthesis steps preceding ureide biosynthesis and catabolism of allantoinic acid. This expression was puzzling considering

virtually no expression of the purine synthesis pathway preceding these enzymatic steps. Minor levels of ureides were measured in the nodules and are perhaps explained by this expression. However, compared to *G. max* the total ureides measured were significantly decreased in all tissue and not what would be expected of a ureide producing legume. For example, in *G. max* and *P. vulgaris* ureide export can make up as much as 80% of fixed N₂ export from the nodules (Rainbird et al., 1984, Atkins & Smith 2007, Collier & Tegeder 2012). In addition, export of ureides at a meaningful rate was deemed unlikely after low and insignificant expression of UPS1 was observed, with an apparent lack of root or leaf total ureide supplementation from the nodules.

This begs the question regarding the purpose of the synthesised ureides, and whether the expression of these enzymes are a relic of past evolutionary ancestry and shared genetic similarities with ureidic legumes. As has been explained in more detail in chapters 3 and 4, expression of urate oxidase may be driven indirectly by urate accumulation for possible ROS scavenging capabilities, because of intensive mitochondrial activity (Sautin & Johnson, 2008, Voß et al., 2022). While allantoate amidohydrolase may be subsequently catabolising allantoic acid for the remobilisation of material, possibly in relation to the onset of nodule senescence. In summary, the low gene expression of the ureide biosynthesis pathway and minor total ureide levels compared to highly expressed amide biosynthesis genes suggests that chickpea preferentially synthesise amides over ureides.

6.2.2 Transport of amino acids and amides in chickpea

RNA sequencing performed in chapter 4 further supported the notion that preferential ureide biosynthesis in chickpea nodules was unlikely. UPS1 and UPS2 were identified but were non-differentially expressed in chickpea nodules during N₂ fixation. There is also convincing evidence to suggest UPS is the sole transporter for ureide transport in legumes (Pélissier et al., 2004, Collier & Tegeder, 2012, Carter & Tegeder, 2016). In contrast, several transporters from known amide and amino acid transporter families were identified and were significantly upregulated in nodules. These genes include AAP (Garneau et al., 2018), CAT (Rentsch et al., 2007, Yang et al., 2014), AVT (Sekito et al., 2014, Tone et al., 2015, Fujiki et al., 2017) and UmamiT (Zhao et al., 2021, Garcia et al., 2023) families. Single cell RNA sequencing from *M. truncatula* and TargetP/WolfPsort analysis also theoretically localised many of these highly upregulated transporters to the nodule parenchyma plasma membrane. This suggests some of these genes facilitate amino acid transport to the vasculature cells prior to nodule export to the xylem.

The most promising of these transporters *CaAAP6*, *CaAVT6A*, *CaAVT6C*, *CaUmamiT9*, *CaUmamiT18* and *CaUmamiT20* were functionally characterized here using a heterologous expression system in *S. cerevisiae* (Besnard et al., 2016). Complementation assays provided evidence to suggest that all but *CaAVT6C* facilitated the transport of the amides glutamine and asparagine, as well as the amino acids glutamate, aspartate and alanine. These transport properties of *CaAAP6* and *CaUmamiTs* were backed up by amino acid transport observations in *PsAAP6* and *GmAAP6* (Garneau et al., 2018, Liu et al., 2020) and reminiscent from similar yeast complementation of *AtUmamiTs* (Besnard et al., 2016, Besnard et al., 2018). Interestingly these results showed that chickpea express genes encoding proteins with broad amino acid transport properties, but further experiments are required to determine more accurate transport preferences for individual amino acids. Most importantly, we now have the foundational data required to design approaches to improve N₂ fixation and whole plant partitioning of amides in chickpea.

6.3 Future Directions

The results of this thesis have identified multiple transporters that are promising targets for future genetic engineering approaches. In particular, the highly expressed UmamiT genes were shown to transport amides when expressed in *S. cerevisiae*. Opportunities to improve N₂ fixation in chickpea could exploit a bottleneck that likely resides in the transport of fixed N₂ from the nodule rather than the efficiency of N₂ fixation itself. This is based on previous studies with other legumes that provide strong evidence for signalling mechanisms where repression or increased export of amides or ureides cause an upregulation of fixed N₂ production (Carter & Tegeder, 2016, Garneau et al., 2018, Lu et al., 2022). The repression of amide export from *P. sativum* using RNAi against AAP6 showed that under shoot N deficiency, systemic signalling caused an increase in nodule activity (Garneau et al., 2018). Whereas overexpression of *GmUPS1* led to a whole plant rebalancing of the N and C status of the plant, resulting in increased plant biomass and N metabolism (Lu et al., 2022). If a UmamiT gene or *CaAAP6* can be overexpressed in a similar manner as per *GmUPS1*, then it is likely that improved export of amides from nodules will lead to an increase in the rate of N₂ fixation to compensate. This may lead to improved N and C remobilisation to the rest of the plant, possibly increasing plant productivity and yield.

However, the identification of multiple highly expressed amino acid transporters raises the question whether chickpea possesses too much redundancy to cause any meaning difference if a single transporter is overexpressed. It would firstly be prudent to expand on the complementation results, possibly in *Xenopus* oocyte expression systems, such as employed by Müller et al., (2015). Most importantly prior to any overexpression studies, the transporter with the greatest affinity for Asn should be identified such as using radiolabelled [¹⁴C] Asn in competitive inhibition and localisation analysis. The gene with the highest Asn affinity would be the best overexpression target given that Asn is typically the primary amino acid in legume nodules making up as much as 65% of the total amino acid pool (Sulieman & Schulze, 2010, Garneau et al., 2018). Localisation of the transporter on the nodule parenchyma will also likely help drive Asn and other amino acids towards the vasculature tissue for nodule export to the roots. With all this in mind the most likely candidates for an overexpression study would be either *CaUmamiT9*, *CaUmamiT18* or *CaUmamiT20*, which are all capable of Asn transport and predictively localised to the parenchyma plasma membrane.

6.3.1 Chickpea tissue culture for genetic modification studies

Once one of the characterised transporters has shown the greatest affinity for Asn transport, an overexpression or knockout study can be performed via chickpea tissue culture to generate stable transformants. The chickpea tissue culture technique outlined by Das Bhowmik et al., (2019) was attempted, briefly outlined in the appendix of this thesis (Appendix 6A), however due to time constraints and future work required mentioned above, genetic modification was not performed. The Das Bhowmik et al., (2019) study builds on previous attempts to generate stable chickpea transformants (Sarmah et al., 2004, Acharjee et al., 2010). I speculate the main reason why chickpea genetic studies in the literature are generally lacking is due to the sheer difficulty and time-consuming nature of this method. Compared to the ease of *Arabidopsis floral dip* (Zhang et al., 2006) and hairy root transformation in soybean and pea (Collier et al., 2005), the chickpea method is a very daunting task with an exceptionally low success rate, if any positive transformants can be generated at all. Indeed, the future of plant transformation may involve the grafting of shoots onto a transgenic donor rootstock, such as was accomplished by Yang et al., (2023), opening up the possibility for effective and robust regeneration of difficult plants such as chickpea.

To provide a summary of the chickpea method, this consists of seed bisections and co-cultivation with agrobacterium harbouring an expression plasmid with kanamycin resistance, following multiple rounds of regeneration on kanamycin selection media. This section can take up to 8-weeks. Most plantlets at this stage would have perished from the stress of tissue culture handling or bleaching of tissue from the kanamycin selection, the seed is also removed from the shoot early into the regeneration stage. On top of this, chimerism of transformants is very common and a significant factor of non-transmission of genes to the next generation. Once plantlets have made it past multiple rounds of growth media selection, they must then be grafted on a newly growing sterile non-transgenic rootstock. For example, a non-transgenic shoot from a newly germinated seed is cut longitudinally from the first hypocotyl then again cut down the length of the shoot from the top, splitting the shoot in half. The transgenic shoot is then inserted between the two halves of the cut shoot from the seed and held together via a silicone ring allowing the two shoots to heal together. This step is exceptionally difficult, however with practice, half of the grafted plants typically survived in my experience post grafting and acclimatization in soil. Overall, the method can take up to 8 months to generate a stable T2 transgenic line.

Using this method, control chickpea plants were successfully regenerated, without any insertion of a transgene. These plants were purely used to practise the method and establish the protocol in a new lab.

Some modification of the protocol was tested, such as a differing light intensity regime during early stages of seed germination and shoot growth (Appendix 6a.3). Additionally multiple different chickpea cultivars were tested, to determine which best suited the tissue culture conditions (Appendix 6a.2).

6.4 An Updated Model of Nitrogen Fixation in Chickpea

The data collated from chickpea ureide assays, RNA sequencing, *M. truncatula* scRNA and *S. cerevisiae* complementation from chapters 3, 4 and 5, respectively of this thesis can be used to construct a model of nitrogen fixation in chickpea nodules (Figure 6.1). The depicted model shows the initial import of sucrose from the plant into the nodule uninfected cells, where synthesised malate is imported to the symbiotic cell bacteroid to fuel nitrogen fixation. Ammonia exported from the bacteroid through the symbiosome membrane protonated to ammonium feeds into the highly upregulated GS/GOGAT cycle responsible in the biosynthesis of the amide Gln and the amino acid Glu. Additional amino acids, Asp and Ala are subsequently synthesised via highly upregulated aminotransferases. While the primary amide in nodule export, Asn is also synthesised via the highly upregulated asparagine synthase.

The entirety of the purine synthesis pathway beginning with Pur1 is non-differentially expressed in chickpea nodules, as such, Gln is likely not exported to the plastid of the uninfected cell at any meaningful rate. Very minor biosynthesis of the ureides allantoin and allantoic acid may occur and subsequently catabolised in the uninfected cell endoplasmic reticulum. Minor ureide biosynthesis likely indicates inactivity of the non-differentially expressed *CaUPS1*.

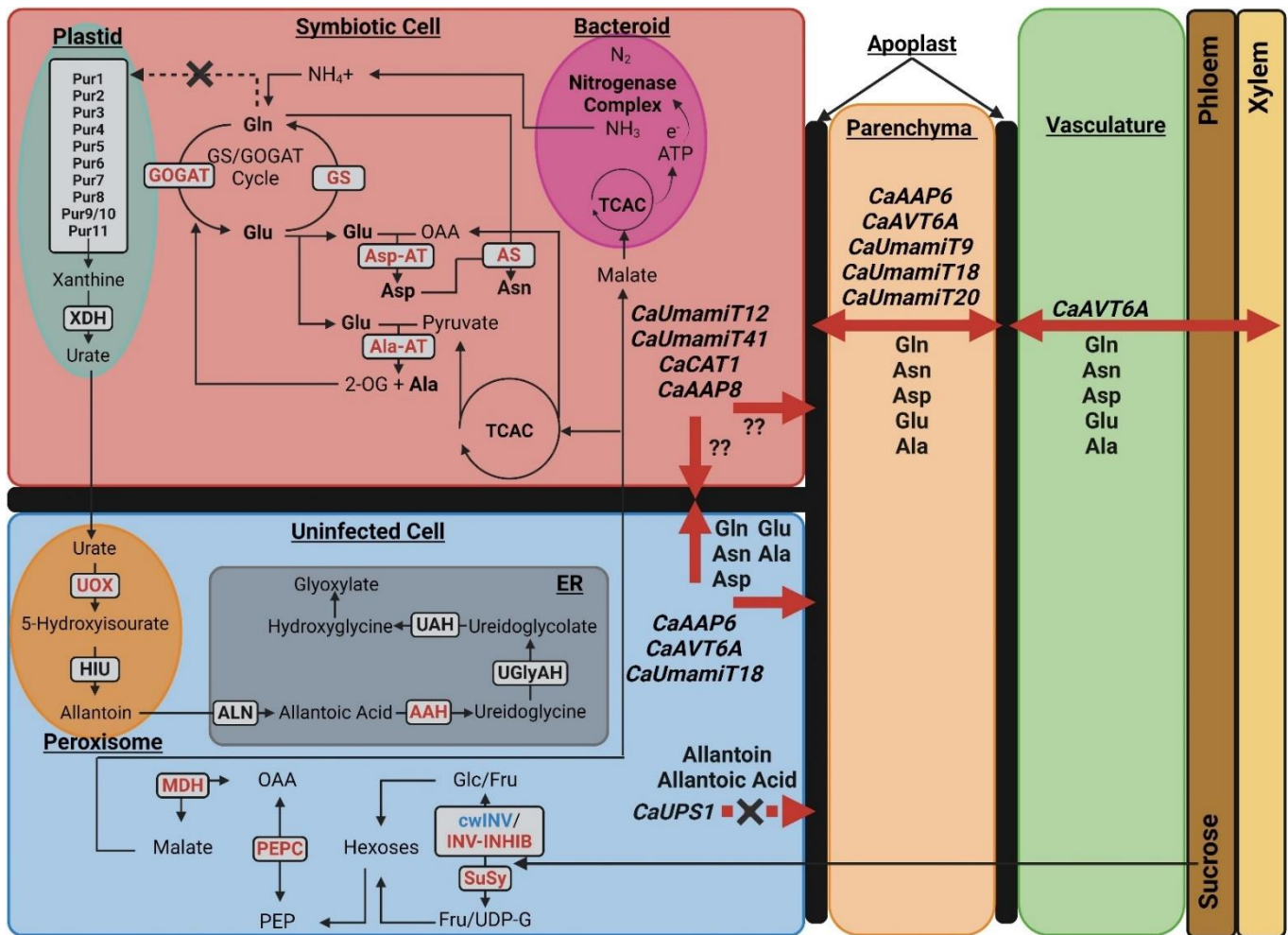


Figure 6.1: Nitrogen fixation model in chickpea nodules depicting the path of sucrose to the biosynthesis of amino acids and ureides with respective transporters.

Upregulation of enzymes depicted in red, down regulation in black. Red arrows represent upregulated transport, red dashed arrow with a cross represents downregulated and unlikely occurrence of transport. Transporters shown were highly expressed during nitrogen fixation from RNAseq, with respective amino acid substrates measured from *S. cerevisiae* complementation. Predicted localization from *M. truncatula* scRNA sequencing. Ammonia (NH₃), Ammonium (NH₄⁺), Glutamine (Gln), glutamate (Glu), aspartate (Asp), asparagine (Asn), Alanine (Ala), 2-oxoglutarate (2-OG), glutamate oxoglutarate aminotransferase (GOGAT), glutamine synthetase (GS), asparagine synthase (AS), aspartate aminotransferase (Asp-AT), Amidophosphoribosyltransferase 1 (Pur1), Phosphoribosylamine glycine ligase (Pur2), Phosphoribosylglycinamide formyltransferase (Pur3), Aminoimidazole RN synthetase (Pur5), Phosphoribosylaminoimidazole carboxylase (Pur6), Succino-aminoimidazole-carboximide RN synthetase (Pur7), Adenylosuccinate lyase (Pur8),

Aminoimidazole-carboximide RN transformylase/IMP cyclohydrolase (Pur9/10), Adenylosuccinate synthetase (Pur11), Xanthine dehydrogenase (XDH), Urate oxidase (UOX), 5 Hydroxyisourate hydrolase (HIU), ureide permease (UPS), Allantoate amidohydrolase (AAH), Allantoinase (ALN), Ureidoglycine aminohydrolase (Ugly-AH), Ureidoglycolate amidohydrolase (UAH), Sucrose synthase (SuSy), fructose (Fru), sucrose-specific invertase (cwINV), glucose (Glc), invertase inhibitor (cwINHIB), phosphoenolpyruvate carboxylase (PEPC), oxaloacetate (OAA), malate dehydrogenase (MDH), Tricarboxylic Acid Cycle (TCAC). Made with Biorender.com.

6.5 Conclusions

The data presented in this thesis convincingly suggests that chickpea indeterminate nodules predominantly synthesize amides as opposed to ureides. Enzymes responsible for amino acid, and in particular amide, biosynthesis were significantly upregulated in fixing nodules. Several highly upregulated transporters in chickpea nodules were also functionally characterized, particularly from the UmamiT family, a newly emerging gene family in the literature. These transporters provide exciting potential targets for future genetic modification experiments to improve nitrogen fixation in chickpea.

Unfortunately, due to unforeseen equipment failures late into the project, amino acid quantification could not be completed in time of writing, however I believe there is substantial evidence to support the findings of this thesis without these data.

This thesis presents the first reports to my knowledge of both the RNAseq dataset focusing on nitrogen fixation in chickpea and subsequent characterization of several chickpea nodule localised amino acid transporters. In summary, this thesis provides useful data and analyses which greatly benefit the field of nitrogen fixation research in chickpea.

Reference List

- Acharjee, S., Sarmah, B. K., Kumar, P. A., Olsen, K., Mahon, R., Moar, W. J., ... & Higgins, T. J. V. (2010). Transgenic chickpeas (*Cicer arietinum* L.) expressing a sequence-modified cry2Aa gene. *Plant Science*, *178*(3), 333-339.
- Agarwal, G., Jhanwar, S., Priya, P., Singh, V. K., Saxena, M. S., Parida, S. K., ... & Jain, M. (2012). Comparative analysis of kabuli chickpea transcriptome with desi and wild chickpea provides a rich resource for development of functional markers. *PLoS one*, *7*(12), e52443.
- Alamillo, J. M., DÍAZ-LEAL, J. L., SÁNCHEZ-MORAN, M. V., & Pineda, M. (2010). Molecular analysis of ureide accumulation under drought stress in *Phaseolus vulgaris* L. *Plant, cell & environment*, *33*(11), 1828-1837.
- Aleman, L., Ortega, J. L., Martinez-Grimes, M., Seger, M., Holguin, F. O., Uribe, D. J., ... & Sengupta-Gopalan, C. (2010). Nodule-enhanced expression of a sucrose phosphate synthase gene member (MsSPSA) has a role in carbon and nitrogen metabolism in the nodules of alfalfa (*Medicago sativa* L.). *Planta*, *231*, 233-244.
- Schulze, J. (2004). How are nitrogen fixation rates regulated in legumes?. *Journal of Plant Nutrition and Soil Science*, *167*(2), 125-137.
- Allaway, D., Ludwig, E. M., Crompton, L. A., Wood, M., Parsons, R., Wheeler, T. R., & Poole, P. S. (2000). Identification of alanine dehydrogenase and its role in mixed secretion of ammonium and alanine by pea bacteroids. *Molecular microbiology*, *36*(2), 508-515.
- Anas, M., Liao, F., Verma, K. K., Sarwar, M. A., Mahmood, A., Chen, Z. L., ... & Li, Y. R. (2020). Fate of nitrogen in agriculture and environment: agronomic, eco-physiological and molecular approaches to improve nitrogen use efficiency. *Biological Research*, *53*, 1-20.
- Angus, J. F., Kirkegaard, J. A., Hunt, J. R., Ryan, M. H., Ohlander, L., & Peoples, M. B. (2015). Break crops and rotations for wheat. *Crop and pasture science*, *66*(6), 523-552.
- Appleby, C. A. (1984). Leghemoglobin and Rhizobium respiration. *Annual Review of Plant Physiology*, *35*(1), 443-478.

- Aranda, P. S., LaJoie, D. M., & Jorcyk, C. L. (2012). Bleach gel: a simple agarose gel for analyzing RNA quality. *Electrophoresis*, *33*(2), 366-369.
- Aranjuelo, I., Molero, G., Erice, G., Avice, J. C., & Nogues, S. (2011). Plant physiology and proteomics reveals the leaf response to drought in alfalfa (*Medicago sativa* L.). *Journal of experimental botany*, *62*(1), 111-123.
- Araújo, S. S., Beebe, S., Crespi, M., Delbreil, B., González, E. M., Gruber, V., ... & Patto, M. C. V. (2015). Abiotic stress responses in legumes: strategies used to cope with environmental challenges. *Critical Reviews in Plant Sciences*, *34*(1-3), 237-280.
- Arrese-Igor Sánchez, C., González García, E., Marino Bilbao, D., Ladrera Fernández, R., Larrainzar Rodríguez, E., & Gil Quintana, E. (2011). Physiological responses of legume nodules to drought. *Plant Stress 5 (Special issue 1): 24-31*.
- Atkins, C. A., & Smith, P. M. C. (2007). Translocation in legumes: assimilates, nutrients, and signaling molecules. *Plant Physiology*, *144*(2), 550-561.
- Atkins, C. and Smith, P. (2000). Ureide synthesis in legume nodules. *Prokaryotic nitrogen fixation: a model system for the analysis of a biological process.*, pp.559-587.
- Badhan, S., Ball, A. S., & Mantri, N. (2021). First report of CRISPR/Cas9 mediated DNA-free editing of 4CL and RVE7 genes in chickpea protoplasts. *International Journal of Molecular Sciences*, *22*(1), 396.
- Baier, M.C., Barsch, A., Küster, H. and Hohnjec, N. (2007). Antisense repression of the *Medicago truncatula* nodule-enhanced sucrose synthase leads to a handicapped nitrogen fixation mirrored by specific alterations in the symbiotic transcriptome and metabolome. *Plant Physiology*, *145*(4), 1600-1618.
- Baral, B., da Silva, J.A.T. and Izaguirre-Mayoral, M.L. (2016). Early signaling, synthesis, transport and metabolism of ureides. *Journal of Plant Physiology*, *193*, 97-109.
- Berry, A. M., Mendoza-Herrera, A., Guo, Y. Y., Hayashi, J., Persson, T., Barabote, R., ... & Pawlowski, K. (2011). New perspectives on nodule nitrogen assimilation in actinorhizal symbioses. *Functional Plant Biology*, *38*(9), 645-652.
- Besnard, J. C. C. (2018). *Identification and Characterization of Amino Acid Exporters in Arabidopsis thaliana* (Doctoral dissertation).

Besnard, J., Pratelli, R., Zhao, C., Sonawala, U., Collakova, E., Pilot, G., & Okumoto, S. (2016). UMAMIT14 is an amino acid exporter involved in phloem unloading in Arabidopsis roots. *Journal of Experimental Botany*, 67(22), 6385-6397.

Besnard, J., Zhao, C., Avice, J. C., Vitha, S., Hyodo, A., Pilot, G., & Okumoto, S. (2018). Arabidopsis UMAMIT 24 and 25 are amino acid exporters involved in transfer of amino acids to the seed. *Journal of Experimental Botany*.

Bianchi, F., van't Klooster, J. S., Ruiz, S. J., & Poolman, B. (2019). Regulation of amino acid transport in *Saccharomyces cerevisiae*. *Microbiology and Molecular Biology Reviews*, 83(4), 10-1128.

Bondada, B. R., Oosterhuis, D. M., Norman, R. J., & Baker, W. H. (1996). Canopy photosynthesis, growth, yield, and boll 15N accumulation under nitrogen stress in cotton. *Crop Science*, 36(1), 127-133.

Bryan, J. K. (1980). Synthesis of the aspartate family and branched-chain amino acids. In *Amino Acids and Derivatives* (pp. 403-452). Academic Press.

Brychkova, G., Alikulov, Z., Fluhr, R. and Sagi, M. (2008). A critical role for ureides in dark and senescence-induced purine remobilization is unmasked in the *Atxdh1* Arabidopsis mutant. *The Plant Journal*, 54(3), 496-509.

Büttner, M. (2010). The Arabidopsis sugar transporter (AtSTP) family: an update. *Plant Biology*, 12, 35-41.

Calvert, H. E., Pence, M. K., Pierce, M., Malik, N. S., & Bauer, W. D. (1984). Anatomical analysis of the development and distribution of *Rhizobium* infections in soybean roots. *Canadian Journal of Botany*, 62(11), 2375-2384.

Carretero-Paulet, L., Chang, T. H., Librado, P., Ibarra-Laclette, E., Herrera-Estrella, L., Rozas, J., & Albert, V. A. (2015). Genome-wide analysis of adaptive molecular evolution in the carnivorous plant *Utricularia gibba*. *Genome Biology and Evolution*, 7(2), 444-456.

Carter, A. M., & Tegeder, M. (2016). Increasing nitrogen fixation and seed development in soybean requires complex adjustments of nodule nitrogen metabolism and partitioning processes. *Current Biology*, 26(15), 2044-2051.

- Carvalho, H., Lescure, N., de Billy, F., Chabaud, M., Lima, L., Salema, R., & Cullimore, J. (2000). Cellular expression and regulation of the *Medicago truncatula* cytosolic glutamine synthetase genes in root nodules. *Plant molecular biology*, *42*, 741-756.
- Castañeda, V., Gil-Quintana, E., Echeverria, A., & González, E. M. (2018). Legume nitrogen utilization under drought stress. *Engineering Nitrogen Utilization in Crop Plants*, 173-184.
- Cernay, C., Makowski, D., & Pelzer, E. (2018). Preceding cultivation of grain legumes increases cereal yields under low nitrogen input conditions. *Environmental chemistry letters*, *16*, 631-636.
- Chahomchuen, T., Hondo, K., Ohsaki, M., Sekito, T., & Kakinuma, Y. (2009). Evidence for Avt6 as a vacuolar exporter of acidic amino acids in *Saccharomyces cerevisiae* cells. *The Journal of General and Applied Microbiology*, *55*(6), 409-417.
- Chandran, N. K., Sriram, S., Prakash, T., & Budhwar, R. (2021). Transcriptome changes in resistant and susceptible rose in response to powdery mildew. *Journal of Phytopathology*, *169*(9), 556-569.
- Chen, S., Zhou, Y., Chen, Y., & Gu, J. (2018). fastp: an ultra-fast all-in-one FASTQ preprocessor. *Bioinformatics*, *34*(17), i884-i890.
- Chen, Y., Tong, S., Jiang, Y., Ai, F., Feng, Y., Zhang, J., ... & Ma, T. (2021). Transcriptional landscape of highly lignified poplar stems at single-cell resolution. *Genome Biology*, *22*, 1-22.
- Cheng, X. G., Nomura, M., Sato, T., Fujikake, H., Ohshima, T., & Tajima, S. (1999). Effect of exogenous NH₄⁺-N supply on distribution of ureide content in various tissues of alfalfa plants, *Medicago sativa*. *Soil Science and Plant Nutrition*, *45*(4), 921-927.
- Cheng, X. G., Nomura, M., Takane, K., Kouchi, H., & Tajima, S. (2000). Expression of two uricase (Nodulin-35) genes in a non-ureide type legume, *Medicago sativa*. *Plant and cell physiology*, *41*(1), 104-109.
- Coletto, I., Pineda, M., Rodiño, A.P., De Ron, A.M. and Alamillo, J.M. (2014). Comparison of inhibition of N₂ fixation and ureide accumulation under water deficit in four common bean genotypes of contrasting drought tolerance. *Annals of botany*, *113*(6), 1071-1082.
- Collier, R., & Tegeder, M. (2012). Soybean ureide transporters play a critical role in nodule development, function and nitrogen export. *The Plant Journal*, *72*(3), 355-367.

- Collier, R., Fuchs, B., Walter, N., Kevin Lutke, W., & Taylor, C. G. (2005). Ex vitro composite plants: an inexpensive, rapid method for root biology. *The Plant Journal*, 43(3), 449-457.
- Dai, X., Zhuang, Z., Boschiero, C., Dong, Y., & Zhao, P. X. (2021). LegumeIP V3: from models to crops—an integrative gene discovery platform for translational genomics in legumes. *Nucleic acids research*, 49(D1), D1472-D1479.
- Dance, I. (2013). A molecular pathway for the egress of ammonia produced by nitrogenase. *Scientific Reports*, 3(1), 3237.
- Das Bhowmik, S. S., Cheng, A. Y., Long, H., Tan, G. Z. H., Hoang, T. M. L., Karbaschi, M. R., ... & Mundree, S. G. (2019). Robust genetic transformation system to obtain non-chimeric transgenic chickpea. *Frontiers in plant science*, 10, 524.
- Das Bhowmik, S.S., Cheng, A.Y., Long, H., Tan, G.Z.H., Hoang, T.M.L., Karbaschi, M.R., Williams, B., Higgins, T.J.V. and Mundree, S.G. (2019). Robust genetic transformation system to obtain non-chimeric transgenic chickpea. *Frontiers in plant science*, 10, 524.
- Dash, S., Campbell, J. D., Cannon, E. K., Cleary, A. M., Huang, W., Kalberer, S. R., ... & Cannon, S. B. (2016). Legume information system (LegumeInfo.org): a key component of a set of federated data resources for the legume family. *Nucleic acids research*, 44(D1), D1181-D1188.
- Day*, D. A., Poole, P. S., Tyerman, S. D., & Rosendahl, L. (2001). Ammonia and amino acid transport across symbiotic membranes in nitrogen-fixing legume nodules. *Cellular and Molecular Life Sciences CMLS*, 58, 61-71.
- Day, D. A., & Udvardi, M. K. (1993). Review article Metabolite Exchange Across Symbiosome Membranes. *Symbiosis*.
- Day, D. A., Price, G. D., & Udvardi, M. K. (1989). Membrane interface of the Bradyrhizobium japonicum–Glycine max symbiosis: peribacteroid units from soyabean nodules. *Functional Plant Biology*, 16(1), 69-84.
- de la Torre, F., Cañas, R. A., Pascual, M. B., Avila, C., & Cánovas, F. M. (2014). Plastidic aspartate aminotransferases and the biosynthesis of essential amino acids in plants. *Journal of experimental botany*, 65(19), 5527-5534.

de la Torre, F., El-Azaz, J., Ávila, C., & Cánovas, F. M. (2014). Deciphering the role of aspartate and prephenate aminotransferase activities in plastid nitrogen metabolism. *Plant Physiology*, *164*(1), 92-104.

Del Castillo, L.D., Hunt, S. and Layzell, D.B. (1994). The role of oxygen in the regulation of nitrogenase activity in drought-stressed soybean nodules. *Plant Physiology*, *106*(3), 949-955.

Denancé, N., Ranocha, P., Oria, N., Barlet, X., Rivière, M. P., Yadeta, K. A., ... & Goffner, D. (2013). *Arabidopsis* *wat1* (walls are thin1)-mediated resistance to the bacterial vascular pathogen, *Ralstonia solanacearum*, is accompanied by cross-regulation of salicylic acid and tryptophan metabolism. *The Plant Journal*, *73*(2), 225-239.

Denancé, N., Szurek, B., & Noël, L. D. (2014). Emerging functions of nodulin-like proteins in non-nodulating plant species. *Plant and cell physiology*, *55*(3), 469-474.

Díaz, P., Borsani, O., Marquez, A.N.T.O.N.I.O. and Monza, J.O.R.G.E. (2005). Nitrogen metabolism in relation to drought stress responses in cultivated and model *Lotus* species. *Lotus newsletter*, *35*(1), 83-92.

Díaz-Leal, J. L., Galvez-Valdivieso, G., Fernandez, J., Pineda, M., & Alamillo, J. M. (2012). Developmental effects on ureide levels are mediated by tissue-specific regulation of allantoinase in *Phaseolus vulgaris* L. *Journal of Experimental Botany*, *63*(11), 4095-4106.

Ding, Y., Kalo, P., Yendrek, C., Sun, J., Liang, Y., Marsh, J.F., Harris, J.M. and Oldroyd, G.E. (2008). Abscisic acid coordinates nod factor and cytokinin signaling during the regulation of nodulation in *Medicago truncatula*. *The Plant Cell*, *20*(10), 2681-2695.

Ditzler, L., van Apeldoorn, D. F., Pellegrini, F., Antichi, D., Bàrberi, P., & Rossing, W. A. (2021). Current research on the ecosystem service potential of legume inclusive cropping systems in Europe. A review. *Agronomy for Sustainable Development*, *41*, 1-13.

Doidy, J., Vidal, U., & Lemoine, R. (2019). Sugar transporters in Fabaceae, featuring SUT MST and SWEET families of the model plant *Medicago truncatula* and the agricultural crop *Pisum sativum*. *PLoS One*, *14*(9), e0223173.

Downie, J.A. (2010). The roles of extracellular proteins, polysaccharides and signals in the interactions of rhizobia with legume roots. *FEMS microbiology reviews*, *34*(2), 150-170.

Duff, S. M., Qi, Q., Reich, T., Wu, X., Brown, T., Crowley, J. H., & Fabbri, B. (2011). A kinetic comparison of asparagine synthetase isozymes from higher plants. *Plant Physiology and Biochemistry*, *49*(3), 251-256.

Faghire, M., Mohamed, F., Taoufiq, K., Fghire, R., Bargaz, A., Mandri, B., ... & Ghoulam, C. (2013). Genotypic variation of nodules' enzymatic activities in symbiotic nitrogen fixation among common bean (*Phaseolus vulgaris* L.) genotypes grown under salinity constraint. *Symbiosis*, *60*, 115-122.

Fang, Z. T., Kapoor, R., Datta, A., & Okumoto, S. (2022). Tissue specific expression of UMAMIT amino acid transporters in wheat. *Scientific Reports*, *12*(1), 1-12.

Farnham, M. W., Miller, S. S., Griffith, S. M., & Vance, C. P. (1990). Aspartate aminotransferase in alfalfa root nodules: II. Immunological distinction between two forms of the enzyme. *Plant Physiology*, *93*(2), 603-610.

Fedorova, E. E. (2023). Rapid Changes to Endomembrane System of Infected Root Nodule Cells to Adapt to Unusual Lifestyle. *International Journal of Molecular Sciences*, *24*(5), 4647.

Ferguson, B. J., Indrasumunar, A., Hayashi, S., Lin, M. H., Lin, Y. H., Reid, D. E., & Gresshoff, P. M. (2010). Molecular analysis of legume nodule development and autoregulation. *Journal of integrative plant biology*, *52*(1), 61-76.

Figuroa, C.M., Feil, R., Ishihara, H., Watanabe, M., Kölling, K., Krause, U., Höhne, M., Encke, B., Plaxton, W.C., Zeeman, S.C. and Li, Z. (2016). Trehalose 6-phosphate coordinates organic and amino acid metabolism with carbon availability. *The Plant Journal*, *85*(3), 410-423.

Fischer, W. N., Loo, D. D., Koch, W., Ludewig, U., Boorer, K. J., Tegeder, M., ... & Frommer, W. B. (2002). Low and high affinity amino acid H⁺-cotransporters for cellular import of neutral and charged amino acids. *The Plant Journal*, *29*(6), 717-731.

Frank, M., Fechete, L. I., Tedeschi, F., Nadzieja, M., Norgaard, M. M. M., Montiel, J., ... & Andersen, S. U. (2022). Single-cell analysis maps distinct cellular responses to rhizobia and identifies the novel infection regulator SYMRKL1 in *Lotus japonicus*. *bioRxiv*.

Fujiki, Y., Teshima, H., Kashiwao, S., Kawano-Kawada, M., Ohsumi, Y., Kakinuma, Y., & Sekito, T. (2017). Functional identification of At AVT 3, a family of vacuolar amino acid transporters, in *Arabidopsis*. *FEBS letters*, *591*(1), 5-15.

- Gálvez, L., González, E.M. and Arrese-Igor, C. (2005). Evidence for carbon flux shortage and strong carbon/nitrogen interactions in pea nodules at early stages of water stress. *Journal of Experimental Botany*, 56(419), 2551-2561.
- Gamas, P., de Carvalho Niebel, F., Lescure, N., & Cullimore, J. V. (1996). Use of a subtractive hybridization approach to identify new *Medicago truncatula* genes induced during root nodule development. *MPMI-Molecular Plant Microbe Interactions*, 9(4), 233-242.
- Garcia, K., Cloghessy, K., Cooney, D. R., Shelley, B., Chakraborty, S., Kafle, A., ... & Pilot, G. (2023). The putative transporter MtUMAMIT14 participates in nodule formation in *Medicago truncatula*. *Scientific Reports*, 13(1), 804.
- García-Calderón, M., Chiurazzi, M., Espuny, M. R., & Márquez, A. J. (2012). Photorespiratory metabolism and nodule function: behavior of *Lotus japonicus* mutants deficient in plastid glutamine synthetase. *Molecular Plant-Microbe Interactions*, 25(2), 211-219.
- Garg, R., Patel, R. K., Jhanwar, S., Priya, P., Bhattacharjee, A., Yadav, G., ... & Jain, M. (2011). Gene discovery and tissue-specific transcriptome analysis in chickpea with massively parallel pyrosequencing and web resource development. *Plant physiology*, 156(4), 1661-1678.
- Garg, R., Sahoo, A., Tyagi, A. K., & Jain, M. (2010). Validation of internal control genes for quantitative gene expression studies in chickpea (*Cicer arietinum* L.). *Biochemical and biophysical research communications*, 396(2), 283-288.
- Garneau, M. G., Tan, Q., & Tegeder, M. (2018). Function of pea amino acid permease AAP6 in nodule nitrogen metabolism and export, and plant nutrition. *Journal of experimental botany*, 69(21), 5205-5219.
- Gaufichon, L., Reisdorf-Cren, M., Rothstein, S. J., Chardon, F., & Suzuki, A. (2010). Biological functions of asparagine synthetase in plants. *Plant Science*, 179(3), 141-153.
- Gavrin, A., Kaiser, B. N., Geiger, D., Tyerman, S. D., Wen, Z., Bisseling, T., & Fedorova, E. E. (2014). Adjustment of host cells for accommodation of symbiotic bacteria: vacuole defunctionalization, HOPS suppression, and TIP1g retargeting in *Medicago*. *The Plant Cell*, 26(9), 3809-3822.

Gebhardt, J. S., Wadsworth, G. J., & Matthews, B. F. (1998). Characterization of a single soybean cDNA encoding cytosolic and glyoxysomal isozymes of aspartate aminotransferase. *Plant molecular biology*, 37, 99-108.

Gebriel, S., Seger, M., Villanueva, F. M., Ortega, J. L., Bagga, S., & Sengupta-Gopalan, C. (2015). Transgenic alfalfa (*Medicago sativa*) with increased sucrose phosphate synthase activity shows enhanced growth when grown under N₂-fixing conditions. *Planta*, 242, 1009-1024.

Gietz, R. D., & Woods, R. A. (2002). Transformation of yeast by lithium acetate/single-stranded carrier DNA/polyethylene glycol method. In *Methods in enzymology* (Vol. 350, pp. 87-96). Academic Press.

Gilbert, D. (2013). Genes of *Litopenaeus vannamei*, white shrimp reconstructed with EvidentialGene. *organism*.

Gil-Quintana, E., Larrainzar, E., Arrese-Igor, C. and González, E.M. (2013). Is N-feedback involved in the inhibition of nitrogen fixation in drought-stressed *Medicago truncatula*?. *Journal of experimental botany*, 64(1), 281-292.

Gil-Quintana, E., Larrainzar, E., Seminario, A., Díaz-Leal, J.L., Alamillo, J.M., Pineda, M., Arrese-Igor, C., Wienkoop, S. and González, E.M. (2013). Local inhibition of nitrogen fixation and nodule metabolism in drought-stressed soybean. *Journal of Experimental Botany*, 64(8), 2171-2182.

Givan, C. V. (1980). Aminotransferases in higher plants. In *Amino acids and derivatives* (pp. 329-357). Academic Press.

González, E.M., Gálvez, L. and Arrese-Igor, C. (2001). Abscisic acid induces a decline in nitrogen fixation that involves leghaemoglobin, but is independent of sucrose synthase activity. *Journal of Experimental Botany*, 52(355), 285-293.

González, E.M., Gordon, A.J., James, C.L. and Arrese-Igor, C. (1995). The role of sucrose synthase in the response of soybean nodules to drought. *Journal of Experimental Botany*, 46(10), 1515-1523.

González-Andrés, F., & James, E. (Eds.). (2016). *Biological nitrogen fixation and beneficial plant-microbe interaction*. Springer.

Gordon, A. J., Thomas, B. J., & Reynolds, P. H. S. (1992). Localization of sucrose synthase in soybean root nodules. *New Phytologist*, 122(1), 35-44.

Gordon, A.J., Minchin, F.R., James, C.L. and Komina, O. (1999). Sucrose synthase in legume nodules is essential for nitrogen fixation. *Plant Physiology*, 120(3), 867-878.

Grabherr, M. G., Haas, B. J., Yassour, M., Levin, J. Z., Thompson, D. A., Amit, I., ... & Regev, A. (2011). Trinity: reconstructing a full-length transcriptome without a genome from RNA-Seq data. *Nature biotechnology*, 29(7), 644.

Graham, P. H., & Vance, C. P. (2003). Legumes: importance and constraints to greater use. *Plant physiology*, 131(3), 872-877.

Graindorge, M., Giustini, C., Jacomin, A. C., Kraut, A., Curien, G., & Matringe, M. (2010). Identification of a plant gene encoding glutamate/aspartate-prephenate aminotransferase: the last homeless enzyme of aromatic amino acids biosynthesis. *FEBS letters*, 584(20), 4357-4360.

Grallath, S., Weimar, T., Meyer, A., Gumy, C., Suter-Grotemeyer, M., Neuhaus, J. M., & Rentsch, D. (2005). The AtProT family. Compatible solute transporters with similar substrate specificity but differential expression patterns. *Plant Physiology*, 137(1), 117-126.

Grant, D., Nelson, R. T., Cannon, S. B., & Shoemaker, R. C. (2010). SoyBase, the USDA-ARS soybean genetics and genomics database. *Nucleic acids research*, 38(suppl_1), D843-D846.

Grant, J. E., Ninan, A., Cripps-Guazzone, N., Shaw, M., Song, J., Petřík, I., ... & Jameson, P. E. (2021). Concurrent overexpression of amino acid permease AAP1 (3a) and SUT1 sucrose transporter in pea resulted in increased seed number and changed cytokinin and protein levels. *Functional Plant Biology*, 48(9), 889-904.

Gruber, N. and Galloway, J.N. (2008). An Earth-system perspective of the global nitrogen cycle. *Nature*, 451(7176), 293-296.

Gu, D., Andreev, K., & Dupre, M. E. (2021). Major trends in population growth around the world. *China CDC weekly*, 3(28), 604.

Gupta, M., Dubey, S., Jain, D., & Chandran, D. (2021). The *Medicago truncatula* sugar transport protein 13 and its Lr67res-like variant confer powdery mildew resistance in legumes via defense modulation. *Plant and Cell Physiology*, 62(4), 650-667.

- Haferkamp, I. (2007). The diverse members of the mitochondrial carrier family in plants. *FEBS letters*, 581(12), 2375-2379.
- Hammes, U. Z., Nielsen, E., Honaas, L. A., Taylor, C. G., & Schachtman, D. P. (2006). AtCAT6, a sink-tissue-localized transporter for essential amino acids in Arabidopsis. *The Plant Journal*, 48(3), 414-426.
- Harrison, J., Pou de Crescenzo, M. A., Sené, O., & Hirel, B. (2003). Does lowering glutamine synthetase activity in nodules modify nitrogen metabolism and growth of *Lotus japonicus*?. *Plant physiology*, 133(1), 253-262.
- Hartmann, K., Peiter, E., Koch, K., Schubert, S. and Schreiber, L. (2002). Chemical composition and ultrastructure of broad bean (*Vicia faba* L.) nodule endodermis in comparison to the root endodermis. *Planta*, 215(1), 14-25.
- Hasegawa, P.M., Bressan, R.A., Zhu, J.K. and Bohnert, H.J. (2000). Plant cellular and molecular responses to high salinity. *Annual review of plant biology*, 51(1), 463-499.
- Hauck, O. K., Scharnberg, J., Escobar, N. M., Wanner, G., Giavalisco, P., & Witte, C. P. (2014). Uric acid accumulation in an Arabidopsis urate oxidase mutant impairs seedling establishment by blocking peroxisome maintenance. *The Plant Cell*, 26(7), 3090-3100.
- Havé, M., Marmagne, A., Chardon, F. and Masclaux-Daubresse, C. (2017). Nitrogen remobilization during leaf senescence: lessons from Arabidopsis to crops. *Journal of Experimental Botany*, 68(10), 2513-2529.
- Hohnjec, N., Perlick, A. M., Pühler, A., & Küster, H. (2003). The *Medicago truncatula* sucrose synthase gene MtSucS1 is activated both in the infected region of root nodules and in the cortex of roots colonized by arbuscular mycorrhizal fungi. *Molecular Plant-Microbe Interactions*, 16(10), 903-915.
- Hruz, T., Laule, O., Szabo, G., Wessendorp, F., Bleuler, S., Oertle, L., ... & Zimmermann, P. (2008). Genevestigator v3: a reference expression database for the meta-analysis of transcriptomes. *Advances in bioinformatics*, 2008.
- Hsiao, T., Mares, T., Waite, K., Yang, J., Kelso, R., Holden, K. and Stoner, R. (2018). Inference of CRISPR edits from Sanger trace data. *BioRxiv*, 251082.

- Hunt, E., Gattolin, S., Newbury, H. J., Bale, J. S., Tseng, H. M., Barrett, D. A., & Pritchard, J. (2010). A mutation in amino acid permease AAP6 reduces the amino acid content of the Arabidopsis sieve elements but leaves aphid herbivores unaffected. *Journal of experimental botany*, *61*(1), 55-64.
- Ibarra-Laclette, Enrique, Eric Lyons, Gustavo Hernández-Guzmán, Claudia Anahí Pérez-Torres, Lorenzo Carretero-Paulet, Tien-Hao Chang, Tianying Lan et al. "Architecture and evolution of a minute plant genome." *Nature* 498, no. 7452 (2013): 94-98.
- Igarashi, D., Miwa, T., Seki, M., Kobayashi, M., Kato, T., Tabata, S., ... & Ohsumi, C. (2003). Identification of photorespiratory glutamate: glyoxylate aminotransferase (GGAT) gene in Arabidopsis. *The Plant Journal*, *33*(6), 975-987.
- Irani, S. and Todd, C.D. (2018). Exogenous allantoin increases Arabidopsis seedlings tolerance to NaCl stress and regulates expression of oxidative stress response genes. *Journal of plant physiology*, *221*, 43-50.
- Jämtgård, S. (2010). *The occurrence of amino acids in agricultural soil and their uptake by plants* (Vol. 2010, No. 2010: 27).
- Jensen, E. S., Peoples, M. B., Boddey, R. M., Gresshoff, P. M., Hauggaard-Nielsen, H., JR Alves, B., & Morrison, M. J. (2012). Legumes for mitigation of climate change and the provision of feedstock for biofuels and biorefineries. A review. *Agronomy for sustainable development*, *32*, 329-364.
- Jhanwar, S., Priya, P., Garg, R., Parida, S. K., Tyagi, A. K., & Jain, M. (2012). Transcriptome sequencing of wild chickpea as a rich resource for marker development. *Plant Biotechnology Journal*, *10*(6), 690-702.
- Ji, Y., Huang, W., Wu, B., Fang, Z., & Wang, X. (2020). The amino acid transporter AAP1 mediates growth and grain yield by regulating neutral amino acid uptake and reallocation in *Oryza sativa*. *Journal of Experimental Botany*, *71*(16), 4763-4777.
- Kapushesky, M., Emam, I., Holloway, E., Kurnosov, P., Zorin, A., Malone, J., ... & Brazma, A. (2010). Gene expression atlas at the European bioinformatics institute. *Nucleic acids research*, *38*(suppl_1), D690-D698.
- Karmann, J., Müller, B., & Hammes, U. Z. (2018). The long and winding road: transport pathways for amino acids in Arabidopsis seeds. *Plant reproduction*, *31*, 253-261.

- Kaur, R., & Prasad, K. (2021). Technological, processing and nutritional aspects of chickpea (*Cicer arietinum*)-A review. *Trends in Food Science & Technology*, *109*, 448-463.
- Kim, D., Langmead, B., & Salzberg, S. L. (2015). HISAT: a fast spliced aligner with low memory requirements. *Nature methods*, *12*(4), 357-360.
- Kim, J. H., Delauney, A. J., & Verma, D. P. S. (1995). Control of de novo purine biosynthesis genes in ureide-producing legumes: induction of glutamine phosphoribosylpyrophosphate amidotransferase gene and characterization of its cDNA from soybean and *Vigna*. *The Plant Journal*, *7*(1), 77-86.
- Kim, J. Y., Symeonidi, E., Pang, T. Y., Denyer, T., Weidauer, D., Bezruczyk, M., ... & Frommer, W. B. (2021). Distinct identities of leaf phloem cells revealed by single cell transcriptomics. *The Plant Cell*, *33*(3), 511-530.
- King, C.A. and Purcell, L.C. (2005). Inhibition of N₂ fixation in soybean is associated with elevated ureides and amino acids. *Plant Physiology*, *137*(4), 1389-1396.
- Kisko, M., Bouain, N., Rouached, A., Choudhary, S. P., & Rouached, H. (2015). Molecular mechanisms of phosphate and zinc signalling crosstalk in plants: Phosphate and zinc loading into root xylem in *Arabidopsis*. *Environmental and Experimental Botany*, *114*, 57-64.
- Komaitis, F., Kalliampakou, K., Botou, M., Nikolaidis, M., Kalloniati, C., Skliros, D., ... & Flemetakis, E. (2020). Molecular and physiological characterization of the monosaccharide transporters gene family in *Medicago truncatula*. *Journal of Experimental Botany*, *71*(10), 3110-3125.
- Kryvoruchko, I. S., Sinharoy, S., Torres-Jerez, I., Sosso, D., Pislariu, C. I., Guan, D., ... & Udvardi, M. K. (2016). MtSWEET11, a nodule-specific sucrose transporter of *Medicago truncatula*. *Plant Physiology*, *171*(1), 554-565.
- Kudapa, H., Garg, V., Chitikineni, A., & Varshney, R. K. (2018). The RNA-Seq-based high resolution gene expression atlas of chickpea (*Cicer arietinum* L.) reveals dynamic spatio-temporal changes associated with growth and development. *Plant, Cell & Environment*, *41*(9), 2209-2225.
- Kumar, S., Bourdes, A., & Poole, P. (2005). De novo alanine synthesis by bacteroids of *Mesorhizobium loti* is not required for nitrogen transfer in the determinate nodules of *Lotus corniculatus*. *Journal of bacteriology*, *187*(15), 5493-5495.

- Kunert, K.J., Vorster, B.J., Fenta, B.A., Kibido, T., Dionisio, G. and Foyer, C.H. (2016). Drought stress responses in soybean roots and nodules. *Frontiers in Plant Science*, 7, 1015.
- Kuzma, M. M., Hunt, S., & Layzell, D. B. (1993). Role of oxygen in the limitation and inhibition of nitrogenase activity and respiration rate in individual soybean nodules. *Plant physiology*, 101(1), 161-169.
- La, H. V., Chu, H. D., Tran, C. D., Nguyen, K. H., Le, Q. T. N., Hoang, C. M., ... & Tran, L. S. P. (2022). Insights into the gene and protein structures of the CaSWEET family members in chickpea (*Cicer arietinum*), and their gene expression patterns in different organs under various stress and abscisic acid treatments. *Gene*, 819, 146210.
- Labun, K., Montague, T.G., Krause, M., Torres Cleuren, Y.N., Tjeldnes, H. and Valen, E. (2019). CHOPCHOP v3: expanding the CRISPR web toolbox beyond genome editing. *Nucleic acids research*, 47(W1), W171-W174.
- Ladrera, R., Marino, D., Larrainzar, E., González, E.M. and Arrese-Igor, C. (2007). Reduced carbon availability to bacteroids and elevated ureides in nodules, but not in shoots, are involved in the nitrogen fixation response to early drought in soybean. *Plant Physiology*, 145(2), 539-546.
- Ladwig, F., Stahl, M., Ludewig, U., Hirner, A. A., Hammes, U. Z., Stadler, R., ... & Koch, W. (2012). Siliques are Red1 from *Arabidopsis* acts as a bidirectional amino acid transporter that is crucial for the amino acid homeostasis of siliques. *Plant Physiology*, 158(4), 1643-1655.
- Larrainzar, E., Wienkoop, S., Scherling, C., Kempa, S., Ladrera, R., Arrese-Igor, C., Weckwerth, W. and González, E.M. (2009). Carbon metabolism and bacteroid functioning are involved in the regulation of nitrogen fixation in *Medicago truncatula* under drought and recovery. *Molecular Plant-Microbe Interactions*, 22(12), 1565-1576.
- Layzell, D. B., Pate, J. S., Atkins, C. A., & Canvin, D. T. (1981). Partitioning of carbon and nitrogen and the nutrition of root and shoot apex in a nodulated legume. *Plant Physiology*, 67(1), 30-36.
- Le Roux, M., Phiri, E., Khan, W., Şakiroğlu, M., Valentine, A., & Khan, S. (2014). Expression of novel cytosolic malate dehydrogenases (cMDH) in *Lupinus angustifolius* nodules during phosphorus starvation. *Journal of plant physiology*, 171(17), 1609-1618.

- Lea, P. J., & Mifflin, B. J. (2010). Nitrogen assimilation and its relevance to crop improvement. *Annual Plant Reviews Volume 42*, 42, 1-40.
- Lea, P. J., Robinson, S. A., & Stewart, G. R. (1990). The enzymology and metabolism of glutamine, glutamate, and asparagine. *The biochemistry of plants*, 16, 121-159.
- Lea, P.J. and Azevedo, R.A. (2007). Nitrogen use efficiency. 2. Amino acid metabolism. *Annals of Applied Biology*, 151(3), 269-275.
- Lee, Y. H., Foster, J., Chen, J., Voll, L. M., Weber, A. P., & Tegeder, M. (2007). AAP1 transports uncharged amino acids into roots of Arabidopsis. *The Plant Journal*, 50(2), 305-319.
- Lescano, C. I., Martini, C., González, C. A., & Desimone, M. (2016). Allantoin accumulation mediated by allantoinase downregulation and transport by Ureide Permease 5 confers salt stress tolerance to Arabidopsis plants. *Plant molecular biology*, 91(4), 581-595.
- Lescano, I., Bogino, M.F., Martini, C., Tessi, T.M., González, C.A., Schumacher, K. and Desimone, M. (2020). Ureide Permease 5 (AtUPS5) Connects Cell Compartments Involved in Ureide Metabolism. *Plant Physiology*, 182(3), 1310-1325.
- Li, X., Staszewski, L., Xu, H., Durick, K., Zoller, M., & Adler, E. (2002). Human receptors for sweet and umami taste. *Proceedings of the National Academy of Sciences*, 99(7), 4692-4696.
- Li, Y., Ran, W., Zhang, R., Sun, S., & Xu, G. (2009). Facilitated legume nodulation, phosphate uptake and nitrogen transfer by arbuscular inoculation in an upland rice and mung bean intercropping system. *Plant and Soil*, 315, 285-296.
- Liao, Y., Smyth, G. K., & Shi, W. (2014). featureCounts: an efficient general purpose program for assigning sequence reads to genomic features. *Bioinformatics*, 30(7), 923-930.
- Liepman, A. H., & Olsen, L. J. (2001). Peroxisomal alanine: glyoxylate aminotransferase (AGT1) is a photorespiratory enzyme with multiple substrates in Arabidopsis thaliana. *The Plant Journal*, 25(5), 487-498.
- Liepman, A. H., Vijayalakshmi, J., Peisach, D., Hulsebus, B., Olsen, L. J., & Saper, M. A. (2019). Crystal structure of photorespiratory alanine: glyoxylate aminotransferase 1 (AGT1) from Arabidopsis thaliana. *Frontiers in Plant Science*, 10, 1229.

Liu, A., Contador, C. A., Fan, K., & Lam, H. M. (2018). Interaction and regulation of carbon, nitrogen, and phosphorus metabolisms in root nodules of legumes. *Frontiers in Plant Science*, *9*, 1860.

Liu, S., Wang, D., Mei, Y., Xia, T., Xu, W., Zhang, Y., ... & Wang, N. N. (2020). Overexpression of GmAAP6a enhances tolerance to low nitrogen and improves seed nitrogen status by optimizing amino acid partitioning in soybean. *Plant biotechnology journal*, *18*(8), 1749-1762.

Liu, Y.H., Offler, C.E. and Ruan, Y.L. (2013). Regulation of fruit and seed response to heat and drought by sugars as nutrients and signals. *Frontiers in Plant Science*, *4*, 282.

Liu, Z., Kong, X., Long, Y., Zhang, H., Jia, J., Qiu, L., ... & Yan, Z. (2022). Integrated single-nucleus and spatial transcriptomics captures transitional states in soybean nodule symbiosis establishment. *bioRxiv*.

Lock, M. (2005). *Legumes of the World* (Vol. 577). G. P. Lewis, B. Schrire, & B. Mackinder (Eds.). Kew: Royal Botanic Gardens.

Lodwig, E., & Poole, P. (2003). Metabolism of Rhizobium bacteroids. *Critical reviews in plant sciences*, *22*(1), 37-78.

Lu, J., Li, X.N., Yang, Y.L., Jia, L.Y., You, J. and Wang, W.R. (2013). Effect of hydrogen peroxide on seedling growth and antioxidants in two wheat cultivars. *Biologia plantarum*, *57*(3), 487-494.

Lu, K., Wu, B., Wang, J., Zhu, W., Nie, H., Qian, J., ... & Fang, Z. (2018). Blocking amino acid transporter Os AAP 3 improves grain yield by promoting outgrowth buds and increasing tiller number in rice. *Plant Biotechnology Journal*, *16*(10), 1710-1722.

Lu, M. Z., Carter, A. M., & Tegeder, M. (2022). Altering ureide transport in nodulated soybean results in whole-plant adjustments of metabolism, assimilate partitioning, and sink strength. *Journal of Plant Physiology*, *269*, 153613.

Lu, M.Z., Snyder, R., Grant, J. and Tegeder, M. (2020). Manipulation of sucrose phloem and embryo loading affects pea leaf metabolism, carbon and nitrogen partitioning to sinks as well as seed storage pools. *The Plant Journal*, *101*(1), 217-236.

Lu, Ming-Zhu, Rachel Snyder, Jan Grant, and Mechthild Tegeder. "Manipulation of sucrose phloem and embryo loading affects pea leaf metabolism, carbon and nitrogen partitioning to sinks as well as seed storage pools." *The Plant Journal* 101, no. 1 (2020): 217-236.

Luo, Z., Liu, H., Li, W., Zhao, Q., Dai, J., Tian, L., & Dong, H. (2018). Effects of reduced nitrogen rate on cotton yield and nitrogen use efficiency as mediated by application mode or plant density. *Field Crops Research*, 218, 150-157.

Maeda, H., & Dudareva, N. (2012). The shikimate pathway and aromatic amino acid biosynthesis in plants. *Annual review of plant biology*, 63, 73-105.

Marino, D., Frendo, P., Ladrera, R., Zabalza, A., Puppo, A., Arrese-Igor, C. and González, E.M. (2007). Nitrogen fixation control under drought stress. Localized or systemic?. *Plant Physiology*, 143(4), 1968-1974.

Masclaux-Daubresse, C., Daniel-Vedele, F., Dechorgnat, J., Chardon, F., Gaufichon, L., & Suzuki, A. (2010). Nitrogen uptake, assimilation and remobilization in plants: challenges for sustainable and productive agriculture. *Annals of botany*, 105(7), 1141-1157.

Masepohl, B., Witty, J. F., Riedel, K. U., Klipp, W., & Puhler, A. (1993). Rhizobium meliloti mutants defective in symbiotic nitrogen fixation affect the oxygen gradient in alfalfa (*Medicago sativa*) root nodules. *Journal of experimental botany*, 44(2), 419-426.

Mathews, A., Carroll, B. J., & Gresshoff, P. M. (1989). Development of Bradyrhizobium infections in supernodulating and non-nodulating mutants of soybean (*Glycine max* [L.] Merrill). *Protoplasma*, 150, 40-47.

Melo, P. M., Silva, L. S., Ribeiro, I., Seabra, A. R., & Carvalho, H. G. (2011). Glutamine synthetase is a molecular target of nitric oxide in root nodules of *Medicago truncatula* and is regulated by tyrosine nitration. *Plant Physiology*, 157(3), 1505-1517.

Merga, B., & Haji, J. (2019). Economic importance of chickpea: Production, value, and world trade. *Cogent Food & Agriculture*, 5(1), 1615718.

Meyer, A., Eskandari, S., Grallath, S., & Rentsch, D. (2006). AtGAT1, a high affinity transporter for γ -aminobutyric acid in *Arabidopsis thaliana*. *Journal of biological chemistry*, 281(11), 7197-7204.

Minchin, F.R. and Witty, J.F. (2005). Respiratory/carbon costs of symbiotic nitrogen fixation in legumes. In *Plant respiration* (pp. 195-205). Springer, Dordrecht.

- Mizukoshi, K., Nishiwaki, T., Ohtake, N., Minagawa, R., Ikarashi, T. and Ohyama, T. (1995). Nitrate transport pathway into soybean nodules traced by tungstate and $^{15}\text{NO}_3$. *Soil Science and Plant Nutrition*, 41(1), 75-88.
- Mokgehle, S. N., Dakora, F. D., & Mathews, C. (2014). Variation in N_2 fixation and N contribution by 25 groundnut (*Arachis hypogaea* L.) varieties grown in different agro-ecologies, measured using ^{15}N natural abundance. *Agriculture, ecosystems & environment*, 195, 161-172.
- Moormann, J., Heinemann, B., & Hildebrandt, T. M. (2022). News about amino acid metabolism in plant–microbe interactions. *Trends in Biochemical Sciences*.
- Moose, S., & Below, F. E. (2009). Biotechnology approaches to improving maize nitrogen use efficiency. In *Molecular genetic approaches to maize improvement* (pp. 65-77). Berlin, Heidelberg: Springer Berlin Heidelberg.
- Moulin, L., Munive, A., Dreyfus, B., & Boivin-Masson, C. (2001). Nodulation of legumes by members of the β -subclass of Proteobacteria. *Nature*, 411(6840), 948-950.
- Müller, B., Fastner, A., Karmann, J., Mansch, V., Hoffmann, T., Schwab, W., ... & Hammes, U. Z. (2015). Amino acid export in developing *Arabidopsis* seeds depends on UmamiT facilitators. *Current Biology*, 25(23), 3126-3131.
- Mulvaney, R.L., Khan, S.A. and Ellsworth, T.R. (2009). Synthetic nitrogen fertilizers deplete soil nitrogen: a global dilemma for sustainable cereal production. *Journal of environmental quality*, 38(6), 2295-2314.
- Mun, T., Bachmann, A., Gupta, V., Stougaard, J., & Andersen, S. U. (2016). Lotus Base: An integrated information portal for the model legume *Lotus japonicus*. *Scientific reports*, 6(1), 1-18.
- Munoz, A., Piedras, P., Aguilar, M., & Pineda, M. (2001). Urea is a product of ureidoglycolate degradation in chickpea. Purification and characterization of the ureidoglycolate urea-lyase. *Plant Physiology*, 125(2), 828-834.
- Naya, L., Ladrera, R., Ramos, J., González, E.M., Arrese-Igor, C., Minchin, F.R. and Becana, M. (2007). The response of carbon metabolism and antioxidant defenses of alfalfa nodules to drought stress and to the subsequent recovery of plants. *Plant Physiology*, 144(2), 1104-1114.

- Newcomb, W. (1976). A correlated light and electron microscopic study of symbiotic growth and differentiation in *Pisum sativum* root nodules. *Canadian Journal of Botany*, *54*(18), 2163-2186.
- Newcomb, W., Sippell, D., & Peterson, R. L. (1979). The early morphogenesis of *Glycine max* and *Pisum sativum* root nodules. *Canadian Journal of Botany*, *57*(23), 2603-2616.
- Nguyen, C. X., Dohnalkova, A., Hancock, C. N., Kirk, K. R., Stacey, G., & Stacey, M. G. (2021). Critical role for uricase and xanthine dehydrogenase in soybean nitrogen fixation and nodule development. *The Plant Genome*, e20171.
- Okumoto, S., Koch, W., Tegeder, M., Fischer, W. N., Biehl, A., Leister, D., ... & Frommer, W. B. (2004). Root phloem-specific expression of the plasma membrane amino acid proton co-transporter AAP3. *Journal of Experimental Botany*, *55*(406), 2155-2168.
- Okumoto, S., Schmidt, R., Tegeder, M., Fischer, W. N., Rentsch, D., Frommer, W. B., & Koch, W. (2002). High affinity amino acid transporters specifically expressed in xylem parenchyma and developing seeds of *Arabidopsis*. *Journal of Biological Chemistry*, *277*(47), 45338-45346.
- Pacios-Bras, C., Schlaman, H. R., Boot, K., Admiraal, P., Mateos Langerak, J., Stougaard, J., & Spaik, H. P. (2003). Auxin distribution in *Lotus japonicus* during root nodule development. *Plant molecular biology*, *52*, 1169-1180.
- Pan, Q., Cui, B., Deng, F., Quan, J., Loake, G. J., & Shan, W. (2016). RTP 1 encodes a novel endoplasmic reticulum (ER)-localized protein in *Arabidopsis* and negatively regulates resistance against biotrophic pathogens. *New Phytologist*, *209*(4), 1641-1654.
- Pappa, V. A., Rees, R. M., Walker, R. L., Baddeley, J. A., & Watson, C. A. (2012). Legumes intercropped with spring barley contribute to increased biomass production and carry-over effects. *The Journal of Agricultural Science*, *150*(5), 584-594.
- Pate, J. S., Atkins, C. A., White, S. T., Rainbird, R. M., & Woo, K. C. (1980). Nitrogen nutrition and xylem transport of nitrogen in ureide-producing grain legumes. *Plant Physiology*, *65*(5), 961-965.
- Pélissier, H. C., Frerich, A., Desimone, M., Schumacher, K., & Tegeder, M. (2004). PvUPS1, an allantoin transporter in nodulated roots of French bean. *Plant Physiology*, *134*(2), 664-675.

Pélissier, H.C. and Tegeder, M. (2007). PvUPS1 plays a role in source–sink transport of allantoin in French bean (*Phaseolus vulgaris*). *Functional Plant Biology*, 34(4), 282-291.

Pélissier, H.C., Frerich, A., Desimone, M., Schumacher, K. and Tegeder, M. (2004). PvUPS1, an allantoin transporter in nodulated roots of French bean. *Plant Physiology*, 134(2), 664-675.

Peng, B., Kong, H., Li, Y., Wang, L., Zhong, M., Sun, L., ... & He, Y. (2014). OsAAP6 functions as an important regulator of grain protein content and nutritional quality in rice. *Nature communications*, 5(1), 4847.

Peng, B., Kong, H., Li, Y., Wang, L., Zhong, M., Sun, L., Gao, G., Zhang, Q., Luo, L., Wang, G. and Xie, W., (2014). OsAAP6 functions as an important regulator of grain protein content and nutritional quality in rice. *Nature communications*, 5(1), 1-12.

Peoples, M. B., Brockwell, J., Herridge, D. F., Rochester, I. J., Alves, B. J. R., Urquiaga, S., ... & Jensen, E. S. (2009). The contributions of nitrogen-fixing crop legumes to the productivity of agricultural systems. *Symbiosis*, 48, 1-17.

Perchlik, M. and Tegeder, M. (2017). Improving plant nitrogen use efficiency through alteration of amino acid transport processes. *Plant physiology*, 175(1), 235-247.

Perchlik, M. and Tegeder, M. (2018). Leaf amino acid supply affects photosynthetic and plant nitrogen use efficiency under nitrogen stress. *Plant physiology*, 178(1), 174-188.

Perchlik, M., Foster, J., & Tegeder, M. (2014). Different and overlapping functions of Arabidopsis LHT6 and AAP1 transporters in root amino acid uptake. *Journal of experimental botany*, 65(18), 5193-5204.

Pierre, O., Engler, G., Hopkins, J., Brau, F., Boncompagni, E., & Herouart, D. (2013). Peribacteroid space acidification: a marker of mature bacteroid functioning in *M. edicago truncatula* nodules. *Plant, Cell & Environment*, 36(11), 2059-2070.

Price, G. D., Day, D. A., & Gresshoff, P. M. (1987). Rapid isolation of intact peribacteroid envelopes from soybean nodules and demonstration of selective permeability to metabolites. *Journal of Plant Physiology*, 130(2-3), 157-164.

Prof. David Edwards (2016): Improved kabuli reference genome. CyVerse Data Commons. Dataset. <http://doi.org/10.7946/P2G596>

- Pueppke, S. G., & Broughton, W. J. (1999). Rhizobium sp. strain NGR234 and R. fredii USDA257 share exceptionally broad, nested host ranges. *Molecular Plant-Microbe Interactions*, 12(4), 293-318.
- Purcell, L.C., Serraj, R., Sinclair, T.R. and De, A. (2004). Soybean N₂ fixation estimates, ureide concentration, and yield responses to drought. *Crop Science*, 44(2), 484-492.
- Quiles, F. A., Galvez-Valdivieso, G., Guerrero-Casado, J., Pineda, M., & Piedras, P. (2019). Relationship between ureidic/amidic metabolism and antioxidant enzymatic activities in legume seedlings. *Plant Physiology and Biochemistry*, 138, 1-8.
- Rachwa-Rosiak, D., Nebesny, E., & Budryn, G. (2015). Chickpeas—composition, nutritional value, health benefits, application to bread and snacks: a review. *Critical reviews in food science and nutrition*, 55(8), 1137-1145.
- Rainbird, R. M., Thorne, J. H., & Hardy, R. W. (1984). Role of amides, amino acids, and ureides in the nutrition of developing soybean seeds. *Plant Physiology*, 74(2), 329-334.
- Ramírez-Tejero, J. A., Jiménez-Ruiz, J., Serrano, A., Belaj, A., León, L., de la Rosa, R., ... & Luque, F. (2021). Verticillium wilt resistant and susceptible olive cultivars express a very different basal set of genes in roots. *BMC genomics*, 22(1), 1-16.
- Ramos, M. L. G., Parsons, R., & Sprent, J. I. (2005). Differences in ureide and amino acid content of water stressed soybean inoculated with Bradyrhizobium japonicum and B. elkanii. *Pesquisa Agropecuária Brasileira*, 40, 453-458.
- Ramos, M.L.G., Gordon, A.J., Minchin, F.R., Sprent, J.I. and Parsons, R. (1999). Effect of water stress on nodule physiology and biochemistry of a drought tolerant cultivar of common bean (*Phaseolus vulgaris* L.). *Annals of Botany*, 83(1), 57-63.
- Ranocha, P., Denancé, N., Vanholme, R., Freydier, A., Martinez, Y., Hoffmann, L., ... & Goffner, D. (2010). Walls are thin 1 (WAT1), an Arabidopsis homolog of Medicago truncatula NODULIN21, is a tonoplast-localized protein required for secondary wall formation in fibers. *The Plant Journal*, 63(3), 469-483.
- Ranocha, P., Dima, O., Nagy, R., Felten, J., Corratgé-Faillie, C., Novák, O., ... & Goffner, D. (2013). Arabidopsis WAT1 is a vacuolar auxin transport facilitator required for auxin homeostasis. *Nature communications*, 4(1), 2625.

- Rao, D. L. N., Giller, K. E., Yeo, A. R., & Flowers, T. J. (2002). The effects of salinity and sodicity upon nodulation and nitrogen fixation in chickpea (*Cicer arietinum*). *Annals of botany*, *89*(5), 563-570.
- Redillas, M.C.F.R., Bang, S.W., Lee, D.K., Kim, Y.S., Jung, H., Chung, P.J., Suh, J.W. and Kim, J.K. (2019). Allantoin accumulation through overexpression of ureide permease1 improves rice growth under limited nitrogen conditions. *Plant biotechnology journal*, *17*(7), 1289-1301.
- Redondo, F. J., de la Pena, T. C., Morcillo, C. N., Lucas, M. M., & Pueyo, J. J. (2009). Overexpression of flavodoxin in bacteroids induces changes in antioxidant metabolism leading to delayed senescence and starch accumulation in alfalfa root nodules. *Plant Physiology*, *149*(2), 1166-1178.
- Rentsch, D., Schmidt, S. and Tegeder, M. (2007). Transporters for uptake and allocation of organic nitrogen compounds in plants. *FEBS letters*, *581*(12), 2281-2289.
- Ricoult, C., Echeverria, L. O., Cliquet, J. B., & Limami, A. M. (2006). Characterization of alanine aminotransferase (AlaAT) multigene family and hypoxic response in young seedlings of the model legume *Medicago truncatula*. *Journal of experimental botany*, *57*(12), 3079-3089.
- Robinson, D. L., Kahn, M. L., & Vance, C. P. (1994). Cellular localization of nodule-enhanced aspartate aminotransferase in *Medicago sativa* L. *Planta*, *192*, 202-210.
- Robinson, D. L., Pathiran, S. M., Gantt, J. S., & Vance, C. P. (1996). Immunogold localization of nodule-enhanced phosphoenolpyruvate carboxylase in alfalfa. *Plant, Cell & Environment*, *19*(5), 602-608.
- Robinson, M. D., McCarthy, D. J., & Smyth, G. K. (2010). edgeR: a Bioconductor package for differential expression analysis of digital gene expression data. *bioinformatics*, *26*(1), 139-140.
- Rocha, M., Sodek, L., Licausi, F., Hameed, M. W., Dornelas, M. C., & Van Dongen, J. T. (2010). Analysis of alanine aminotransferase in various organs of soybean (*Glycine max*) and in dependence of different nitrogen fertilisers during hypoxic stress. *Amino Acids*, *39*, 1043-1053.
- Rolfe, B. G., & Gresshoff, P. M. (1988). Genetic analysis of legume nodule initiation. *Annual Review of Plant Physiology and Plant Molecular Biology*, *39*(1), 297-319.
- Roux, B., Rodde, N., Jardinaud, M. F., Timmers, T., Sauviac, L., Cottret, L., ... & Gamas, P. (2014). An integrated analysis of plant and bacterial gene expression in symbiotic root nodules using laser-capture microdissection coupled to RNA sequencing. *The Plant Journal*, *77*(6), 817-837.

- Ruffel, S., Freixes, S., Balzergue, S., Tillard, P., Jeudy, C., Martin-Magniette, M.L., Van Der Merwe, M.J., Kakar, K., Gouzy, J., Fernie, A.R. and Udvardi, M. (2008). Systemic signaling of the plant nitrogen status triggers specific transcriptome responses depending on the nitrogen source in *Medicago truncatula*. *Plant physiology*, 146(4), 2020-2035.
- Russnak, R., Konczal, D., & McIntire, S. L. (2001). A family of yeast proteins mediating bidirectional vacuolar amino acid transport. *Journal of Biological Chemistry*, 276(26), 23849-23857.
- Ryan, E., & Fottrell, P. F. (1974). Subcellular localization of enzymes involved in the assimilation of ammonia by soybean root nodules. *Phytochemistry*, 13(12), 2647-2652.
- Saier Jr, M. H., Reddy, V. S., Tsu, B. V., Ahmed, M. S., Li, C., & Moreno-Hagelsieb, G. (2016). The transporter classification database (TCDB): recent advances. *Nucleic acids research*, 44(D1), D372-D379.
- Sakagishi, Y. (1995). Alanine aminotransferase (ALT). *Nihon rinsho. Japanese journal of clinical medicine*, 53(5), 1146-1150.
- Sánchez-Vioque, R., Clemente, A., Vioque, J., Bautista, J., & Millán, F. J. F. C. (1999). Protein isolates from chickpea (*Cicer arietinum* L.): chemical composition, functional properties and protein characterization. *Food Chemistry*, 64(2), 237-243.
- Sanders, A., Collier, R., Trethewy, A., Gould, G., Sieker, R. and Tegeder, M. (2009). AAP1 regulates import of amino acids into developing Arabidopsis embryos. *The Plant Journal*, 59(4), 540-552.
- Santiago, J. P., & Tegeder, M. (2016). Connecting source with sink: the role of Arabidopsis AAP8 in phloem loading of amino acids. *Plant Physiology*, 171(1), 508-521.
- Sarmah, B. K., Moore, A., Tate, W., Molvig, L., Morton, R. L., Rees, D. P., ... & Higgins, T. J. V. (2004). Transgenic chickpea seeds expressing high levels of a bean α -amylase inhibitor. *Molecular Breeding*, 14, 73-82.
- Sarmah, B.K., Moore, A., Tate, W., Molvig, L., Morton, R.L., Rees, D.P., Chiaiese, P., Chrispeels, M.J., Tabe, L.M. and Higgins, T.J.V. (2004). Transgenic chickpea seeds expressing high levels of a bean α -amylase inhibitor. *Molecular Breeding*, 14(1), 73-82.
- Sautin, Y. Y., & Johnson, R. J. (2008). Uric acid: the oxidant-antioxidant paradox. *Nucleosides, Nucleotides, and Nucleic Acids*, 27(6-7), 608-619.

- Schenck, C. A., Chen, S., Siehl, D. L., & Maeda, H. A. (2015). Non-plastidic, tyrosine-insensitive prephenate dehydrogenases from legumes. *Nature Chemical Biology*, *11*(1), 52-57.
- Schenck, C. A., Westphal, J., Jayaraman, D., Garcia, K., Wen, J., Mysore, K. S., ... & Maeda, H. A. (2020). Role of cytosolic, tyrosine-insensitive prephenate dehydrogenase in *Medicago truncatula*. *Plant Direct*, *4*(5), e00218.
- Schnorr, K.M., Laloue, M. and Hirel, B. (1996). Isolation of cDNAs encoding two purine biosynthetic enzymes of soybean and expression of the corresponding transcripts in roots and root nodules. *Plant molecular biology*, *32*(4), 751-757.
- Schubert, M., Koteyeva, N. K., Wabnitz, P. W., Santos, P., Büttner, M., Sauer, N., ... & Pawlowski, K. (2011). Plasmodesmata distribution and sugar partitioning in nitrogen-fixing root nodules of *Datisca glomerata*. *Planta*, *233*, 139-152.
- Schwacke, R., Ponce-Soto, G. Y., Krause, K., Bolger, A. M., Arsova, B., Hallab, A., ... & Usadel, B. (2019). MapMan4: a refined protein classification and annotation framework applicable to multi-omics data analysis. *Molecular plant*, *12*(6), 879-892.
- Schwember, A. R., Schulze, J., Del Pozo, A., & Cabeza, R. A. (2019). Regulation of symbiotic nitrogen fixation in legume root nodules. *Plants*, *8*(9), 333.
- Schwenke, G. D., Herridge, D. F., Scheer, C., Rowlings, D. W., Haigh, B. M., & McMullen, K. G. (2015). Soil N₂O emissions under N₂-fixing legumes and N-fertilised canola: a reappraisal of emissions factor calculations. *Agriculture, Ecosystems & Environment*, *202*, 232-242.
- Sekito, T., Chardwiriyaapreecha, S., Sugimoto, N., Ishimoto, M., Kawano-Kawada, M., & Kakinuma, Y. (2014). Vacuolar transporter Avt4 is involved in excretion of basic amino acids from the vacuoles of *Saccharomyces cerevisiae*. *Bioscience, Biotechnology, and Biochemistry*, *78*(6), 969-975.
- Sekito, T., Fujiki, Y., Ohsumi, Y., & Kakinuma, Y. (2008). Novel families of vacuolar amino acid transporters. *IUBMB life*, *60*(8), 519-525.
- Serventi, F., Ramazzina, I., Lamberto, I., Puggioni, V., Gatti, R., & Percudani, R. (2010). Chemical basis of nitrogen recovery through the ureide pathway: formation and hydrolysis of S-ureidoglycine in plants and bacteria. *ACS Chemical Biology*, *5*(2), 203-214.

- Silvente, S., Camas, A., & Lara, M. (2003). Molecular cloning of the cDNA encoding aspartate aminotransferase from bean root nodules and determination of its role in nodule nitrogen metabolism. *Journal of experimental botany*, *54*(387), 1545-1551.
- Silvente, S., Sobolev, A.P. and Lara, M. (2012). Metabolite adjustments in drought tolerant and sensitive soybean genotypes in response to water stress. *PLoS One*, *7*(6), e38554.
- Singh, S., Singh, I., Kapoor, K., Gaur, P. M., Chaturvedi, S. K., Singh, N. P., & Sandhu, J. S. (2014). Chickpea. *Broadening the genetic base of grain legumes*, 51-73.
- Smith, P. M., & Atkins, C. A. (2002). Purine biosynthesis. Big in cell division, even bigger in nitrogen assimilation. *Plant Physiology*, *128*(3), 793-802.
- Snowden, C. J., Thomas, B., Baxter, C. J., Smith, J. A. C., & Sweetlove, L. J. (2015). A tonoplast Glu/Asp/GABA exchanger that affects tomato fruit amino acid composition. *The Plant Journal*, *81*(5), 651-660.
- Soussana, J.F. and Tallec, T. (2010). Can we understand and predict the regulation of biological N₂ fixation in grassland ecosystems?. *Nutrient Cycling in Agroecosystems*, *88*(2), 197-213.
- Sprent, J. I., & James, E. K. (2007). Legume evolution: where do nodules and mycorrhizas fit in?. *Plant physiology*, *144*(2), 575-581.
- Stagnari, F., Maggio, A., Galieni, A., & Pisante, M. (2017). Multiple benefits of legumes for agriculture sustainability: an overview. *Chemical and Biological Technologies in Agriculture*, *4*, 1-13.
- Stein, L. Y., & Klotz, M. G. (2016). The nitrogen cycle. *Current Biology*, *26*(3), R94-R98.
- Stein, O., & Granot, D. (2019). An overview of sucrose synthases in plants. *Frontiers in plant science*, *10*, 95.
- Su, Y. H., Frommer, W. B., & Ludewig, U. (2004). Molecular and functional characterization of a family of amino acid transporters from Arabidopsis. *Plant physiology*, *136*(2), 3104-3113.
- Sugiyama, A., Saida, Y., Yoshimizu, M., Takanashi, K., Sosso, D., Frommer, W. B., & Yazaki, K. (2017). Molecular characterization of LjSWEET3, a sugar transporter in nodules of Lotus japonicus. *Plant and Cell Physiology*, *58*(2), 298-306.

- Sujkowska, M., Górská-Czekaj, M., Bederska, M., & Borucki, W. (2011). Vacuolar organization in the nodule parenchyma is important for the functioning of pea root nodules. *Symbiosis*, *54*, 1-16.
- Sulieman S, Fischinger S, Schulze J. (2008). N-feedback regulation of N₂ fixation in *Medicago truncatula* under P-deficiency. *Gen Appl Plant Physiol* *34*: 33–54
- Sulieman, S. (2011). Does GABA increase the efficiency of symbiotic N₂ fixation in legumes?. *Plant signaling & behavior*, *6*(1), 32-36.
- Sulieman, S. and Schulze, J. (2010). The efficiency of nitrogen fixation of the model legume *Medicago truncatula* (Jemalong A17) is low compared to *Medicago sativa*. *Journal of Plant Physiology*, *167*(9), 683-692.
- Sulieman, S. and Tran, L.S.P. (2013). Asparagine: an amide of particular distinction in the regulation of symbiotic nitrogen fixation of legumes. *Critical Reviews in Biotechnology*, *33*(3), 309-327.
- Sulieman, S., & Schulze, J. (2010). Phloem-derived γ -aminobutyric acid (GABA) is involved in upregulating nodule N₂ fixation efficiency in the model legume *Medicago truncatula*. *Plant, Cell & Environment*, *33*(12), 2162-2172.
- Sulieman, S., & Tran, L. S. P. (2013). Asparagine: an amide of particular distinction in the regulation of symbiotic nitrogen fixation of legumes. *Critical Reviews in Biotechnology*, *33*(3), 309-327.
- Sulieman, S., Fischinger, S. A., Gresshoff, P. M., & Schulze, J. (2010). Asparagine as a major factor in the N-feedback regulation of N₂ fixation in *Medicago truncatula*. *Physiologia Plantarum*, *140*(1), 21-31.
- Sulieman, S., Sheteiwy, M. S., Abdelrahman, M., & Tran, L. S. P. (2024). γ -Aminobutyric acid (GABA) in N₂-fixing-legume symbiosis: Metabolic flux and carbon/nitrogen homeostasis in responses to abiotic constraints. *Plant Physiology and Biochemistry*, 108362.
- Svennerstam, H., Jämtgård, S., Ahmad, I., Huss-Danell, K., Näsholm, T., & Ganeteg, U. (2011). Transporters in *Arabidopsis* roots mediating uptake of amino acids at naturally occurring concentrations. *New Phytologist*, *191*(2), 459-467.

Swarup, R., Kargul, J., Marchant, A., Zadik, D., Rahman, A., Mills, R., ... & Bennett, M. J. (2004). Structure-function analysis of the presumptive Arabidopsis auxin permease AUX1. *The Plant Cell*, *16*(11), 3069-3083.

Tajima, S., Nomura, M., & Kouchi, H. (2004). Ureide biosynthesis in legume nodules. *Frontiers in Bioscience*, *9*(1-3), 1374.

Takagi, H., Ishiga, Y., Watanabe, S., Konishi, T., Egusa, M., Akiyoshi, N., Matsuura, T., Mori, I.C., Hirayama, T., Kaminaka, H. and Shimada, H. (2016). Allantoin, a stress-related purine metabolite, can activate jasmonate signaling in a MYC2-regulated and abscisic acid-dependent manner. *Journal of experimental botany*, *67*(8), 2519-2532.

Takagi, H., Watanabe, S., Tanaka, S., Matsuura, T., Mori, I.C., Hirayama, T., Shimada, H. and Sakamoto, A. (2018). Disruption of ureide degradation affects plant growth and development during and after transition from vegetative to reproductive stages. *BMC plant biology*, *18*(1), 1-16.

Takanashi, K., Sasaki, T., Kan, T., Saida, Y., Sugiyama, A., Yamamoto, Y., & Yazaki, K. (2016). A dicarboxylate transporter, LjALMT4, mainly expressed in nodules of *Lotus japonicus*. *Molecular Plant-Microbe Interactions*, *29*(7), 584-592.

Takanashi, K., Takahashi, H., Sakurai, N., Sugiyama, A., Suzuki, H., Shibata, D., ... & Yazaki, K. (2012). Tissue-specific transcriptome analysis in nodules of *Lotus japonicus*. *Molecular plant-microbe interactions*, *25*(7), 869-876.

Tan, Q., Grennan, A.K., Pélissier, H.C., Rentsch, D. and Tegeder, M. (2008). Characterization and expression of French bean amino acid transporter PvAAP1. *Plant science*, *174*(3), 348-356.

Tang, Y., Zhang, Z., Lei, Y., Hu, G., Liu, J., Hao, M., ... & Wu, J. (2019). Cotton WATs modulate SA biosynthesis and local lignin deposition participating in plant resistance against *Verticillium dahliae*. *Frontiers in Plant Science*, *10*, 526.

Tegeder, M. (2014). Transporters involved in source to sink partitioning of amino acids and ureides: opportunities for crop improvement. *Journal of Experimental Botany*, *65*(7), 1865-1878.

Tegeder, M., & Hammes, U. Z. (2018). The way out and in: phloem loading and unloading of amino acids. *Current Opinion in Plant Biology*, *43*, 16-21.

- Tegeder, M., & Masclaux-Daubresse, C. (2018). Source and sink mechanisms of nitrogen transport and use. *New phytologist*, 217(1), 35-53.
- Temple, S. J., Vance, C. P., & Gantt, J. S. (1998). Glutamate synthase and nitrogen assimilation. *Trends in plant science*, 3(2), 51-56.
- The, S. V., Snyder, R., & Tegeder, M. (2021). Targeting nitrogen metabolism and transport processes to improve plant nitrogen use efficiency. *Frontiers in Plant Science*, 11, 628366.
- Thu, S.W., Lu, M.Z., Carter, A.M., Collier, R., Gandin, A., Sitton, C.C. and Tegeder, M. (2020). Role of ureides in source-to-sink transport of photoassimilates in non-fixing soybean. *Journal of Experimental Botany*.
- Todd, C. D., Tipton, P. A., Blevins, D. G., Piedras, P., Pineda, M., & Polacco, J. C. (2006). Update on ureide degradation in legumes. *Journal of Experimental Botany*, 57(1), 5-12.
- Tone, J., Yamanaka, A., Manabe, K., Murao, N., Kawano-Kawada, M., Sekito, T., & Kakinuma, Y. (2015). A vacuolar membrane protein Avt7p is involved in transport of amino acid and spore formation in *Saccharomyces cerevisiae*. *Bioscience, biotechnology, and biochemistry*, 79(2), 190-195.
- Tone, J., Yoshimura, A., Manabe, K., Murao, N., Sekito, T., Kawano-Kawada, M., & Kakinuma, Y. (2015). Characterization of Avt1p as a vacuolar proton/amino acid antiporter in *Saccharomyces cerevisiae*. *Bioscience, biotechnology, and biochemistry*, 79(5), 782-789.
- Touraine, B. (2004). Nitrate uptake by roots-transporters and root development. In *Nitrogen Acquisition and Assimilation in Higher Plants*. 1-34. Springer, Dordrecht.
- Trepp, G. B., Plank, D. W., Stephen Gantt, J., & Vance, C. P. (1999). NADH-glutamate synthase in alfalfa root nodules. Immunocytochemical localization. *Plant physiology*, 119(3), 829-838.
- Tsuchimatsu, T., Kakui, H., Yamazaki, M., Marona, C., Tsutsui, H., Hedhly, A., ... & Shimizu, K. K. (2020). Adaptive reduction of male gamete number in the selfing plant *Arabidopsis thaliana*. *Nature Communications*, 11(1), 2885.
- Udvardi, M. K., & Day, D. A. (1997). Metabolite transport across symbiotic membranes of legume nodules. *Annual review of plant biology*, 48(1), 493-523.

- Udvardi, M. K., Price, G. D., Gresshoff, P. M., & Day, D. A. (1988). A dicarboxylate transporter on the peribacteroid membrane of soybean nodules. *FEBS letters*, *231*(1), 36-40.
- Udvardi, M. K., Salom, C. L., & Day, D. A. (1988). Transport of L-glutamate across the bacteroid membrane but not the peribacteroid membrane from soybean root nodules. *Molecular plant-microbe interactions*, *1*(6), 250-254.
- Udvardi, M., & Poole, P. S. (2013). Transport and metabolism in legume-rhizobia symbioses. *Annual review of plant biology*, *64*, 781-805.
- Urwat, U., Zargar, S. M., Ahmad, S. M., & Ganai, N. A. (2021). Insights into role of STP13 in sugar driven signaling that leads to decrease in photosynthesis in dicot legume crop model (*Phaseolus vulgaris* L.) under Fe and Zn stress. *Molecular Biology Reports*, *48*, 2527-2531.
- Vadez, V., Sinclair, T.R., Serraj, R. and Purcell, L.C. (2000). Manganese application alleviates the water deficit-induced decline of N₂ fixation. *Plant, Cell & Environment*, *23*(5), 497-505.
- Valentine, A.J., Benedito, V.A. and Kang, Y. (2018). Legume nitrogen fixation and soil abiotic stress: from physiology to genomics and beyond. *Annual Plant Reviews online*, 207-248.
- Vance, C. P. (2000). Amide biosynthesis in root nodules of temperate legumes. *Prokaryotic nitrogen fixation: a model system for the analysis of a biological process.*, 589-607.
- Vance, C. P. (2008). Carbon and nitrogen metabolism in legume nodules. *Nitrogen-fixing leguminous symbioses*, 293-320.
- Vance, C. P., & Gantt, J. S. (1992). Control of nitrogen and carbon metabolism in root nodules. *Physiologia Plantarum*, *85*(2), 266-274.
- Varshney, R. K., Song, C., Saxena, R. K., Azam, S., Yu, S., Sharpe, A. G., ... & Cook, D. R. (2013). Draft genome sequence of chickpea (*Cicer arietinum*) provides a resource for trait improvement. *Nature biotechnology*, *31*(3), 240-246.
- Vessey, J. K. (2003). Plant growth promoting rhizobacteria as biofertilizers. *Plant and soil*, *255*, 571-586.
- Vessey, J. K., Pawlowski, K., & Bergman, B. (2005). Root-based N₂-fixing symbioses: legumes, actinorhizal plants, *Parasponia* sp. and cycads. *Plant and soil*, *274*, 51-78.

- Voß, L., Heinemann, K. J., Herde, M., Medina-Escobar, N., & Witte, C. P. (2022). Enzymes and cellular interplay required for flux of fixed nitrogen to ureides in bean nodules. *Nature Communications*, *13*(1), 5331.
- Waese, J., Fan, J., Pasha, A., Yu, H., Fucile, G., Shi, R., ... & Provard, N. J. (2017). ePlant: visualizing and exploring multiple levels of data for hypothesis generation in plant biology. *The Plant Cell*, *29*(8), 1806-1821.
- Wang, J., Wu, B., Lu, K., Wei, Q., Qian, J., Chen, Y., & Fang, Z. (2019). The amino acid permease 5 (OsAAP5) regulates tiller number and grain yield in rice. *Plant Physiology*, *180*(2), 1031-1045.
- Wang, L., Lu, Q., Wen, X. and Lu, C. (2015). Enhanced sucrose loading improves rice yield by increasing grain size. *Plant Physiology*, *169*(4), 2848-2862.
- Wang, M., & Maeda, H. A. (2018). Aromatic amino acid aminotransferases in plants. *Phytochemistry Reviews*, *17*, 131-159.
- Watanabe, S., Matsumoto, M., Hakomori, Y., Takagi, H., Shimada, H. and Sakamoto, A. (2014). The purine metabolite allantoin enhances abiotic stress tolerance through synergistic activation of abscisic acid metabolism. *Plant, cell & environment*, *37*(4), 1022-1036.
- Weigelt, K., Küster, H., Radchuk, R., Müller, M., Weichert, H., Fait, A., Fernie, A.R., Saalbach, I. and Weber, H. (2008). Increasing amino acid supply in pea embryos reveals specific interactions of N and C metabolism, and highlights the importance of mitochondrial metabolism. *The Plant Journal*, *55*(6), 909-926.
- Werner, A. K., & Witte, C. P. (2011). The biochemistry of nitrogen mobilization: purine ring catabolism. *Trends in plant science*, *16*(7), 381-387.
- Werner, A. K., Medina-Escobar, N., Zulawski, M., Sparkes, I. A., Cao, F. Q., & Witte, C. P. (2013). The ureide-degrading reactions of purine ring catabolism employ three amidohydrolases and one aminohydrolase in Arabidopsis, soybean, and rice. *Plant Physiology*, *163*(2), 672-681.
- Werner, A. K., Romeis, T., & Witte, C. P. (2010). Ureide catabolism in Arabidopsis thaliana and Escherichia coli. *Nature chemical biology*, *6*(1), 19-21.

Werner, A. K., Sparkes, I. A., Romeis, T., & Witte, C. P. (2008). Identification, biochemical characterization, and subcellular localization of allantoate amidohydrolases from Arabidopsis and soybean. *Plant Physiology*, *146*(2), 418.

Werner, A.K. and Witte, C.P. (2011). The biochemistry of nitrogen mobilization: purine ring catabolism. *Trends in plant science*, *16*(7), 381-387.

Werner, G.D., Cornwell, W.K., Sprent, J.I., Kattge, J. and Kiers, E.T. (2014). A single evolutionary innovation drives the deep evolution of symbiotic N₂-fixation in angiosperms. *Nature communications*, *5*(1), 1-9.

Witty, J.F., Minchin, F.R., Skøt, L. and Sheehy, J.E. (1986). Nitrogen fixation and oxygen in legume root nodules. *Oxford surveys of plant molecular and cell biology*, *3*, 275-314.

Wojtyła, Ł., Lechowska, K., Kubala, S. and Garnczarska, M. (2016). Different modes of hydrogen peroxide action during seed germination. *Frontiers in plant science*, *7*, 66.

Wong, D. C. (2020). Network aggregation improves gene function prediction of grapevine gene co-expression networks. *Plant molecular biology*, *103*, 425-441.

Xu, J. J., Fang, X., Li, C. Y., Yang, L., & Chen, X. Y. (2020). General and specialized tyrosine metabolism pathways in plants. *Abiotech*, *1*, 97-105.

Yang, H., Bogner, M., Stierhof, Y. D., & Ludewig, U. (2010). H⁺-independent glutamine transport in plant root tips. *PLoS One*, *5*(1), e8917.

Yang, H., Krebs, M., Stierhof, Y. D., & Ludewig, U. (2014). Characterization of the putative amino acid transporter genes AtCAT2, 3 & 4: the tonoplast localized AtCAT2 regulates soluble leaf amino acids. *Journal of plant physiology*, *171*(8), 594-601.

Yang, H., Stierhof, Y. D., & Ludewig, U. (2015). The putative Cationic Amino Acid Transporter 9 is targeted to vesicles and may be involved in plant amino acid homeostasis. *Frontiers in plant science*, *6*, 212.

Yang, L., Machin, F., Wang, S., Saploura, E., & Kragler, F. (2023). Heritable transgene-free genome editing in plants by grafting of wild-type shoots to transgenic donor rootstocks. *Nature Biotechnology*, *41*(7), 958-967.

- Yang, X., Wang, X., Wei, M., Hikosaka, S., & Goto, E. (2011). Changes of glutamine and asparagine content in cucumber seedlings in response to nitrate stress.
- Yao, X., Nie, J., Bai, R., & Sui, X. (2020). Amino acid transporters in plants: Identification and function. *Plants*, *9*(8), 972.
- Yarnes, S. C., & Sengupta-Gopalan, C. (2009). Sucrose synthase levels do not limit or regulate carbon transfer in the arbuscular mycorrhizal symbiosis. *Journal of Plant Interactions*, *4*(2), 113-117.
- Ye, Q., Zhu, F., Sun, F., Wang, T. C., Wu, J., Liu, P., ... & Wang, T. (2022). Differentiation trajectories and biofunctions of symbiotic and un-symbiotic fate cells in root nodules of *Medicago truncatula*. *Molecular Plant*, *15*(12), 1852-1867.
- Ye, Q., Zhu, F., Sun, F., Wang, T. C., Wu, J., Liu, P., ... & Wang, T. (2022). Differentiation trajectories and biofunctions of symbiotic and un-symbiotic fate cells in root nodules of *Medicago truncatula*. *Molecular Plant*, *15*(12), 1852-1867.
- Yesbergenova, Z., Yang, G., Oron, E., Soffer, D., Fluhr, R. and Sagi, M. (2005). The plant Mo-hydroxylases aldehyde oxidase and xanthine dehydrogenase have distinct reactive oxygen species signatures and are induced by drought and abscisic acid. *The Plant Journal*, *42*(6), 862-876.
- Yim, A. K. Y., Wong, J. W. H., Ku, Y. S., Qin, H., Chan, T. F., & Lam, H. M. (2015). Using RNA-Seq data to evaluate reference genes suitable for gene expression studies in soybean. *PLoS one*, *10*(9), e0136343.
- Yoshioka, H., Gregerson, R. G., Samac, D. A., Hoevens, K. C., Trepp, G., Gantt, J. S., & Vance, C. P. (1999). Aspartate aminotransferase in alfalfa nodules: localization of mRNA during effective and ineffective nodule development and promoter analysis. *Molecular plant-microbe interactions*, *12*(4), 263-274.
- Yu, Y., Xue, L., & Yang, L. (2014). Winter legumes in rice crop rotations reduces nitrogen loss, and improves rice yield and soil nitrogen supply. *Agronomy for sustainable development*, *34*, 633-640.
- Zammit, A., & Copeland, L. (1993). Immunocytochemical localisation of nodule-specific sucrose synthase in soybean nodules. *Functional Plant Biology*, *20*(1), 25-32.
- Zhang, L., Garneau, M. G., Majumdar, R., Grant, J., & Tegeder, M. (2015). Improvement of pea biomass and seed productivity by simultaneous increase of phloem and embryo loading with amino acids. *The Plant Journal*, *81*(1), 134-146.

Zhang, L., Tan, Q., Lee, R., Trethewy, A., Lee, Y. H., & Tegeder, M. (2010). Altered xylem-phloem transfer of amino acids affects metabolism and leads to increased seed yield and oil content in Arabidopsis. *The Plant Cell*, 22(11), 3603-3620.

Zhang, Q., Lee, J., Pandurangan, S., Clarke, M., Pajak, A., & Marsolais, F. (2013). Characterization of Arabidopsis serine: glyoxylate aminotransferase, AGT1, as an asparagine aminotransferase. *Phytochemistry*, 85, 30-35.

Zhang, X., Henriques, R., Lin, S. S., Niu, Q. W., & Chua, N. H. (2006). Agrobacterium-mediated transformation of Arabidopsis thaliana using the floral dip method. *Nature protocols*, 1(2), 641-646.

Zhao, C., Pratelli, R., Yu, S., Shelley, B., Collakova, E., & Pilot, G. (2021). Detailed characterization of the UMAMIT proteins provides insight into their evolution, amino acid transport properties, and role in the plant. *Journal of Experimental Botany*, 72(18), 6400-6417.

Zhao, J., Chen, J., Beillouin, D., Lambers, H., Yang, Y., Smith, P., ... & Zang, H. (2022). Global systematic review with meta-analysis reveals yield advantage of legume-based rotations and its drivers. *Nature Communications*, 13(1), 4926.

Zhou, T., Yue, C. P., Huang, J. Y., Cui, J. Q., Liu, Y., Wang, W. M., ... & Hua, Y. P. (2020). Genome-wide identification of the amino acid permease genes and molecular characterization of their transcriptional responses to various nutrient stresses in allotetraploid rapeseed. *BMC plant biology*, 20(1), 1-22.

Appendix 3A:

Appendix 3A.1: Acetylene reduction assay and nodule dry weight

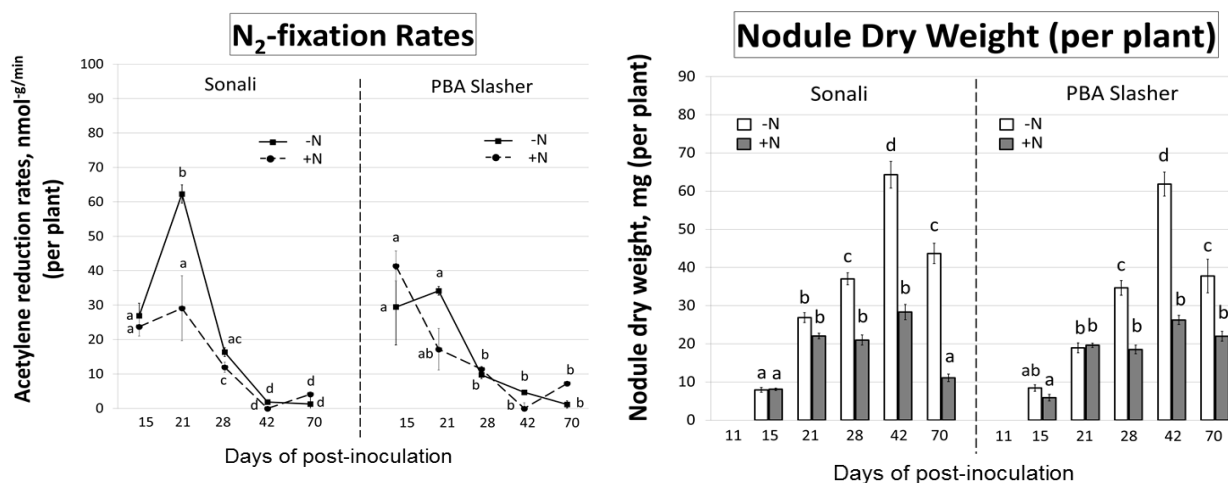


Figure 3a.1 Acetylene reduction assay depicts plummeting nitrogen fixation rates post 20 DAI despite increasing nodule dry weight. Evgenia Ovchinnikova & Ella Brear, 2017 (Unpublished Data).

Cicer arietinum L. 'PBA Sonali' and 'PBA Slasher' was used in all experiments. Surface sterilization of chickpea seeds was done with 3% (v/v) sodium hypochlorite for 1 min three times, followed by 70% ethanol for 30 s and rinsed with sterile water five times. After inoculation with *Mesorhizobium cicer* CC1192) at planting and 10 days later, seed germination was carried out in trays embedded with wet tissue paper for 72 h and kept moist with water misting. After 3d, young seedlings with similar radical lengths and germination stage were sown individually in a pot filled with a built potting soil consisting of Narellan river sand and Cocopeat mixed at a 60:40 ratio, respectively. The plants were supplied with two different nutrient solutions: **Solution 1:** 2.5 mM NH₄NO₃, 0.5 mM MgSO₄, 0.5 mM KH₂PO₄, 25 μM H₃BO₃, 2 μM MnSO₄·H₂O, 2 μM ZnSO₄·7H₂O, 5 μM CuSO₄·5H₂O, 5 μM Na₂MoO₄·2H₂O, 5 mM KCl, 0.1 mM Fe-EDTA, 0.1 mM Fe-EDDHA and **Solution 2:** -N solution using a similar recipe without added N were used. Experiment conducted funded by the Legumes for sustainable agriculture, supervised by Brent Kaiser, Penny Smith, Andrew Merchant and Murray Unkovich. Data collection and analysis performed by Evgenia Ovchinnikova and Ella Brear. Written approval from Brent Kaiser and Penny Smith to include this data here.

Appendix 3A.2: *GmPur1* expression in leaf and root tissue

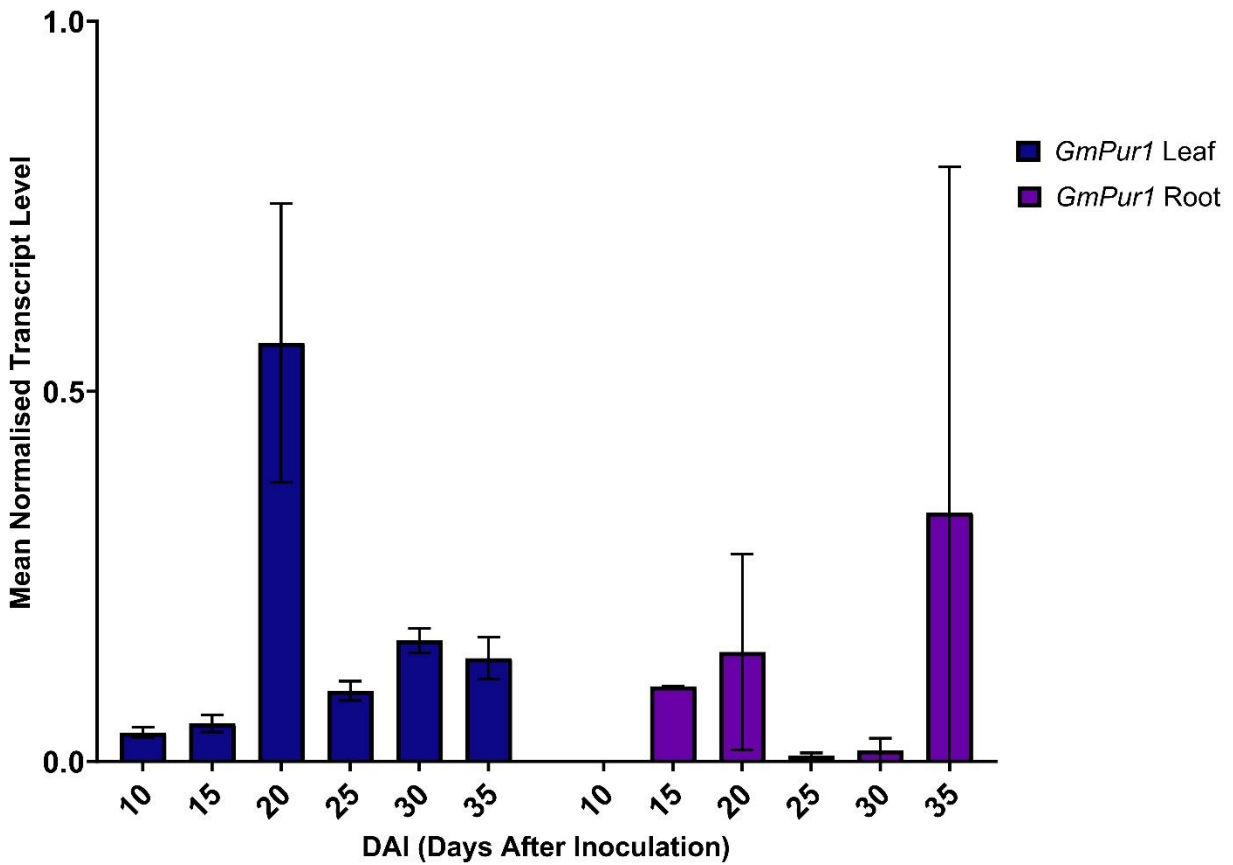


Figure 3a.2: *GmPur1* exhibited insignificant expression in both leaf and root tissues from 10 to 35 DAI, suggesting nodule localised function.

Transcript levels measured in nodule cDNA from 20 to 35 DAI in 5-day intervals and normalised against *GmELF1B* & *GmACT11* (N = 3). Plants grown in sand supplemented with 0.5 mM KNO₃. Statistical significance calculated for transcript level of *GmPur1* between harvest intervals via Two-Way ANOVA with multiple comparisons test (Tukey) (*<0.05, **<0.005, ***<0.0005).

Appendix 3A.3: *CaUPS1* & *CaPur1* expression in chickpea grown with high and low N supplementation

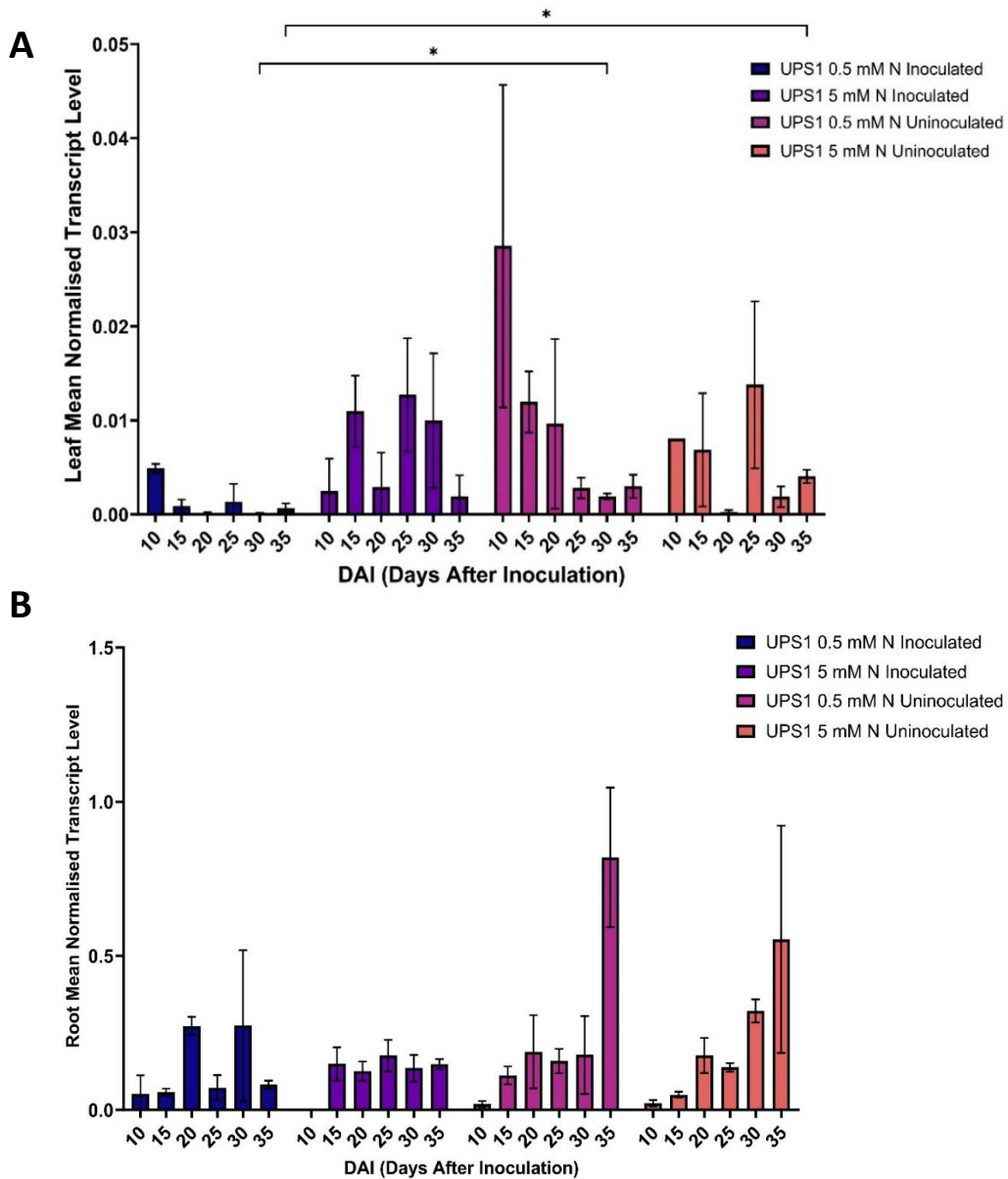


Figure 3a.3: *CaUPS1* exhibited significantly inconsistent expression in root and insignificant expression in leaf tissue.

Transcript levels measured in leaf and root cDNA from 10 to 35 DAI in 5-day intervals and normalised against *CaEif* & *CaHSP90*, (N = 3). Statistical significance calculated for transcript level of *CaUPS1* between harvest intervals via Two-Way ANOVA with multiple comparisons test (Tukey) (*<0.05, **<0.005, ***<0.0005). Plants grown in sand supplemented with either 0.5 mM or 5 mM KNO₃, with rhizobia applied or withheld.

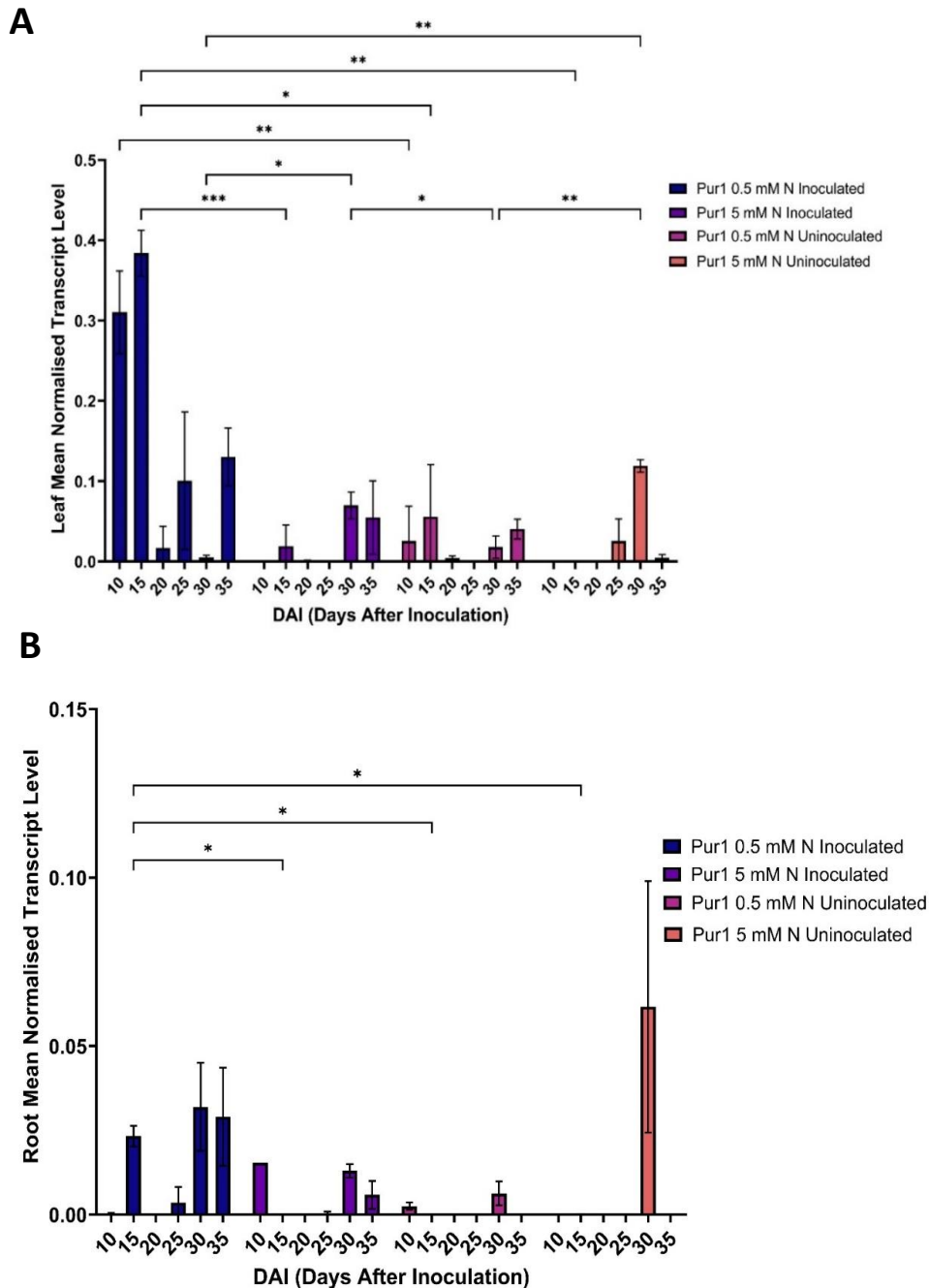


Figure 3a.4: *CaPur1* exhibited negligible expression in chickpea leaf and root tissue.

Transcript levels measured in leaf and root cDNA from 10 to 35 DAI in 5-day intervals and normalised against *CaEiF* & *CaHSP90*, (N = 3). Statistical significance calculated for transcript level of *CaPur1* between harvest intervals via Two-Way ANOVA with multiple comparisons test (Tukey) (*<0.05, **<0.005, ***<0.0005). Plants grown in sand supplemented with either 0.5 mM or 5 mM KNO_3 , with rhizobia applied or withheld.

Appendix 3A.4: Total ureide summary data in chickpea leaf, root and nodule tissues

Table 3a.1: Mean total ureides (nmols/mg Dry Weight) in leaf, root and nodule tissue over 10 to 35 DAI for chickpea and soybean.

Mean Total Ureides (nmols/mg Dry Weight)						
DAI (Days After Inoculation)	Soybean Leaf	Soybean Root	Soybean Nodule	Chickpea Leaf	Chickpea Root	Chickpea Nodule
10	154.80	164.65	0.00	21.76	3.71	0.00
15	86.10	96.86	0.00	22.12	7.29	0.00
20	61.24	26.07	56.92	15.29	13.90	20.09
25	67.36	22.77	72.90	12.67	1.35	32.24
30	66.02	39.66	136.07	7.77	0.00	26.71
35	45.67	58.31	144.19	14.97	3.14	13.21

Table 3a.2: Mean total ureides (nmols/mg Dry Weight) in leaf, root and nodule tissue from plants inoculated (Green) or uninoculated (Orange), treated with either high N (KNO₃) or low N (KNO₃).

Mean Total Ureides (nmols/mg Dry Weight)									
DAI (Days After Inoculation)	Low N Leaf	Low N Root	High N Leaf	High N Root	High N Leaf	High N Root	Low N Leaf	Low N Root	Low N Nodule
10	11.71	7.43	40.35	13.99	6.85	24.76	21.76	3.71	0.00
15	6.70	7.31	43.66	22.56	32.54	21.35	22.12	7.29	1.79
20	4.77	36.18	8.44	3.19	31.68	7.97	15.29	13.90	20.09
25	7.81	0.49	49.76	18.93	39.28	13.65	12.67	1.35	32.24
30	37.56	13.02	156.23	64.38	25.03	17.58	7.77	0.00	26.71
35	23.37	17.57	60.29	54.17	25.72	18.96	14.97	3.14	13.21

Appendix 4A

Appendix 4A.1: Pearson's correlation analysis

Table 4a.1: Results of the Pearson's correlation analysis displaying most and least correlated (r) groups for all 16 samples.

	Nod 1 Fixing	Nod 2 Fixing	Nod 3 Fixing	Nod 4 Fixing	Nod 1 PRE-FIXING	Nod 2 PRE-FIXING	Nod 3 PRE-FIXING	Nod 4 PRE-FIXING	Root 1 Fixing	Root 2 Fixing	Root 3 Fixing	Root 4 Fixing	Root1 PRE-FIXING	Root2 PRE-FIXING	Root1 PRE-fixing	Root1 PRE-fixing
Nod 1 Fixing	1.00	0.99	0.99	0.99	0.84	0.77	0.71	0.80	0.38	0.40	0.41	0.36	0.36	0.37	0.41	0.37
Nod 2 Fixing	0.99	1.00	0.99	1.00	0.79	0.71	0.66	0.74	0.38	0.41	0.41	0.38	0.36	0.37	0.40	0.37
Nod 3 Fixing	0.99	0.99	1.00	0.99	0.84	0.77	0.73	0.80	0.37	0.40	0.41	0.36	0.35	0.36	0.39	0.37
Nod 4 Fixing	0.99	1.00	0.99	1.00	0.79	0.70	0.66	0.74	0.38	0.39	0.40	0.37	0.35	0.37	0.40	0.37
Nod 1 PRE-FIXING	0.84	0.79	0.84	0.79	1.00	0.91	0.80	0.92	0.27	0.29	0.31	0.27	0.25	0.26	0.29	0.28
Nod 2 PRE-FIXING	0.77	0.71	0.77	0.70	0.91	1.00	0.90	0.99	0.27	0.30	0.31	0.27	0.24	0.25	0.30	0.26

Nod 3 PRE- FIXING	0.71	0.66	0.73	0.66	0.80	0.90	1.00	0.90	0.32	0.36	0.38	0.33	0.31	0.30	0.34	0.44
Nod 4 PRE- FIXING	0.80	0.74	0.80	0.74	0.92	0.99	0.90	1.00	0.33	0.36	0.38	0.32	0.29	0.31	0.35	0.32
Root1Fi xing	0.38	0.38	0.37	0.38	0.27	0.27	0.32	0.33	1.00	0.94	0.97	0.93	0.94	0.96	0.96	0.90
Root2 Fixing	0.40	0.41	0.40	0.39	0.29	0.30	0.36	0.36	0.94	1.00	0.96	0.95	0.88	0.92	0.89	0.89
Root 3 Fixing	0.41	0.41	0.41	0.40	0.31	0.31	0.38	0.38	0.97	0.96	1.00	0.92	0.91	0.93	0.92	0.89
Root 4 Fixing	0.36	0.38	0.36	0.37	0.27	0.27	0.33	0.32	0.93	0.95	0.92	1.00	0.86	0.89	0.87	0.86
Root 1 PRE- FIXING	0.36	0.36	0.35	0.35	0.25	0.24	0.31	0.29	0.94	0.88	0.91	0.86	1.00	0.98	0.98	0.93
Root 2 PRE- FIXING	0.37	0.37	0.36	0.37	0.26	0.25	0.30	0.31	0.96	0.92	0.93	0.89	0.98	1.00	0.99	0.94
Root 3 PRE- FIXING	0.41	0.40	0.39	0.40	0.29	0.30	0.34	0.35	0.96	0.89	0.92	0.87	0.98	0.99	1.00	0.92
Root 4 PRE- FIXING	0.37	0.37	0.37	0.37	0.28	0.26	0.44	0.32	0.90	0.89	0.89	0.86	0.93	0.94	0.92	1.00

Appendix 4A.2: Unique and shared differentially expressed gene interactions between comparisons

Many of the upregulated DEGs for each of the four comparisons were not unique to individual comparison, with multiple interactions identified. For upregulated DEGs, a total of 9566 genes were unique to each of the four comparisons, whereas 3954 shared interactions between two comparisons (Figure 4a.1C). Of the 1541 and 423 upregulated DEGs for C1 and C2 respectively, 105 genes shared increased expression in nodule and root tissue between early to peak N-fixation (Figure 4a.1A). Similarly, C1 of nodule tissue shared 731 and 338 unique upregulated genes with C3 and C4, respectively (Figure 4a.1A). In contrast, in roots the C2 comparison, had fewer unique shared upregulated DEGs, C2 with only 26 and 54 genes shared with C3 and C4, respectively (Figure 4a.1A). Early fixing and peak fixing nodule and root tissue (C3 & C4) had the largest number of shared genes - 2700 from the 3663 and 3939 upregulated genes from the respective comparisons (Figure 4a.1A).

Analysis of the overlap interactions between three comparisons revealed a total of 376 upregulated DEGs (Figure 4a.1C). Of these, 337 were shared between C1, C3 and C4, indicating a large overlap between the N-fixing nodule tissue sampled for C1 and either early- or peak-fixing nodule and root tissue used in comparisons C3 and C4 (Figure 4a.1A). The remaining gene interactions identified showed 22 genes shared between C2, C3 and C4, 10 between C1, C2 and C3 and lastly 7 between C1, C2 and C4 (Figure 4a.1A). When considering all four comparisons, only six genes were upregulated in all of them (Figure 4a.1C).

Unsurprisingly, the sum of unique and all shared upregulated gene interactions was much greater in comparisons C3 and C4 (7495 and 7403, respectively), compared to those in comparison C2 in which only 653 total gene elements were evident (Figure 4a.1B). Importantly, C1 (the comparison of early to peak N-fixing nodules) was found to have a total of 3075 upregulated gene elements reflecting the many important developmental, metabolic and transport functions involved in N-fixation (Figure 4a.1B).

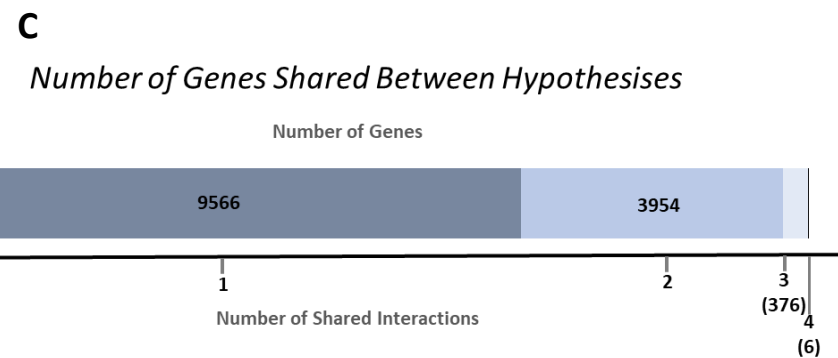
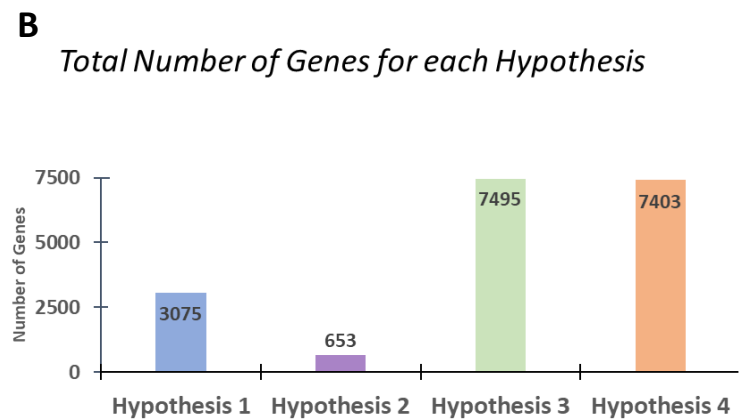
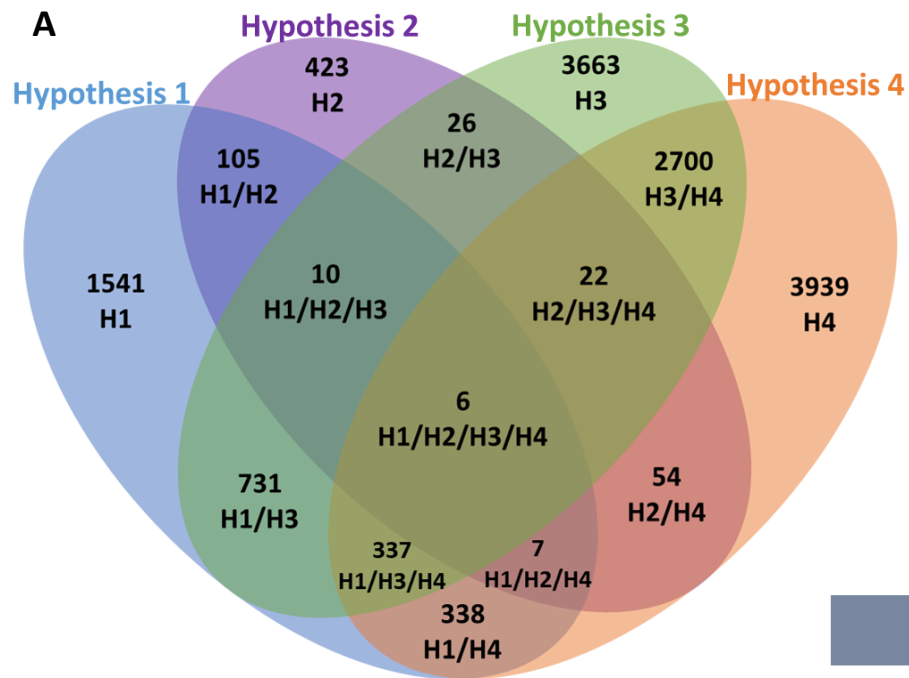


Figure 4a.1: Interactions between each comparison for upregulated DEGs (>1 Log₂ Fold change).

(A) Venn four-way diagram displaying the shared upregulated genes between each comparison. (B) The total number of shared gene matches for each comparison. (C) Total number of genes specific to each comparison (1), or shared by two, three or four comparisons.

A similar trend was observed for the number of downregulated DEGs between each comparison: C3 and C4 had a considerably larger shared pool of significantly downregulated genes than C1 and C2 (Figure 4a.2A). C2 exhibited 592 downregulated genes compared to its 423 upregulated genes (Figure 4a.2A). Conversely, C1 showed a larger number of upregulated genes to downregulated genes at 1541 and 879, respectively (Figure 4a.2A). This would be expected when considering a period of heightened nodule function during nitrogen fixation and will be further explored through gene ontology analysis in the following section.

The same trend was seen for the total number of significant shared gene elements for downregulated genes when two distinct plant tissues are compared: C3 and C4 show a considerably higher total compared to C1 and C2 (4664, 5231, 879 and 592, respectively; Figure 4a.2B). Despite an increase in significantly upregulated genes for C1, the total number of downregulated genes for each comparison was 11366, compared to the 9566 found to be upregulated (Figure 4a.2C). The number of genes that displayed two interactions i.e., a gene overlapping between any two comparisons, was 5200 compared to 3954 for significant downregulated to upregulated genes, respectively (Figure 4a.2C).

Importantly, C1 shared the most significantly downregulated gene elements with C3 (356) and 214 for interactions with C1, C3 and C4 (Figure 4a.2A). The least number of interactions shared with C1 was 91 genes between C1 and C2 and 51 genes between C1, C2 and C3 (Figure 4a.2A). It was reasonable to assume that the lowest number of up and downregulated gene overlaps would occur between nodule and root tissues of C1 and C2, considering the different metabolic nature of the two tissues.

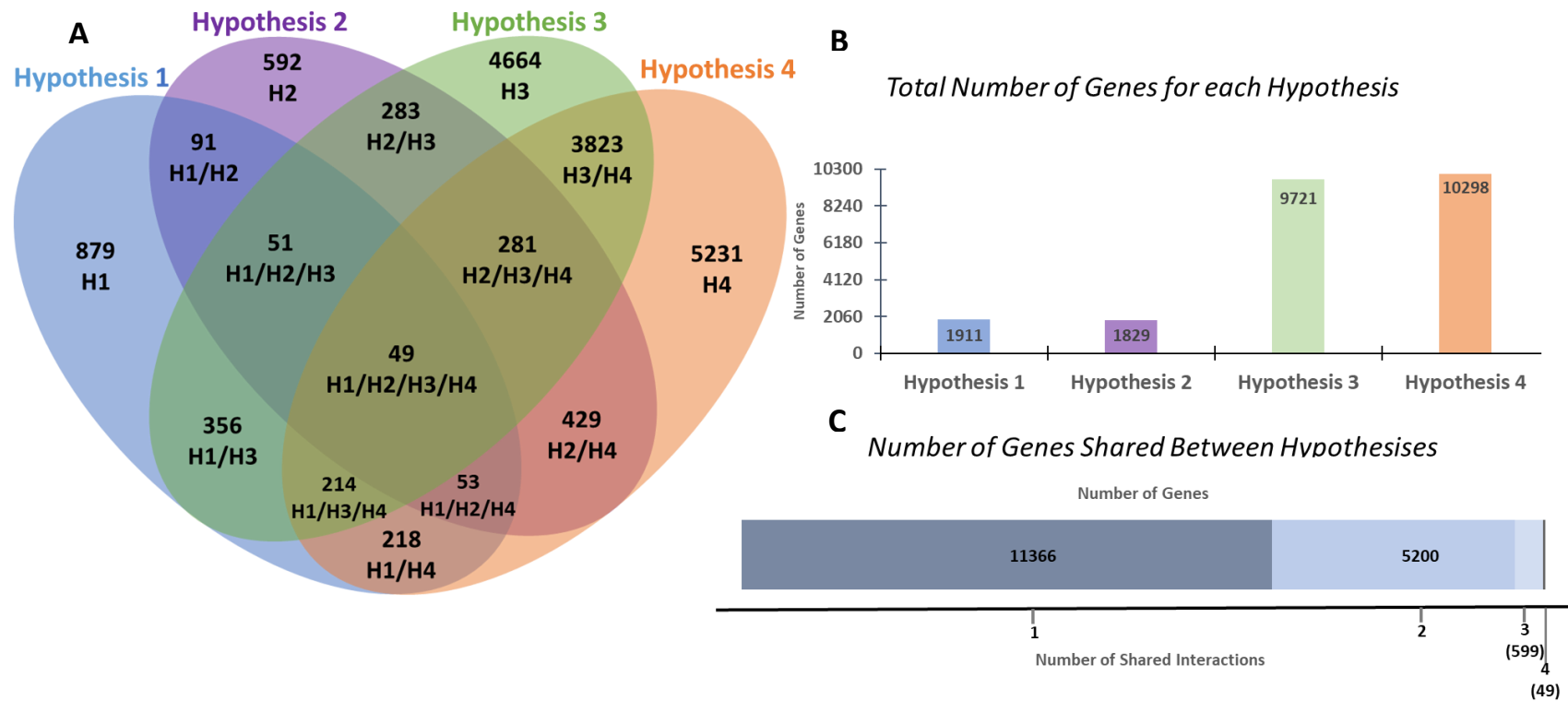


Figure 4a.2: Interactions between each comparison for downregulated DEGs (<-1 Log₂ Fold change).

(A) Venn four-way diagram displaying the shared downregulated genes between each comparison. (B) The total number of shared gene matches for each comparison. (C) Total number of genes specific to each comparison (1), or shared by two, three or four comparisons.

The UpSet plot depicted in figure 6 shows the intersections of DEGs between up and downregulated genes separately for each comparison; there were an increasingly fewer number of DEGs as the number of intersections increased from two to four (Figure 4a.3B). Notably, downregulated genes in peak N-fixing tissue (C3) had the largest number of DEG intersections with early-fixing downregulated genes of C4 (Figure 4a.3B), followed closely by the intersection of upregulated peak N-fixing (C3) with upregulated early N-fixing (C4) tissues (Figure 4a.3B). The largest number of DEGs from a three-way intersection, although considerably less than the two-way intersections, was seen between upregulated DEGs from peak-fixing roots (C3), early-fixing tissue (C4) and N-fixing nodule peak tissue (C1) (Figure 4a.3B).

When identifying intersections of most importance to nitrogen fixation in C1, the largest number of DEG interactions were observed between upregulated DEGs from C1 and C3 (Figure 4a.3B), closely followed by upregulated DEGs from C1, C4 and C3 and, lastly, upregulated DEGs from C1 and downregulated DEGs from C3 and C4 (Figure 4a.3B). A similar number of interactions of downregulated DEGs C1 was also observed between C1, C3 and C4 (Figure 6B). A relationship was observed between intersecting DEGs of fixing and pre-fixing tissues where if a gene was downregulated in fixing tissues (C3), that same gene was also downregulated in pre-fixing tissues (C4) and the same for upregulated genes (Figure 4a.3). For example, the largest number of intersection events by a significant amount occurred between the respective down or upregulated genes of C3 and C4, which was expected when considering the larger pool of DEGs as seen in the volcano plots in figure 3A-D.

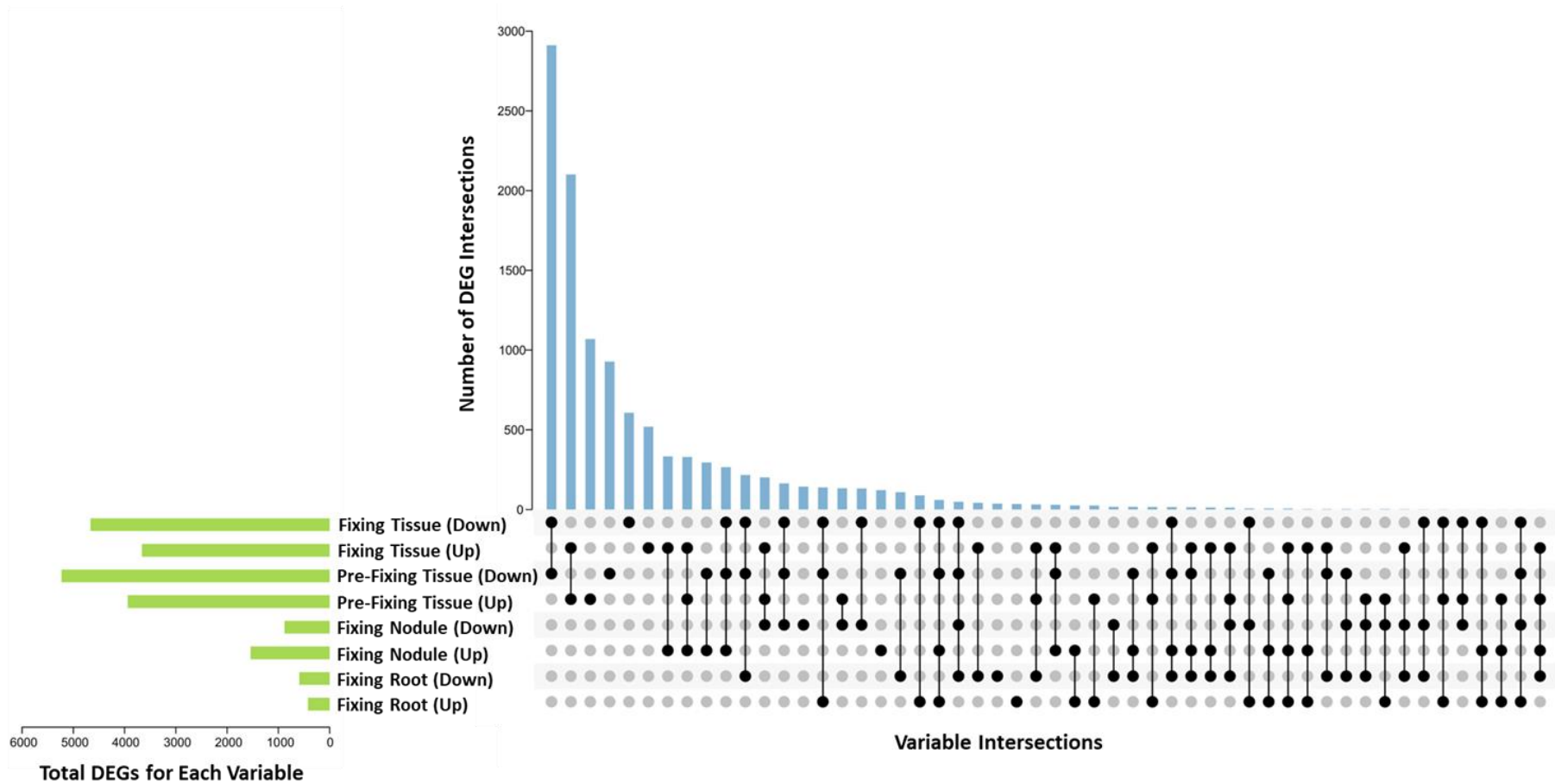


Figure 4a.3: UpSet plot of gene interactions between each variable (Up or Downregulated genes) within each comparison.

(A) The total number of up or downregulated DEGs for each variable, including non-unique genes. **(B)** Total number of DEG intersections between other comparison variables and matrix representation of interactions. Single dots indicate the number of unique genes to the variable, multiple dots connected by a line indicate one or more variable intersections. Fixing nodule represents comparison 1 (18-25 DAI nodule), Fixing root; comparison 2 (18-25DAI root), Fixing tissue; comparison 3 (25 DAI nodule and root), Pre-Fixing tissue; comparison 4 (18 DAI nodule and root).

Appendix 4A.3: Gene summary list for each transporter gene family analysed in the RNAseq database

Table 4a.2: Summary amino acid permease transporters DEG in chickpea.

Data displayed as Log₂ fold change as a heatmap with corresponding average FPKM for each gene. Data presented for all nodule and root comparisons, 18 DAI (Early-Fixing) and 25 (Peak-Fixing). Genes in red were presented in chapter 2.

Gene	RNAseq Accession	Average FPKM				Log ₂ Fold Change							
		25 DAI Nodule	18 DAI Nodule	25 DAI Root	18 DAI Root	Nodule 18 DAI to 25 DAI	FDR	Root 18 DAI to 25 DAI	FDR	Nodule 25 DAI to Root 25 DAI	FDR	Nodule 18 DAI to Root 18 DAI	FDR
AAP1	NonamEVm006690t1	38.017	22.633	0.451	0.758	0.750	0.007	-0.686	0.236	6.377	0.000	4.941	0.000
AAP2	NonamEVm006072t1	14.857	8.579	20.937	19.660	0.793	0.000	0.089	0.548	-0.495	0.000	-1.199	0.000
AAP2	NonamEVm006087t1	0.460	0.744	2.655	9.467	-0.663	0.269	-1.828	0.000	-2.529	0.000	-3.694	0.000
AAP2	NonamEVm006557t1	0.467	0.464	6.499	7.620	0.026	0.977	-0.232	0.348	-3.782	0.000	-4.039	0.000
AAP2	NonamEVm005391t1	0.012	0.012	0.169	0.353	0.078	0.994	-1.097	0.189	-3.424	0.010	-4.599	0.000
AAP3	NonamEVm006278t1	6.866	1.048	10.492	11.104	2.720	0.000	-0.082	0.696	-0.611	0.001	-3.414	0.000
AAP3	NonamEVm006048t1	0.562	0.847	19.300	21.834	-0.589	0.192	-0.181	0.503	-5.096	0.000	-4.688	0.000
AAP6.1	NonamEVm006231t1	4.173	14.148	79.152	71.099	-1.758	0.000	0.154	0.668	-4.241	0.000	-2.329	0.000
AAP6.2	NonamEVm006610t1	21.855	1.990	0.099	0.109	3.498	0.000	-0.091	0.982	7.738	0.000	4.149	0.000
AAP6.3	NonamEVm006553t1	74.924	60.553	78.384	103.829	0.307	0.008	-0.405	0.002	-0.065	0.508	-0.778	0.000
AAP7	NonamEVm006112t1	3.556	1.838	1.661	1.573	0.950	0.003	0.100	0.799	1.094	0.000	0.245	0.357

AAP7	NonamEVm006780t1	5.662	7.059	4.378	4.057	-0.317	0.038	0.106	0.560	0.371	0.010	0.794	0.000
AAP7	NonamEVm006701t1	1.065	1.748	2.706	3.613	-0.713	0.127	-0.415	0.353	-1.349	0.002	-1.051	0.008
AAP7	NonamEVm009679t1	16.734	19.481	42.183	74.479	-0.219	0.166	-0.820	0.000	-1.334	0.000	-1.936	0.000
APP8	NonamEVm017381t1	0.000	0.102	0.073	0.083	-3.360	0.079	-0.177	0.928	-2.887	0.089	0.296	0.799
AAP8	NonamEVm006524t1	58.762	70.514	17.949	19.051	-0.263	0.121	-0.090	0.683	1.711	0.000	1.884	0.000
AAP8	NonamEVm006734t1	3.315	3.732	12.071	16.916	-0.169	0.342	-0.486	0.006	-1.864	0.000	-2.182	0.000
AAP8	NonamEVm014751t1	0.176	0.236	0.000	0.023	-0.390	0.784	-1.519	0.503	4.219	0.021	3.091	0.040

Table 4a.3: Summary cationic amino acid transporter DEGs in chickpea.

Data displayed as Log₂ fold change as a heatmap with corresponding average FPKM for each gene. Data presented for all nodule and root comparisons, 18 DAI (Early-Fixing) and 25 (Peak-Fixing). Genes in red were presented in chapter 2.

Gene	RNAseq Accession	Average FPKM				Log ₂ Fold Change							
		25 DAI Nodule	18 DAI Nodule	25 DAI Root	18 DAI Root	Nodule 18 DAI to 25 DAI	FDR	Root 18 DAI to 25 DAI	FDR	Nodule 25 DAI to Root 25 DAI	FDR	Nodule 18 DAI to Root 18 DAI	FDR
CAT1	NonamEVm004038t1	90.975	29.154	0.101	0.139	1.643	0.000	-0.289	0.854	9.804	0.000	7.872	0.000
CAT1	NonamEVm003928t1	2.598	1.980	9.118	11.526	0.387	0.035	-0.337	0.041	-1.808	0.000	-2.533	0.000
CAT1	NonamEVm006139t1	11.929	16.269	0.399	0.744	-0.446	0.059	-0.901	0.049	4.871	0.000	4.416	0.000
CAT1	NonamEVm015458t1	0.525	0.621	0.825	0.641	-0.238	0.530	0.370	0.313	-0.649	0.039	-0.042	0.919
CAT1	NonamEVm020720t1	5.321	5.864	0.385	0.584	-0.136	0.836	-0.680	0.528	3.692	0.000	3.147	0.000
CAT2	NonamEVm003627t1	13.211	4.724	28.955	28.234	1.485	0.000	0.034	0.922	-1.132	0.000	-2.583	0.000

CAT2	NonamEVm003398t1	0.125	0.195	0.215	0.336	-0.626	0.317	-0.655	0.232	-0.752	0.152	-0.781	0.093
CAT4	NonamEVm003271t1	9.951	6.035	13.709	13.681	0.724	0.000	0.002	1.000	-0.462	0.000	-1.183	0.000
CAT5	NonamEVm003988t1	14.301	13.857	2.325	1.900	0.046	0.793	0.295	0.115	2.620	0.000	2.869	0.000
CAT6	NonamEVm004235t1	10.175	18.057	3.576	3.223	-0.827	0.000	0.153	0.379	1.508	0.000	2.488	0.000
CAT7	NonamEVm004186t1	3.296	8.366	5.985	10.219	-1.342	0.000	-0.769	0.000	-0.860	0.000	-0.288	0.041
CAT8	NonamEVm003957t1	9.401	5.250	13.971	12.964	0.844	0.000	0.107	0.518	-0.572	0.000	-1.309	0.000
CAT9	NonamEVm003907t1	3.973	2.615	5.520	5.899	0.602	0.000	-0.095	0.542	-0.475	0.001	-1.173	0.000
CAT	NonamEVm003161t1	22.440	23.342	6.621	6.399	-0.057	0.600	0.049	0.706	1.761	0.000	1.867	0.000

Table 4a.4: Summary usually multiple amino acids transport in and out transporter DEGs in chickpea.

Data displayed as Log₂ fold change as a heatmap with corresponding average FPKM for each gene. Data presented for all nodule and root comparisons, 18 DAI (Early-Fixing) and 25 (Peak-Fixing). Genes in red were presented in chapter 2.

Gene	RNAseq Accession	Average FPKM				Log ₂ Fold Change							
		25 DAI Nodule	18 DAI Nodule	25 DAI Root	18 DAI Root	Nodule 18 DAI to 25 DAI	FDR	Root 18 DAI to 25 DAI	FDR	Nodule 25 DAI to Root 25 DAI	FDR	Nodule 18 DAI to Root 18 DAI	FDR
UmamiT2	NonamEVm008762t1	15.631	20.345	6.341	7.881	-0.380	0.003	-0.310	0.027	1.301	0.000	1.370	0.000
UmamiT2	NonamEVm011915t1	1.763	2.456	5.968	6.352	-0.475	0.031	-0.090	0.695	-1.758	0.000	-1.374	0.000
UmamiT4	NonamEVm009780t1	0.000	0.031	2.479	5.635	-2.501	0.314	-1.178	0.015	-8.651	0.000	-7.328	0.000
UmamiT7	NonamEVm010118t1	1.747	3.290	0.160	0.180	-0.913	0.012	-0.261	0.743	3.411	0.000	4.063	0.000

UmamiT7	NonamEVm014496t1	0.213	0.315	0.016	0.117	-0.578	0.590	-2.248	0.190	3.187	0.019	1.517	0.109
UmamiT9	NonamEVm008756t1	10.318	1.454	16.265	23.600	2.865	0.000	-0.539	0.084	-0.657	0.017	-4.060	0.000
UmamiT9	NonamEVm008436t1	212.514	25.304	119.216	95.693	3.073	0.000	0.316	0.508	0.834	0.028	-1.923	0.000
UmamiT9	NonamEVm010058t1	53.114	92.489	5.478	4.592	-0.800	0.000	0.257	0.088	3.277	0.000	4.334	0.000
UmamiT9	NonamEVm008589t1	93.703	112.236	0.419	0.671	-0.260	0.640	-0.490	0.717	7.803	0.000	7.573	0.000
UmamiT12	NonamEVm009081t1	1.536	0.000	3.489	1.818	7.972	0.000	0.949	0.058	-1.185	0.009	-8.207	0.000
UmamiT12	NonamEVm010199t1	78.385	80.060	36.651	34.174	-0.030	0.850	0.098	0.531	1.096	0.000	1.225	0.000
UmamiT18	NonamEVm008729t1	8.036	0.181	242.277	134.750	5.456	0.000	0.846	0.004	-4.914	0.000	-9.524	0.000
UmamiT18	NonamEVm010982t1	90.948	21.904	94.803	103.042	2.058	0.000	-0.122	0.799	-0.060	0.860	-2.240	0.000
UmamiT20	NonamEVm009098t1	2.708	0.000	11.572	0.707	9.195	0.000	3.967	0.000	-2.095	0.000	-7.323	0.000
UmamiT20	NonamEVm013126t1	70.787	3.473	70.748	34.915	4.354	0.000	1.016	0.031	0.000	1.000	-3.338	0.000
UmamiT20	NonamEVm018348t1	0.364	0.954	15.885	26.305	-1.358	0.078	-0.730	0.035	-5.401	0.000	-4.773	0.000
UmamiT20	NonamEVm016381t1	0.313	0.282	7.993	11.492	0.202	0.833	-0.526	0.129	-4.629	0.000	-5.357	0.000
UmamiT21	NonamEVm010543t1	4.675	6.963	1.223	1.434	-0.574	0.003	-0.242	0.294	1.932	0.000	2.264	0.000
UmamiT21	NonamEVm008630t1	0.362	0.511	0.379	0.528	-0.488	0.481	-0.531	0.445	-0.078	0.902	-0.121	0.836
UmamiT21	NonamEVm009886t1	1.782	1.575	0.526	1.350	0.179	0.608	-1.376	0.002	1.753	0.000	0.198	0.495
UmamiT22	NonamEVm009135t1	5.148	6.653	5.264	4.435	-0.372	0.048	0.254	0.215	-0.033	0.852	0.593	0.001
UmamiT24.1	NonamEVm019805t1	60.275	26.606	1.311	1.321	1.183	0.000	0.058	0.941	5.511	0.000	4.387	0.000
UmamiT23.1	NonamEVm008823t1	104.540	26.623	0.271	0.483	1.974	0.002	-0.750	0.456	8.589	0.000	5.864	0.000
UmamiT23.2	NonamEVm008815t1	88.047	46.142	0.254	0.281	0.933	0.003	-0.014	1.000	8.423	0.000	7.475	0.000

UmamiT23	NonamEVm007274t1	9.190	16.054	1.377	2.921	-0.803	0.048	-1.087	0.041	2.733	0.000	2.449	0.000
UmamiT24.2	NonamEVm013792t1	23.719	9.342	0.612	0.614	1.350	0.001	0.112	0.917	5.257	0.000	4.020	0.000
UmamiT24.3	NonamEVm010584t1	39.189	57.290	0.097	0.334	-0.547	0.355	-1.532	0.364	8.631	0.000	7.646	0.000
UmamiT25	NonamEVm008752t1	9.639	24.186	0.066	0.069	-1.326	0.000	0.242	0.912	7.041	0.000	8.610	0.000
UmamiT25	NonamEVm012993t1	0.000	0.000	0.156	0.174	0.000	1.000	-0.177	0.930	-4.084	0.066	-4.261	0.047
UmamiT32	NonamEVm017894t1	6.051	0.689	0.117	0.142	3.165	0.000	-0.302	0.801	5.659	0.000	2.192	0.002
UmamiT32	NonamEVm009794t1	0.012	0.054	1.017	2.086	-1.835	0.193	-1.032	0.018	-5.884	0.000	-5.081	0.000
UmamiT32	NonamEVm010400t1	0.045	0.072	0.731	0.593	-0.569	0.704	0.259	0.729	-3.859	0.000	-3.031	0.001
UmamiT34	NonamEVm017785t1	5.746	25.361	0.139	0.027	-2.141	0.000	1.665	0.436	5.272	0.000	9.078	0.000
UmamiT34	NonamEVm017123t1	1.891	8.949	0.042	0.000	-2.235	0.001	2.067	0.384	5.183	0.000	9.486	0.000
UmamiT34	NonamEVm014288t1	136.264	85.106	0.295	0.547	0.680	0.066	-0.646	0.688	8.802	0.000	7.475	0.000
UmamiT34	NonamEVm009633t1	0.780	1.020	1.868	1.967	-0.392	0.534	-0.057	0.945	-1.257	0.016	-0.921	0.055
UmamiT36	NonamEVm009968t1	0.925	0.154	21.918	6.075	2.511	0.005	1.839	0.000	-4.552	0.000	-5.224	0.000
UmamiT38	NonamEVm010044t1	0.018	0.063	0.366	0.759	-1.543	0.307	-1.026	0.094	-3.922	0.000	-3.405	0.000
UmamiT40	NonamEVm010442t1	6.208	4.231	6.841	6.858	0.550	0.000	-0.005	0.988	-0.140	0.170	-0.694	0.000
UmamiT40	NonamEVm013104t1	4.958	6.832	50.796	88.792	-0.465	0.022	-0.805	0.000	-3.356	0.000	-3.696	0.000
UmamiT40	NonamEVm010001t1	0.194	0.451	0.130	0.391	-1.160	0.161	-1.556	0.076	0.533	0.522	0.137	0.844
UmamiT41	NonamEVm009547t1	16.250	6.148	13.559	12.611	1.406	0.000	0.101	0.621	0.261	0.088	-1.044	0.000
UmamiT41	NonamEVm013420t1	17.882	5.695	25.978	31.669	1.651	0.000	-0.286	0.120	-0.539	0.001	-2.476	0.000
UmamiT41	NonamEVm009943t1	55.448	16.058	52.181	55.400	1.790	0.000	-0.087	0.712	0.087	0.606	-1.789	0.000

UmamiT41	NonamEVm010286t1	0.742	1.447	4.111	6.660	-0.937	0.020	-0.700	0.027	-2.453	0.000	-2.215	0.000
UmamiT41	NonamEVm012861t1	1.485	1.011	5.261	7.060	0.570	0.142	-0.427	0.158	-1.827	0.000	-2.825	0.000
UmamiT46	NonamEVm010524t1	3.670	2.590	9.191	10.427	0.497	0.026	-0.181	0.395	-1.324	0.000	-2.002	0.000
UmamiT	NonamEVm023303t1	116.683	54.445	0.319	1.031	1.100	0.031	-1.579	0.089	8.492	0.000	5.813	0.000
UmamiT/WAT1	NonamEVm009059t1	5.488	20.534	18.090	14.031	-1.903	0.000	0.368	0.115	-1.719	0.000	0.552	0.006
UmamiT/WAT1	NonamEVm012029t1	29.585	7.970	4.302	11.922	1.897	0.000	-1.470	0.000	2.775	0.000	-0.592	0.031
UmamiT/WAT1	NonamEVm022285t1	0.172	0.196	0.073	0.122	-0.120	0.966	-0.506	0.816	1.126	0.424	0.740	0.580
WAT1	NonamEVm008236t1	0.733	0.974	2.520	1.948	-0.414	0.036	0.375	0.030	-1.780	0.000	-0.992	0.000
WAT1	NonamEVm008701t1	5.215	6.150	34.508	37.685	-0.235	0.173	-0.127	0.458	-2.723	0.000	-2.616	0.000

Table 4a.5: Summary amino acid vacuolar transporter DEGs in chickpea.

Data displayed as Log₂ fold change as a heatmap with corresponding average FPKM for each gene. Data presented for all nodule and root comparisons, 18 DAI (Early-Fixing) and 25 (Peak-Fixing). Genes in red were presented in chapter 2.

Gene	RNAseq Accession	Average FPKM				Log ₂ Fold Change							
		25 DAI Nodule	18 DAI Nodule	25 DAI Root	18 DAI Root	Nodule 18 DAI to 25 DAI	FDR	Root 18 DAI to 25 DAI	FDR	Nodule 25 DAI to Root 25 DAI	FDR	Nodule 18 DAI to Root 18 DAI	FDR
AVT1A	NonamEVm005713t1	20.216	7.253	0.931	1.340	1.483	0.000	-0.508	0.286	4.430	0.000	2.440	0.000
AVT1A	NonamEVm004820t1	1.059	0.256	1.045	0.462	2.014	0.032	1.188	0.183	0.018	0.984	-0.808	0.352
AVT1C	NonamEVm004850t1	7.235	9.573	47.895	42.052	-0.406	0.081	0.187	0.443	-2.726	0.000	-2.133	0.000

AVT1C	NonamEVm025048t1	4.875	6.067	14.524	14.021	-0.309	0.282	0.061	0.854	-1.573	0.000	-1.203	0.000
AVT1C	NonamEVm014805t1	1.526	1.349	3.112	2.877	0.176	0.594	0.127	0.695	-1.025	0.000	-1.074	0.000
AVT1C	NonamEVm011932t1	4.777	4.936	12.211	12.715	-0.045	0.848	-0.054	0.814	-1.355	0.000	-1.364	0.000
AVT1D	NonamEVm011461t1	2.723	0.578	0.041	0.131	2.222	0.001	-1.615	0.179	5.823	0.000	1.986	0.006
AVT1H	NonamEVm006560t1	0.844	0.161	0.990	3.180	2.348	0.001	-1.689	0.002	-0.238	0.586	-4.275	0.000
AVT1I	NonamEVm006906t1	1.135	2.230	0.386	0.282	-0.967	0.016	0.366	0.533	1.540	0.001	2.873	0.000
AVT1I	NonamEVm008307t1	5.495	3.298	1.005	1.305	0.742	0.016	-0.384	0.324	2.449	0.000	1.323	0.000
AVT1I	NonamEVm007346t1	1.506	2.274	2.330	2.948	-0.601	0.075	-0.338	0.324	-0.626	0.038	-0.362	0.188
AVT1J	NonamEVm008281t1	4.198	8.538	0.273	0.278	-1.025	0.015	0.052	0.971	3.924	0.000	5.002	0.000
AVT3A	NonamEVm013912t1	0.115	0.089	0.112	0.098	0.453	0.780	0.073	0.977	0.063	0.962	-0.318	0.803
AVT3C	NonamEVm007786t1	54.646	35.239	106.601	69.410	0.633	0.000	0.618	0.000	-0.964	0.000	-0.979	0.000
AVT6A	NonamEVm006714t1	248.157	71.694	204.932	92.142	1.791	0.000	1.153	0.000	0.276	0.063	-0.362	0.017
AVT6A	NonamEVm006637t1	0.025	0.305	0.091	0.022	-3.166	0.018	1.874	0.227	-1.576	0.231	3.464	0.004
AVT6A	NonamEVm006670t1	0.915	1.069	4.487	4.981	-0.213	0.487	-0.153	0.509	-2.288	0.000	-2.228	0.000
AVT6B	NonamEVm006759t1	16.845	13.517	22.181	16.343	0.318	0.005	0.440	0.001	-0.397	0.000	-0.275	0.006
AVT6C.1	NonamEVm006953t1	23.550	1.488	13.307	5.389	4.010	0.000	1.298	0.003	0.822	0.009	-1.890	0.000
AVT6C.2	NonamEVm007499t1	42.712	9.078	26.979	39.172	2.236	0.000	-0.539	0.035	0.662	0.003	-2.112	0.000
AVT6C	NonamEVm006935t1	0.615	0.089	5.699	6.674	2.809	0.014	-0.231	0.690	-3.194	0.000	-6.234	0.000
AVT6E	NonamEVm006057t1	17.497	20.750	12.411	13.904	-0.246	0.074	-0.161	0.297	0.495	0.001	0.579	0.000

Table 4a.6: Summary sucrose transporter DEGs in chickpea.

Data displayed as Log₂ fold change as a heatmap with corresponding average FPKM for each gene. Data presented for all nodule and root comparisons, 18 DAI (Early-Fixing) and 25 (Peak-Fixing). Genes in red were presented in chapter 2.

Gene	RNAseq Accession	Average FPKM				Log ₂ Fold Change							
		25 DAI Nodule	18 DAI Nodule	25 DAI Root	18 DAI Root	Nodule 18 DAI to 25 DAI	FDR	Root 18 DAI to 25 DAI	FDR	Nodule 25 DAI to Root 25 DAI	FDR	Nodule 18 DAI to Root 18 DAI	FDR
SWEET1	NonamEVm015941t1	21.053	2.018	0.033	0.008	3.408	0.000	1.894	0.491	9.221	0.000	7.707	0.000
SWEET1	NonamEVm017858t1	15.373	23.543	7.195	7.826	-0.617	0.037	-0.121	0.766	1.090	0.001	1.586	0.000
SWEET2	NonamEVm017715t1	95.700	49.270	0.272	0.573	0.960	0.023	-0.904	0.474	8.432	0.000	6.569	0.000
SWEET2	NonamEVm014609t1	9.976	9.794	5.634	7.111	0.026	0.934	-0.336	0.150	0.826	0.000	0.464	0.017
SWEET2	NonamEVm024023t1	15.401	15.003	0.328	0.129	0.043	0.966	1.373	0.503	5.490	0.000	6.820	0.000
SWEET3	NonamEVm014110t1	0.097	0.102	0.997	0.654	0.082	0.979	0.574	0.434	-3.217	0.001	-2.725	0.003
SWEET5	NonamEVm019167t1	0.307	0.190	0.081	0.038	0.669	0.486	0.938	0.539	1.800	0.045	2.069	0.058
SWEET5	NonamEVm019342t1	0.183	0.210	0.089	0.213	-0.188	0.926	-1.228	0.420	0.935	0.480	-0.105	0.933
SWEET7	NonamEVm006345t1	22.192	12.036	1.892	1.318	0.884	0.000	0.523	0.006	3.550	0.000	3.189	0.000
SWEET13	NonamEVm013888t1	10.280	44.696	36.408	112.786	-2.117	0.000	-1.631	0.000	-1.821	0.000	-1.335	0.000
SWEET14	NonamEVm013603t1	152.520	214.567	0.876	1.016	-0.492	0.423	-0.107	0.941	7.445	0.000	7.830	0.000
SWEET14	NonamEVm012338t1	0.000	0.000	1.233	1.191	0.000	1.000	0.032	0.989	-7.469	0.002	-7.437	0.002

SWEET17	NonamEVm017794t1	0.605	1.368	2.316	2.914	-1.178	0.002	-0.332	0.268	-1.934	0.000	-1.088	0.000
Bidirectional sugar transporter N3	NonamEVm013733t1	44.477	152.055	11.163	13.515	-1.773	0.000	-0.273	0.432	1.991	0.000	3.491	0.000
Bidirectional sugar transporter N3	NonamEVm013796t1	3.337	14.899	3.117	2.306	-2.158	0.000	0.400	0.402	0.098	0.802	2.655	0.000
Bidirectional sugar transporter N3	NonamEVm013270t1	0.171	0.040	0.292	0.457	1.908	0.295	-0.699	0.556	-0.763	0.493	-3.370	0.015

Table 4a.7: Summary nitrate transporter DEGs in chickpea.

Data displayed as Log₂ fold change as a heatmap with corresponding average FPKM for each gene. Data presented for all nodule and root comparisons, 18 DAI (Early-Fixing) and 25 (Peak-Fixing). Genes in red were presented in chapter 2.

Gene	RNAseq Accession	Average FPKM						Log ₂ Fold Change					
		25 DAI Nodule	18 DAI Nodule	25 DAI Root	18 DAI Root	Nodule 18 DAI to 25 DAI	FDR	Root 18 DAI to 25 DAI	FDR	Nodule 25 DAI to Root 25 DAI	FDR	Nodule 18 DAI to Root 18 DAI	FDR
High-affinity nitrate transporter 2.5	Nonam EVm00 5626t1	17.733	25.559	70.127	18.419	-0.525	0.047	1.926	0.000	-1.983	0.000	0.468	0.046
High-affinity nitrate transporter 2.1	Nonam EVm00 5099t1	111.34 2	2.619	482.08 9	187.61 2	5.430	0.000	1.361	0.016	-2.114	0.000	-6.183	0.000
High-affinity nitrate transporter 3.1	Nonam EVm01 6161t1	19.902	26.288	266.92 4	107.71 2	-0.401	0.116	1.308	0.000	-3.745	0.000	-2.036	0.000
NRT1/ PTR 1.2	Nonam EVm00 3969t1	4.923	8.725	2.073	2.579	-0.824	0.000	-0.312	0.185	1.243	0.000	1.755	0.000

NRT1/ PTR 1.2	Nonam EVm00 3277t1	18.974	13.446	19.411	24.471	0.497	0.003	-0.336	0.039	-0.033	0.813	-0.865	0.000
NRT1/ PTR 1.2	Nonam EVm00 4065t1	8.108	6.340	6.077	12.382	0.357	0.049	-1.027	0.000	0.415	0.013	-0.969	0.000
NRT1/ PTR 1.2	Nonam EVm00 4066t1	23.076	18.855	0.358	0.398	0.293	0.274	-0.090	0.911	6.016	0.000	5.634	0.000
NRT1/ PTR 2.10	Nonam EVm01 9470t1	5.079	8.295	3.400	4.040	-0.707	0.003	-0.257	0.317	0.576	0.008	1.026	0.000
NRT1/ PTR 2.11	Nonam EVm00 3682t1	5.576	5.981	4.994	5.091	-0.101	0.385	-0.030	0.849	0.159	0.119	0.230	0.026
NRT1/ PTR 2.13	Nonam EVm00 3655t1	53.987	30.735	16.056	12.056	0.813	0.000	0.410	0.021	1.749	0.000	1.347	0.000
NRT1/ PTR 2.13	Nonam EVm00 3937t1	0.097	0.335	0.073	0.244	-1.769	0.056	-1.618	0.101	0.338	0.737	0.489	0.476

NRT1/ PTR 2.13	Nonam EVm00 3884t1	1.859	3.202	0.122	0.149	-0.789	0.099	-0.087	0.959	3.866	0.000	4.568	0.000
NRT1/ PTR 2.6	Nonam EVm00 4795t1	0.112	0.097	3.697	2.743	0.265	0.844	0.424	0.358	-4.989	0.000	-4.830	0.000
NRT1/ PTR 2.8	Nonam EVm00 3734t1	3.140	2.729	0.207	0.537	0.197	0.611	-1.310	0.027	3.880	0.000	2.372	0.000
NRT1/ PTR 2.9	Nonam EVm00 4602t1	3.447	0.455	0.070	0.029	2.936	0.000	1.080	0.422	5.501	0.000	3.645	0.000
NRT1/ PTR 2.9	Nonam EVm00 3844t1	9.990	6.137	12.303	10.482	0.706	0.052	0.229	0.574	-0.302	0.329	-0.778	0.018
NRT1/ PTR 2.9	Nonam EVm01 8956t1	3.086	4.154	3.250	3.058	-0.424	0.318	0.061	0.924	-0.073	0.853	0.412	0.251
NRT1/ PTR 3.1	Nonam EVm00 3601t1	101.95 7	73.250	5.866	5.893	0.478	0.054	-0.001	1.000	4.115	0.000	3.637	0.000

NRT1/ PTR 3.1	Nonam EVm00 4169t1	99.698	77.503	2.755	2.871	0.363	0.058	-0.052	0.881	5.172	0.000	4.756	0.000
--------------------------	--------------------------	--------	--------	-------	-------	-------	-------	--------	-------	-------	-------	-------	-------

Gene	RNAseq Accession	Average FPKM					Log2 Fold Change						
		25 DAI Nodule	18 DAI Nodule	25 DAI Root	18 DAI Root	Nodule 18 DAI to 25 DAI	FDR	Root 18 DAI to 25 DAI	FDR	Nodule 25 DAI to Root 25 DAI	FDR	Nodule 18 DAI to Root 18 DAI	FDR
NRT1/ PTR 3.1	NonamEVm007748t1	11.973	11.624	22.785	21.226	0.042	0.829	0.102	0.578	-0.929	0.000	-0.869	0.000
NRT1/ PTR 4.2	NonamEVm017017t1	0.000	0.113	0.139	0.083	-3.352	0.173	0.552	0.770	-3.593	0.089	0.311	0.839
NRT1/ PTR 4.2	NonamEVm024982t1	0.000	0.219	0.000	0.000	-3.008	0.220	0.000	1.000	0.000	1.000	3.008	0.127
NRT1/ PTR 4.3	NonamEVm004157t1	0.849	1.262	8.221	7.186	-0.562	0.037	0.193	0.367	-3.272	0.000	-2.517	0.000
NRT1/ PTR 4.3	NonamEVm004015t1	0.397	0.754	7.236	6.742	-0.948	0.224	0.095	0.890	-4.165	0.000	-3.122	0.000
NRT1/ PTR 4.3	NonamEVm011160t1	0.065	0.043	0.233	0.000	0.589	0.741	4.821	0.011	-1.722	0.102	2.509	0.140
NRT1/ PTR 4.3	NonamEVm003522t1	1.144	2.087	5.180	9.432	-0.865	0.004	- 0.861	0.002	-2.178	0.000	-2.173	0.000
NRT1/ PTR 4.4	NonamEVm011413t1	0.929	2.732	0.038	0.018	-1.540	0.004	1.018	0.571	4.363	0.000	6.922	0.000
NRT1/ PTR 4.5	NonamEVm004212t1	8.419	8.854	38.134	28.793	-0.072	0.756	0.405	0.055	-2.180	0.000	-1.703	0.000
NRT1/ PTR 4.5	NonamEVm004007t1	0.000	0.000	0.127	2.059	0.000	1.000	- 3.993	0.001	-5.105	0.018	-9.098	0.000
NRT1/ PTR 4.6	NonamEVm020362t1	0.080	0.427	0.027	0.087	-2.244	0.078	- 1.328	0.473	1.216	0.433	2.132	0.042

NRT1/ PTR 4.6	NonamEVm007078t1	0.049	0.165	0.050	0.335	-1.720	0.210	-	0.035	-0.061	0.970	-0.914	0.287
								2.573					
NRT1/ PTR 4.6	NonamEVm004201t1	82.933	68.022	11.058	6.270	0.287	0.242	0.821	0.008	2.906	0.000	3.441	0.000
NRT1/ PTR 4.6	NonamEVm019506t1	0.050	0.044	0.098	0.000	0.083	0.992	2.538	0.215	-0.723	0.653	1.732	0.294
NRT1/ PTR 4.6	NonamEVm004243t1	1.230	1.751	6.569	6.267	-0.510	0.191	0.057	0.902	-2.411	0.000	-1.844	0.000
NRT1/ PTR 5.1	NonamEVm0044005t1	1.546	1.616	0.442	0.221	-0.065	0.836	0.942	0.018	1.794	0.000	2.801	0.000
NRT1/ PTR 5.10	NonamEVm023163t1	7.385	13.562	41.707	59.201	-0.885	0.001	-	0.009	-2.493	0.000	-2.114	0.000
								0.505					
NRT1/ PTR 5.10	NonamEVm004773t1	13.176	11.313	26.736	21.046	0.220	0.013	0.345	0.001	-1.021	0.000	-0.896	0.000
NRT1/ PTR 5.2	NonamEVm003788t1	154.404	21.298	0.361	0.171	2.861	0.000	1.158	0.225	8.722	0.000	7.019	0.000
NRT1/ PTR 5.2	NonamEVm004889t1	6.203	1.273	0.145	0.145	2.303	0.000	-	0.929	5.378	0.000	2.961	0.000
								0.113					
NRT1/ PTR 5.2	NonamEVm003809t1	179.135	24.963	0.139	0.152	2.846	0.000	0.110	0.976	10.321	0.000	7.585	0.000
NRT1/ PTR 5.2	NonamEVm013297t1	0.349	0.163	0.272	0.229	1.084	0.053	0.235	0.716	0.358	0.431	-0.491	0.326
NRT1/ PTR 5.2	NonamEVm003960t1	31.384	17.393	0.037	0.160	0.856	0.072	-	0.460	9.583	0.000	7.010	0.000
								1.718					

NRT1/ PTR 5.2	NonamEVm015708t1	0.243	0.212	0.238	0.156	0.185	0.814	0.569	0.440	0.032	0.961	0.417	0.492
NRT1/ PTR 5.4	NonamEVm004293t1	13.913	23.716	17.787	22.745	-0.769	0.000	-	0.004	-0.354	0.001	0.059	0.522
NRT1/ PTR 5.4	NonamEVm012900t1	0.357	0.456	0.887	1.810	-0.335	0.586	-	0.031	-1.291	0.009	-1.966	0.000
NRT1/ PTR 5.6	NonamEVm004115t1	0.687	1.189	1.672	1.109	-0.787	0.117	0.585	0.235	-1.276	0.006	0.096	0.829

Gene	RNAseq Accession	Average FPKM					Log2 Fold Change						
		25 DAI Nodule	18 DAI Nodule	25 DAI Root	18 DAI Root	Nodule 18 DAI to 25 DAI	FDR	Root 18 DAI to 25 DAI	FDR	Nodule 25 DAI to Root 25 DAI	FDR	Nodule 18 DAI to Root 18 DAI	FDR
NRT1/ PTR 5.6	NonamEVm017222t1	0.445	0.288	9.979	4.444	0.555	0.678	1.137	0.046	-4.429	0.000	-3.847	0.000
NRT1/ PTR 5.6	NonamEVm003885t1	0.315	0.293	6.284	4.824	0.150	0.834	0.373	0.260	-4.308	0.000	-4.085	0.000
NRT1/ PTR 5.8	NonamEVm004768t1	4.946	4.704	10.080	8.397	0.073	0.688	0.261	0.117	-1.027	0.000	-0.839	0.000
NRT1/ PTR 6.1	NonamEVm004485t1	0.037	0.093	0.199	0.269	-1.208	0.265	-0.459	0.488	-2.304	0.005	-1.555	0.014
NRT1/ PTR 6.2	NonamEVm004114t1	0.076	0.123	1.561	3.264	-0.733	0.437	-1.066	0.011	-4.291	0.000	-4.624	0.000
NRT1/ PTR 6.3	NonamEVm003915t1	0.560	0.156	37.042	21.390	1.866	0.062	0.790	0.042	-6.044	0.000	-7.120	0.000
NRT1/ PTR 6.3	NonamEVm009485t1	2.969	1.301	7.599	25.262	1.187	0.003	-1.727	0.000	-1.358	0.000	-4.272	0.000
NRT1/ PTR 6.4	NonamEVm004117t1	0.200	0.019	8.927	19.786	3.183	0.004	-1.151	0.000	-5.448	0.000	-9.782	0.000
NRT1/ PTR 7.1	NonamEVm004230t1	107.730	53.996	0.174	0.237	0.997	0.007	-0.317	0.819	9.261	0.000	7.947	0.000
NRT1/ PTR 7.3	NonamEVm003807t1	101.593	4.233	44.958	21.242	4.596	0.000	1.081	0.032	1.176	0.006	-2.339	0.000
NRT1/ PTR 7.3	NonamEVm023618t1	4.148	0.241	1.918	1.509	4.115	0.000	0.346	0.435	1.110	0.003	-2.660	0.000

NRT1/ PTR 7.3	NonamEVm003941t1	8.500	5.397	12.629	31.136	0.656	0.016	-1.300	0.000	-0.572	0.015	-2.528	0.000
NRT1/ PTR 7.3	NonamEVm004101t1	5.395	4.990	4.525	3.690	0.114	0.562	0.305	0.134	0.253	0.125	0.444	0.011
NRT1/ PTR 7.3	NonamEVm003938t1	0.220	0.188	0.276	0.412	0.199	0.804	-0.532	0.410	-0.326	0.567	-1.056	0.058
NRT1/ PTR 8.1	NonamEVm009025t1	0.311	0.109	0.181	0.255	1.464	0.131	-0.418	0.688	0.742	0.323	-1.140	0.184
NRT1/ PTR 8.1	NonamEVm004029t1	0.805	0.614	0.170	0.115	0.418	0.462	0.581	0.513	2.213	0.001	2.376	0.001
NRT1/ PTR 8.1	NonamEVm018959t1	0.208	0.096	0.170	0.149	1.015	0.474	0.185	0.919	0.240	0.828	-0.590	0.634
NRT1/ PTR 8.2	NonamEVm004312t1	18.759	9.694	25.660	30.605	0.947	0.005	-0.253	0.462	-0.452	0.097	-1.652	0.000
NRT1/ PTR 8.3	NonamEVm022266t1	6.380	2.780	6.091	8.763	1.181	0.000	-0.527	0.044	0.066	0.776	-1.642	0.000
NRT1/ PTR 8.3	NonamEVm004044t1	5.314	4.415	19.992	23.553	0.265	0.051	-0.237	0.072	-1.911	0.000	-2.413	0.000
NRT1/ PTR 8.3	NonamEVm007853t1	0.104	0.060	0.471	0.191	0.657	0.600	1.203	0.125	-2.084	0.009	-1.538	0.087
NRT1/ PTR 8.3	NonamEVm018616t1	0.000	0.000	0.661	0.107	0.000	1.000	2.362	0.063	-5.402	0.004	-3.040	0.111

Table 4a.8: Summary ureide permease DEGs in chickpea.

Data displayed as Log₂ fold change as a heatmap with corresponding average FPKM for each gene. Data presented for all nodule and root comparisons, 18 DAI (Early-Fixing) and 25 (Peak-Fixing). Genes in red were presented in chapter 2.

Gene	RNAseq Accession	Average FPKM				Log ₂ Fold Change							
		25 DAI Nodule	18 DAI Nodule	25 DAI Root	18 DAI Root	Nodule 18 DAI to 25 DAI	FDR	Root 18 DAI to 25 DAI	FDR	Nodule 25 DAI to Root 25 DAI	FDR	Nodule 18 DAI to Root 18 DAI	FDR
UPS1	NonamEVm012124t1	36.905	19.731	30.768	37.945	0.908	0.009	-0.301	0.415	0.262	0.366	-0.947	0.003
UPS1	NonamEVm025171t1	10.718	6.282	8.286	10.970	0.774	0.017	-0.401	0.231	0.369	0.174	-0.805	0.006
UPS2	NonamEVm008463t1	33.063	26.021	41.199	39.125	0.346	0.005	0.075	0.577	-0.317	0.004	-0.588	0.000

Appendix 4a: Single cell mRNA relative expression and cell count data

Table 4a.9: ScRNA cell cluster relative gene expression and Log2 relative expression.

Cell Cluster Relative Gene Expression

Gene	MIX	NP	Uic2	NF1	PI	NA1	UN1	NA2	Uic1	UN2	NF2	IF	VA
NRT2.1	1.00	1.14	1.00	1.73	1.29	1.00	1.00	1.06	1.00	1.00	1.90	1.00	1.00
AAP1	1.05	1.00	1.00	1.72	1.14	1.00	1.00	1.00	1.00	1.17	1.00	1.82	0.00
AAP2	1.07	4.22	3.04	1.09	1.45	1.32	1.14	2.09	1.51	1.15	1.24	1.07	2.14
AAP3	1.09	5.18	3.35	1.00	1.15	1.10	1.00	1.54	1.73	1.14	1.00	1.00	2.70
AAP7	1.00	1.00	1.33	0.00	1.50	0.00	0.00	1.33	1.00	0.00	0.00	0.00	0.00
AAP7.2	1.00	1.13	1.18	1.00	0.00	2.00	1.00	0.00	1.00	0.00	0.00	1.00	0.00
AAP8	1.00	1.29	1.00	0.00	2.00	0.00	0.00	0.00	0.00	0.00	0.00	1.00	0.00
AVT1A	1.00	1.00	1.00	1.00	1.50	1.00	0.00	1.00	1.00	0.00	1.00	0.00	1.50
AVT3C	1.06	2.06	2.37	1.05	1.19	1.45	1.00	1.89	1.39	1.00	1.00	1.11	1.50
AVT6A	1.15	6.22	10.35	1.45	1.73	1.33	1.22	1.54	2.74	1.22	1.47	1.50	3.15
AVT6C.1	1.00	1.12	1.27	1.20	1.00	1.00	1.00	1.00	1.50	1.00	1.00	0.00	1.00
AVT6C.2	1.04	1.72	1.52	1.06	1.25	1.17	1.00	1.54	1.18	1.31	1.00	1.10	1.86
CAT1	1.05	1.08	1.11	1.40	1.56	1.10	1.00	1.07	1.00	1.05	2.45	1.54	1.00
CAT2	1.00	1.10	1.00	1.00	1.00	1.00	1.00	1.00	1.00	1.00	0.00	1.00	1.00
At5g07050-2	1.11	24.02	1.10	1.06	1.10	1.00	2.18	1.09	1.13	1.00	1.00	1.00	1.00
At4g08290-1	1.00	10.00	1.00	1.00	0.00	0.00	1.00	0.00	0.00	0.00	0.00	0.00	0.00
At4g08300-1	1.06	27.98	1.23	1.17	1.07	1.00	2.57	1.00	1.00	1.00	1.25	1.00	1.00
At1g25270-2	1.00	3.14	1.50	1.00	0.00	1.00	1.17	0.00	1.00	0.00	0.00	0.00	0.00
At3g28050-2	1.00	1.47	1.23	2.00	1.00	1.00	1.00	1.00	1.00	1.25	1.29	1.00	1.00
At2g37460	1.04	1.11	1.00	2.01	1.49	1.00	1.00	1.00	1.00	1.11	1.31	1.20	1.00

At1g68170-1	1.00	3.14	1.50	1.00	0.00	1.00	1.17	0.00	1.00	0.00	0.00	0.00	0.00
At1g68170-2	1.00	1.21	1.33	1.07	1.14	1.00	1.25	1.09	1.11	1.00	1.33	1.00	1.00
At1g68170-3	1.00	22.58	1.00	1.00	0.00	0.00	1.12	1.00	1.00	0.00	0.00	0.00	1.00
BT1-2	1.03	1.64	1.77	1.21	1.11	1.10	1.00	1.00	1.12	1.00	1.00	1.18	1.00
BT1-3	1.02	1.20	1.11	1.15	1.00	1.00	1.00	1.13	1.00	1.14	1.17	1.09	1.00
MTCC-1	1.01	1.25	1.15	1.13	1.30	1.00	1.00	1.25	1.00	1.22	1.17	1.13	1.00
MTCC-6	1.10	4.91	3.76	1.38	1.81	1.45	1.18	1.42	1.32	1.50	2.00	1.35	2.14
MTCC-7	1.01	1.73	1.19	1.16	1.27	1.21	1.00	1.31	1.12	1.11	1.20	1.00	1.00
MTCC-9	1.08	1.56	1.17	1.28	1.48	1.30	1.03	1.40	1.17	1.07	1.05	1.20	1.00
MTCC-10	1.10	4.76	2.08	1.35	1.92	1.64	1.00	2.16	2.58	1.18	1.46	1.75	1.34
MTCC-11	1.36	6.59	4.27	3.34	2.86	1.80	1.30	2.42	2.59	1.64	1.75	2.51	1.56

Cell Cluster Relative Gene Expression (Log₂)

Gene	MIX	NP	UiC2	NF1	PI	NA1	UN1	NA2	UiC1	UN2	NF2	IF	VA
NRT2.1	0.00	0.19	0.00	0.79	0.36	0.00	0.00	0.08	0.00	0.00	0.92	0.00	0.00
AAP1	0.07	0.00	0.00	0.78	0.19	0.00	0.00	0.00	0.00	0.22	0.00	0.86	0.00
AAP2	0.10	2.08	1.60	0.12	0.54	0.40	0.19	1.07	0.60	0.20	0.30	0.10	1.10
AAP3	0.12	2.37	1.74	0.00	0.21	0.14	0.00	0.63	0.79	0.19	0.00	0.00	1.43
AAP7	0.00	0.00	0.42	0.00	0.58	0.00	0.00	0.42	0.00	0.00	0.00	0.00	0.00
AAP7.2	0.00	0.18	0.24	0.00	0.00	1.00	0.00	0.00	0.00	0.00	0.00	0.00	0.00
AAP8	0.00	0.37	0.00	0.00	1.00	0.00	0.00	0.00	0.00	0.00	0.00	0.00	0.00
AVT1A	0.00	0.00	0.00	0.00	0.58	0.00	0.00	0.00	0.00	0.00	0.00	0.00	0.58
AVT3C	0.08	1.04	1.24	0.07	0.25	0.54	0.00	0.92	0.47	0.00	0.00	0.14	0.58
AVT6A	0.20	2.57	3.27	0.54	0.79	0.42	0.28	0.62	1.45	0.29	0.55	0.58	1.66
AVT6C.1	0.00	0.16	0.34	0.26	0.00	0.00	0.00	0.00	0.58	0.00	0.00	0.00	0.00
AVT6C.2	0.06	0.78	0.61	0.08	0.32	0.23	0.00	0.62	0.24	0.39	0.00	0.14	0.90
CAT1	0.07	0.11	0.14	0.49	0.64	0.14	0.00	0.10	0.00	0.07	1.29	0.63	0.00
CAT2	0.00	0.13	0.00	0.00	0.00	0.00	0.00	0.00	0.00	0.00	0.00	0.00	0.00
At5g07050-2	0.15	0.51	0.13	0.09	0.14	0.00	1.13	0.13	0.17	0.00	0.00	0.00	0.00
At4g08290-1	0.00	3.32	0.00	0.00	0.00	0.00	0.00	0.00	0.00	0.00	0.00	0.00	0.00
At4g08300-1	0.08	1.84	0.30	0.22	0.10	0.00	0.98	0.00	0.00	0.00	0.32	0.00	0.00
At1g25270-2	0.00	1.65	0.58	0.00	0.00	0.00	0.22	0.00	0.00	0.00	0.00	0.00	0.00

At3g28050-2	0.00	0.55	0.30	1.00	0.00	0.00	0.00	0.00	0.00	0.32	0.36	0.00	0.00
At2g37460	0.05	0.15	0.00	1.01	0.58	0.00	0.00	0.00	0.00	0.15	0.39	0.26	0.00
At1g68170-1	0.00	1.65	0.58	0.00	0.00	0.00	0.22	0.00	0.00	0.00	0.00	0.00	0.00
At1g68170-2	0.00	0.28	0.41	0.10	0.19	0.00	0.32	0.13	0.15	0.00	0.42	0.00	0.00
At1g68170-3	0.00	3.39	0.00	0.00	0.00	0.00	0.16	0.00	0.00	0.00	0.00	0.00	0.00
BT1-2	0.04	0.72	0.82	0.28	0.14	0.14	0.00	0.00	0.16	0.00	0.00	0.24	0.00
BT1-3	0.03	0.26	0.15	0.20	0.00	0.00	0.00	0.17	0.00	0.19	0.22	0.13	0.00
MTCC-1	0.02	0.32	0.20	0.17	0.37	0.00	0.00	0.32	0.00	0.29	0.22	0.17	0.00
MTCC-6	0.14	2.29	1.91	0.47	0.86	0.53	0.24	0.51	0.40	0.58	1.00	0.43	1.09
MTCC-7	0.01	0.79	0.26	0.22	0.35	0.27	0.00	0.39	0.16	0.14	0.26	0.00	0.00
MTCC-9	0.11	0.64	0.23	0.36	0.57	0.37	0.05	0.49	0.23	0.10	0.07	0.27	0.00
MTCC-10	0.14	2.25	1.06	0.43	0.94	0.72	0.00	1.11	1.37	0.24	0.55	0.81	0.42
MTCC-11	0.44	2.70	2.09	1.74	1.52	0.85	0.38	1.27	1.38	0.71	0.81	1.33	0.64
AAP6.2	0.02	2.18	1.11	0.11	0.00	0.23	0.00	0.49	0.75	0.00	0.14	0.26	0.58

Table 4a.10: ScRNA cell cluster cell count and square root cell count.

Gene	Cell Cluster Total Cell Count												
	MIX	NP	Uic2	NF1	PI	NA1	UN1	NA2	Uic1	UN2	NF2	IF	VA
NRT2.1	41	21	6	11	7	7	6	17	2	5	39	4	2

AAP1	96	18	9	166	28	6	6	9	9	6	5	44	0
AAP2	314	631	324	47	77	90	43	128	68	27	17	28	56
AAP3	145	492	128	22	13	40	12	35	44	7	4	9	40
AAP7	1	2	3	0	2	0	0	3	1	0	0	0	0
AAP7.2	4	52	38	2	0	1	2	0	1	0	0	1	0
AAP8	5	17	11	0	1	0	0	0	0	0	0	1	0
AVT1A	4	12	10	1	4	1	0	3	4	0	1	0	2
AVT3C	71	354	174	21	32	22	4	57	36	6	9	19	8
AVT6A	645	739	631	178	130	78	79	87	115	76	60	76	79
AVT6C.1	12	17	56	5	1	2	1	3	2	4	2	0	1
AVT6C.2	193	353	145	36	44	23	13	72	28	26	6	20	36
CAT1	199	51	38	131	105	10	20	14	10	21	42	59	4
CAT2	16	52	23	4	7	2	2	8	2	2	0	2	2
At5g07050-2	102	55	21	16	10	10	169	11	8	3	9	7	1
At4g08290-1	7	7	1	1	0	0	11	0	0	0	0	0	0
At4g08300-1	107	49	35	18	14	5	205	4	13	6	4	3	4
At1g25270-2	2	14	4	1	0	1	6	0	2	0	0	0	0
At3g28050-2	16	94	43	1	3	3	3	11	7	4	7	2	3
At2g37460	196	53	29	207	98	22	22	14	12	27	26	51	7
At1g68170-1	2	14	4	1	0	1	6	0	2	0	0	0	0

At1g68170-2	82	90	79	29	21	4	4	22	9	6	3	11	3
At1g68170-3	7	12	2	1	0	0	17	2	1	0	0	0	1
BT1-2	79	163	95	33	19	10	3	10	17	7	7	11	8
BT1-3	42	101	28	33	15	4	2	8	5	7	6	11	3
MTCC-1	68	171	54	32	27	14	7	20	9	9	6	8	3
MTCC-6	585	432	282	92	102	85	55	45	62	54	45	20	59
MTCC-7	108	212	36	31	62	29	8	35	17	19	5	13	3
MTCC-9	294	248	111	106	116	61	29	70	29	27	20	44	12
MTCC-10	502	597	279	117	142	101	40	129	77	38	39	69	38
MTCC-11	1556	905	562	410	282	224	164	215	185	139	122	164	71

Cell Cluster Cell Count (Square Root)

Gene	MIX	NP	UiC2	NF1	PI	NA1	UN1	NA2	UiC1	UN2	NF2	IF	VA
NRT2.1	6.40	4.58	2.45	3.32	2.65	2.65	2.45	4.12	1.41	2.24	6.24	2.00	1.41
AAP1	9.80	4.24	3.00	12.88	5.29	2.45	2.45	3.00	3.00	2.45	2.24	6.63	0.00
AAP2	17.72	25.12	18.00	6.86	8.77	9.49	6.56	11.31	8.25	5.20	4.12	5.29	7.48
AAP3	12.04	22.18	11.31	4.69	3.61	6.32	3.46	5.92	6.63	2.65	2.00	3.00	6.32
AAP7	1.00	1.41	1.73	0.00	1.41	0.00	0.00	1.73	1.00	0.00	0.00	0.00	0.00
AAP7.2	2.00	7.21	6.16	1.41	0.00	1.00	1.41	0.00	1.00	0.00	0.00	1.00	0.00

AAP8	2.24	4.12	3.32	0.00	1.00	0.00	0.00	0.00	0.00	0.00	0.00	1.00	0.00
AVT1A	2.00	3.46	3.16	1.00	2.00	1.00	0.00	1.73	2.00	0.00	1.00	0.00	1.41
AVT3C	8.43	18.81	13.19	4.58	5.66	4.69	2.00	7.55	6.00	2.45	3.00	4.36	2.83
AVT6A	25.40	27.18	25.12	13.34	11.40	8.83	8.89	9.33	10.72	8.72	7.75	8.72	8.89
AVT6C.1	3.46	4.12	7.48	2.24	1.00	1.41	1.00	1.73	1.41	2.00	1.41	0.00	1.00
AVT6C.2	13.89	18.79	12.04	6.00	6.63	4.80	3.61	8.49	5.29	5.10	2.45	4.47	6.00
CAT1	14.11	7.14	6.16	11.45	10.25	3.16	4.47	3.74	3.16	4.58	6.48	7.68	2.00
CAT2	4.00	7.21	4.80	2.00	2.65	1.41	1.41	2.83	1.41	1.41	0.00	1.41	1.41
At5g07050-2	10.10	7.42	4.58	4.00	3.16	3.16	13.00	3.32	2.83	1.73	3.00	2.65	1.00
At4g08290-1	2.65	2.65	1.00	1.00	0.00	0.00	3.32	0.00	0.00	0.00	0.00	0.00	0.00
At4g08300-1	10.34	7.00	5.92	4.24	3.74	2.24	14.32	2.00	3.61	2.45	2.00	1.73	2.00
At1g25270-2	1.41	3.74	2.00	1.00	0.00	1.00	2.45	0.00	1.41	0.00	0.00	0.00	0.00
At3g28050-2	4.00	9.70	6.56	1.00	1.73	1.73	1.73	3.32	2.65	2.00	2.65	1.41	1.73
At2g37460	14.00	7.28	5.39	14.39	9.90	4.69	4.69	3.74	3.46	5.20	5.10	7.14	2.65
At1g68170-1	1.41	3.74	2.00	1.00	0.00	1.00	2.45	0.00	1.41	0.00	0.00	0.00	0.00
At1g68170-2	9.06	9.49	8.89	5.39	4.58	2.00	2.00	4.69	3.00	2.45	1.73	3.32	1.73
At1g68170-3	2.65	3.46	1.41	1.00	0.00	0.00	4.12	1.41	1.00	0.00	0.00	0.00	1.00
BT1-2	8.89	12.77	9.75	5.74	4.36	3.16	1.73	3.16	4.12	2.65	2.65	3.32	2.83
BT1-3	6.48	10.05	5.29	5.74	3.87	2.00	1.41	2.83	2.24	2.65	2.45	3.32	1.73
MTCC-1	8.25	13.08	7.35	5.66	5.20	3.74	2.65	4.47	3.00	3.00	2.45	2.83	1.73

MTCC-6	24.19	20.78	16.79	9.59	10.10	9.22	7.42	6.71	7.87	7.35	6.71	4.47	7.68
MTCC-7	10.39	14.56	6.00	5.57	7.87	5.39	2.83	5.92	4.12	4.36	2.24	3.61	1.73
MTCC-9	17.15	15.75	10.54	10.30	10.77	7.81	5.39	8.37	5.39	5.20	4.47	6.63	3.46
MTCC-10	22.41	24.43	16.70	10.82	11.92	10.05	6.32	11.36	8.77	6.16	6.24	8.31	6.16
MTCC-11	39.45	30.08	23.71	20.25	16.79	14.97	12.81	14.66	13.60	11.79	11.05	12.81	8.43

Appendix 5A

Appendix 5a.1: Primers used for yeast cloning pipeline and PCR setup conditions

Table 5a.1: Primers to amplify chickpea amino acid genes, primer Tm °C, annealing temp °C and product size (bp).

Gene	Primer Name	Sequence (5'-3')	Tm (°C)	Anneal at (°C) Q5*	Product size (bp)
AAP6.2	AAP6_2_Fwd	ATGGCACAGAGTAGC TTCTC	68	67	1407
	AAP6_2_Rev	TCAATTAGTCTGGAA GGGC	66		
AVT6A	AVT6A_Fwd	ATGACAATTGGTAATC TTGC	62	63	1398
	AVT6A_Rev	TCATTTCGCGGAAGT TTTG	68		
AVT6C.2	AVT6C_2_Fwd	ATGTCGCCGTCTGCC GGAG	78	65	1308
	AVT6C_2_Rev	TTATGACTTGCTACTT AAAGCATTG	64		
CAT1	CAT1_Fwd	ATGAGTAATGAAAAC ACAGAAGG	64	65	1761
	CAT1_Rev	CTAATTTGACTTTCT TCCTCTCC	64		
CAT2	CAT2_Fwd	ATGGGTGTTTCGGTT GG	68	62	1839
	CAT2_Rev	TTAAGTTTCAGCTTCT TGAC	61		
UmamiT9	UmamiT9_Fwd	ATGGCCTCAGAAAAT TCAAAC	65	64	1212
	UmamiT9_Rev	TCAAGCATTGTTTGT TGG	63		

UmamiT12	UmamiT12_Fwd	ATGACAATCATGATGG AGAGG	66	63	1056
	UmamiT12_Rev	CTAATTCGGTAAAACA GGTTC	62		
UmamiT18	UmamiT18_Fwd	ATGACGGATGTATGTG ATAAAATG	64	64	1152
	UmamiT18_Rev	TTATGGTTTGACATTT TTTCCTG	63		
UmamiT20	UmamiT20_Fwd	ATGGGTGGACTAACA TATTGTG	66	66	1179
	UmamiT20_Rev	CTATGTGCTTGATCCT TTGAC	65		
UmamiT23.1	UmamiT23_1_Fwd	ATGGTTAAATTATTGG ATGTTAAAG	60	61	1176
	UmamiT23_1_Rev	TCAAGTAGTGTTGCC ATC	64		
UmamiT41	UmamiT41_Fwd	ATGGCAATAAGACATT GGTAC	64	64	1077
	UmamiT41_Rev	TCAACTCTGATCAGTT TTATAGC	63		

Table 5a.2: PCR setup to amplify amino acid transporter gene sequences using Q5 high-fidelity polymerase.

Reaction Setup	Volumes (μ l)	
	x1	x13
5x Q5 Reaction Buffer	5	65
10 mM dNTPs	0.5	6.5
10 μ M F/R Primers	2.5	32.5
Template cDNA	1	13
Q5 Polymerase	0.25	3.25
H ₂ O To 25 μ l	15.75	240.75
Total Volume	25.0	325

Step	Temp (°C)	Time (Mins)	Cycles
Initial Denaturation	98	0.30	x1
Gradient Annealing	98	0.10	x30
	61-67	0.30	
	72	1.00	
Final Extension	72	5.00	x1

Table 5a.3: PCR Primers to anneal attB sites in one overhanging PCR step, using during pDR196 cloning. Red text indicates primer overhang.

Gene	Primer Name	Sequence (5'-3')	Tm (°C)	Anneal at (°C) *Phusion	Gradient Anneal at (°C)
AAP6.2	AAP6_2_attbF	GGGGACAAGTTTGTACAAAAA AGCAGGCTGGATGGCACAGAG TAGC	63	61	56
	AAP6_2_attbR	GGGGACCACTTTGTACAAGAA AGCTGGGTGTCAATTAGTCTGG AAGGG	66		
AVT6A	AVT6A_attbF	GGGGACAAGTTTGTACAAAAA AGCAGGCTGGATGACAATTGGT AATCTTG	58	59	54
	AVT6A_attbR	GGGGACCACTTTGTACAAGAA AGCTGGGTGTCATTCGCGCGAA GTTTTG	68		
AVT6C.2	AVT6C_2_attbF	GGGGACAAGTTTGTACAAAAA AGCAGGCTGGATGTCGCCGTCT GCCGG	77	61	56
	AVT6C_2_attbR	GGGGACCACTTTGTACAAGAA AGCTGGGTGTTATGACTTGCTA CTTAAAGC	62		
CAT1	CAT1_attbF	GGGGACAAGTTTGTACAAAAA AGCAGGCTGGATGAGTAATGA AAACAC	54	54	50
	CAT1_attbR	GGGGACCACTTTGTACAAGAA AGCTGGGTGCTAATTTGACTTT CTTCC	56		
CAT2	CAT2_attbF	GGGGACAAGTTTGTACAAAAA AGCAGGCTGGATGGGTGTTTC GG	60	57	52
	CAT2_attbR	GGGGACCACTTTGTACAAGAA AGCTGGGTGTTAAGTTTCAGCT TCTTG	58		
UmamiT9	UmamiT9_attbF	GGGGACAAGTTTGTACAAAAA AGCAGGCTGGATGGCCTCAGA AAATTC	61	60	55

	UmamiT9_attbR	GGGGACCACTTTGTACAAGAA AGCTGGGTGTC AAGCATTTGTT TGTTG	63		
UmamiT12	UmamiT12_attbF	GGGGACAAGTTTGTACAAAAA AGCAGGCTGGATGACAATCATG ATGGAG	60	58	53
	UmamiT12_attbR	GGGGACCACTTTGTACAAGAA AGCTGGGTGCTAATTCGGTAAA ACAGG	59		
UmamiT18	UmamiT18_attbF	GGGGACAAGTTTGTACAAAAA AGCAGGCTGGATGACGGATGT ATGTG	60	58	53
	UmamiT18_attbR	GGGGACCACTTTGTACAAGAA AGCTGGGTGTTATGGTTTGACA TTTTTC	57		
UmamiT20	UmamiT20_attbF	GGGGACAAGTTTGTACAAAAA AGCAGGCTGGATGGGTGGACT AAC	58	56	51
	UmamiT20_attbR	GGGGACCACTTTGTACAAGAA AGCTGGGTGCTATGTGCTTGAT CC	57		
UmamiT23.1	UmamiT23_1_attbF	GGGGACAAGTTTGTACAAAAA AGCAGGCTGGATGGTTAAATTA TTGGATG	55	56	51
	UmamiT23_1_attbR	GGGGACCACTTTGTACAAGAA AGCTGGGTGTC AAGTAGTGTTG CCATC	64		
UmamiT41	UmamiT41_attbF	GGGGACAAGTTTGTACAAAAA AGCAGGCTGGATGGCAATAAG ACATTGG	61	61	56
	UmamiT41_attbR	GGGGACCACTTTGTACAAGAA AGCTGGGTGTC AACTCTGATCA GTTTTATAG	60		

Table 5a.4: PCR setup to anneal attB cloning sites using Phusion polymerase to previously amplified amino acid transporter gene sequences as template.

Reaction Setup	Volumes (μ l)	
	x1	x13
5x Phusion HF Buffer	4	48
10 mM dNTPs	0.4	4.8
10 μ M F/R Primers	1	12
Template cDNA	3	36
Phusion Polymerase	0.2	2.4
H ₂ O To 25 μ l	16.4	196.8
Total Volume	25.0	325

Step	Temp (°C)	Time (Mins)	Cycles
Initial Denaturation	98	0.30	x1
Gradient Annealing	98	0.10	X40
	56-50	0.30	
	72	1.00	
Final Extension	72	10.00	x1

Table 5a.5: PCR primers for attB site annealing using two PCR steps for cloning into pYESdest52. Red text indicated primer overhang.

Gene	Primer Name	Sequence (5'-3')	Tm (°C)	Anneal at (°C) *Phusion	Gradient Anneal at (°C)
AAP3	AAP3_F	ATGGTTGAGAACAATGGTCACC ACC	67	66	61
	AAP3_R	TCAATAGGTGGTTTTGAATGGC TT	63		
	AAP3_Overlap_F	CAAAAAAGCAGGCTGGATGGT TGAGAACAATGG	53		
	AAP3_Overlap_R	CAAGAAAGCTGGGTGTCATAG GTGGTTTTG	49	53	48
AAP6	AAP6_F	ATGCACATAGAAGCTCAAG	57	61	56
	AAP6_R	TTATTGTTCTCCTTTGAAGGG	57		
	AAP6_Overlap_F	TACAAAAAAGCAGGCTGGATG CACATAGAAGCTC	57	59	54
	AAP6_Overlap_R	TACAAGAAAGCTGGGTGTTATT GTTCTCCTTTGAAG	55		
AVT6C	AVT6C_F	ATGAAAACACAAAGCGAT	55	55	50
	AVT6C_R	CTAGGTACTAAAAAGCTTAT	51		
	AVT6C_Overlap_F	TACAAAAAAGCAGGCTGGATG AAAACACAAAGCG	57	60	55
	AVT6C_Overlap_R	ACAAGAAAGCTGGGTGCTAGG TACTAAAAAGCT	56		
MTCC11	MTCC11_F	ATGGTTGATCAGGTTTCAGC	59	61	56
	MTCC11_R	TCAGGCATTTTATTCTTGAATA AG	57		
	MTCC11_Overlap_F	TACAAAAAAGCAGGCTGGATG GTTGATCAGGTTTC	57		

		TACAAGAAAGCTGGGTGCAG	59	54
	MTCC11_Overlap_R	GCATTTTATTCTTG	55	
Attb site	attB1_F	GGGGACAAGTTTGTACAAAAA	51	
		AGCAGGCTGG		55
	attB1_R	GGGGACCACTTTGTACAAGAA	53	50
		AGCTGGGTG		

Appendix 5a.2: PCR amplification of amino acid transporters

Chickpea amino acid gene sequences were successfully amplified from nodule cDNA using PCR run with Phusion high fidelity polymerase via primers designed (Table 5a.1) to amplify the gene coding region by annealing at the start and stop codons (Figure 5a.1A). Gene fragments appeared at the respective approximate sizes (Table 5a.1) on the gel with minor size discrepancy compared to the DNA ladder (Figure 5a.1A). However, the size patterns of each linear DNA fragment on the agarose gel matches the respected sizes differences of each gene. For example, CAT1 and CAT2 in lanes five & six were larger than AVT6C in lane four. The PCR was repeated with an annealing temperature 5°C to reduce the occurrence of unintended off target amplified products on the agarose gel (Figure 5a.1B). Amplified genes were subsequently gel purified using the Wizard® SV Gel and PCR Clean-Up System to remove any residual primer, enzyme and dNTPs which may interfere with downstream PCR steps.

Following gene amplification, attB cloning sites adaptors were annealed to the 5' and 3' ends of the linear template via overhanging primers containing the attB sequence. Due to the large length of the required overhanging primers to anneal the attB site, the PCR was very inefficient at amplifying the desired product requiring 40 cycles to generate enough product after PCR purification for BP Gateway® cloning. Similarly high annealing temperatures, some cases over 60°C (Table 5a.3) was required, as there was little room for primer binding site optimisation. Indeed, there was large primer dimer because of the inefficient PCR, present at the bottom of the agarose gel (Figure 5a.2). This was subsequently removed through a gel purification after excision of the desired band using the Wizard® SV Gel and PCR Clean-Up System prior to performing the BP cloning reaction into pDONR. As seen in the agarose gel in Figure 5a.3, whereby secondary off target bands and primer dimer were removed.

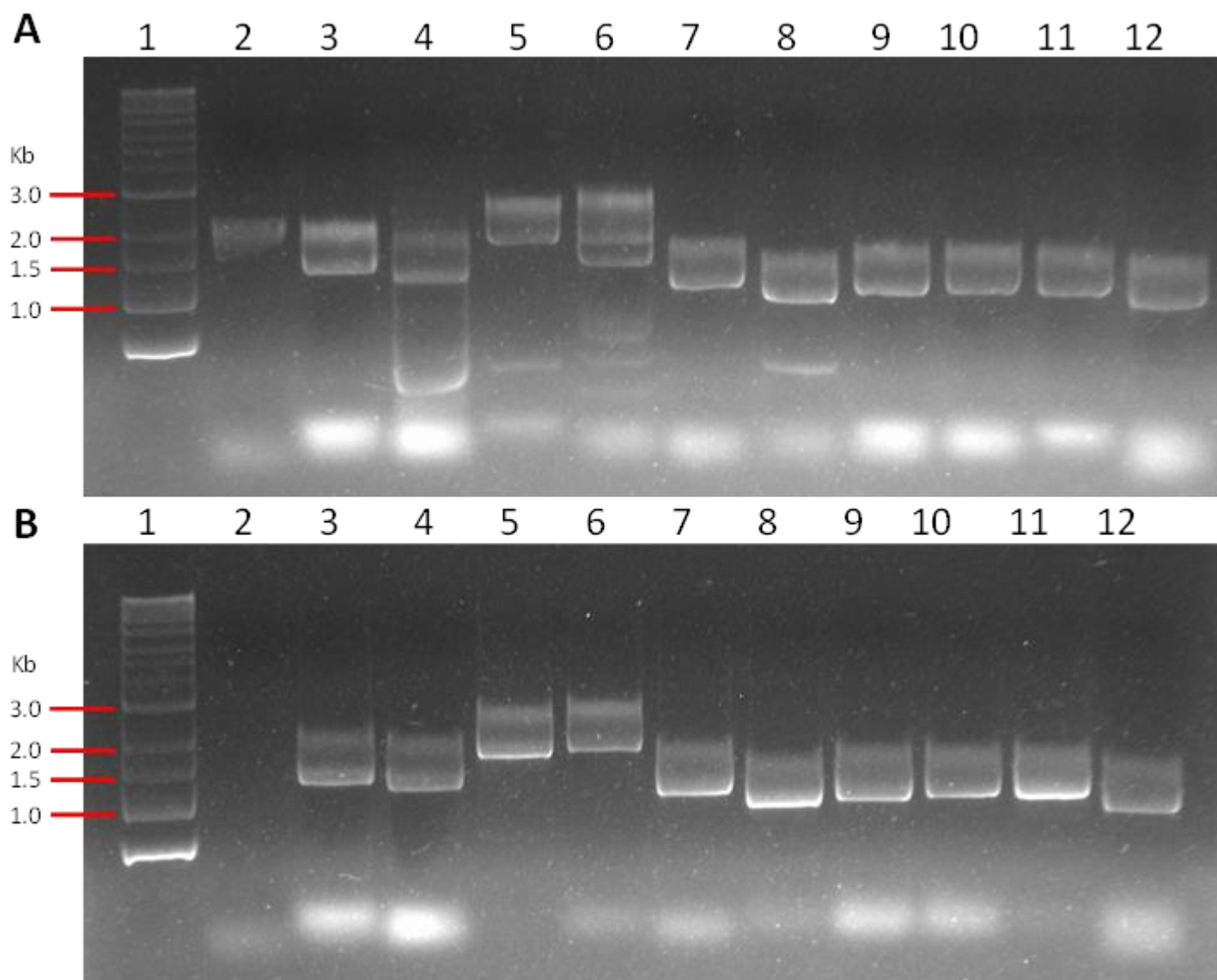


Figure 5a.1: Agarose gel electrophoresis of amino acid transporter gene PCR amplifications.

Performed using chickpea nodule cDNA as template with gene specific primers (Table 5a.1) designed to amplify gene coding region, designed using SnapGene software. PCR run with Phusion high fidelity polymerase. Product run on a 1% agarose gel visualised with GelRed and run for ~1 hour. PCR run with annealing steps at two different respective temperatures separated by 5 °C for each gene; (A) PCR annealing steps 5 °C lower than (B) (Table 5a.2). Lane 1: NEB 1 kb DNA Ladder; Lane 2: *CaAAP6.2*; Lane 3: *CaAVT6A*; Lane 4: *CaAVT6C.2*; Lane 5: *CaCAT1*; Lane 6: *CaCAT2*; Lane 7: *CaUmamiT9*; Lane 8: *CaUmamait12*; Lane 9: *CaUmamiT18*; Lane 10: *CaUmamiT20*; Lane 11: *CaUmamiT23.1*; Lane 12: *CaUmamiT41*.

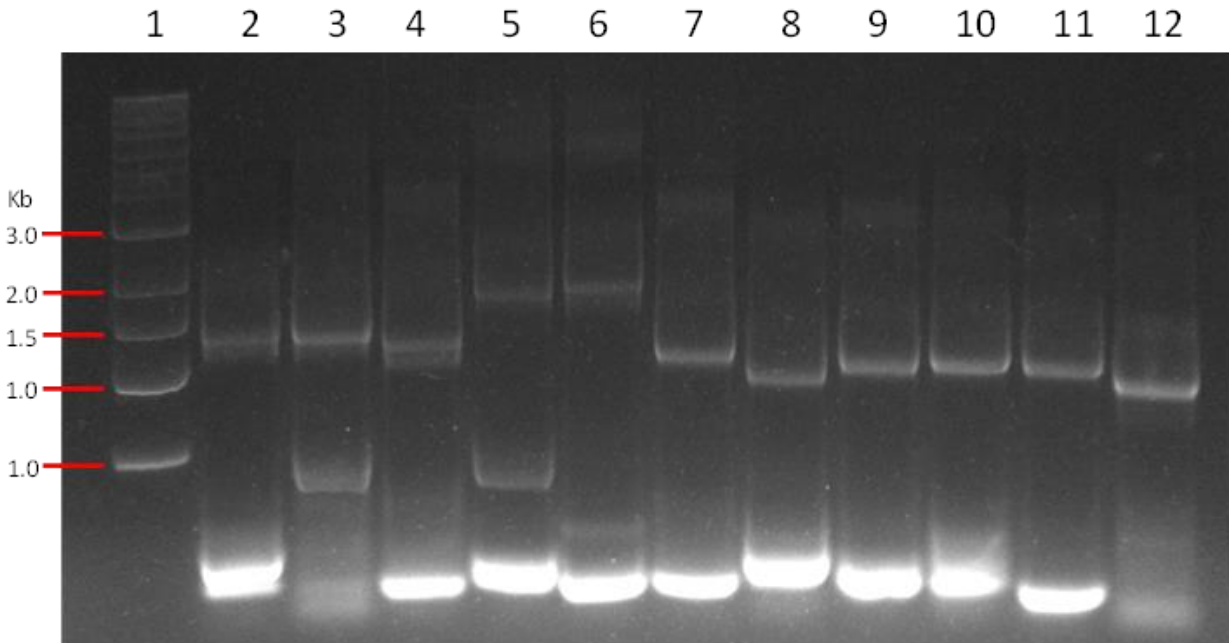


Figure 5a.2: Agarose gel electrophoresis of PCR step, annealing attB cloning sites to amino acid transporter gene sequences.

PCR performed using previously amplified amino acid transporter gene sequences as template and primers with overhanging attB cloning sites. PCR run with Phusion high fidelity polymerase. Product run on a 1% agarose gel visualised with GelRed and run for ~1 hour. Lane 1: NEB 1 kb DNA ladder; Lane 2: *CaAAP6.2*; Lane 3: *CaAVT6A*; Lane 4: *CaAVT6C.2*; Lane 5: *CaCAT1*; Lane 6: *CaCAT2*; Lane 7: *CaUmamiT9*; Lane 8: *CaUmamiT12*; Lane 9: *CaUmamiT18*; Lane 10: *CaUmamiT20*; Lane 11: *CaUmamiT23.1*; Lane 12: *CaUmamiT41*.

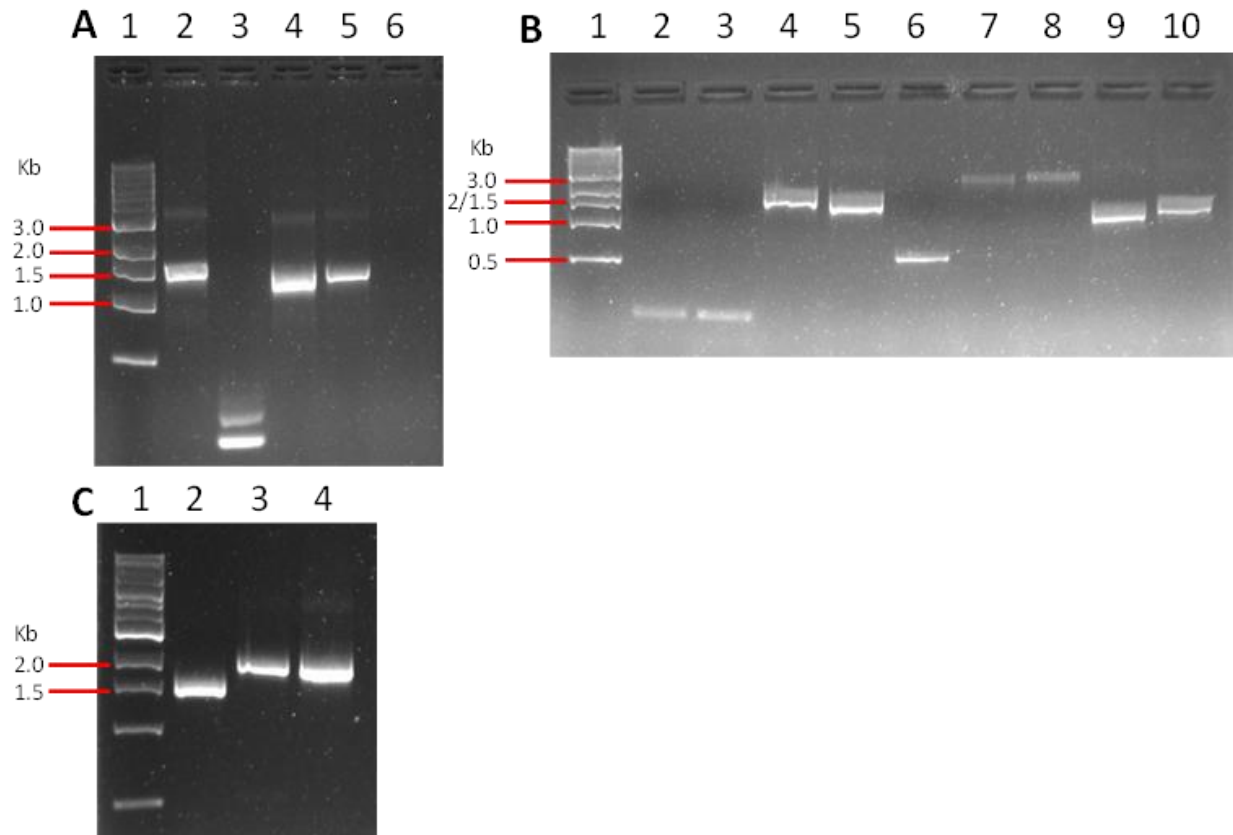


Figure 5a.3: Agarose gel electrophoresis of gel purified attB sites annealed to chickpea amino acid transporter gene sequences.

Purification performed using Wizard® SV Gel and PCR Clean-Up System. PCR run with Phusion high fidelity polymerase. Product run on a 1% agarose gel visualised with GelRed and run for ~1 hour. **(A)** Lane 1: NEB 1 kb DNA ladder; Lane 2: *CaUmamiT9*; Lane 3: *CaUmamiT12*; Lane 4: *CaUmamiT18*; Lane 5: *CaUmamiT20*; Lane 6: *CaUmamiT23.1*. **(B)** Lane 1: NED 1 kb DNA ladder; Lane 2: *CaAAP6.2*; Lane 3: *CaAAP6.2*; Lane 4: *CaAVT6A*; Lane 5: *CaAVT6C.2*; Lane 6: *CaCAT1*; Lane 7: *CaCAT1*; Lane 8: *CaCAT2*; Lane 9: *CaUmamiT12*; Lane 10: *CaUmamiT23.1*. **(C)** Lane 1: NEB 1 kb DNA ladder; Lane 2: *CaAAP6.2*; Lane 3: *CaCAT1*; Lane 4: *CaCAT2*.

Appendix 5a.3: BP Gateway® cloning of chickpea transporters into pDONR

The BP clonase cloning reaction to integrate the chickpea amino acid genes with attB sites into pDONR was setup as Table 5a.6, as per the Invitrogen Gateway BP Clonase II Enzyme Mix manual (2.7.4). Reactions were left at 25°C overnight followed by 1 µl proteinase K solution (2 µg/µl) incubated for 10 minutes at 37°C to terminate the reaction. The total pDONR recombination reaction (6 µl) was then transformed into inhouse made chemical-competent DH5α cells (2.1.6), via heat-shock transformation and spread-plated on kanamycin selection agar media (2.1.8). Successful recombination of amino acid genes into the pDONR plasmid between the attB sites will remove the lethal *ccdB* gene, yielding transformants harbouring CaAA genes.

Successful recombination of CaAA genes into pDONR was observed after the appearance of colonies in kanamycin selection media. Colony purification using the Wizard® Plus SV Minipreps DNA Purification System and subsequently visualised on an agarose gel showed the appearance of supercoiled plasmid likely harbouring, *CaUmamiT9* colony 1 (C1) & C2, *CaUmamiT18* C1 & C2 and *CaUmamiT41* in Figure 5a.4A; *CaAVT6A* and *CaAVT6C* in Figure 5a.4B; *CaUmamiT9* and two additional colonies for *CaUmamiT20* in Figure 5a.4C. Sanger sequencing using m13 forward and reverse primers flanking the insert region also confirmed the presence of *CaAVT6A*, *CaAVT6C*, *CaUmamiT9*, *CaUmamiT18* and *CaUmamiT20* (Figures 3a.5 – 3a.9). *CaAAP6*-pDNOR was successfully sequenced in the following section, Figure 5a.15, for LR recombination into firstly pYESdest52 prior to pDR196 here. Whereas *CaUmamiT41*-pDONR was not sequenced due to time constraints but was still attempted in downstream LR recombination into pDR196.

Table 5a.6: BP recombination reaction setup to clone amino acid genes into the pDONR entry plasmid.

Gene	Bp Length w/attb Sites	ng/μl After Purification	PCR Templated Added (15-150 ng)	pDONR Added (150 ng)	BP Clonase	TE (pH 8) to final vol. of 5μl
AAP6	1469	15	1.6	0.65	1	1.7
AVT6A	1460	15	1.6	0.65	1	1.7
AVT6C	1370	18	1.3	0.65	1	2.1
CAT1	1823	25	1.2	0.65	1	2.1
CAT2	1901	25	1.3	0.65	1	2.1
UMAMIT9	1274	12	1.8	0.65	1	1.6
umamit12	1118	12	1.5	0.65	1	1.8
umamit18	1214	12	1.7	0.65	1	1.7
umamit20	1241	20	1.0	0.65	1	2.3
umamit23	1238	10	2.0	0.65	1	1.3
umamit41	1139	70	0.3	0.65	1	3.1

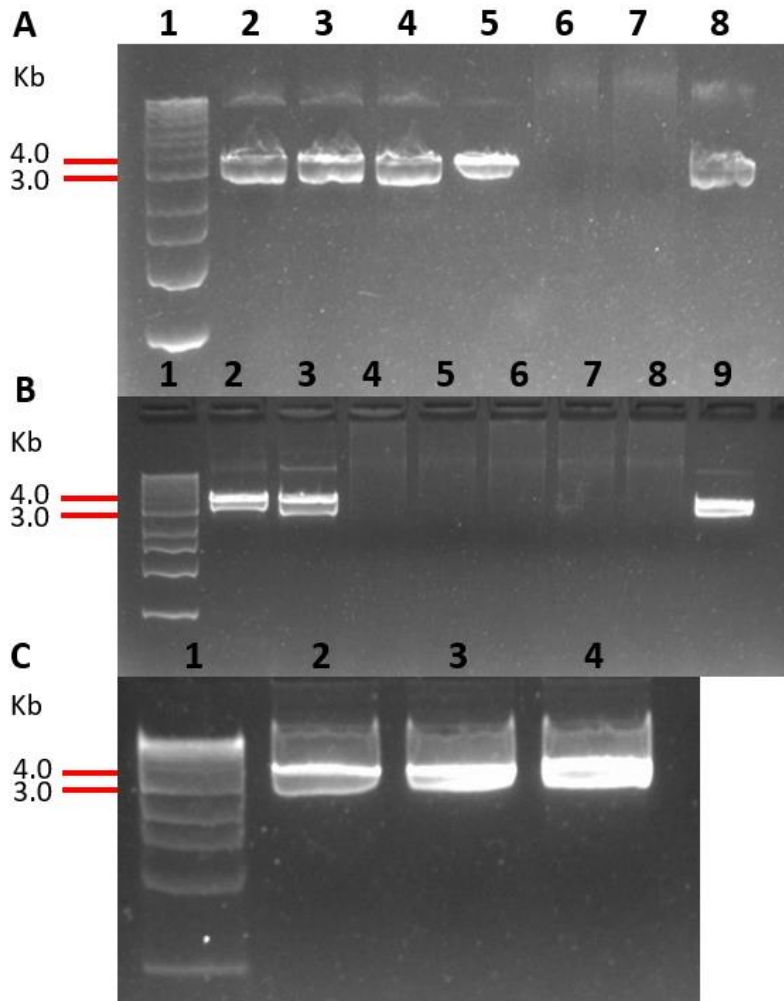


Figure 5a.4: Agarose gel electrophoresis of purified pDONR entry plasmids harbouring chickpea amino acid transporter genes inserted via BP clonase.

Purification performed using Wizard® Plus SV Minipreps DNA Purification System. BP clonase reaction of chickpea amino acid genes with annealed attB sites into the pDONR entry plasmids. Product run on a 1% agarose gel visualised with GelRed Product run on a 1% agarose gel visualised with GelRed and run for ~1 hour. **(A)** Lane 1: Promega 1 kb DNA ladder; Lane 2: *CaUmamiT9*-pDONR C1; Lane 3: *CaUmamiT9*-pDONR C2; Lane 4: *CaUmamiT18*-pDONR C1; Lane 5: *CaUmamiT18*-pDONR C2; Lane 6: *CaUmamiT20*-pDONR C1; Lane 7: *CaUmamiT20*-pDONR C1; Lane 8: *CaUmamiT41*-pDONR C1. **(B)** Lane 1: Promega 1 kb DNA ladder; Lane 2: *CaAVT6A*-pDONR C1; Lane 3: *CaAVT6C*-pDONR C1; Lane 4: *CaCAT1*-pDONR C1; Lane 5: *CaCAT2*-pDONR C1; Lane 6: *CaUmamiT12*-pDONR C1; Lane 7: *CaUmamiT20*-pDONR C1; Lane 8: *CaUmamiT23*-pDONR C1; Lane 9: *CaUmamiT41*-pDONR. **(C)** Lane 1: Promega 1 kb DNA ladder; Lane 2: *CaUmamiT20*-pDONR C1; Lane 3: *CaUmamiT20*-pDONR C2; Lane 4: *CaUmamiT9*-pDONR C1.



Figure 5a.5: Sanger sequencing confirmation of BP clonase reaction to yield the *CaAVT6A*-pDONR plasmid.

Sequence contains the *CaAVT6A* gene sequence with resulting attL and attR sites post integration into the pDONR plasmid. Gene sequence in red and flanking attB altered cloning sites in black.



Figure 5a.6: Sanger sequencing confirmation of BP clonase reaction to yield the *CaAVT6C*-pDONR plasmid.

Sequence contains the *CaAVT6C* gene sequence with resulting attL and attR sites post integration into the pDONR plasmid. Gene sequence in red and flanking attB altered cloning sites in black.

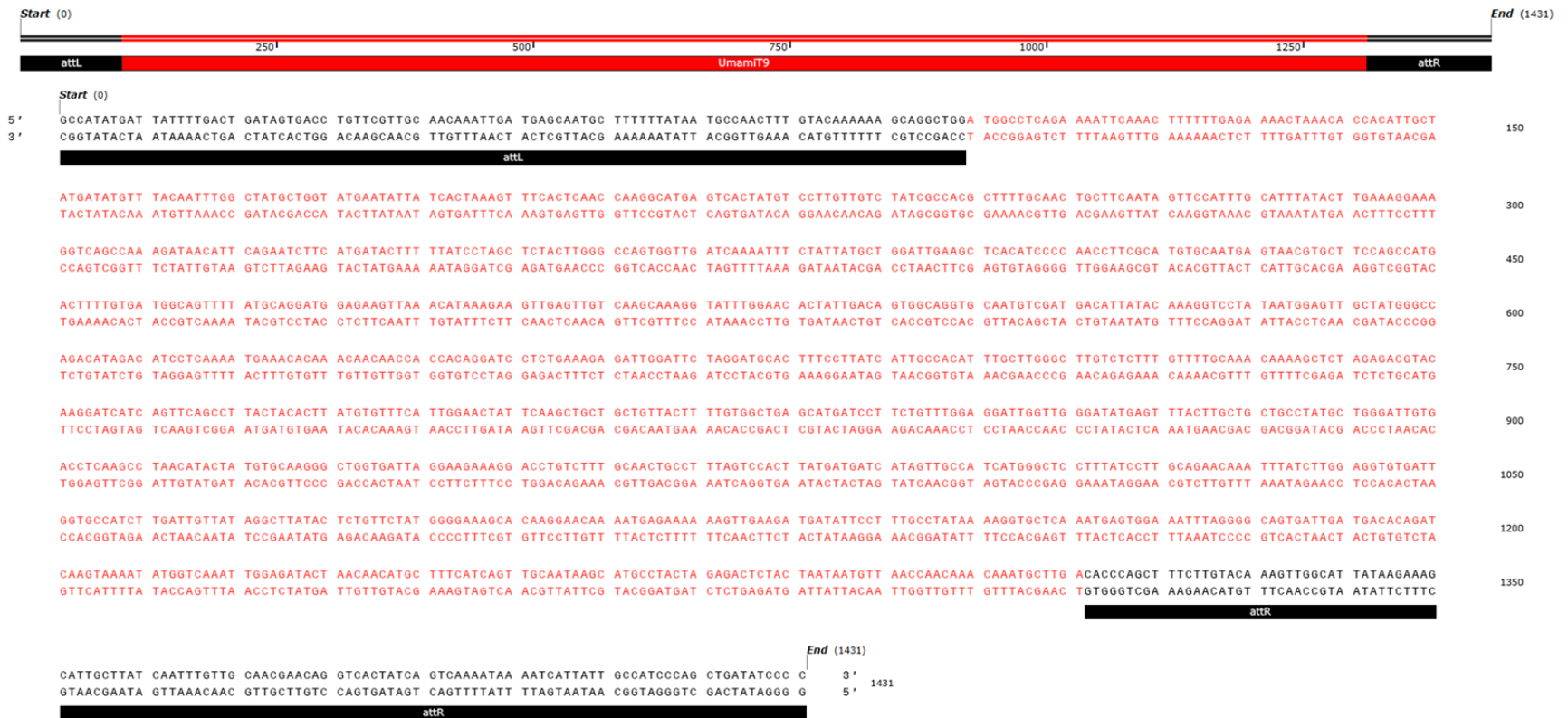


Figure 5a.7: Sanger sequencing confirmation of BP clonase reaction to yield the *CaUmamiT9*-pDONR plasmid.

Sequence contains the *CaUmamiT9* gene sequence with resulting *attL* and *attR* sites post integration into the pDONR plasmid. Gene sequence in red and flanking *attB* altered cloning sites in black.



Figure 5a.8: Sanger sequencing confirmation of BP clonase reaction to yield the *CaUmamiT18*-pDONR plasmid.

Sequence contains the *CaUmamiT18* gene sequence with resulting attL and attR sites post integration into the pDONR plasmid. Gene sequence in red and flanking attB altered cloning sites in black.



Figure 5a.9: Sanger sequencing confirmation of BP clonase reaction to yield the *CaUmamiT20*-pDONR plasmid.

Sequence contains the *CaUmamiT20* gene sequence with resulting attL and attR sites post integration into the pDONR plasmid. Gene sequence in red and flanking attB altered cloning sites in black.

Appendix 5a.4: LR gateway[®] cloning of chickpea transporters into pDR196

After successful verification of *CaAVT6A*, *CaAVT6C*, *CaUmamiT9*, *CaUmamiT18* and *CaUmamiT20* within pDONR, a LR II clonase reaction was setup (Table 5a.7) to recombine the amino acid genes into pDR196 (Figure 5a.11), a yeast expression vector. *CaAAP6* and *CaAVT6C* were performed under 1 µl clonase reactions, whereas the following genes of Table 5a.7 were setup as half reactions to conserve reagents. Reaction were setup and performed as the product specifications (Invitrogen™ Gateway Technology® User Guide) with minor amendments (2.7.5). Post recombination the reaction mix was transformed into DH5α cells via heat-shock and plated on Ampicillin 50 µg/ml selection media, with the resulting colonies purified and visualised on an agarose gel (Figure 5a.10).

Four purified colonies of *CaAAP6*, as expected generated supercoiled and nicked plasmid DNA as the smaller and larger band, respectively (Figure 5a.10A). Similarly, three *CaUmamiT9*, two *CaAVT6A*, *CaUmamiT18*, *CaUmamiT20* and *CaUmamiT41* colony purifications all generated supercoiled and nicked plasmid DNA (Figure 5a.10B). All purifications on the gel were of similar size to the empty pDR196 plasmid in lane 7, which would be expected after the recombination of the amino acid genes and removal of the lethal *ccdB* selection gene between the *attB* sites. Unlike the pDR196 with a chickpea gene, the empty vector without successful recombination would not grow on selection media without the removal of the lethal *ccdB* gene. Cloned pDR196 plasmids were subsequently transformed via lithium acetate (LiAc) method (Gietz & Woods 2002) (2.8.2) into *S. cerevisiae* strains, 23344c (parental) and 22Δ10AA (10 amino acid knockout mutant) (Bensard et al., 2016).

Table 5a.7: LR clonase II recombination reaction setup to clone amino acid genes into the pDR196 destination plasmid.

Gene	Entry conc. (ng/uL)	Entry len. (bp)	Dest. vector	Dest. conc. (ng/uL)	Dest. len. (bp)	Entry added (fmol)	Dest. added (fmol)	Entry to add (uL)	Dest. to add (uL)	TE to add (uL)	LR Mix II to add (uL)	Final reaction (uL)
AAP6	83	3947	pDR196	114	8117	12.74	12.76	0.4	0.60	3.0	1	5
AVT6C	77	3923	pDR196	114	8117	11.89	12.76	0.4	0.60	3.0	1	5
UT9	38	3772	pDR196	45	8117	7.02	6.99	0.46	0.83	0.70	0.5	2.5
UT18	31	3712	pDR196	45	8117	6.95	6.99	0.55	0.83	0.61	0.5	2.5
UT20	34	3739	pDR196	45	8117	6.88	6.99	0.5	0.83	0.66	0.5	2.5
UT41	31	3637	pDR196	45	8117	7.10	6.99	0.55	0.83	0.61	0.5	2.5
AVT6A	38	3958	pDR196	45	8117	6.98	6.99	0.48	0.83	0.68	0.5	2.5

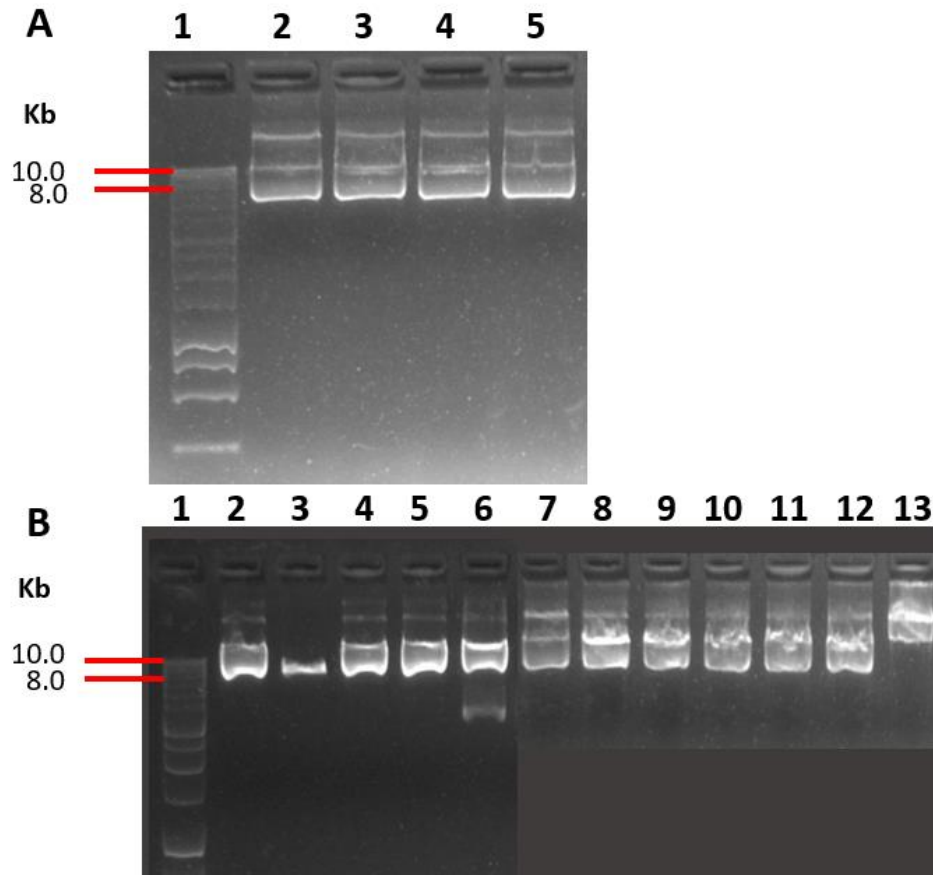


Figure 5a.10: Agarose gel electrophoresis of purified pDR196 destination expression clones harbouring chickpea amino acid transporter genes inserted via LR II clone.

Purification performed using Wizard® Plus SV Minipreps DNA Purification System. LR II clone reaction of pDONR expression clones with inserted chickpea amino acid genes ligated into pDR196 destination plasmid. Product run on a 1% agarose gel visualised with GelRed Product run on a 1% agarose gel visualised with GelRed and run for ~1 hour. **(A)** Lane 1: Promega 1 kb DNA ladder; Lane 2: *CaAAP6*-pDR196 C1; Lane 3: *CaAAP6*-pDR196 C2; Lane 4: *CaAAP6*-pDR196 C3; Lane 5: *CaAAP6*-pDR196 C4. **(B)** Lane 1: Promega 1 kb DNA ladder; Lane 2: *CaUmamiT9*-pDR196 C1; Lane 3: *CaUmamiT9*-pDR196 C2; Lane 4: *CaUmamiT9*-pDR196 C3; Lane 5: *CaAVT6A*-pDR196 C1; Lane 6: *CaAVT6A*-pDR196 C2; Lane 7: Empty pDR196; Lane 8: *CaUmamiT18*-pDR196 C1; Lane 9: *CaUmamiT18*-pDR196 C2; Lane 10: *CaUmamiT20*-pDR196 C1; Lane 11: *CaUmamiT20*-pDR196 C2; Lane 12: *CaUmamiT41*-pDR196 C1; Lane 13: *CaUmamiT41*-pDR196 C2.

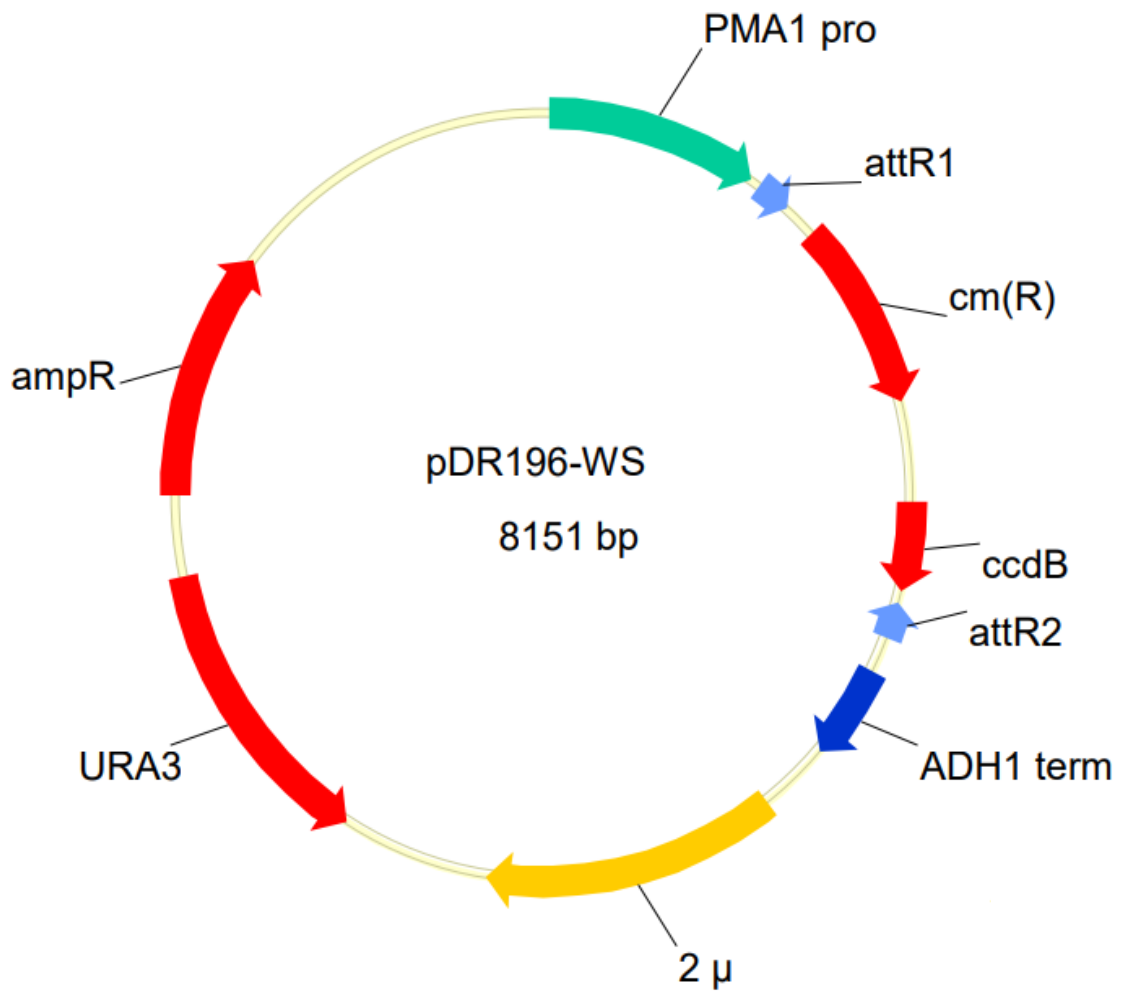


Figure 5a.11: pDR196 destination yeast expression vector (Besnard et al., 2018).

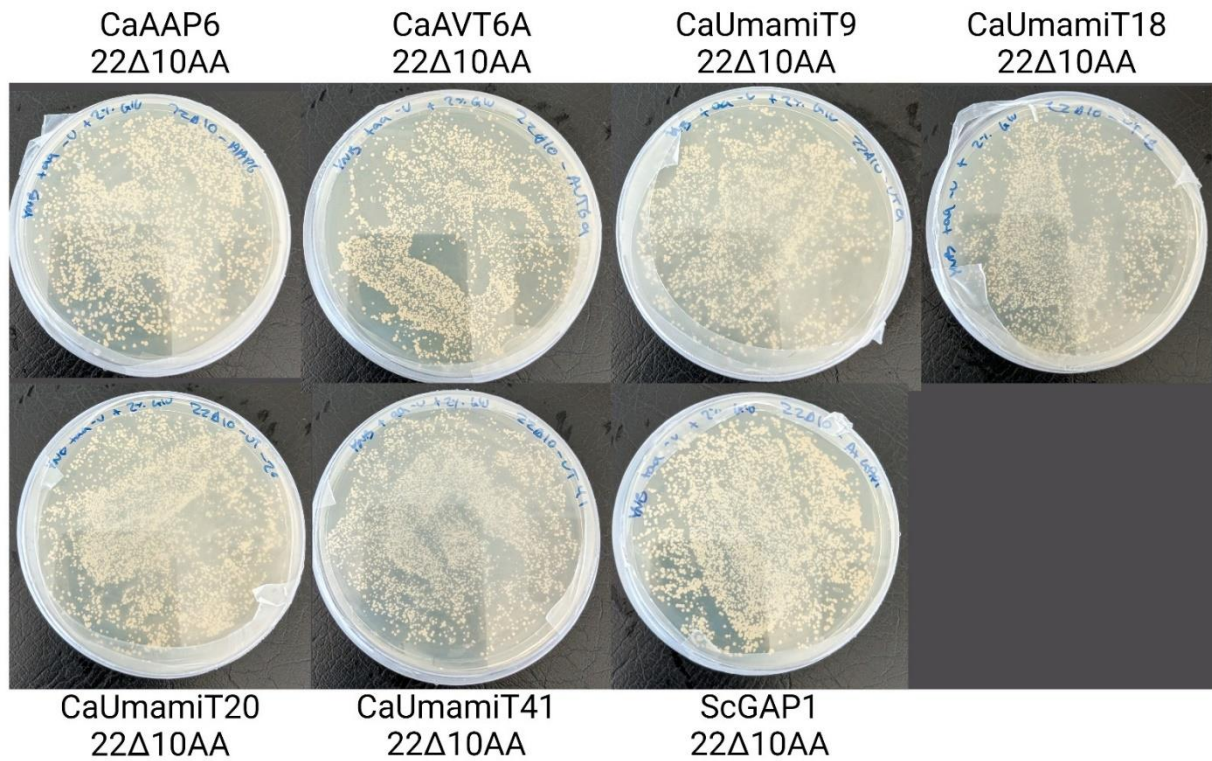


Figure 5a.12: Transformation of pDR196 expressing chickpea and *ScGAP1* positive control amino acid transporter genes into *S. cerevisiae* 22Δ10AA strain.

Appendix 5a.5: Setup of the pYESdest52 expression system

Prior to performing yeast expression analysis in pDR196, the pYESdest52 was used differing by an inducible galactose promoter of the GAL1 gene as opposed to glucose in pDR196 to compare efficiency of both systems (Figure 5a.13). The pYESdest52 used is a gateway destination vector for expression in *S. cerevisiae* harbouring ampicillin antibiotic resistance.

The PCR pipeline here was performed as previously, whereby *CaAAP3*, *CaAAP6*, *CaAVT6C* and *CaMTCC11* were amplified via nodule cDNA and respective attB sites annealed by overhanging PCR primers (Figure 5a.14A). Here however, the attB site addition was performed by two overhanging PCR steps to improve primer binding efficiency (Table 5a.5). Agarose gel electrophoresis of purified linear DNA gene templates of *CaAAP3*, *CaAAP6*, *CaAVT6C* and *CaMTCC11* showed successful PCR annealing of attB sites via two overhanging primer PCR steps (Figure 5a.14B-C).

BP cloning and DH5 α heat-shock transformation of *CaAAP6* and *CaAVT6C* into pDONR was successfully validated via sanger sequencing of purified colonies grown on kanamycin 50 μ g/ml selection media (Figure 5a.14-15). *CaAAP3* sanger sequencing was unsuccessful with very low Q20 bases and sequence intensity, however, was still attempted for LR II clonase recombination into pYESdest52. *CaMTCC11* was not sequenced or used in downstream cloning due to time constraints, LR II clonase reagent scarcity and associated cost.

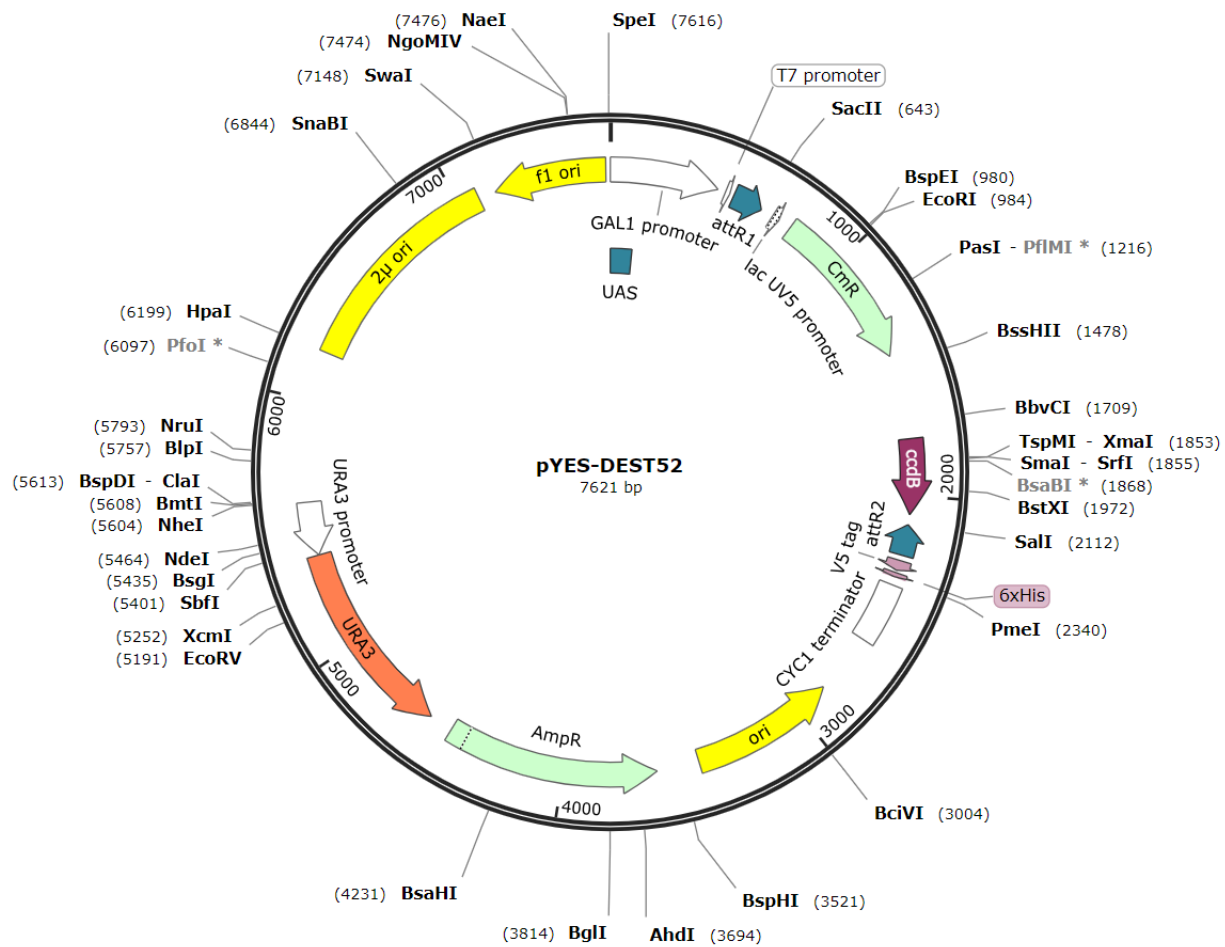


Figure 5a.13: SnapGene® viewer plasmid schematical map of the pYESdest52 yeast expression system.

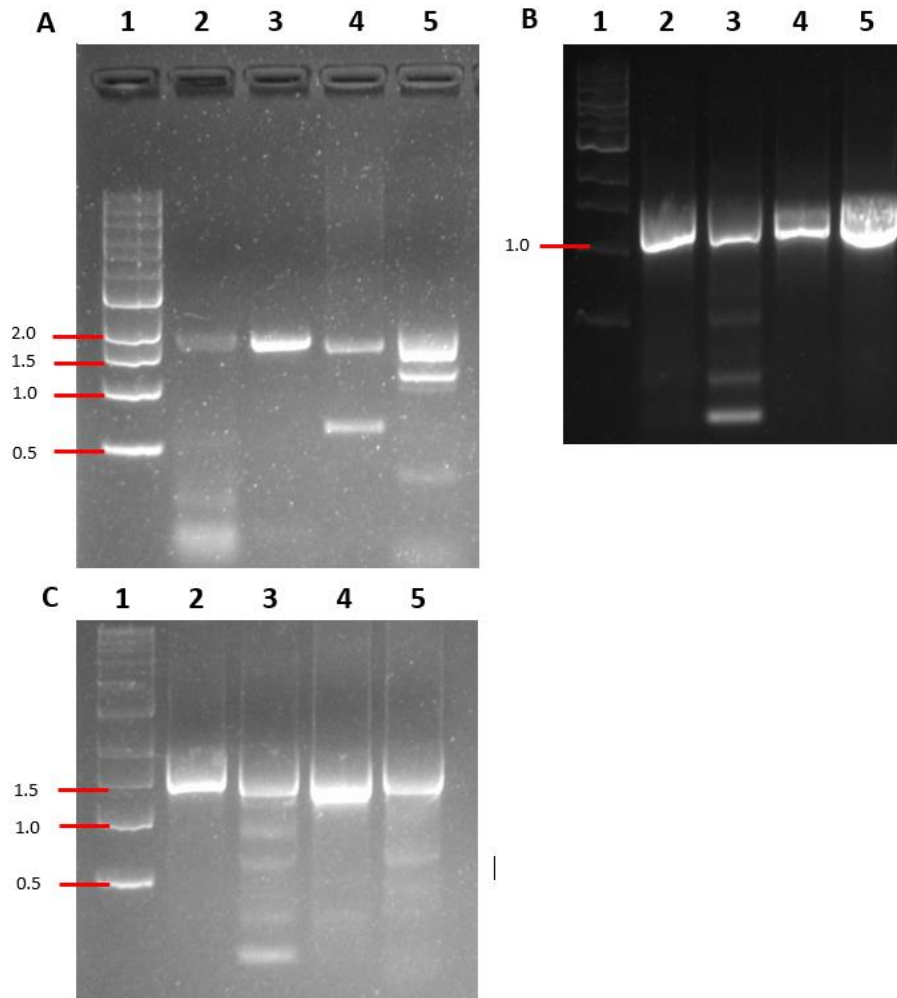


Figure 5a.14: Agarose gel electrophoresis of PCR pipeline for BP/LR setup displaying purified PCR product.

PCR pipeline run with Phusion high fidelity polymerase beginning with (A) amino acid genes amplified from nodule cDNA, (B) overlapping PCR step 1 to anneal attB cloning site, (C) step 2 of attB cloning site annealing. PCR product purification performed using Wizard® SV Gel and PCR Clean-Up System. Product run on a 1% agarose gel visualised with GelRed and run for ~1 hour. (A) Lane 1: NEB 1 kb DNA ladder; Lane 2: Amplified *CaAAP3*; Lane 3: Amplified *CaAAP6*; Lane 4: Amplified *CaAVT6C*; Lane 5: Amplified *CaMTCC11*. (B) Lane 1: NEB 1 kb DNA ladder; Lane 2: Overlapping attB *CaAAP3* PCR product; Lane 3: Overlapping attB *CaAAP6* PCR product; Lane 4: Overlapping attB *CaAVT6C* PCR product; Lane 5: Overlapping attB *CaMTCC11* PCR product. (C) Lane 1: NEB 1 kb DNA ladder; Lane 2: attB *CaAAP3* template; Lane 3: attB *CaAAP6* template; Lane 4: attB *CaAVT6C* template; Lane 5: attB *CaMTCC11* template.



Figure 5a.15: Sanger sequencing confirmation of BP clonase reaction to yield the *CaAAP6*-pDONR plasmid.

Sequence contains the *CaAAP6* gene sequence with resulting attL and attR sites post integration into the pDONR plasmid. Gene sequence in red and flanking attB altered cloning sites in black.

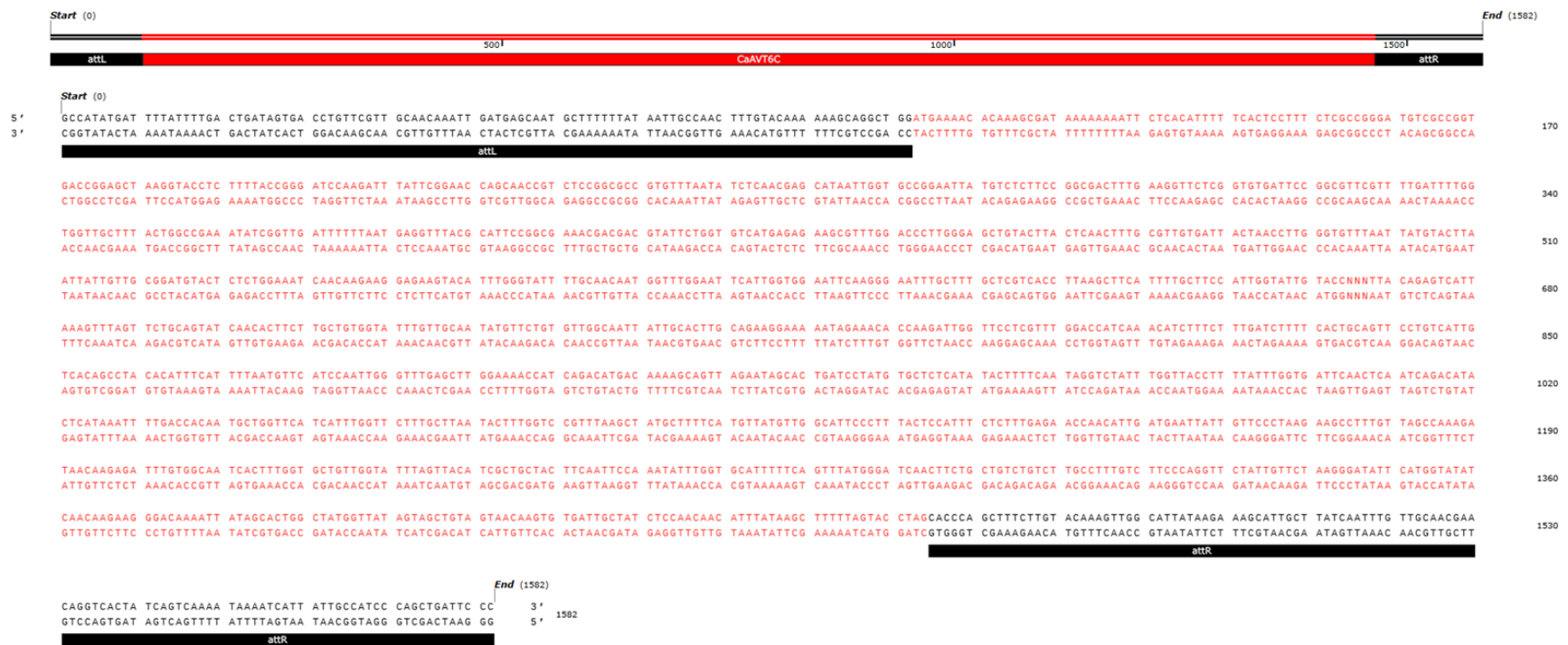


Figure 5a.16: Sanger sequencing confirmation of BP clonase reaction to yield the *CaAVT6C*-pDONR plasmid.

Sequence contains the *CaAVT6C* gene sequence with resulting attL and attR sites post integration into the pDONR plasmid. Gene sequence in red and flanking attB altered cloning sites in black.

Appendix 5a.6: Restriction digest validation of pYESdest52 expression clones

Restriction digests of pYESdest52 plasmids containing chickpea amino acid genes were conducted to validate LR cloning reaction (Figure 5a.17). Double digest of *CaAAP3*-pYESdest52 using NdeI & PstI in lane two produced linear DNA bands at approximately 4 kb & 3.5 kb, close to the approximate predicted outcome of two bands at 3.8 kb & 3.6 kb (Figure 5a.17 & Table 5a.8). Lanes three to five with three different purified colonies of *CaAAP6*-pYESdest52 digested with NdeI was successful, observed with two linear DNA bands at approximately 4.0 kb & 3.8 kb (Figure 5a.17). The digestion of *CaAAP6*-pYESdest52 was predicted to generate two linear DNA fragments of 3963 & 3657 bp in length (Table 5a.8). Lane four however, likely contained the pYESdest52 plasmid which had recombined on itself without the insertion of *CaAAP6*, which would generate a single linear DNA fragment at 5890 bp in length, like what was observed in the agarose gel (Figure 5a.17). Restriction digestion of colony 1 harbouring *CaAVT6C*-pYESdest52 also generated two separated linear DNA bands at approximately 3 kb & 5-6 kb (Figure 5a.17). The first fragment was expected, close to the expected result of 2920 bp, however the larger predicted band of 4645 bp was smaller than the observed DNA fragment in the gel (Figure 5a.17 & Table 5a.8). This result still generated two separated bands of approximately what was expected and may indicate a successful recombination into pYESdest52. Irrespective of this result, *CaAAP6*-pYESdest52 and *CaAVT6C*-pYESdest52 were used for downstream transformation into *S. cerevisiae* strains 23344c (Parental) and 22Δ10AA (Mutant).

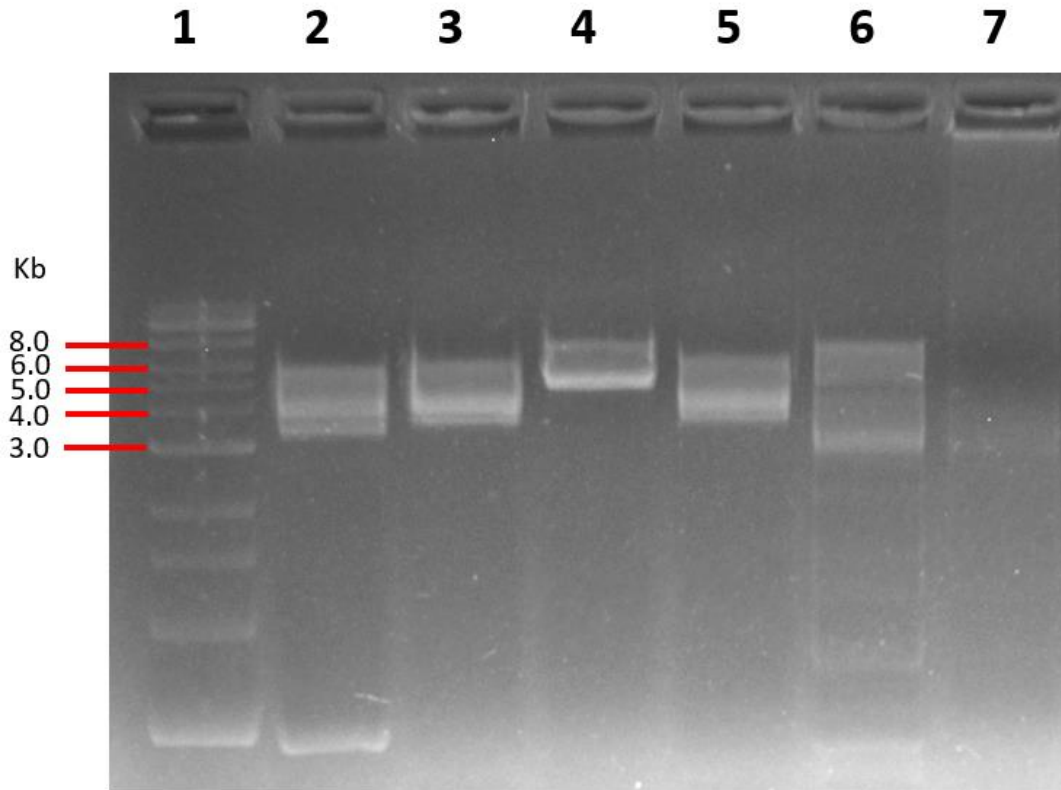


Figure 5a.17: Agarose gel electrophoresis of purified colonies of pYESdest52 plasmids harbouring chickpea amino acid transporters digested via restriction enzymes.

Restriction digests performed with restriction enzyme sites on the pYESdest52 plasmids and gene insert to generate two fragments. Product run on a 1% agarose gel visualised with GelRed and run for ~1 hour. Lane 1: NEB 1 kb DNA ladder; Lane 2: *CaAAP3*-pYESdest52 C1 cut with NdeI & PstI; Lane 3: *CaAAP6*-pYESdest52 C1 cut with NdeI; Lane 4: *CaAAP6*-pYESdest52 C2 cut with NdeI; Lane 5: *CaAAP6*-pYESdest52 C3 cut with NdeI; Lane 6: *CaAVT6C*-pYESdest52 C1 cut with NdeI & BamHI; Lane 7: *CaAVT6C*-pYESdest52 C2 cut with NdeI & BamHI.

Table 5a.8: Predicted restriction digest outcome of pYESdest52 harbouring chickpea amino acid genes.

Gene	Restriction Enzymes	Gene Size (Bp)	Plasmid Size w/Gene (Bp)	DNA Fragment 1 Size (Bp)	DNA Fragment 2 Size (Bp)
AAP3	NdeI + PstI	1464	7354	3856	3651
AAP6	NdeI	1407	7297	3963	3657
AVT6C	NdeI + BamHI	1423	7313	2920	4645

Appendix 5a.7: Validation of the parental wild type 23344c *S. cerevisiae* control strains in liquid growth assays

The parental wild type 23344c *S. cerevisiae* strain harboring the six chickpea amino acid transporters was measured under liquid assay conditions as a positive control prior to complementation assays with the mutant 22Δ10AA strain. Seven amino acids were examined: Gln, Asn, Glu, Asp, Ala, Tyr and GABA under three concentrations of 1, 3 and 6 mM. Liquid assays were prepared and conducted as stated in (2.8.6). In summary single colonies of either the mutant or parental strain carrying chickpea gene insert were bulked on solid YNB media plates containing the synthetic amino acid minus uracil drop out media and later grown overnight in the equivalent liquid media diluted to an OD600 of 1 following washing of the pellet to remove residual AAs. Liquid assays were then conducted using a SPECTROstar Nano BMG microplate reader with 20 μl of the diluted culture in 180 μl of liquid YNB media supplemented with 1, 3 or 6 mM of one of the seven amino acids.

Growth of the parental 23344c strains expressing each of the six chickpea genes as well as the *ScGAP1* positive control and empty pDR196 vector negative control were validated with the two amides, Gln and Asn at concentrations of 1, 3 and 6 mM (Figure 5a.23, 5a.24). *CaAVT6C-23344c*, *CaUmamiT9-23344c*, *CaUmamiT18-23344c*, *CaUmamiT20-23344c*, *CaUmamiT41-23344c*, *ScGAP1-23344c* and pDR196 all grew at an increasing rate from 1 to 6 mM on both Gln and Asn. A linear growth phase was reached at approximately 10 hours into the 48-hour assay, plateauing at approximately 20 hours for 6 mM, 30 hours at 3 mM and ~48 hours for 1 mM (Figures 5a.23, 5a.24). Parental strains all grew effectively under control conditions with (NH₄)₂SO₄ as the sole N source. *CaAAP6-23344c* displayed an unusual growth phenotype where initiation of a linear growth rate was delayed as the concentration of either Gln or Asn increased from 1 mM to 6 mM (Figures 5a.23, 5a.24). This lagging growth rate was also observed when grown with Tyr but not Glu, Asp, Ala and GABA (Figure 5a.18-5a.22). All parentals were also run under liquid assay conditions containing Glu, Asp, Ala, Tyr and GABA at 1, 3 and 6 mM concentrations and exhibited near identical growth curves as with Gln and Asp (Figure 5a.18-5a.22).

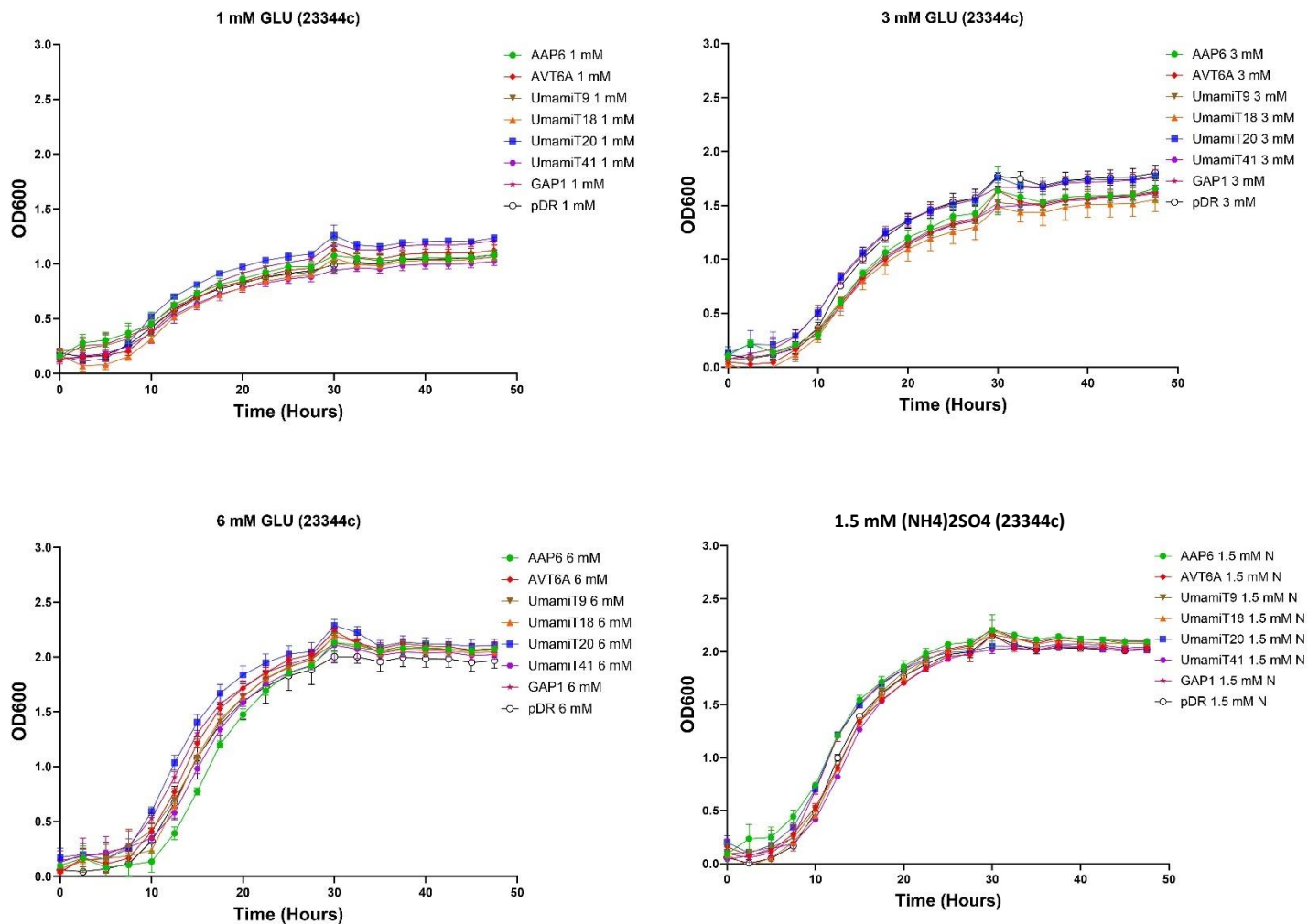


Figure 5a.18: Glutamate Liquid 48h growth assay of the parental (23344c) *S. cerevisiae* strain harbouring six chickpea amino acid genes, *ScGAP1* positive control and empty pDR196 negative control.

Assay measured at OD600 at three separate concentrations of Glu (1, 3 & 6 mM) and 1.5 mM (NH₄)₂SO₄ as a N control. *S. cerevisiae* 23344c transformants harboring amino acid genes and the empty pDR196 control grown overnight in 2% glucose, 50 mM citric acid buffer and YNB (pH 6.2) supplemented with yeast synthetic amino acid minus uracil drop out medium, washed twice with sterile milli-Q water and diluted to an OD600 of 1. Assay performed with a 1:10 dilution of culture (20 µl) to liquid YNB (180 µl) made as previously, replacing synthetic amino acid medium with Glu and run at 30°C with shaking. N = 3

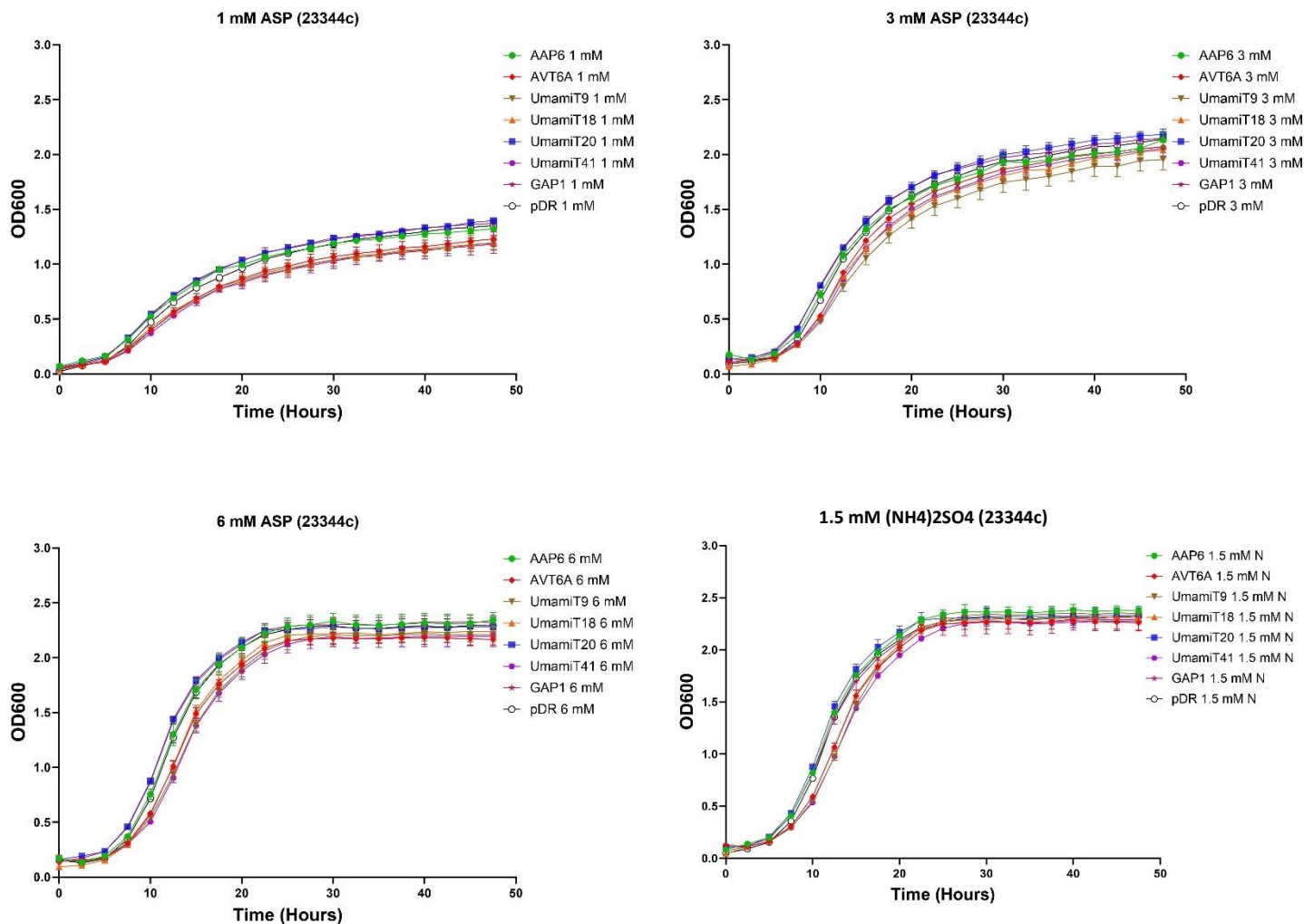


Figure 5a.19: Aspartate Liquid 48h growth assay of the parental (23344c) *S. cerevisiae* strain harboring six chickpea amino acid genes, *ScGAP1* positive control and empty pDR196 negative control.

Assay measured at OD600 at three separate concentrations of Asp (1, 3 & 6 mM) and 1.5 mM (NH₄)₂SO₄ as a N control. *S. cerevisiae* 23344c transformants harboring amino acid genes and the empty pDR196 control grown overnight in 2% glucose, 50 mM citric acid buffer and YNB (pH 6.2) supplemented with yeast synthetic amino acid minus uracil drop out medium, washed twice with sterile milli-Q water and diluted to an OD600 of 1. Assay performed with a 1:10 dilution of culture (20 μ l) to liquid YNB (180 μ l) made as previously, replacing synthetic amino acid medium with Asp and run at 30 $^{\circ}$ c with shaking. N = 3

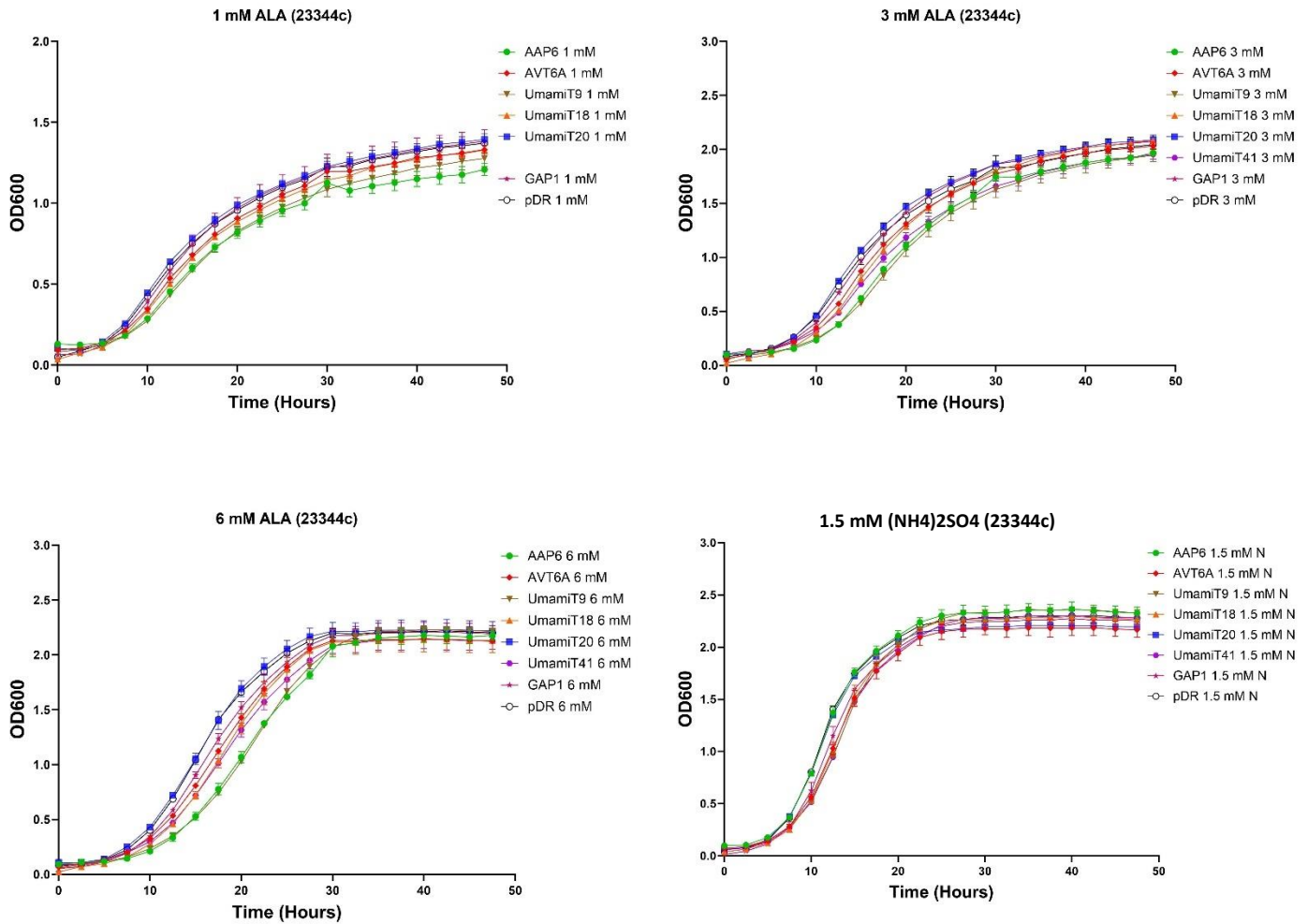


Figure 5a.20: Alanine Liquid 48h growth assay of the parental (23344c) *S. cerevisiae* strain harboring six chickpea amino acid genes, *ScGAP1* positive control and empty pDR196 negative control.

Assay measured at OD600 at three separate concentrations of ALA (1, 3 & 6 mM) and 1.5 mM (NH₄)₂SO₄ as a N control. *S. cerevisiae* 23344c transformants harboring amino acid genes and the empty pDR196 control grown overnight in 2% glucose, 50 mM citric acid buffer and YNB (pH 6.2) supplemented with yeast synthetic amino acid minus uracil drop out medium, washed twice with sterile milli-Q water and diluted to an OD600 of 1. Assay performed with a 1:10 dilution of culture (20 μ l) to liquid YNB (180 μ l) made as previously, replacing synthetic amino acid medium with Ala and run at 30 $^{\circ}$ c with shaking. N = 3

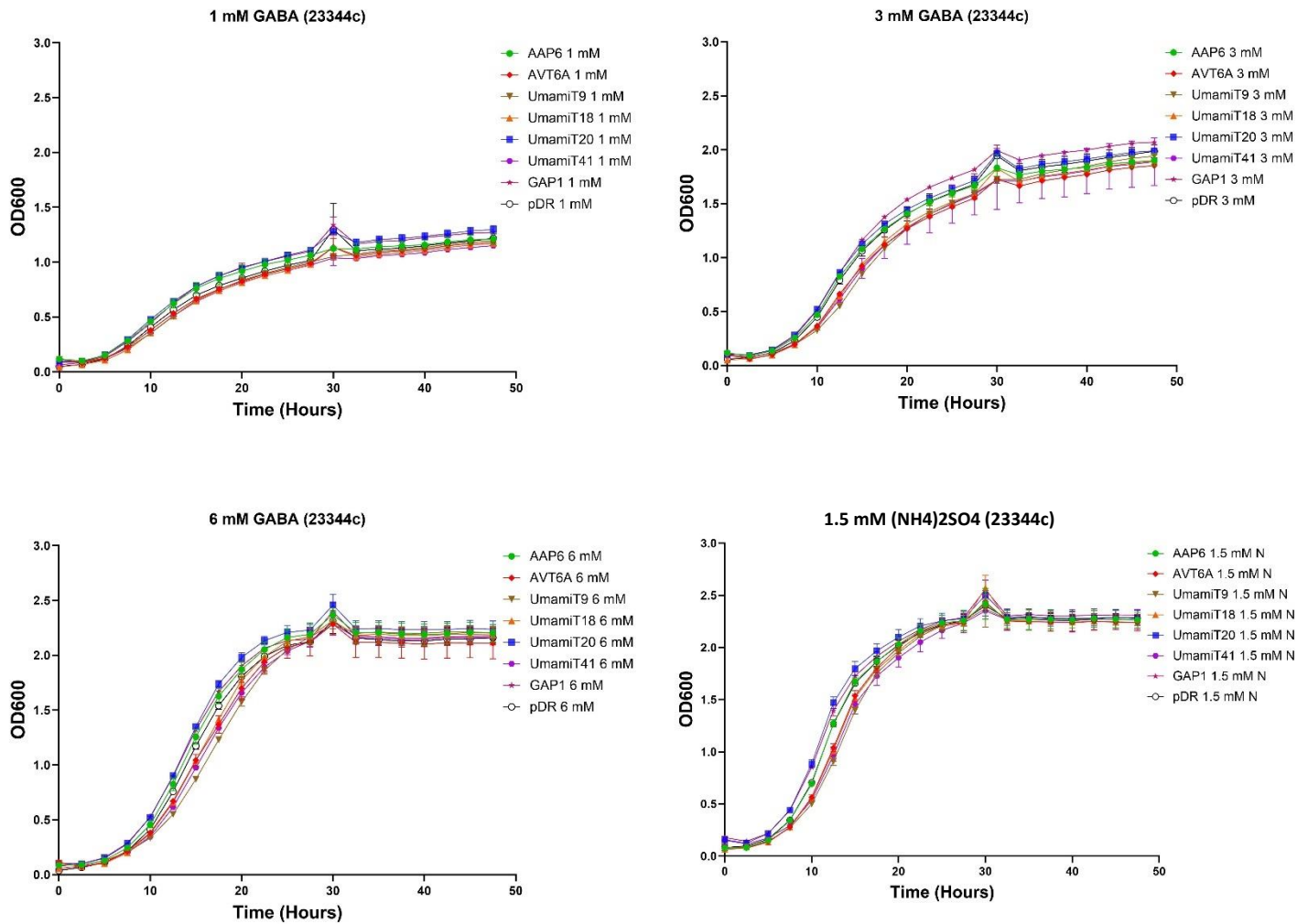


Figure 5a.21: GABA Liquid 48h growth assay of the parental (23344c) *S. cerevisiae* strain harboring six chickpea amino acid genes, *ScGAP1* positive control and empty pDR196 negative control.

Assay measured at OD600 at three separate concentrations of GABA (1, 3 & 6 mM) and 1.5 mM $(\text{NH}_4)_2\text{SO}_4$ as a N control. *S. cerevisiae* 23344c transformants harboring amino acid genes and the empty pDR196 control grown overnight in 2% glucose, 50 mM citric acid buffer and YNB (pH 6.2) supplemented with yeast synthetic amino acid minus uracil drop out medium, washed twice with sterile milli-Q water and diluted to an OD600 of 1. Assay performed with a 1:10 dilution of culture (20 μl) to liquid YNB (180 μl) made as previously, replacing synthetic amino acid medium with GABA and run at 30°C with shaking. N = 3

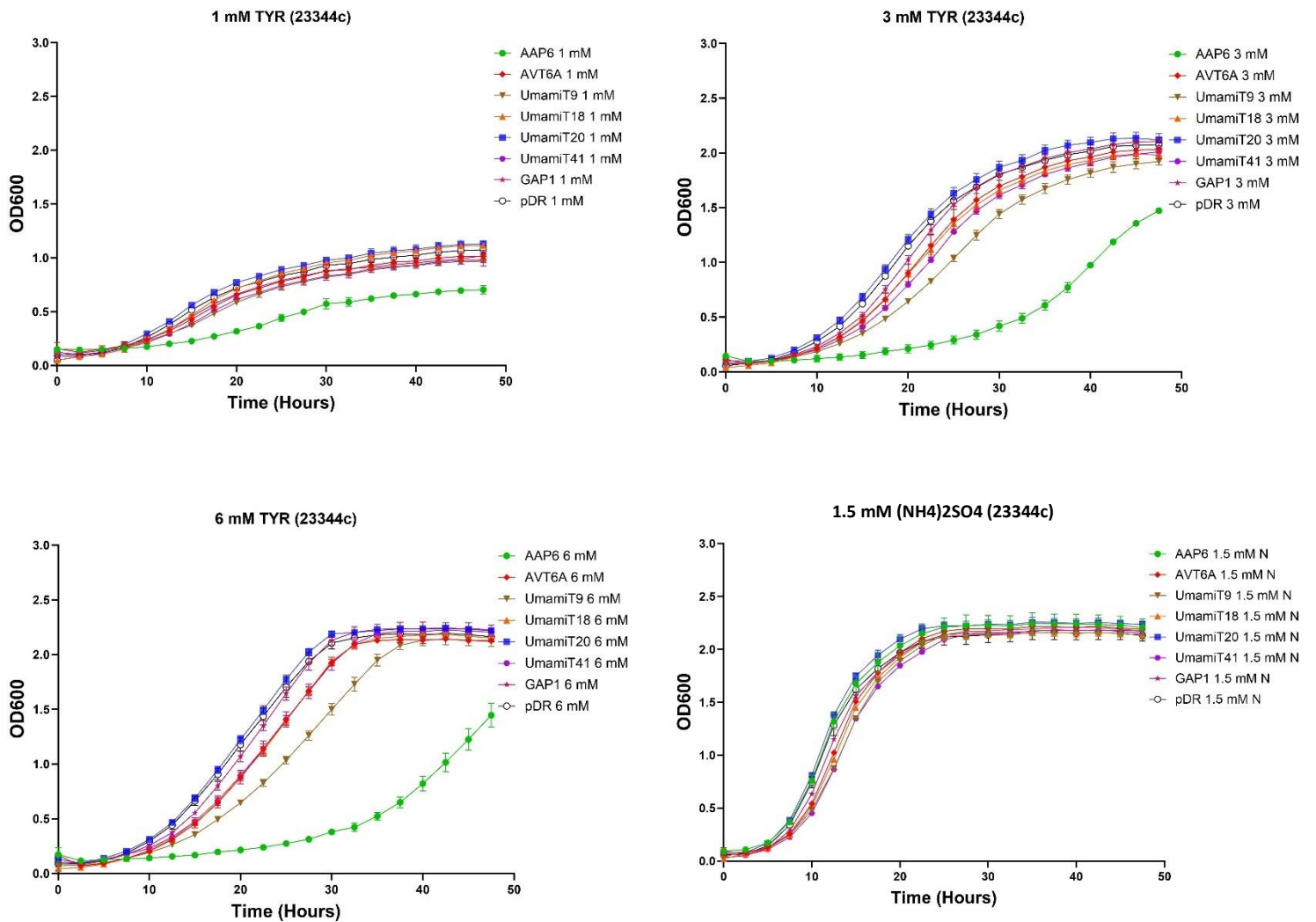


Figure 5a.22: Tyrosine Liquid 48h growth assay of the parental (23344c) *S. cerevisiae* strain harboring six chickpea amino acid genes, *ScGAP1* positive control and empty pDR196 negative control.

Assay measured at OD600 at three separate concentrations of Tyr (1, 3 & 6 mM) and 1.5 mM (NH₄)₂SO₄ as a N control. *S. cerevisiae* 23344c transformants harboring amino acid genes and the empty pDR196 control grown overnight in 2% glucose, 50 mM citric acid buffer and YNB (pH 6.2) supplemented with yeast synthetic amino acid minus uracil drop out medium, washed twice with sterile milli-Q water and diluted to an OD600 of 1. Assay performed with a 1:10 dilution of culture (20 μ l) to liquid YNB (180 μ l) made as previously, replacing synthetic amino acid medium with Tyr and run at 30 $^{\circ}$ c with shaking. N = 3

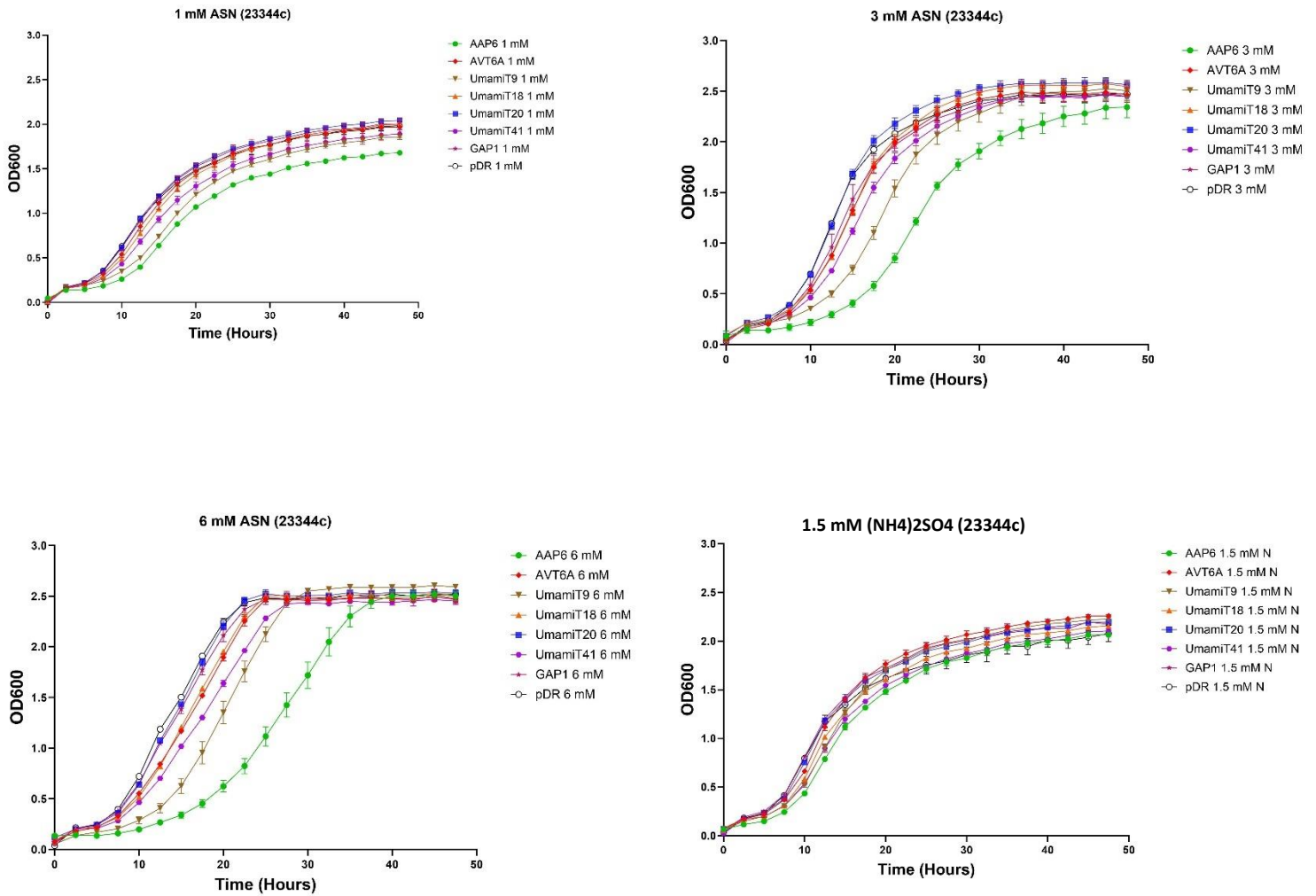


Figure 5a.23: Asparagine Liquid 48h growth assay of the parental (23344c) *S. cerevisiae* strain expressing six chickpea amino acid genes, *ScGAP1* positive control and empty pDR196 negative control.

Assay measured at OD600 at three separate concentrations of Asn (1, 3 & 6 mM) and 1.5 mM (NH₄)₂SO₄ as a N control. *S. cerevisiae* 23344c transformants expressing amino acid genes and the empty pDR196 control grown overnight in 2% glucose, 50 mM citric acid and YNB (pH 6.2) supplemented with yeast synthetic amino acid minus uracil drop out medium, washed twice with sterile milli-Q water and diluted to an OD600 of 1. Assay performed with a 1:10 dilution of culture (20 μ l) to liquid YNB (180 μ l) made as previously, replacing synthetic amino acid medium with Asn and run at 30°C with shaking. N = 3

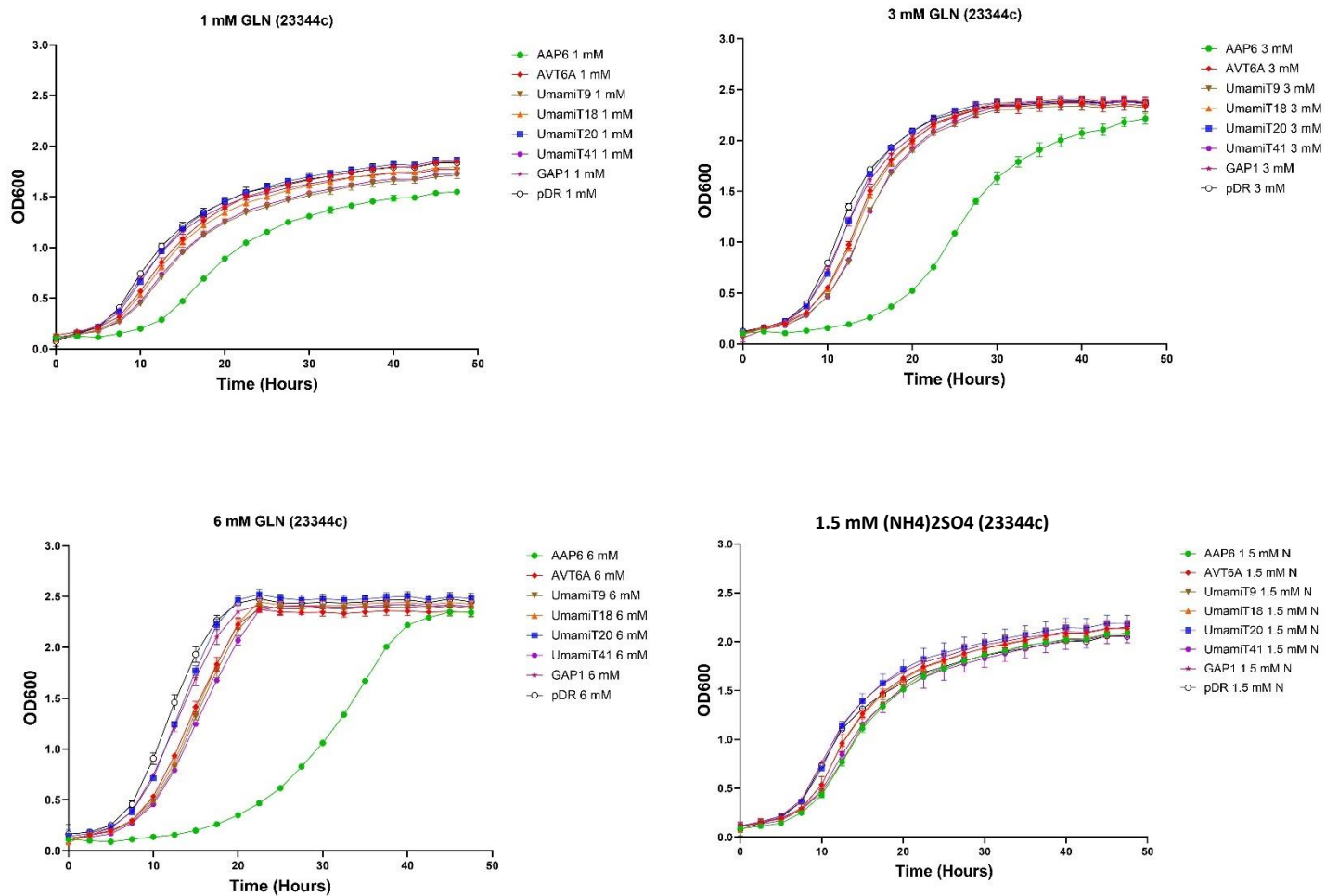


Figure 5a.24: Glutamine Liquid 48h growth assay of the parental (23344c) *S. cerevisiae* strain expressing six chickpea amino acid genes, *ScGAP1* positive control and empty pDR196 negative control.

Assay measured at OD600 at three separate concentrations of Gln (1, 3 & 6 mM) and 1.5 mM (NH₄)₂SO₄ as a N control. *S. cerevisiae* 23344c transformants expressing amino acid genes and the empty pDR196 control grown overnight in 2% glucose, 50 mM citric acid buffer and YNB (pH 6.2) supplemented with yeast synthetic amino acid minus uracil drop out medium, washed twice with sterile milli-Q water and diluted to an OD600 of 1. Assay performed with a 1:10 dilution of culture (20 µl) to liquid YNB (180 µl) made as previously, replacing synthetic amino acid medium with Gln and run at 30°C with shaking. N = 3

Appendix 5a.7: Pre-optimized Amide liquid growth assay complementation of the mutant 22Δ10AA yeast strain

First round of amino acid complementation liquid growth assays in the yeast mutant (22Δ10AA) strain were conducted using the amides Gln & Asn with the six chickpea amino acid genes, *ScGAP1* positive control and the empty pDR196 vector. *S. cerevisiae* strain harboring amino acid genes were first grown on YNB medium (pH 6.2) supplemented with yeast synthetic amino acid minus uracil drop out medium, followed by an overnight inoculation and diluted to an OD600 of 1 prior to grown in liquid YNB supplemented with either Gln or Asn (2.8.6). Liquid assay panels were accompanied by relative to empty vector growth rates (Log_{10}) calculated to compensate for any growth of the empty pDR196-22Δ10AA negative control.

Initial liquid assays conducted for 48 hours at pH 6.2 showed that *CaAAP6*-22Δ10AA, *AVT6A*-22Δ10AA *CaUmamiT9*-22Δ10AA and *CaUmamiT18*-22Δ10AA rescued the amino acid *S. cerevisiae* mutant when supplemented with both Asn and Gln supplementation as the sole nitrogen source (Figures 3a.25, 3a.26). *CaAAP6*-22Δ10AA grew best at 1 mM Gln compared to 3 and 6 mM, with a significantly (p -value <0.01) greater Log_{10} growth rate relative to the empty pDR196 control (Figure 5a.25). Perhaps higher concentrations of Gln are toxic to the mutant strain but not the parental which has several transporters to compensate for an increasing concentration. *CaUmamiT9*-22Δ10AA and *ScGAP1*-22Δ10AA both exhibited a significantly increased growth rate at 3 mM, compared to 6 mM and 1 mM Gln, respectively (Figure 5a.25). In comparison the relative growth rate of the mutants grown with the amide Asn did not significantly differ from the *ScGAP1*-22Δ10AA positive control in a concentration dependent manner at 1, 3 and 6 mM (Figure 5a.26). As had been observed previously on the spot plate assays (Figure 5.13) the empty vector control exhibited minor growth under 3 and 6 mM Gln (Figure 5a.26).

Following the successful complementation with the amides Gln and Asn for the 22Δ10AA mutant strain expressing *CaAAP6*, *CaAVT6A*, *CaUmamiT9* and *CaUmamiT18*, the assay was further optimized to generate more consistently reproducible results. For example, on occasion the mutant strains displayed highly variable growth rates even when cultured from the same original colony and regrown from glycerol stocks. To solve this, an additional step was applied to select for, and drive expression of the chickpea transporter gene cloned into the yeast mutant. Following culturing yeast cells of the mutant strain on a streak plate supplemented with the synthetic amino acid minus uracil medium, cells were again serial diluted on a spot plate containing an amino acid with which complementation had been observed for the gene. The resulting yeast cells from the spot plate were subsequently used to inoculate

the overnight culture for liquid growth assays. This method generated more repeatable and consistent assay results. To prevent any false positives using this technique where the mutant may revert to the parental state, the empty vector pDR196-22Δ10AA was inoculated overnight after growth on a $(\text{NH}_4)_2\text{SO}_4$ control plate.

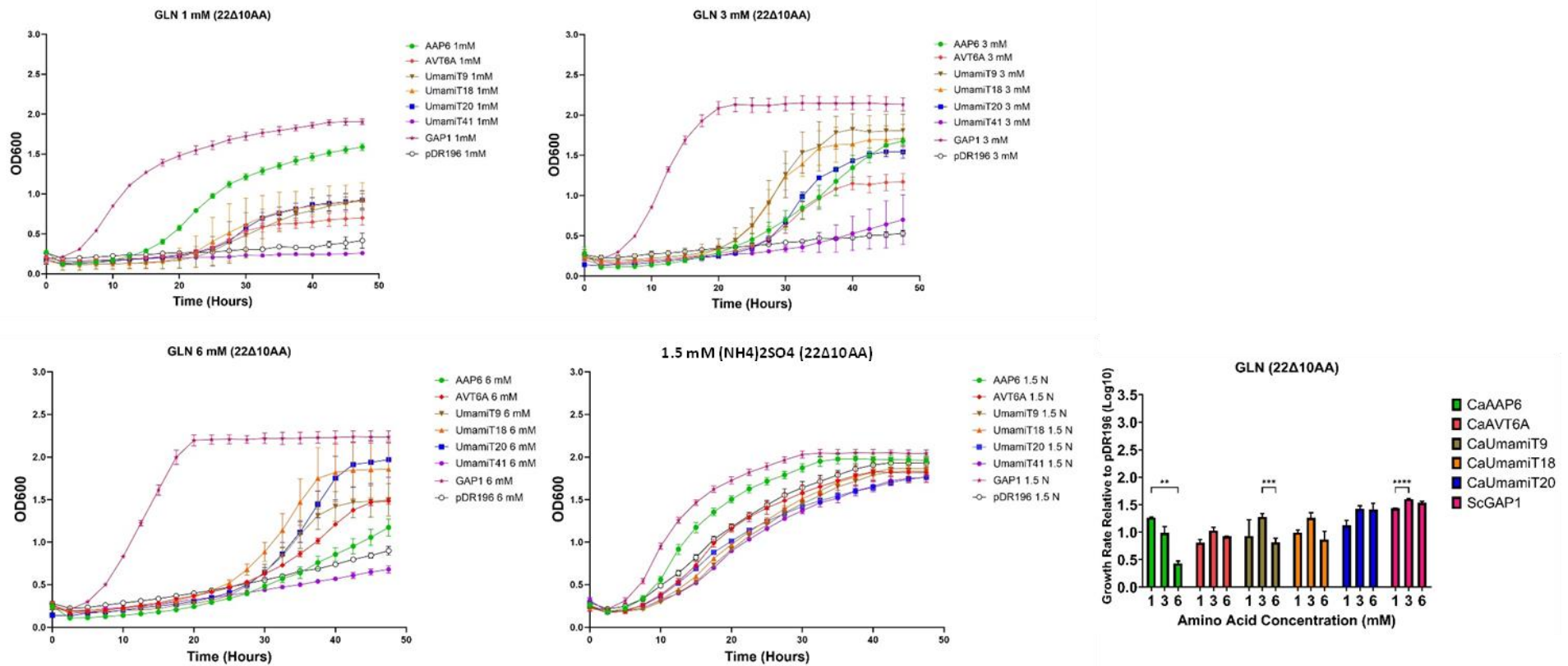


Figure 5a.25: Glutamine Liquid 48h growth assay of the mutant (22Δ10AA) *S. cerevisiae* strain expressing five chickpea amino acid genes, *ScGAP1* positive control and empty pDR196 negative control.

Assay measured at OD600 at three separate concentrations of Gln (1, 3 & 6 mM) and 1.5 mM (NH₄)₂SO₄ as a N control. A single colony of *S. cerevisiae* 22Δ10AA transformants expressing amino acid genes and the empty pDR196 control grown overnight in 2% glucose, 50 mM citric acid buffer and YNB (pH 6.2) supplemented with yeast synthetic amino acid minus uracil drop out medium, washed twice with sterile milli-Q water and diluted to an OD600 of 1. Assay performed with a 1:10 dilution of culture (20 μl) to liquid YNB (180 μl) made as previously, replacing synthetic amino acid medium with Gln, and run at 30°C with shaking. Relative growth rates for genes at differing Gln concentrations statistical significance calculated via Two-Way ANOVA with multiple comparisons test (Tukey) (*<0.01, **<0.001, ***<0.0001). N = 3

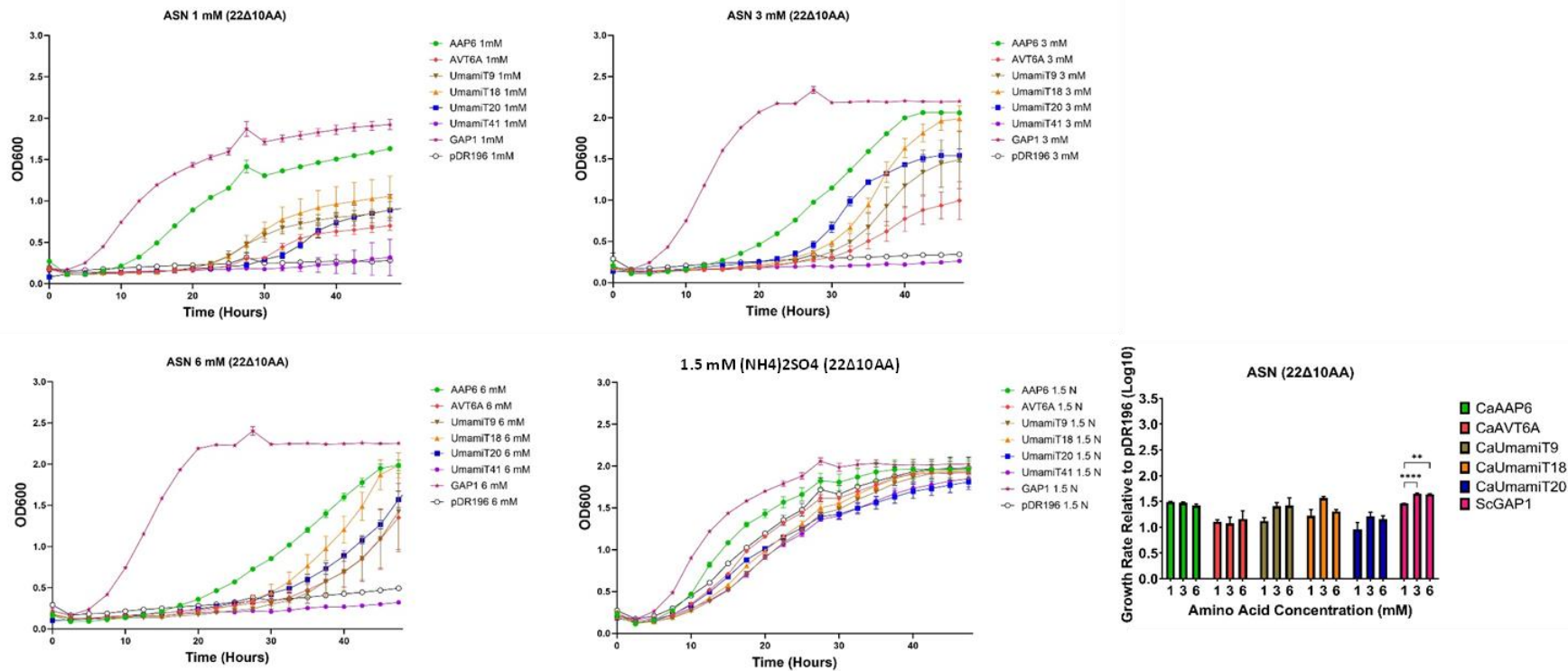


Figure 5a.26: Asparagine liquid 48h growth assay of the mutant (22Δ10AA) *S. cerevisiae* strain expressing five chickpea amino acid genes, *ScGAP1* positive control and empty pDR196 negative control.

Assay measured at OD600 at three separate concentrations of Asn (1, 3 & 6 mM) and 1.5 mM (NH₄)₂SO₄ as a N control. A single colony of *S. cerevisiae* 22Δ10AA transformants expressing amino acid genes and the empty pDR196 control grown overnight in 2% glucose, 50 mM citric acid buffer and YNB (pH 6.2) supplemented with yeast synthetic amino acid minus uracil drop out medium, washed twice with sterile milli-Q water and diluted to an OD600 of 1. Assay performed with a 1:10 dilution of culture (20 μl) to liquid YNB (180 μl) made as previously, replacing synthetic amino acid medium with Asn, and run at 30°C with shaking. Relative growth rates for genes at differing Asn concentrations statistical significance calculated via Two-Way ANOVA with multiple comparisons test (Tukey) (*<0.01, **<0.001, ***<0.0001). N = 3

Appendix 5a.8 Effect of decreasing pH on the mutant 22Δ10AA strain grown with (NH₄)₂SO₄

All mutants grown in the presence of (NH₄)₂SO₄ rescued the knockout mutant at a pH of 4, 5 and 6 without any notable pH related effect on growth (Figure 5a.27). The empty pDR196 vector control did show a minor growth penalty at pH 6 compared to pH 4 and 5 (Figure 5a.27).

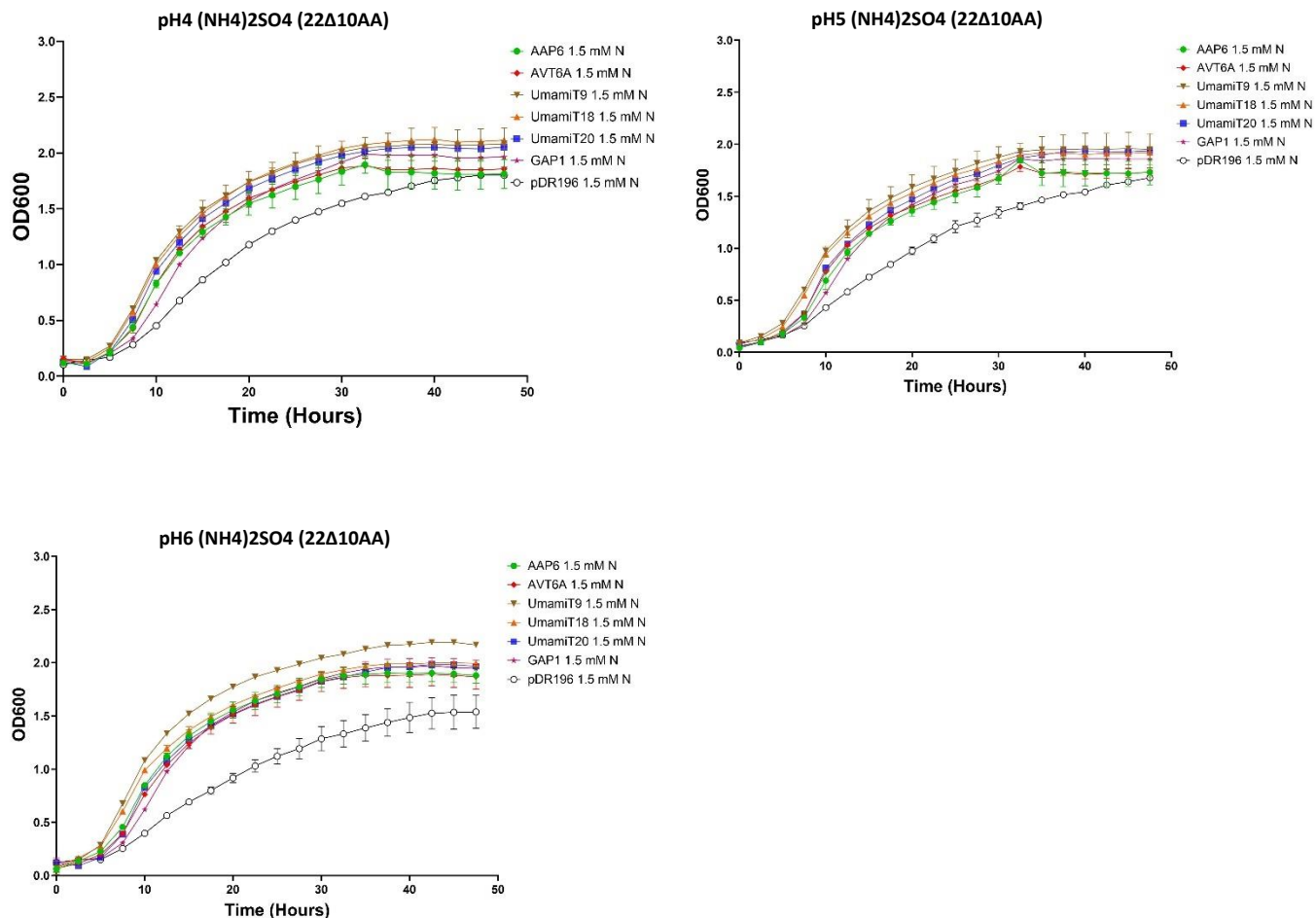


Figure 5a.27: PH dependent complementation control $(\text{NH}_4)_2\text{SO}_4$ in the *S. cerevisiae* mutant (22Δ10AA) strain expressing five chickpea amino acid genes, *ScGAP1* positive control and empty pDR196 negative control.

Assay measured at OD600 under increasingly acidic conditions (pH 6, 5 & 4) when supplemented with 1.5 mM $(\text{NH}_4)_2\text{SO}_4$ as a N control. *S. cerevisiae* 22Δ10AA transformants expressing amino acid genes and the empty pDR196 control grown overnight in 2% glucose, 50 mM citric acid buffer and YNB (pH 6.2) supplemented with yeast synthetic amino acid minus uracil drop out medium, washed twice with sterile milli-Q water and diluted to an OD600 of 1. Assay performed with a 1:10 dilution of culture (20 μl) to liquid YNB (180 μl) made as previously, replacing synthetic amino acid medium with 1.5 mM $(\text{NH}_4)_2\text{SO}_4$, and run at 30°C with shaking. Statistical significance calculated for relative growth rates of each gene compared at the three pH levels via Two-Way ANOVA with multiple comparisons test (Tukey) (*<0.01, **<0.001, ***<0.0001). N = 3

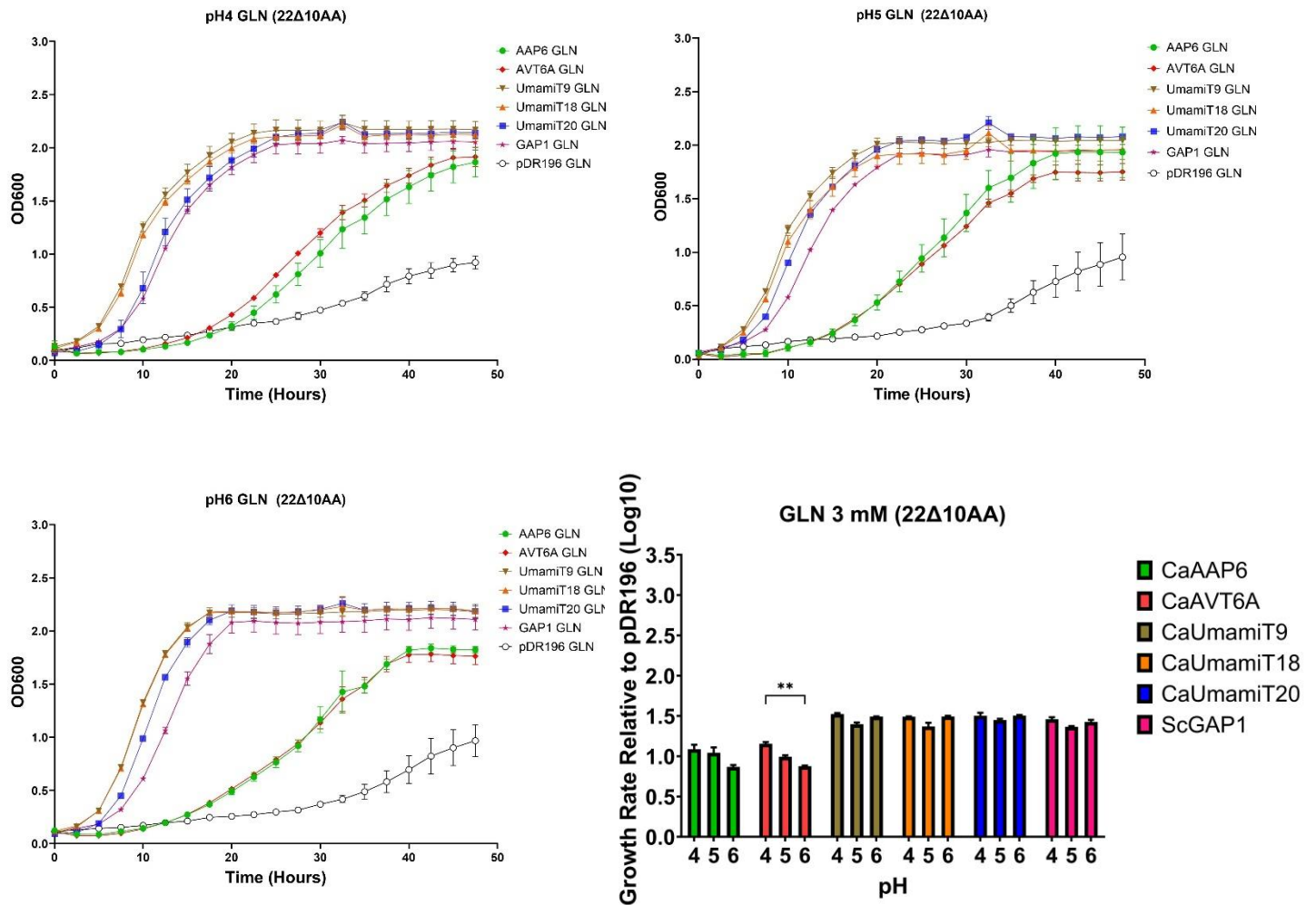


Figure 5a.28: PH dependent complementation of glutamine in the *S. cerevisiae* mutant (22Δ10AA) strain expressing five chickpea amino acid genes, *ScGAP1* positive control and empty pDR196 negative control.

Assay measured at OD600 under increasingly acidic conditions (pH 6, 5 & 4) when supplemented with 3 mM Gln. *S. cerevisiae* 22Δ10AA transformants expressing amino acid genes and the empty pDR196 control grown overnight in 2% glucose, 50 mM citric acid buffer and YNB (pH 6.2) supplemented with yeast synthetic amino acid minus uracil drop out medium, washed twice with sterile milli-Q water and diluted to an OD600 of 1. Assay performed with a 1:10 dilution of culture (20 μl) to liquid YNB (180 μl) made as previously, replacing synthetic amino acid medium with 3 mM Gln, and run at 30°C with shaking. Statistical significance calculated for relative growth rates of each gene compared at the three pH levels via Two-Way ANOVA with multiple comparisons test (Tukey) (*<0.01, **<0.001, ***<0.0001).

N = 3

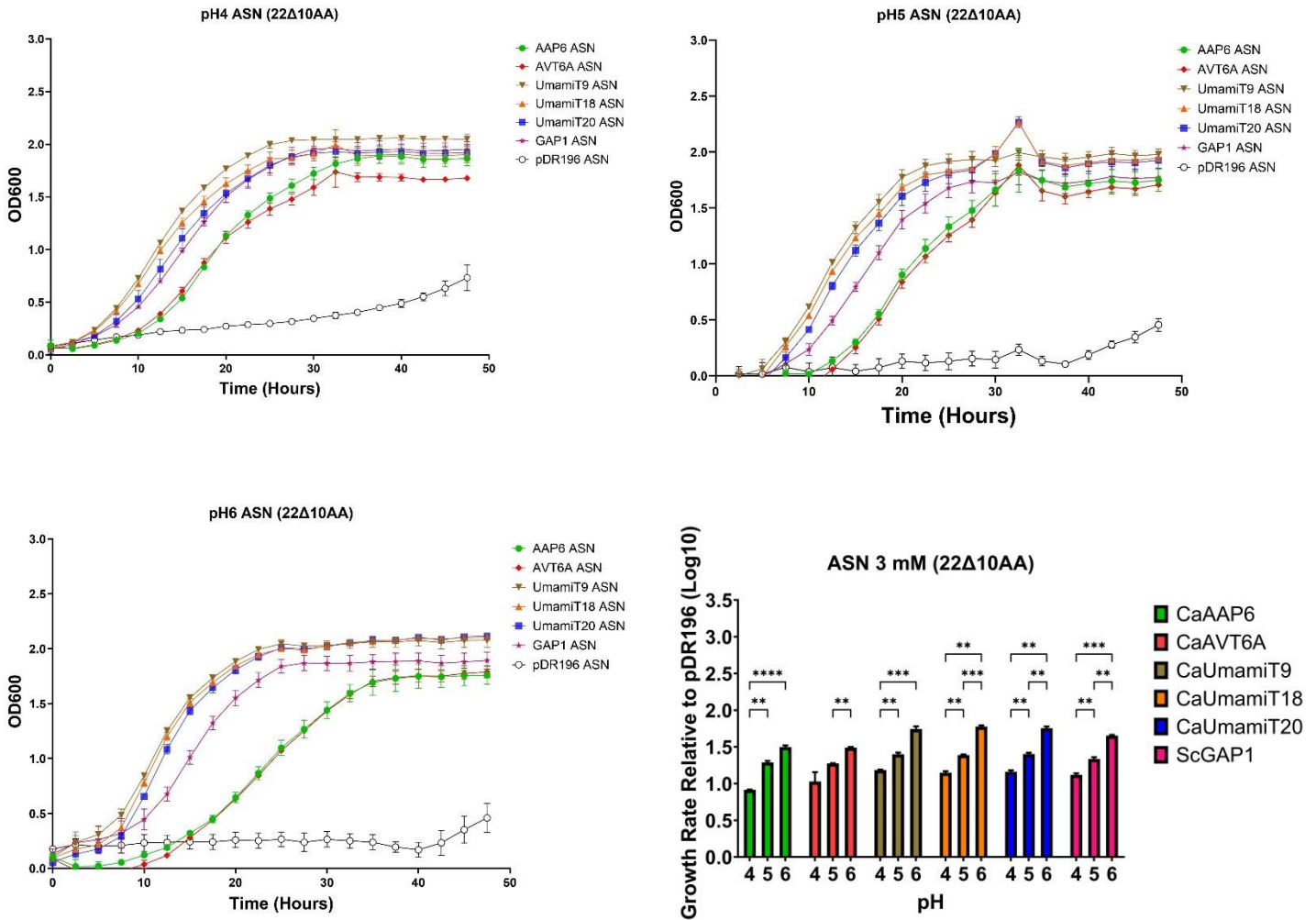


Figure 5a.29: PH dependent complementation of asparagine in the *S. cerevisiae* mutant (22Δ10AA) strain expressing five chickpea amino acid genes, *ScGAP1* positive control and empty pDR196 negative control.

Assay measured at OD600 under increasingly acidic conditions (pH 6, 5 & 4) when supplemented with 3 mM Asn. *S. cerevisiae* 22Δ10AA transformants expressing amino acid genes and the empty pDR196 control grown overnight in 2% glucose, 50 mM citric acid buffer and YNB (pH 6.2) supplemented with yeast synthetic amino acid minus uracil drop out medium, washed twice with sterile milli-Q water and diluted to an OD600 of 1. Assay performed with a 1:10 dilution of culture (20 μl) to liquid YNB (180 μl) made as previously, replacing synthetic amino acid medium with 3 mM Asn, and run at 30°C with shaking. Statistical significance calculated for relative growth rates of each gene compared at the three pH levels via Two-Way ANOVA with multiple comparisons test (Tukey) (*<0.01, **<0.001, ***<0.0001).

N = 3

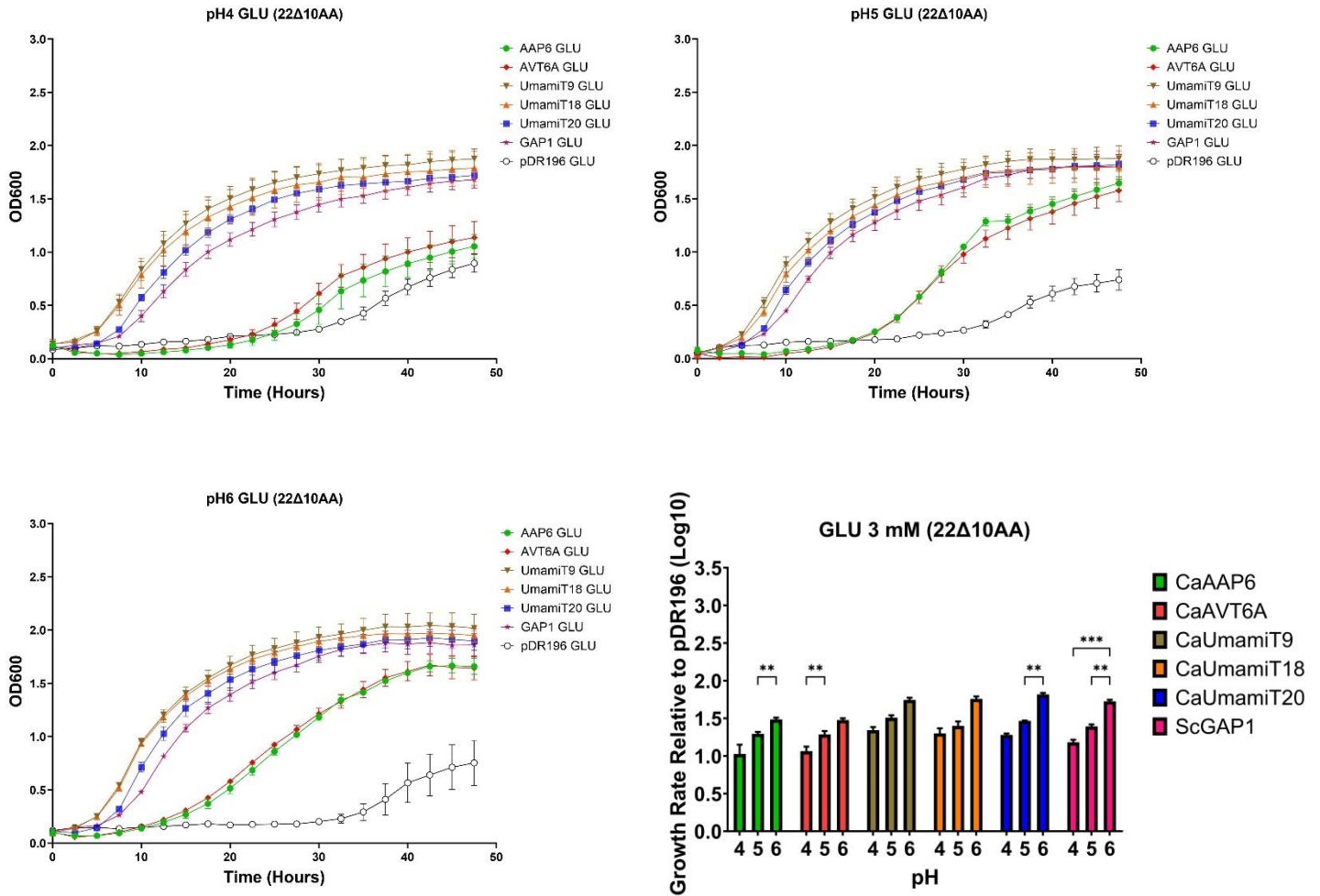


Figure 5a.30: PH dependent complementation of glutamate in the *S. cerevisiae* mutant (22Δ10AA) strain expressing five chickpea amino acid genes, *ScGAP1* positive control and empty pDR196 negative control.

Assay measured at OD600 under increasingly acidic conditions (pH 6, 5 & 4) when supplemented with 3 mM Glu. *S. cerevisiae* 22Δ10AA transformants expressing amino acid genes and the empty pDR196 control grown overnight in 2% glucose, 50 mM citric acid buffer and YNB (pH 6.2) supplemented with yeast synthetic amino acid minus uracil drop out medium, washed twice with sterile milli-Q water and diluted to an OD600 of 1. Assay performed with a 1:10 dilution of culture (20 μl) to liquid YNB (180 μl) made as previously, replacing synthetic amino acid medium with 3 mM Glu, and run at 30°C with shaking. Statistical significance calculated for relative growth rates of each gene compared at the three pH levels via Two-Way ANOVA with multiple comparisons test (Tukey) (*<0.01, **<0.001, ***<0.0001).

N = 3

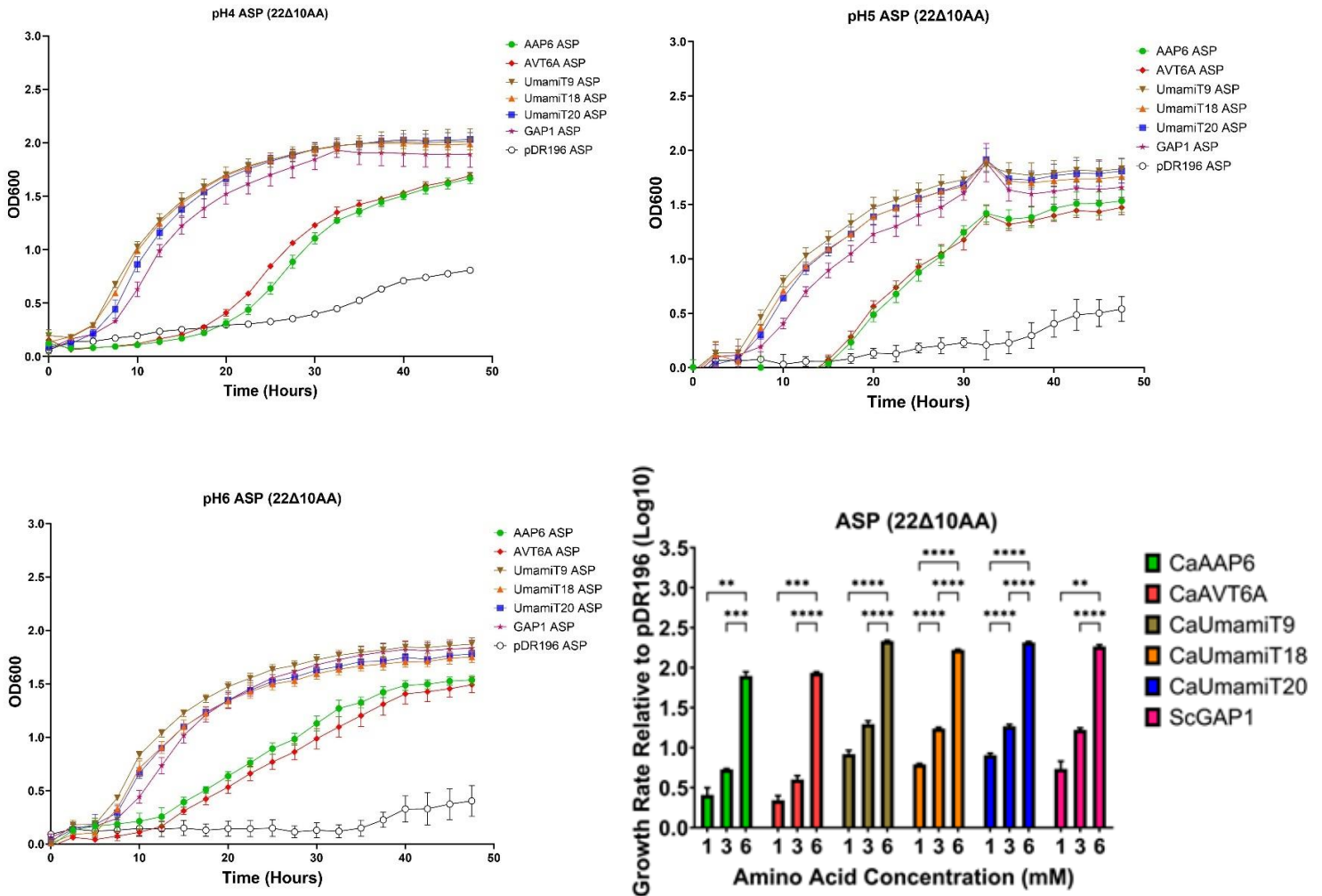


Figure 5a.31: PH dependent complementation of aspartate in the *S. cerevisiae* mutant (22Δ10AA) strain expressing five chickpea amino acid genes, *ScGAP1* positive control and empty pDR196 negative control.

Assay measured at OD600 under increasingly acidic conditions (pH 6, 5 & 4) when supplemented with 3 mM Asp. *S. cerevisiae* 22Δ10AA transformants expressing amino acid genes and the empty pDR196 control grown overnight in 2% glucose, 50 mM citric acid buffer and YNB (pH 6.2) supplemented with yeast synthetic amino acid minus uracil drop out medium, washed twice with sterile milli-Q water and diluted to an OD600 of 1. Assay performed with a 1:10 dilution of culture (20 μl) to liquid YNB (180 μl) made as previously, replacing synthetic amino acid medium with 3 mM Asp, and run at 30°C with shaking. Statistical significance calculated for relative growth rates of each gene compared at the three pH levels via Two-Way ANOVA with multiple comparisons test (Tukey) (*<0.01, **<0.001, ***<0.0001).

N = 3

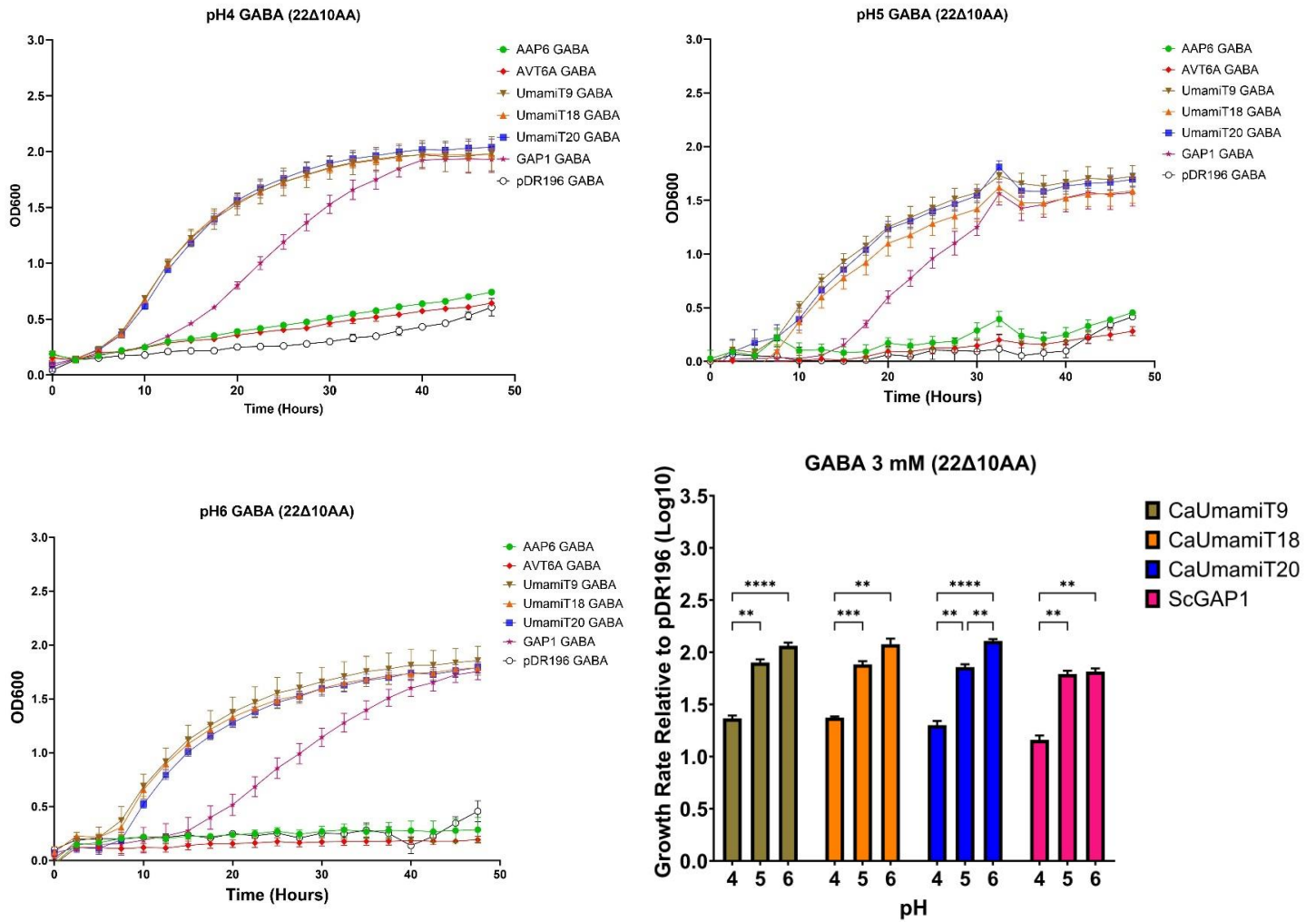


Figure 5a.32: PH dependent complementation of GABA in the *S. cerevisiae* mutant (22Δ10AA) strain expressing five chickpea amino acid genes, *ScGAP1* positive control and empty pDR196 negative control.

Assay measured at OD600 under increasingly acidic conditions (pH 6, 5 & 4) when supplemented with 3 mM GABA. *S. cerevisiae* 22Δ10AA transformants expressing amino acid genes and the empty pDR196 control grown overnight in 2% glucose, 50 mM citric acid buffer and YNB (pH 6.2) supplemented with yeast synthetic amino acid minus uracil drop out medium, washed twice with sterile milli-Q water and diluted to an OD600 of 1. Assay performed with a 1:10 dilution of culture (20 μl) to liquid YNB (180 μl) made as previously, replacing synthetic amino acid medium with 3 mM GABA, and run at 30°C with shaking. Statistical significance calculated for relative growth rates of each gene compared at the three pH levels via Two-Way ANOVA with multiple comparisons test (Tukey) (*<0.01, **<0.001, ***<0.0001).

N = 3

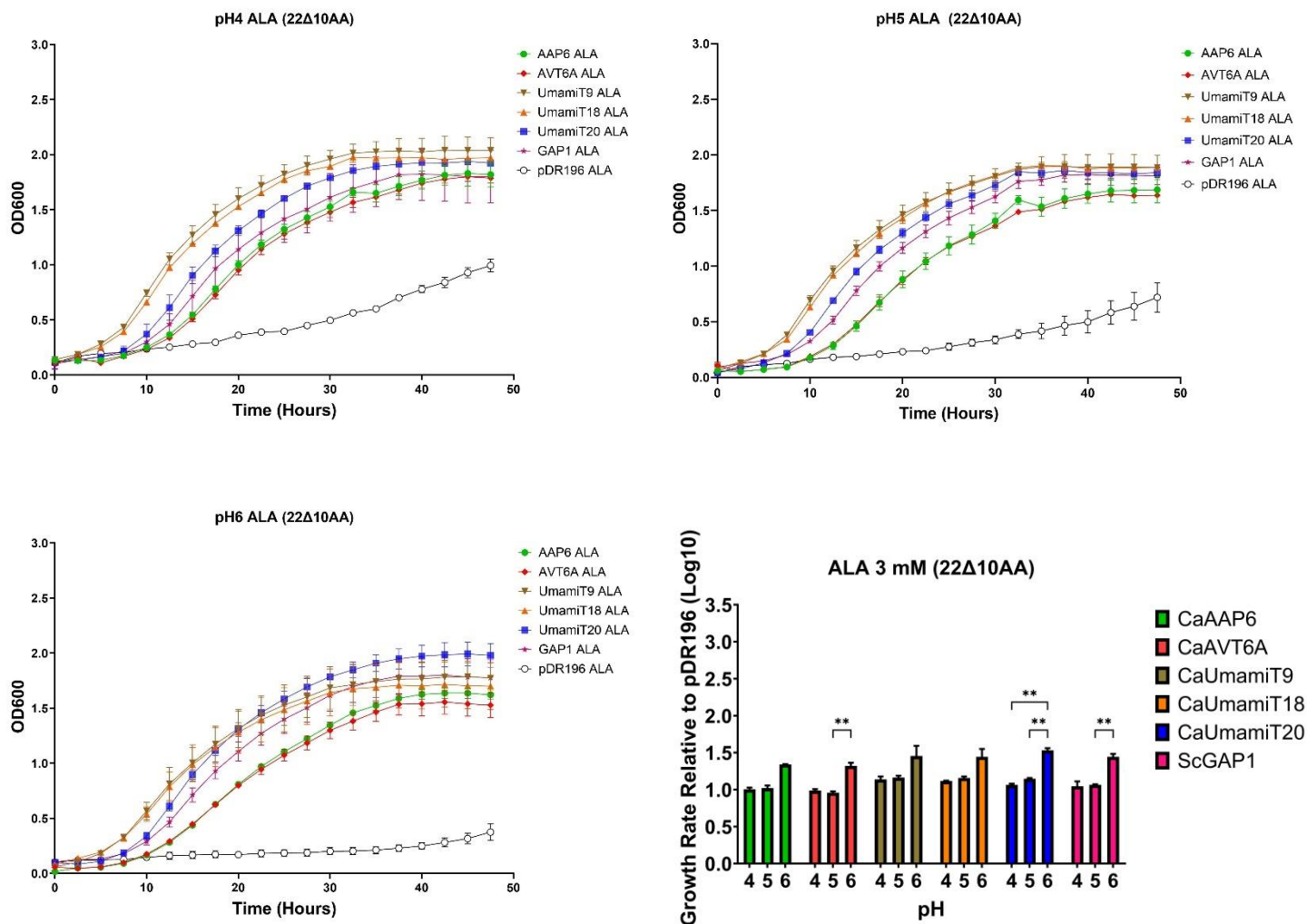


Figure 5a.33: PH dependent complementation of alanine in the *S. cerevisiae* mutant (22Δ10AA) strain expressing five chickpea amino acid genes, *ScGAP1* positive control and empty pDR196 negative control.

Assay measured at OD600 under increasingly acidic conditions (pH 6, 5 & 4) when supplemented with 3 mM Ala. *S. cerevisiae* 22Δ10AA transformants expressing amino acid genes and the empty pDR196 control grown overnight in 2% glucose, 50 mM citric acid buffer and YNB (pH 6.2) supplemented with yeast synthetic amino acid minus uracil drop out medium, washed twice with sterile milli-Q water and diluted to an OD600 of 1. Assay performed with a 1:10 dilution of culture (20 μl) to liquid YNB (180 μl) made as previously, replacing synthetic amino acid medium with 3 mM Ala, and run at 30°C with shaking. Statistical significance calculated for relative growth rates of each gene compared at the three pH levels via Two-Way ANOVA with multiple comparisons test (Tukey) (*<0.01, **<0.001, ***<0.0001).

N = 3

Appendix 6A

Appendix 6a.1: Chickpea tissue culture method overview

See Das Bhowmik et al., (2019) for a detailed description of the method. In summary, this consists of seed bisections and co-cultivation with agrobacterium harboring an expression plasmid with kanamycin resistance, following multiple rounds of regeneration on kanamycin selection media (Figure 6a.1). This section can take up to 8-weeks. Once plantlets have made it past multiple rounds of growth media selection, they must then be grafted on a newly growing sterile non-transgenic seedstock (Figure 6a.2). A non-transgenic shoot from a newly germinated seed is cut longitudinally from the first hypocotyl then again cut down the length of the shoot from the top, splitting the shoot in half. The transgenic shoot is then inserted between the two halves of the cut shoot from the seed and held together via a silicone ring allowing the two shoots to heal together (Figure 6a.2B). From here the plantlet is acclimatized and grown in soil until the generation of T2 seed.

Table 6a.1: Regeneration media composition for chickpea tissue culture.

Chemical	Quantities (per L)			
	MS0	RS1	RS2	RS3
200 X MS Iron	5 mL	5 mL	5 mL	5 mL
200 X MS EDTA	5 mL	5 mL	5 mL	5 mL
200 X MS Micro	5mL	5mL	5mL	5mL
20 X MS Macro	50 mL	50 mL	50 mL	50 mL
100 X MS Vitamins	10 mL	10 mL	10 mL	10 mL
Sucrose	30 g	30 g	30 g	30 g
Myo-inositol	0.1 g	0.1 g	0.1 g	0.1 g
MES Hydrate	0.59 g	0.59 g	0.59 g	0.59 g
Agar	8 g	8 g	8 g	8 g
6-Benzyl-aminopurine (Stock: 1mg/ml)	-	1 ml	0.5ml	0.1ml
Kinetin (Stock: 1mg/mL)	-	0.5ml	0.5ml	0.1ml
Napthalene acetic acid (Stock: 1mg/ml)	-	0.05ml	-	-
Kanamycin		200 mg/L	200 mg/L	200 mg/L
Timentin		100 mg/L	100 mg/L	100 mg/L

Table 6a.2: B5 co-cultivation media composition for chickpea tissue culture.

Chemical	Quantities (per L)			
	MS0	RS1	RS2	RS3
200 X MS Iron	5 mL	5 mL	5 mL	5 mL
200 X MS EDTA	5 mL	5 mL	5 mL	5 mL
200 X MS Micro	5mL	5mL	5mL	5mL
20 X MS Macro	50 mL	50 mL	50 mL	50 mL
100 X MS Vitamins	10 mL	10 mL	10 mL	10 mL
Sucrose	30 g	30 g	30 g	30 g
Myo-inositol	0.1 g	0.1 g	0.1 g	0.1 g
MES Hydrate	0.59 g	0.59 g	0.59 g	0.59 g
Agar	8 g	8 g	8 g	8 g
6-Benzyl-aminopurine (Stock: 1mg/ml)	-	1 ml	0.5ml	0.1ml
Kinetin (Stock: 1mg/mL)	-	0.5ml	0.5ml	0.1ml
Napthalene acetic acid (Stock: 1mg/ml)	-	0.05ml	-	-
Kanamycin		200 mg/L	200 mg/L	200 mg/L
Timentin		100 mg/L	100 mg/L	100 mg/L

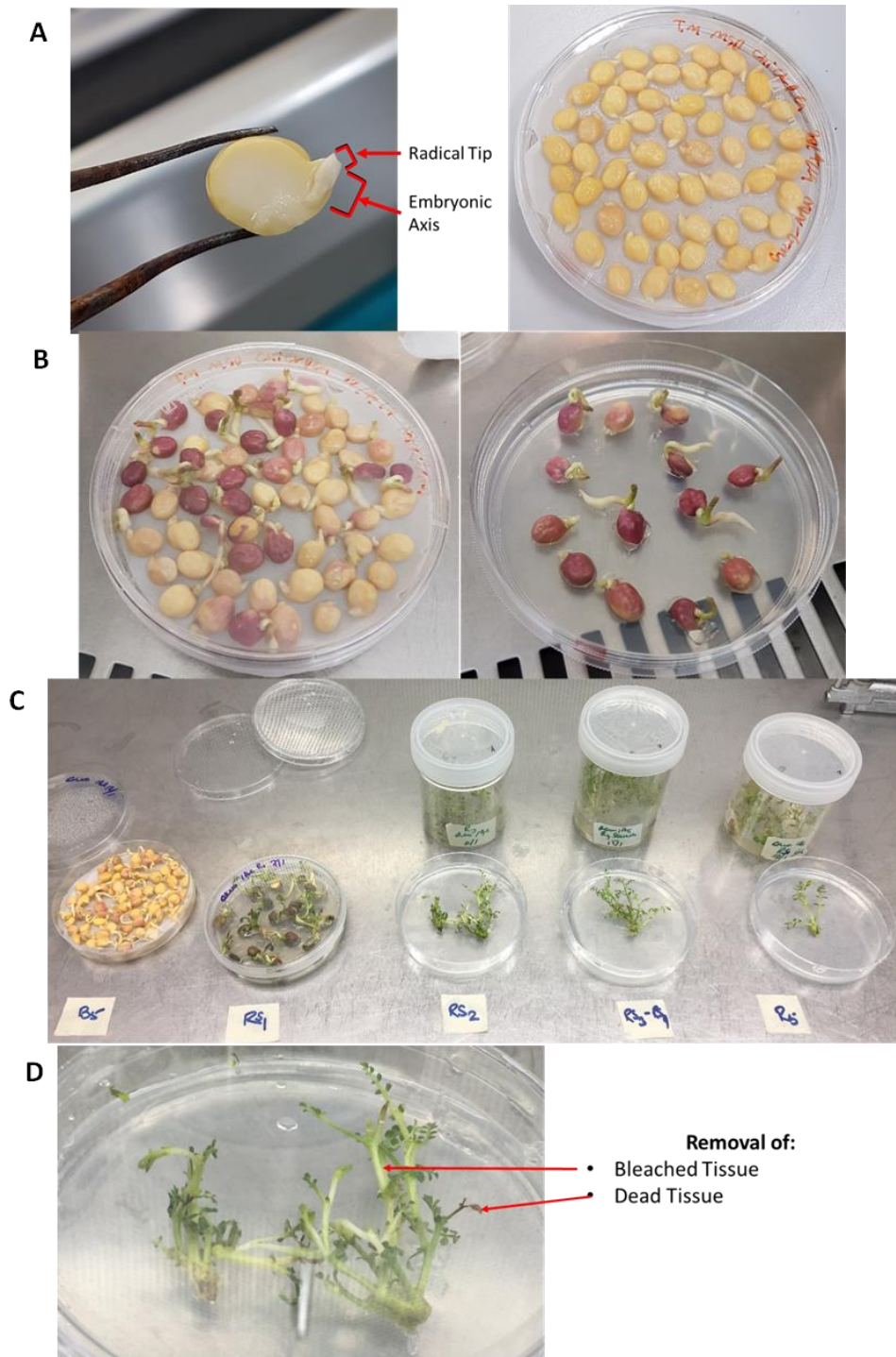


Figure 6a.1: Chickpea tissue culture workflow.

(A) Seed bisection and co-cultivation on B5 media, (B) embryonic development on B5 media and transition to regeneration cycle 1 (RS1) media, (C) summary of each regeneration cycle, (D) preparation of explant at each regeneration cycle.

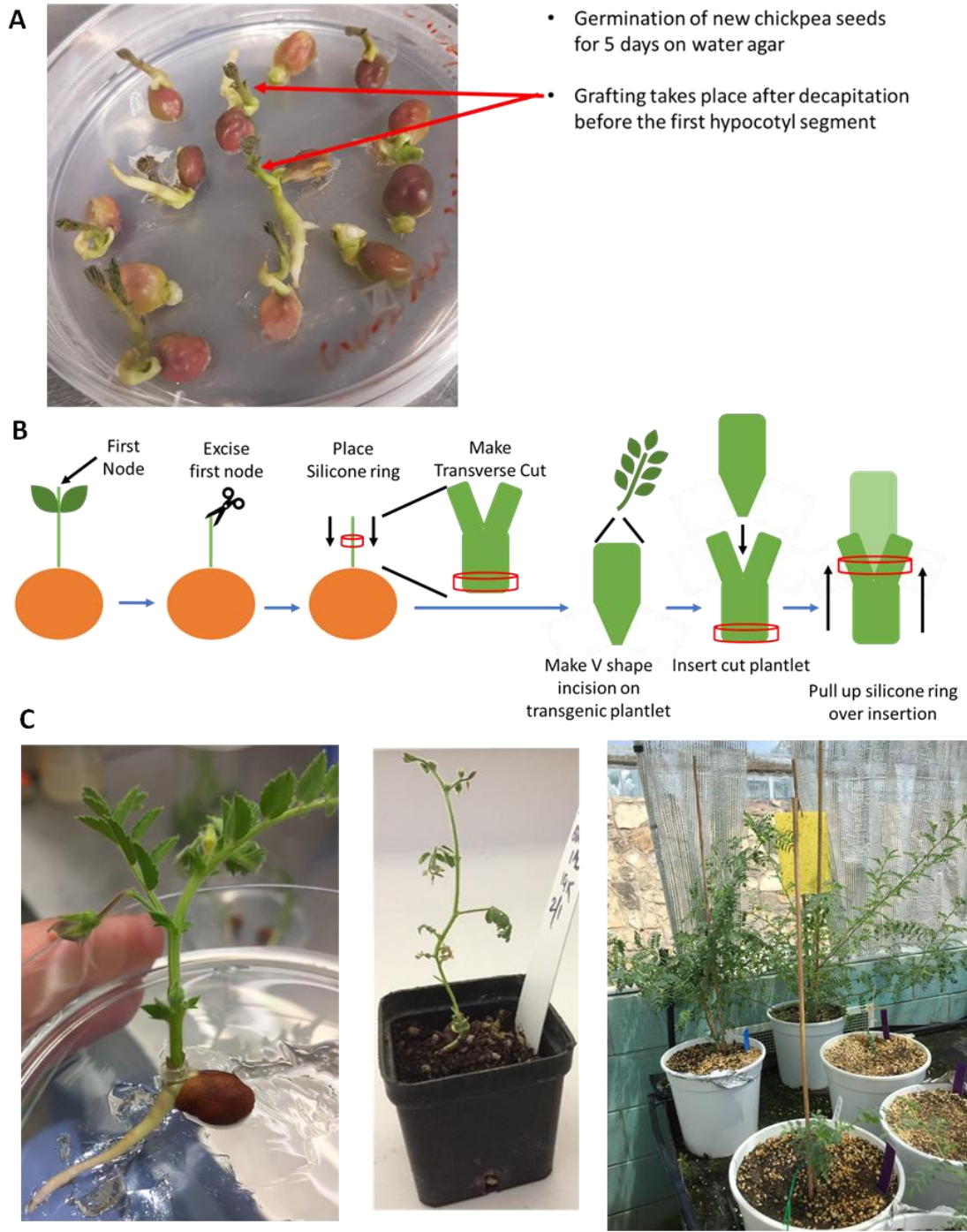


Figure 6a.2: Grafting of transgenic explants on newly grown rootstock.

(A) Germination of non-transgenic rootstock, prior to grafting. (B) Depiction of the grafting process. (C) Grafted plantlet and subsequent acclimatisation steps.

Appendix 6a.2: Multiple chickpea cultivar tissue culture test

(Only hatrick seeds were not bulked at Flinders)

(Control) Hatrick (Desi): Very easy bisection, though appears to have the highest frequency of discolouration/damaged seed coat probably due to the sterilising process.

Rupali (Desi): Slow to bisect, difficult to remove seed coat.

Jimbour (Desi): Easy to bisect.

Slasher (Desi): Relatively easy to bisect.

Striker (Desi): Relatively easy to bisect, like hatrick in appearance and bisection.

Yubileny (Kabuli): Very hard to remove seed coat. The seed coat is very thin. Was easier to bisect the seed then remove the coat by hand but adds an additional contamination concern.

Genesis (Kabuli): Very similar to Yubileny with a very thin seed coat but if the seed is kept wet by the MSO media then the seed coat slides off easy. It may even be unnecessary to remove the coat.

Summary of bisections: The ease of the bisection process of Hatrick (Control) makes it a more capable variety in terms of time-efficiency. The bisection is usually the most time consuming step and is critical to produce as many replicates as possible to counteract the loss of explants due to no germination, bleaching of non-transgenic tissue and necrosis within the subsequent steps and to overcome the limited (~1%) transformation efficiency of the method. Hatrick was the chosen cultivar in the original method and hence used as a control.

Other promising cultivars were Jimbour, Slasher and Striker all of which were relatively easy to perform the bisection process on, in terms of removal of the external seed coat. Rupali was slightly more difficult due the underside of the coat sticking to the seed, making it difficult remove and in-turn making the process more time-consuming. This may be due to poor seed quality, however all the cultivars apart from hatrick were all control plants from a previous experiment all watered to 80% field capacity. It is unlikely the seeds were harvested prematurely as there were no obvious signs of any unmaturing seeds which is generally observed as a green seed. It is also possible that the Rupali seeds were too dry during the bisection which can cause the seed coat to stick. This could be overcome by keeping the seeds moist by pouring a small volume of the MSO media on the petri dish used when performing the bisection.

The poor performers were notably the only Kabuli varieties Genesis and Yubileny, suggesting their incompatibility to this method. This was due to their very thin seed coat, making it difficult to remove in some cases. This was overcome by either removing the coat by hand after bisection or keeping the seed moist allowing it to slide off easier.

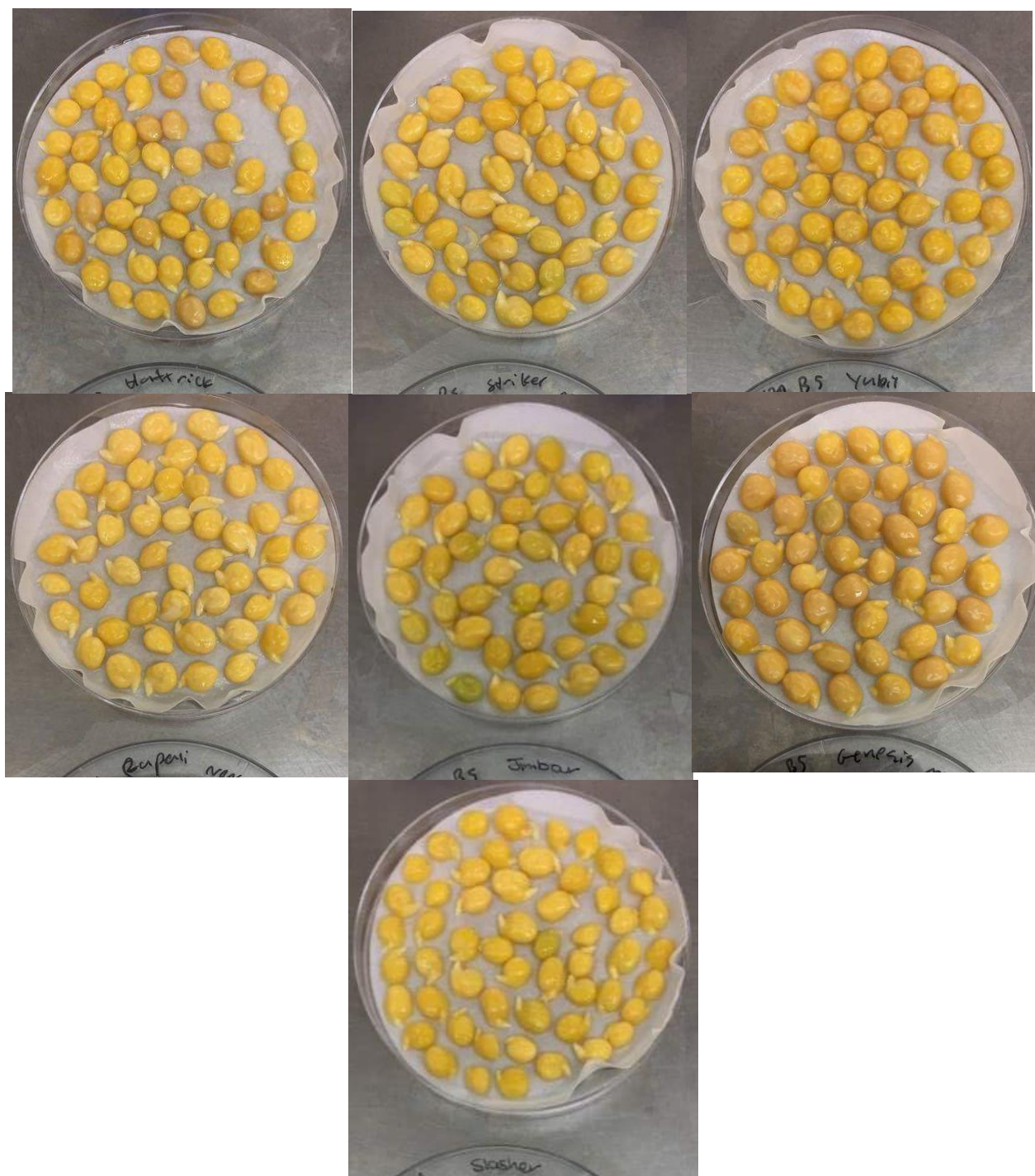


Figure 6a.3: Bisections of all 7 cultivars placed on B5 co-cultivation media.

Jimbar contained some slightly green seeds (~5), suggesting they were unmaturred when harvested and may affect the germination/shoot generation in the following step. Striker was similar, however only a couple appeared slightly green.



Figure 6a.4: Germination of multiple chickpea cultivars on B5 media.

(A) Day 3 after bisection, ordered from most shoot germination to least. Notably the last 2 Genesis and Yubil are both Kabuli cultivars. Rupali germinated seeds were transferred to RS1 media on day 3. Hattrick, Jim and Striker on day 4, Slasher day 6. (B) Day 4 germination of Hattrick, Jim and Striker (Left to Right).

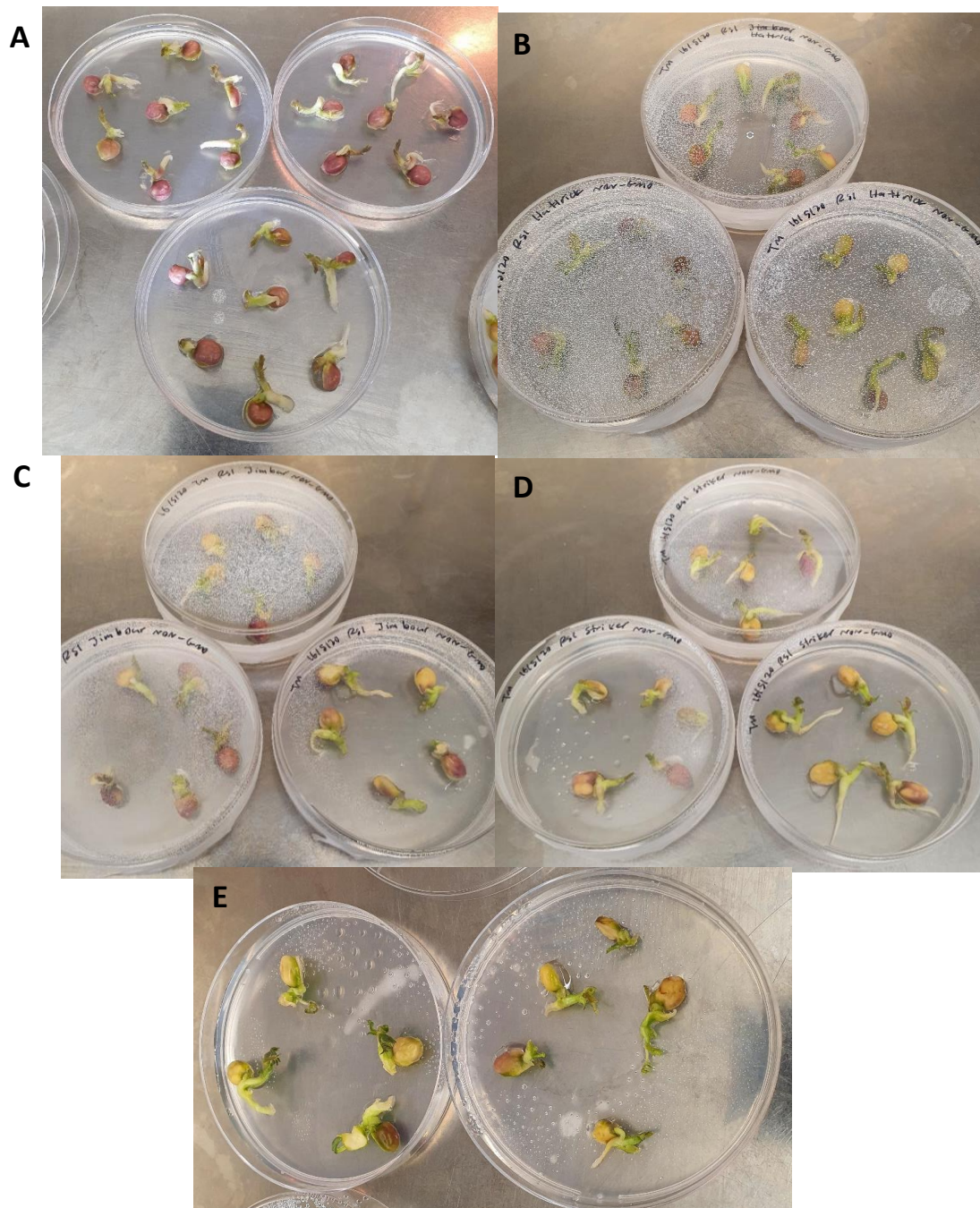


Figure 6a.5: Transition of bisected seeds to regeneration cycle 1 media (RS1).

(A) Rupali, Day 3; (B) Hatrick, Day 4; (C) Jimbour, Day 4; (D) Striker, Day 4; (E) Slasher, Day 6.

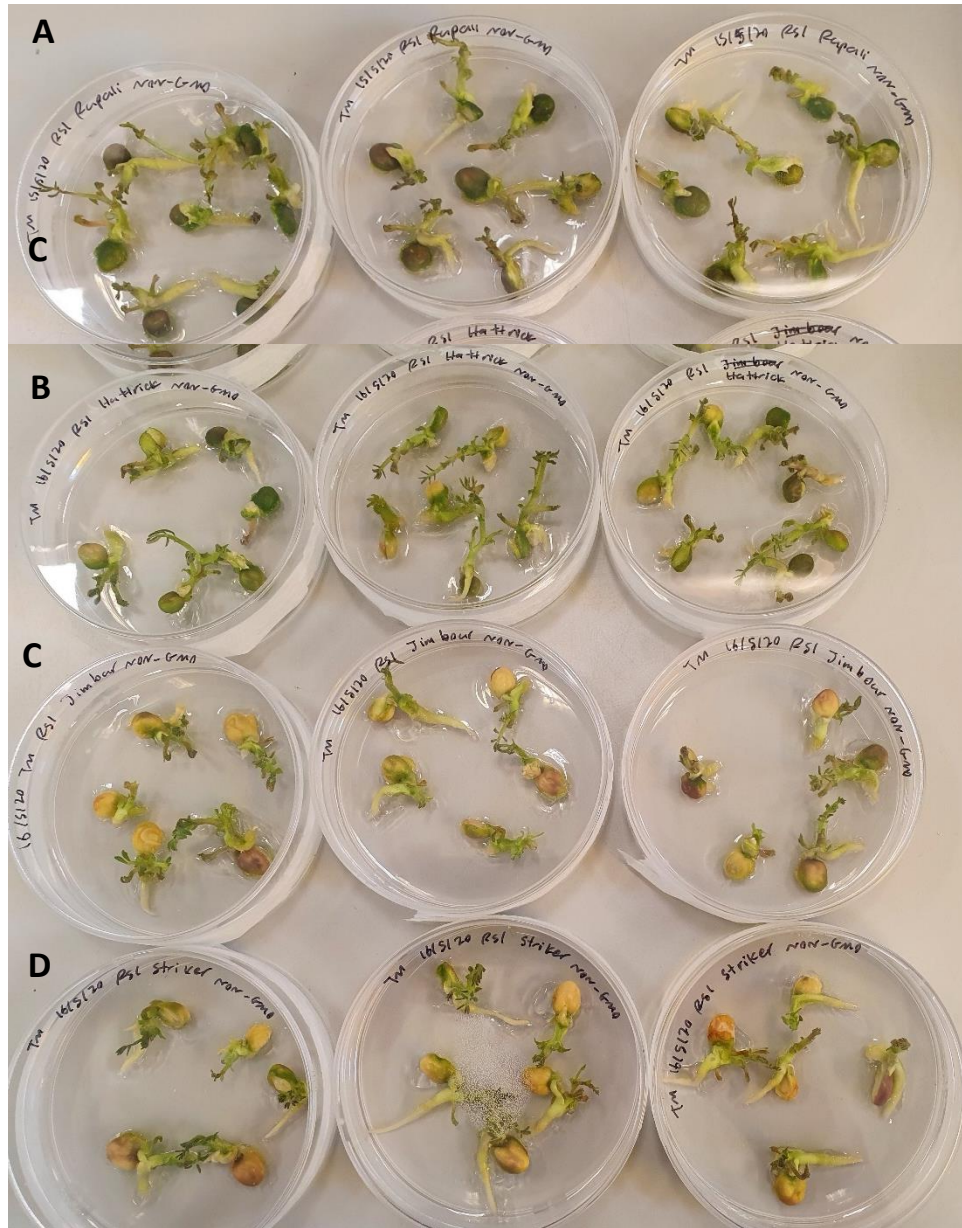


Figure 6a.6: Day 6 progression of explant growth after transition to RS1 media.

(A) Rupali, (B) Hatrick, (C) Jimbour, (D) Striker.

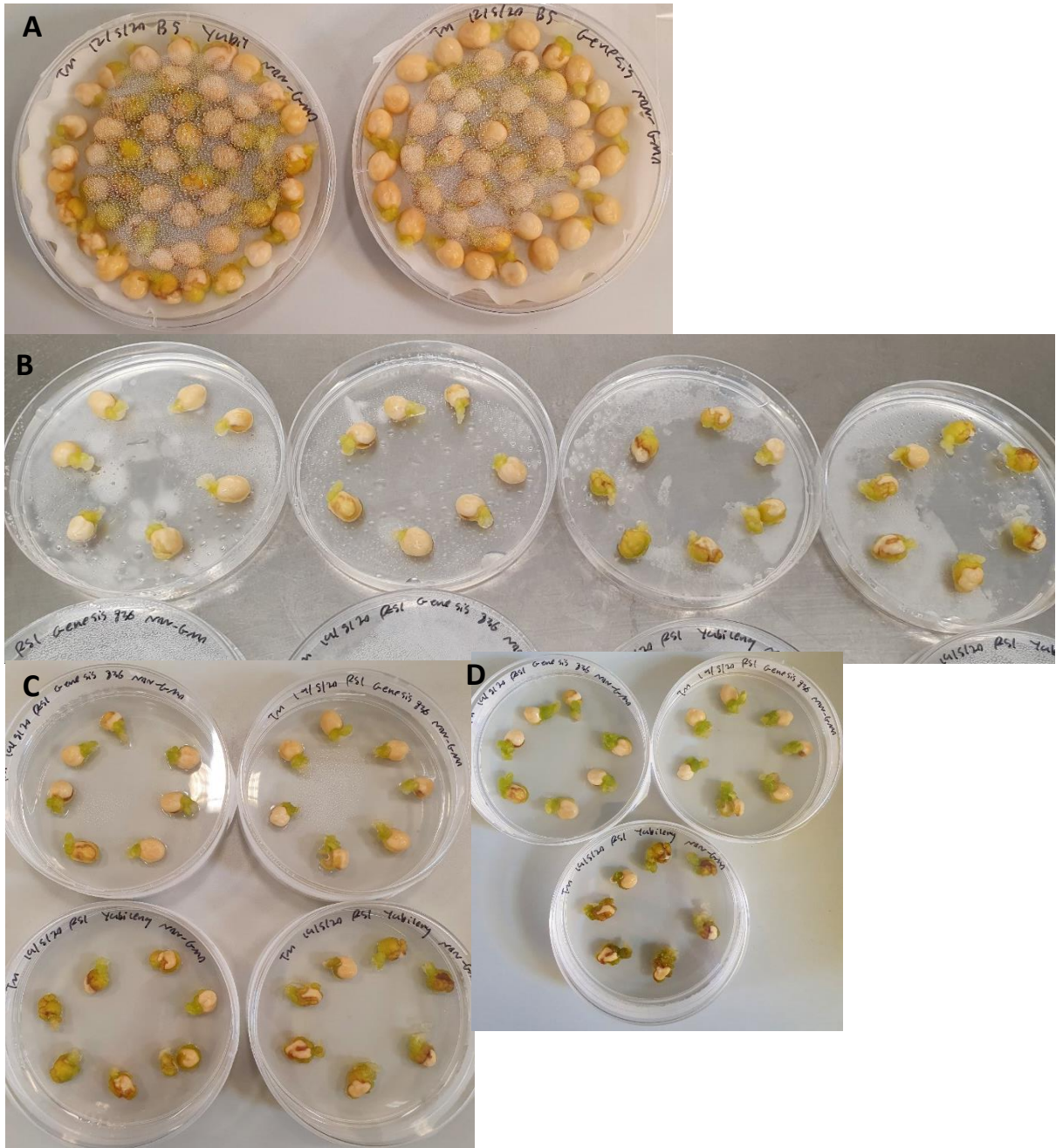


Figure 6a.7: Progression of Genesis and Yubileny transferred from (A) B5 media RS1 media after (B) 7 days, (C) 9 days and (D) 13 days.

Very slow germination and no shoot growth. Seeds appear to be forming a green callus instead of a shoot. Shoot growth is typically seen on day 3 however, both the Kabuli varieties have not produced a shoot only a green callus.

Genesis and yubileny appear to be incompatible to this tissue culture method. There was no sign of shoot growth after 13 days on RS1 media when shoot growth is typically seen at day 3. Shoots may emerge from the callus eventually, however, will be too time-consuming to be an effective cultivar. This does provide an opportunity to regenerate Kabuli cultivars from callus, something which could be explored in the future.

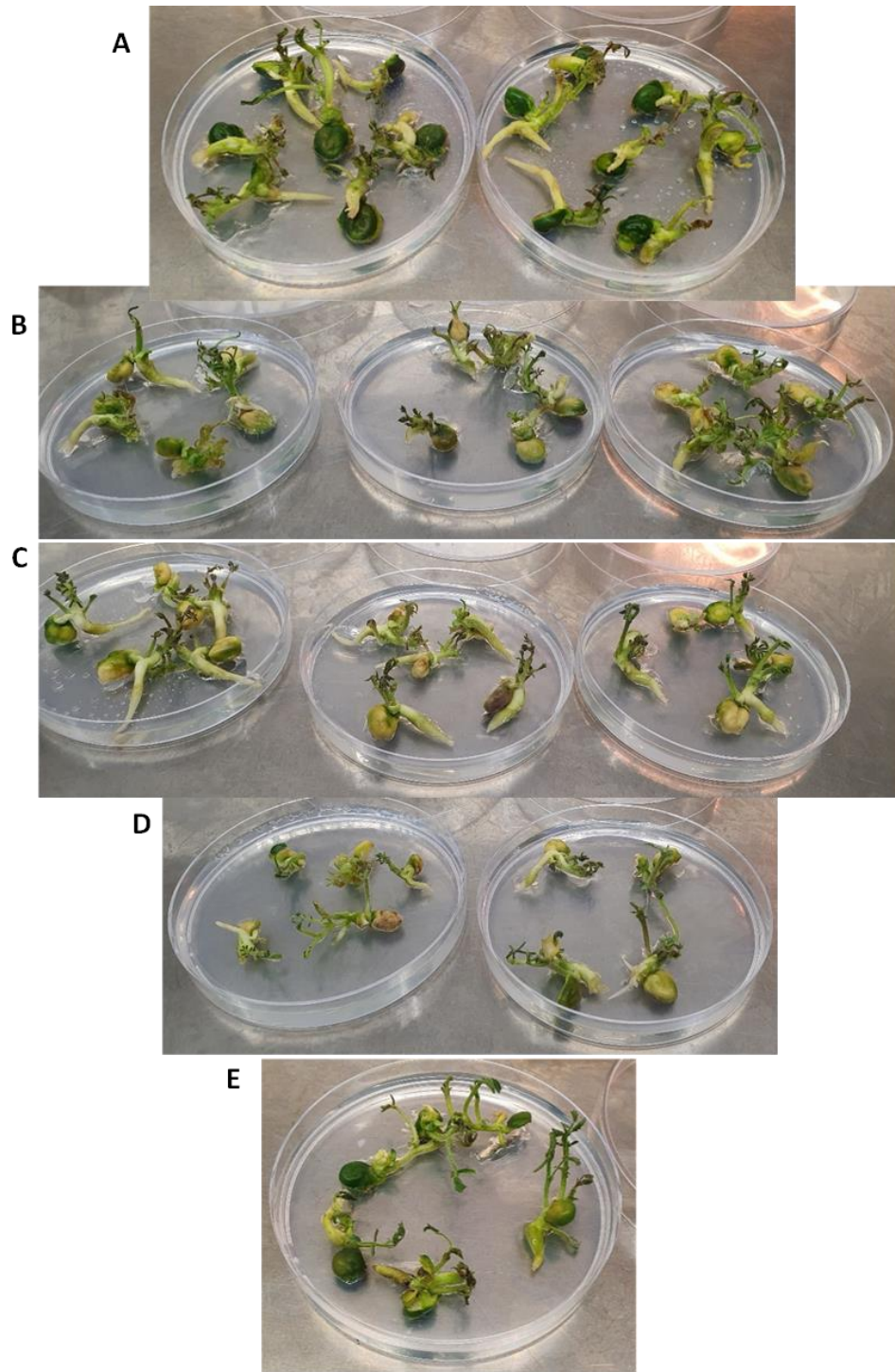


Figure 6a.8: Day 9 growth of cultivars prior to RS2, still on RS1 (A) Rupali, (B) Jimbour, (C) Striker, (D) Slasher, (E) Hatrick.



Figure 6a.9: (A) Day 9 transition of cultivars to larger magenta containers in RS1 media (Slasher – Rupali – Striker – Jimbour – Hattrick), (B) day 13 transition to RS2 media.

Table 6a.3: Summary of cultivar performance under chickpea tissue culture

Cultivar	Bisection Difficulty	Germination Frequency (On B5 Media After 3 Days)	Shoot Elongation (B5 to RS1 Transition)	Explant Quality (Transition to RS2)
Hattrick (Control)	Very Easy/Fast	64%	Day 4	Good
Rupali	Hard/Slow	85%	Day 3	Moderate
Jimbour	Easy/Fast	40%	Day 4	Moderate
Slasher	Easy/Moderate	22%	Day 6	Poor
Striker	Easy/Fast	36%	Day 4	Poor
Yubileny	Very Hard*/Slow	0%	Day 7+	NA
Genesis 826	Easy/Moderate	0%	Day 7+	NA

*Yubileny difficulty could be overcome by keeping the seed moist

*Germination frequency assumes roughly 50-55 (35-40 for Kabuli) bisections placed on B5 media.

Appendix 6a.3: Light intensity experiments

The 300PAR plates do seem to have less efficient germination and shoot quality. Red light and 70PAR look relatively similar, but 70PAR have slightly better-looking shoots (Figure 6a.11). PAR 70 had the greenest shoots and appeared to grow the fastest over the five-day period. PAR300 still germinated but showed some signs of stress with some browning of the shoots, particularly when compared to the 70 PAR tissue. They also showed minor signs of stunted growth. RED light seeds grew slightly slower than the 70 PAR seeds and showed no obvious signs of stress.

70 PAR: A lot of tissue browning (Leaf), but no chlorosis

RED: A lot of browning of tissue and chlorosis possibly due to the more intense light

300PAR: Not as much browning and currently no chlorosis.

Summary of light experiment: 1 week into RS1 all light treatments showed stress. 70PAR had slightly more tissue browning and minor slower growth than RED and 300PAR. Whereas RED and 300 PAR were relatively the same with less browning than the 70PAR but also had minor anthocyanin reddening of some leaves as well as minor chlorosis (light browning, instead of the normal browning) of leaf tissue. Overall, the 300PAR and RED seemed to be better at this stage. Perhaps starting plants at 70 then increasing light intensity would be an effective light treatment over time.

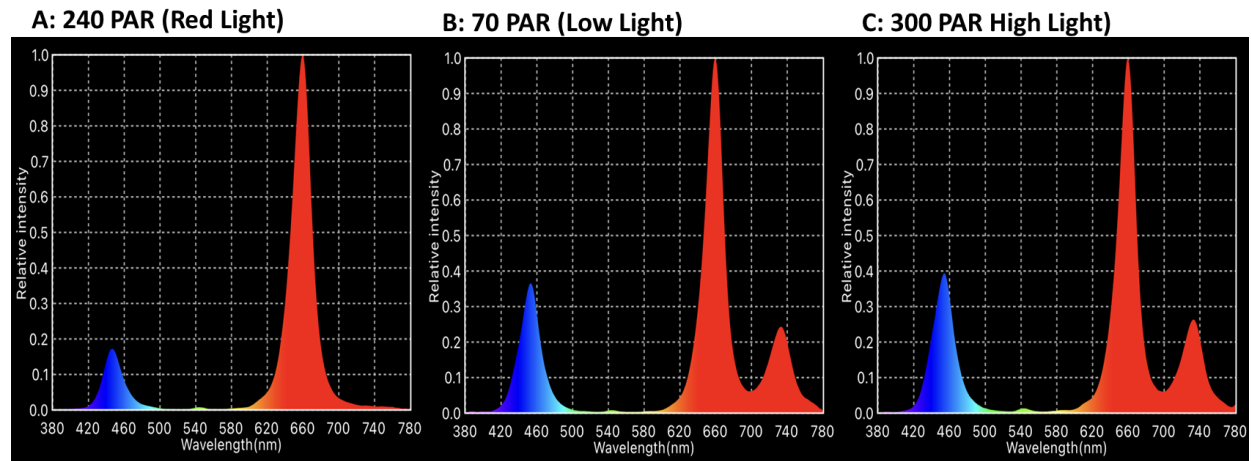


Figure 6a.10: Spectra wavelength using during light intensity experiments.

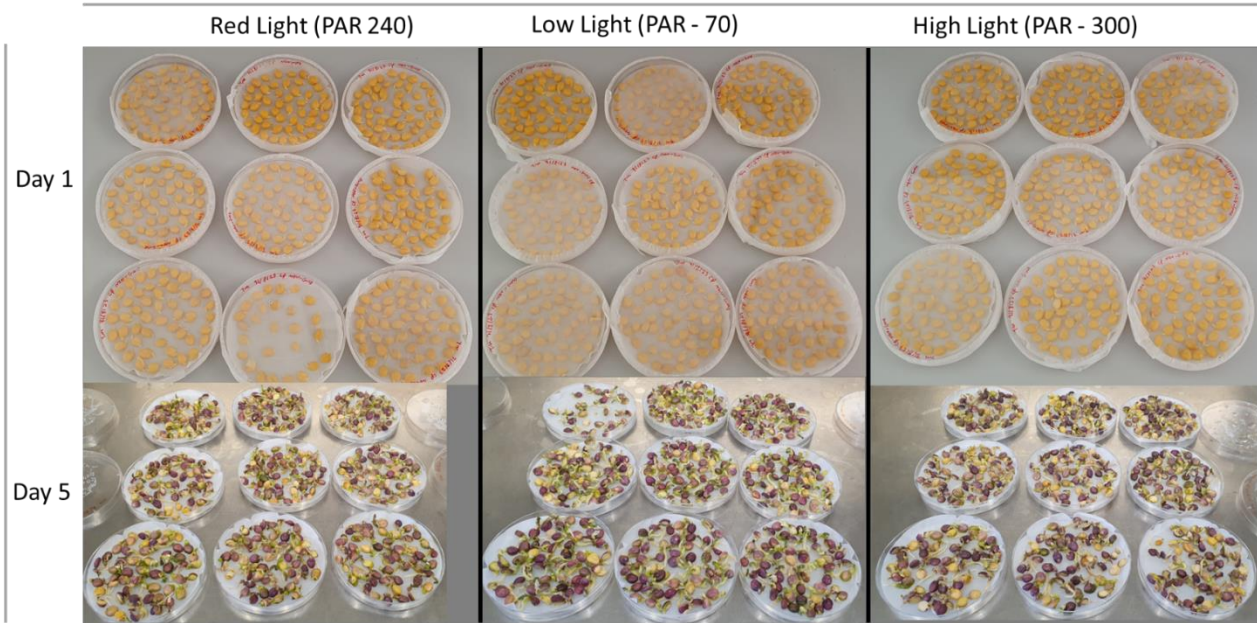


Figure 6a.11: RS1 transition to RS2.

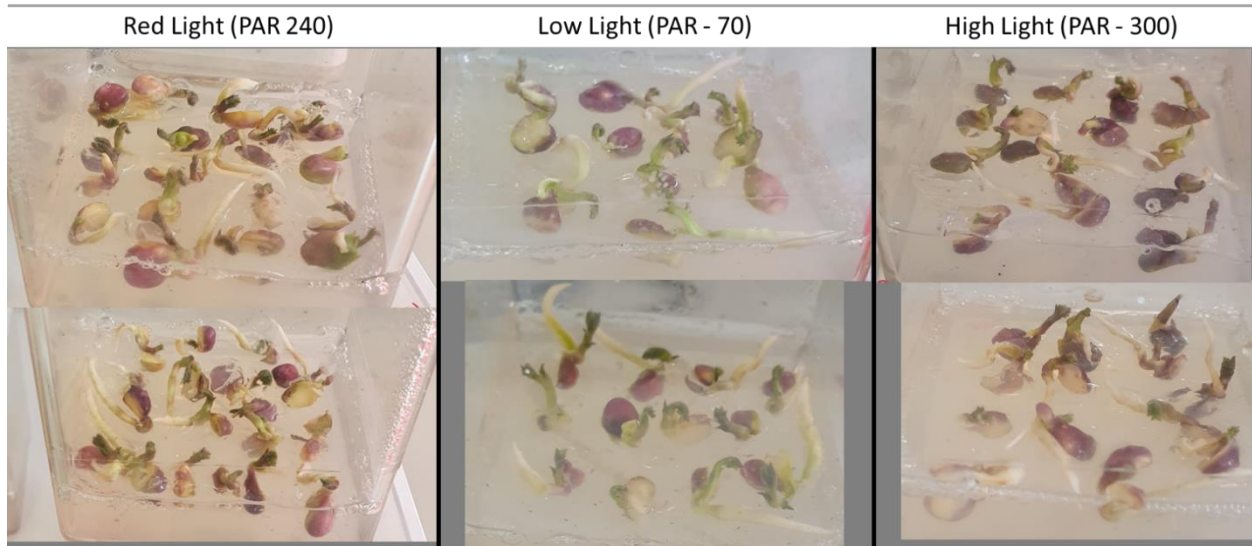


Figure 6a.12: Light experiment showing bisected seeds to RS1 media transition.

Table 6a.4: B5 to RS1 transition including seed counts and effect of light conditions on transition efficiency (%).

Light condition	Seed count at bisection	Seeds transferred to RS1	Efficiency (%)
Red light (par - 240)	450	163	36
Low light (par - 70)	424	206	49
High light (par - 300)	450	138	31

*50 seeds per plate, except one low light plate of 24 seeds

Table 6a.5: RS1 to RS2 transition including seed counts and effect of light conditions on transition efficiency (%).

Light condition	Plantlets at RS1	Plantlets transferred to RS2	Efficiency (%)
Red light (PAR - 240)	163	60	37
Low light (PAR - 70)	206	54	26
High light (PAR - 300)	138	62	45

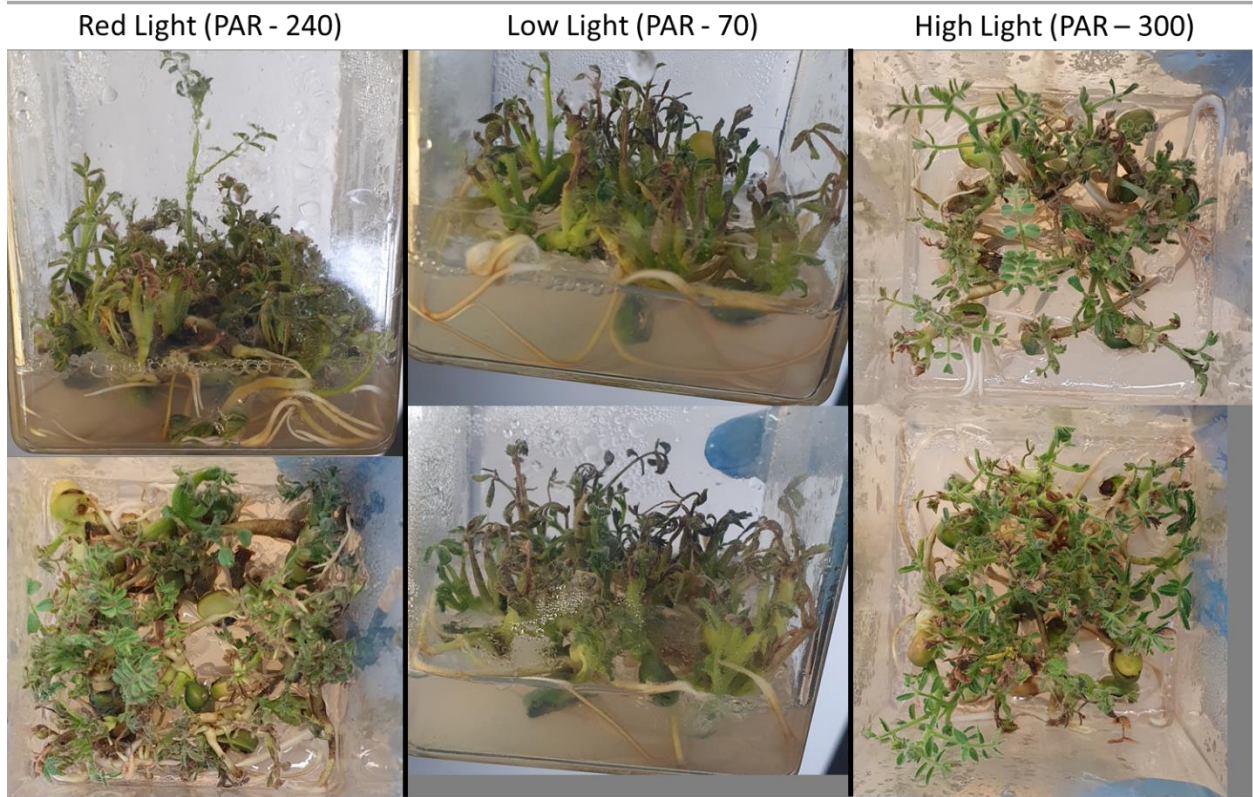


Figure 6a.13: Plantlets at the end of RS1 cycle grown with red (PAR-240), low (PAR-70) and high (PAR-300) light conditions.

Red Light (PAR - 240)



Low Light (PAR - 70)



High Light (PAR - 300)



Figure 6a.14: Plantlets transitioned from RS1 to RS2 grown with red (PAR-240), low (PAR-70) and high (PAR-300) light conditions.

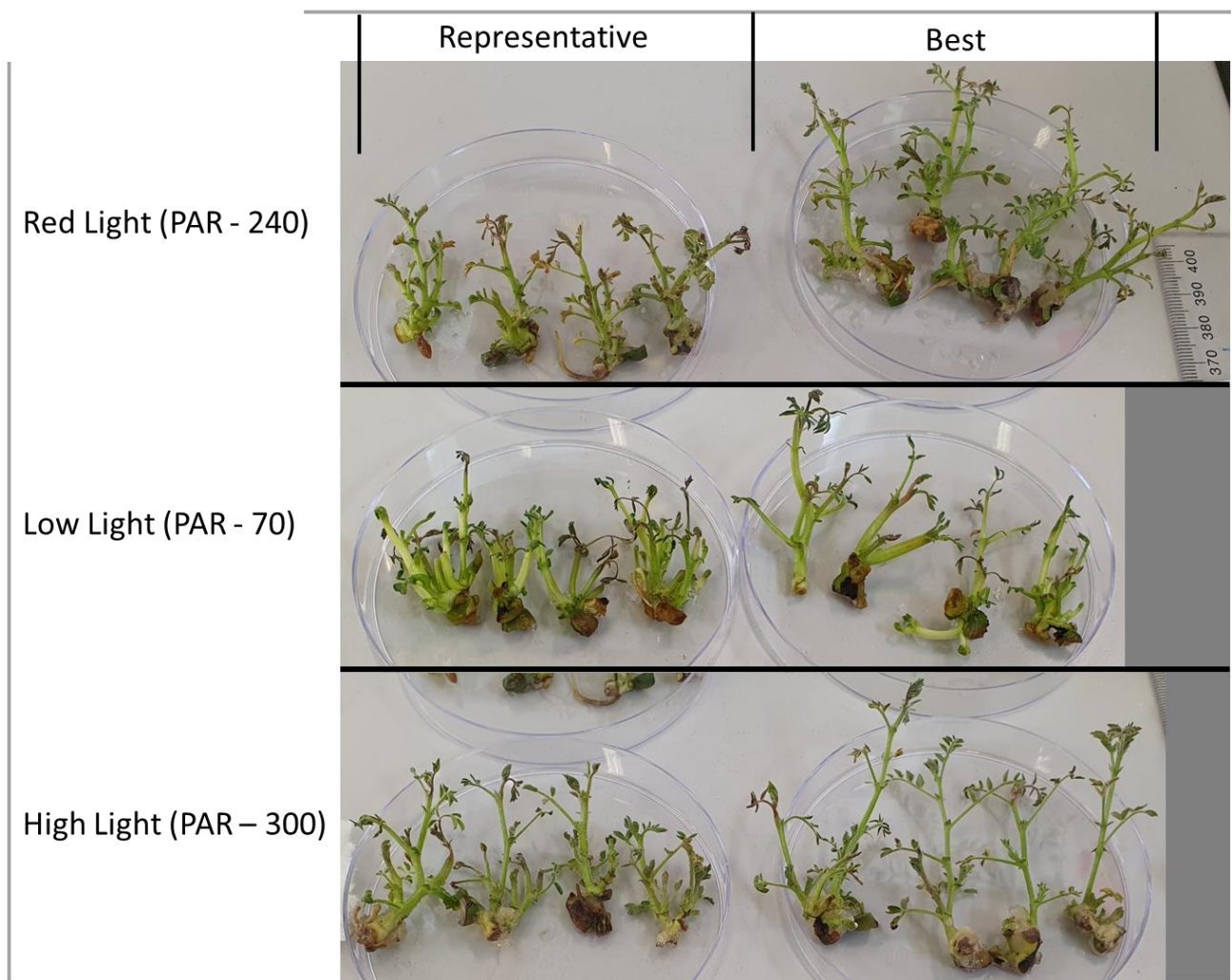


Figure 6a.15: Tissue quality at the end of RS2 when grown with red (PAR-240), low (PAR-70) and high (PAR-300) light conditions.